MALARIA TRANSMISSION BIOLOGY

EDITED BY: Rhoel Dinglasan, Matthias Marti, Isabelle Morlais and Brandon Keith Wilder

PUBLISHED IN: Frontiers in Microbiology and Frontiers in Cellular and Infection Microbiology

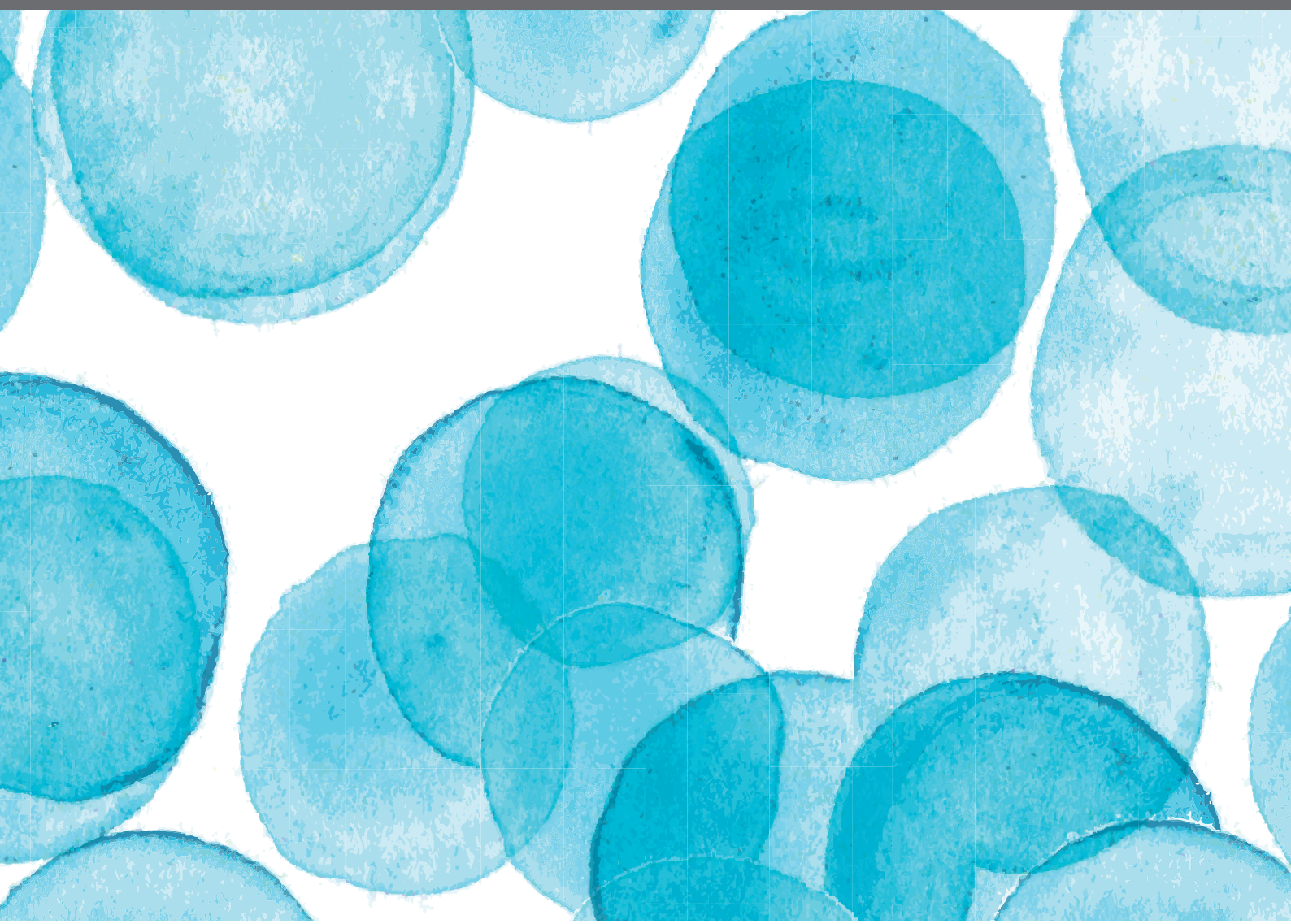

frontiers Research Topics

ISSN 1664-8714
ISBN 978-2-88966-422-1
DOI 10.3389/978-2-88966-422-1

About Frontiers

Frontiers is more than just an open-access publisher of scholarly articles: it is a pioneering approach to the world of academia, radically improving the way scholarly research is managed. The grand vision of Frontiers is a world where all people have an equal opportunity to seek, share and generate knowledge. Frontiers provides immediate and permanent online open access to all its publications, but this alone is not enough to realize our grand goals.

Frontiers Journal Series

The Frontiers Journal Series is a multi-tier and interdisciplinary set of open-access, online journals, promising a paradigm shift from the current review, selection and dissemination processes in academic publishing. All Frontiers journals are driven by researchers for researchers; therefore, they constitute a service to the scholarly community. At the same time, the Frontiers Journal Series operates on a revolutionary invention, the tiered publishing system, initially addressing specific communities of scholars, and gradually climbing up to broader public understanding, thus serving the interests of the lay society, too.

Dedication to Quality

Each Frontiers article is a landmark of the highest quality, thanks to genuinely collaborative interactions between authors and review editors, who include some of the world's best academicians. Research must be certified by peers before entering a stream of knowledge that may eventually reach the public - and shape society; therefore, Frontiers only applies the most rigorous and unbiased reviews.
Frontiers revolutionizes research publishing by freely delivering the most outstanding research, evaluated with no bias from both the academic and social point of view. By applying the most advanced information technologies, Frontiers is catapulting scholarly publishing into a new generation.

What are Frontiers Research Topics?

Frontiers Research Topics are very popular trademarks of the Frontiers Journals Series: they are collections of at least ten articles, all centered on a particular subject. With their unique mix of varied contributions from Original Research to Review Articles, Frontiers Research Topics unify the most influential researchers, the latest key findings and historical advances in a hot research area! Find out more on how to host your own Frontiers Research Topic or contribute to one as an author by contacting the Frontiers Editorial Office: researchtopics@frontiersin.org

MALARIA TRANSMISSION BIOLOGY

Topic Editors:
Rhoel Dinglasan, University of Florida, United States
Matthias Marti, University of Glasgow, United Kingdom
Isabelle Morlais, Institut de Recherche Pour le Développement (IRD), France
Brandon Keith Wilder, Oregon Health and Science University, United States

The malaria parasite life cycle is complex and includes an obligatory developmental stage in its mosquito vector host. This transition from human-host to mosquito-host to human-host involves multiple developmental stages and divergent host tissues. Over the years, the research focus on the asexual stage parasites, which causes the symptoms of the disease, has transitioned towards a renewed focus on the transmission forms (or gametocytes), the only stages transmittable to the mosquito vector through ingestion of an infected blood meal. Analysis of sporozoite-liver interactions that result in the establishment of parasitic infection in the mammalian host has become an important research focus, and we now have a greater appreciation of the fascinating development of the sporozoites of the mosquito midgut wall and its travel to the salivary glands prior to inoculation into the mammalian dermis. This Research Topic embraces the full transition of the malaria parasite between its two obligatory hosts in what is termed as "malaria transmission biology".

Of note are the critical, enabling technologies and experimental systems that have been developed over the recent decade and have opened up significant new avenues for exploring the multi-stage, and multi-step processes that comprise malaria transmission biology. From uncovering that gametocyte development occurs in the bone marrow to quantifying the influence of both human host metabolism and parasite genetics on mosquito infection, it is clear that malaria transmission biology has entered an exciting era of discovery. Importantly, recent maturation of humanized liver mice and more sophisticated in vitro platforms have allowed more accurate recapitulations of the mosquito-to-skin-to-liver stages of human malaria infection. This allows both observation and study of the biological nuances of parasite vector-to-mammalian host transmission as well as interventions which can inhibit or block this stage of transmission. Paired with observations from clinical trials and the field, we can better understand exactly which parameters in which systems are most relevant for translation and biology.

Citation: Dinglasan, R., Marti, M., Morlais, I., Wilder, B. K., eds. (2021). Malaria Transmission Biology. Lausanne: Frontiers Media SA.
doi: 10.3389/978-2-88966-422-1

Table of Contents

frontiers in Cellular and Infection Microbiology

BRIEF RESEARCH REPORT
published: 03 July 2019
doi: 10.3389/fcimb.2019.00238

Protein *O*-Fucosyltransferase 2 Is Not Essential for *Plasmodium berghei* Development

Silvia Sanz[1,2,3], Eleonora Aquilini[4], Rebecca E. Tweedell[2,3], Garima Verma[2,3], Timothy Hamerly[2,3], Bernadette Hritzo[2], Abhai Tripathi[2], Marta Machado[4], Thomas S. Churcher[5], João A. Rodrigues[4], Luis Izquierdo[1] and Rhoel R. Dinglasan[2,3]**

[1] ISGlobal, Barcelona Centre for International Health Research (CRESIB), Hospital Clínic-Universitat de Barcelona, Barcelona, Spain, [2] Department of Molecular Microbiology and Immunology, Johns Hopkins Bloomberg School of Public Health, Baltimore, MD, United States, [3] Department of Infectious Diseases and Immunology, The University of Florida Emerging Pathogens Institute, Gainesville, FL, United States, [4] Instituto de Medicina Molecular, Unidade de Malária, Universidade de Lisboa, Lisbon, Portugal, [5] Department of Infectious Disease Epidemiology, MRC Centre for Outbreak Analysis and Modelling, Imperial College London, London, United Kingdom

OPEN ACCESS

Edited by:
Paul R. Gilson,
Burnet Institute, Australia

Reviewed by:
Carlos A. Buscaglia,
National Council for Scientific and Technical Research (CONICET), Argentina
Sabrina Absalon,
Boston Children's Hospital, Harvard Medical School, United States
Ashley Vaughan,
Seattle Children's Research Institute, United States

***Correspondence:**
Luis Izquierdo
luis.izquierdo@isglobal.org
Rhoel R. Dinglasan
rdinglasan@epi.ufl.edu

Specialty section:
This article was submitted to Parasite and Host, a section of the journal Frontiers in Cellular and Infection Microbiology

Received: 05 April 2019
Accepted: 17 June 2019
Published: 03 July 2019

Citation:
Sanz S, Aquilini E, Tweedell RE, Verma G, Hamerly T, Hritzo B, Tripathi A, Machado M, Churcher TS, Rodrigues JA, Izquierdo L and Dinglasan RR (2019) Protein O-Fucosyltransferase 2 Is Not Essential for Plasmodium berghei Development. Front. Cell. Infect. Microbiol. 9:238. doi: 10.3389/fcimb.2019.00238

Thrombospondin type I repeat (TSR) domains are commonly *O*-fucosylated by protein *O*-fucosyltransferase 2 (PoFUT2), and this modification is required for optimal folding and secretion of TSR-containing proteins. The human malaria parasite *Plasmodium falciparum* expresses proteins containing TSR domains, such as the thrombospondin-related anonymous protein (TRAP) and circumsporozoite surface protein (CSP), which are *O*-fucosylated. TRAP and CSP are present on the surface of sporozoites and play essential roles in mosquito and human host invasion processes during the transmission stages. Here, we have generated PoFUT2 null-mutant *P. falciparum* and *Plasmodium berghei* (rodent) malaria parasites and, by phenotyping them throughout their complete life cycle, we show that PoFUT2 disruption does not affect the growth through the mosquito stages for both species. However, contrary to what has been described previously by others, *P. berghei* PoFUT2 null mutant sporozoites showed no deleterious motility phenotypes and successfully established blood stage infection in mice. This unexpected result indicates that the importance of *O*-fucosylation of TSR domains may differ between human and RODENT malaria parasites; complicating our understanding of glycosylation modifications in malaria biology.

Keywords: *Plasmodium falciparum*, *Plasmodium berghei*, *O*-fucosylation, protein *O*-fucosyltransferase 2, oocyst, sporozoite

INTRODUCTION

Malaria is one of the most important human parasitic diseases, causing ~219 million new cases and more than 400,000 deaths every year (WHO, 2018). It is caused by a protozoan apicomplexan parasite of the genus *Plasmodium*, with *Plasmodium falciparum* regarded as the deadliest species. *Plasmodium* parasites are transmitted by female *Anopheles* mosquitoes. After the bite of an infected mosquito, motile sporozoites are injected into the human dermis; from there, they travel through blood vessels to the liver and infect hepatocytes. A week later, the infected hepatocyte ruptures and releases merozoites that reach the blood circulation and invade erythrocytes initiating cyclical asexual reproduction. A small percentage of blood stage parasites become sexually committed cells

known as gametocytes, which are taken up during a mosquito blood meal. Once in the mosquito midgut, gametocytes develop into gametes, fertilization takes place, and zygotes are formed. These zygotes develop into motile ookinetes that traverse the mosquito midgut wall to form oocysts. Each oocyst can develop into thousands of sporozoites that invade the mosquito salivary glands and are ready to infect another human host (Menard et al., 2013).

Thrombospondin type 1 repeat (TSR) domains are small (50–60 amino acid residues) cysteine-knot motifs with 3 conserved disulfide bonds that play important roles in cell adhesion and motility (Adams and Tucker, 2000; Tan et al., 2002). *Plasmodium* parasites express several TSR domain-containing proteins throughout the different stages of their life cycle that are critical for host cell recognition, motility, and invasion (Morahan et al., 2009). These proteins include circumsporozoite protein (CSP) and thrombospondin-related anonymous protein (TRAP) in the sporozoite stage and circumsporozoite and TRAP-related protein (CTRP) in the ookinete stage (Wengelnik et al., 1999; Coppi et al., 2011; Mathias et al., 2013). Antibodies against these proteins inhibit host cell invasion and block the progression of the parasite's life cycle (Chattopadhyay et al., 2003; Li et al., 2004). Hence, TSR domain-containing proteins are potentially important vaccine targets (Moorthy et al., 2004). Indeed, the licensed malaria vaccine RTS,S (Mosquirix) is based on CSP (RTS,S Clinical Trials Partnership, 2015).

TSR domains are *O*-fucosylated by protein *O*-fucosyltransferase 2 (PoFUT2) (Luo et al., 2006; Leonhard-Melief and Haltiwanger, 2010). That fucose can be further elongated with a glucose residue, generating an *O*-linked disaccharide (Kozma et al., 2006). This modification is important for the secretion of TSR domain-containing proteins (Ricketts et al., 2007; Wang et al., 2007; Vasudevan and Haltiwanger, 2014). A recent report demonstrated that CSP and TRAP TSR domains are also *O*-fucosylated in the *Plasmodium* sporozoite stage (Swearingen et al., 2016). A homolog of PoFUT2 is conserved in all the *Plasmodium* species sequenced (Cova et al., 2015), and the parasite synthesizes the GDP-fucose (GDP-Fuc) precursor required for *O*-fucosylation (Sanz et al., 2013, 2016; López-Gutiérrez et al., 2017). In a recent study, Lopaticki et al. (2017) characterized the *P. falciparum* protein *O*-fucosyltransferase (PoFUT2) and showed that it is involved in the *O*-fucosylation of parasite TSR domains. The authors reported that PoFUT2 genetic disruption in *P. falciparum* resulted in a reduction in the ability of ookinetes to traverse the mosquito midgut to form oocysts. They also provided evidence showing that mosquitoes infected with ΔPoFUT2 parasites harbored significantly fewer sporozoites in the mosquito salivary glands compared to mosquitoes infected with the wild type *P. falciparum* parental line, NF54. Finally, they assessed the infectivity of salivary gland sporozoites by analyzing their motility, cell traversal activity, and hepatocyte invasion and by carrying out co-infection experiments using wild type and mutant parasites in a humanized chimeric liver mouse model; these assays revealed an apparent lower fitness of ΔPoFUT2 parasites in completing development in the mosquito and infecting mammalian hepatocytes compared to wild type NF54. Here, we report a robust study that differs from the central results of the previous report and reveals that under laboratory conditions, that PoFUT2 is not essential for murine parasite development and transmission.

MATERIALS AND METHODS

Ethics Statement

The human blood used for mosquito blood meals and *P. falciparum* culture was collected from a pool of pre-screened donors under an IRB-approved protocol at Johns Hopkins University (Protocol NA00019050) or obtained commercially from anonymous donors through Interstate Blood Bank or Banc de Sang i Teixits (Catalonia, Spain), after approval from the Comitè Ètic Investigació Clínica Hospital Clínic de Barcelona, making informed consent not applicable. Animal experiments were approved by the Portuguese official veterinary department for welfare licensing and the Instituto de Medicina Molecular Animal Ethics Committee. All animal experiments were performed in strict compliance to the guidelines of the institution's animal ethics committee and the Federation of European Laboratory Animal Science Associations (FELASA).

P. falciparum Asexual Parasite Culture and Transfection

P. falciparum NF54 parasites (*Pf*WT) (a kind gift of Teun Bousema, Radboud University Nijmegen Medical Center) were cultured with human B^+ erythrocytes (2–4% hematocrit) in complete culture medium (RPMI media [Sigma] supplemented with 10% AB^+ human serum or 0.5% Albumax II), incubated at 37°C in an atmosphere of 92% N_2, 3% O_2, and 5% CO_2 using standard methods (Trager and Jensen, 1976). *Pf*WT parasites were transfected by schizont nucleofection as described previously (Moon et al., 2013). After the appearance of resistant parasites, on/off drug cycling with WR22910 using 2-week cycles was used, followed by negative selection with 5-fluorocytosine (5FCyt) to select double recombinant parasites. Integrant clonal parasites were obtained by limiting dilution.

P. falciparum Transfection Construct

pCC1-*Pf*PoFUT2 transfection construct (Maier et al., 2006) consisted of two fragments of ≈ 850 and ≈ 960 bp, respectively, from different regions of the *Pf*PoFUT2 locus. F1 (nucleotides from −361 to +479 of the *Pf*PoFUT2 locus) and F2 (nucleotides from +1363 to 630 after the *Pf*PoFUT2 locus) fragments were amplified with primers pf3 (CAATGGCCCCTTTCCGCGGTCT TATGTCTTATTCTCATTTTGCTT) and pf4 (AGATCTTCGG ACTAGTCTTTTTGTAGCTGCAAGGGGG) for fragment F1, and pf5 (ATCGATAACTCCATGGTGAGCAATGGATTTGT ACAAGGT) and pf6 (CAGGCGCCAGCCTAGGTCAAGTGC AAGGGTTCTTTT) for fragment F2. The construct generated would integrate into the PoFUT2 locus, disrupting it by double crossover homologous recombination (**Figure 1A**).

P. falciparum Southern Blotting and PCR Analysis

Two μg of genomic DNA (gDNA) from *Pf*WT, SRΔPoFUT2 (single recombinant parasites before 5FCyt selection), and

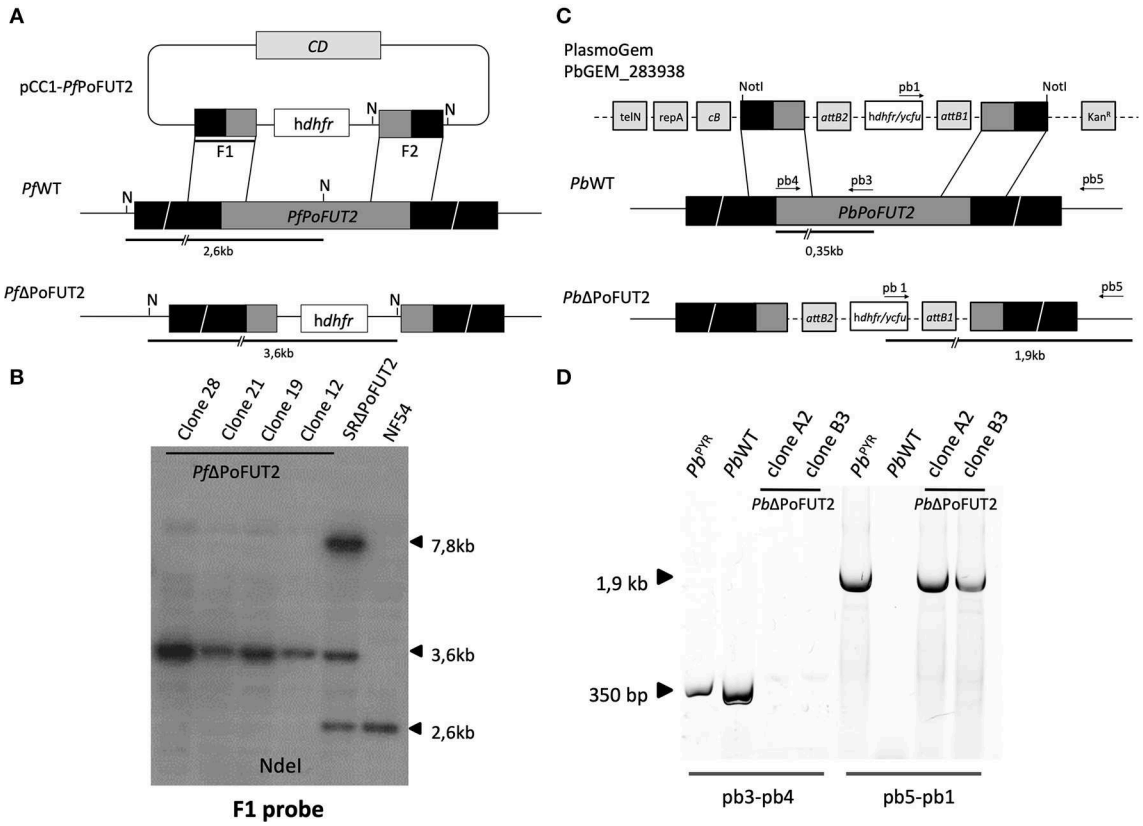

FIGURE 1 | PoFUT2 transfection constructs and integration events in human and rodent malaria parasites. **(A)** Scheme of the transfection plasmid (pCC1-*Pf*PoFUT2) used to target and disrupt *Pf*PoFUT2 in *P.falciparum* NF54 parasites (*Pf*WT) and the expected double crossover recombination event (*Pf*ΔPoFUT2). Black boxes represent upstream and downstream DNA sequence flanking the *Pf*PoFUT2 gene locus. Position of NdeI (N) sites, position of F1 probe (thick black line) and predicted length of the restriction fragments (thick black lines) are shown. **(B)** Southern blot of NdeI digested genomic DNA from *Pf*WT, SRΔPoFUT2, and *Pf*ΔPoFUT2 parasite clones hybridized with the F1 probe. SR refers to single recombinant parasites before negative selection with 5-FCyt. A 7.8Kb band (size of the pCC1-*Pf*PoFUT2 plasmid) can be also observed in SRΔPoFUT2 lane. **(C)** Scheme of the PlasmoGem transfection plasmid (PbGEM-283938) used to disrupt *Pb*PoFUT2 in *Pb*WT parasites and the expected double crossover recombination events (*Pb*ΔPoFUT2). Black boxes represent upstream and downstream DNA sequence flanking the *Pb*PoFUT2 gene locus. Position of NotI, predicted length of PCR fragments (black lines), and position of primers pb1, pb3, pb4, and pb5 are shown. TelN refers to telomerase, RepA to helicase, *cB* to arabinose-inducible origin, and Kan^R to the kanamycin resistance cassette. *att*B1 and *att*B2 are the recombination sequences for the Gateway technology. **(D)** Genotype analysis of *P. berghei* transfectants. PCR using genomic DNA from *Pb*WT, pyrimethamine-resistant population (Pb^{PYR}) and *Pb*ΔPoFUT2 clones as template were done using primers pb3 and pb4, and pb5 and pb1for wild type locus and integration (*Pb*PoFUT2 disruption), respectively.

Pf ΔPoFUT2 (*P. falciparum* PoFUT2 null mutant; four different clones) were digested with NdeI and probed with ^{32}P (Perkin Elmer)-labeled F1 (**Figure 1B**).

Mice

BALB/c and C57BL/6 mice (6–8 weeks of age) were purchased from Charles River and housed in the rodent facility of Instituto de Medicina Molecular (Lisbon, Portugal).

Plasmodium berghei Transfection, Cloning, and PCR Genotyping

Transfection experiments were performed using *Plasmodium berghei* ANKA strain 2.34 parasites (Janse et al., 2006). The PoFUT2 knockout vector PbGEM-283938 was obtained from the PlasmoGEM resource (Pfander et al., 2011) (http://plasmogem.sanger.ac.uk). The final knockout construct was digested with NotI to release the fragment for transfection (**Figure 1C**). The pyrimethamine-resistant parasite population (Pb^{PYR}) containing the correct genomic integration substituting PoFUT2 gene (*Pb*ΔPoFUT2) was cloned by injecting one parasite per mouse (BALB/c male mice, 6–8 weeks of age) to obtain *Pb*ΔPoFUT2. *hu-dhfr* cassette integration conveying resistance to pyrimethamine was tested using primers pb1 (CATACTAGCCATTTTATGTG), pb3 (AGCACCACGGGGGAAGGACT), pb4 (ATGCAAAAACGTCTTCCCTT), and pb5 (TCGAGCAACGATAAAATGCCT) (**Figure 1D**).

P. falciparum Gametocyte Cultures and Mosquito Infection

Pf WT and *Pf* ΔPoFUT2 were diluted to 0.5% mixed stage asexual parasites and 4% hematocrit with complete culture media and cultured at 37°C using the candle jar method (Trager and Jensen, 1976). The media was exchanged daily from day 1 to day 17 to allow for gametocyte maturation from stage I through stage V.

Standard membrane feeding assays (SMFA) were performed on day 15–18 post-culture initiation. Approximately 60 female *An. stephensi* (SDA-500) or *An. gambiae* (KEELE) mosquitoes were distributed into pint-sized cups and starved of sugar and water for ≈ 12 h prior to feeding. *Pf*WT and *Pf* ΔPoFUT2 gametocyte cultures were pelleted and diluted to 0.03 or 0.3% gametocytemia with human blood at 50% hematocrit. Blood was washed with RPMI media and brought to 50% hematocrit with heat-inactivated AB serum. Gametocytemic blood was kept at 37°C until feeding. Approximately 250–300 μL of gametocytemic blood was dispensed into a water-jacketed membrane feeder at 37°C, and mosquitoes were allowed to feed for a minimum of 45 min. After blood feeding, non-blood fed mosquitoes were removed. Blood fed mosquitoes were kept at 26°C and 70% humidity with a 12-h light:dark cycle. Mosquitoes were provided a 10% sucrose solution for energy.

P. berghei Mosquito Infections

An. stephensi mosquitoes were bred at the insectary of the Instituto de Medicina Molecular. For mosquito infection, female BALB/c mice were intraperitoneally injected with *P. berghei* wild type (*Pb*WT) and *Pb*ΔPoFUT2 mutant lines. Three to 5 days post-infection, the number of exflagellation events was determined using a Zeiss Axioskop 2 light microscope and a counting grid. If > 1 exflagellation event per field of view was observed, mice were anesthetized with a mixture of 10% ketamine and 2% xylazin in phosphate buffered saline (PBS) (100 μL per 20 g mouse body weight i.p.) and fed to *An. stephensi* mosquitoes. Unfed mosquitoes were removed, and fed mosquitoes were maintained at 19–22°C in 50–80% relative humidity. Mosquitoes were used 10–23 days post infection for further experiments.

Oocyst Counting and Imaging

For *P. falciparum* oocyst counting, mosquito midguts were dissected 8 to 10 days post-feeding; midguts were stained with 0.2% mercurochrome in water for 9 min. Midguts were placed on a slide with a drop of PBS, overlaid with a coverslip, and examined for oocysts using brightfield microscopy at 200× total magnification. Each midgut was imaged with ProGres CapturePro software to measure oocyst diameter, ensuring oocyst in all planes were visible. Six biological replicates with two technical replicates each were analyzed. *P. berghei* infected midguts were collected and stained with 0.5% mercurochrome 10 days post-feeding. Oocysts were counted to determine the intensity of infection (number of oocysts per midgut). Twelve experiments were carried out, and generalized mixed effect models (GLMM) were used for or statistical analysis.

Sporozoite Purification and Counting

On day 14 post-feeding, 30 mosquitoes infected with each *P. falciparum* line (*Pf*WT and *Pf* ΔPoFUT2) were dissected to obtain salivary glands. Each pair of salivary glands was kept in 100 μL PBS in a 1.5 mL tube. The tubes were spun at 1,200 × g for 3 min at room temperature (RT). The salivary gland pellet was gently crushed and vortexed for 3 s to resuspend the salivary gland contents. The tubes were spun again and sporozoites were counted blindly on a Zeiss Axioskop 2 microscope using a hemocytometer and averaging counts from 2 fields. Unpaired *t*-test was run using GraphPad (version 5.00). Three biological replicates with two technical replicates each were performed. *P. berghei* sporozoites (*Pb*WT and *Pb*ΔPoFUT2) were collected 21–24 days post-feeding from infected *An. stephensi* females bred at Instituto de Medicina Molecular. Salivary glands were dissected and kept in non-supplemented RPMI media at 4°C. Salivary glands were then smashed in a microcentrifuge tube. To eliminate mosquito debris and isolate sporozoites, samples were filtered using a 70 μm strainer. Sporozoites were counted in a Neubauer chamber using an Olympus CKX41 inverted microscope. Six experiments were performed using GLMM for statistical analysis.

P. berghei Gliding Motility Assays

For gliding motility analysis, 20,000 *P. berghei* sporozoites isolated from infected mosquito salivary glands were deposited on glass slides coated with anti-CSP monoclonal antibody (3D11 mouse mAb, 10 μg/mL final concentration) and incubated at 37°C for 1 h. Sporozoites were subsequently fixed in 4% paraformaldehyde for 10 min and blocked with 1% bovine serum albumin (BSA) in PBS for 1 h at RT. Parasites were stained with 3D11 antibody (10 μg/mL) for 1 h at RT, followed by three PBS washes. Sporozoites were further incubated (1:250) with goat anti-mouse AlexaFluor 488 (Jackson ImmunoResearch Laboratories). Three additional PBS washes were carried out. Sporozoites associated with CSP trails were visualized by fluorescence microscopy using a Zeiss Axiovert 200M microscope. Quantification was performed by counting the number of sporozoites performing < 3 circles, ≥ 3 and ≤ 10 circles, and > 10 circles.

Human Hepatoma Cell Culture and *in vitro* Infection With *P. berghei* Parasites

Human hepatoma Huh7 cells were cultured in RPMI 1640 media supplemented with 10% v/v fetal bovine serum, 0.1 mM non-essential amino acids, 50 μg/mL penicillin/streptomycin, 2 mM glutamine, and 1 mM HEPES (final concentrations) at pH 7 and maintained at 37°C with 5% CO_2.

For *in vitro* hepatic infections, cells were seeded on glass coverslips the day before infection. Sporozoite addition was followed by 5 min centrifugation at 1,800 × g. 48 h post-infection, cells were fixed for 20 min at RT and incubated with permeabilization/blocking solution (0.1% v/v Triton X-100, 1% w/v BSA in PBS) for 30 min at RT. Parasites were stained with an anti-UIS4 antibody (dilution 1:1,000, SICGEN # AB0042-200) for 1 h at RT, washed three times, and further incubated with anti-mouse AlexaFluor 488 secondary antibody (1:400 dilution) in the presence of Hoechst 33258 (1:1,000 dilution, Thermo Fisher Scientific) for nuclear staining. Coverslips were mounted on microscope slides with Fluoromount (SouthernBiotech). Widefield images for size determination were acquired with a Zeiss Axiovert 200M microscope. Images were processed with ImageJ software (version 1.47).

Sporozoite traversing activity was examined using a standard cell-wounding and membrane repair assay. Huh7 cells (1.0×10^4 per well) were seeded in 96-well plates the day before infection.

Sporozoites were added to cells for 2 h in the presence of 0.5 mg/mL FITC-labeled dextran (Thermo Fisher Scientific). Cells were collected for flow cytometry analysis 48 h post-infection and analyzed on a Becton Dickinson LSR Fortessa flow cytometer with the DIVA software (version 6.2). Analysis was carried out using the FlowJo software (version 6.4.7, FlowJo).

P. berghei Sporozoite Infectivity to Mice

For transmission experiments, naïve C57BL/6 mice were exposed to 10 mosquitoes infected with *Pb*WT or *Pb*ΔPoFUT2 for 30 min; 5 mice were used per parasite clone. Parasitemias were followed daily by counting Giemsa stained smears from a drop of tail blood. Animals were monitored daily for clinical signs of cerebral malaria (head deviation, convulsions, ataxia, and paraplegia). Mice were euthanized when required, according to the approved protocol, to avoid further stress and pain.

Statistical Analyses

GLMM was applied as described previously (Churcher et al., 2012) to test for differences between the prevalence of oocysts (assuming a binomial distribution error structure) and the average number of oocysts per mosquito (assuming a negative binomial distribution) (Bolker et al., 2012; Churcher et al., 2012). GraphPad Prism version 6 was used for standard statistical analyses as indicated in the respective sections above.

RESULTS

Creation of *Plasmodium* PoFUT2 Null Mutants (*Pf*ΔPoFUT2 and *Pb*ΔPoFUT2)

To study the function of PoFUT2 in *Plasmodium* parasites, we knocked out this gene in the human malaria parasite *P. falciparum*. *P. falciparum* PoFUT2 (*Pf*PoFUT2) was disrupted by double crossover recombination using a targeting construct (pCC1-*Pf*PoFUT2; Maier et al., 2006) that replaced the gene with a *hu-dhfr* selection cassette in the *P. falciparum* NF54 line, the same parasite line used by Lopaticki et al. (Lopaticki et al., 2017). To add robustness to our experimental data, a similar approach was used to ablate *P. berghei* PoFUT2 (*Pb*PoFUT2) in ANKA strain 2.34 parasites, using the available PlasmoGEM resource PbGEM-283938 plasmid (Pfander et al., 2011). After cloning *hu-dhfr* resistant parasites by limiting dilution, PCR or Southern blot analyses confirmed PoFUT2 disruption in two clones from both *Plasmodium* species (**Figure 1**). As reported (Lopaticki et al., 2017), the ability to produce PoFUT2 null-mutant parasites demonstrates that the gene is not essential for asexual blood stage growth in culture or in a rodent model of infection.

Oocyst Infection of Mosquito Midguts Is Similar in *Pf*ΔPoFUT2 and *Pf*WT

Considering the importance of TSR domain-containing proteins such as CTRP, CSP, and TRAP in the mosquito stages of parasite development, we examined the function of PoFUT2 throughout the complete life cycle of *Plasmodium*. Notably, CTRP is an ookinete surface protein containing 7 TSR domains and 5 conserved *O*-fucosylation motifs that plays a critical role in *Plasmodium* invasion of the *Anopheles* midgut (Dessens et al., 1999). To understand the importance of PoFUT2 for oocyst infection, we infected *An. gambiae* mosquitoes with *Pf*WT and *Pf*ΔPoFUT2 gametocyte cultures. Recognizing the inherent variation from experiment to experiment when using SMFA for mosquito infections (Churcher et al., 2012), we conducted 12 experiments to capture the entire variation in oocyst development in the mosquito midgut.

We quantified the *P. falciparum* oocyst numbers on the *An. gambiae* midgut wall following *Pf*WT or *Pf*ΔPoFUT2 parasite infection (**Figure 2A**). GLMM was used to test for differences between the average number of oocysts (assuming a negative binomial distribution) and oocyst prevalence (assuming a binomial distribution; Churcher et al., 2012). An average difference between *Pf*WT and *Pf*ΔPoFUT2 parasites was calculated by including replicate number as a random effect, which accounts for differences in infectivity between the replicates. There was no significant difference in *P. falciparum* oocyst intensity (P value $= 0.517$) and prevalence (P value $= 0.963$) (**Figure 2B**). Furthermore, the diameter and mean size of *P. falciparum* oocysts were comparable for *Pf*WT and *Pf*ΔPoFUT2 parasites (**Supplementary Figures 1A–D**). Six biological replicates (with two technical replicates each) were performed with *P. falciparum* parasites.

PoFUT2 Is Not Required for *An. gambiae* Salivary Gland Infection by Sporozoites

CSP is an important sporozoite surface protein with a single *O*-fucosylation site in the TSR domain. We quantified the number of sporozoites per salivary gland pair at day 14 post-blood feeding for *P. falciparum*. Three biological replicates (with two technical replicates each for a total of 6 experiments) were performed with *P. falciparum* (**Supplementary Figure S2A**). Using a GLMM approach, we observed that *Anopheles* mosquitoes carrying null-mutant or wild type parasites showed comparable numbers of salivary gland sporozoites (intensity counts P value $= 0.446$, prevalence P value $= 0.645$). Hence, PoFUT2 does not play a critical role for parasite maturation in oocysts or salivary gland colonization.

PoFUT2 Is Not Essential in a Murine Malaria Model

To examine the cross-species role of PoFUT2, additional functional assays were carried out with *P. berghei* parasites lacking PoFUT2 (*Pb*ΔPoFUT2). The murine malaria model allows for the use of non-transgenic mice, which are infected routinely by *P. berghei* sporozoites. We infected *An. stephensi* mosquitoes with *Pb*WT and *Pb*ΔPoFUT2 parasites and examined oocyst intensity and prevalence, salivary gland sporozoite characteristics, and *in vivo* infection of mice. In the *P. berghei-An. stephensi* model, there was no significant difference in *P. berghei* oocyst intensity (P value $= 0.656$) and prevalence (P value $= 0.962$); which corroborated our *P. falciparum* results in *An. gambiae*

Sporozoite motility assays (**Figure 2C**) and *in vitro* hepatic infection experiments with *Pb*ΔPoFUT2 mutant parasites (**Supplementary Figures 2B,C**) produced comparable results

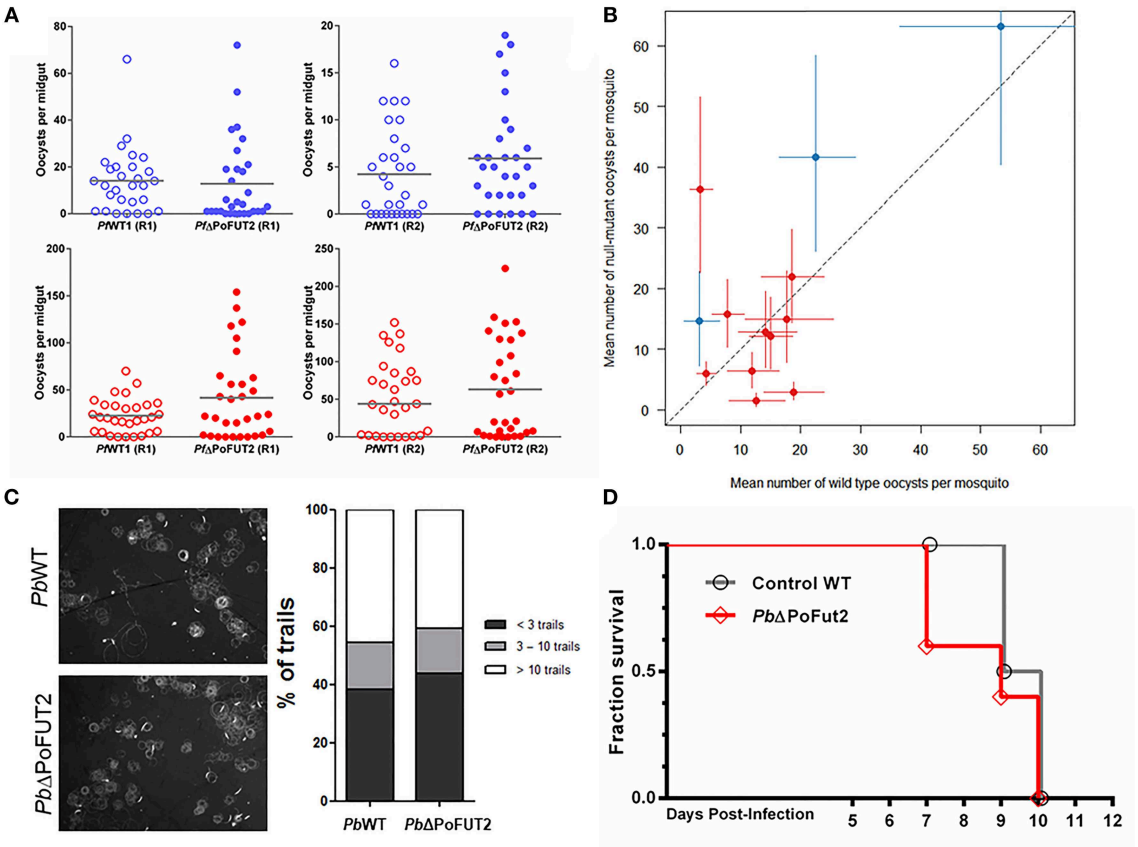

FIGURE 2 | Wild type and PoFUT2 mutant *Plasmodium* parasites demonstrate comparable infectiousness to mosquitoes but exhibit species-specific difference in infection phenotypes for mosquito-mammal transmission. **(A)** *An. gambiae* female mosquitoes ($N = 30$ per group) were fed with *Pf*WT (open) and *Pf*ΔPoFUT2 (closed), and oocyst number per midgut was counted 8 days post-feed for two gametocyte concentrations: 0.03% (blue) and 0.3% (red). Two representative replicate experiments at each gametocyte concentration (R1, R2) are shown. Horizontal bars indicate the mean oocyst number per midgut. **(B)** Generalized Linear Mix Model statistical analysis of the mean oocyst intensity and infection prevalence from SMFAs performed with *Pf*WT or *Pf*ΔPoFUT2 in either 0.03% gametocytemia (blue) or 0.3% gametocytemia (red). Black dotted line indicates no difference between the two groups of mosquitoes; colored vertical, and horizontal lines denote 95% confidence intervals for the point estimates. **(C)** Motility assays were performed for *Pb*WT and *Pb*ΔPoFUT parasites to monitor CSP trails (left panels). The number of trails for each sporozoite was classified as < 3 circles (dark gray), 3–10 circles (light gray), or > 10 circles (white; right panel). **(D)** C57BL/6 mice were infected by mosquito direct feeding with *Pb*WT (gray line) or *Pb*ΔPoFUT2 (red line) and monitored for patency (blood stage infection) and subsequent survival.

between WT and null-mutant parasites. Finally, two independent experiments performed with *P. berghei* showed that *Pb*ΔPoFUT2 sporozoites were able to infect C57BL/6 mice in mosquito "bite-back" direct feeding experiments (**Figure 2D**). For *Pb*WT (gray lines, **Figure 2D**), 4/5 mice succumbed to cerebral malaria (2 at day 9 and 2 at day 10) and the fifth mouse that remained alive with high parasitemia was sacrificed on day 10. For *Pb*ΔPoFUT2 (red lines, **Figure 2D**), 4/5 mice succumbed to cerebral malaria (2 at day 7, 1 at day 9, and 1 at day 10) and the fifth mouse that remained alive with high parasitemia was sacrificed on day 10. Comparable sporozoite numbers developed in mosquitoes for both *Pb*WT and *Pb*ΔPoFUT2 (**Table 1**), akin to what was observed for *P. falciparum* (**Supplementary Figure 2A**). The apparent reduction in sporozoites/salivary gland pair in Experiment A is not reproducible (as shown in Experiment B), underscoring the variation in the system. These results demonstrated that *Pb*ΔPoFUT2 mutants are fully infectious and able to progress through skin passage, hepatocyte infection, and intrahepatic or liver stage development.

TABLE 1 | *Plasmodium berghei* WT and *Pb*ΔPoFUT2 "bite back" infections in mice.

Expt	*Pb*WT (N)	% Infected mice (n/N)	*Pb*ΔPoFUT2 (N)	% Infected mice (n/N)
A	114,000/mosquito (13)	100% (5/5)	65,019/mosquito (13)	100% (5/5)
B	133,750/mosquito (10)	100% (5/5)	148,255/mosquito (10)	100% (5/5)

DISCUSSION

O-fucosylation, the process of adding a fucose residue to the -OH side chain of serines or threonines in TSR cysteine-rich domains (Leonhard-Melief and Haltiwanger, 2010), is

mediated by PoFUT2 *O*-fucosyltransferase (Valero-González et al., 2016). The *O*-fucosylation of *P. falciparum* CSP and TRAP sporozoite proteins has been recently demonstrated (Swearingen et al., 2016). Considering the relevance of these and other TSR domain-containing proteins for *Plasmodium* invasion and motility (Morahan et al., 2009), we created a PoFUT2 null-mutant in human and rodent parasites to completely assess the effect of PoFUT2 disruption throughout the parasite life cycle. We observed that PoFUT2 was not required for either *P. falciparum* or *P. berghei* infection of *Anopheles* mosquitoes by counting the number of oocysts per midgut. These data are in clear contrast to the reported observation by Lopaticki et al. (2017), which pooled data from replicate assays. Pooling data without statistical support may generate misleading results, as there can be large variability in average oocyst counts between replicates (as seen in **Figure 2B**) with single studies biasing overall estimates. However, testing differences using robust and adequate GLMMs is more appropriate to analyze SMFA assays (Churcher et al., 2012), which have a high variability risk due to the use of different sources of blood, cages, or feeders and the generation of highly dispersed data. GLMM, a multi-level analysis enabling the estimation of a fixed effect (number of oocysts) while allowing the level of infection in different assays to vary at random, is the statistical model of choice for assessing parasite infectiousness to mosquito vectors (Churcher et al., 2015; Kapulu et al., 2015).

Remarkably, our primary parasite-mosquito model pits an African parasite (NF54) with an African mosquito vector (*An. gambiae* KEELE), which represents the closest natural combination in laboratory studies. *An. stephensi* (SDA-500) has also been the customary laboratory vector for *P. berghei* studies. Although other groups have used *An. stephensi-P. falciparum* (NF54) combinations, we have found that the overall mean oocyst intensity tends to be lower than what is observed for *An. gambiae-P. falciparum*. We tested two gametocyte densities of 0.03 and 0.3% to determine whether any potential phenotypes would be observed at lower parasite densities during mosquito infection. In both cases, no reductions in oocyst development were observed. Therefore, in our hands PoFUT2 disruption did not affect oocyst development in the most relevant parasite-mosquito species combinations in a laboratory setting for both human and murine malaria models.

CSP and TRAP are important sporozoite TSR domain-containing proteins which are *O*-fucosylated by PoFUT2 (Swearingen et al., 2016). However, *Plasmodium* PoFUT2 null-mutants and wild type parasites showed comparable numbers of sporozoites in mosquito salivary glands. Furthermore, sporozoite motility, and infectivity was similar in *Pb*WT and *Pb*ΔPoFUT2 parasites, in agreement with mouse infectivity data. Interestingly, TRAP secretion appears to have been partly affected in the work published by Lopaticki et al. (2017). This is not surprising, as it is known that the intensity of attenuated PoFUT2-ablation phenotypes are protein-specific (Vasudevan et al., 2015). However, the ookinete and sporozoite infectivity in mosquitoes and vertebrates, respectively, remains unchanged; indicating that functional redundancy or the presence of multiple parasite "invasins" ensures the success of the malaria parasite during transmission. As Lopaticki et al. (2017), mention in their study, the absence of many genes necessary for classical glycosylation in *Plasmodium* genomes (von Itzstein et al., 2008; Cova et al., 2015), together with some contradictory results (Kimura et al., 1996; Gowda et al., 1997), fueled the debate about the existence of protein glycosylation in the malaria parasite, with the exception of glycosylphosphatidylinositol anchors (Naik et al., 2000). Recently, studies are casting new light on this issue (Bushkin et al., 2010; Sanz et al., 2013, 2016; Swearingen et al., 2016; López-Gutiérrez et al., 2017). Additionally, recent work exploring the function of PoFUT2 in *Toxoplasma gondii*, a *Plasmodium* related parasite, also revealed discrepancies in the effect of PoFUT2 null mutants on microneme protein 2 secretion and host cell attachment and invasion (Bandini et al., 2019; Gas-Pascual et al., 2019; Khurana et al., 2019). Our results suggest that within *Plasmodia*, nuanced differences with respect to developmental biology and host preference can also result in the observation of diverse phenotypes, which in this case is specific to *O*-fucosylation of sporozoite TSR domain-containing proteins. Taking into account previous and current controversies about the glycobiology of *Plasmodium* and our experimental results reported here, we note that caution must be exercised before considering protein *O*-fucosylation as a strict requirement for the efficient infection of mosquito and vertebrate hosts for all *Plasmodium* species.

DATA AVAILABILITY

All datasets generated for this study are included in the manuscript and/or the Supplementary Files.

AUTHOR CONTRIBUTIONS

SS, RD, and LI conceived the work. SS and EA knocked out and genotyped *Plasmodium falciparum* and *Plasmodium berghei* lines, respectively. SS, RD, RT, AT, BH, TH, and GV conducted the oocyst and sporozoite experiments with *P. falciparum* strains. EA, MM, and JR were responsible for *P. berghei* experiments. SS, LI, and RD outlined the manuscript. TC and RD performed SMFAs GLMM statistical analyses. All authors contributed to the writing and review of this manuscript.

FUNDING

This work was funded by National Institutes of Health (grant 1R21AI115063-01).

ACKNOWLEDGMENTS

Authors thank funding from National Institutes of Health (1R21AI115063-01, supporting SS, RD, and LI) as well as the Bloomberg Family Foundation/Johns Hopkins Malaria Research Institute and the UF Rising/Preeminence Program and the Emerging Pathogens Institute at the University of Florida (RD). EA, JR, and LI are members of the GlycoPar-EU FP7 funded Marie Curie Initial Training Network (GA 608295),

and LI is also supported by the Spanish Ministry of Economy (FEDER SAF2016-76080-R). ISGlobal is a member of the CERCA Programme, Generalitat de Catalunya. SS thanks for funding from Boehringer Ingelheim Fonds and EMBO (ASTF 598–2015) for supporting exchanges. The authors thank P. Eggleston and H. Hurd for the *An. gambiae* (KEELE) line. The authors also thank M. Ramírez, M. Cova, and B. López-Gutiérrez for technical support, advice, assistance, and useful suggestions.

SUPPLEMENTARY MATERIAL

The Supplementary Material for this article can be found online at: https://www.frontiersin.org/articles/10.3389/fcimb.2019.00238/full#supplementary-material

Supplementary Figure 1 | Oocyst development as a proxy-measure for successful ookinete invasion of the mosquito midgut epithelium is not impacted in *Pf*ΔPoFUT2 parasites. **(A,B)** Brightfield images of mercurochrome-stained *Pf*WT or *Pf*ΔPoFUT2 oocysts. **(C,D)** The range of *Plasmodium falciparum* oocyst diameters within individually mosquitoes (μm) **(C)** and the mean diameter of oocysts for all infected mosquitoes (μm) **(D)** of the *Pf*WT (white) and *Pf*ΔPoFUT2 (gray) oocyst is represented. Unpaired *t*-test *P* value = 0.6897. The horizontal bar indicates the mean oocyst diameter.

Supplementary Figure 2 | Sporozoite development, motility, and infection of hepatocytes by null-mutant parasites is unaffected. **(A)** *P. falciparum* sporozoites (*Pf*WT and *Pf*ΔPoFUT2) were counted on day 14 post-blood feeding. Two representative experiments of six total are shown. **(B)** *in vitro* hepatocyte infection of Huh7 cells normalized to *Pb*WT infection as 100%. Mann-Whitney *U* test *P* value = 0.1716. **(C)** Exoerythrocytic form (EEF) size in Huh7 hepatocyte cell infection model with *Pb*WT and *Pb*ΔPoFUT2 sporozoites. Unpaired *t*-test *P* value = 0.3931.

REFERENCES

Adams, J. C., and Tucker, R. P. (2000). The thrombospondin type 1 repeat (TSR) superfamily: diverse proteins with related roles in neuronal development. *Dev. Dyn.* 218, 280–299. doi: 10.1002/(SICI)1097-0177(200006)218:2<280::AID-DVDY4>3.0.CO;2-0

Bandini, G., Leon, D. R., Hoppe, C. M., Zhang, Y., Agop-Nersesian, C., Shears, M. J., et al. (2019). O-Fucosylation of thrombospondin-like repeats is required for processing of microneme protein 2 and for efficient host cell invasion by *Toxoplasma gondii* tachyzoites. *J. Biol. Chem.* 294, 1967–1983. doi: 10.1074/jbc.RA118.005179

Bolker, B., Skaug, H., Magnusson, A., and Nielsen, A. (2012). *Getting Started With the glmmADMB Package.* Available online at: http://glmmadmb.r-forge.r-project.org/glmmADMB.pdf

Bushkin, G. G., Ratner, D. M., Cui, J., Banerjee, S., Duraisingh, M. T., Jennings, C. V., et al. (2010). Suggestive evidence for Darwinian selection against asparagine-linked glycans of *Plasmodium falciparum* and *Toxoplasma gondii*. *Eukaryot. Cell* 9, 228–241. doi: 10.1128/EC.00197-09

Chattopadhyay, R., Rathore, D., Fujioka, H., Kumar, S., de la Vega, P., Haynes, D., et al. (2003). PfSPATR, a *Plasmodium falciparum* protein containing an altered thrombospondin type I repeat domain is expressed at several stages of the parasite life cycle and is the target of inhibitory antibodies. *J. Biol. Chem.* 278, 25977–25981. doi: 10.1074/jbc.M300865200

Churcher, T. S., Blagborough, A. M., Delves, M., Ramakrishnan, C., Kapulu, M. C., Williams, A. R., et al. (2012). Measuring the blockade of malaria transmission–an analysis of the standard membrane feeding assay. *Int. J. Parasitol.* 42, 1037–1044. doi: 10.1016/j.ijpara.2012.09.002

Churcher, T. S., Trape, J. F., and Cohuet, A. (2015). Human-to-mosquito transmission efficiency increases as malaria is controlled. *Nat. Commun.* 6:6054. doi: 10.1038/ncomms7054

Coppi, A., Natarajan, R., Pradel, G., Bennett, B. L., James, E. R., Roggero, M. A., et al. (2011). The malaria circumsporozoite protein has two functional domains, each with distinct roles as sporozoites journey from mosquito to mammalian host. *J. Exp. Med.* 208, 341–356. doi: 10.1084/jem.20101488

Cova, M., Rodrigues, J. A., Smith, T. K., and Izquierdo, L. (2015). Sugar activation and glycosylation in Plasmodium. *Malar. J.* 14:427. doi: 10.1186/s12936-015-0949-z

Dessens, J. T., Beetsma, A. L., Dimopoulos, G., Wengelnik, K., Crisanti, A., Kafatos, F. C., et al. (1999). CTRP is essential for mosquito infection by malaria ookinetes. *EMBO J.* 18, 6221–6227. doi: 10.1093/emboj/18.22.6221

Gas-Pascual, E., Ichikawa, H. T., Sheikh, M. O., Serji, M. I., Deng, B., Mandalasi, M., et al. (2019). CRISPR/Cas9 and glycomics tools for *Toxoplasma* glycobiology. *J. Biol. Chem.* 294, 1104–1125. doi: 10.1074/jbc.RA118.006072

Gowda, D. C., Gupta, P., and Davidson, E. A. (1997). Glycosylphosphatidylinositol anchors represent the major carbohydrate modification in proteins of intraerythrocytic stage *Plasmodium falciparum*. *J. Biol. Chem.* 272, 6428–6439. doi: 10.1074/jbc.272.10.6428

Janse, C. J., Ramesar, J., and Waters, A. P. (2006). High-efficiency transfection and drug selection of genetically transformed blood stages of the rodent malaria parasite *Plasmodium berghei*. *Nat. Protoc.* 1, 346–356. doi: 10.1038/nprot.2006.53

Kapulu, M. C., Da, D. F., Miura, K., Li, Y., Blagborough, A. M., Churcher, T. S., et al. (2015). Comparative assessment of transmission-blocking vaccine candidates against *Plasmodium falciparum*. *Sci. Rep.* 5:11193. doi: 10.1038/srep11193

Khurana, S., Coffey, M. J., John, A., Uboldi, A. D., Huynh, M. H., Stewart, R. J., et al. (2019). Protein O-fucosyltransferase 2–mediated O-glycosylation of the adhesin MIC2 is dispensable for *Toxoplasma gondii* tachyzoite infection. *J. Biol. Chem.* 294, 1541–1553. doi: 10.1074/jbc.RA118.005357

Kimura, E. A., Couto, A. S., Peres, V. J., Casal, O. L., and Katzin, A. M. (1996). N-linked glycoproteins are related to schizogony of the intraerythrocytic stage in *Plasmodium falciparum*. *J. Biol. Chem.* 271, 14452–14461. doi: 10.1074/jbc.271.24.14452

Kozma, K., Keusch, J. J., Heggemann, B., Luther, K. B., Klein, D., Hess, D., et al. (2006). Identification and characterization of abeta1,3-glucosyltransferase that synthesizes the Glc-beta1,3-Fuc disaccharide on thrombospondin type 1 repeats. *J. Biol. Chem.* 281, 36742–36751. doi: 10.1074/jbc.M605912200

Leonhard-Melief, C., and Haltiwanger, R. S. (2010). O-Fucosylation of thrombospondin type 1 repeats. *Methods Enzymol.* 480, 401–416. doi: 10.1016/S0076-6879(10)80018-7

Li, F., Templeton, T. J., Popov, V., Comer, C. E., Tsuboi, T., Torii, M., et al. (2004). *Plasmodium* ookinete-secreted proteins secreted through a common micronemal pathway are targets of blocking malaria transmission. *J. Biol. Chem.* 279, 26635–26644. doi: 10.1074/jbc.M401385200

Lopaticki, S., Yang, A. S. P., John, A., Scott, N. E., Lingford, J. P., O'Neill, M. T., et al. (2017). Protein O-fucosylation in *Plasmodium falciparum* ensures efficient infection of mosquito and vertebrate hosts. *Nat. Commun.* 8:561. doi: 10.1038/s41467-017-00571-y

López-Gutiérrez, B., Dinglasan, R. R., and Izquierdo, L. (2017). Sugar nucleotide quantification by liquid chromatography tandem mass spectrometry reveals a distinct profile in *Plasmodium falciparum* sexual stage parasites. *Biochem. J.* 474, 897–905. doi: 10.1042/BCJ20161030

Luo, Y., Nita-Lazar, A., and Haltiwanger, R. S. (2006). Two distinct pathways for O-fucosylation of epidermal growth factor-like or thrombospondin type 1 repeats. *J. Biol. Chem.* 281, 9385–9392. doi: 10.1074/jbc.M511974200

Maier, A. G., Braks, J. M., Waters, A. P., and Cowman, A. F. (2006). Negative selection using yeast cytosine deaminase/uracil phosphoribosyl transferase in *Plasmodium falciparum* for targeted gene deletion by double crossover recombination. *Mol. Biochem. Parasitol.* 150, 118–121. doi: 10.1016/j.molbiopara.2006.06.014

Mathias, D. K., Pastrana-Mena, R., Ranucci, E., Tao, D., Ferruti, P., Ortega, C., et al. (2013). A small molecule glycosaminoglycan mimetic blocks *Plasmodium* invasion of the mosquito midgut. *PLoS Pathog.* 9:e1003757. doi: 10.1371/journal.ppat.1003757

Menard, R., Tavares, J., Cockburn, I., Markus, M., Zavala, F., and Amino, R. (2013). Looking under the skin: the first steps in malarial infection and immunity. *Nat. Rev. Microbiol.* 11, 701–12. doi: 10.1038/nrmicro3111

Moon, R. W., Hall, J., Rangkuti, F., Ho, Y. S., Almond, N., Mitchell, G. H., et al. (2013). Adaptation of the genetically tractable malaria pathogen *Plasmodium knowlesi* to continuous culture in human erythrocytes. *Proc. Natl. Acad. Sci. U. S. A.* 110, 531–536. doi: 10.1073/pnas.1216457110

Moorthy, V. S., Imoukhuede, E. B., Milligan, P., Bojang, K., Keating, S., Kaye, P., et al. (2004). A randomised, double-blind, controlled vaccine efficacy trial of DNA/MVA ME-TRAP against malaria infection in Gambian adults. *PLoS Med.* 1:e33. doi: 10.1371/journal.pmed.0010033

Morahan, B. J., Wang, L., and Coppel, R. L. (2009). No TRAP, no invasion. *Trends Parasitol.* 25, 77–84. doi: 10.1016/j.pt.2008.11.004

Naik, R. S., Branch, O. H., Woods, A. S., Vijaykumar, M., Perkins, D. J., Nahlen, B. L., et al. (2000). Glycosylphosphatidylinositol anchors of Plasmodium falciparum: molecular characterization and naturally elicited antibody response that may provide immunity to malaria pathogenesis. *J. Exp. Med.* 192, 1563–1576. doi: 10.1084/jem.192.11.1563

Pfander, C., Anar, B., Schwach, F., Otto, T. D., Brochet, M., Volkmann, K., et al. (2011). A scalable pipeline for highly effective genetic modification of a malaria parasite. *Nat. Methods* 8, 1078–1082. doi: 10.1038/nmeth.1742

Ricketts, L. M., Dlugosz, M., Luther, K. B., Haltiwanger, R. S., and Majerus, E. M. (2007). O-fucosylation is required for ADAMTS13 secretion. *J. Biol. Chem.* 282, 17014–17023. doi: 10.1074/jbc.M.700317200

RTS,S Clinical Trials Partnership (2015). Efficacy and safety of RTS,S/AS01 malaria vaccine with or without a booster dose in infants and children in Africa: final results of a phase 3, individually randomised, controlled trial. *Lancet* 386, 31–45. doi: 10.1016/S0140-6736(15)60721-8

Sanz, S., Bandini, G., Ospina, D., Bernabeu, M., Marino, K., Fernandez-Becerra, C., et al. (2013). Biosynthesis of GDP-fucose and other sugar nucleotides in the blood stages of *Plasmodium falciparum*. *J. Biol. Chem.* 288, 16506–16517. doi: 10.1074/jbc.M112.439828

Sanz, S., López-Gutiérrez, B., Bandini, G., Damerow, S., Absalon, S., Dinglasan, R. R., et al. (2016). The disruption of GDP-fucose de novo biosynthesis suggests the presence of a novel fucose-containing glycoconjugate in *Plasmodium* asexual blood stages. *Sci. Rep.* 6:37230. doi: 10.1038/srep37230

Swearingen, K. E., Lindner, S. E., Shi, L., Shears, M. J., Harupa, A., Hopp, C. S., et al. (2016). Interrogating the *Plasmodium* sporozoite surface: identification of surface-exposed proteins and demonstration of glycosylation on CSP and TRAP by mass spectrometry-based proteomics. *PLoS Pathog.* 12:e1005606. doi: 10.1371/journal.ppat.1005606

Tan, K., Duquette, M., Liu, J. H., Dong, Y., Zhang, R., Joachimiak, A., et al. (2002). Crystal structure of the TSP-1 type 1 repeats: a novel layered fold and its biological implication. *J. Cell Biol.* 159, 373–382. doi: 10.1083/jcb.200206062

Trager, W., and Jensen, J. B. (1976). Human malaria parasites in continuous culture. *Science* 193, 673–675. doi: 10.1126/science.781840

Valero-González, J., Leonhard-Melief, C., Lira-Navarrete, E., Jiménez-Osés, G., Hernández-Ruiz, C., Pallarés, M. C., et al. (2016). A proactive role of water molecules in acceptor recognition by protein O-fucosyltransferase 2. *Nat. Chem. Biol.* 12, 240–246. doi: 10.1038/nchembio.2019

Vasudevan, D., and Haltiwanger, R. S. (2014). Novel roles for O-linked glycans in protein folding. *Glycoconj. J.* 31, 417–426. doi: 10.1007/s10719-014-9556-4

Vasudevan, D., Takeuchi, H., Johar, S. S., Majerus, E., and Haltiwanger, R. S. (2015). Peters plus syndrome mutations disrupt a noncanonical ER quality-control mechanism. *Curr. Biol.* 25, 286–295. doi: 10.1016/j.cub.2014.11.049

von Itzstein, M., Plebanski, M., Cooke, B. M., and Coppel, R. L. (2008). Hot, sweet and sticky: the glycobiology of *Plasmodium falciparum*. *Trends Parasitol.* 24, 210–218. doi: 10.1016/j.pt.2008.02.007

Wang, L. W., Dlugosz, M., Somerville, R. P., Raed, M., Haltiwanger, R. S., and Apte, S. S. (2007). O-fucosylation of thrombospondin type 1 repeats in ADAMTS-like-1/punctin-1 regulates secretion: implications for the ADAMTS superfamily. *J. Biol. Chem.* 282, 17024–17031. doi: 10.1074/jbc.M701065200

Wengelnik, K., Spaccapelo, R., Naltaz, S., Robson, K. J., Janse, C. J., Bistoni, F., et al. (1999). The A-domain and the thrombospondin-related motif of *Plasmodium falciparum* TRAP are implicated in the invasion process of mosquito salivary glands. *EMBO J.* 18, 5195–5204. doi: 10.1093/emboj/18.19.5195

WHO (2018). *World Malaria Report 2018*. Geneva, Switzerland: World Health Organization.

Conflict of Interest Statement: The authors declare that the research was conducted in the absence of any commercial or financial relationships that could be construed as a potential conflict of interest.

frontiers in Microbiology

ORIGINAL RESEARCH
published: 18 July 2019
doi: 10.3389/fmicb.2019.01580

A Gut Symbiotic Bacterium *Serratia marcescens* Renders Mosquito Resistance to *Plasmodium* Infection Through Activation of Mosquito Immune Responses

*Liang Bai[1,2], Lili Wang[2,3], Joel Vega-Rodríguez[4], Guandong Wang[2,3] and Sibao Wang[2]**

[1]School of Life Science and Technology, Tongji University, Shanghai, China, [2]CAS Key Laboratory of Insect Developmental and Evolutionary Biology, CAS Center for Excellence in Molecular Plant Sciences, Institute of Plant Physiology and Ecology, Shanghai Institutes for Biological Sciences, Chinese Academy of Sciences, Shanghai, China, [3]University of Chinese Academy of Sciences, Beijing, China, [4]Laboratory of Malaria and Vector Research, National Institute of Allergy and Infectious Diseases, National Institutes of Health, Rockville, MD, United States

OPEN ACCESS

Edited by:
Rhoel Dinglasan,
University of Florida, United States

Reviewed by:
Isabelle Morlais,
Institut de Recherche pour le Développement (IRD), France
Sandrine Eveline Nsango,
University of Douala, Cameroon
Mathilde Gendrin,
Institut Pasteur de la Guyane, French Guiana

***Correspondence:**
Sibao Wang
sbwang@sibs.ac.cn

Specialty section:
This article was submitted to Infectious Diseases, a section of the journal Frontiers in Microbiology

Received: 15 March 2019
Accepted: 25 June 2019
Published: 18 July 2019

Citation:
Bai L, Wang L, Vega-Rodríguez J, Wang G and Wang S (2019) A Gut Symbiotic Bacterium Serratia marcescens Renders Mosquito Resistance to Plasmodium Infection Through Activation of Mosquito Immune Responses. Front. Microbiol. 10:1580. doi: 10.3389/fmicb.2019.01580

The malaria development in the mosquito midgut is a complex process that results in considerable parasite losses. The mosquito gut microbiota influences the outcome of pathogen infection in mosquitoes, but the underlying mechanisms through which gut symbiotic bacteria affect vector competence remain elusive. Here, we identified two *Serratia* strains (Y1 and J1) isolated from field-caught female *Anopheles sinensis* from China and assessed their effect on *Plasmodium* development in *An. stephensi*. Colonization of *An. stephensi* midgut by *Serratia* Y1 significantly renders the mosquito resistant to *Plasmodium berghei* infection, while *Serratia* J1 has no impact on parasite development. Parasite inhibition by *Serratia* Y1 is induced by the activation of the mosquito immune system. Genome-wide transcriptomic analysis by RNA-seq shows a similar pattern of midgut gene expression in response to *Serratia* Y1 and J1 in sugar-fed mosquitoes. However, 24 h after blood ingestion, *Serratia* Y1 modulates more midgut genes than *Serratia* J1 including the c-type lectins (CTLs), CLIP serine proteases and other immune effectors. Furthermore, silencing of several *Serratia* Y1-induced anti-*Plasmodium* factors like the thioester-containing protein 1 (TEP1), fibrinogen immunolectin 9 (FBN9) or leucine-rich repeat protein LRRD7 can rescue parasite oocyst development in the presence of *Serratia* Y1, suggesting that these factors modulate the *Serratia* Y1-mediated anti-*Plasmodium* effect. This study enhances our understanding of how gut bacteria influence mosquito-*Plasmodium* interactions.

Keywords: *Anopheles* mosquito, gut symbiont, antiparasitic defense, malaria transmission, immune activation

INTRODUCTION

Malaria continues to be one of the most devastating infectious diseases and a major public health problem in tropical and subtropical regions. The increase in mosquito insecticide resistance and parasite drug resistance, combined with the lack of an effective vaccine, have stalled the steady reduction in global malaria cases (World Health Organization, 2018), making the development of new malaria interventions a global priority.

Malaria is caused by *Plasmodium* parasites and is transmitted to humans by *Anopheles* mosquitoes. The most severe bottleneck during *Plasmodium* development occurs in the mosquito midgut, where the majority of ingested parasites are killed (Vaughan et al., 1992; Ghosh et al., 2000; Pradel, 2007; Simon et al., 2009). The malaria parasite encounters a hostile environment in the mosquito midgut and undergoes a chain of complex developmental transitions that are required for successful transmission (Smith et al., 2014). Several reports have shown that the mosquito midgut microbiota affects mosquito susceptibility to parasite infection (Pumpuni et al., 1993, 1996; Dong et al., 2009; Cirimotich et al., 2011; Boissiere et al., 2012; Gendrin and Christophides, 2013; Bahia et al., 2014; Smith et al., 2014; Stathopoulos et al., 2014). Diverse species of bacteria colonize the midgut of both laboratory-reared and field caught mosquitoes, and some can inhibit *Plasmodium* development (Pumpuni et al., 1996; Straif et al., 1998; Gonzalez-Ceron et al., 2003). Likewise, elimination of the gut bacteria with antibiotics renders the mosquito more susceptible to *Plasmodium* infection, which can be reverted by reintroduction of bacteria in the midgut (Dong et al., 2009; Gendrin et al., 2015). However, the mechanisms by which the specific gut bacteria negatively impact malaria parasite development in the mosquito midgut are not completely understood.

The number of bacteria in the mosquito midgut increases exponentially within 24 h of a blood meal ingestion (Pumpuni et al., 1996; Wang et al., 2012), resulting in induction of the midgut immune responses (Dong et al., 2009; Meister et al., 2009). This immune activation can also modulate the mosquito defense against the malaria parasite (Meister et al., 2005, 2009; Bahia et al., 2014). RNA transcription profiling of microbe-free aseptic and septic mosquitoes identified many genes up-regulated by gut bacteria, including several anti-*Plasmodium* factors (Dong et al., 2009). Although, there is overlap between the mosquito antibacterial and anti-malarial immune responses, some antibacterial immune genes have no impact on *Plasmodium* development (Dimopoulos et al., 1997; Oduol et al., 2000; Dong et al., 2006, 2009). In addition, the effect of the gut microbiota on *Plasmodium* infection may be exerted through direct interactions with bacteria-produced anti-*Plasmodium* factors or by the formation of a physical barrier that blocks the parasite's access to the midgut epithelium (Cirimotich et al., 2011; Bando et al., 2013; Bahia et al., 2014; Song et al., 2018). Conversely, a positive correlation was reported between the presence of *Enterobacteriaceae* bacteria in the midgut of field-caught mosquitoes and the *Plasmodium falciparum* infection status (Boissiere et al., 2013). These indicate that the effect of mosquito gut bacteria on parasite infection is complex and may depend on species-specific or strain-specific interactions.

In this study, we examined the influence of two *Serratia* strains isolated from field-caught *Anopheles sinensis*, the main malaria vector in Asia, on *Plasmodium* infection. *Serratia* strain Y1 inhibited *Plasmodium berghei* infection in *An. stephensi* mosquitoes, whereas *Serratia* strain J1 had no impact on parasite infection. Gene expression and RNA interference analysis show that the inhibition of *Plasmodium* by *Serratia* Y1 is mediated by the bacterial activation of the mosquito immune system. Understanding the interactions and mechanisms through which gut commensal bacteria actively shape mosquito immunity may yield new insights into vector-pathogen interactions and may help in the development of new vector-based disease interventions.

MATERIALS AND METHODS

Ethics Statement

This study was carried out in strict accordance with the guidelines of the Shanghai Institutes for Biological Sciences Animal Care and Use Committee, and all animal work was approved by the committee.

Mosquito Rearing, Oral Bacterial Introduction and Infection With *Plasmodium berghei*

Anopheles stephensi (Nijmegen strain) and *An. sinensis* (Jiangsu strain) mosquitoes were maintained at 27°C with 70 ± 5% relative humidity under 12 h/12 h day-night cycle. Adult mosquitoes were maintained on 10% (w/v) sucrose. The larvae were reared on cat food pellets and ground fish food supplement. Axenic female mosquitoes were generated *via* treatment with oral antibiotics as previously described (Wei et al., 2017). Female mosquitoes were reared with 10% sucrose solution containing penicillin (10 unit/ml), streptomycin (10 μg/ml) and gentamicin (15 μg/ml). Three days after antibiotic treatment, the antibiotic solution was replaced by sterile water, and mosquitoes were starved for 8 h and fed for 24–48 h on a cotton pad soaked with a 5% sucrose solution containing *Serratia* bacteria at a final concentration of 10^7 CFU/ml. The control group was only given 5% sucrose solution without any bacteria. The mosquitoes were allowed to feed on wild-type *P. berghei*-mCherry (Graewe et al., 2009) infected mouse. On each experiment, control and experimental groups were fed on the same infected mouse. Fully engorged mosquitoes were separated within 24 h and provided with a cotton pad soaked with 5% (w/v) sterile sucrose solution that was replaced twice a day. Oocyst numbers in midguts were determined on day 10 after infection, stained with 0.1% (w/v) mercurochrome.

Direct PCR Amplification of the 16S rRNA Gene was Performed From the Isolated Bacteria

16S rRNA Gene Cloning and Sequencing

A fragment of approximately 1.5 kb of the 16S rRNA gene was PCR amplified from isolated bacteria from the mosquito midgut using the following primers: 27F (5′-AGAGTTT

GATCMTGGCTCAG-3′) and 1492R (5′-GGTTACCTTGTT ACGACTT-3′). PCR mixtures used to amplify bacterial sequences contained about 50 ng DNA; 0.4 mM each dNTP; 2.5 U Taq DNA polymerase; 3 mM MgCl2 (50 mM magnesium chloride); 1X PCR buffer (200 mM Tris, pH 8.4, 500 mM KCl); 25 pmol of each primer and sterile water to a final volume of 50 µl. PCR amplification was carried out with the following conditions: 95°C for 3 min; 35 cycles at 95°C for 15 s, 58°C for 30 s and 72°C for 2 min, and a final extension at 72°C for 5 min. Reactions were carried out in an ProFlex PCR System (Applied Biosystems). Amplification products were analyzed by electrophoresis on a 1% agarose gel and visualized under UV light after staining with ethidium bromide. PCR products were purified using the Wizard® SV Gel and PCR Clean-Up System (Promega, Madison, WI, USA) according to the manufacturer recommendations. Purified PCR products were cloned into a pGEM-T easy vector according to manufacturer instructions and transformed into competent DH5α *Escherichia coli* cells by heat-shock for 90 s. Recombinant colonies were identified using blue and white screening on LB agar medium containing 100 µg/ml ampicillin, 2 mM IPTG, and 0.004% X-gal. The plates were incubated at 37°C overnight. The white colonies were selected and cultured in Luria-Bertani (LB) broth complemented with 100 µg/ml ampicillin. Plasmid extraction were done using an alkaline lysis method. The 16S rRNA gene was sequenced by Sangon Biotech (Shanghai, China) Co., Ltd. The sequences obtained were compared with GenBank database for bacterial species identification.

Generation of Fluorescent Strains of *Serratia* Y1 and J1

To integrate an enhanced fluorescent protein gene (*egfp*) into the chromosome of *Serratia* Y1 and J1, the transposon plasmid pBAM2-GFP (Wang et al., 2017) was transformed into a donor strain *E. coli* S17-1λpir. Freshly cultured transformed donor strain and the recipient strains (*Serratia* Y1 and J1) cells were washed and resuspended with 10 mM MgSO4 solution to a final OD600 of 0.1 of each strain, mixed (1:1) and co-cultured on Luria-Bertani (LB) agar plates at 37°C for conjugation mating. After 5 h incubation, the fluorescence gene was mobilized and integrated into the genome of the recipient strain *Serratia* Y1 and J1. The co-culture was seriously diluted and plated on LB agar plates containing 100 µg/ml of kanamycin. The plates were incubated overnight at 30°C and fluorescent colonies were identified under fluorescent microscopy.

Colonization of *Serratia* Y1 and J1 in the Mosquito Midgut

To test colonization of *Serratia* Y1 and J1 in adult *An. sinensis* and *An. Stephensi* mosquitoes, GFP-labeled *Serratia* strains (Y1-GFP and J1-GFP) were used in this assay. The bacteria were cultured overnight in LB broth medium at 30°C, washed twice in sterile 1 × PBS and resuspended in 5% sterile sucrose solution to obtain 1×10^7 cells/ml. The bacteria were introduced into 2 day-old female mosquitoes by feeding on a cotton pad moistened with bacterial suspension for 24–48 h. Two days later, the mosquitoes were allowed to feed on a non-infected mouse. Before and post-blood meal, 10 mosquitoes were collected at different time points, and were surface-sterilized by washing in 75% ethanol for 3 min and then rinsing them in sterile PBS three times. The midguts were dissected under sterile conditions and homogenized in 100 µl sterile PBS. The bacterial load was determined by plating 10-fold serial dilutions of the homogenates on LB agar plates containing 100 µg/ml of kanamycin and incubating the plates overnight at 30°C. The fluorescent colonies were counted by fluorescent microscopy.

RNA Extraction and Transcriptome Sequencing

Serratia Y1 and J1 were separately fed to 3-day-old aseptic mosquitoes in a sugar meal for 24–48 h, then mosquitoes were allowed to feed on non-infected blood. About 50 female mosquitoes were collected from two biological replicates before (0 h) and 24 h after blood meal. The aseptic females that did not feed on Y1 and J1bacteria were used as the controls. Mosquito midguts were dissected in ice-cold PBS and total RNA was extracted using Direct-zol RNA Miniprep Kit (The Epigenetics Company, USA) followed by RNase-free DNase I treatment. Messenger RNA (mRNA) was purified, and reverse-transcribed into cDNA libraries using the NEBNext® Ultra™ RNA Library Prep Kit for Illumina® (NEB, Boston, Massachusetts, USA). The cDNA libraries were sequenced on an Illumina HiSeq 2000 platform.

Assembly and Annotation of Transcriptomes

Before assembling the clean reads, the raw reads were preprocessed using filter-fq software. For the transcriptome analysis, the clean reads were aligned in paired-end mode against the *Anopheles stephensi* SDA-500 genome[1] using HISAT v0.1.6-beta and assembled with Cufflinks with the default settings[2]. The gene annotation was performed by FunCat[3]. Secreted proteins were predicted by SignalP 3.0[4].

Differential Expression Genes, Clustering and Functional Enrichment Analysis

Differential expression genes (DEGs) were identified for each time point, which were compared to the data of the control group using Cuffdiff. Differential expression was detected using log2 (fold change) ≥ 1.0 and adjusted $p < 0.05$. The combined transcriptomes were used as the background to search for GO terms enriched within the DEGs using http://bioinfo.cau.edu.cn/agriGO/ and a $p < 0.01$ as the parameters for determining significantly enriched terms. Similarly, pathways significantly enriched with the DEGs were identified by mapping all DEGs to terms in the KEGG database using KOBAS2.0 with a $p < 0.05$.

[1]https://www.vectorbase.org/organisms/anopheles-stephensi
[2]http://cole-trap-nell-lab.github.io/cufflinks/
[3]ftp://ftpmips.gsf.de/FGDB/
[4]http://www.cbs.dtu.dk/services/SignalP/

Validation of DEGs by qRT-PCR Analysis

First-strand cDNA was synthesized from total RNA using the PrimeScript RT Reagent Kit with gDNA Eraser (Takara) according to the manufacturer's instructions. Quantitative real-time PCR (qRT-PCR) analysis was performed with the PikoReal 96 (Thermo, USA) using the AceQ qPCR SYBR Green Master Mix (Vazyme). The housekeeping As S7 gene was used as an endogenous control. The primers are shown in **Supplementary Table S2**.

Double-Stranded RNA Synthesis and Gene Silencing in Adult Mosquitoes

Forward and reverse primers with T7 promoter sequence (5′-TAATACGACTCACTATAGGG-3′) were used to amplify the fragment of the enhanced green fluorescent protein (eGFP) gene from plasmid pBacRMCE-Ac5-EGFP (**Supplementary Table S3**). Fragments of the *Rel1*, *Rel2*, *TEP1*, *FBN9*, and *LRRD7* genes were amplified from *An. stephensi* cDNA. Purified PCR products were used as template for *in vitro* double-strand RNA (dsRNA) transcription using the MEGAscript RNAi Kit (Thermo Fisher Scientific). Pure dsRNAs were diluted to approximately 3 μg/μl in DEPC-water. Two-day-old female mosquitoes were intrathoracically injected with 138 nl of either dsRel1, dsRel2, dsTEP1, dsFBN9, dsLRRD7, or dsGFP as a control. The silencing efficiency was evaluated by qPCR at selected time points after injection.

Statistical Analysis

Significant difference in oocyst intensity between two samples was analyzed using the Mann-Whitney test. The statistics were performed using GraphPad Prism version 5.00 for Windows (GraphPad Software). $p < 0.05$ was considered to be statistically significant.

RESULTS

Effect of *Serratia* Strains on *Plasmodium Berghei* Infection in the Mosquito

We isolated two dominant *Serratia* strains, termed Y1 and J1, from the midguts of field-collected adult female *An. sinensis* mosquitoes in China. The 16S rRNA gene sequence showed 99% similarity to *Serratia marcescens*. The two *Serratia* strains, Y1 and J1, could stably colonize the midgut of both *An. sinensis* and *An. stephensi* mosquitoes, and rapidly proliferate by more than 200-fold 24 h after a blood meal (**Figure 1A**). These two strains did not significantly affect mosquito survival whether the mosquitoes fed on sugar or blood (**Supplementary Figure S1**).

The downstream analyses were performed in *An. stephensi* because it is difficult to maintain *An. sinensis* under laboratory conditions. Investigation of the effect of the two *Serratia* strains on *Plasmodium* development in the midgut of *An. stephensi*

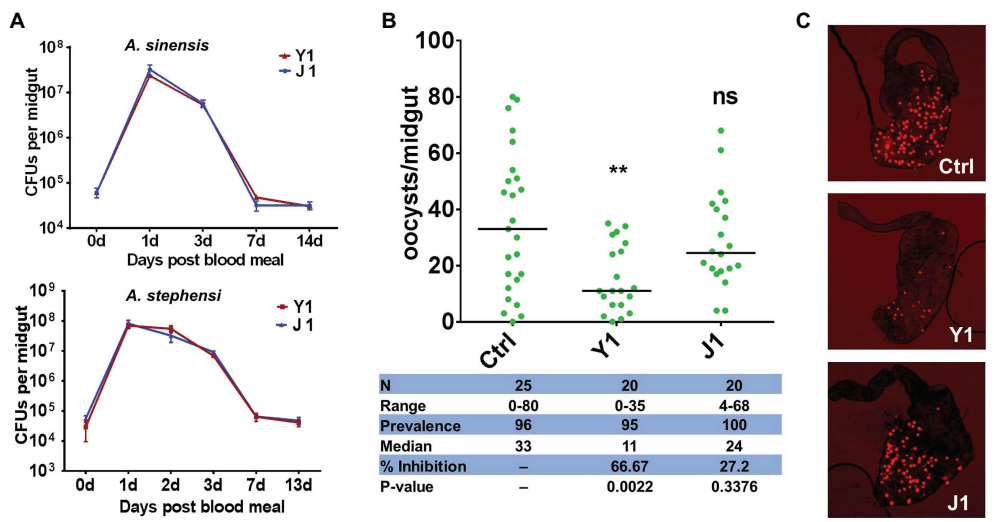

FIGURE 1 | Effect of different *Serratia* strains on *Plasmodium berghei* oocyst development. **(A)** *Serratia* strains Y1 and J1 stably colonize the midgut of female *An. sinensis* and *An. stephensi* mosquitoes and rapidly proliferate after a blood meal. The eGFP-tagged strains Y1-GFP and J1-GFP were fed to 3-day-old female *An. sinensis* and *An. stephensi* mosquitoes in a 5% sugar meal for 24 h, then mosquitoes were allowed to feed on a blood meal. Fluorescent bacteria colony-forming units (CFUs) were determined by plating serially diluted homogenates of midguts on LB agar plates containing 100 mg/ml of kanamycin. Data were pooled from three biological replicates (shown are means ± SEM). **(B)** Oocyst infection intensity in *An. stephensi* mosquitoes colonized with *Serratia* Y1 or J1 after feeding on *P. berghei* mCherry infected mice. Each dot represents the oocysts number from individual midguts, and the horizontal lines indicate the median number of oocysts. Inhibition = [(# of oocyst in control group – # of oocyst in experimental group)/# of mosquitoes in control group] × 100; Median, median oocyst number per midgut; N, number of mosquitoes analyzed; Prevalence, percentage of mosquitoes carrying at least one oocyst; Range, range of oocyst numbers per midgut. The experiments were repeated three times with similar results (**Supplementary Figure S2**). The Mann-Whitney test was used to determine significance in oocysts numbers, $^{**}p < 0.01$. **(C)** mCherry oocysts in the midgut epithelium of mosquitoes that had been fed with only sugar solution (top panel), *Serratia* Y1 (center panel) or J1 (bottom panel).

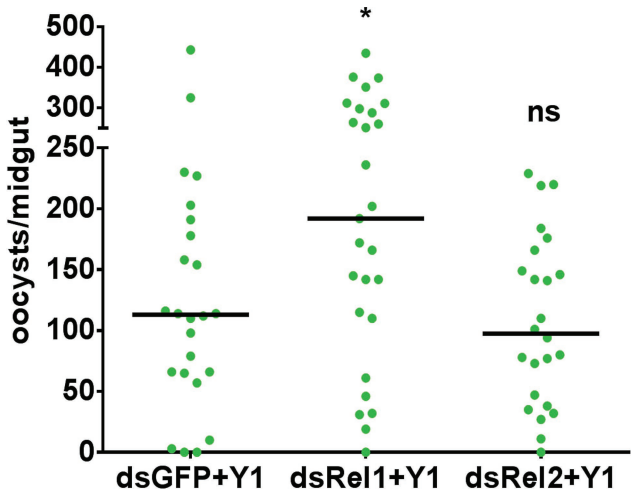

N	24	26	24
Range	0-443	0-435	0-229
Prevalence	91.67	96.15	95.83
Median	113	192	101
% Inhibition	—	- 69.91	10.62
P-value	—	0.0416	0.3829

FIGURE 2 | Effect of *Rel1* and *Rel2* silencing on the *Serratia* Y1-mediated anti-*Plasmodium* activity. *Rel1* and *Rel2* were silenced in *An. stephensi* mosquitoes by systemic injection of dsGFP, dsRel1 or dsRel2 RNA. The injected mosquitoes were fed on a sugar meal containing *Serratia* Y1. Three days later, all mosquito groups were allowed to feed on the same *P. berghei* infected mouse. The injected double-stranded RNA (ds) and presence (Y1) of *Serratia* Y1 are indicated below each column. Each dot represents the number of oocysts from an individual midgut, and the horizontal lines indicate the median number of oocysts. The experiments were repeated three times with similar results (**Supplementary Figure S3**). The Mann-Whitney test was used to determine significance in oocysts numbers, $^*p < 0.05$.

show that *Serratia* Y1 significantly reduced oocyst formation ($p < 0.001$), while *Serratia* J1 did not affect *P. berghei* oocyst formation (**Figures 1B,C; Supplementary Figure S2**). Thus, we identified two mosquito *S. marcescens* strains, one of them inhibiting *Plasmodium* infection in the mosquito midgut.

Serratia Y1 Inhibits *Plasmodium* Development Through Activation of the Mosquito Immune System

To test whether *Serratia* Y1 exerts the parasite inhibitory effect through stimulation of the mosquito immune system, we used RNA interference (RNAi) to silence the expression of Rel1 and Rel2, the NF-κB transcription factors of Toll and IMD signaling pathways that regulate mosquito innate immunity, respectively. We compared the oocyst numbers in the midguts of *An. stephensi* mosquito cohorts that had been injected with double-stranded RNA either for GFP (dsGFP), dsRel1 or dsRel2. Inhibition of the Toll pathway by Rel1 knockdown significantly increased *P. berghei* infection in mosquitoes fed with Y1 (**Figure 2; Supplementary Figure S3**). Silencing of Rel2 did not rescue *P. berghei* oocyst development in the presence of Y1 (**Figure 2; Supplementary Figure S3**). These results suggested that *Serratia* Y1 exerts its anti-*Plasmodium* activity through the activation of the Toll immune pathway.

Mosquito Global Transcriptome Responses to *Serratia* Challenge

To gain a better understanding of the differences in the mosquito immune response to *Serratia* Y1 and J1, we compared the midgut gene transcriptional profile of mosquitoes colonized by *Serratia* Y1 or J1 before (0 h) and 24 h after a blood meal. RNA-seq data from six RNA libraries are summarized in **Supplementary Table S1**. Genome-wide transcriptomic profiles showed a similar pattern of midgut gene expression in response to *Serratia* Y1 and J1 in sugar-fed mosquitoes (**Figure 3A**). A total of 375 genes were differentially regulated in the *Serratia* Y1 challenged group ($p < 0.05$), of which 225 genes were up-regulated and 150 genes were down-regulated (**Figure 3C**). In the *Serratia* J1 challenged group, 357 genes were differentially regulated including 223 up-regulated and 134 down-regulated genes (**Figures 3A,C**). The majority of the DEGs (257 genes) had similar expression pattern between the two groups (**Figure 3C**). At 24 h post-blood meal, *Serratia* Y1 modulated 370 DGEs while *Serratia* J1 regulated only 252 DGEs (**Figures 3B,C**). Interestingly, a total of 146 upregulated and 3 downregulated genes were specific for the *Serratia* challenged Y1 group. However, the *Serratia* J1 challenged group only showed 7 upregulated and 24 downregulated genes specific to this group (**Figures 3B,C**). This indicates that *Serratia* Y1 regulates more genes in the midgut after the mosquito takes a blood meal than *Serratia* J1.

Gene Ontology (GO) enrichment analysis was performed to show the potential biological function of the differentially expressed genes. For 0 h before blood meal, we found that, 7 of 48 gene functional groups (14.6%) belonging to extracellular matrix, extracellular region part, extracellular space and transcription regulator were only enriched in the *Serratia* J1 challenged group, while 37 gene functional groups (77%) were enriched in both Y1 and J1 groups (**Supplementary Figure S4**). At 24 h post-blood meal, 19 of 50 GO terms (38%) were only presented in the *Serratia* Y1 challenged group (**Supplementary Figure S5**). KEGG classification was also used to analyze the corresponding metabolic pathways involved in the regulation of mosquito genes induced by *Serratia* challenge. Before blood meal, 39 and 42 pathways of level 2 were enriched in the *Serratia* Y1 challenged group and the *Serratia* J1 challenged group, respectively (**Supplementary Figure S6A**). At 24 h post-blood meal, 42 and 34 pathways of level 2 were enriched in the *Serratia* Y1 challenged group and the *Serratia* J1 challenged group, respectively (**Supplementary Figure S6B**). Pathways including global and overview maps, signal transduction, immune system, transport and catabolism, signaling molecules and interaction, amino acid metabolism, digestive system and endocrine system were overrepresented in the *Serratia* Y1 challenged group (**Supplementary Figure S6B**).

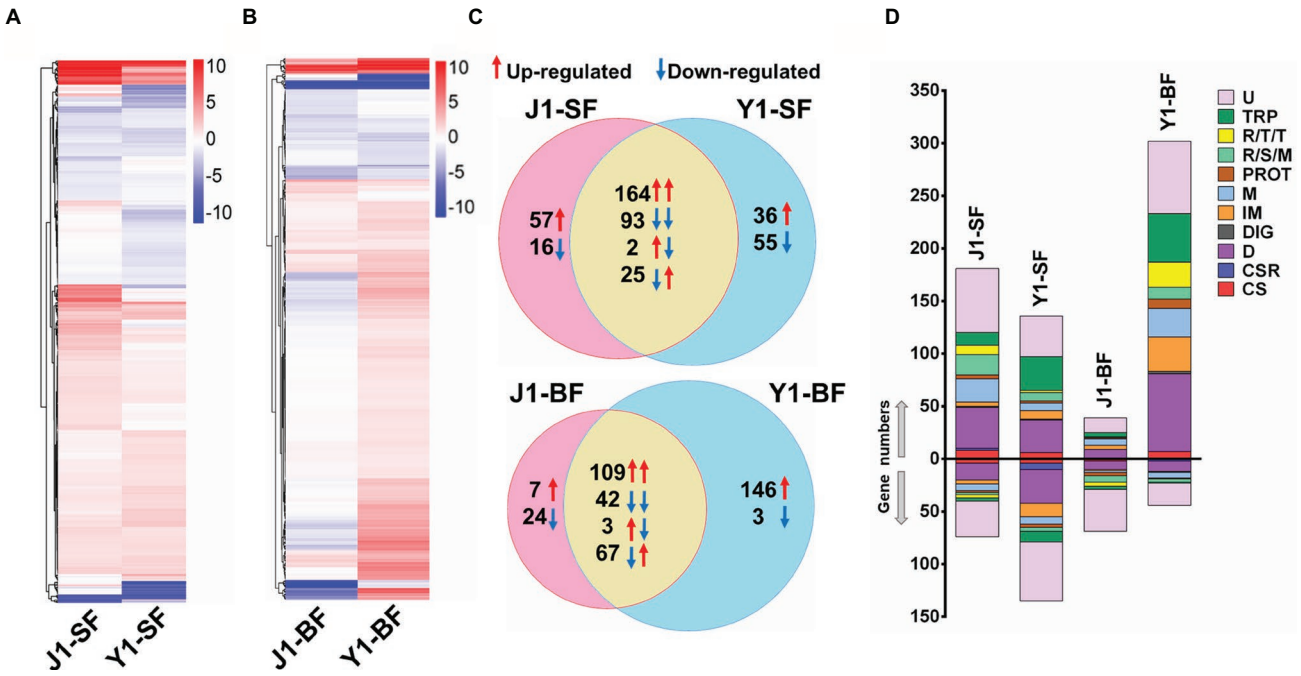

FIGURE 3 | Comparative analysis of transcriptional profiles in mosquito midguts challenged with *Serratia* Y1 or J1. **(A,B)** Heat maps and hierarchical clustering analysis of differentially expressed genes (DEGs) in the midgut of *An. stephensi* mosquitoes fed with *Serratia* Y1 or J1 before (SF, sugar fed) and 24 h after blood meal (BF, blood fed). DEGs in each group were identified with log 2 (fold change) of ≥1 ($p < 0.05$) by comparison of transcript abundance between bacteria challenged and aseptic mosquitoes. Colors from white to red indicate up-regulation; colors from white to blue indicate down-regulation. **(C)** Venn diagram showing the number of shared and specific DEGs in the midgut of mosquitoes fed with *Serratia* Y1 or J1 before and 24 h after blood meal. Red and blue arrows indicate the mosquitoes challenged with *Serratia* Y1 and J1, respectively. **(D)** Global gene regulation in the different groups. Proportions and numbers of genes belonging to distinct functional groups were up- (red arrow) or down-regulated (blue arrow) in the corresponding groups. U, unknown functions; TRP, transport; R/T/T, replication, transcription, translation; R/S/M, oxidoreductive, stress-related and mitochondrial; PROT, proteolysis; M, metabolism; IM, immunity; DIG, digestion; D, diverse; CSR, chemosensory protein; CS, cytoskeletal, structural.

Serratia Y1 Modulates Mosquito Immune Genes

Given that *Serratia* Y1 exerts anti-*Plasmodium* activity by stimulating the mosquito immune pathway (**Figure 2**), the expression profiles of genes involved in mosquito immunity were further analyzed. In sugar-fed mosquitoes, the number of immune regulated genes was similar between *Serratia* Y1 and *Serratia* J1 colonized mosquitoes (**Figure 3D**). At 24 h post-blood meal, there were marked differences in immune gene regulation between *Serratia* Y1 and J1 challenged groups. A total of 33 immunity genes were up-regulated in mosquitoes fed with *Serratia* Y1. However, in mosquitoes fed with *Serratia* J1 only 4 immune genes were up-regulated and 1 down-regulated (**Figure 3D**). In mosquitoes challenged by *Serratia* Y1, the antimicrobial immune genes with the highest upregulation were *Defensin 1*(*DEF1*), *Cecropins 1* (*CEC1*), *Cecropins 2* (*CEC2*) and *Gambicin 1* (*GAM1*). In addition, except for CLIPD 2 and CLIPA 3, all other genes encoding the CLIP family were up-regulated by *Serratia* Y1 (**Figure 4A**). The expression profiles of CTL family genes were also differently regulated in the midgut of mosquitoes fed with *Serratia* Y1 and J1 (**Figure 4B**).

Serratia Y1 Modulates the Anti-*Plasmodium* Effector Genes

To validate the RNA-seq results, we focused on the transcriptional regulation of several potent anti-*Plasmodium* and anti-bacterial effector genes encoding the thioester-containing protein 1 (TEP1), *Anopheles Plasmodium* responsive leucine-rich repeat protein (APL1A), leucine-rich repeat protein LRRD7, fibrinogen immunolectin 9 (FBN9), *Plasmodium* protective c-type lectin 4 (CTL4) and Gambicin (GAM1). All these genes were differentially regulated in the midgut of mosquitoes fed with *Serratia* Y1 at 24 h post-blood meal (**Figure 5A**). Real-time quantitative PCR (qPCR) confirmed that *TEP1*, *APL1A*, *LRRD7*, *FBN9*, and *GAM1* were significantly up-regulated, while the protective agonist *CTL4* gene was significantly down-regulated in the mosquitoes fed with Y1 at 24 h post-blood meal (**Figures 5A–C**). The other two antimicrobial peptides (*DEF1* and *CEC1*) were also significantly up-regulated (**Figure 5D**).

To establish further evidence that *Serratia* Y1 impacts *P. berghei* infection through activation of anti-*Plasmodium* effector genes, we chose three induced potent anti-*Plasmodium* factors, TEP1, FBN9, and LRRD7 for validation in mosquitoes colonized with *Serratia* Y1. Midgut mRNA levels for *TEP1*, *FBN9*, and *LRRD7* in the dsRNAs-injected mosquitoes were

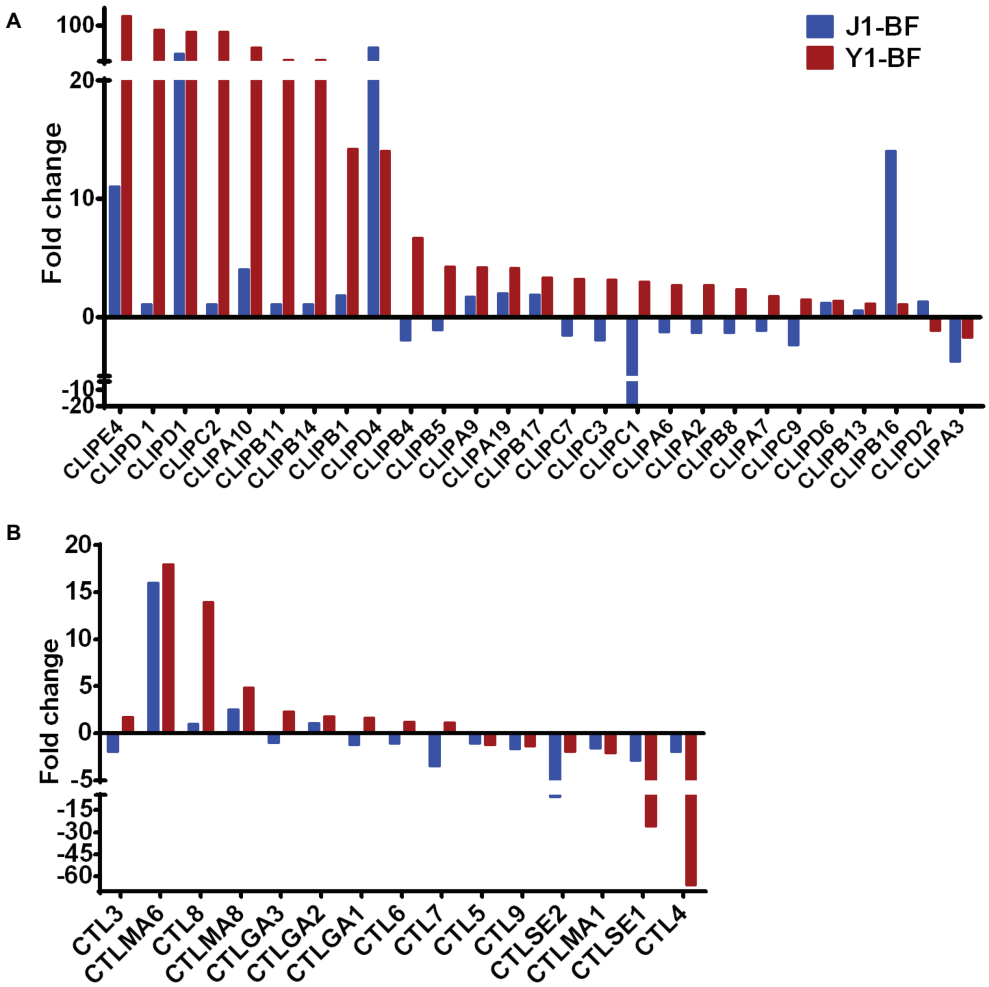

FIGURE 4 | Transcript abundance of CLIP and CTL family genes. **(A)** Fold change in transcript levels of the CLIP family genes in the midgut of mosquitoes fed with *Serratia* Y1 or J1, as compared with the aseptic control mosquitoes. **(B)** Fold change in transcript levels of the CTL family in the midgut of mosquitoes fed with *Serratia* Y1 or J1, relative to the aseptic mosquitoes.

markedly reduced compared to the dsGFP treated control (**Supplementary Figure S7**). Silencing of the three effector genes resulted in a significant increase of oocyst numbers when compared to the dsGFP -injected control in the *Serratia* Y1 colonized mosquitoes (**Figure 6; Supplementary Figure S8**). This result indicates that the depletion of dsTEP1, dsFBN9, or dsLRRD7 significantly reverses the refractoriness conferred by *Serratia* Y1 infection.

DISCUSSION

Mosquito gut bacteria form a resident community that has co-evolved with the insect host. In addition to playing important roles in digestion and harvesting energy, commensal bacteria are important factors determining the outcome of pathogen infection. Other mechanisms such as induction of mosquito innate immune responses have also been proposed, although the exact effect and mode of action by individual commensal bacteria are largely unknown. Interestingly, the presence, outgrowth, or loss of certain bacterial components of gut microbiota correlates with increased or decreased susceptibility to *Plasmodium* and dengue virus infection (Apte-Deshpande et al., 2012, 2014; Boissiere et al., 2012; Bahia et al., 2014). A previous study also showed that different strains of the same bacterial species can induce different outcomes on *Plasmodium* infections (Bando et al., 2013), indicating that the effect of gut bacteria on *Plasmodium* infection is complex and may involve species-specific or strain-specific interactions. In this study, we identified two mosquito symbiotic *Serratia* strains, from field caught *An. sinensis* mosquitoes, with different effect on *Plasmodium* development. *Serratia* Y1 shows anti-*Plasmodium* activity, but *Serratia* J1 does not influence parasite development in the midgut of mosquitoes. In mosquitoes, anti-*Plasmodium* and antibacterial immune defenses are largely controlled by the Toll and Imd immune signaling pathways, and the Toll pathway seems to be most efficient against the rodent parasite

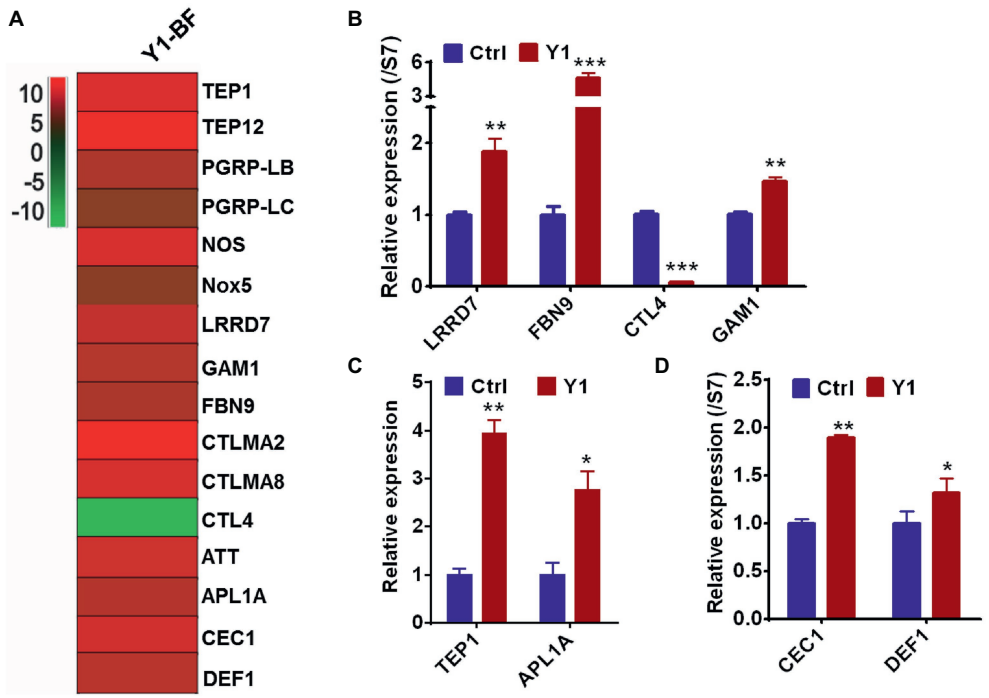

FIGURE 5 | *Serratia* Y1 elicits expression of immune genes in the midgut of mosquitoes 24 h post-blood meal. **(A)** Fold change in transcript levels of immune marker genes in the midgut of Y1-containing mosquitoes 24 h post-blood meal obtained from RNA-seq data. **(B)** Relative expression of immune factor genes (*LRRD7, FBN9, CTL4,* and *GAM1*) in the midgut of mosquitoes 24 h post-blood meal detected by qPCR. **(C)** Relative expression of *TEP1* and *APL1A* in the midgut of mosquitoes 24 h post-blood meal detected by qPCR. **(D)** Relative expression of *DEF1* and *CEC1* in the midgut of mosquitoes 24 h post-blood meal detected by qPCR. mRNA levels of the tested genes were normalized to that of the housekeeping gene S7. Error bars indicate SD of three technical replicates. Experiments were repeated three times with similar results, $^{*}p < 0.05$; $^{**}p < 0.01$; $^{***}p < 0.001$.

P. berghei (Meister et al., 2005, 2009; Garver et al., 2009). Some immune factors and AMP genes are regulated by both Toll and Imd pathways (Luna et al., 2006). This dual activation may be modulated by independent stimulation or by cross-regulation of the two signaling pathways (De Gregorio et al., 2002). Previous study also showed that the Toll and Imd pathways can interact synergistically and activate innate immune responses in *Drosophila*, demonstrating that cross-regulation of the two pathways occur (Tanji et al., 2007). Our findings also show that *Serratia* Y1 and J1 induce some genes that are regulated by both Toll and Imd pathways. We further showed that *Serratia* Y1 indirectly antagonizes *P. berghei* infection through activation of the mosquito Toll immune pathway.

Since the midgut is the primary site of response to the invading *Plasmodium*, identification of factors regulated by gut bacteria would provide insight into the mechanisms of how commensal bacteria activate immune-mediated anti-*Plasmodium* activity. Toward this we investigated the influence of *Serratia* Y1- or J1 on the mosquito midgut transcriptome. Before blood meal, the number of regulated immune genes in the *Serratia* Y1 and J1 groups was very similar, which may indicate that the mosquitoes modulate similar basal immune responses to limit the over-proliferation of the symbiotic bacteria and maintain gut homeostasis. Normally, when mosquitoes ingest sugar, the symbiotic bacteria in the midgut are kept at a relatively low level (Pumpuni et al., 1996; Wang et al., 2012). This healthy status requires mosquitoes to deploy basal immunity to maintain a symbiotic relationship with the bacteria (Wei et al., 2017). The gut microbiota and the host mosquito have adapted to coexist during long-term adaptive coevolution, which may be the reason why the gene expression patterns of the *Serratia* Y1 and J1 mosquitoes are similar when they feed on sugar.

After ingestion of a *Plasmodium* infected blood meal by the mosquito, the parasite undergoes sexual development in the midgut lumen to form a motile ookinete that invades the midgut epithelium around 24–26 h after blood feeding (Sinden and Billingsley, 2001; Baton and Ranford-Cartwright, 2005). The bacterial numbers in the mosquito midgut also increase by 100- to 1,000-fold 24 h after a blood meal (Cirimotich et al., 2011), activating the mosquito immune system to limit the over-proliferation of gut bacteria (Dong et al., 2009). We found that the c-type lectins (CTLs) and CLIP serine proteases were were up-regulated in the *Serratia* Y1 group. Many CLIP family genes have been showed to affect *Plasmodium* development. CLIPA2, A5 and A7 suppress parasite melanization, and CLIPA2 and CLIPA5 interact synergistically to block ookinete invasion (Barillas-Mury, 2007), while CLIPB3, B4, B8 and B17 promote ookinete

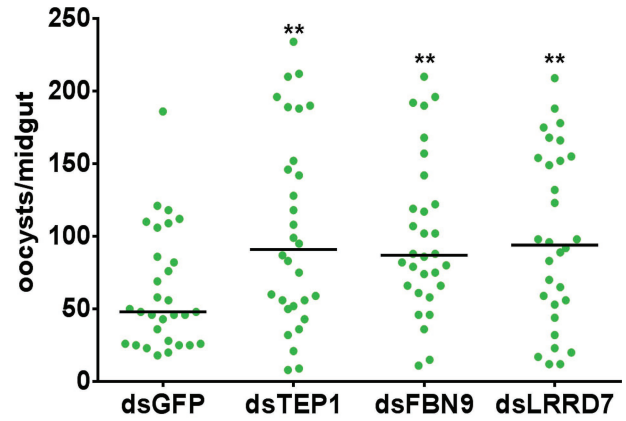

N	30	30	30	30
Range	18-186	8-234	11-210	12-209
Prevalence	100	100	100	100
Median	48	91	88	94
% Inhibition	–	-89.6	-83.3	-95.8
P-value	–	0.0046	0.0036	0.0073

FIGURE 6 | Oocyst loads following silencing of *TEP1*, *FBN9* and *LRRD7* genes. *An. stephensi* female mosquitoes were injected with dsRNA solution for *TEP1*, *FBN9*, *LRRD7* or *GFP* as a control. Injected mosquitoes were colonized with *Serratia* Y1 and then fed on a *P. berghei* infected mouse 3 days after dsRNA injection. Mosquito midguts were dissected 10 days post-blood feeding to determine the number of oocysts per mosquito. Each dot represents the number of oocysts from individual midguts, and the horizontal lines indicate the median number of oocysts. The experiments were repeated three times with similar results (**Supplementary Figure S8**). The Mann-Whitney test was used to determine significance in oocysts numbers, $^{**}p < 0.01$.

invasion (Volz et al., 2006). CLIPB14 and CLIPB15 are also involved in killing *Plasmodium* ookinetes and participate in the response against bacteria (Volz et al., 2005). Interestingly, expression of CTL4 was severely down-regulated in the *Serratia* Y1 challenged mosquitoes at 24 h post-blood meal. CTL 4 and CTLMA 2 are present in the hemolymph and up-regulated 24 h after blood ingestion and can protect the rodent *Plasmodium* ookinetes from destruction (Osta et al., 2004). FBN9, a member of the fibrinogen domain immunolectin family (FBN), was up-regulated in the *Serratia* Y1 fed mosquitoes at 24 h post-blood meal. A previous study suggested that FBN9 interacts with gram-positive and gram-negative bacteria and also affects *Plasmodium* development (Dong and Dimopoulos, 2009). The complement-like protein TEP1 and the leucine-rich repeat (LRR) protein APL1, which mediate lysis of *Plasmodium* parasites in the mosquito midgut (Blandin et al., 2008; Garver et al., 2009; Dong et al., 2011), were also up-regulated in the *Serratia* Y1 group at 24 h post-blood meal. Other factors including LRRD7, TEP12, NOX5, PGRP-LB, NOS and PGRP-LC, which had been shown to affect *Plasmodium* infection (Luckhart et al., 1998; Dong et al., 2006; Meister et al., 2009; Oliveira Gde et al., 2012), were also up-regulated in the *Serratia* Y1 group at 24 h post-blood meal. We further demonstrated that silencing of *TEP1*, *FBN9*, or *LRRD7* markedly reverses the parasite inhibition conferred by *Serratia* Y1 infection. Previous studies reported that these three genes can strongly influence both *P. falciparum* and *P. berghei* development (Blandin et al., 2004; Dong et al., 2006). Taken together, *Serratia* Y1 elicited a strong immune response in the mosquito midgut after taking a blood meal and knock-down of several highly elicited immune genes induced a significant increase of *P. berghei* oocysts, further confirming that *Serratia* Y1 interferes with *P. berghei* development by eliciting the mosquito's immune response.

In summary, our data shows that *Serratia* Y1 inhibits *Plasmodium* development through stimulation of the mosquito immunity. Our work establishes an important framework of knowledge for further investigations into the molecular interactions between gut bacteria, *Anopheles* mosquitoes and pathogens, which would enhance our understanding of how gut bacteria inhibit *Plasmodium* development in the midgut of mosquitoes.

DATA AVAILABILITY

RNA sequencing datasets from this work were deposited in the National Center for Biotechnology Information Sequence Read Archive (accession no. PRJNA520745).

AUTHOR CONTRIBUTIONS

SW conceived the study. SW and LB designed the experiments. LB performed the majority of experiments and generated fluorescent strains and performed transcriptome analysis. LB and GW performed RNAi analysis. LW and JV-R discussed results and provided advice. LB and SW analyzed the data. JV-R edited the manuscript. LB, LW, and SW wrote the manuscript.

FUNDING

This work was supported by grants from the National Natural Science Foundation of China (grants 31830086, 31772534, 31472044, 31501703 to SW), the Key Research Program of the Chinese Academy of Sciences (grant KFZD-SW-219 to SW), the Strategic Priority Research Program of Chinese Academy of Sciences (grant XDB11010500 to SW), and One Hundred Talents Program of the Chinese Academy of Sciences (grant 2013OHTP01 to SW). The funders had no role in study design, data collection, and interpretation, or the decision to submit the work for publication.

SUPPLEMENTARY MATERIAL

The Supplementary Material for this article can be found online at: https://www.frontiersin.org/articles/10.3389/fmicb.2019.01580/full#supplementary-material

REFERENCES

Apte-Deshpande, A., Paingankar, M., Gokhale, M. D., and Deobagkar, D. N. (2012). *Serratia odorifera* a midgut inhabitant of *Aedes aegypti* mosquito enhances its susceptibility to dengue-2 virus. *PLoS One* 7:e40401. doi: 10.1371/journal.pone.0040401

Apte-Deshpande, A. D., Paingankar, M. S., Gokhale, M. D., and Deobagkar, D. N. (2014). *Serratia odorifera* mediated enhancement in susceptibility of *Aedes aegypti* for chikungunya virus. *Indian J. Med. Res.* 139, 762–768. Available at: https://www.ncbi.nlm.nih.gov/pmc/articles/PMC4140042/

Bahia, A. C., Dong, Y., Blumberg, B. J., Mlambo, G., Tripathi, A., BenMarzouk-Hidalgo, O. J., et al. (2014). Exploring *Anopheles* gut bacteria for *Plasmodium* blocking activity. *Environ. Microbiol.* 16, 2980–2994. doi: 10.1111/1462-2920.12381

Bando, H., Okado, K., Guelbeogo, W. M., Badolo, A., Aonuma, H., Nelson, B., et al. (2013). Intra-specific diversity of *Serratia marcescens* in *Anopheles* mosquito midgut defines *Plasmodium* transmission capacity. *Sci. Rep.* 3:1641. doi: 10.1038/srep01641

Barillas-Mury, C. (2007). CLIP proteases and *Plasmodium* melanization in *Anopheles gambiae*. *Trends Parasitol.* 23, 297–299. doi: 10.1016/j.pt.2007.05.001

Baton, L. A., and Ranford-Cartwright, L. C. (2005). How do malaria ookinetes cross the mosquito midgut wall? *Trends Parasitol.* 21, 22–28. doi: 10.1016/j.pt.2004.11.001

Blandin, S. A., Marois, E., and Levashina, E. A. (2008). Antimalarial responses in *Anopheles gambiae*: from a complement-like protein to a complement-like pathway. *Cell Host Microbe* 3, 364–374. doi: 10.1016/j.chom.2008.05.007

Blandin, S., Shiao, S. H., Moita, L. F., Janse, C. J., Waters, A. P., Kafatos, F. C., et al. (2004). Complement-like protein TEP1 is a determinant of vectorial capacity in the malaria vector *Anopheles gambiae*. *Cell* 116, 661–670. doi: 10.1016/s0092-8674(04)00173-4

Boissiere, A., Gimonneau, G., Tchioffo, M. T., Abate, L., Bayibeki, A., Awono-Ambene, P. H., et al. (2013). Application of a qPCR assay in the investigation of susceptibility to malaria infection of the M and S molecular forms of *An. gambiae* s.s. in Cameroon. *PLoS One* 8:e54820. doi: 10.1371/journal.pone.0054820

Boissiere, A., Tchioffo, M. T., Bachar, D., Abate, L., Marie, A., Nsango, S. E., et al. (2012). Midgut microbiota of the malaria mosquito vector *Anopheles gambiae* and interactions with *Plasmodium falciparum* infection. *PLoS Pathog.* 8:e1002742. doi: 10.1371/journal.ppat.1002742

Cirimotich, C. M., Dong, Y., Clayton, A. M., Sandiford, S. L., Souza-Neto, J. A., Mulenga, M., et al. (2011). Natural microbe-mediated refractoriness to *Plasmodium* infection in *Anopheles gambiae*. *Science* 332, 855–858. doi: 10.1126/science.1201618

De Gregorio, E., Spellman, P. T., Tzou, P., Rubin, G. M., and Lemaitre, B. (2002). The Toll and Imd pathways are the major regulators of the immune response in *Drosophila*. *EMBO J.* 21, 2568–2579. doi: 10.1093/emboj/21.11.2568

Dimopoulos, G., Richman, A., Muller, H. M., and Kafatos, F. C. (1997). Molecular immune responses of the mosquito *Anopheles gambiae* to bacteria and malaria parasites. *Proc. Natl. Acad. Sci. USA* 94, 11508–11513. doi: 10.1073/pnas.94.21.11508

Dong, Y., Aguilar, R., Xi, Z., Warr, E., Mongin, E., and Dimopoulos, G. (2006). *Anopheles gambiae* immune responses to human and rodent *Plasmodium parasite* species. *PLoS Pathog.* 2:e52. doi: 10.1371/journal.ppat.0020052

Dong, Y., Das, S., Cirimotich, C., Souza-Neto, J. A., McLean, K. J., and Dimopoulos, G. (2011). Engineered *Anopheles* immunity to *Plasmodium* infection. *PLoS Pathog.* 7:e1002458. doi: 10.1371/journal.ppat.1002458

Dong, Y., and Dimopoulos, G. (2009). *Anopheles* fibrinogen-related proteins provide expanded pattern recognition capacity against bacteria and malaria parasites. *J. Biol. Chem.* 284, 9835–9844. doi: 10.1074/jbc.M807084200

Dong, Y., Manfredini, F., and Dimopoulos, G. (2009). Implication of the mosquito midgut microbiota in the defense against malaria parasites. *PLoS Pathog.* 5:e1000423. doi: 10.1371/journal.ppat.1000423

Garver, L. S., Dong, Y., and Dimopoulos, G. (2009). Caspar controls resistance to *Plasmodium falciparum* in diverse *Anopheline* species. *PLoS Pathog.* 5:e1000335. doi: 10.1371/journal.ppat.1000335

Gendrin, M., and Christophides, G. (2013). The *Anopheles* mosquito microbiota and their impact on pathogen transmission. 525–539. *INTECH*. doi: 10.5772/55107

Gendrin, M., Rodgers, F. H., Yerbanga, R. S., Ouédraogo, J. B., Basáñez, M. G., Cohuet, A., et al. (2015). Antibiotics in ingested human blood affect the mosquito microbiota and capacity to transmit malaria. *Nat. Commun.* 6, 1–7. doi: 10.1038/ncomms6921

Ghosh, A., Edwards, M. J., and Jacobs-Lorena, M. (2000). The journey of the malaria parasite in the mosquito: hopes for the new century. *Parasitol. Today* 16, 196–201. doi: 10.1016/S0169-4758(99)01626-9

Gonzalez-Ceron, L., Santillan, F., Rodriguez, M. H., Mendez, D., and Hernandez-Avila, J. E. (2003). Bacteria in midguts of field-collected *Anopheles albimanus* block *Plasmodium vivax* sporogonic development. *J. Med. Entomol.* 40, 371–374. doi: 10.1603/0022-2585-40.3.371

Graewe, S., Retzlaff, S., Struck, N., Janse, C. J., and Heussler, V. T. (2009). Going live: a comparative analysis of the suitability of the RFP derivatives RedStar, mCherry and tdTomato for intravital and in vitro live imaging of *Plasmodium* parasites. *Biotechnol. J.* 4, 895–902. doi: 10.1002/biot.200900035

Luckhart, S., Vodovotz, Y., Cui, L., and Rosenberg, R. (1998). The mosquito *Anopheles stephensi* limits malaria parasite development with inducible synthesis of nitric oxide. *Proc. Natl. Acad. Sci. USA* 95, 5700–5705. doi: 10.1073/pnas.95.10.5700

Luna, C., Hoa, N. T., Lin, H., Zhang, L., Nguyen, H. L., Kanzok, S. M., et al. (2006). Expression of immune responsive genes in cell lines from two different *Anopheline* species. *Insect Mol. Biol.* 15, 721–729. doi: 10.1111/j.1365-2583.2006.00661.x

Meister, S., Agianian, B., Turlure, F., Relogio, A., Morlais, I., Kafatos, F. C., et al. (2009). *Anopheles gambiae* PGRPLC-mediated defense against bacteria modulates infections with malaria parasites. *PLoS Pathog.* 5:e1000542. doi: 10.1371/journal.ppat.1000542

Meister, S., Kanzok, S. M., Zheng, X. L., Luna, C., Li, T. R., Hoa, N. T., et al. (2005). Immune signaling pathways regulating bacterial and malaria parasite infection of the mosquito *Anopheles gambiae*. *Proc. Natl. Acad. Sci. USA* 102, 11420–11425. doi: 10.1073/pnas.0504950102

Oduol, F., Xu, J. N., Niare, O., Natarajan, R., and Vernick, K. D. (2000). Genes identified by an expression screen of the vector mosquito *Anopheles gambiae* display differential molecular immune response to malaria parasites and bacteria. *Proc. Natl. Acad. Sci. USA* 97, 11397–11402. doi: 10.1073/pnas.180060997

Oliveira Gde, A., Lieberman, J., and Barillas-Mury, C. (2012). Epithelial nitration by a peroxidase/NOX5 system mediates mosquito antiplasmodial immunity. *Science* 335, 856–859. doi: 10.1126/science.1209678

Osta, M. A., Christophides, G. K., and Kafatos, F. C. (2004). Effects of mosquito genes on *Plasmodium* development. *Science* 303, 2030–2032. doi: 10.1126/science.1091789

Pradel, G. (2007). Proteins of the malaria parasite sexual stages: expression, function and potential for transmission blocking strategies. *Parasitology* 134, 1911–1929. doi: 10.1017/S0031182007003381

Pumpuni, C. B., Beier, M. S., Nataro, J. P., Guers, L. D., and Davis, J. R. (1993). *Plasmodium falciparum*: inhibition of sporogonic development in *Anopheles stephensi* by gram-negative bacteria. *Exp. Parasitol.* 77, 195–199. doi: 10.1006/expr.1993.1076

Pumpuni, C. B., Demaio, J., Kent, M., Davis, J. R., and Beier, J. C. (1996). Bacterial population dynamics in three anopheline species: the impact on *Plasmodium* sporogonic development. *Am. J. Trop. Med. Hyg.* 54, 214–218. doi: 10.4269/ajtmh.1996.54.214

Simon, N., Scholz, S. M., Moreira, C. K., Templeton, T. J., Kuehn, A., Dude, M. A., et al. (2009). Sexual stage adhesion proteins form multi-protein complexes in the malaria parasite *Plasmodium falciparum*. *J. Biol. Chem.* 284, 14537–14546. doi: 10.1074/jbc.M808472200

Sinden, R. E., and Billingsley, P. F. (2001). *Plasmodium* invasion of mosquito cells: hawk or dove? *Trends Parasitol.* 17, 209–211. doi: 10.1016/S1471-4922(01)01928-6

Smith, R. C., Vega-Rodriguez, J., and Jacobs-Lorena, M. (2014). The *Plasmodium* bottleneck: malaria parasite losses in the mosquito vector. *Mem. Inst. Oswaldo Cruz* 109, 644–661. doi: 10.1590/0074-0276130597

Song, X., Wang, M., Dong, L., Zhu, H., and Wang, J. (2018). PGRP-LD mediates *A. stephensi* vector competency by regulating homeostasis of microbiota-induced peritrophic matrix synthesis. *PLoS Pathog.* 14:e1006899. doi: 10.1371/journal.ppat.1006899

Stathopoulos, S., Neafsey, D. E., Lawniczak, M. K., Muskavitch, M. A., and Christophides, G. K. (2014). Genetic dissection of *Anopheles gambiae* gut epithelial responses to *Serratia marcescens*. *PLoS Pathog.* 10:e1003897. doi: 10.1371/journal.ppat.1003897

Straif, S. C., Mbogo, C. N., Toure, A. M., Walker, E. D., Kaufman, M., Toure, Y. T., et al. (1998). Midgut bacteria in *Anopheles gambiae* and *An. funestus* (Diptera: Culicidae) from Kenya and Mali. *J. Med. Entomol.* 35, 222–226. doi: 10.1093/jmedent/35.3.222

Tanji, T., Hu, X., Weber, A. N., and Ip, Y. T. (2007). Toll and IMD pathways synergistically activate an innate immune response in *Drosophila melanogaster*. *Mol. Cell. Biol.* 27, 4578–4588. doi: 10.1128/MCB.01814-06

Vaughan, J. A., Noden, B. H., and Beier, J. C. (1992). Population dynamics of *Plasmodium falciparum* sporogony in laboratory-infected *Anopheles gambiae*. *J. Parasitol.* 78, 716–724. doi: 10.2307/3283550

Volz, J., Muller, H. M., Zdanowicz, A., Kafatos, F. C., and Osta, M. A. (2006). A genetic module regulates the melanization response of *Anopheles* to *Plasmodium*. *Cell. Microbiol.* 8, 1392–1405. doi: 10.1111/j.1462-5822.2006.00718.x

Volz, J., Osta, M. A., Kafatos, F. C., and Muller, H. M. (2005). The roles of two clip domain serine proteases in innate immune responses of the malaria vector *Anopheles gambiae*. *J. Biol. Chem.* 280, 40161–40168. doi: 10.1074/jbc.M506191200

Wang, S., Dos-Santos, A. L. A., Huang, W., Liu, K. C., Oshaghi, M. A., Wei, G., et al. (2017). Driving mosquito refractoriness to *Plasmodium falciparum* with engineered symbiotic bacteria. *Science* 357, 1399–1402. doi: 10.1126/science.aan5478

Wang, S., Ghosh, A. K., Bongio, N., Stebbings, K. A., Lampe, D. J., and Jacobs-Lorena, M. (2012). Fighting malaria with engineered symbiotic bacteria from vector mosquitoes. *Proc. Natl. Acad. Sci. USA* 109, 12734–12739. doi: 10.1073/pnas.1204158109

Wei, G., Lai, Y., Wang, G., Chen, H., Li, F., and Wang, S. (2017). Insect pathogenic fungus interacts with the gut microbiota to accelerate mosquito mortality. *Proc. Natl. Acad. Sci. USA* 114, 5994–5999. doi: 10.1073/pnas.1703546114

World Health Organization (2018). "World malaria report 2018" in *Geneva Switzerland WHO*. Available at: www.who.int/malaria/publications/worldmalariareport-2018/en/

Conflict of Interest Statement: The authors declare that the research was conducted in the absence of any commercial or financial relationships that could be construed as a potential conflict of interest.

frontiers in Cellular and Infection Microbiology

BRIEF RESEARCH REPORT
published: 24 July 2019
doi: 10.3389/fcimb.2019.00266

Distinct Functional Contributions by the Conserved Domains of the Malaria Parasite Alveolin IMC1h

Michael P. Coghlan[1,2], *Annie Z. Tremp*[1], *Sadia Saeed*[1], *Cara K. Vaughan*[2] *and Johannes T. Dessens*[1]*

[1] *Department of Infection Biology, London School of Hygiene and Tropical Medicine, London, United Kingdom,* [2] *Institute of Structural and Molecular Biology, School of Biological Sciences, Birkbeck, London, United Kingdom*

Invasive, motile life cycle stages (zoites) of apicomplexan parasites possess a cortical membrane skeleton composed of intermediate filaments with roles in zoite morphogenesis, tensile strength and motility. Its building blocks include a family of proteins called alveolins that are characterized by conserved "alveolin" domains composed of tandem repeat sequences. A subset of alveolins possess additional conserved domains that are structurally unrelated and the roles of which remain unclear. In this structure-function analysis we investigated the functional contributions of the "alveolin" vs. "non-alveolin" domains of IMC1h, a protein expressed in the ookinete and sporozoite life cycle stages of malaria parasites and essential for parasite transmission. Using allelic replacement in *Plasmodium berghei,* we show that the alveolin domain is responsible for targeting IMC1h to the membrane skeleton and, consequently, its deletion from the protein results in loss of function manifested by abnormally-shaped ookinetes and sporozoites with reduced tensile strength, motility and infectivity. Conversely, IMC1h lacking its non-alveolin conserved domain is correctly targeted and can facilitate tensile strength but not motility. Our findings support the concept that the alveolin module contains the properties for filament formation, and show for the first time that tensile strength makes an important contribution to zoite infectivity. The data furthermore provide new insight into the underlying molecular mechanisms of motility, indicating that tensile strength is mechanistically uncoupled from locomotion, and pointing to a role of the non-alveolin domain in the motility-enhancing properties of IMC1h possibly by engaging with the locomotion apparatus.

Keywords: ***Plasmodium*, cytoskeleton, ookinete, sporozoite, motility, transmission**

OPEN ACCESS

Edited by:
Rhoel Dinglasan,
University of Florida, United States

Reviewed by:
JUN Miao,
University of South Florida, United States
Arun Kumar Kota,
University of Hyderabad, India
Joel Vega-Rodriguez,
National Institute of Allergy and Infectious Diseases (NIAID), United States

***Correspondence:**
Johannes T. Dessens
johannes.dessens@lshtm.ac.uk

Specialty section:
This article was submitted to Parasite and Host, a section of the journal Frontiers in Cellular and Infection Microbiology

Received: *06 March 2019*
Accepted: *08 July 2019*
Published: *24 July 2019*

Citation:
Coghlan MP, Tremp AZ, Saeed S, Vaughan CK and Dessens JT (2019) Distinct Functional Contributions by the Conserved Domains of the Malaria Parasite Alveolin IMC1h. Front. Cell. Infect. Microbiol. 9:266. doi: 10.3389/fcimb.2019.00266

INTRODUCTION

Plasmodium species, the causative agents of malaria, have a complex life cycle in vertebrate host and mosquito vector. Parasite-infected erythrocytes multiply via an asexual replication cycle called schizogony to release merozoites that infect new red blood cells. A small percentage of these develop into sexual stage precursor cells (gametocytes) which, after uptake with the blood meal of a feeding mosquito, begin a rapid process of gamete formation and fertilization inside the mosquito midgut.

The resultant zygotes undergo meiosis and transform into elongated forms termed ookinetes, which traverse the midgut epithelium and then round up to form the oocysts. In the following weeks, young oocysts grow and divide by a process known as sporogony to generate hundreds of daughter cells named sporozoites. After egress from the oocyst, sporozoites invade and inhabit the salivary glands, and are transmitted to new hosts by mosquito bite to first infect liver cells from which new malaria blood stage infections are initiated to complete the life cycle.

The merozoite, ookinete, and sporozoite constitute the three motile and invasive stages in the *Plasmodium* life cycle. These so-called "zoite" stages possess a characteristic cortical structure termed the pellicle. The pellicle is defined by a double membrane structure termed the inner membrane complex (IMC) situated directly underneath the plasma membrane, which is equivalent to a sutured system of flattened sacs or alveoli (Bannister et al., 2000; Morrissette and Sibley, 2002; Santos et al., 2009). On the cytoplasmic face of the IMC, and tightly associated with it, sits a network of intermediate filaments termed the subpellicular network (SPN), a viscoelastic membrane skeleton that supports the IMC and provides tensile strength to the cell (Mann and Beckers, 2001). A family of IMC1 proteins, now called alveolins, have been identified as major components of the SPN (Mann and Beckers, 2001; Khater et al., 2004). Members of the alveolin family are found in apicomplexans and chromerids, as well as in ciliates and dinoflagellate algae, which together with the apicomplexans form the Alveolata superphylum (Gould et al., 2008). The alveolins are part of a larger class of proteins called epiplastins that aside alveolates have also been identified in euglenids, glaucophytes and cryptophytes (Goodenough et al., 2018). In the genus *Plasmodium*, 13 conserved and syntenic alveolin family members have thus far been identified that are differentially expressed among the three different zoites stages (Al-Khattaf et al., 2015; Kaneko et al., 2015). In addition, two PhIL1 interacting proteins: PIP2 and PIP3, show structural homology with alveolins (Kono et al., 2013; Parkyn Schneider et al., 2017).

It has been shown in the rodent malaria species *P. berghei* that disruption of the alveolins IMC1a, IMC1b, or IMC1h gives rise to morphological aberrations that are accompanied by reduced tensile strength of the zoite stages in which they are expressed. The same null mutant parasites also display motility defects, indicating that these alveolins also participate in parasite locomotion through an as yet unknown mechanism (Khater et al., 2004; Tremp et al., 2008; Tremp and Dessens, 2011; Volkmann et al., 2012). The SPN effectively separates the main cytosol from a smaller cortical cytoplasm that contains the molecular machinery that drives apicomplexan zoite motility, invasion and egress. Motility of apicomplexan zoites relies on an actinomyosin motor system that is situated in the space between the plasma membrane and the IMC. The conventional model is that the molecular motor and its auxiliary proteins is linked to cell surface adhesins via actin filaments and bridging proteins, and is internally anchored into the IMC. Motor force drives the actin filaments and adhesins rearward, thereby creating a traction force that propels the cell in the opposite direction against a substrate (Frenal et al., 2010). The IMC is underlain by the rigid yet flexible SPN, and this is most likely how alveolins assert their role in motility, either indirectly by providing mechanical support to the IMC, or through interactions with components of the motility apparatus.

The structural homologies between alveolin proteins are largely confined to conserved domains containing tandem repeat sequences (Al-Khattaf et al., 2015), herein referred to as "alveolin" domains. A subset of alveolins possess additional conserved modules that are structurally unrelated to the archetypal "alveolin" module. The roles of these "non-alveolin" domains in protein function are poorly understood. In this study, we investigated the functional contributions of the "alveolin" vs. "non-alveolin" modules of IMC1h, using the rodent malaria parasite species *P. berghei* and a strategy of allelic replacement and GFP tagging. IMC1h is expressed in both the ookinete and sporozoite life cycle stages of the parasite, where it carries out equivalent roles (Tremp and Dessens, 2011; Volkmann et al., 2012), thus allowing our investigations to be conducted across two distinct zoite stages. The results obtained indicate that the two IMC1h modules play distinct parts in facilitating morphogenesis, tensile strength and motility. The implications of these results are discussed in the context of parasite infectivity.

MATERIALS AND METHODS

Animal Use

Experiments were conducted in 6–8 weeks old female CD1 mice, specific pathogen free and maintained in filter cages. Animal welfare was assessed daily and animals were humanely killed upon reaching experimental or humane endpoints. Mice were infected with parasites by intraperitoneal injection, or by infected mosquito bite on anesthetized animals. Parasitemia was monitored regularly by collecting of a small drop of blood from a superficial tail vein. Drugs were administered by intraperitoneal injection or where possible were supplied in drinking water. Parasitized blood was harvested by cardiac bleed under general anesthesia without recovery.

Gene Targeting Vectors

To delete domain 1 of IMC1h (amino acids 103 to 306) primers IMC1hdeltadomain1-F (GAGGTTCACAATATTTGAA TAACAATCAAGCACA) and IMC1hdeltadomain1-R (AAAT ATTGTGAACCTCCATACAAAGTGTGTT) were used to PCR amplify plasmid pLP-IMC1h/GFP (Tremp and Dessens, 2011). Template plasmid was removed after the PCR by *Dpn*I digestion, and the PCR product was circularized by in-fusion, to give plasmid pLP-IMC1hΔ1. This mutation deletes 205 amino acids from the IMC1h::GFP fusion protein (**Figure 1**). The same approach was used to delete domain 2 (amino acids 397 to 504), using primers IMC1hdeltadomain2-F (ATAATTCGGT TAAAGCTATCCAGAAAAACAT) and IMC1hdeltadomain2-R (GCTTTAACCGAATTATTTTGTCTATAATCCATATTTGA) to give plasmid pLP-IMC1hΔ2. This mutation deletes 109 amino acids from the IMC1h::GFP fusion protein (**Figure 1**).

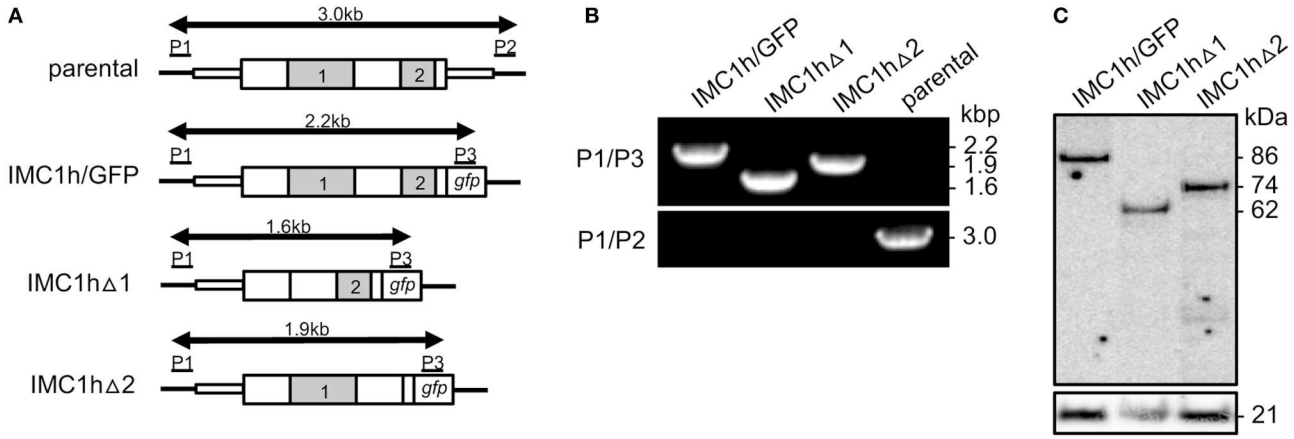

FIGURE 1 | Generation and genotyping of IMC1h mutants. **(A)** Schematic diagram of the parental and modified *imc1h* alleles. The *imc1h* gene is indicated with coding sequence (wide bars) and 5′ and 3′ untranslated regions (narrow bars). The relative positions of domains 1 and 2 are indicated (gray). Also shown are the *gfp* module, positions of primers P1–P3 used for diagnostic PCR amplification, and the predicted lengths of the amplicons (arrows). **(B)** PCR with primers P1 and P3 diagnostic for integration of the modified, GFP-tagged *imc1h* alleles into the *imc1h* locus, or with primers P1 and P2 diagnostic for absence/presence of the unmodified parental *imc1h* allele. Amplicon sizes (kb) are indicated on the right-hand side and correspond to those depicted in **(A)**. **(C)** Western blot analysis of purified ookinetes (∼ 50,000 per lane) of IMC1h mutant parasite lines using anti-GFP antibodies, showing successful expression of IMC1h::GFP fusion proteins. Identified band sizes reflect the introduced domain deletions in IMC1h, resulting in proteins of 86 kDa (IMC1h/GFP), 62 kDa (IMC1hΔ1), and 74 kDa (IMC1hΔ2). The ookinete surface protein Pbs21 is shown as a loading control.

Generation and Genotyping of Genetically Modified Parasites

Parasite transfection, pyrimethamine selection and dilution cloning were performed as previously described (Waters et al., 1997). Prior to performing transfections, plasmid DNA was double-digested with KpnI and SacII to remove the plasmid backbone. Genomic DNA extraction was performed as previously described (Dessens et al., 1999). After transfection, drug resistant parasites were subjected to limiting dilution cloning. Integration of the GFP-tagged IMC1h-encoding sequence into the *imc1h* locus was confirmed by diagnostic PCR across the 5' integration site with primers P1 (CCATTTTTA TGTTGAGCTTGAG) and P3 (GTGCCCATTAACCATCACC) (**Figure 1**). The absence of the unmodified *imc1h* allele in the clonal parasite lines was confirmed by diagnostic PCR with primers P1 and P2 (TTCTATAATCTTTAATTGTTCAGAA ATGTG) (**Figure 1**).

Sporozoite Size Measurements

Images of individual midgut sporozoites were captured by microscopy on Zeiss LSM510 inverted laser scanning confocal microscope. Using Zeiss LSM image browser software the circumference was measured from which the occupied surface area ("footprint") was calculated as a measure of cell size. Statistical analysis was carried out using Student's *t*-test.

Zoite Motility

Ookinete motility was assessed essentially as previously described (Moon et al., 2009). Aliquots of neat ookinete cultures were added to equal volumes of Matrigel (BD Biosciences) on ice, mixed thoroughly, spotted onto a microscope slide, and covered with a cover slip. After sealing with nail varnish, the Matrigel was allowed to set at room temperature for 30 min before analysis. Sporozoites were gently released from ∼ 20 salivary glands in 200 μl RPMI medium in a Dounce homogenizer on ice. Following addition of an equal volume of RPMI supplemented with 20% fetal bovine serum, the sporozoites were transferred to an Eppendorf tube and collected by centrifugation in a swing-out rotor for 10 min at 1,000 × g at 4°C, followed by removal of excess supernatant. Aliquots of resuspended sporozoites were mixed with an equal volume of Matrigel on ice before transfer to microscope slides. After sealing the cover slip with nail varnish, the Matrigel was allowed to set at room temperature for 30 min before analysis. Cells were examined and time-lapse images taken on a Zeiss Axioplan II microscope. Movies were analyzed with ImageJ using the Manual Tracking plugin. Statistical analysis was carried out using ANOVA and Tukey's multiple comparison.

Osmotic Shock and Viability Assays

Ookinetes in neat culture were subjected to hypo-osmotic shock of 0.5 × normal osmotic strength by adding an equal volume of water. Sporozoites were released from oocyst-infected midguts at 15 days post-infection and were subjected to 0.33 × normal osmotic strength by adding two equal volumes of water. After 5 min, normal osmotic conditions were restored by adding an appropriate amount of 10 × PBS. Cell viability was scored by fluorescence microscopy in the presence of 0.5% propidium iodide and 1% Hoechst 33258. Ookinetes whose nuclei stained positive for both propidium iodide and Hoechst were scored as non-viable, whereas ookinetes whose nuclei stained positive only for Hoechst were scored as viable. Values were normalized to 100% viability in untreated cells.

Mosquito Infection

At 6 days before infecting mosquitoes, mice were injected intraperitoneally with phenylhydrazine (6 mg/ml in PBS, 10 μl/g body weight) to induce reticulocytosis. At 3 days before mosquito feeding, mice were infected intraperitoneally with 10^7 parasitized red blood cells. The day of the feed, parasitemia and gametocytemia were checked by using a Giemsa-stained blood film. Mice were anesthetized and placed on a cage containing up to 50 starved female mosquitoes. Insects were allowed to blood feed in a draft-free, darkened environment at room temperature for 15 min. The day after feeding, unfed or partially fed mosquitoes (i.e., those unlikely to be infected) were removed if desired. For sporozoite transmission, the prevalence of infection of mosquito batches was determined and combined with the number of blood meal-positive insects after feeding to estimate the number of sporozoite-infected mosquitoes that fed.

RESULTS

Generation and Genotyping of IMC1h Mutants

Multiple alignment of amino acid sequences of IMC1h orthologs from different *Plasmodium* species clearly reveals the presence of its single conserved "alveolin" module (domain 1), as well as a conserved carboxy-terminal module that is structurally unrelated (domain 2) (Tremp and Dessens, 2011). We previously generated and characterized parasites lines stably expressing IMC1h::GFP from the native *imc1h* promoter (named IMC1h/GFP) (Tremp and Dessens, 2011). To study the role of domains 1 and 2 we used the same allelic replacement strategy, generating transgenic parasites lines that express IMC1h::GFP without domain 1 (named IMC1hΔ1) or IMC1h::GFP lacking domain 2 (named IMC1hΔ2) (**Figure 1A**). Diagnostic PCR with primers P1 and P3 (**Figure 1A**) of clonal parasite lines amplified expected products of ∼ 2.2, 1.6, and 1.9 kb from parasite lines IMC1h/GFP, IMC1hΔ1, and IMC1hΔ2, respectively, confirming integration of the modified *imc1h* alleles into the *imc1h* locus (**Figure 1B**). Moreover, amplification with primers P1 and P2 (**Figure 1A**) amplified an ∼ 3 kb product only from the parental parasite, confirming absence of the unmodified *imc1h* allele in the transgenic lines (**Figure 1B**). Western blot analysis of purified ookinete samples using anti-GFP antibodies showed comparable expression levels of IMC1h::GFP fusion proteins in all three parasite lines, with protein sizes of the IMC1h::GFP fusion proteins corresponding to the introduced amino acid deletions in IMC1h (**Figure 1C**). This indicated that the truncated IMC1h proteins are stably expressed in ookinetes and confirms the successful introduction of the domain 1 and domain 2 deletions.

Ookinete-Specific Subcellular Localization of Mutant IMC1h::GFP and Cell Shape

To study the subcellular localization of the truncated IMC1h::GFP fusion proteins in parasite lines IMC1hΔ1 and IMC1hΔ2, live ookinetes were examined for GFP fluorescence. As described previously (Tremp and Dessens, 2011), ookinetes expressing full-length IMC1h::GFP had normal shape and displayed a predominantly cortical localization of GFP fluorescence (**Figure 2A**), consistent with the recruitment of IMC1h to the SPN. Both IMC1hΔ1 and IMC1hΔ2 ookinetes were misshapen, lacking the typical crescent shape and possessing a bulging area in the center (**Figure 2A**) similar to the shape of IMC1h-KO ookinetes (Tremp and Dessens, 2011). This indicates that domain 1 and domain 2 are both required for IMC1h to facilitate normal ookinete morphogenesis. Subcellular localization of GFP fluorescence was markedly different between IMC1hΔ1 and IMC1hΔ2 ookinetes: while the GFP signal in IMC1hΔ2 ookinetes was predominantly found at the cell cortex like in IMC1h/GFP ookinetes, IMC1hΔ1 ookinetes displayed only cytoplasmic fluorescence (**Figure 2A**). These observations show that domain 1 is required for recruitment of IMC1h to the SPN.

Motility, Tensile Strength, and Infectivity of IMC1h Mutant Ookinetes

As the truncated IMC1h::GFP fusion protein expressed in IMC1hΔ1 ookinetes fails to reach its site of action: the SPN (**Figure 2A**), this parasite is effectively an IMC1h null mutant. Indeed, assessment of ookinete motility in Matrigel revealed that IMC1hΔ1 ookinetes had a significantly lower average speed to that of IMC1h/GFP ookinetes (**Figure 2B**), as was reported for IMC1h null mutants (Tremp and Dessens, 2011). IMC1hΔ2 ookinetes also had a significantly lower average speed than IMC1h/GFP ookinetes, that was comparable to that of IMC1hΔ1 ookinetes (**Figure 2B**). The manner of ookinete movement as judged by their 3D trajectories was also examined: this showed that IMC1h/GFP ookinetes moved in a clearly helical fashion, while the trajectories of both IMC1hΔ1 and IMC1hΔ2 ookinetes were much more linear (**Figure 2C**). Similar differences were reported between wildtype and IMC1h null mutant ookinetes (Volkmann et al., 2012; Kan et al., 2014). Examination of videos of 3D ookinete movement showed that the abnormally shaped ookinetes of parasite lines IMC1hΔ1 and IMC1hΔ2 still possessed mildly helical movement albeit with a smaller radius, explaining why their trajectories appeared more linear (**Videos S1–S3**). These collective findings indicate that deletion of either domain 1 or domain 2 from IMC1h results in a loss-of-function phenotype with respect to ookinete motility.

We also assessed tensile strength of ookinetes using a hypo-osmotic shock assay. Hypo-osmotic conditions cause the cells to draw in water and swell, and the degree of hypo-osmotic stress a cell can tolerate is a measure of its tensile strength (Menke and Jockusch, 1991). In this assay, IMC1hΔ2 ookinetes were significantly more resistant to hypo-osmotic shock than their IMC1hΔ1 counterparts (**Figure 2D**), indicating that IMC1hΔ2 ookinetes have superior tensile strength to IMC1hΔ1 ookinetes. Thus, IMC1h lacking domain 2 is able to facilitate tensile strength above null mutant levels.

To assess the effects of the IMC1h module deletions on parasite infectivity, we infected *Anopheles stephensi* mosquitoes and recorded oocyst numbers as a measure of ookinete infectivity (**Table 1**). Reproducibly, both IMC1hΔ1 and IMC1hΔ2 ookinetes gave rise to statistically significantly

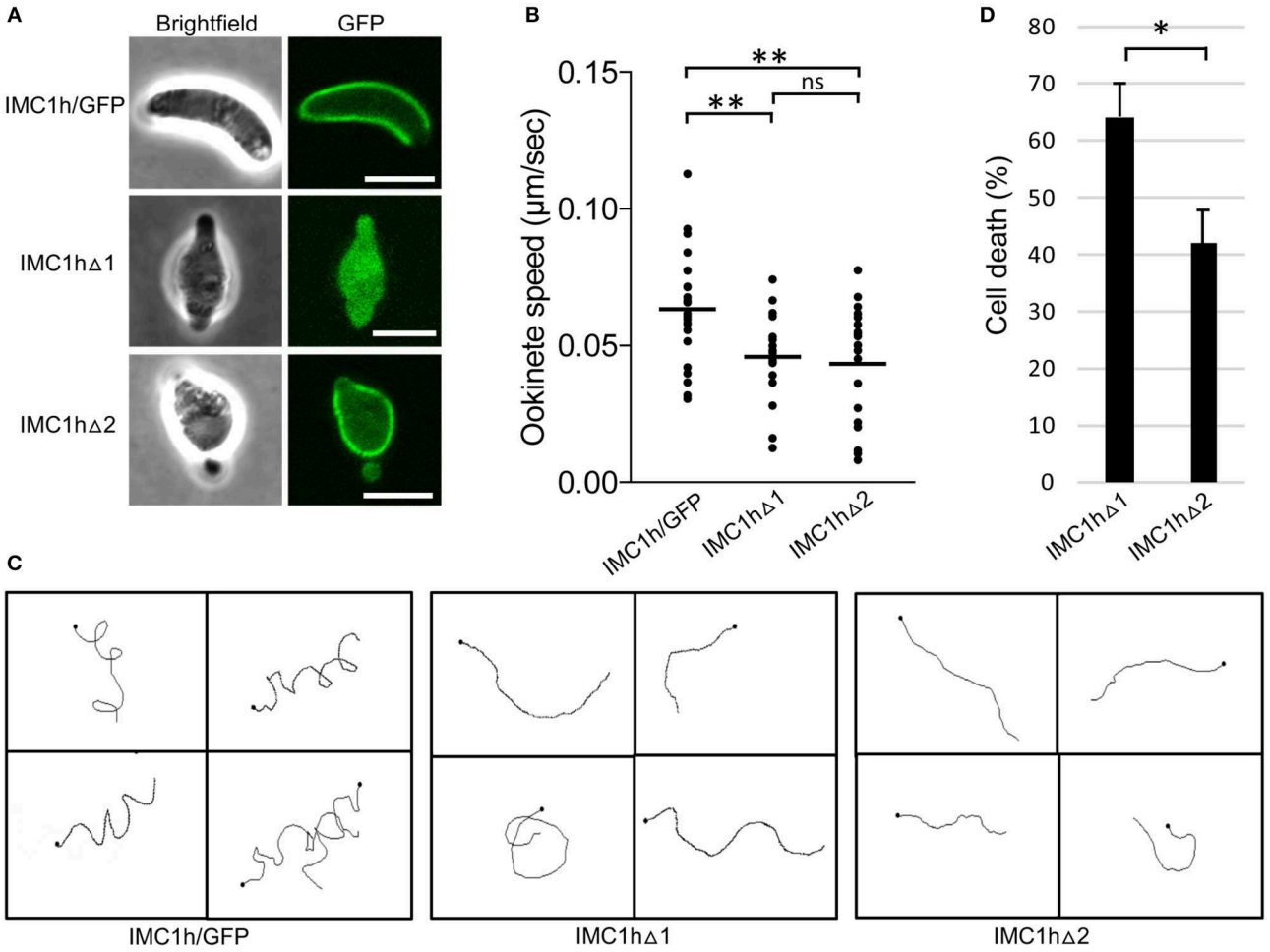

FIGURE 2 | Ookinete-specific subcellular localization of IMC1h::GFP in IMC1h mutants, and their phenotypes. **(A)** Confocal GFP fluorescence and brightfield images of ookinetes of IMC1h mutant parasite lines. Note that IMC1hΔ2 ookinetes have abnormal shape, but display normal cortical localization of the GFP fusion protein. Scale bar = 5 µm. **(B)** Ookinete speed expressed in µm/sec. Images were captured every 10 s over a 10 min period. Plot is based on pooled data from two independent experiments and >60 ookinetes analyzed. Horizontal lines mark mean values. **statistically significant differences ($P < 0.05$). ns, not significant. **(C)** Representative images of reconstructed 3D movement patterns from time-lapse movies of IMC1h mutants in Matrigel. The trajectories reveal the much straighter movement of IMC1hΔ1 and IMC1hΔ2 ookinetes compared to the helical movement of IMC1h/GFP ookinetes. **(D)** Percentage cell death after hypo-osmotic shock (0.5 × normal strength for 5 min). Cell death inversely correlates to tensile strength. *statistically significant differences ($P < 0.05$). Error bars indicate S.E.M. values from four independent experiments.

($P < 0.05$, *t*-test) reduced oocyst numbers compared to IMC1h/GFP control parasites (**Table 1**), indicating that they are less infective than their wildtype counterparts. IMC1hΔ2 ookinetes produced significantly higher oocyst numbers than IMC1hΔ1 ookinetes in one experiment (Experiment II, **Table 1**), indicating that they are more infective than their IMC1hΔ1 counterparts.

Sporozoite-Specific Subcellular Localization of Mutant IMC1h::GFP and Cell Shape

Sporozoites of parasite line IMC1hΔ1 were misshapen possessing a bulging area (**Figure 3A**), similar to IMC1h null mutant sporozoites (Tremp and Dessens, 2011). Like IMC1hΔ1 ookinetes (**Figure 2A**), these sporozoites displayed only cytoplasmic fluorescence (**Figure 3A**) reflecting absence of SPN targeting. By contrast, the large majority (95%, $n = 100$) of IMC1hΔ2 midgut sporozoites had a normal crescent shape and displayed cortical localization of GFP fluorescence (**Figure 3A**) indicative of normal SPN targeting as observed in IMC1hΔ2 ookinetes (**Figure 2A**). Assessment of sporozoite sizes revealed that IMC1hΔ1 sporozoites had a significantly smaller average size than IMC1hΔ2 sporozoites ($P < 0.001$), which in turn were significantly smaller than IMC1h/GFP sporozoites ($P < 0.005$) (IMC1hΔ1 footprint: 6.9 ± 0.16 µm^2; IMC1hΔ2 footprint: 8.5 ± 0.14 µm^2; IMC1h/GFP footprint; 10.0 ± 0.42 µm^2; $n = 30$). Interestingly, IMC1hΔ2 sporozoites lost their normal shape during transition from the midgut to the salivary glands, resulting in salivary gland sporozoites possessing a bulging area (**Figure 3A**). These combined observations indicate that IMC1hΔ2

TABLE 1 | Development of IMC1h mutant parasite lines in *Anopheles stephensi*.

Experiment	Parasite line	Infection prevalence[a]	Mean ± SEM oocyst number[b]	Median oocyst number	Mean salivary gland sporozoite number[c]	Salivary gland sporozoites per oocyst[d]
I	IMC1h/GFP	80 (15)	90 ± 19	82	n/a	n/a
	IMC1hΔ1	27 (15)	8.8 ± 5	5	n/a	n/a
	IMC1hΔ2	60 (15)	4.7 ± 1	4	n/a	n/a
II	IMC1h/GFP	100 (15)	102 ± 22	62	7,230 (13)	71
	IMC1hΔ1	100 (15)	7.9 ± 2.3	5	300 (20)	38
	IMC1hΔ2	100 (15)	32 ± 7.3	25	2,300 (20)	72
III	IMC1h/GFP	100 (21)	104 ± 25	48	n/a	n/a
	IMC1hΔ1	100 (21)	27 ± 6.5	20	625 (20)	23
	IMC1hΔ2	100 (22)	39 ± 10	26	2,760 (20)	70
IV	IMC1h/GFP	83 (24)	132 ± 26	85	7,968 (15)	60
	IMC1hΔ1	88 (24)	37 ± 7.3	19	528 (15)	14
	IMC1hΔ2	78 (27)	35 ± 6.8	20	2,496 (15)	71

[a] *Percentage of mosquitoes with at least one oocyst. (n) denotes the total number of mosquitoes analyzed.*
[b] *Oocysts were counted between 9 and 11 days post infection. Only infected insects were included.*
[c] *Average number of sporozoites per mosquito was calculated from (n) pooled salivary glands.*
[d] *Average number of sporozoites per mosquito divided by mean oocyst number.*

parasites possess an intermediate phenotype with respect to sporozoite morphogenesis.

Tensile Strength, Motility, and Infectivity IMC1h Mutant Sporozoites

Tensile strength assessment of midgut sporozoites indicated that IMC1hΔ2 sporozoites had higher tensile strength than their IMC1hΔ1 counterparts, but lower tensile strength than IMC1h/GFP sporozoites (**Figure 3B**). Both IMC1hΔ1 and IMC1hΔ2 sporozoites had similar average speed that was significantly reduced compared to that of their IMC1h/GFP counterparts (**Figure 3C**). The manner of sporozoite 3D movement as judged by their trajectories in Matrigel was also different between the parasite lines examined: while IMC1h/GFP sporozoites moved in a predominantly circular fashion in Matrigel, the trajectories of IMC1hΔ1 and IMC1hΔ2 sporozoites were more meandering and less circular (**Figure 3D**), as indeed was reported for IMC1h null mutants (Volkmann et al., 2012). These collective observations indicate that deletion of either domain 1 or domain 2 from IMC1h results in a loss-of-function phenotype with respect to sporozoite motility.

Sporozoite infectivity to the mosquito was assessed by counting salivary gland sporozoite numbers 3 weeks post-infection. Assuming a linear correlation between the number of oocyst and the number of sporozoites produced, these data indicated that IMC1hΔ2 sporozoites were almost three times more infective to salivary glands than IMC1hΔ1 sporozoites ($P < 0.05$, *t*-test), and had similar efficacy to IMC1h/GFP sporozoites in colonizing the salivary glands (**Table 1**). This is consistent with previous findings that IMC1h null mutant sporozoites are less invasive than their wildtype counterparts (Tremp and Dessens, 2011; Volkmann et al., 2012). Despite their presence in salivary glands, we failed to transmit IMC1hΔ1 and IMC1hΔ2 sporozoites by mosquito bite to naive mice, indicating that their infectivity to the mammalian host by natural route of transmission is compromised.

DISCUSSION

Plasmodium alveolins have important roles in morphogenesis, tensile strength and motility of the zoite stages, and in many cases their disruption leads to loss of parasite fitness, infectivity and transmission (Khater et al., 2004; Tremp et al., 2008, 2014; Tremp and Dessens, 2011). Here, we present data from a structure-function analysis of the alveolin IMC1h, aimed to determine the contributions of its "alveolin" and "non-alveolin" modules to protein function. This was based on a research strategy of allelic replacement of *imc1h* with modified versions of the gene fused to a GFP module for localization purposes. Our results demonstrate that the alveolin module of IMC1h is necessary for targeting the protein to the cortical membrane skeleton. This is in full agreement with a report showing that the alveolin domain of TgIMC3 can target YFP to the SPN of *Toxoplasma gondii* in a wildtype parasite background (Anderson-White et al., 2011). Our data show furthermore that the alveolin domain of IMC1h is sufficient to increase tensile strength above null mutant levels. Given the filamentous nature of the SPN (Mann and Beckers, 2001), the assembly or incorporation of the alveolins into such structures is likely to be a prerequisite for the provision of mechanical strength. Hence, our findings strongly suggest that the alveolin module contains the properties for intermediate filament formation, consistent with the fact that it is found in all alveolins and indeed is the distinguishing feature of this protein family. The processes of filament formation and SPN recruitment could be mechanistically linked as proposed (Tremp et al., 2017).

Previous studies have shown that knockout of IMC1a, IMC1b, or IMC1h reduced motility and tensile strength at the same time (Khater et al., 2004; Tremp et al., 2008; Tremp and Dessens,

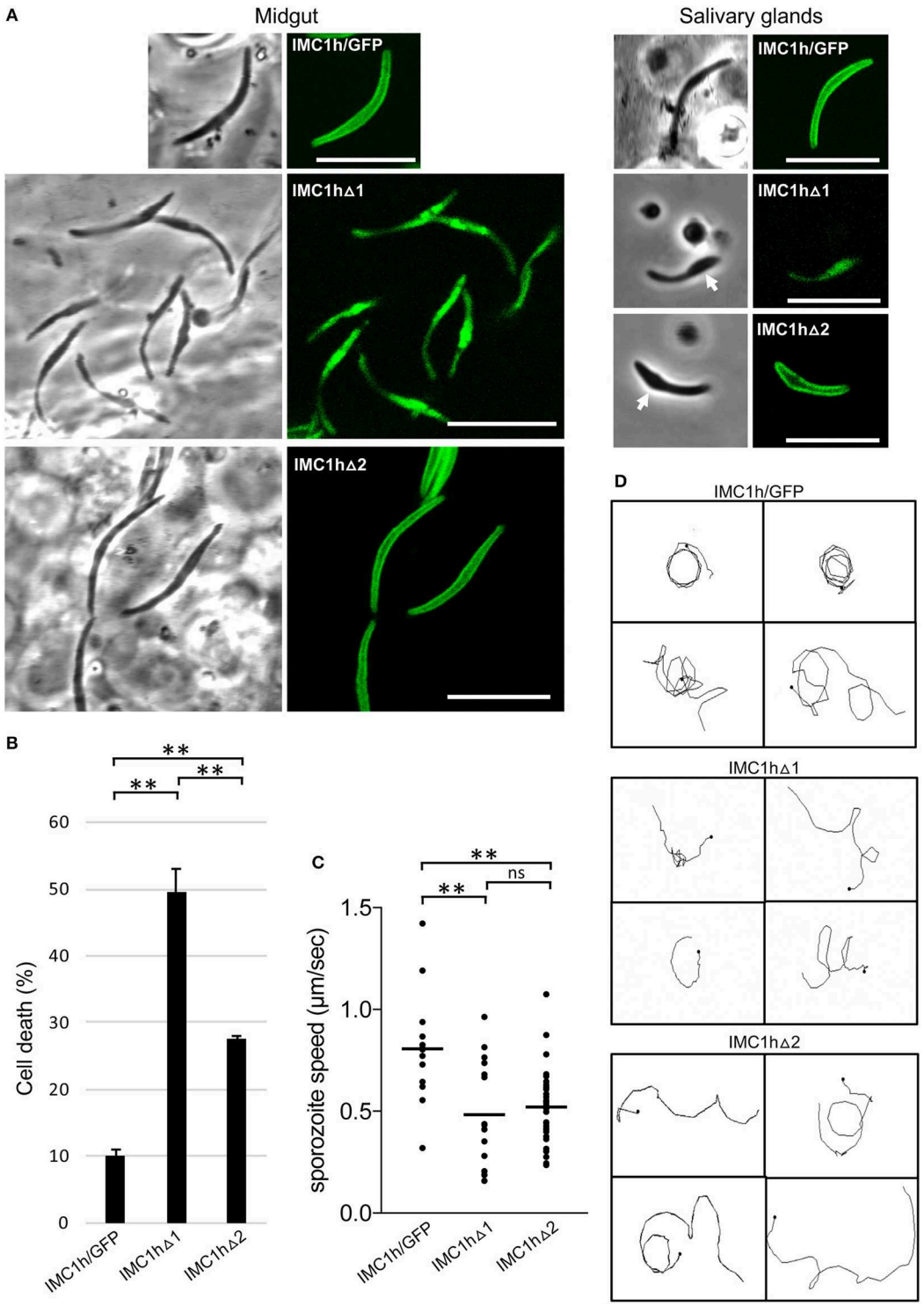

FIGURE 3 | Sporozoite-specific subcellular localization of IMC1h::GFP in IMC1h mutants, and their phenotypes. **(A)** Confocal GFP fluorescence and brightfield images of sporozoites of IMC1h mutant parasite lines. Note that IMC1hΔ2 sporozoites display normal cortical localization of the GFP fusion protein and have normal shape in midguts, but abnormal shape with bulging area (white arrow) in salivary glands. Scale bar = 10 µm. **(B)** Percentage cell death after hypo-osmotic shock (0.33 × normal strength for 5 min). Cell death inversely correlates to tensile strength. *statistically significant differences ($P < 0.05$). Error bars indicate S.E.M. values from two experiments. **(C)** Sporozoite speed expressed in µm/s. Images were captured every 10 s over a 2 min period. Plot is based on pooled data from two independent experiments and >60 sporozoites analyzed. Horizontal lines mark mean values. **statistically significant differences ($P < 0.005$). ns, not significant. **(D)** Representative images of reconstructed 3D movement patterns from time-lapse movies of IMC1h mutants in Matrigel. The trajectories reveal the more meandering movement of IMC1hΔ1 and IMC1hΔ2 sporozoites compared to the more circular movement of IMC1h/GFP sporozoites.

2011). For this reason, it has not been previously possible to dissect the individual contributions of tensile strength and motility to zoite infectivity. This study shows that zoites of parasite line IMC1hΔ2 are better at infecting mosquito tissues than the equivalent IMC1hΔ1 parasites (**Table 1**). As IMC1hΔ1 and IMC1hΔ2 zoites do not differ discernibly in their motilities, their differences in tensile strength are likely to be the cause of their distinct invasive capacities. These experiments thus show for the first time that tensile strength is an important contributor to zoite infectivity in the mosquito. Cell rigidity and flexibility are likely to be important when ookinetes escape the blood meal in the midgut lumen and cross the peritrophic matrix and midgut epithelium, a process that has been described to cause major cell constrictions (Vernick et al., 1999; Han et al., 2000), and the same can be envisaged in sporozoites when entering mosquito salivary glands.

IMC1hΔ2 sporozoites are larger than IMC1hΔ1 sporozoites and smaller than wildtype sporozoites, and they display normal shape when first formed. These observations indicate that IMC1h without its non-alveolin module causes an intermediate phenotype with regards to sporozoite morphogenesis. Interestingly, mutations of putative amino- or carboxy-terminal palmitoylation sites of the sporozoite-specific alveolin IMC1a have also been shown to affect sporozoite shape and size, being in between that of null mutant and wildtype sporozoites (Al-Khattaf et al., 2017). Collectively, these findings point to a fundamental role of the alveolins in determining sporozoite size and shape. The mechanisms by which alveolins participate in zoite morphogenesis remain poorly understood and, interestingly, knockouts of other SPN proteins that are structurally unrelated to alveolins such as G2 and PhIL1 cause similar cell shape abnormalities (Barkhuff et al., 2011; Tremp et al., 2013). Zoite morphogenesis is concurrent with the formation of the IMC and SPN structures (Hu et al., 2002; Tremp et al., 2008), and one possibility is that this is a highly constrained process that is very sensitive to structural disruption of any SPN component.

The apparent lack of correlation between motility and tensile strength (**Figures 2**, **3**) indicates that these two processes are in fact mechanistically uncoupled. This corroborates previous findings that IMC1h null mutant ookinetes have comparably reduced speed to similarly misshapen G2 null mutant ookinetes, despite these two parasite lines possessing different tensile strengths (Tremp et al., 2013). Thus, these observations support a role of IMC1h in motility through interactions with the motility apparatus, possibly via IMC-resident bridging proteins, rather than by simply contributing mechanical support to the IMC. Furthermore, our finding that IMC1hΔ2 parasites fail to rescue the IMC1h null mutant phenotype with respect to motility points to an involvement of the non-alveolin domain of IMC1h in the motility process. We therefore postulate that domain 2 is the part of IMC1h that engages with the motility apparatus, while the alveolin module is primarily involved in filament formation, SPN recruitment and viscoelasticity. Comparative alveolin interactome studies using IMC1hΔ2, IMC1hΔ1, and IMC1h/GFP ookinetes are underway to test this hypothesis and identify candidate IMC proteins interacting with domain 2. In this context, it is also worth noting that the other two alveolins with demonstrated roles in motility: IMC1a and IMC1b, also possess a conserved carboxy-terminal domain that has no structural relationship to the alveolin module (Khater et al., 2004; Tremp et al., 2008), and which may fulfill a similar role in motility to domain 2 of IMC1h.

Both ookinetes and sporozoites possess chirality, which is thought to be responsible for the circular nature of their directional movement (Kudryashev et al., 2012; Kan et al., 2014). During circular forward movement in Matrigel, ookinetes also rotate on their axis resulting in a helical, corkscrew-like 3D trajectory. By contrast, sporozoites possess dorsoventral polarity (Kudryashev et al., 2012) and helical movement is largely missing, explaining their predominantly circular directional movement in both 2D and 3D environments. Previous studies showed that the simultaneous absence of the alveolins IMC1h and IMC1b did not further affect ookinete cell shape, but further reduced ookinete speed and tensile strength compared with the respective single mutants, indicating that these two alveolins operate autonomously and contribute to motility independently of cell shape (Tremp and Dessens, 2011). We show here that the deletion of domains 1 or 2 from IMC1h not only reduces ookinete and sporozoite speed, but also alters their 3D movement to a markedly more linear fashion compared to that of their counterparts expressing full-length IMC1h. Nonetheless, examination of IMC1h mutant ookinetes reveals that the underlying motion remains mildly helical (**Videos S1**–**S3**), indicating that the biomechanics of movement have remained fundamentally the same as those of normal-shaped ookinetes. Changes in ookinete shape resulting from IMC1h knockout reduce the level of chirality and it was proposed that this determines the way in which these cells move in a 3D environment (Kan et al., 2014). The same could apply to the IMC1h mutant zoites described here. Consolidating the entire spectrum of motility observations, a model is emerging whereby zoite speed is largely cell shape-independent, whilst 3D movement is affected by the shape of the cells.

Salivary gland sporozoite numbers indicate that the infectivity of IMC1hΔ2 sporozoites to the mosquito is higher than that of IMC1hΔ1 sporozoites (**Table 1**), despite both mutant sporozoite populations possessing similar motility defects. These observations suggest that motility makes a relatively minor contribution to the sporozoites' invasive power. This is consistent with findings that IMC1h null mutant sporozoites have similar *in vitro* hepatoma cell transmigration and infection rates to their wildtype counterparts, despite having significantly reduced speed (∼ 2-fold) and more meandering movement patterns (Volkmann et al., 2012). Heat shock protein 20 null mutant sporozoites, which can move only very slowly, are also able to invade hepatocytes at the same efficiency as wild-type sporozoites, indicating that at least rapid gliding is not essential for efficient invasion (Montagna et al., 2012). The invasive power of IMC1hΔ2 sporozoites with regards to salivary glands was however not reflected in a greater infectivity to the mouse, as we were repeatedly unable to transmit these parasites by the normal route of mosquito bite. IMC1h null mutants are not naturally transmissible, but are infective to

mice when injected intravenously (Volkmann et al., 2012). These collective observations thus identify traversal of the dermis as a major bottleneck for sporozoite infection of the mammalian host.

DATA AVAILABILITY

All datasets generated for this study are included in the manuscript and/or the **Supplementary Files**.

ETHICS STATEMENT

This study was carried out in accordance with the Laboratory Animal Science Association guidelines. All laboratory animal work was approved by the Animal Welfare and Ethical Review Board of the London School of Hygiene and Tropical Medicine, and by the United Kingdom Home Office. Work was carried out in accordance with the United Kingdom Animals (Scientific Procedures) Act 1986 implementing European Directive 2010/63 for the protection of animals used for experimental purposes.

AUTHOR CONTRIBUTIONS

JD and CV contributed conception and design of the study. MC, AT, SS, and JD performed experiments and interpreted results. MC wrote the first draft of the manuscript. All authors contributed to manuscript revision, read, and approved the submitted version.

FUNDING

This research was jointly funded by the UK Medical Research Council (MRC) and the UK Department for International Development (DFID) under the MRC/DFID Concordat agreement (reference MR/P021611), and by grants from the Wellcome Trust (reference 088449) and the UK Biotechnology and Biological Sciences Research Council (reference BB/M001598). MC was sponsored by the London Interdisciplinary Doctoral Programme funded by the UK Biotechnology and Biological Sciences Research Council (reference BB/M009513/1).

SUPPLEMENTARY MATERIAL

The Supplementary Material for this article can be found online at: https://www.frontiersin.org/articles/10.3389/fcimb.2019.00266/full#supplementary-material

Video S1 | Time lapse movie of a representative IMC1h/GFP ookinete in Matrigel.

Video S2 | Time lapse movie of a representative IMC1hΔ1 ookinete in Matrigel.

Video S3 | Time lapse movie of a representative IMC1hΔ2 ookinete in Matrigel.

REFERENCES

Al-Khattaf, F. S., Tremp, A. Z., and Dessens, J. T. (2015). *Plasmodium alveolins* possess distinct but structurally and functionally related multi-repeat domains. *Parasitol. Res.* 115, 631–639. doi: 10.1007/s00436-014-4226-9

Al-Khattaf, F. S., Tremp, A. Z., El-Houderi, A., and Dessens, J. T. (2017). The *Plasmodium alveolin* IMC1a is stabilised by its terminal cysteine motifs and facilitates sporozoite morphogenesis and infectivity in a dose-dependent manner. *Mol. Biochem. Parasitol.* 211, 48–56. doi: 10.1016/j.molbiopara.2016.09.004

Anderson-White, B. R., Ivey, F. D., Cheng, K., Szatanek, T., Lorestani, A., Beckers, C. J., et al. (2011). A family of intermediate filament-like proteins is sequentially assembled into the cytoskeleton of *Toxoplasma gondii*. *Cell Microbiol.* 13, 18–31. doi: 10.1111/j.1462-5822.2010.01514.x

Bannister, L. H., Hopkins, J. M., Fowler, R. E., Krishna, S., and Mitchell, G. H. (2000). A brief illustrated guide to the ultrastructure of *Plasmodium falciparum* asexual blood stages. *Parasitol. Today* 16, 427–433. doi: 10.1016/S0169-4758(00)01755-5

Barkhuff, W. D., Gilk, S. D., Whitmarsh, R., Tilley, L. D., Hunter, C., and Ward, G. E. (2011). Targeted disruption of TgPhIL1 in *Toxoplasma gondii* results in altered parasite morphology and fitness. *PLoS ONE* 6:e23977. doi: 10.1371/journal.pone.0023977

Dessens, J. T., Beetsma, A. L., Dimopoulos, G., Wengelnik, K., Crisanti, A., Kafatos, F. C., et al. (1999). CTRP is essential for mosquito infection by malaria ookinetes. *EMBO J.* 18, 6221–6227. doi: 10.1093/emboj/18.22.6221

Frenal, K., Polonais, V., Marq, J. B., Stratmann, R., Limenitakis, J., and Soldati-Favre, D. (2010). Functional dissection of the apicomplexan glideosome molecular architecture. *Cell Host Microbe* 8, 343–357. doi: 10.1016/j.chom.2010.09.002

Goodenough, U., Roth, R., Kariyawasam, T., He, A., and Lee, J. H. (2018). Epiplasts: membrane skeletons and epiplastin proteins in euglenids, glaucophytes, cryptophytes, ciliates, dinoflagellates, and apicomplexans. *mBio* 9:18. doi: 10.1128/mBio.02020-18

Gould, S. B., Tham, W. H., Cowman, A. F., Mcfadden, G. I., and Waller, R. F. (2008). Alveolins, a new family of cortical proteins that define the protist infrakingdom Alveolata. *Mol. Biol. Evol.* 25, 1219–1230. doi: 10.1093/molbev/msn070

Han, Y. S., Thompson, J., Kafatos, F. C., and Barillas-Mury, C. (2000). Molecular interactions between *Anopheles stephensi* midgut cells and *Plasmodium berghei*: the time bomb theory of ookinete invasion of mosquitoes. *EMBO J.* 19, 6030–6040. doi: 10.1093/emboj/19.22.6030

Hu, K., Mann, T., Striepen, B., Beckers, C. J., Roos, D. S., and Murray, J. M. (2002). Daughter cell assembly in the protozoan parasite *Toxoplasma gondii*. *Mol. Biol. Cell* 13, 593–606. doi: 10.1091/mbc.01-06-0309

Kan, A., Tan, Y. H., Angrisano, F., Hanssen, E., Rogers, K. L., Whitehead, L., et al. (2014). Quantitative analysis of *Plasmodium* ookinete motion in three dimensions suggests a critical role for cell shape in the biomechanics of malaria parasite gliding motility. *Cell Microbiol.* 16, 734–750. doi: 10.1111/cmi.12283

Kaneko, I., Iwanaga, S., Kato, T., Kobayashi, I., and Yuda, M. (2015). Genome-wide identification of the target genes of AP2-O, a *Plasmodium* AP2-family transcription factor. *PLoS Pathog.* 11:e1004905. doi: 10.1371/journal.ppat.1004905

Khater, E. I., Sinden, R. E., and Dessens, J. T. (2004). A malaria membrane skeletal protein is essential for normal morphogenesis, motility, and infectivity of sporozoites. *J. Cell Biol.* 167, 425–432. doi: 10.1083/jcb.200406068

Kono, M., Prusty, D., Parkinson, J., and Gilberger, T. W. (2013). The apicomplexan inner membrane complex. *Front. Biosci.* 18, 982–992. doi: 10.2741/4157

Kudryashev, M., Munter, S., Lemgruber, L., Montagna, G., Stahlberg, H., Matuschewski, K., et al. (2012). Structural basis for chirality and directional motility of *Plasmodium sporozoites*. *Cell Microbiol.* 14, 1757–1768. doi: 10.1111/j.1462-5822.2012.01836.x

Mann, T., and Beckers, C. (2001). Characterization of the subpellicular network, a filamentous membrane skeletal component in the parasite *Toxoplasma gondii*. *Mol. Biochem. Parasitol.* 115, 257–268. doi: 10.1016/S0166-6851(01)00289-4

Menke, A., and Jockusch, H. (1991). Decreased osmotic stability of dystrophin-less muscle cells from the mdx mouse. *Nature* 349, 69–71. doi: 10.1038/349069a0

Montagna, G. N., Buscaglia, C. A., Munter, S., Goosmann, C., Frischknecht, F., Brinkmann, V., et al. (2012). Critical role for heat shock protein 20 (HSP20) in migration of malarial sporozoites. *J. Biol. Chem.* 287, 2410–2422. doi: 10.1074/jbc.M111.302109

Moon, R. W., Taylor, C. J., Bex, C., Schepers, R., Goulding, D., Janse, C. J., et al. (2009). A cyclic GMP signalling module that regulates gliding motility in a malaria parasite. *PLoS Pathog.* 5:e1000599. doi: 10.1371/journal.ppat.1000599

Morrissette, N. S., and Sibley, L. D. (2002). Cytoskeleton of apicomplexan parasites. *Microbiol. Mol. Biol. Rev.* 66, 21–38. doi: 10.1128/MMBR.66.1.21-38.2002

Parkyn Schneider, M., Liu, B., Glock, P., Suttie, A., Mchugh, E., Andrew, D., et al. (2017). Disrupting assembly of the inner membrane complex blocks *Plasmodium falciparum* sexual stage development. *PLoS Pathog.* 13:e1006659. doi: 10.1371/journal.ppat.1006659

Santos, J. M., Lebrun, M., Daher, W., Soldati, D., and Dubremetz, J. F. (2009). Apicomplexan cytoskeleton and motors: key regulators in morphogenesis, cell division, transport and motility. *Int. J. Parasitol.* 39, 153–162. doi: 10.1016/j.ijpara.2008.10.007

Tremp, A. Z., Al-Khattaf, F. S., and Dessens, J. T. (2014). Distinct temporal recruitment of *Plasmodium alveolins* to the subpellicular network. *Parasitol. Res.* 113, 4177–4188. doi: 10.1007/s00436-014-4093-4

Tremp, A. Z., Al-Khattaf, F. S., and Dessens, J. T. (2017). Palmitoylation of *Plasmodium alveolins* promotes cytoskeletal function. *Mol. Biochem. Parasitol.* 213, 16–21. doi: 10.1016/j.molbiopara.2017.02.003

Tremp, A. Z., Carter, V., Saeed, S., and Dessens, J. T. (2013). Morphogenesis of *Plasmodium zoites* is uncoupled from tensile strength. *Mol. Microbiol.* 89, 552–564. doi: 10.1111/mmi.12297

Tremp, A. Z., and Dessens, J. T. (2011). Malaria IMC1 membrane skeleton proteins operate autonomously and participate in motility independently of cell shape. *J. Biol. Chem.* 286, 5383–5391. doi: 10.1074/jbc.M110.187195

Tremp, A. Z., Khater, E. I., and Dessens, J. T. (2008). IMC1b is a putative membrane skeleton protein involved in cell shape, mechanical strength, motility, and infectivity of malaria ookinetes. *J. Biol. Chem.* 283, 27604–27611. doi: 10.1074/jbc.M801302200

Vernick, K. D., Fujioka, H., and Aikawa, M. (1999). *Plasmodium gallinaceum*: a novel morphology of malaria ookinetes in the midgut of the mosquito vector. *Exp. Parasitol.* 91, 362–366. doi: 10.1006/expr.1998.4388

Volkmann, K., Pfander, C., Burstroem, C., Ahras, M., Goulding, D., Rayner, J. C., et al. (2012). The alveolin IMC1h is required for normal ookinete and sporozoite motility behaviour and host colonisation in *Plasmodium berghei*. *PLoS ONE* 7:e41409. doi: 10.1371/journal.pone.0041409

Waters, A. P., Thomas, A. W., Van Dijk, M. R., and Janse, C. J. (1997). Transfection of malaria parasites. *Methods* 13, 134–147. doi: 10.1006/meth.1997.0506

Conflict of Interest Statement: The authors declare that the research was conducted in the absence of any commercial or financial relationships that could be construed as a potential conflict of interest.

frontiers in Cellular and Infection Microbiology

ORIGINAL RESEARCH
published: 10 September 2019
doi: 10.3389/fcimb.2019.00316

Expression and Localization Profiles of Rhoptry Proteins in *Plasmodium berghei* Sporozoites

Naohito Tokunaga[1†‡], *Mamoru Nozaki*[1†‡], *Mayumi Tachibana*[1], *Minami Baba*[1], *Kazuhiro Matsuoka*[1‡], *Takafumi Tsuboi*[2], *Motomi Torii*[1] *and Tomoko Ishino*[1*]

[1] *Division of Molecular Parasitology, Proteo-Science Center, Ehime University, Toon, Japan,* [2] *Division of Malaria Research, Proteo-Science Center, Ehime University, Matsuyama, Japan*

OPEN ACCESS

Edited by:
Rhoel Dinglasan, University of Florida, United States

Reviewed by:
Scott E. Lindner, Pennsylvania State University, United States
Friedrich Frischknecht, Heidelberg University, Germany

***Correspondence:**
Tomoko Ishino
tishino@m.ehime-u.ac.jp

[†] *These authors have contributed equally to this work*

[‡] ***Present address:***
Naohito Tokunaga, Division of Analytical Bio-Medicine, The Advanced Research Support Center (ADRES), Ehime University, Matsuyama, Japan
Mamoru Nozaki, Plant and Cell Engineering Laboratory, Graduate School of Engineering, Toyama Prefectural University, Imizu, Japan
Kazuhiro Matsuoka, Department of Infectious Diseases and Immunology, Clinical Research Center, National Hospital Organization Nagoya Medical Center, Nagoya, Japan

Specialty section:
This article was submitted to Parasite and Host, a section of the journal Frontiers in Cellular and Infection Microbiology

Received: *25 June 2019*
Accepted: *22 August 2019*
Published: *10 September 2019*

In the *Plasmodium* lifecycle two infectious stages of parasites, merozoites, and sporozoites, efficiently infect mammalian host cells, erythrocytes, and hepatocytes, respectively. The apical structure of merozoites and sporozoites contains rhoptry and microneme secretory organelles, which are conserved with other infective forms of apicomplexan parasites. During merozoite invasion of erythrocytes, some rhoptry proteins are secreted to form a tight junction between the parasite and target cell, while others are discharged to maintain subsequent infection inside the parasitophorous vacuole. It has been questioned whether the invasion mechanisms mediated by rhoptry proteins are also involved in sporozoite invasion of two distinct target cells, mosquito salivary glands and mammalian hepatocytes. Recently we demonstrated that rhoptry neck protein 2 (RON2), which is crucial for tight junction formation in merozoites, is also important for sporozoite invasion of both target cells. With the aim of comprehensively describing the mechanisms of sporozoite invasion, the expression and localization profiles of rhoptry proteins were investigated in *Plasmodium berghei* sporozoites. Of 12 genes representing merozoite rhoptry molecules, nine are transcribed in oocyst-derived sporozoites at a similar or higher level compared to those in blood-stage schizonts. Immuno-electron microscopy demonstrates that eight proteins, namely RON2, RON4, RON5, ASP/RON1, RALP1, RON3, RAP1, and RAMA, localize to rhoptries in sporozoites. It is noteworthy that most rhoptry neck proteins in merozoites are localized throughout rhoptries in sporozoites. This study demonstrates that most rhoptry proteins, except components of the high-molecular mass rhoptry protein complex, are commonly expressed in merozoites and sporozoites in *Plasmodium* spp., which suggests that components of the invasion mechanisms are basically conserved between infective forms independently of their target cells. Combined with sporozoite-stage specific gene silencing strategies, the contribution of rhoptry proteins in invasion mechanisms can be described.

Keywords: malaria, *Plasmodium*, merozoite, sporozoite, rhoptry, immuno-electron microscopy

INTRODUCTION

During the malaria lifecycle, three invasive forms, ookinetes, sporozoites, and merozoites, invade different types of cells in mosquito vectors and mammalian hosts. Among them, sporozoites, which transmit malaria disease from mosquitoes to mammalian hosts, firstly invade mosquito salivary glands prior to be injected into the mammalian skin during a blood meal. Sporozoites actively migrate through the skin to enter blood vessels and finally infect hepatocytes, where they develop into several thousand merozoites within a parasitophorous vacuole membrane (PVM). Merozoites invade erythrocytes by similarly forming a PVM, while ookinetes, the invasive form which develops in the midgut lumen after fertilization, simply traverse midgut epithelial cells without PVM formation.

The apical structures of invasive stage parasites in the phylum Apicomplexa are well-conserved as having microneme and rhoptry secretory organelles, which store proteins discharged prior to or post-invasion. Micronemes in the highly motile sporozoite and ookinete stages contain proteins involved in motility and cell traversal (Sultan et al., 1997; Yuda and Ishino, 2004; Kariu et al., 2006). In the case of the non-motile merozoite stage parasites micronemal proteins, such as merozoite surface proteins (MSPs), are involved in attachment to erythrocytes (Kadekoppala and Holder, 2010). Rhoptries are present only in infective stage parasites, such as *Plasmodium* merozoites and sporozoites which proliferate inside the PVM, and are absent in ookinetes, raising the possibility that rhoptry secretory proteins are involved in cell infection (reviewed in Baum et al., 2008; Frenal et al., 2017).

Rhoptry protein profiling has been conducted and characterized mainly in the related apicomplexans *Toxoplasma* tachyzoites and *Plasmodium* merozoites, and are classified into two protein groups based on their localization in rhoptry neck or rhoptry bulb (Bradley et al., 2005; Counihan et al., 2013). Rhoptry neck protein 2 (RON2), RON4, and RON5 are discharged as a complex prior to invasion and inserted into the target cellular membrane. The complex then interacts with apical merozoite protein 1 (AMA1) on the parasite plasma membrane to form a tight junction between the parasite and its target cell, a step which is essential for *Plasmodium* merozoite and *Toxoplasma* tachyzoite invasion of target cells (Alexander et al., 2005; Lebrun et al., 2005; Besteiro et al., 2009; Cao et al., 2009). Rhoptry bulb proteins are discharged subsequent to rhoptry neck proteins, to develop inside the parasitophorous vacuole. Many rhoptry bulb proteins are species specific, in contrast to rhoptry neck proteins which are largely conserved between *Plasmodium* and *Toxoplasma*, such as components for the RON complex which is crucial for invasion by both parasites (Boothroyd and Dubremetz, 2008; Zuccala et al., 2012; Counihan et al., 2013; Kemp et al., 2013).

It has been studied whether tight junction formation mechanisms are critical for *Plasmodium* sporozoite invasion of mosquito salivary gland and mammalian hepatocyte target cells. This hypothesis is supported by the finding that the components of the RON complex, RON2, RON4, and RON5, are also expressed in sporozoites (Tufet-Bayona et al., 2009; Mutungi et al., 2014; Risco-Castillo et al., 2014). Moreover, a peptide inhibiting the interaction between AMA1 and RON2 reduced the *P. falciparum* sporozoite infection ability of cultured hepatocytes (Yang et al., 2017), and a conditional knockdown of RON2 or RON4 resulted in a reduction in sporozoite invasion ability (Giovannini et al., 2011; Ishino et al., 2019).

A comprehensive analysis of rhoptry proteins during sporozoite invasion using the sporozoite-stage specific knockdown system first requires the detailed profiling of rhoptry proteins in sporozoites. To date, about thirty rhoptry proteins have been classified in *P. falciparum* (reviewed in Counihan et al., 2013). In the present study, 12 proteins were selected as merozoite rhoptry proteins commonly expressed among *Plasmodium* spp.—i.e., expressed in both human and rodent malaria parasites—to examine their expression and localization in sporozoites. To achieve this goal, transgenic parasites were generated in *P. berghei* expressing target rhoptry proteins tagged with c-Myc tag at their C-terminus. Immuno-electron microscopy revealed that eight out of 12 candidate proteins are also localized to sporozoite rhoptries.

MATERIALS AND METHODS

Parasites and Mosquitoes

A transgenic *Plasmodium berghei* ANKA parasite line was used in this study which constitutively expresses GFP under the control of the *elongation factor 1A* (*ef1α*) promoter without any drug resistance gene (Franke-Fayard et al., 2004), kindly given by Dr. Janse. Cryopreserved *P. berghei* ANKA infected erythrocytes were intraperitoneally injected into female ICR mice (4–6 weeks old, CLEA Japan, Tokyo, Japan) to obtain asexual stage parasites. To harvest mature schizonts, infected mouse erythrocytes with 0.5–1% parasitemia were cultured for 16 h and purified using Nycoprep 1.077 solution (Axis-Shield Diagnostics, Dundee, UK; Janse et al., 2006b). *Anopheles stephensi* SDA strain (*An. stephensi*) mosquitoes were maintained on a 5% sucrose solution during adult stages at 25°C. After feeding on *P. berghei* infected ICR mice, fully engorged mosquitoes were selected and kept at 20°C until dissection under a 12 h-light/12 h-dark cycle. All animal experimental protocols were approved by the Institutional Animal Care and Use Committee of Ehime University and the experiments were conducted according to the Ethical Guidelines for Animal Experiments of Ehime University.

Abbreviations: AMA1, apical merozoite protein 1; *An*, *Anopheles*; ASP, apical sushi protein; ef1α, elongation factor 1A; GPI, glycosylphosphatidylinositol; IFA, immunofluorescent assay; IEM, immuno-electron microscopy; *Pb*, *P. berghei*; RAMA, rhoptry associated membrane antigen; PBS-MT, PBS containing 5% non-fat dry milk and 0.01% Tween 20; PBS-BT, PBS containing 0.4% Block Ace and 0.01% Tween 20; PVM, parasitophorous vacuole membrane; RALP1, rhoptry-associated leucine zipper-like protein 1; RAP1, rhoptry-associated protein 1; RhopH, high-molecular mass rhoptry protein; RON2, rhoptry neck protein; RT-PCR, reverse transcription-PCR; SPECT2, sporozoite protein essential for cell traversal 2.

Real Time Reverse Transcription (RT)-PCR Analysis

Purified schizonts and infected-mosquito tissues (midguts and salivary glands) were collected in RNAlater (Thermo Fisher Scientific, San Jose, CA, USA) and stored at 4°C until RNA isolation. Total RNA was extracted using an RNeasy kit (Qiagen, GmbH, Hilden, Germany) and treated with DNaseI (Qiagen). Reverse transcription was conducted using a PrimeScript RT reagent Kit (Takara Bio, Otsu, Japan) with gDNA Eraser. Real-time RT-PCR reactions were performed using SYBR Premix Ex Taq (Takara Bio). The primer sequences used are listed in **Supplementary Table S1**. Real time PCR was performed using a TaKaRa PCR Thermal Cycler Dice (Takara Bio). Relative gene expressions were normalized by *ef1α* (PBANKA_1133300) mRNA levels and were compared using the delta, delta-Ct method (Pfaffl, 2001; Ishino et al., 2019).

Generation of c-Myc-Tagged Rhoptry Protein Expressing Transgenic Parasites

To generate transgenic parasites expressing a rhoptry protein tagged with c-Myc at its C-terminus, the native locus of the targeted rhoptry molecule in the WT-GFP genome was replaced by single crossover homologous recombination with an expression cassette of the C-terminus of the rhoptry protein fused with a c-Myc tag, similar to the generation of RON2-c-Myc expressing parasites (Ishino et al., 2019). Schematic representation of the transgenic vector construction is shown in **Supplementary Figure S1**. Approximately 1,000–2,000 base pair of DNA fragments including the C-terminus of each rhoptry protein were amplified with specific primers (sequences of primers used in this study were listed in **Supplementary Table S1**) by PCR from genomic DNA of WT-GFP. Amplified PCR fragments of RAP1, RhopH1A, RhopH2, and RhopH3 were inserted into the pL0033 plasmid (BEI Resources, Manassas, VA, USA) at SacII and NcoI sites just before the c-Myc tag coding region, and these plasmids were then linearized at endogenous HpaI, SpeI, and XbaI sites, respectively (see **Supplementary Figure S1A**). RON5 and RALP1 fragments were inserted into an NdeI site disrupted pL0033 vector, which was linearized at an endogenous NdeI site (see **Supplementary Figure S1B**). To introduce XbaI recognition sites for linearization into the PCR fragments of RON3 and RON4, site directed mutagenesis was performed to introduce mutations without amino acid substitution as follows: RON3, 5716A > T and 5717G > C; and RON4, 1711T > C. Using the same strategy, the endogenous NcoI site in the amplified RON6 fragment was disrupted, to avoid interference with ligation into the SacII and NcoI sites of pL0033 (1878C > A). These DNA fragments were inserted into the pL0033 plasmid at SacII and NcoI sites, which were linearized at an introduced XbaI site for RON3 and RON4, and at an endogenous BamHI site for RON6 (see **Supplementary Figure S1C**). Electroporation of 10–15 μg linearized DNA into schizont-enriched WT-GFP and selection of transgenic parasites were performed as described (Janse et al., 2006a). DNA integration occurs at the target locus in the WT-GFP genome by single crossover homologous recombination as illustrated in **Supplementary Figure S2**. DNA integration into the target locus was confirmed by PCR genotyping and transgenic parasites were cloned by limiting dilution.

Antibody Production

DNA fragments encoding amino acids 25–694 of ASP/RON1 and 899–1,072 of RON3 were amplified from *P. berghei* schizont cDNA by PCR and inserted into pEU-E01-GST-(TEV)-N1 (CellFree Sciences, Matsuyama, Japan) at EcoRV and BamHI sites to produce recombinant ASP/RON1 proteins and at XhoI and BamHI sites to produce recombinant RON3 with GST tag at their N-terminus. The GST-tagged recombinant proteins were produced using the wheat germ cell-free protein expression system (CellFree Sciences) and purified using a glutathione-Sepharose 4B column (GE Healthcare UK, Buckinghamshire, UK; Tsuboi et al., 2008). Purified GST-tagged recombinant proteins were used for immunization of Japanese white rabbits with Freund's adjuvant. Immunizations were done three times at 3-week intervals with 250 μg recombinant protein and the antisera were collected 14 days after the last immunization (Kitayama Labes, Ina, Japan). Anti-RON2 antibodies and anti-RAMA antibodies used in the study were prepared previously (Ishino et al., 2019).

Western Blotting Analysis

Purified schizonts were treated with 0.08% saponin for 15 min on ice and the schizont pellets were resuspended in sample buffer solution for SDS-PAGE (nacalai tesque, Kyoto, Japan) containing 5% 2-mercaptoethanol. Sporozoites collected from midguts of infected mosquitoes at days 24–26 post-feeding were purified by density gradient centrifugation using 17% Accudenz solution (Accurate Chemical & Scientific Corporation, NY, United States; Kennedy et al., 2012). Sporozoite pellets were resuspended in sample buffer containing 5% 2-mercaptoethanol. Proteins were separated by SDS-PAGE using 5–20% gradient acrylamide gels (ATTO, Tokyo, Japan) and electroblotted onto polyvinylidene difluoride (PVDF) membranes. The PVDF membranes were blocked with Blocking One (nacalai tesque) overnight at 4°C and then incubated with primary antibodies (1:100 anti-c-Myc rabbit antibodies (A-14), Santa Cruz Biotechnology, Santa Cruz, CA, USA; 1:2,500, anti-ASP/RON1, RON3, or RAMA rabbit antibodies) diluted in PBS containing 0.01% Tween-20 (PBST) for 2 h at room temperature. After washing with PBST, the membranes were incubated with secondary antibodies conjugated to horseradish peroxidase (HRP; 1:30,000, Biosource, Camarillo, CA, USA) for 30 min at room temperature. Chemiluminescence detection was performed by adding Immobilon Western Chemiluminescent HRP Substrate (Merck Millipore, Darmstadt, Germany), and the signal was detected using ImageQuant LAS 4000 (GE Healthcare UK).

Indirect Immunofluorescence Assay

Thin smears of purified schizonts were prepared on glass slides and fixed with cold acetone for 3 min. Sporozoites collected from midgut and salivary gland at day 24–26 post-feeding were seeded on 8-well multi-well slides, then air-dried and

fixed with cold acetone for 3 min. The slides of schizonts and sporozoites were blocked with PBS containing 10% fetal calf serum at 37°C for 30 min and incubated with primary antibodies (1:50 for anti-c-Myc mouse monoclonal antibodies (9E10), 1:100 for anti-c-Myc rabbit antibodies (A-14), and 1:200 for anti RON2, ASP/RON1, and RAMA rabbit polyclonal antibodies) in blocking solution at 37°C for 2 h, followed by Alexa Fluor 488–conjugated goat anti-rabbit IgG and Alexa Fluor 568-conjugated goat anti-mouse IgG (Thermo Fisher Scientific) at 37°C for 30 min. Nuclei were stained with 1 mg/ml of 4′,6-diamidino-2-phenylindole (DAPI). The samples were mounted in ProLong Gold antifade reagent (Thermo Fisher Scientific) and observed with an inverted fluorescence microscope (Axio Observer Z1, Carl Zeiss, Oberkochen, Germany).

Immuno-Transmission Electron Microscopy

Cultivated schizonts of WT-GFP or transgenic parasites expressing c-Myc tagged rhoptry proteins were purified by density gradient centrifugation. Infected midguts (day 17 or 21 post-feeding) or salivary glands (day 24 or 26 post-feeding) were dissected. The samples were fixed in 1% paraformaldehyde, 0.2% glutaraldehyde and embedded in LR-White resin (Polyscience, PA, USA). Ultrathin sections were blocked in PBS containing 5% non-fat dry milk and 0.01% Tween 20 (PBS-MT), then incubated at 4°C overnight with anti-c-Myc antibody (Santa Cruz biotechnology) or specific antibodies against ASP/RON1 (1:25), RAMA (1:100), or RON3 (1:200). The sections were washed with PBS containing 0.4% Block Ace (Yukijirushi, Tokyo, Japan) and 0.01% Tween 20 (PBS-BT), and the grids were incubated for 1 h at 37°C with goat anti-rabbit IgG conjugated with 15 nm gold particles (GE Healthcare) diluted 1:20 in PBS-MT, rinsed with PBS-BT, and fixed in 2% glutaraldehyde for 10 min at 4°C to stabilize the gold particles. The sections were then stained with 2% uranyl acetate in 50% methanol and lead citrate. Samples were examined using a transmission electron microscope (JEM-1230; JEOL, Tokyo, Japan).

Gene IDs

The sequence information of genes in this article can be found in the PlasmoDB database (PlasmoDB.org) under the following gene ID numbers: *ron2,* PBANKA_1315700; *ron4,* PBANKA_0932000; *ron5,* PBANKA_0713100; *ron6*, PBANKA_0311700; *ralp1*, PBANKA_0619700; *asp/ron1,* PBANKA_1003600; *rap1*, PBANKA_1032100; *ron3*, PBANKA_1464900; *rama*, PBANKA_0804500; *rhoph1a*, PBANKA_1400600; *rhoph2*, PBANKA_0830200; and *rhoph3*, PBANKA_0416000.

RESULTS

Selection of *Plasmodium* Rhoptry Proteins

In this study a rodent malaria parasite line, *P. berghei* ANKA strain expressing GFP under the control of *ef1α* promoter (WT-GFP; Janse et al., 2006a), was used to characterize rhoptry proteins in both merozoites and sporozoites. From the catalog of known *P. falciparum* rhoptry proteins (Counihan et al., 2013), 12 molecules whose orthologous genes exist in *P. berghei* were selected to compare their expression between merozoites and sporozoites. RON2, a sporozoite rhoptry protein demonstrated as transcribed predominantly in oocyst-derived sporozoites (Ishino et al., 2019), was included as a positive control. Among 12 selected proteins, six are conserved across the Apicomplexa phylum and another six are specific to *Plasmodium* spp. Gene IDs in *P. berghei* together with those of the orthologous genes in *P. falciparum* and in *Toxoplasma gondii* are listed in **Table 1** (Aurrecoechea et al., 2009).

Expression Profiling of Rhoptry Molecules in Schizonts and Developing Sporozoites

Firstly, the mRNA expression levels of the selected genes during sporozoite development in mosquito bodies were compared by real-time RT-PCR analysis with transcript levels in schizonts. Sporozoites, formed within oocysts on midguts of mosquitoes, are released into hemolymph and then invade salivary glands prior to being inoculated into mammalian skin with saliva. Since *P. berghei* sporozoite formation inside oocysts starts at days 10–14 post-feeding (Thathy et al., 2002; Ferguson et al., 2014), parasite-infected midguts were collected at days 9, 13, and 17 post-feeding. In addition, salivary glands of infected mosquitoes were collected at day 17 post-feeding. As a control, schizont-rich infected erythrocytes were purified and harvested. Relative mRNA amounts of selected genes were examined by real-time RT-PCR, normalized by *ef1α* mRNA expression.

Six molecules categorized as encoding rhoptry neck proteins in merozoites (*ron2*, *ron4*, *ron5*, *ron6*, *rhoptry-associated leucine zipper-like protein 1 (ralp1)*, and *apical sushi protein* (*asp*)/*ron1*) are also transcribed in sporozoites (**Figure 1A**). Among six genes encoding rhoptry proteins localized to the bulb region in merozoites, *rhoptry-associated protein 1* (*rap1)*, *ron3*, and *rhoptry associated membrane antigen* (*rama)* are also transcribed in sporozoites (**Figure 1B**); while the other three, encoding the components of the high-molecular mass rhoptry protein complex (RhopH complex; Kaneko et al., 2001, 2005; Ling et al., 2003, 2004; Vincensini et al., 2008; Comeaux et al., 2011; Nguitragool et al., 2011; Counihan et al., 2017; Ito et al., 2017; Sherling et al., 2017), are transcribed far less in sporozoites than in schizonts (**Figure 1C**). This data raises the possibility that RhopH1A, RhopH2, and RhopH3 may play roles predominantly in merozoites. In contrast, *ron5*, *ron6, asp*/*ron1,* and *ron3* are predominantly transcribed in sporozoites vs. schizonts. The transcripts of rhoptry molecules expressed in sporozoites increase during sporozoite maturation in oocysts. After sporozoite invasion of salivary glands, the transcript amounts of *ron2*, *ron4*, *rap1, ron3*, and *rama* are significantly decreased, while transcripts of *ron5*, *ron6*, *ralp1*, and *asp1*/*ron1* remain high or increase. In salivary gland sporozoites, *ron5* and *ron6* are the highest transcribed among rhoptry molecules; however, their amounts remain ∼200-fold less than that of a micronemal molecule, *sporozoite protein essential for cell traversal 2* (*spect2;* Ishino et al., 2005), whose transcription is strongly enhanced after sporozoites invade salivary glands (**Figure 1D**). These results demonstrate that most merozoite

TABLE 1 | The list of rhoptry proteins examined in this study.

	P. berghei		*P. falciparum*		*T. gondii*	References
	ID	Expression in sporozoite*	ID	Merozoite	ID	
RON2	PBANKA_1315700	Rhoptry	PF3D7_1452000	Neck	TGME49_300100	Cao et al., 2009; Ishino et al., 2019
RON4	PBANKA_0932000	Rhoptry	PF3D7_1116000	Neck	TGME49_229010	Richard et al., 2010
RON5	PBANKA_0713100	Rhoptry	PF3D7_0817700	Neck	TGME49_311470	Richard et al., 2010
RON6	PBANKA_0311700	Apical end	PF3D7_0214900	Neck	TGME49_297960	Proellocks et al., 2009
RALP1	PBANKA_0619700	Rhoptry	PF3D7_0722200	Neck	No ortholog	Haase et al., 2008; Ito et al., 2013
ASP/RON1	PBANKA_1003600	Rhoptry	PF3D7_0405900	Neck	TGME49_310010	Srivastava et al., 2010
RON3	PBANKA_1464900	Rhoptry	PF3D7_1252100	Bulb	TGME49_223920	Ito et al., 2011
RAP1	PBANKA_1032100	Rhoptry	PF3D7_1410400	Bulb	No ortholog	Riglar et al., 2011
RAMA	PBANKA_0804500	Rhoptry	PF3D7_0707300	Bulb	No ortholog	Topolska et al., 2004
RhopH1A	PBANKA_1400600	Not detected	3 paralogues	Bulb	No ortholog	Kaneko et al., 2001
RhopH2	PBANKA_0830200	Not detected	PF3D7_0929400	Bulb	No ortholog	Counihan et al., 2017
RhopH3	PBANKA_0416000	Not detected	PF3D7_0905400	Bulb	No ortholog	Sherling et al., 2017

**Localization in sporozoites determined by IEM (except for RON6 which was detected by IFA) in this study.*

rhoptry molecules, except for those encoding RhopH complex components, are expressed in both infective stages, merozoites and sporozoites.

Expression of Rhoptry Proteins in Sporozoites

To comprehensively examine protein expression patterns of rhoptry proteins in merozoites and sporozoites, transgenic parasite lines were generated by single-crossover homologous recombination to express each rhoptry protein fused with a C-terminal c-Myc tag (see Material and methods). Ten transgenic parasite lines were successfully isolated. Specific antibodies against recombinant protein were prepared for ASP/RON1 and RAMA, since they are predicted to have C-terminal glycosylphosphatidylinositol (GPI) anchored domains (Gilson et al., 2006) and therefore the modification of their C-terminal structure might disrupt their function (see **Supplementary Figure S3**). Specific antibodies against the middle region of RON3 were also prepared, because it was demonstrated that a 40 kDa fragment of C-terminal RON3 is cleaved during schizont maturation in *P. falciparum* (Ito et al., 2011).

Protein lysates of 1.5×10^5 schizonts and oocyst-derived sporozoites of each transgenic parasite line expressing c-Myc tagged rhoptry protein or WT-GFP were analyzed by western blotting using anti-c-Myc antibodies or specific antibodies against ASP/RON1, RAMA, and RON3. In schizonts all examined c-Myc tagged rhoptry proteins, except for RON3, were detected at the expected size of full-length (indicated by closed arrowheads, **Figures 2A,B**), demonstrating that c-Myc fused rhoptry proteins are successfully expressed. In addition, the processed forms of RON4 and RALP1 were detected at ∼60 and 40 kDa (indicated by open arrowheads). In the case of RON3, anti-c-Myc antibodies detected ∼40 kDa fragment as reported in *P. falciparum*, while anti-RON3 antibodies recognized two bands, near 250 kDa, corresponding to the full-length and processed RON3. It was confirmed that a roughly 40 kDa fragment of the C-terminal region in RON3 is cleaved in *P. berghei* mature schizonts as well as in *P. falciparum*. Antibodies against ASP/RON1 and RAMA recognized corresponding proteins at the size of expected full- and processed-proteins, confirming the specificity of these antibodies.

RhopH1A and RhopH3 proteins were not detected in sporozoites, while RhopH2 was detected as a far weaker band compared to that in schizonts, which is in good agreement with the transcriptional data (**Figure 2C**). In addition, RON2 production in sporozoites was significantly less than in schizonts. Proteolysis patterns are conserved between schizonts and sporozoites, although the ratio of uncleaved protein is less in oocyst-derived sporozoites than in schizonts. Since it takes longer for sporozoite maturation in oocysts than merozoites in schizonts, proteolysis of rhoptry proteins might be enhanced in sporozoites.

Protein Localization of Rhoptry Molecules in Merozoites and Sporozoites

Rhoptry proteins in *P. falciparum* merozoites and *T. gondii* tachyzoites are categorized according to their detailed localization in rhoptries; specifically, rhoptry neck proteins (RON2, RON4, RON5, RON6, ASP/RON1, and RALP1) and rhoptry bulb proteins (RON3, RAP1, RAMA, RhopH1A, RhopH2, and RhopH3) (Counihan et al., 2013; Kemp et al., 2013). All rhoptry proteins examined in this study were confirmed to localize to the apical end region of *P. berghei* merozoites, similar to the RON2 marker signal, by immunofluorescent assay (IFA) using anti-c-Myc or specific antibodies (**Figure 3**, left columns). By comparison to RON2 localization, RON4, RON5, RON6, ASP/RON1, and RALP1 were suggested to be localized to the rhoptry neck region. This indicates that the C-terminal c-Myc tagging does not interfere

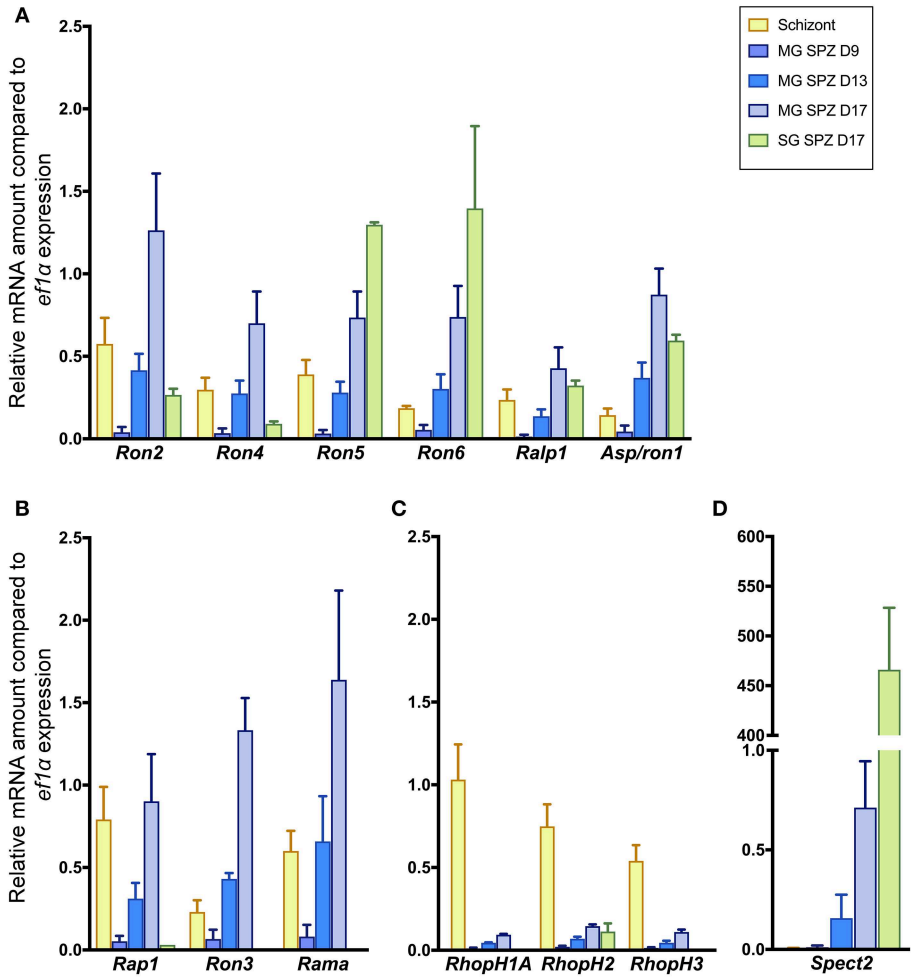

FIGURE 1 | Transcriptional analyses of rhoptry genes in sporozoites and schizonts. Total RNA was extracted from parasite-infected mosquito midguts at days 9, 13, and 17 post-feeding (MG SPZ D9, MG SPZ D13, and MG SPZ D17); and salivary glands at day 17 post-feeding (SG SPZ D17). Total RNA was also extracted from schizont-enriched infected erythrocytes (Schizont). The mean values of relative mRNA amounts of each molecule, normalized by *ef1α* mRNA expression, are plotted as bar graphs with standard deviations from three independent experiments. **(A)** A group of molecules categorized as rhoptry neck proteins in merozoites. All examined molecules are transcribed in both merozoites and sporozoites. **(B)** A group of molecules categorized as rhoptry bulb proteins in merozoites whose transcriptions are detected in both merozoites and sporozoites. **(C)** A group of molecules categorized as rhoptry bulb proteins in merozoites whose transcriptions occur dominantly in merozoites. **(D)** Transcription profile of a typical micronemal protein, SPECT2, required for sporozoite migration toward hepatocytes after inoculation in the skin. Its transcript level drastically increases after sporozoite invasion of salivary glands.

with proper rhoptry protein localization. Additionally, their localization was examined in sporozoites collected from midguts and salivary glands (**Figure 3**, right columns). Specific signals corresponding to RhopH1A and RhopH3 were barely detected in sporozoites by IFA, confirming the western blotting data. The signal for RhopH2 was detected as a diffuse pattern in the cytoplasm of sporozoites. Taking into consideration the western blotting result, a small amount of RhopH2 is also expressed in sporozoites; however, it is not localized to rhoptries. Other examined proteins were detected at the apical end of sporozoites from both midguts and salivary glands, demonstrating that these proteins were transported to the apical region during sporozoite formation in oocysts and maintained even after sporozoite invasion of salivary glands.

Eight Proteins Are Localized to Rhoptries in Sporozoites

To determine the precise localization of rhoptry proteins, immuno-electron microscopy (IEM) was performed using schizont stage merozoites and oocyst sporozoites. In *P. berghei* merozoites, RON2, RON4, RON5, RALP1, and ASP/RON1, which are categorized as rhoptry neck proteins in *Pf* merozoites, were confirmed to localize to the rhoptry neck region (**Figure 4A**). In addition, RAP1, RON3, RhopH1A, RhopH2, and RhopH3 are observed in the rhoptry bulb region, as reported for *Pf* merozoites (**Figure 4B**). RAMA is observed on the rhoptry membrane at the bulb region. RON6 could not be detected by anti-c-Myc antibodies, possibly because its protein amount in merozoites is not sufficient to be observed by IEM. This is the first

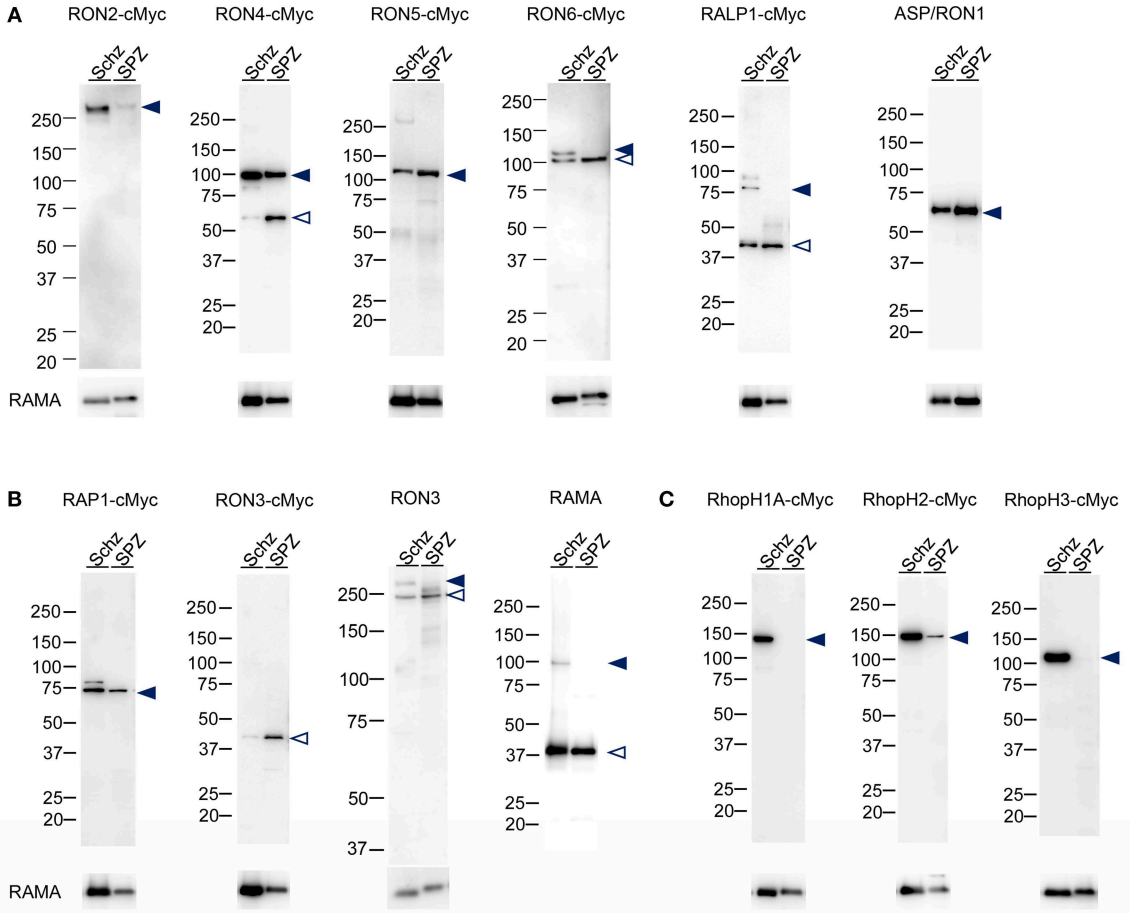

FIGURE 2 | Western blot analyses of rhoptry proteins in schizonts and sporozoites. Proteins were extracted from schizonts purified after *in vitro* culture of parasite infected erythrocytes (Schz) or sporozoites purified from midguts at days 24–26 post-feeding (SPZ). Each lane contains proteins from 1.5×10^5 schizonts or sporozoites of transgenic parasites expressing c-Myc tagged rhoptry proteins or WT-GFP. Target proteins were detected by western blotting using anti c-Myc antibodies or specific antibodies against ASP/RON1, RON3, or RAMA. The transgenic parasite lines used as antigens are indicated above panels; for example, RON2-cMyc. When specific antibodies were used to detect target molecules in WT-GFP parasites, the name of the target molecule is instead indicated. Closed- and open- arrowheads demonstrate the expected full-length and cleaved target proteins, respectively. The sizes of protein markers (kDa) are indicated on the left of each image. **(A)** Expression patterns of proteins categorized as rhoptry neck proteins in merozoites. ASP/RON1 was detected using rabbit specific antibodies as it contains a C-terminal GPI-anchor domain and is likely refractory to C-terminal c-Myc integration. **(B)** Expression patterns of proteins which are categorized as rhoptry bulb proteins in merozoites and transcribed in both merozoites and sporozoites. In the case of RON3, anti-c-Myc antibodies only recognized a roughly 40 kDa protein (RON3-cMyc), demonstrating that the C-terminal region was cleaved in both merozoites and sporozoites. Specific anti-RON3 antibodies detected full-length and cleaved forms of RON3 (RON3). **(C)** Expression patterns of proteins which are categorized as rhoptry bulb proteins in merozoites and predominantly transcribed in schizonts. Consistent with transcription analyses, the protein amounts of RhopH1A, RhopH2, and RhopH3 are far less in sporozoites than those in merozoites, indicated by closed arrowheads.

comprehensive demonstration of rhoptry protein localization in *Plasmodium* merozoites.

In sporozoites formed inside oocysts, it was confirmed that three components for the RhopH complex do not accumulate in rhoptries, as expected from the observation of far less amounts of transcripts and proteins in sporozoites compared to merozoites (**Figure 4C**). Other than the RhopH complex, all proteins examined are localized to rhoptries in sporozoites as well as in merozoites. However, most proteins are distributed throughout rhoptries in sporozoites, despite their sub-localization in merozoites, suggesting that sub-compartmentation in rhoptries might be different between merozoites and sporozoites. This is consistent with the observation that the sub-localization of RON11 in rhoptries differs between merozoites and sporozoites (**Figure 4A**, Bantuchai et al., 2019). Only ASP/RON1 tends to accumulate in the thinner part in rhoptries near the tip of sporozoites. It is not clear whether RAMA localizes to the rhoptry membrane in sporozoites as in merozoites, as the maximum width of rhoptries is shorter in sporozoites than in merozoites. Matured sporozoites are released into the haemocoel followed by invasion of salivary glands. It was reported that, although morphologically similar, sporozoites in salivary glands show higher infectivity to the liver than sporozoites developed inside oocysts (Vanderberg, 1975); and accordingly transcription of

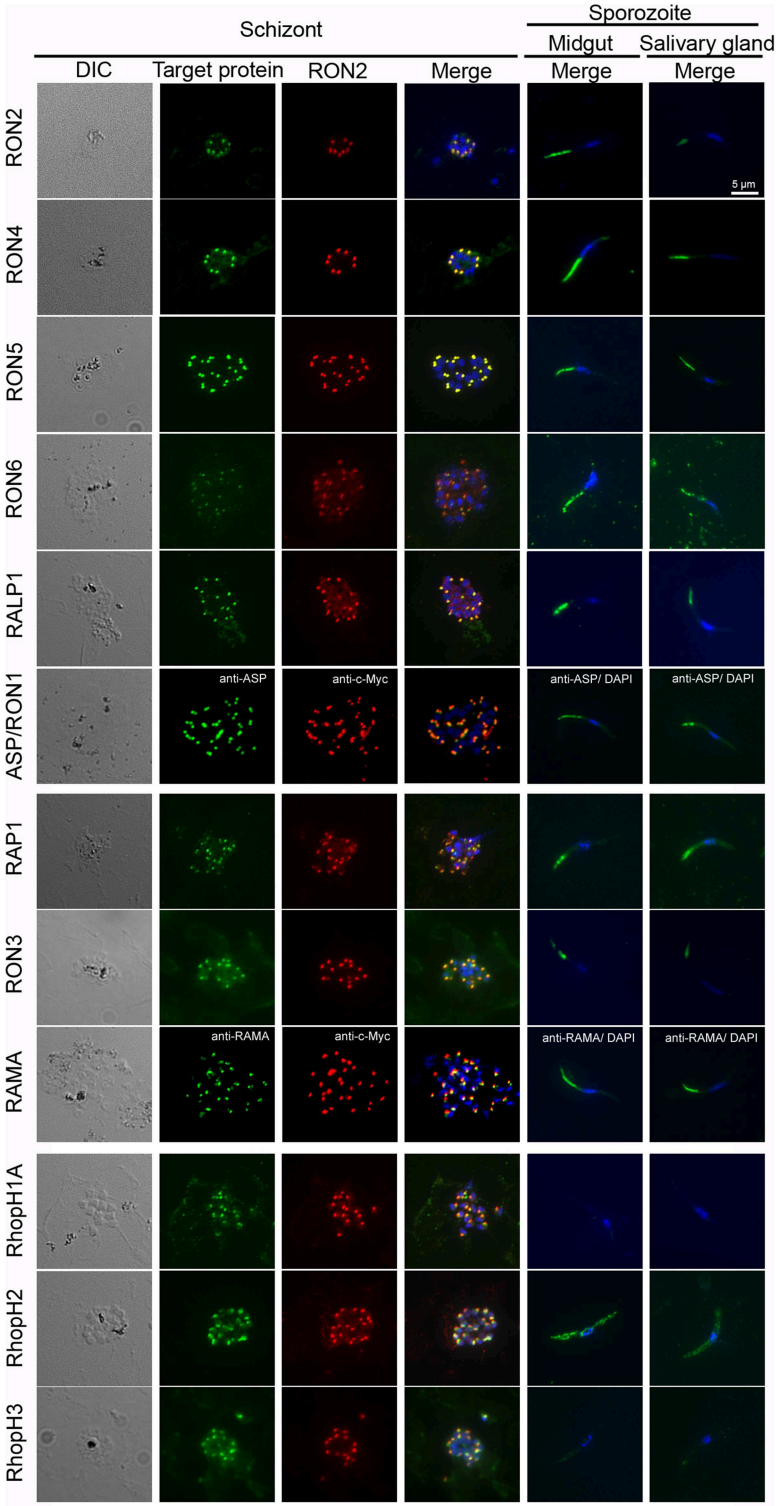

FIGURE 3 | Expression pattern of rhoptry proteins in merozoites and sporozoites. Schizonts and sporozoites collected from midguts or salivary glands at day 24–26 post-feeding were fixed with acetone on glass slides. In schizonts, anti-c-Myc antibodies were used to detect target c-Myc fused rhoptry protein (shown in green) in each transgenic parasite, which is compared with the localization pattern of RON2 (shown in red) and nuclei (blue) stained by anti-RON2 antibodies and DAPI, respectively. To detect ASP/RON1 and RAMA, RON2-c-Myc transgenic parasites were used as antigens and target proteins and RON2 was detected by specific antibodies (green) and anti-c-Myc antibodies (red). Differential interference contrast (DIC) images are shown in the left panels. In sporozoites (right two panels), the localization of target proteins (green) and nuclei (blue) are shown in the merged images. Bar indicates 5 μm.

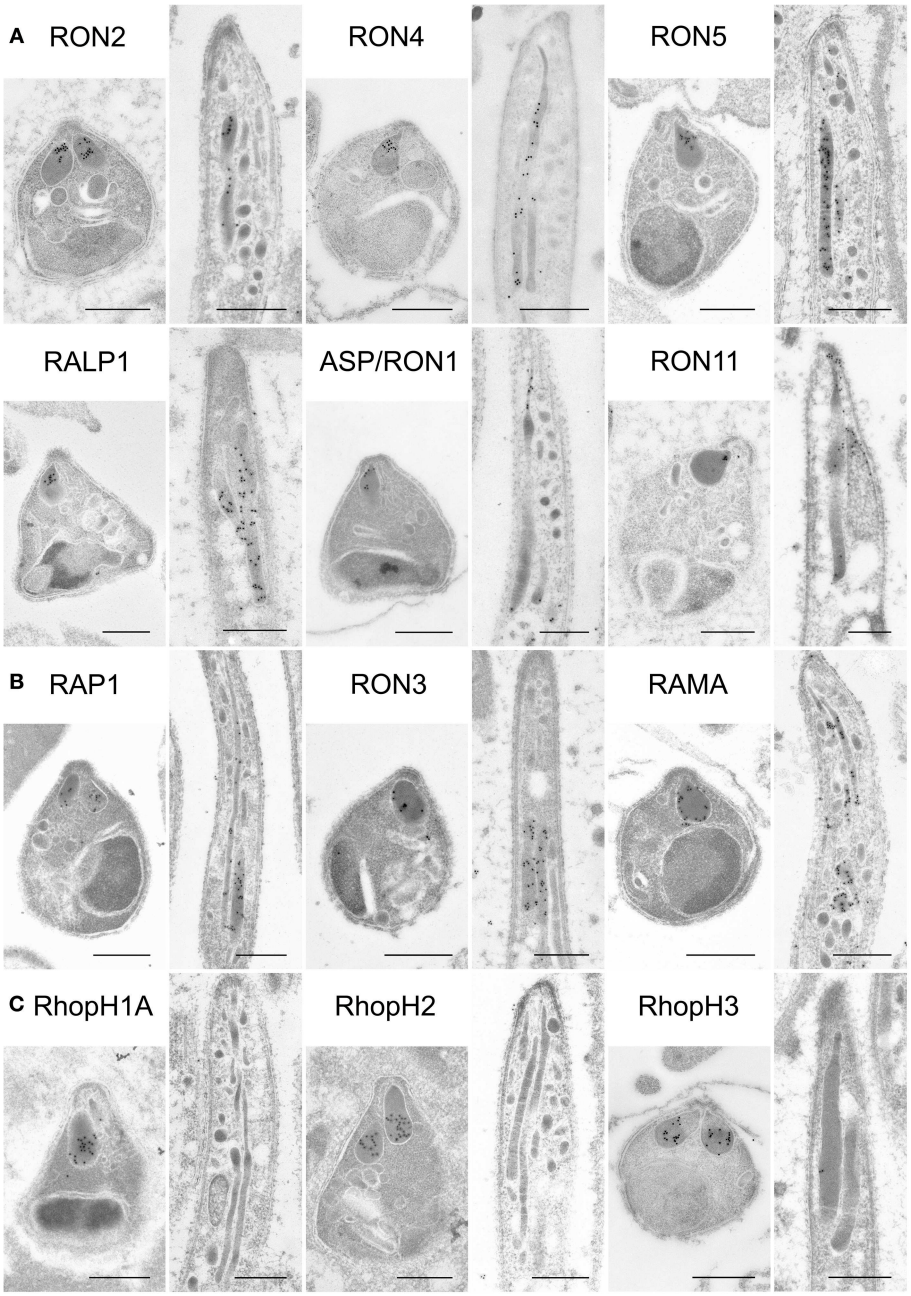

FIGURE 4 | Localization analyses of rhoptry proteins in merozoites and sporozoites by immuno-electron microscopy. Longitudinally sectioned merozoites in cultivated schizonts and oocyst-derived sporozoites (at day 17 or 21 post-feeding) of each transgenic parasite line or WT-GFP were prepared for IEM analyses. Target proteins were detected by incubation with anti-c-Myc rabbit antibodies or specific antibodies against ASP/RON1 or RAMA, followed by secondary antibodies conjugated to gold particles. **(A)** A group of rhoptry proteins categorized as rhoptry neck proteins in merozoites. All examined proteins are confirmed to be localized to the rhoptry neck region in *P. berghei* merozoites. In contrast, most of them, except ASP/RON1, are distributed throughout rhoptries in sporozoites, as demonstrated previously regarding RON11. **(B)** A group of proteins expressed both in merozoites and sporozoites and categorized as rhoptry bulb proteins in merozoites. It is noteworthy that RAMA localizes to the rhoptry membrane in merozoites. In sporozoites, they are distributed in the rhoptry body region. **(C)** A group of proteins categorized as rhoptry bulb proteins in merozoites, which are produced predominantly in merozoites. IEM confirmed that none of them, RhopH1A, RhopH2, and RhopH3, are localized to rhoptries in sporozoites, despite their clear localization to the rhoptry bulb in merozoites. Bars, 500 nm.

some genes are upregulated or downregulated after sporozoite invasion of salivary glands (Kaiser et al., 2004; Mikolajczak et al., 2008; Tarun et al., 2008; Zhang et al., 2010). To determine rhoptry protein localization in liver infective sporozoites, salivary glands of transgenic parasites or WT-GFP infected mosquitoes were fixed for IEM analyses (**Figure 5**). RON2, RON4, RON5, RALP1, RAP1, and RAMA were detected in rhoptries of sporozoites residing in salivary glands, indicating that rhoptry proteins

reside in rhoptries after sporozoite invasion of salivary glands, presumably available for subsequent invasion of hepatocytes in mammalian hosts. ASP/RON1 and RON3 could not be detected by anti-ASP/RON1 or anti-c-Myc antibodies, which might due to less target or c-Myc tagged protein amounts in salivary gland sporozoites.

DISCUSSION

In this study it is demonstrated that most rhoptry proteins reported in merozoites are expressed in sporozoites, with the exception of components of the RhopH complex. Together with three reported proteins, RAP2/3, RON11, and RON12 (Tufet-Bayona et al., 2009; Bantuchai et al., 2019; Oda-Yokouchi et al., 2019), nine rhoptry proteins are demonstrated to be commonly expressed in the infective stages of *P. berghei*. Our results on mRNA expression in schizonts and sporozoites of rhoptry molecules are mostly confirmed by single cell RNA-seq analyses in *P. berghei* (Reid et al., 2018). The orthologs of these proteins in *P. yoelii*, another rodent malaria parasite, are transcribed in oocyst-derived sporozoites (Tarun et al., 2008) and their proteins, except for RALP1, were detected in salivary gland residing sporozoites (Lindner et al., 2013). In addition, the orthologous proteins in the human malaria parasite *Plasmodium falciparum* were detected in salivary gland residing sporozoites (Lindner et al., 2013). Taken together, our finding that the most rhoptry proteins, except for RhopH complex components, are expressed in both merozoites and sporozoites indicates conservation of expression among *Plasmodium* species.

It is noteworthy that all examined commonly expressed rhoptry proteins localize to the neck region in merozoites, that is RON2, RON4, RON5, RALP1, ASP1/RON1, RON11, and RON12; while some rhoptry bulb proteins, RhopH1A, RhopH2, and RhopH3, are expressed predominantly in merozoites. The orthologs of proteins localized to the rhoptry neck are highly conserved across the infective stages of apicomplexan parasites, such as *Plasmodium*, *Toxoplasma*, *Babesia*, and *Cryptosporidium*; however, proteins localized to the rhoptry bulb tend to be species specific. Since it has been proposed that rhoptry neck proteins, such as RON2, RON4, and RON5, are discharged to form the tight junction between parasites and host cells, this invasion mechanism could be conserved across the Apicomplexa phylum. Recently it was reported that the *Toxoplasma* genome contains paralogous genes for RON2 and AMA1, selectively expressed in sporozoites, suggesting that *Toxoplasma* has developed stage-specific invasion mechanisms (Poukchanski et al., 2013). Since the *Plasmodium* genome contains only one set of genes encoding RON2 and AMA1, it would be interesting to examine whether the rhoptry neck protein complex is formed during sporozoite invasion of mosquito salivary glands and mammalian hepatocytes. In contrast, it has been revealed that many of the *Toxoplasma* rhoptry bulb proteins are involved in interaction with host signaling pathways (Lim et al., 2012) and interference with host immunity after invasion (Fentress et al., 2010; Ong et al., 2010; Steinfeldt et al., 2010; Yamamoto et al., 2011; Niedelman et al., 2012). These mechanisms are likely host cell-specific adaptations, and therefore the expression of rhoptry bulb proteins might be variable among parasites species and stages. As most rhoptry proteins are refractory to gene disruption in both *Plasmodium* and *Toxoplasma,* the sporozoite-specific gene knockdown system by promoter swapping is a powerful tool to reveal functions of rhoptry proteins in sporozoites (Ishino et al., 2019). To differentiate the conserved- or specific-mechanisms of invasion among species or infective stages would give clues to understand the comprehensive molecular basis of parasite infection.

The mRNA amounts of ASP/RON1 and RON3 are clearly greater in sporozoites than in schizonts. This suggests that ASP/RON1 and RON3 might mainly have roles or additional roles in sporozoites. Indeed, unlike other rhoptry proteins, ASP/RON1 is dispensable for parasite proliferation during the intraerythrocytic stage in *P. berghei* (Bushell et al., 2017). Understanding its function in sporozoites would reveal the different contributions of rhoptry proteins depending on infective stages or target host cells.

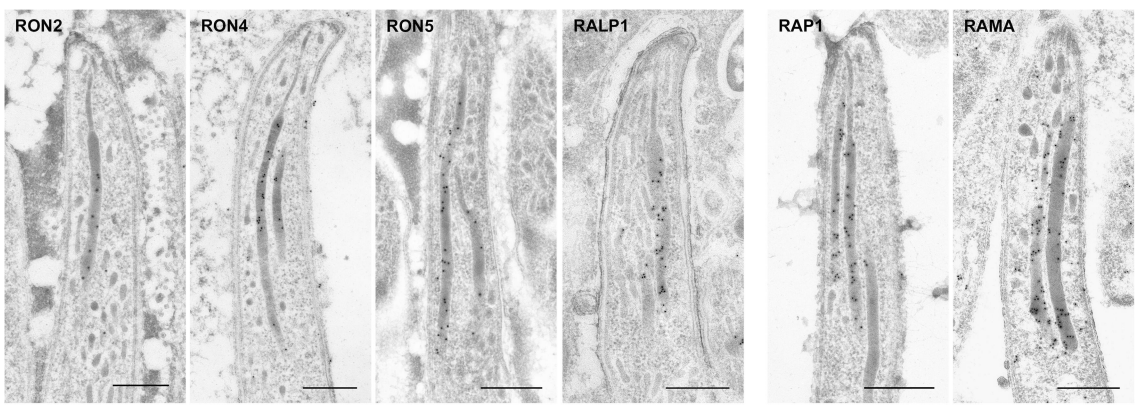

FIGURE 5 | Localization of rhoptry proteins in sporozoites residing in mosquito salivary glands. Salivary glands of parasite infected mosquitoes were harvested at day 24 or 26 post-feeding and fixed for IEM. Target proteins were detected by anti-c-Myc antibodies or specific antibodies against ASP/RON1 or RAMA. All examined rhoptry proteins, despite their sub-localization in merozite rhoptries, are distributed throughout rhoptries in sporozoites residing in salivary glands, as well as oocyst-derived sporozoites. Bars, 500 nm.

This is the first profiling data showing the expression and localization of rhoptry proteins in both merozoites and sporozoites by immuno-electron microscopy. By generation of transgenic parasite lines expressing c-Myc tagged rhoptry proteins, comprehensive localization analyses by immuno-electron microscopy could be performed using anti-c-Myc antibodies, thus overcoming the difficulty to obtain specific and high titer antibodies against *Plasmodium* proteins. The c-Myc tag, a peptide of 10 amino acids and ∼1,200 Da, is relatively small and unlikely to interfere with protein folding and function following addition to the C-terminus of target proteins that do not possess a C-terminal GPI-anchor domain. All the transgenic parasite lines, in which native rhoptry proteins were replaced by c-Myc tagged rhoptry proteins, proliferate normally during the intra-erythrocytic stage. Considering that most rhoptry proteins are refractory to gene deletion due to their necessity for parasite proliferation in the blood stage (Tufet-Bayona et al., 2009; Giovannini et al., 2011; Counihan et al., 2013; Bushell et al., 2017), this indicates that c-Myc tagging at the C-terminus of each protein doesn't affect rhoptry protein localization and function. This c-Myc tagging application combined with IEM will facilitate the observation of protein trafficking and discharge; for example, by overcoming the difficulties in producing specific antibodies with high titer.

In merozoites of *P. berghei* ANKA, as well as in *P. falciparum*, RON2, RON4, RON5, RALP1, and ASP /RON1 are localized to the rhoptry neck, while RAP1, RON3, RAMA, RhopH1A, RhopH2, and RhopH3 are localized to the rhoptry bulb. It has been proposed that sub-localization of rhoptry proteins reflects the order of discharge during merozoite invasion; that is, rhoptry neck proteins are secreted prior to invasion and followed by release of rhoptry bulb proteins (Zuccala et al., 2012). In this study we demonstrate that rhoptry neck proteins are also expressed in sporozoites; however, their localization, except for ASP/RON1, is not restricted to the rhoptry neck. This observation is in good agreement with reports demonstrating that the localization of the rhoptry proteins RON11 and RON12 differ between merozoites and sporozoites (Bantuchai et al., 2019; Oda-Yokouchi et al., 2019). RON2 in sporozoites is required for salivary gland invasion as well as hepatocyte infection (Ishino et al., 2019), which is not the case for RON2 in merozoites involved in erythrocyte invasion, supporting that localization in sporozoite rhoptries might be different from that in merozoites. Further analyses will reveal whether the protein secretion mechanisms and/or timing is different between merozoites and sporozoites. In addition, the same strategy can be used to address protein secretion mechanisms, such as how proteins might be transported to but differentially localized within rhoptries in sporozoites vs. merozoites.

DATA AVAILABILITY

All datasets generated for this study are included in the manuscript/**Supplementary Files**.

ETHICS STATEMENT

All animal experimental protocols were approved by the Institutional Animal Care and Use Committee of Ehime University and the experiments were conducted according to the Ethical Guidelines for Animal Experiments of Ehime University.

AUTHOR CONTRIBUTIONS

NT, MTo, and TI conceived and designed the experiments. NT, MN, MTa, MB, KM, MTo, and TI performed the experiments and analyzed the data. MN, MTo, and TI wrote manuscript. NT, MTa, MB, KM, and TT critically reviewed it.

FUNDING

This work was supported in part by JSPS KAKENHI (JP22590379, JP23790459, JP24390101, and JP19H03459) and Takeda Science Foundation.

ACKNOWLEDGMENTS

We are grateful to Dr. Chris J. Janse, Leiden University, for supplying the *Plasmodium berghei* ANKA parasites expressing GFP under the control of *ef1α* promoter. The following reagents were obtained through BEI Resources, NIAID, NIH: Plasmid pL0033, for generation of transgenic parasites expressing c-Myc tagged rhoptry proteins in *Plasmodium berghei*, and MRA-802, contributed by Dr. Andrew P. Waters. This study was supported by the Division of Analytical Bio-Medicine, the Advanced Research Support Center (ADRES), Ehime University. We also thank A. Konishi and S. Sadaoka for rearing mice and technical support. We would like to thank Dr. Thomas Templeton for critical reading of the manuscript.

SUPPLEMENTARY MATERIAL

The Supplementary Material for this article can be found online at: https://www.frontiersin.org/articles/10.3389/fcimb.2019.00316/full#supplementary-material

REFERENCES

Alexander, L., Mital, J., Ward, G. E., Bradley, P., and Boothroyd, J. C. (2005). Identification of the moving junction complex of *Toxoplasma gondii*: a collaboration between distinct secretory organelles. *PLoS Pathog.* 1:e17. doi: 10.1371/journal.ppat.0010017

Aurrecoechea, C., Brestelli, J., Brunk, B. P., Dommer, J., Fischer, S., Gajria, B., et al. (2009). PlasmoDB: a functional genomic database for malaria parasites. *Nucleic Acids Res.* 37, D539–D543. doi: 10.1093/nar/gkn814

Bantuchai, S., Nozaki, M., Thongkukiatkul, A., Lorsuwannarat, N., Tachibana, M., Baba, M., et al. (2019). Rhoptry neck protein 11 has crucial roles during malaria parasite sporozoite invasion of salivary glands and hepatocytes. *Int. J. Parasitol.* 49, 725–735. doi: 10.1016/j.ijpara.2019.05.001

Baum, J., Gilberger, T. W., Frischknecht, F., and Meissner, M. (2008). Host-cell invasion by malaria parasites: insights from *Plasmodium*

and Toxoplasma. *Trends Parasitol.* 24, 557–563. doi: 10.1016/j.pt.2008.08.006

Besteiro, S., Michelin, A., Poncet, J., Dubremetz, J. F., and Lebrun, M. (2009). Export of a *Toxoplasma gondii* rhoptry neck protein complex at the host cell membrane to form the moving junction during invasion. *PLoS Pathog.* 5:e1000309. doi: 10.1371/journal.ppat.1000309

Boothroyd, J. C., and Dubremetz, J. F. (2008). Kiss and spit: the dual roles of Toxoplasma rhoptries. *Nat. Rev. Microbiol.* 6, 79–88. doi: 10.1038/nrmicro1800

Bradley, P. J., Ward, C., Cheng, S. J., Alexander, D. L., Coller, S., Coombs, G. H., et al. (2005). Proteomic analysis of rhoptry organelles reveals many novel constituents for host-parasite interactions in *Toxoplasma gondii*. *J. Biol. Chem.* 280, 34245–34258. doi: 10.1074/jbc.M504158200

Bushell, E., Gomes, A. R., Sanderson, T., Anar, B., Girling, G., Herd, C., et al. (2017). Functional profiling of a *Plasmodium* genome reveals an abundance of essential genes. *Cell* 170, 260–272.e8. doi: 10.1016/j.cell.2017.06.030

Cao, J., Kaneko, O., Thongkukiatkul, A., Tachibana, M., Otsuki, H., Gao, Q., et al. (2009). Rhoptry neck protein RON2 forms a complex with microneme protein AMA1 in *Plasmodium falciparum* merozoites. *Parasitol. Int.* 58, 29–35. doi: 10.1016/j.parint.2008.09.005

Comeaux, C. A., Coleman, B. I., Bei, A. K., Whitehurst, N., and Duraisingh, M. T. (2011). Functional analysis of epigenetic regulation of tandem RhopH1/clag genes reveals a role in *Plasmodium falciparum* growth. *Mol. Microbiol.* 80, 378–390. doi: 10.1111/j.1365-2958.2011.07572.x

Counihan, N. A., Chisholm, S. A., Bullen, H. E., Srivastava, A., Sanders, P. R., Jonsdottir, T. K., et al. (2017). *Plasmodium falciparum* parasites deploy RhopH2 into the host erythrocyte to obtain nutrients, grow and replicate. *Elife* 6:e23217. doi: 10.7554/eLife.23217

Counihan, N. A., Kalanon, M., Coppel, R. L., and de Koning-Ward, T. F. (2013). Plasmodium rhoptry proteins: why order is important. *Trends Parasitol.* 29, 228–236. doi: 10.1016/j.pt.2013.03.003

Fentress, S. J., Behnke, M. S., Dunay, I. R., Mashayekhi, M., Rommereim, L. M., Fox, B. A., et al. (2010). Phosphorylation of immunity-related GTPases by a *Toxoplasma gondii*-secreted kinase promotes macrophage survival and virulence. *Cell Host Microbe.* 8, 484–495. doi: 10.1016/j.chom.2010.11.005

Ferguson, D. J., Balaban, A. E., Patzewitz, E. M., Wall, R. J., Hopp, C. S., Poulin, B., et al. (2014). The repeat region of the circumsporozoite protein is critical for sporozoite formation and maturation in *Plasmodiu*m. *PLoS ONE* 9:e113923. doi: 10.1371/journal.pone.0113923

Franke-Fayard, B., Trueman, H., Ramesar, J., Mendoza, J., van der Keur, M., van der Linden, R., et al. (2004). A *Plasmodium berghei* reference line that constitutively expresses GFP at a high level throughout the complete life cycle. *Mol. Biochem. Parasitol.* 137, 23–33. doi: 10.1016/j.molbiopara.2004.04.007

Frenal, K., Dubremetz, J. F., Lebrun, M., and Soldati-Favre, D. (2017). Gliding motility powers invasion and egress in Apicomplexa. *Nat. Rev. Microbiol.* 15, 645–660. doi: 10.1038/nrmicro.2017.86

Gilson, P. R., Nebl, T., Vukcevic, D., Moritz, R. L., Sargeant, T., Speed, T. P., et al. (2006). Identification and stoichiometry of glycosylphosphatidylinositol-anchored membrane proteins of the human malaria parasite *Plasmodium falciparum*. *Mol. Cell Proteomics* 5, 1286–1299. doi: 10.1074/mcp.M600035-MCP200

Giovannini, D., Spath, S., Lacroix, C., Perazzi, A., Bargieri, D., Lagal, V., et al. (2011). Independent roles of apical membrane antigen 1 and rhoptry neck proteins during host cell invasion by apicomplexa. *Cell Host Microbe* 10, 591–602. doi: 10.1016/j.chom.2011.10.012

Haase, S., Cabrera, A., Langer, C., Treeck, M., Struck, N., Herrmann, S., et al. (2008). Characterization of a conserved rhoptry-associated leucine zipper-like protein in the malaria parasite *Plasmodium falciparum*. *Infect. Immun.* 76, 879–887. doi: 10.1128/IAI.00144-07

Ishino, T., Chinzei, Y., and Yuda, M. (2005). A *Plasmodium* sporozoite protein with a membrane attack complex domain is required for breaching the liver sinusoidal cell layer prior to hepatocyte infection. *Cell Microbiol.* 7, 199–208. doi: 10.1111/j.1462-5822.2004.00447.x

Ishino, T., Murata, E., Tokunaga, N., Baba, M., Tachibana, M., Thongkukiatkul, A., et al. (2019). Rhoptry neck protein 2 expressed in *Plasmodium* sporozoites plays a crucial role during invasion of mosquito salivary glands. *Cell Microbiol.* 21:e12964. doi: 10.1111/cmi.12964

Ito, D., Han, E. T., Takeo, S., Thongkukiatkul, A., Otsuki, H., Torii, M., et al. (2011). Plasmodial ortholog of *Toxoplasma gondii* rhoptry neck protein 3 is localized to the rhoptry body. *Parasitol. Int.* 60, 132–138. doi: 10.1016/j.parint.2011.01.001

Ito, D., Hasegawa, T., Miura, K., Yamasaki, T., Arumugam, T. U., Thongkukiatkul, A., et al. (2013). RALP1 is a rhoptry neck erythrocyte-binding protein of *Plasmodium falciparum* merozoites and a potential blood-stage vaccine candidate antigen. *Infect. Immun.* 81, 4290–4298. doi: 10.1128/IAI.00690-13

Ito, D., Schureck, M. A., and Desai, S. A. (2017). An essential dual-function complex mediates erythrocyte invasion and channel-mediated nutrient uptake in malaria parasites. *Elife* 6:e23485. doi: 10.7554/eLife.23485

Janse, C. J., Franke-Fayard, B., and Waters, A. P. (2006a). Selection by flow-sorting of genetically transformed, GFP-expressing blood stages of the rodent malaria parasite, *Plasmodium berghe*i. *Nat. Protoc.* 1, 614–623. doi: 10.1038/nprot.2006.88

Janse, C. J., Ramesar, J., and Waters, A. P. (2006b). High-efficiency transfection and drug selection of genetically transformed blood stages of the rodent malaria parasite *Plasmodium berghe*i. *Nat. Protoc.* 1, 346–356. doi: 10.1038/nprot.2006.53

Kadekoppala, M., and Holder, A. A. (2010). Merozoite surface proteins of the malaria parasite: the MSP1 complex and the MSP7 family. *Int. J. Parasitol.* 40, 1155–1161. doi: 10.1016/j.ijpara.2010.04.008

Kaiser, K., Matuschewski, K., Camargo, N., Ross, J., and Kappe, S. H. (2004). Differential transcriptome profiling identifies *Plasmodium* genes encoding pre-erythrocytic stage-specific proteins. *Mol. Microbiol.* 51, 1221–1232. doi: 10.1046/j.1365-2958.2003.03909.x

Kaneko, O., Tsuboi, T., Ling, I. T., Howell, S., Shirano, M., Tachibana, M., et al. (2001). The high molecular mass rhoptry protein, RhopH1, is encoded by members of the clag multigene family in *Plasmodium falciparum* and *Plasmodium yoeli*i. *Mol. Biochem. Parasitol.* 118, 223–231. doi: 10.1016/S0166-6851(01)00391-7

Kaneko, O., Yim Lim, B. Y., Iriko, H., Ling, I. T., Otsuki, H., Grainger, M., et al. (2005). Apical expression of three RhopH1/Clag proteins as components of the *Plasmodium falciparum* RhopH complex. *Mol. Biochem. Parasitol.* 143, 20–28. doi: 10.1016/j.molbiopara.2005.05.003

Kariu, T., Ishino, T., Yano, K., Chinzei, Y., and Yuda, M. (2006). CelTOS, a novel malarial protein that mediates transmission to mosquito and vertebrate hosts. *Mol. Microbiol.* 59, 1369–1379. doi: 10.1111/j.1365-2958.2005.05024.x

Kemp, L. E., Yamamoto, M., and Soldati-Favre, D. (2013). Subversion of host cellular functions by the apicomplexan parasites. *FEMS Microbiol. Rev.* 37, 607–631. doi: 10.1111/1574-6976.12013

Kennedy, M., Fishbaugher, M. E., Vaughan, A. M., Patrapuvich, R., Boonhok, R., Yimamnuaychok, N., et al. (2012). A rapid and scalable density gradient purification method for *Plasmodium* sporozoites. *Malar J.* 11:421. doi: 10.1186/1475-2875-11-421

Lebrun, M., Michelin, A., El Hajj, H., Poncet, J., Bradley, P. J., Vial, H., et al. (2005). The rhoptry neck protein RON4 re-localizes at the moving junction during *Toxoplasma gondii* invasion. *Cell Microbiol.* 7, 1823–1833. doi: 10.1111/j.1462-5822.2005.00646.x

Lim, D. C., Cooke, B. M., Doerig, C., and Saeij, J. P. (2012). Toxoplasma and *Plasmodium* protein kinases: roles in invasion and host cell remodelling. *Int. J. Parasitol.* 42, 21–32. doi: 10.1016/j.ijpara.2011.11.007

Lindner, S. E., Swearingen, K. E., Harupa, A., Vaughan, A. M., Sinnis, P., Moritz, R. L., et al. (2013). Total and putative surface proteomics of malaria parasite salivary gland sporozoites. *Mol. Cell Proteomics* 12, 1127–1143. doi: 10.1074/mcp.M112.024505

Ling, I. T., Florens, L., Dluzewski, A. R., Kaneko, O., Grainger, M., Yim Lim, B. Y., et al. (2004). The *Plasmodium falciparum* clag9 gene encodes a rhoptry protein that is transferred to the host erythrocyte upon invasion. *Mol. Microbiol.* 52, 107–118. doi: 10.1111/j.1365-2958.2003.03969.x

Ling, I. T., Kaneko, O., Narum, D. L., Tsuboi, T., Howell, S., Taylor, H. M., et al. (2003). Characterisation of the rhoph2 gene of *Plasmodium falciparum* and *Plasmodium yoeli*i. *Mol. Biochem. Parasitol.* 127, 47–57. doi: 10.1016/S0166-6851(02)00302-X

Mikolajczak, S. A., Silva-Rivera, H., Peng, X., Tarun, A. S., Camargo, N., Jacobs-Lorena, V., et al. (2008). Distinct malaria parasite sporozoites reveal transcriptional changes that cause differential tissue infection competence in the mosquito vector and mammalian host. *Mol. Cell. Biol.* 28, 6196–6207. doi: 10.1128/MCB.00553-08

Mutungi, J. K., Yahata, K., Sakaguchi, M., and Kaneko, O. (2014). Expression and localization of rhoptry neck protein 5 in merozoites and sporozoites of *Plasmodium yoelii*. *Parasitol. Int*. 63, 794–801. doi: 10.1016/j.parint.2014.07.013

Nguitragool, W., Bokhari, A. A., Pillai, A. D., Rayavara, K., Sharma, P., Turpin, B., et al. (2011). Malaria parasite clag3 genes determine channel-mediated nutrient uptake by infected red blood cells. *Cell* 145, 665–677. doi: 10.1016/j.cell.2011.05.002

Niedelman, W., Gold, D. A., Rosowski, E. E., Sprokholt, J., K., Lim, D., Farid Arenas, A., et al. (2012). The rhoptry proteins ROP18 and ROP5 mediate *Toxoplasma gondii* evasion of the murine, but not the human, interferon-gamma response. *PLoS Pathog*. 8:e1002784. doi: 10.1371/journal.ppat.1002784

Oda-Yokouchi, Y., Tachibana, M., Iriko, H., Torii, M., Ishino, T., and Tsuboi, T. (2019). Plasmodium RON12 localizes to the rhoptry body in sporozoites. *Parasitol. Int*. 68, 17–23. doi: 10.1016/j.parint.2018.10.001

Ong, Y. C., Reese, M. L., and Boothroyd, J. C. (2010). Toxoplasma rhoptry protein 16 (ROP16) subverts host function by direct tyrosine phosphorylation of STAT6. *J. Biol. Chem*. 285, 28731–28740. doi: 10.1074/jbc.M110.112359

Pfaffl, M. W. (2001). A new mathematical model for relative quantification in real-time RT-PCR. *Nucleic Acids Res*. 29:e45. doi: 10.1093/nar/29.9.e45

Poukchanski, A., Fritz, H. M., Tonkin, M. L., Treeck, M., Boulanger, M. J., and Boothroyd, J. C. (2013). *Toxoplasma gondii* sporozoites invade host cells using two novel paralogues of RON2 and AMA1. *PLoS ONE* 8:e70637. doi: 10.1371/journal.pone.0070637

Proellocks, N. I., Kats, L. M., Sheffield, D. A., Hanssen, E., Black, C. G., Waller, K. L. et al. (2009). Characterisation of PfRON6, *a Plasmodium falciparum* rhoptry neck protein with a novel cysteine-rich domain. *Int. J. Parasitol*. 39, 683–692. doi: 10.1016/j.ijpara.2008.11.002

Reid, A. J., Talman, A. M., Bennett, H. M., Gomes, A. R., Sanders, M. J., Illingworth, C. J. R., et al. (2018). Single-cell RNA-seq reveals hidden transcriptional variation in malaria parasites. *Elife* 7:e33105. doi: 10.7554/eLife.33105

Richard, D., MacRaild, C. A., Riglar, D. T., Chan, J. A., Foley, M., Baum, J., et al. (2010). Interaction between *Plasmodium falciparum* apical membrane antigen 1 and the rhoptry neck protein complex defines a key step in the erythrocyte invasion process of malaria parasites. *J. Biol. Chem*. 285, 14815–14822. doi: 10.1074/jbc.M109.080770

Riglar, D. T., Richard, D., Wilson, D. W., Boyle, M. J., Dekiwadia, C., Turnbull, L., et al. (2011). Super-resolution dissection of coordinated events during malaria parasite invasion of the human erythrocyte. *Cell Host Microbe* 9, 9–20. doi: 10.1016/j.chom.2010.12.003

Risco-Castillo, V., Topcu, S., Son, O., Briquet, S., Manzoni, G., and Silvie, O. (2014). CD81 is required for rhoptry discharge during host cell invasion by *Plasmodium yoelii* sporozoites. *Cell Microbiol*. 16, 1533–1548. doi: 10.1111/cmi.12309

Sherling, E. S., Knuepfer, E., Brzostowski, J. A., Miller, L. H., Blackman, M. J., and van Ooij, C. (2017). The *Plasmodium falciparum* rhoptry protein RhopH3 plays essential roles in host cell invasion and nutrient uptake. *Elife* 6:e23239. doi: 10.7554/eLife.23239

Srivastava, A., Singh, S., Dhawan, S., Mahmood Alam, M., Mohmmed, A., and Chitnis, C. E. (2010). Localization of apical sushi protein in *Plasmodium falciparum* merozoites. *Mol. Biochem. Parasitol*. 174, 66–69. doi: 10.1016/j.molbiopara.2010.06.003

Steinfeldt, T., Konen-Waisman, S., Tong, L., Pawlowski, N., Lamkemeyer, T., Sibley, L. D., et al. (2010). Phosphorylation of mouse immunity-related GTPase (IRG) resistance proteins is an evasion strategy for virulent *Toxoplasma gondii*. *PLoS Biol*. 8:e1000576. doi: 10.1371/journal.pbio.1000576

Sultan, A. A., Thathy, V., Frevert, U., Robson, K. J., Crisanti, A., Nussenzweig, V., et al. (1997). TRAP is necessary for gliding motility and infectivity of *Plasmodium* sporozoites. *Cell* 90, 511–522. doi: 10.1016/S0092-8674(00)80511-5

Tarun, A. S., Peng, X., Dumpit, R. F., Ogata, Y., Silva-Rivera, H., Camargo, N., et al. (2008). A combined transcriptome and proteome survey of malaria parasite liver stages. *Proc. Natl. Acad. Sci. U. S. A.* 105, 305–310. doi: 10.1073/pnas.0710780104

Thathy, V., Fujioka, H., Gantt, S., Nussenzweig, R., Nussenzweig, V., and Menard, R. (2002). Levels of circumsporozoite protein in the *Plasmodium* oocyst determine sporozoite morphology. *EMBO J.* 21, 1586–1596. doi: 10.1093/emboj/21.7.1586

Topolska, A. E., Lidgett, A., Truman, D., Fujioka, H., and Coppel, R. L. (2004). Characterization of a membrane-associated rhoptry protein of *Plasmodium falciparum*. *J. Biol. Chem*. 279, 4648–4656. doi: 10.1074/jbc.M307859200

Tsuboi, T., Takeo, S., Iriko, H., Jin, L., Tsuchimochi, M., Matsuda, S., et al. (2008). Wheat germ cell-free system-based production of malaria proteins for discovery of novel vaccine candidates. *Infect. Immun*. 76, 1702–1708. doi: 10.1128/IAI.01539-07

Tufet-Bayona, M., Janse, C. J., Khan, S. M., Waters, A. P., Sinden, R. E., and Franke-Fayard, B. (2009). Localisation and timing of expression of putative *Plasmodium berghei* rhoptry proteins in merozoites and sporozoites. *Mol. Biochem. Parasitol*. 166, 22–31. doi: 10.1016/j.molbiopara.2009.02.009

Vanderberg, J. P. (1975). Development of infectivity by the *Plasmodium berghei* sporozoite. *J. Parasitol*. 61, 43–50. doi: 10.2307/3279102

Vincensini, L., Fall, G., Berry, L., Blisnick, T., and Braun Breton, C. (2008). The RhopH complex is transferred to the host cell cytoplasm following red blood cell invasion by *Plasmodium falciparum*. *Mol. Biochem. Parasitol*. 160, 81–89. doi: 10.1016/j.molbiopara.2008.04.002

Yamamoto, M., Ma, J. S., Mueller, C., Kamiyama, N., Saiga, H., Kubo, E., et al. (2011). ATF6beta is a host cellular target of the *Toxoplasma gondii* virulence factor ROP18. *J. Exp. Med*. 208, 1533–1546. doi: 10.1084/jem.20101660

Yang, A. S. P., Lopaticki, S., O'Neill, M. T., Erickson, S. M., Douglas, D. N., Kneteman, N. M., et al. (2017). AMA1 and MAEBL are important for *Plasmodium falciparum* sporozoite infection of the liver. *Cell Microbiol*. 19:e12745 doi: 10.1111/cmi.12745

Yuda, M., and Ishino, T. (2004). Liver invasion by malarial parasites–how do malarial parasites break through the host barrier? *Cell Microbiol*. 6, 1119–1125. doi: 10.1111/j.1462-5822.2004.00474.x

Zhang, M., Fennell, C., Ranford-Cartwright, L., Sakthivel, R., Gueirard, P., Meister, S., et al. (2010). The *Plasmodium* eukaryotic initiation factor-2alpha kinase IK2 controls the latency of sporozoites in the mosquito salivary glands. *J. Exp. Med*. 207, 1465–1474. doi: 10.1084/jem.20091975

Zuccala, E. S., Gout, A. M., Dekiwadia, C., Marapana, D. S., Angrisano, F., Turnbull, L., et al. (2012). Subcompartmentalisation of proteins in the rhoptries correlates with ordered events of erythrocyte invasion by the blood stage malaria parasite. *PLoS ONE* 7:e46160. doi: 10.1371/journal.pone.0046160

Conflict of Interest Statement: The authors declare that the research was conducted in the absence of any commercial or financial relationships that could be construed as a potential conflict of interest.

Citation: Tokunaga N, Nozaki M, Tachibana M, Baba M, Matsuoka K, Tsuboi T, Torii M and Ishino T (2019) Expression and Localization Profiles of Rhoptry Proteins in Plasmodium berghei Sporozoites. Front. Cell. Infect. Microbiol. 9:316. doi: 10.3389/fcimb.2019.00316

frontiers in Microbiology

ORIGINAL RESEARCH
published: 13 September 2019
doi: 10.3389/fmicb.2019.02134

Fueling Open Innovation for Malaria Transmission-Blocking Drugs: Hundreds of Molecules Targeting Early Parasite Mosquito Stages

Michael Delves[1,2], M. Jose Lafuente-Monasterio[3], Leanna Upton[2], Andrea Ruecker[2,4,5], Didier Leroy[6], Francisco-Javier Gamo[3] and Robert Sinden[2]*

[1] Department of Infection Biology, Faculty of Infectious and Tropical Diseases, London School of Hygiene & Tropical Medicine, London, United Kingdom, [2] Department of Life Sciences, Imperial College London, London, United Kingdom, [3] Diseases of the Developing World (DDW), GlaxoSmithKline, Tres Cantos, Spain, [4] Mahidol Oxford Tropical Medicine Research Unit, Faculty of Tropical Medicine, Mahidol University, Bangkok, Thailand, [5] Centre for Tropical Medicine and Global Health, Nuffield Department of Medicine, University of Oxford, Oxford, United Kingdom, [6] Medicines for Malaria Venture, Geneva, Switzerland

OPEN ACCESS

Edited by:
Isabelle Morlais, Institut de Recherche pour le Développement (IRD), France

Reviewed by:
Mathieu Gissot, Centre National de la Recherche Scientifique (CNRS), France
Juan Diego Maya, University of Chile, Chile

***Correspondence:**
Michael Delves
michael.delves@lshtm.ac.uk

Specialty section:
This article was submitted to Infectious Diseases, a section of the journal Frontiers in Microbiology

Received: *20 June 2019*
Accepted: *30 August 2019*
Published: *13 September 2019*

Citation:
Delves M, Lafuente-Monasterio MJ, Upton L, Ruecker A, Leroy D, Gamo F-J and Sinden R (2019) Fueling Open Innovation for Malaria Transmission-Blocking Drugs: Hundreds of Molecules Targeting Early Parasite Mosquito Stages. Front. Microbiol. 10:2134. doi: 10.3389/fmicb.2019.02134

Background: Despite recent successes at controlling malaria, progress has stalled with an estimated 219 million cases and 435,000 deaths in 2017 alone. Combined with emerging resistance to front line antimalarial therapies in Southeast Asia, there is an urgent need for new treatment options and novel approaches to halt the spread of malaria. *Plasmodium*, the parasite responsible for malaria propagates through mosquito transmission. This imposes an acute bottleneck on the parasite population and transmission-blocking interventions exploiting this vulnerability are recognized as vital for malaria elimination.

Methods: 13,533 small molecules with known activity against *Plasmodium falciparum* asexual parasites were screened for additional transmission-blocking activity in an *ex vivo Plasmodium berghei* ookinete development assay. Active molecules were then counterscreened in dose response against HepG2 cells to determine their activity/cytotoxicity window and selected non-toxic representative molecules were fully profiled in a range of transmission and mosquito infection assays. Furthermore, the entire dataset was compared to other published screens of the same molecules against *P. falciparum* gametocytes and female gametogenesis.

Results: 437 molecules inhibited *P. berghei* ookinete formation with an $IC_{50} < 10$ μM. of which 273 showed >10-fold parasite selectivity compared to activity against HepG2 cells. Active molecules grouped into 49 chemical clusters of three or more molecules, with 25 doublets and 94 singletons. Six molecules representing six major chemical scaffolds confirmed their transmission-blocking activity against *P. falciparum* male and female gametocytes and inhibited *P. berghei* oocyst formation in the standard membrane feeding assay at 1 μM. When screening data in the *P. berghei* development ookinete assay was compared to published screens of the same library in assays against *P. falciparum* gametocytes and female gametogenesis, it was established that

each assay identified distinct, but partially overlapping subsets of transmission-blocking molecules. However, selected molecules unique to each assay show transmission-blocking activity in mosquito transmission assays.

Conclusion: The *P. berghei* ookinete development assay is an excellent high throughput assay for efficiently identifying antimalarial molecules targeting early mosquito stage parasite development. Currently no high throughput transmission-blocking assay is capable of identifying all transmission-blocking molecules.

Keywords: malaria, transmission, ookinete, drug, screening

INTRODUCTION

Malaria is still a disease of devastating medical and economic impact affecting nearly half of the world's population. *Plasmodium*, the apicomplexan parasite responsible for malaria has a complex life cycle requiring both vertebrate hosts and mosquitoes. With every round of asexual replication within the blood, a proportion of cells are triggered to undergo an alternative developmental pathway and transform into mosquito-transmissible male and female gametocytes. When a mosquito bites, these gametocytes are taken up in the bloodmeal and within minutes transform into male and female gametes in the mosquito midgut. Fertilization ensues and the resultant zygote develops into a motile ookinete around 22 h after feeding. The ookinete migrates to and through the midgut wall forming an oocyst and infecting the mosquito. Parasites then further develop into sporozoites that migrate to the salivary glands ready to infect a new human host.

With the exception of tafenoquine and 8-aminoquinolines, all antimalarial drugs have been developed primarily to target the pathogenic asexual stage of the parasite life cycle. Consequently, they have variable activity against other parasite stages possessing divergent cell biology (Delves M. et al., 2012; Plouffe et al., 2016). In order to achieve local elimination and global eradication of malaria, reducing parasite transmission is essential (Rabinovich et al., 2017). At the point of seeking treatment, malarial patients frequently already possess mosquito-infectious male and female gametocyte stage parasites, therefore a patient can be treated and "cured" of their infection but still be able to pass parasites on to mosquitoes and perpetuate the disease (Eziefula et al., 2013). In addition, a significant proportion of the population in malaria-endemic areas have asymptomatic infections and harbor submicroscopic levels of gametocytes which contribute to the persistence of malaria. As gametocytes develop and reside within the human host, gametocyte-targeted transmission-blocking drugs can be administered directly to the patient (Burrows et al., 2017). However, the reduced and divergent metabolism of the gametocyte leaves them insensitive to most antimalarial treatments (Delves M. et al., 2012; Plouffe et al., 2016). Given that the mosquito bloodmeal is composed primarily of blood, transmission-blocking drugs administered to the patient can also access and target early mosquito stage parasite development when the parasite "reawakens" its metabolism and displays more targetable cell biology. However, such a strategy requires drugs with long half-lives so that efficacious concentrations can be maintained within every mosquito bite where infectious gametocytes are present. Alternatively, recent data has shown surfaces treated with the transmission-blocking antimalarial atovaquone are effective at delivering an efficacious dose directly to the mosquito through contact exposure (Paton et al., 2019).

In 2010, GlaxoSmithKline (GSK) reported and released the chemical structures of 13,533 molecules from within their compound library with activity against *P. falciparum* asexual development (Gamo et al., 2010). Since then, the Tres Cantos Antimalarial Set (TCAMS) has been extensively screened in a range of high throughput assays against different parasite stages (Almela et al., 2015; Raphemot et al., 2015; Miguel-Blanco et al., 2017) and yielded new antimalarial candidate molecules (Sanz et al., 2011; Calderón et al., 2012; Williamson et al., 2016). To date, little is known about their activity on early parasite development in the mosquito. Using the rodent malaria model *P. berghei* and an established *ex vivo* ookinete development assay (Pb ODA) which simulates the first 22 h of parasite development in the mosquito (Delves M.J. et al., 2012), we report the screening, identification and profiling of new transmission-blocking molecules.

RESULTS

Screening of the TCAMS Library in the Pb ODA

The Pb ODA introduces gametocyte-infected mouse blood to compound-treated "ookinete medium" that simultaneously stimulates gametogenesis *ex vivo*. The readout of this assay is parasite expression of GFP under the control of an ookinete-specific promoter (CTRP) which is detected in a fluorescence plate reader. Therefore, this assay can measure the ability of a compound to inhibit parasite development from the onset of gametogenesis to ookinete formation – approximately the first 22 h of mosquito stage development.

The entire TCAMS library was screened in the Pb ODA at 1 μM in duplicate independent experiments (**Figure 1**). A relatively lenient cut-off of >50% inhibition in one or both replicates was selected as the assay "primary-hit" criterion to permit even weakly active compounds to be investigated. Under these conditions, 550 compounds were identified (**Supplementary Table S1**). 513 of these compounds were available for resupply and were retested in dose response in

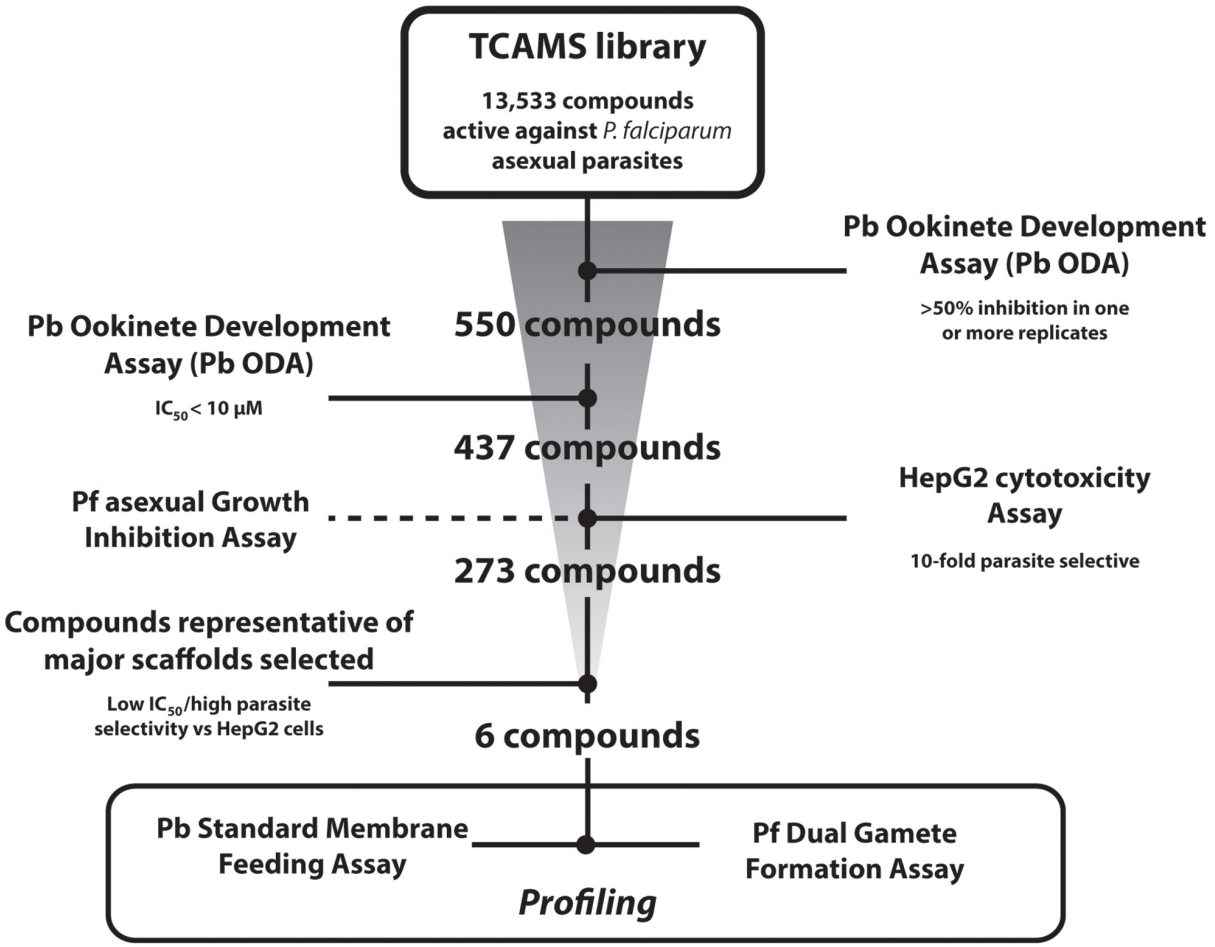

FIGURE 1 | Screening Progression Cascade. The Tres Cantos Antimalarial Set (TCAMS) was screened in the *P. berghei* ookinete development assay (Pb ODA) at 1 μM in duplicate identifying 550 compounds showing >50% inhibition. 437 compounds were reconfirmed in dose response to have an IC_{50} < 10 μM. Active compounds were counterscreened against *P. falciparum* asexuals and HepG2 cells. Six potent and parasite-selective compounds representing major chemical scaffolds were selected and studied in detail.

at least triplicate independent experiments which confirmed an IC_{50} < 10 μM for 437 of them. Compounds with >70% inhibition in the primary screen exhibited a false positive discovery rate of 4.96% (**Supplementary Tables S1, S2**). Compounds with 50–69% inhibition in the primary screen, however, showed a false positive discovery rate of 31.66%, suggesting future Pb ODA screens should adopt a more stringent hit criteria of >70% inhibition. One compound with a pyridone scaffold (TCMDC-135461) exhibited a sub-nanomolar IC_{50} of < 0.2 nM (the lowest concentration tested in the dose response analysis). 21 additional compounds exhibited low-nanomolar IC_{50}s < 100 nM and a further 162 compounds possessed IC_{50}s < 1 μM (**Supplementary Table S2**).

Initial Profiling

The molecules active against *P. berghei* ookinete development were counter-screened for activity against *P. falciparum* asexual development in the growth inhibition assay (GIA), and additionally screened against HepG2 cells to determine cytotoxicity (**Supplementary Table S2**). 92 compounds were more potent against HepG2 cells than against ookinete development and therefore were inferred to be cytotoxic (**Figure 2A**). 77 compounds were slightly parasite selective (1 to 10-fold more active against ookinete development), 190 showed good selectivity (>10 to 100-fold) and 83 were highly selective (>100-fold). After eliminating the cytotoxic compounds, the activity of those remaining were compared to activity in the Pf GIA (**Figure 2B**). Not a single compound had greater than 8-fold selectivity for *P. berghei* ookinetes over *P. falciparum* asexuals. Given that the TCAMS library is comprised entirely of compounds shown to have activity against *P. falciparum* asexuals, this is unsurprising; indeed 320 out of 441 compounds were more active against asexuals than ookinete development (**Figure 2B**).

Chemical Clustering Analysis

Molecular frameworks and fingerprint cluster analyses were used to structurally characterize the 437 confirmed hits, identifying 49 clusters and 128 singletons (**Figure 3** and

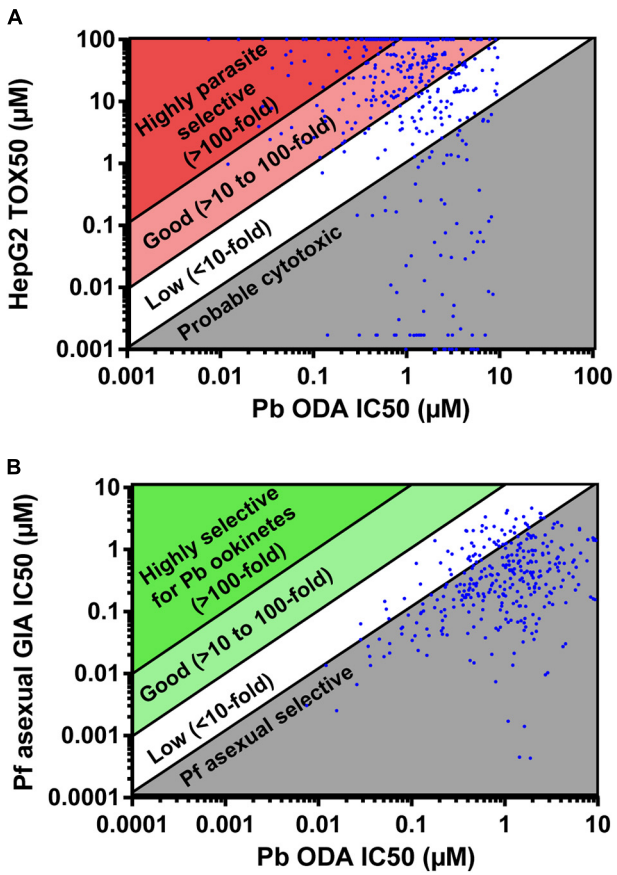

FIGURE 2 | Parasite selectivity and stage specificity. IC_{50}s of active compounds were determined in the *P. berghei* ookinete development assay (Pb ODA). **(A)** These were then compared to Tox_{50} values against HepG2 cells to determine parasite selectivity. **(B)** In parallel, to determine parasite stage specificity, Pb ODA IC_{50}s were compared to corresponding activity in the *P. falciparum* asexual inhibition growth assay (Pf GIA).

Supplementary Table S2). In addition, many clusters contained compounds that shared a common functional scaffold and were grouped into seven different families comprising of pyridones, cyclic diaminopyrimidines, pyridyl derivatives, diaminopyrimidines, quinolones, tetrahydroisoquinolines, and benzodiazoles. The majority of compounds in the cyclic diaminopyrimidine group were found to be cytotoxic, however, most members of the other groups showed >10-fold parasite selectivity.

Profiling the Transmission-Blocking Properties of Selected Molecules

Exemplar molecules from the remaining six families showing high potency and parasite selectivity were selected for detailed parasitological profiling: TCMDC-135461 (pyridone); TCMDC-135907 (pyridyl derivative); TCMDC-134114 (diaminopyrimidine); TCMDC-137173 (quinolone); TCMDC-125849 (tetrahydroisoquinoline); TCMDC-124514 (benzodiazole) (**Figure 4**).

The selected molecules were evaluated for their ability to prevent mosquito transmission at 1 μM in *P. berghei* standard membrane feeding assays (Pb SMFA) (**Figure 5A** and **Supplementary Table S3**). Relative activity in the Pb SMFA broadly matched their activity in the Pb ODA, albeit with reduced potency. TCMDC-137173 and TCMDC-134114 both displayed low nanomolar activity in the Pb ODA (IC_{50}s < 60 nM). This translated into a 97–100% inhibition of oocyst intensity at 1 μM in the Pb SMFA. TCMDC-125849, TCMDC-135907 and TCMDC-124514 were less active in the Pb ODA (IC_{50}s > 250 nM) which translated into a 9–71% inhibition of oocyst intensity at 1 μM in the Pb SMFA. TCMDC-135461, the pyridone compound with the most potent activity in the Pb ODA was tested in the Pb SMFA in dose response at 1 μM, 100 nM, and 10 nM (**Figure 5B** and **Supplementary Table S4**). At 1 μM, no oocysts were observed in any mosquitoes. At 100 nM, oocyst intensity was reduced by 77.9% (±11.8% standard error of the mean – SEM). At 10 nM, oocyst intensity was inhibited by 43% (±13.7% SEM). Taken together, based upon the direct comparison of these six compounds in the Pb ODA and Pb SMFA, it would appear that a Pb ODA IC_{50} of at least ∼60 nM translates into a near-total transmission-blockade in mosquito feeds at 1 μM and should set the approximate threshold onward progression of molecules in future screens.

To ensure that data obtained using a rodent malaria parasite shows applicability to human malaria-infective species, the six molecules were tested in an established *P. falciparum* Dual Gamete Formation Assay (Pf DGFA). The Pf DGFA evaluates the ability of test molecules to prevent male and female gametocytes from differentiating into gametes *in vitro*, which is the first step of parasite development in the mosquito (Ruecker et al., 2014; Delves et al., 2018). Activity in the Pf DGFA has been shown to be highly predictive of activity in *P. falciparum* SMFAs which are technically difficult and expensive to perform (Ruecker et al., 2014; Baragaña et al., 2015). At 1 μM a diverse range of activities was observed against male and female *P. falciparum* gametocytes (**Figure 5C** and **Supplementary Table S4**). TCMDC-135461 and TCMDC-137173 – the two most potent compounds in the Pb ODA showed 75.4 and 76.7% inhibition of male gametocyte functional viability respectively, but low activity against female gametocytes (27.4 and 21.0% inhibition respectively). This indicates that these compounds are more active against male gametocytes than female gametocytes. TCMDC-134114 gave 97.0% inhibition of male gametocyte functional viability and was not active against female gametocytes – suggesting a male-specific mode of action. In contrast, TCMDC-125849 and TCMDC-124514 showed activity against both male (65.5 and 95.6% inhibition respectively) and female (99.3 and 90.7% inhibition respectively) gametocytes suggesting a mode of action targeting biochemical pathways fundamental to both gametocyte sexes. Finally, TCMDC-135907 showed little-to-no activity in the Pf DGFA, perhaps suggesting that this compound targets parasite development post-gamete formation (hence active in the Pb ODA and not Pf DGFA).

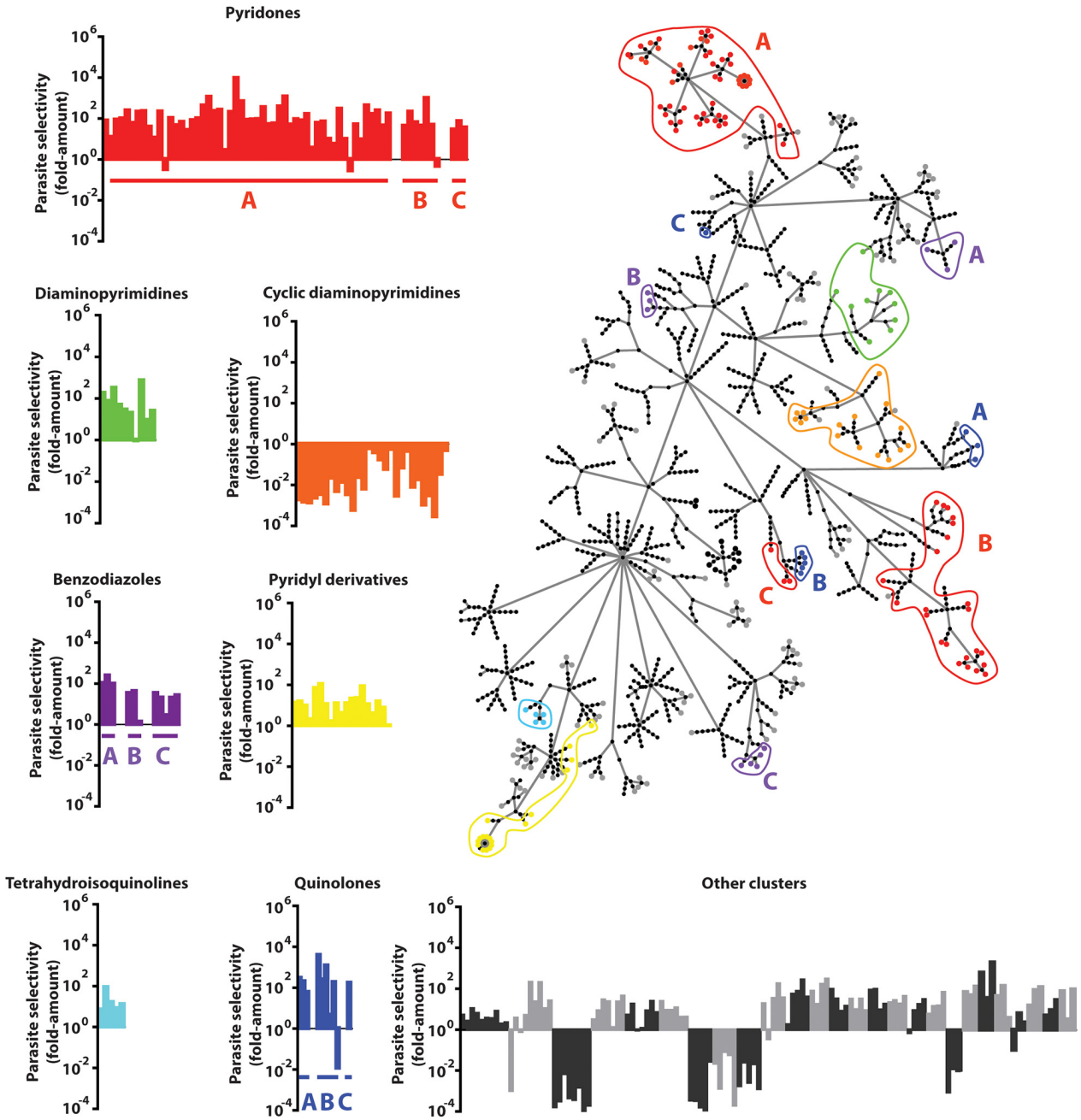

FIGURE 3 | Compound Clustering. Compounds active in the *P. berghei* ookinete development assay (Pb ODA) were clustered using the FragFP algorithm and visualized as a dendrogram. Terminal nodes represent individual compounds and linking nodes represent FragFP similarity toward the single central point in 0.1 unit increments. Colored regions highlight compounds possessing common major scaffolds. Graphs indicate the individual parasite selectivity (HepG2 IC_{50}/Pb ODA IC_{50}) of members of each scaffold.

Comparison to Other Transmission-Blocking Assays

With regards to potential for transmission-blocking, the TCAMS library has also been previously screened against purified *P. falciparum* late stage (stages IV-V) gametocytes in an ATP depletion assay (Pf GC-ATP) (Almela et al., 2015), and purified *P. falciparum* female gametocytes in a female gametogenesis assay (Pf FGAA) (Miguel-Blanco et al., 2017). In the Pf GC-ATP assay, the TCAMS were initially screened at 5 μM and yielded 363 molecules with an IC_{50} < 10 μM, and in the Pf FGAA they were screened at 2 μM, yielding 405 active compounds. In parallel, both studies also performed counterscreens against HepG2 cells for cytotoxicity. Combining these data with the Pb ODA screen results reported here and only considering molecules

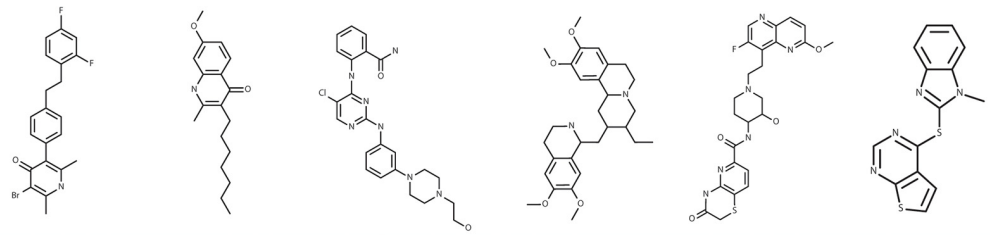

Compound ID	TCMDC-135461	TCMDC-137173	TCMDC-134114	TCMDC-125849	TCMDC-135907	TCMDC-124514
Molecular scaffold	pyridone	quinolone	diaminopyrimidine	tetrahydroisoquinoline	pyridyl derivative	benzodiazole
Putative mode of action	Cyt bc_1 inhibitor	Cyt bc_1 inhibitor	antifolate	protein synthesis inhibitor	unknown	coenzyme-A biosynthesis inhibitor
IC_{50} Pb ODA (nM)	0.2	24.8	55.8	268.2	381.0	397.6
IC_{50} Pf Asexual (nM)	3.1	35.2	21.5	41.9	2022.3	187.6
IC_{50} HepG2 (μM)	>100	>100	41.7	24.0	42.2	>100
% inhibition Pb SMFA 1 μM (±SEM)	100 (0)	98.41 (0.92)	96.98 (0.56)	71.39 (3.58)	56.25 (7.75)	9.07 (22.41)
% inhibition Pf DGFA (male) 1 μM (±SEM)	75.40 (7.88)	76.72 (7.06)	99.71 (0.20)	65.46 (4.92)	17.43 (16.33)	95.61 (1.86)
% inhibition Pf DGFA (female) 1 μM (±SEM)	27.45 (29.02)	21.02 (13.56)	-14.68 (13.72)	99.34 (0.25)	1.82 (10.22)	90.69 (5.60)

FIGURE 4 | Parasitological profiling. Six compounds representative of each of the major chemical scaffolds (pyridones, cyclic diaminopyrimidines, pyridyl derivatives, diaminopyrimidines, quinolones, tetrahydroisoquinolines and benzodiazoles) with potent activity against ookinetes and high parasite selectivity were selected for profiling in the *P. berghei* standard membrane feeding assay (Pb SMFA) and *P. falciparum* Dual Gamete Formation Assay (Pf DGFA).

with a >10-fold parasite specificity in their respective assay gives a collection of transmission-blocking molecules with a range of different phenotypes (**Figure 6** and **Supplementary Table S5**). Nevertheless, molecules from all three assays have demonstrated transmission-blocking activity in mosquito feeds (Almela et al., 2015; Miguel-Blanco et al., 2017; Colmenarejo et al., 2018).

DISCUSSION

The TCAMS library is the largest collection of antimalarial molecules in the public domain and has sparked several major antimalarial drug discovery campaigns. Antimalarial molecules that have additional transmission-blocking activity have the potential to make a significant contribution to malaria elimination and eradication and are prioritized for development (Burrows et al., 2017). The Pb ODA is a simple and relatively inexpensive assay that can characterize the transmission-blocking activity of hundreds of molecules with the gametocyte infected blood of a single mouse (compared to Pb SMFAs which can evaluate ∼2 molecules per mouse). It correlates well with SMFA data and the majority of identified molecules are also active against *P. falciparum* sexual stages.

TCMDC-135461, the representative pyridone molecule selected for profiling was the most potent molecule active in the Pb ODA but was less active against male and female gametocytes in the Pf DGFA. Other pyridones are known to act by targeting the parasite respiratory chain by inhibiting cytochrome bc_1 (Capper et al., 2015). Supporting this activity, mitochondrial respiration is essential for mosquito stage parasite development (Goodman et al., 2016) and other cytochrome bc_1 inhibitors such as atovaquone are established transmission-blocking molecules (Fowler et al., 1995). However, phase-1 clinical trials of the pyridone antimalarial molecule GSK932121 were halted after it showed acute cardiotoxicity in rats, thought to be through inhibition of mammalian cytochrome bc_1 (Capper et al., 2015). This suggests higher selectivity is required for other pyridones to be used as orally administered antimalarials. Recently, contact exposure of mosquitoes to atovaquone has shown to inhibit parasite development in the mosquito (Paton et al., 2019). This reinforces the potential of parasite cytochrome bc_1 inhibitors as transmission blocking agents. Given the extreme potency of TCMDC-135461, indoor residual spraying and/or baited sugar traps may be a practical, efficacious and safer method of utilizing this class of molecules to elicit a transmission-blocking response. TCMDC-134114, the representative diaminopyrimidine molecule was also potent in the Pb ODA and Pb SMFA. Interestingly it had male gametocyte-specific activity in the Pf DGFA. The diaminopyrimidine scaffold is found in many molecules targeting dihydrofolate reductase (DHFR), such as the antimalarial pyrimethamine. DHFR is required for parasite folate biosynthesis which is essential for generating the nucleotides required for DNA replication (Heinberg and Kirkman, 2015). Male gametogenesis requires three rounds of endomitosis to generate eight male gametes. In addition, ookinete development requires one round of meiosis. Therefore, activity in the Pb ODA (which includes male gametogenesis and ookinete development) and male-specific activity against gametocytes in the Pf DGFA is consistent with this mode of action for TCMDC-134114. Datamining the chemical structure of TCMDC-137173 (the

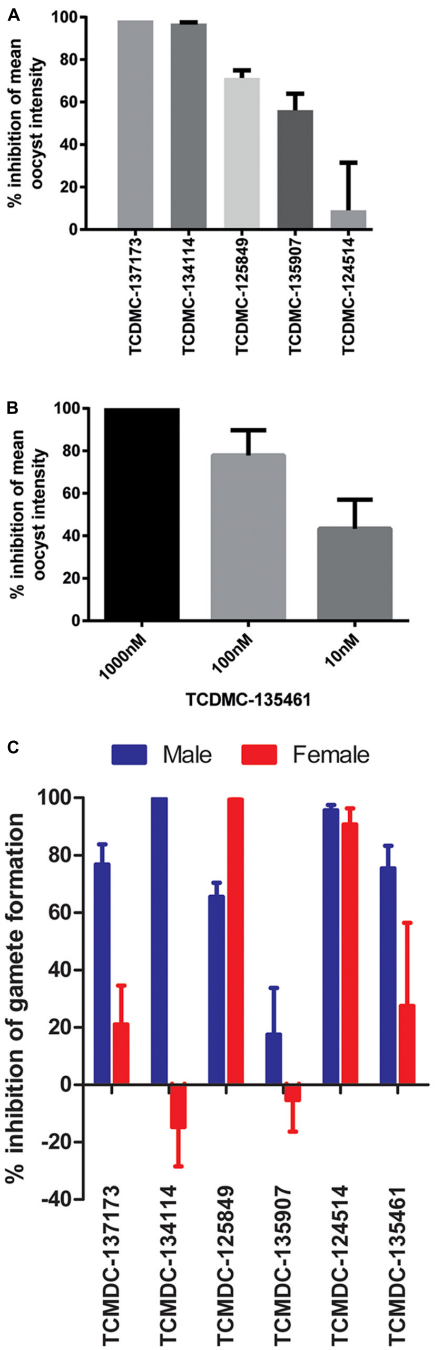

FIGURE 5 | Activity in other transmission-blocking assays. The six selected molecules were evaluated in the *P. berghei* standard membrane feeding assay (Pb SMFA). **(A)** Five molecules were tested at 1 μM to confirm transmission-blocking activity (n = 48–53 mosquitoes per treatment). Bars represent the mean of three biological repeats, error bars indicate the standard error of the mean (SEM) **(B)** The most potent compound in the Pb ODA, TCDMC-135461, was investigated over a range of concentrations in Pb SMFAs (n = 22–83 mosquitoes per condition). Bars represent the mean of three biological repeats, error bars indicate the standard error of the mean (SEM). **(C)** Additionally, the compounds were tested against male and female *P. falciparum* gametocytes at 1 μM in the Pf DGFA. Bars represent the mean of at least three biological repeats, error bars indicate the standard error of the mean (SEM).

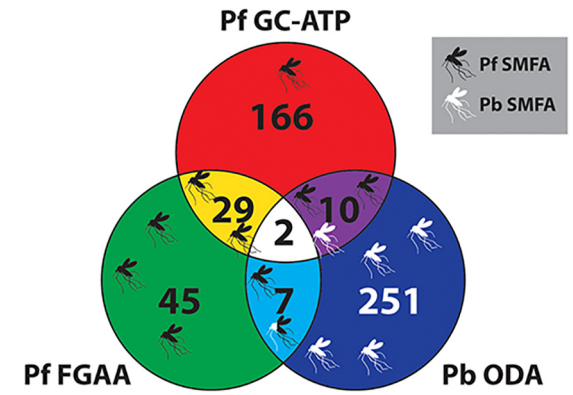

FIGURE 6 | Venn diagram comparing the TCAMS transmission-blocking across three transmission-blocking assay. Active compounds from the *P. berghei* ookinete development assay (Pb ODA) were compared with published activity against *P. falciparum* late stage gametocytes and *P. falciparum* female gametogenesis (Almela et al., 2015; Miguel-Blanco et al., 2017). To ensure parasite specificity, to be classed as active in a particular assay, parasite selectivity had to be greater than ten-fold compared to HepG2 cells **(Supplementary Table S5)**. Where specific compounds have been reported to block transmission in mosquito feeds, this has been mapped onto the Venn diagram as mosquitoes. Their position on the diagram indicates their activity profile in the three assays and the color represents Pf SMFA (Black), Pb SMFA (White) or both (Black and White).

representative quinolone compound) revealed that it is the established antimalarial quinolone endochin which was first reported in 1948 (Doggett et al., 2012). Since then, several endochin-like antimalarials have been developed, however, poor oral bioavailability has hampered their clinical progress (Nilsen et al., 2013; Miley et al., 2015). Like the pyridones, TCMDC-137173/endochin targets the parasite mitochondrial cytochrome bc_1 complex and therefore displays a transmission-blocking profile similar to TCMDC-135461. TCMDC-125849, the representative tetrahydroisoquinoline was moderately active in the Pb ODA with an IC_{50} of 268 nM. Reflecting this, it gave only 71.4% inhibition of oocyst intensity in the Pb SMFA at 1 μM. Supporting this level of transmission-blocking activity, 2 μM TCMDC-125849 reportedly gives 100% inhibition of oocyst intensity and total inhibition of male gametogenesis in *P. falciparum* (Colmenarejo et al., 2018). The chemical structure of TCMDC-125849 closely resembles emetine – a known antiprotozoal compound which inhibits protein synthesis (Toyé et al., 1977; Wong et al., 2014). Supporting this hypothesis of targeting such a fundamental biological pathway, 1 μM TCMDC-125849 inhibited both male and female gametogenesis (**Figure 5C**). In particular, female gametogenesis was inhibited by 99.3%. The female readout of the Pf DGFA relies on antibody detection of female gamete expression of Pfs25, which is held under translational repression in the female gametocyte. Therefore, inhibition of protein synthesis by TCMDC-125849 would be predicted to strongly reduce Pfs25 expression as observed. The representative benzodiazole TCMDC-124514 was also moderately active in the Pb ODA with an IC_{50} of 397 nM which was reflected by low inhibition of oocyst intensity (9.1%

inhibition) in the Pb SMFA. Interestingly at 1 μM it potently inhibited both male and female gametogenesis suggesting it targets biology fundamental to both gametocyte sexes. In support of this, TCMDC-124514 has been hypothesized to be a Coenzyme A biosynthesis inhibitor (Weidner et al., 2017) which would both affect energy and lipid metabolism – both fundamental pathways within the parasite. The difference in species activity suggest that TCMDC-124514 is more active against *P. falciparum* than *P. berghei*. The representative pyridyl derivative, TCMDC-135907 showed moderate activity in the Pb ODA with an IC_{50} of 381 nM, which again was reflected incomplete inhibition at 1 μM in the Pb SMFA. There is no data in the literature to suggest a mode of action for this compound, however, data presented here suggests it targets the parasite after gamete formation.

When comparing the activities of several high throughput transmission assays against the TCAMS collection, it is clear to see that no single assay is sufficient to identify all transmission-blocking molecules. Likely this is due to the distinct (but overlapping) cell biology that they interrogate. To date, a high throughput assay that incorporates the entire cell biology of transmission does not exist. Therefore, to maximize the discovery of new transmission-blocking antimalarials, it would be prudent to use several assays and not rely on the data generated by a single assay alone.

MATERIALS AND METHODS

Compound Handling

The TCAMS library was provided in duplicate on assay-ready 384 well plates by GSK. 50 nl of each compound in 100% DMSO was stamped into each well with one column containing DMSO-only (negative control) and one column containing cycloheximide at a final assay concentration of 10 μM (positive control). Assay plates were stored at −20°C until used. Compounds selected for further investigation were supplied by GSK as 10 mM stock solutions in 100% DMSO.

P. berghei Ookinete Development Assay (Pb ODA)

All work involving laboratory animals was performed in accordance with the EU regulations EU Directive 86/609/EEC and within the regulations of the United Kingdom Animals (Scientific Procedures) Act 1986. The Pb ODA was performed exactly as described in Delves M.J. et al. (2012). Female T0 mice were treated with an intraperitoneal (ip) injection of 200 μl 6 mg/ml phenylhydrazine to induce hyperreticulocytosis. Three days later, the treated mice were infected with approximately 10^8 parasites by ip injection of blood from a donor mouse infected with *Plasmodium berghei* expressing GFP under the control of the ookinete-specific CTRP promoter (Vlachou et al., 2004). Three days afterward, the presence of high levels of gametocytes were confirmed by stimulating and observing male gametogenesis (exflagellation). A drop of blood was sampled from the tail of each mouse and mixed with ookinete medium (RPMI medium with 25 mM HEPES, 2 mM L-glutamine, 2 g/l sodium bicarbonate, 50 mg/l hypoxanthine and 100 μM anthurenic acid, adjusted to pH 7.4, plus 20% FBS) under a coverslip on a glass slide. Ten minutes later vigorously beating exflagellation centers were observed by phase contrast microscopy and invariably showed >10 centers per field at ×40 objective. Infected mice were anesthetized in batches of five, rapidly exsanguinated, blood pooled and immediately transferred to ookinete medium at a 1:20 dilution. 50 μl of blood/medium was then rapidly dispensed into each well of the assay plates using a Multidrop Combi automated dispenser (Thermo Scientific) and the plates incubated in a humidified incubator at 19°C in the dark for 22 h. GFP fluorescence was then measured in a fluorescence plate reader (BMG Labtech FluoSTAR Omega) and inhibition of ookinete production calculated in relation to the positive and negative controls using the formula:% inhibition of ookinete production = 100 − [(well_fluorescence − positive_control)/(negative_control − positive_control) × 100].

Compound Clustering and Computational Analysis

Clustering was performed following the computational methods described in Gamo et al. (2010). Briefly, molecular frameworks were calculated using an in-house implementation of the algorithm described previously (Bemis and Murcko, 1996). Compounds were also classified in chemical families using the Daylight fingerprint methods with a Tanimoto similarity index of 0.85, following the procedures in the Daylight Information Systems manual (Daylight Chemical Information Systems, 2019). The dendrogram in **Figure 3** was constructed using data obtained from the FragFP clustering algorithm performed within OSIRIS DataWarrior Version 04.07.03 and visualized using Cytoscape Version 3.7.1.

P. berghei Standard Membrane Feeding Assays (Pb SMFAs)

Membrane feeding assays were performed essentially as described in Ramakrishnan et al. (2013). Briefly, a phenylhydrazine-treated mouse (see above) was infected with blood from a donor mouse infected with *P. berghei* 507 parasites that constitutively express GFP throughout the parasite life cycle (Janse et al., 2006). Three days later the infected mouse was rapidly exsanguinated and the parasite-infected blood diluted at 1:10 dilution in naïve mouse blood pre-warmed to 37°C. Working as quickly as possible, the blood mix was divided into 500 μl aliquots and mixed with test compounds or DMSO alone at appropriate concentrations (final DMSO concentration of 0.2%) and immediately added to plastic water-jacketed membrane feeders and fed to *Anopheles stephensi* SDA 500 strain mosquitoes. After the feed, mosquitoes were maintained at 19°C/80% relative humidity overnight before unfed mosquitoes were removed. Fed mosquitoes continued to be maintained on 8% fructose (w/v)/0.05% (w/v) p-aminobenzoic acid for 7 days before their midguts were dissected out and oocyst burden quantified using fluorescence microscopy and semi-automated counting analysis (Delves and Sinden, 2010). Data presented is the mean of three independent experiments.

P. falciparum Dual Gamete Formation Assay (Pf DGFA)

Compounds were tested exactly as described in Ruecker et al. (2014) in the carry-over assay format. Briefly, functionally mature stage V male and female gametocytes were generated by seeding *P. falciparum* NF54 strain asexual cultures at 1% parasitemia and 4% hematocrit and replacing culture medium (RPMI medium with 25 mM HEPES, 2 mM L-glutamine, 2 g/l sodium bicarbonate, 50 mg/l hypoxanthine plus 10% human serum) daily for 14 days whilst maintaining a constant temperature of 37°C and a gas mix of 3% CO_2, 5%O_2, 92% N_2. Gametocyte cultures were diluted to 25 million cells/ml (including erythrocytes) and 200 μl added to each well of a round-bottomed 96 well plate containing test compounds. Plates also contained DMSO negative and 20 μM methylene blue positive control wells. After a 24 h incubation at 37°C, gametogenesis was stimulated by transferring the gametocytes to a flat-bottomed 96 well plate containing 10 μl of ookinete medium at room temperature. Twenty minutes later, the emergence of male gametes was recorded microscopically using phase contrast and ×10 objective lens. The plate was then further incubated at 26°C for another 24 h to allow emerged female gametes to maximally express Pfs25 on their cell surface. An anti-Pfs25 antibody (Mab 4B7) conjugated to the Cy3 fluorophore was added to the plates and female gametes detected by live fluorescence microscopy at ×10 objective. Data was then processed using custom image analysis algorithms and percent inhibition in respect to positive (methylene blue) and negative (DMSO) controls was calculated. Data presented is the mean of four independent biological repeats.

P. falciparum Asexual Growth Inhibition Assay (Pf GIA)

The asexual activity of active compounds was tested in dose response with parasite lactate dehydrogenase (LDH) activity used as a readout of parasite viability as described in Gamo et al. (2010). Briefly, 3D7-strain *P. falciparum* asexual parasites were diluted to 0.25% parasitemia, 2% hematocrit in culture medium composed of RPMI medium with 25 mM HEPES, 2% D-sucrose, 0.3% L-glutamine, 150 μM hypoxanthine plus 5% albumax. 25 μl of parasite inoculum was then dispensed into each well of a 384 well plate containing test compounds and positive (50 μM chloroquine) and negative (DMSO) controls. Plates were incubated for 72 h at 37°C in a 5% CO_2, 5%O_2, 90% N_2 environment before being frozen at −70°C. Plates were then thawed and 70 μl of reaction mix (143 mM sodium L-lactate, 143 mM 3-acetyl pyridine adenine dinucleotide, 178.75 mM Nitro Blue tetrazolium chloride, 286 mg/ml diaphorase (2.83 U/ml), 0.7% Tween 20, 100 mM Tris–HCl pH 8.0) was added to each well using a Multidrop Combi automated dispenser. Plates were shaken to mix and then absorbance at 650 nm was measured after 10 min incubation at room temperature. Percent inhibition of asexual growth was then calculated with respect to positive and negative controls. Data presented is the mean of three independent biological replicates.

HepG2 Cytotoxicity Assay

The activity of active compounds against HepG2 cells was performed as described in Delves et al. (2018). Briefly, HepG2 cells were seeded onto compound-treated 384 well plates at a density of 2,500 cells per well in Minimal Essential Medium (MEM) plus 10% fetal bovine serum and 1% non-essential amino acids solution (NEAA). Cells were incubated with test compounds or 50 μM doxorubicin (positive) and DSMO (negative) controls at 37°C for 48 h in a humidified 5% CO_2 atmosphere. Plates were then treated with Resazurin to a final concentration of 45 μM for 4 h. Cell viability was then measured in a fluorescent plate reader and percent inhibition calculated with respect to positive and negative controls.

DATA AVAILABILITY

All datasets generated for this study are included in the manuscript and/or **Supplementary Files**.

ETHICS STATEMENT

The animal study was reviewed and approved by Imperial College Animal Welfare Ethical Review Body.

AUTHOR CONTRIBUTIONS

MD, RS, F-JG, and DL designed the study. MD performed the Pb ookinete assay. ML-M performed the chemical clustering analysis. MD and LU performed the Pb SMFAs. AR performed the Pf DGFA.

FUNDING

This work was supported by a grant to RS from the Medicines for Malaria Venture (#MMV 08/2800/01). MD was funded by a Wellcome/LSHTM ISSF Fellowship.

ACKNOWLEDGMENTS

We would like to acknowledge Mark Tunnicliff for provision of mosquitoes and Dolores Jimenez-Alfaro for providing support in compound handling and platemap design.

SUPPLEMENTARY MATERIAL

The Supplementary Material for this article can be found online at: https://www.frontiersin.org/articles/10.3389/fmicb.2019.02134/full#supplementary-material

REFERENCES

Almela, M. J., Lozano, S., Lelièvre, J., Colmenarejo, G., Coterón, J. M., Rodrigues, J., et al. (2015). A new set of chemical starting points with *Plasmodium falciparum* transmission-blocking potential for antimalarial drug discovery. *PLoS One* 10:e0135139. doi: 10.1371/journal.pone.0135139

Baragaña, B., Hallyburton, I., Lee, M. C. S., Norcross, N. R., Grimaldi, R., Otto, T. D., et al. (2015). A novel multiple-stage antimalarial agent that inhibits protein synthesis. *Nature* 522, 315–320. doi: 10.1038/nature14451

Bemis, G. W., and Murcko, M. A. (1996). the properties of known drugs. 1. molecular frameworks. *J. Med. Chem.* 39, 2887–2893.

Burrows, J. N., Duparc, S., Gutteridge, W. E., Hooft van Huijsduijnen, R., Kaszubska, W., Macintyre, F., et al. (2017). New developments in anti-malarial target candidate and product profiles. *Malar. J.* 16:26. doi: 10.1186/s12936-016-1675-x

Calderón, F., Vidal-Mas, J., Burrows, J., de la Rosa, J. C., Jiménez-Díaz, M. B., Mulet, T., et al. (2012). A divergent sar study allows optimization of a potent 5-ht2c inhibitor to a promising antimalarial scaffold. *ACS Med. Chem. Lett.* 3, 373–377. doi: 10.1021/ml300008j

Capper, M. J., O'Neill, P. M., Fisher, N., Strange, R. W., Moss, D., Ward, S. A., et al. (2015). Antimalarial 4(1H)-pyridones bind to the Qi site of cytochrome bc1. *Proc. Natl. Acad. Sci. U.S.A.* 112, 755–760. doi: 10.1073/pnas.1416611112

Colmenarejo, G., Lozano, S., González-Cortés, C., Calvo, D., Sanchez-Garcia, J., Matilla, J. P., et al. (2018). Predicting transmission blocking potential of anti-malarial compounds in the mosquito feeding assay using *Plasmodium falciparum* male gamete inhibition assay. *Sci. Rep.* 8, 7764–7764. doi: 10.1038/s41598-018-26125-w

Daylight Chemical Information Systems, (2019). *Dlight Theory Manual*. Available at: https://www.daylight.com/dayhtml/doc/theory/index.html (Accessed May 20, 2019).

Delves, M. J., Miguel-Blanco, C., Matthews, H., Molina, I., Ruecker, A., Yahiya, S., et al. (2018). A high throughput screen for next-generation leads targeting malaria parasite transmission. *Nat. Commun.* 9:3805. doi: 10.1038/s41467-018-05777-2

Delves, M. J., Ramakrishnan, C., Blagborough, A. M., Leroy, D., Wells, T. N. C., and Sinden, R. E. (2012). A high-throughput assay for the identification of malarial transmission-blocking drugs and vaccines. *Int. J. Parasitol.* 42, 999–1006. doi: 10.1016/j.ijpara.2012.08.009

Delves, M., Plouffe, D., Scheurer, C., Meister, S., Wittlin, S., Winzeler, E. A., et al. (2012). The activities of current antimalarial drugs on the life cycle stages of *Plasmodium*: a comparative study with human and rodent parasites. *PLoS Med.* 9:e1001169. doi: 10.1371/journal.pmed.1001169

Delves, M. J., and Sinden, R. E. (2010). A semi-automated method for counting fluorescent malaria oocysts increases the throughput of transmission blocking studies. *Malar. J.* 9:35. doi: 10.1186/1475-2875-9-35

Doggett, J. S., Nilsen, A., Forquer, I., Wegmann, K. W., Jones-Brando, L., Yolken, R. H., et al. (2012). Endochin-like quinolones are highly efficacious against acute and latent experimental toxoplasmosis. *PNAS* 109, 15936–15941.

Eziefula, A. C., Bousema, T., Yeung, S., Kamya, M., Owaraganise, A., Gabagaya, G., et al. (2013). Single dose primaquine for clearance of *Plasmodium falciparum* gametocytes in children with uncomplicated malaria in Uganda: a randomised, controlled, double-blind, dose-ranging trial. *Lancet Infect. Dis.* 14, 130–139. doi: 10.1016/S1473-3099(13)70268-8

Fowler, R. E., Sinden, R. E., and Pudney, M. (1995). Inhibitory activity of the anti-malarial atovaquone (566C80) against ookinetes, oocysts, and sporozoites of *Plasmodium berghei*. *J. Parasitol.* 81, 452–458.

Gamo, F.-J., Sanz, L. M., Vidal, J., de Cozar, C., Alvarez, E., Lavandera, J.-L., et al. (2010). Thousands of chemical starting points for antimalarial lead identification. *Nature* 465, 305–310. doi: 10.1038/nature09107

Goodman, C. D., Siregar, J. E., Mollard, V., Vega-Rodríguez, J., Syafruddin, D., Matsuoka, H., et al. (2016). Parasites resistant to the antimalarial atovaquone fail to transmit by mosquitoes. *Science* 352, 349–353. doi: 10.1126/science.aad9279

Heinberg, A., and Kirkman, L. (2015). The molecular basis of antifolate resistance in *Plasmodium falciparum*: looking beyond point mutations. *Ann. N. Y. Acad. Sci. U.S.A.* 1342, 10–18. doi: 10.1111/nyas.12662

Janse, C. J., Franke-Fayard, B., and Waters, A. P. (2006). Selection by flow-sorting of genetically transformed, GFP-expressing blood stages of the rodent malaria parasite, *Plasmodium berghei*. *Nat. Protoc.* 1, 614–623.

Miguel-Blanco, C., Molina, I., Bardera, A. I., Díaz, B., de Las Heras, L., Lozano, S., et al. (2017). Hundreds of dual-stage antimalarial molecules discovered by a functional gametocyte screen. *Nat. Commun.* 8, 15160. doi: 10.1038/ncomms15160

Miley, G. P., Pou, S., Winter, R., Nilsen, A., Li, Y., Kelly, J. X., et al. (2015). ELQ-300 prodrugs for enhanced delivery and single-dose cure of malaria. *Antimicrob. Agents Chemother.* 59, 5555–5560. doi: 10.1128/AAC.01183-15

Nilsen, A., LaCrue, A. N., White, K. L., Forquer, I. P., Cross, R. M., Marfurt, J., et al. (2013). Quinolone-3-diarylethers: a new class of antimalarial drug. *Sci. Transl. Med.* 5:177ra37. doi: 10.1126/scitranslmed.3005029

Paton, D. G., Childs, L. M., Itoe, M. A., Holmdahl, I. E., Buckee, C. O., and Catteruccia, F. (2019). Exposing *Anopheles* mosquitoes to antimalarials blocks *Plasmodium parasite* transmission. *Nature* 567, 239–243. doi: 10.1038/s41586-019-0973-1

Plouffe, D. M., Wree, M., Du, A. Y., Meister, S., Li, F., Patra, K., et al. (2016). High-throughput assay and discovery of small molecules that interrupt malaria transmission. *Cell Host Microbe* 19, 114–126. doi: 10.1016/j.chom.2015.12.001

Rabinovich, R. N., Drakeley, C., Djimde, A. A., Hall, B. F., Hay, S. I., Hemingway, J., et al. (2017). malERA: an updated research agenda for malaria elimination and eradication. *PLoS Med.* 14:e1002456. doi: 10.1371/journal.pmed.1002456

Ramakrishnan, C., Delves, M. J., Lal, K., Blagborough, A. M., Butcher, G., Baker, K. W., et al. (2013). Laboratory maintenance of rodent malaria parasites. *Methods Mol. Biol.* 923, 51–72.

Raphemot, R., Lafuente-Monasterio, M. J., Gamo-Benito, F. J., Clardy, J., and Derbyshire, E. R. (2015). Discovery of dual stage malaria inhibitors with new targets. *Antimicrob. Agents Chemother.* 60, 1430–1437. doi: 10.1128/AAC.02110-15

Ruecker, A., Mathias, D. K., Straschil, U., Churcher, T. S., Dinglasan, R. R., Leroy, D., et al. (2014). A male and female gametocyte functional viability assay to identify biologically relevant malaria transmission-blocking drugs. *Antimicrob. Agents Chemother.* 58, 7292–7302. doi: 10.1128/AAC.03666-14

Sanz, L. M., Jiménez-Díaz, M. B., Crespo, B., De-Cozar, C., Almela, M. J., Angulo-Barturen, I., et al. (2011). Cyclopropyl carboxamides a novel chemical class of antimalarial agents identified in a phenotypic screen. *Antimicrob. Agents Chemother.* 55, 5740–5745. doi: 10.1128/AAC.05188-11

Toyé, P. J., Sinden, R. E., and Canning, E. U. (1977). The action of metabolic inhibitors on microgametogenesis in Plasmodium yoelii nigeriensis. *Z. Parasitenkd* 53, 133–141.

Vlachou, D., Zimmermann, T., Cantera, R., Janse, C. J., Waters, A. P., and Kafatos, F. C. (2004). Real-time, in vivo analysis of malaria ookinete locomotion and mosquito midgut invasion. *Cell. Microbiol.* 6, 671–685.

Weidner, T., Lucantoni, L., Nasereddin, A., Preu, L., Jones, P. G., Dzikowski, R., et al. (2017). Antiplasmodial dihetarylthioethers target the coenzyme A synthesis pathway in *Plasmodium falciparum* erythrocytic stages. *Malar. J.* 16:192. doi: 10.1186/s12936-017-1839-3

Williamson, A. E., Ylioja, P. M., Robertson, M. N., Antonova-Koch, Y., Avery, V., Baell, J. B., et al. (2016). Open source drug discovery: highly potent antimalarial compounds derived from the tres cantos arylpyrroles. *ACS Cent. Sci.* 2, 687–701.

Wong, W., Bai, X., Brown, A., Fernandez, I. S., Hanssen, E., Condron, M., et al. (2014). Cryo-EM structure of the *Plasmodium falciparum* 80S ribosome bound to the anti-protozoan drug emetine. *eLife* 3:e03080. doi: 10.7554/eLife.03080

Conflict of Interest Statement: F-JG and ML-M are employed by GlaxoSmithKline.

The remaining authors declare that the research was conducted in the absence of any commercial or financial relationships that could be construed as a potential conflict of interest.

frontiers in Microbiology

ORIGINAL RESEARCH
published: 20 September 2019
doi: 10.3389/fmicb.2019.02193

An MFS-Domain Protein Pb115 Plays a Critical Role in Gamete Fertilization of the Malaria Parasite *Plasmodium berghei*

Fei Liu[1], Qingyang Liu[1], Chunyun Yu[1], Yan Zhao[1], Yudi Wu[1], Hui Min[1,2], Yue Qiu[3], Ying Jin[4], Jun Miao[2], Liwang Cui[2] and Yaming Cao[1]**

[1] Department of Immunology, College of Basic Medical Sciences, China Medical University, Shenyang, China, [2] Department of Internal Medicine, Morsani College of Medicine, University of South Florida, Tampa, Tampa, FL, United States, [3] The First Hospital of China Medical University, Shenyang, China, [4] Liaoning Research Institute of Family Planning, Shenyang, China

Sexual reproduction is an essential process in the *Plasmodium* life cycle and a vulnerable step for blocking transmission from the human host to mosquitoes. In this study, we characterized the functions of a conserved cell membrane protein P115 in the rodent malaria parasite *Plasmodium berghei* ANKA. Pb115 was expressed in both asexual stages (schizonts) and sexual stages (gametocytes, gametes, and ookinetes), and was localized on the plasma membrane of gametes and ookinetes. In *P. berghei*, genetic deletion of *Pb115* (Δ*pb115*) did not affect asexual multiplication, nor did it affect gametocyte development or exflagellation of the male gametocytes. However, mosquitoes fed on Δ*pb115*-infected mice showed 74% reduction in the prevalence of infection and 96.5% reduction in oocyst density compared to those fed on wild-type *P. berghei*-infected mice. The Δ*pb115* parasites showed significant defects in the interactions between the male and female gametes, and as a result, very few zygotes were formed in ookinete cultures. Cross fertilization with the male-defective Δ*pbs48/45* line and the female-defective Δ*pfs47* line further indicated that the fertilization defects of the Δ*pb115* lines were present in both male and female gametes. We evaluated the transmission-blocking potential of Pb115 by immunization of mice with a recombinant Pb115 fragment. *In vivo* mosquito feeding assay showed Pb115 immunization conferred modest, but significant transmission reducing activity with 44% reduction in infection prevalence and 39% reduction in oocyst density. Our results described functional characterization of a conserved membrane protein as a fertility factor in *Plasmodium* and demonstrated transmission-blocking potential of this antigen.

Keywords: *Plasmodium berghei*, yeast protein expression, gamete, gamete interaction, transmission-blocking

OPEN ACCESS

Edited by:
Isabelle Morlais,
Institut de Recherche pour le Développement (IRD), France

Reviewed by:
Gabriele Pradel,
RWTH Aachen University, Germany
Kai Matuschewski,
Humboldt University of Berlin, Germany
Sonja Frölich,
The University of Adelaide, Australia

****Correspondence:***
Liwang Cui
lcui@health.usf.edu
Yaming Cao
ymcao@cmu.edu.cn

Specialty section:
This article was submitted to Infectious Diseases, a section of the journal Frontiers in Microbiology

Received: *31 March 2019*
Accepted: *06 September 2019*
Published: *20 September 2019*

Citation:
Liu F, Liu Q, Yu C, Zhao Y, Wu Y, Min H, Qiu Y, Jin Y, Miao J, Cui L and Cao Y (2019) An MFS-Domain Protein Pb115 Plays a Critical Role in Gamete Fertilization of the Malaria Parasite Plasmodium berghei. Front. Microbiol. 10:2193. doi: 10.3389/fmicb.2019.02193

INTRODUCTION

Malarial incidence has significantly decreased in recent years due to a range of actions, including the deployment of insecticide-treated nets, indoor residual spraying and artemisinin-based combination therapies (Bhatt et al., 2015). Nevertheless, recent World Health Organization reports showed that the global progress toward malaria elimination has stalled (World Health Organization [WHO], 2018). To achieve global elimination of malaria, an integrated malaria control strategy and novel interventions are needed, which may include measures that interrupt and inhibit disease transmission.

During the complex life cycle of malaria parasite, sexual stages are obligative for the transmission of the parasite from the human host to the mosquitoes. Male and female gametocytes formed in the human blood, after ingestion by a female anopheline mosquito, undergo gametogenesis to form gametes, which then fuse to form zygotes. Later, zygotes mature into ookinetes, which penetrate the midgut epithelium to differentiate into oocysts.

Transmission from the human host to the mosquito represents a major population bottleneck in the life cycle of the parasite (Vaughan, 2007). Transmission-blocking vaccines (TBVs) target this bottleneck by eliciting antibodies that inhibit the fusion of the male and female gametes (pre-fertilization) and maturation from zygotes to ookinetes (post-fertilization). To date, a substantial number of antigens expressed during sexual development have been studied for their TBV potentials (Nikolaeva et al., 2015; Wu et al., 2015; Delves et al., 2018), but only three antigens, namely the pre-fertilization antigens Pfs48/45 (Kocken et al., 1993; Outchkourov et al., 2008; Chowdhury et al., 2009) and Pfs230 (Williamson et al., 1993; Lee et al., 2017; Tachibana et al., 2019), as well as the post-fertilization antigen Pfs25 (Kaslow et al., 1988; Shimp et al., 2013; Talaat et al., 2016; Sagara et al., 2018) and its ortholog Pvs25 in *Plasmodium vivax* (Tsuboi et al., 1998; Sagara et al., 2018), have been extensively investigated as lead vaccine candidates. However, all these TBV candidates are conformational antigens containing multiple disulfide bridges, and the production of correctly folded antigens is an important challenge (Sauerwein and Bousema, 2015). Therefore, continuous efforts on TBV antigen discovery are warranted.

The deciphering of *Plasmodium* genomes has provided an unprecedented opportunity for large-scale functional studies toward a better understanding of the fundamental developmental biology of the parasite (Gardner et al., 2002; Hall et al., 2005). This has also fueled the functional screening of potential TBV antigens during ookinete development in the more genetically amenable rodent parasite *Plasmodium berghei* (Ecker et al., 2008). Using a similar strategy, we identified Pb115, an evolutionarily conserved, putative membrane protein that is expressed in both asexual and sexual stages of the malaria parasites. Through genetic manipulation studies in *P. berghei*, we found that the mutant parasites lacking *Pb115* had a major defect in ookinete formation, resulting in transmission failure to the mosquitoes. Genetic crosses revealed that both male and female gametes require this protein for gamete recognition and attachment. Immunization of mice with the recombinant Pb115 protein induced strong antibody responses that effectively blocked formation of ookinetes, highlighting the TBV potential of this protein.

MATERIALS AND METHODS

Mice, Parasites, and Mosquitoes

Six-to-eight-week old female BALB/c mice were purchased from Beijing Animal Institute (Beijing, China). The *P. berghei* ANKA strain 2.34 was maintained by serial passage and used for challenge infections as described previously (Blagborough and Sinden, 2009). Adult female *Anopheles stephensi* mosquitoes (Hor strain) were reared in an insectary under 25°C, 50–80% humidity and a 12 h light/dark cycle, and fed 10% (w/v) glucose solution-soaked cotton balls. All animal experiments were approved by the animal ethics committee of China Medical University.

Sequence Analysis

To identify genes encoding potential ookinete surface proteins, we searched the malaria database PlasmoDB[1] for proteins expressed in ookinetes with a putative signal peptide or at least one transmembrane domain. We identified a gene *PBANKA_0931000*, which encodes a putative protein of 115 kDa, henceforth designated as Pb115. The sequences of its orthologs in other *Plasmodium* species were retrieved from PlasmoDB and aligned using the ClustalW multiple sequence alignment program.

Generation of Transgenic Parasites

The HA-tagging and gene-knockout (KO) targeting vectors for *Pb115* (PbGEM-290856 and PbGEM-290848) were acquired from PlasmoGEM (Wellcome Trust Sanger Institute, Cambridge, United Kingdom). HA-tagged (pb115-HA) and *Pb115* KO (Δ*pb115*) parasite lines were generated by homologous recombination as previously described (Braks et al., 2006). To obtain schizonts for transfection, parasitized red blood cells (RBCs) were collected from mice at day 4 after infection and cultured at 37°C overnight in the culture medium [RPMI 1640, 20% (v/v) fetal calf serum, and 50 mg/L penicillin and streptomycin] at 0.5 mL blood/50 mL medium. The culture was then fractionated on a 55% (v/v) Nycodenz cushion to purify the schizonts (Dempsey et al., 2013). Linearized plasmids were transfected into the schizonts using Nucleofector II (Lonza, Stockholm, Sweden), and the parasite suspension was intravenously injected into two BALB/c mice through the tail vein. At 24 h after injection, mice were treated with pyrimethamine (0.07 mg/ml) via drinking water for 3–4 days. PCR was used to identify the desired integration events in transfected parasites using integration-specific primers (**Supplementary Table S1**). For tagging, the HA tag was inserted at the C-terminus of the *pb115* gene, and for KO, the open reading frame of *pb115* was replaced with an *hdhfr* expression cassette. Parasites were cloned by limiting dilution. Primers for 5′ or 3′ recombination fragments and integration-specific PCR are listed in **Supplementary Table S1**.

Expression of Recombinant Pb115 (rPb115) and Immunization

A 205 amino acid (aa) fragment of the Pb115 (aa 756–960) was expressed in the yeast *Pichia pastoris*. Briefly, the Pb115 DNA fragment was amplified using primers CGT ACGTACAAAATATTAAAACTATTTTTTCATCATTT and TTGCGGCCGCTCTTGCCTTCCAATATATGGTAAATATTAG (restriction sites underlined) and cloned into the pPIC3.5K(+His) plasmid. A positive yeast strain was cultured in 1 L of BMMG medium and rPb115 expression was induced with

[1] http://www.plasmodb.org

methanol. Yeast cells were collected by centrifugation and lysed using an ATS high pressure homogenizer (ATS Engineering Inc., Germany). Recombinant proteins were purified with the Ni-NTA column (Novagen, Germany). The quality of purified protein was analyzed by SDS-PAGE.

To generate antisera against Pb115, 6–8-week old female BALB/c mice (n = 5) were immunized with 50 μg of purified rPb115 emulsified with complete Freund's adjuvant. Mice were then given two booster injections at 2-week intervals with 25 μg of protein, each emulsified with incomplete Freund's adjuvant. Mice in the control group (n = 5) were immunized with adjuvant formulations in phosphate buffered saline (PBS, pH 7.0). Two weeks after the final immunization, blood was collected from mice via cardiac puncture and allowed to clot at room temperature to obtain the antisera. An enzyme-linked immunoassay (ELISA) was used to analyze the antibody titers as previously described (Chan et al., 2014).

Western Blot

Western blots were performed with parasite lysates and protein fractions of different developmental stages. Purified schizonts, gametocytes, and ookinetes were treated with 0.15% saponin (Sigma) in PBS for 10 min on ice. Parasites were collected by centrifugation and washed once with PBS. Parasite proteins were collected following repeated extraction in PBS containing 1% Triton X-100, 2% SDS and protease inhibitors (Roche, Basel, Switzerland) for 30 min at room temperature. Lysates of non-infected erythrocytes and Δ*pb115* ookinetes were used as negative controls. For subcellular protein fractionation, plasma membrane (PM) and cytoplasm of the parasites were separated using the Minute™ Plasma Membrane Protein Isolation and Cell Fractionation Kit (Invent Biotechnologies Inc., United States) according to the manufacturer's instructions. Protein concentration was determined using the BCA method, and equal amounts of protein lysates or cellular fractions (10 μg) were separated in 6% SDS-PAGE gels. For Western blots, proteins were transferred to a 0.22 μm polyvinylidene difluoride membrane (Bio-Rad, Hercules, CA, United States). The membrane was blocked with 5% non-fat milk in TBS buffer containing 0.1% Tween 20 (TBST) for 2 h, and then probed with anti-rPb115 antisera at 1:1000 or the anti-HA monoclonal antibody (mAb) at 1:1000 (Invitrogen, Carlsbad, CA, United States) for 2 h. Mouse anti-PbHsp70 antiserum (1:1000) was used as a control to estimate protein loading. After washing three times with TBST, bound primary antibodies were detected with HRP-conjugated goat anti-mouse antibodies (Invitrogen) diluted 1:10,000 in TBST. After three washes with TBST, proteins on the blot were visualized using a Pierce ECL Western Blotting Kit (Thermo Fisher Scientific). Band intensities were measured by ImageJ and the relative expression levels of Pb115 protein were normalized against those of PbHsp70 for the corresponding stages.

Indirect Immunofluorescence Assay

For Indirect Immunofluorescence Assay (IFA), HA-tagged or wild-type (WT) parasites were fixed with 4% paraformaldehyde and 0.0075% glutaraldehyde in PBS for 20 min at room temperature and rinsed with 50 mM glycine in PBS. To differentiate internal and external protein localizations, cells were either permeabilized with 0.1% Triton X-100/PBS for 10 min or directly processed without permeabilization. To liberate schizonts and gametocytes from the enveloping RBC and parasitophorous vacuole membranes, schizonts and gametocytes were treated with 0.05% saponin/PBS for 3 min at 37°C prior to fixation. Without further membrane permeabilization, cells were washed in PBS and then treated with 0.1 mg/ml of sodium borohydride in PBS for 10 min to reduce the free aldehyde groups (Tonkin et al., 2004). After blocking with PBS containing 3% BSA/PBS at 37°C for 1 h, WT and Pb115-HA parasites were incubated with mouse anti-rPb115 antisera (1:500) and mouse anti-HA mAb (1:500, Invitrogen), respectively, at 37°C for 1 h. Cells were co-incubated with rabbit antisera against PbMSP1, Pbg377, α-tubulin and PSOP25 as stage-specific markers for schizonts, female gametocytes/gametes, male gametocytes/gametes, and ookinetes, respectively. Then the slides were washed three times with PBS and incubated with polyclonal Alexa Flour 488-conjugated goat-anti-mouse IgG secondary antibodies (1:500, Invitrogen) and Alexa Flour 555-conjugated goat-anti-rabbit IgG secondary antibodies (1:500, Cell signaling), respectively, at 37°C for 30 min. Parasite nuclei were stained with 4, 6-diamidino-2-phenylindole (DAPI, Invitrogen) at a final concentration of 1 μg/mL. As negative controls, WT ookinete smears were incubated mouse anti-HA mAb (1:1000, Invitrogen) and control sera obtained from mice immunized with adjuvant emulsified in PBS as primary antibodies, or secondary antibodies alone. Slides were mounted with ProLong® Gold antifade reagent (Invitrogen) and observed under a Nikon C2 fluorescence confocal laser scanning microscope.

Phenotypic Analysis of Δ*pb115*

To study the functions of Pb115 during the *Plasmodium* development, mice in each group were injected with either 1×10^6 WT *P. berghei*- or Δ*pb115*-infected RBCs (iRBCs) (Clone 1 and Clone 2). Parasitemia and mortality of mice were monitored daily. To determine the effect on parasite sexual development, mice were pre-treated with 0.2 mL of 6 mg/mL phenylhydrazine for 3 days before injection of iRBCs. On day 3 after infection, gametocytemia and the gametocyte sex ratio were determined by Giemsa-stained tail blood smears (Guttery et al., 2014). At least 100 mature gametocytes were quantified as males and females to determine the gametocyte sex ratio (Liu et al., 2018). Exflagellation centers of male gametocytes and male–female gametes interactions were quantified as previously described (Tewari et al., 2010). In short, 10 μL tail blood from infected mice was added to 40 μL standard ookinete medium (RPMI 1640 with 50 mg/L penicillin, 50 mg/L streptomycin, 100 mg/L neomycin, 20% [v/v] heat-inactivated fetal calf serum [FCS], pH 8.0). Fifteen minutes after induction of gamete formation at 25°C, 1 μL of culture was placed on a coverslip (Matsunami Glass Ind., Ltd., Japan) and analyzed under a light microscope (40× objective). The exflagellation centers were counted as an exflagellating male gametocyte with four red blood cells in 10 min. Male–female gametes interactions were counted as the males attached females for more than 3 s during a period

of 20 min in 10 fields (40× objective) (van Dijk et al., 2010). To count the macrogamete numbers, ookinete culture was set up as described above. After incubation at 25°C for 15 min, 1 μL of culture were placed on a coverslip and female gametes were stained with mouse anti-Pbs21 antibody (1:1000) without permeabilization. The numbers of female gametes in 1 μL of culture were counted under a fluorescence microscope (100× oil objective). The culture was further incubated at 19°C; 1 μL of culture was taken out at 2 h and 24 h to determine the number of zygotes and ookinetes, respectively (Tewari et al., 2010). To determine whether defects of Δ*pb115* lines were female- or male-specific, *Pbs47* KO (Δ*pbs47*) and *Pbs48/45* KO (Δ*pbs48/45*) lines were used in an *in vitro* cross-fertilization assay as described (van Dijk et al., 2010; Zhu et al., 2019). At 3 days post infection, equal numbers of mature gametocytes of different clones were mixed and incubated for 24 h. The numbers of ookinetes were counted as described above (100× oil objective).

To determine the subsequent development, mosquito feeding experiment was performed with mice that were infected three days earlier with either the WT or Δ*pb115 P. berghei*. Four-day-old female *A. stephensi* mosquitoes (∼100/mouse) starved for 6 h were allowed to feed on infected mice for 30 min. Unfed mosquitoes were then removed and fed mosquitoes were maintained at 19–22°C and in 50–80% relative humidity. Ten days after feeding, up to 50 mosquitoes were dissected in each group. The midguts of mosquitoes were removed and stained with 0.5% mercurochrome (Sigma-Aldrich). Oocysts were counted to determine the prevalence (number of infected mosquitoes) and intensity of infection (number of oocysts per positive midgut).

Quantification of Transmission-Blocking Activity

Transmission-blocking activity (TBA) of anti-rPb115 antisera was estimated using both *in vitro* ookinete conversion and *in vivo* mosquito feeding assays (Kou et al., 2016). In short, phenylhydrazine pre-treated mice were injected with 1×10^6 WT iRBCs. Three days post-infection, parasitemia was counted by Giemsa staining, and 10 μL gametocyte-infected blood were mixed with 90 μL ookinete culture medium containing 10% anti-Pb115 mouse sera or control sera (immunized with adjuvants only) incubated at 19°C for 2 h to count zygote numbers and 24 h to count ookinete numbers. Mosquito-feeding experiments were carried out as described previously (Zheng et al., 2017). Immunized mice with rPb115 protein or control mice were pre-treated with 0.2 mL of 6 mg/mL phenylhydrazine for 3 days. Five mice from each group were injected with 1×10^6 WT iRBCs, and mosquitoes were fed on immunized mice at day 3 after infection. Ten days after blood meal, the prevalence and intensity of infection in mosquitoes were determined.

Statistical Analysis

Statistical comparison between groups (IgG levels, parasitemia, gametocytemia, and ookinete numbers) was performed by Student's *t* test using the GraphPad Prism software. The intensity of mosquito infection (oocysts/midgut) was analyzed using the Mann–Whitney *U* test, while infection prevalence was analyzed by Fisher's exact test using SPSS version 21.0. Survival of mice infected with WT or Δ*pb115* parasites was compared by using the Kaplan–Meyer's method. All data were from three independent experiments.

RESULTS

P115 Is Highly Conserved Among *Plasmodium* Species

PBANKA_0931000 (Pb115) is among a group of genes with the following features: conserved in *Plasmodium* genomes; sexual-stage expression; and containing the sequence for a putative signal peptide or at least one transmembrane domain (Zheng et al., 2016). The *Pb115* gene is located on chromosome 9 and encodes a protein of 978 aa with a predicted size of 115 kDa. As shown in the predicted protein features in PlasmoDB, the predicted protein contains a membrane lipoprotein lipid attachment site at the N-terminus and a major facilitator superfamily (MFS) general substrate transporter domain (*P* value 1.05e-14) near the C terminus (**Supplementary Figure S1**). The encoded protein contains 12 transmembrane domains, six within the MFS domain. Multiple sequence alignment showed that this protein is highly conserved among *Plasmodium* species (**Supplementary Figure S2**).

Pb115 Is Expressed in Both Asexual and Sexual Stages

Expression of the ortholog of *Pb115* in *Plasmodium falciparum* (*PF3D7_1117000*), as demonstrated by RNA-seq analysis, was mainly in schizonts during the asexual intraerythrocytic development cycle (Plasmodb.org). The *PF3D7_1117000* mRNA was also detected during sexual development and was almost equally abundant in male and female gametocytes (Lasonder et al., 2016). To study Pb115 protein expression during *P. berghei* development, we generated a recombinant Pb115 fragment, which was used to generate antibodies directed against the protein. For this, the 205 aa MFS domain from aa 756 to aa 960 (**Supplementary Figure S1**) was expressed in yeast and purified using the Ni-NTA column. SDS-PAGE of the purified recombinant protein (rPb115) showed a relatively homogenous protein band with a molecular weight of ∼23 kDa (**Figure 1A**), which agreed with the predicted size of the MFS domain. The rPb115 protein was used to immunize 6–8-week-old female BALB/c mice. Two weeks after the third immunization, the immune sera contained a significantly higher antibody titer against the rPb115 fragment than the adjuvant control sera (**Supplementary Figure S3**). The antisera were used to probe lysates from purified *P. berghei* schizonts, gametocytes and cultured ookinetes in Western blots. Compared with the erythrocyte lysate control, the anti-rPb115 antisera specifically recognized a protein of approximately 115 kDa in the three developmental stages, consistent with the predicted molecular size of Pb115. Using HSP70 for protein loading control, Pb115 showed similar expression levels in all these

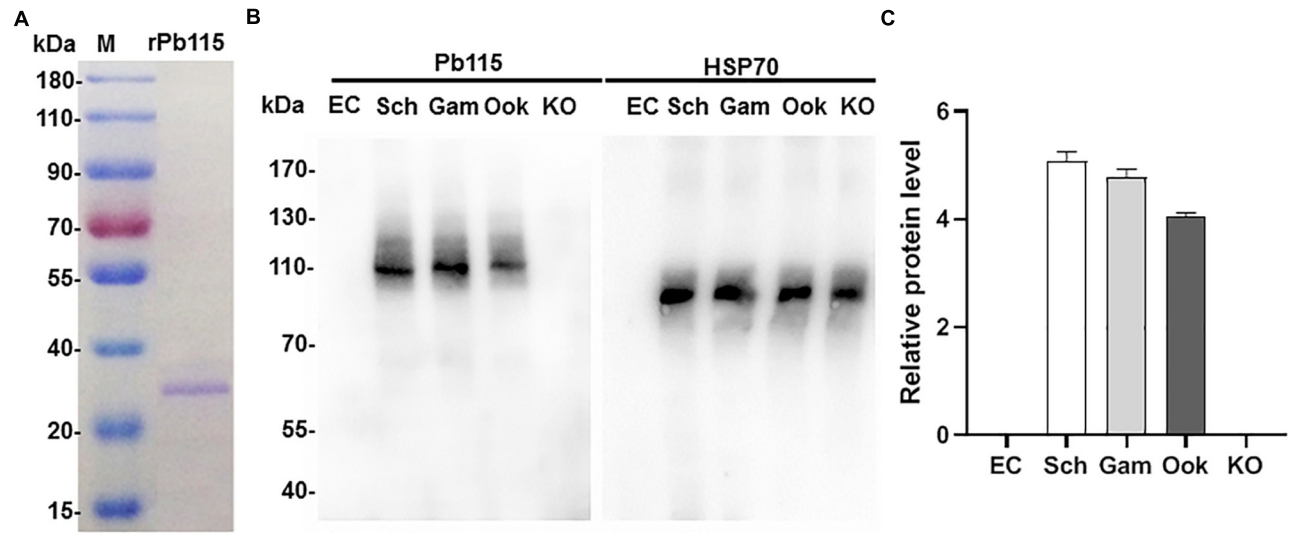

FIGURE 1 | Recombinant Pb115 protein purification and detection of Pb115 expression during parasite development. **(A)** Purified recombinant Pb115 protein was subjected to electrophoresis on a 12% polyacrylamide gel, and the proteins were stained with Coomassie Brilliant Blue. M: PageRuler Prestained Protein Ladder in kDa. **(B)** Representative Western blot of Pb115 in asexual- and sexual-stage parasites. Lysates of schizonts (Sch), gametocytes (Gam), ookinetes (Ook), and Δ*pb115* parasites (KO) at 10 μg/lane were probed with mouse anti-Pb115 sera (1:500). The Δ*pb115* parasite protein extract was a mixture of 7 μg asexual-stage proteins and 3 μg ookinete proteins. Protein loading was estimated by Western blot with the anti-Hsp70 sera (1:1000). Non-infected erythrocytes (EC) were used as negative control. **(C)** The Pb115 relative protein levels in schizonts (Sch), gametocytes (Gam), ookinetes (Ook), and KO parasites were estimated by using ImageJ analysis of replicate Western blots shown in **(B)**. Data were normalized against the PbHsp70 bands of the respective stages.

three stages examined (**Figure 1B**). ImageJ analysis of the band intensities in three replicated Western blots showed a slight lower Pb115 abundance in ookinetes than in schizonts and gametocytes (**Figure 1C**).

To further verify that the anti-rPb115 sera indeed identified the Pb115 protein, we generated a *P. berghei* parasite line with the endogenous Pb115 tagged with HA at its C-terminus. Correct fusion of the *Pb115* gene with the HA tag was confirmed by diagnostic integration PCR (**Supplementary Figure S4**). Western blotting with the anti-HA mAb identified a protein band of ∼115 kDa, similar to the size of the protein identified by the anti-Pb115 antisera. No specific protein bands were detected in lysates from non-infected erythrocytes and WT ookinetes (**Supplementary Figure S4**). Similarly, Pb115-HA protein level in ookinetes was slightly lower than those in schizonts and gametocytes.

Pb115 Is Localized on the Plasma Membrane of Gametes and Ookinetes

The presence of multiple transmembrane domains in Pb115 suggests that this protein might be associated with membrane structures in the parasites. To detect membrane association of Pb115, we separated the parasite PM with the cytoplasm and performed Western blots using the anti-Pb115 antisera. In schizonts and gametocytes, Pb115 was detected in both the cytoplasm and PM fractions, with Pb115 appearing more abundant in the PM fractions (**Supplementary Figure S5**). Interestingly, in ookinetes, Pb115 was mainly detected in the PM fraction. Using the same procedure, we evaluated the subcellular distribution of Pb115 in the Pb115-HA parasite line using the anti-HA mAb. The results obtained using both the WT and Pb115-HA lines were highly comparable (**Supplementary Figure S5**).

We further examined Pb115 expression and localization in more detail by IFA. In WT parasites, IFA with the anti-rPb115 sera detected Pb115 protein expression in schizonts, gametocytes, gametes, and ookinetes (**Figure 2**), whereas fluorescence was almost undetectable in rings, trophozoites and sporozoites (data not shown). As negative controls, IFA with control mouse sera or without primary antibodies did not produce fluorescence signals (**Figure 2**). In both schizonts and gametocytes, Pb115 fluorescence dispersed throughout the cytoplasm, sometimes with a speckled appearance. In female gametes, the Pb115 signal was found to be associated with the PM only, whereas in male gametes, it was associated with both the flagella and the residual body (**Figure 2**). Consistent with the Western analysis showing primary association of Pb115 with the PM in ookinetes, IFA also showed association of Pb115 with the PM of ookinetes with the signals partially being co-localized with those of PSOP25. To differentiate internal from external membrane localization, IFA was performed without membrane permeabilization. In this case, schizonts and gametocytes were not labeled, indicating that the Pb115 protein was not localized outside of the membrane of the iRBC (**Figure 2**). During gamete development, the female gametes showed a similar localization pattern regardless of membrane permeabilization status, demonstrating external membrane localization of the Pb115 on female gametes. Similarly, in male gametes, the fluorescent signals were detected on both residual bodies and

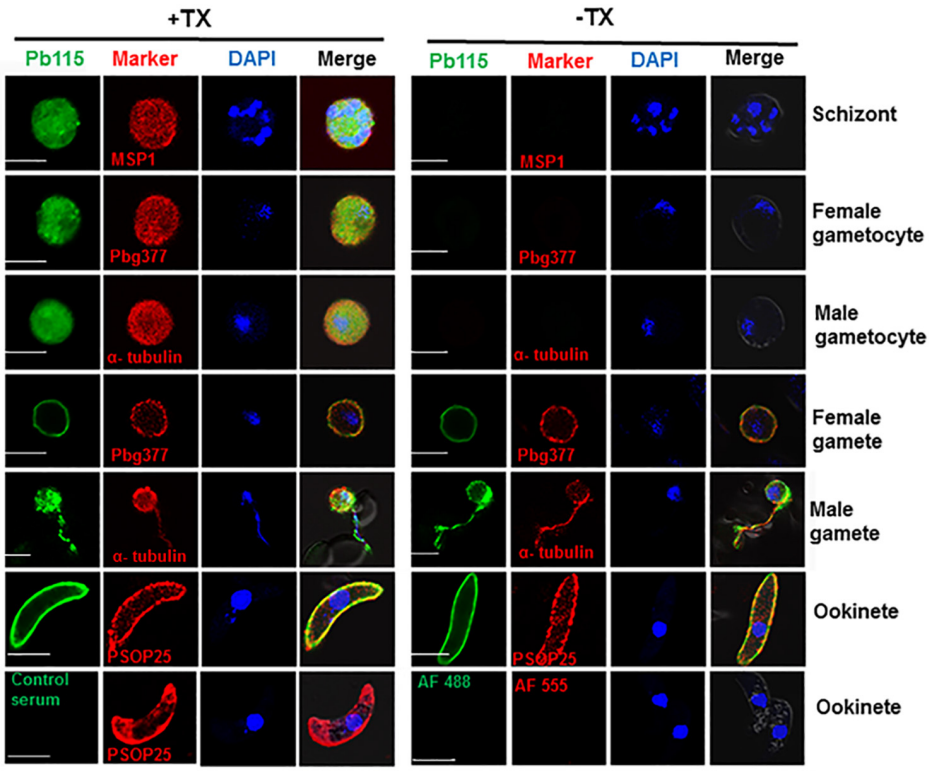

FIGURE 2 | Representative IFA images of Pb115 in WT *P. berghei* with (+TX) or without (–TX) membrane permeabilization. Parasites were incubated with anti-Pb115 sera (1: 500) as the primary antibodies (green). The parasites were also labeled with antibodies against the marker proteins for different stages (PbMSP1 for schizonts, Pbg377 for female gametocytes and gametes, α-tubulin for male gametocytes and gametes, and PSOP25 for ookinetes). Nuclei were stained with DAPI (1 μg/mL) (blue). The bottom panel shows two negative controls: WT ookinetes (+TX) labeled with the control serum or only with the secondary antibodies (AF488, Alexa Fluor 488, and AF555, Alexa Fluor 555). Merge, Alexa Flour 488 + Alexa Flour 555 + DAPI. Bar, 5 μm. Data are representatives of three independent experiments.

flagella-like male gametes. Again, Pb115 was clearly localized on the PM of ookinetes (**Figure 2**). IFA with developmental stages of the Pb115-HA line using anti-HA mAb showed highly similar patterns of Pb115 localization (**Supplementary Figure S6**).

To further demonstrate the PM association of Pb115 in schizonts and gametocytes, parasites were liberated from the enveloping RBC and parasitophorous vacuole membranes via mild saponin treatment. Subsequent IFA showed that Pb115 was localized at the peripheral PM in both male and female gametocytes (**Supplementary Figure S7A**). This localization pattern was further confirmed using the Pb115-HA line probed with the anti-HA mAb (**Supplementary Figure S7B**). Collectively, these data indicated that Pb115 was expressed from schizonts to ookinetes, and Pb115 retained PM localization from gametes through ookinete development. Given that the Pb115 antisera were generated against the C-terminus and HA was also tagged to the C-terminus, these localization patterns suggest that the Pb115 C-terminus was external to the PM.

Pb115 Is Needed for Gamete Attachment

To investigate the function of Pb115 in *P. berghei* development, the *pb115* gene was knocked out by homologous recombination. Integration-specific PCR was used to confirm the KO lines (**Supplementary Figures S8A,B**). In addition, the lack of Pb115 protein expression in a KO line was confirmed by Western blot analysis (**Figures 1B,C**) and IFA (**Supplementary Figure S8C**). Two Δ*pb115* lines were selected from two independent transfection experiments and used for phenotype analysis. The effect of the *pb115* KO on parasite development was examined during blood-stage infection and in mosquitoes. Although Pb115 was expressed in schizonts, deletion of *pb115* did not affect asexual blood-stage multiplication of the parasites ($P > 0.05$; **Figure 3A**), nor did it impact the survival of infected mice ($P > 0.05$, Kaplan–Meier's survival analysis; **Figure 3B**). With regard to sexual stages, there were no differences in gametocytemia and sex ratio between the WT and Δ*pb115* lines ($P > 0.05$; **Figures 3C,D**). Furthermore, the Δ*pb115* parasites showed no defects in gametogenesis, as the numbers of exflagellation centers and macrogamete numbers were all comparable between the WT and the Δ*pb115* lines ($P > 0.05$; **Figures 4A,B**). Using *in vitro* assays, we then evaluated whether *pb115* KO affected the fertilization and subsequent sexual development process. During our *in vitro* culture of ookinetes, the zygote numbers formed at 2 h and ookinete numbers at 24 h in the two Δ*pb115* clones suffered similar levels of reduction (∼95%) compared to the WT parasites ($P < 0.01$; **Figures 4C,D**),

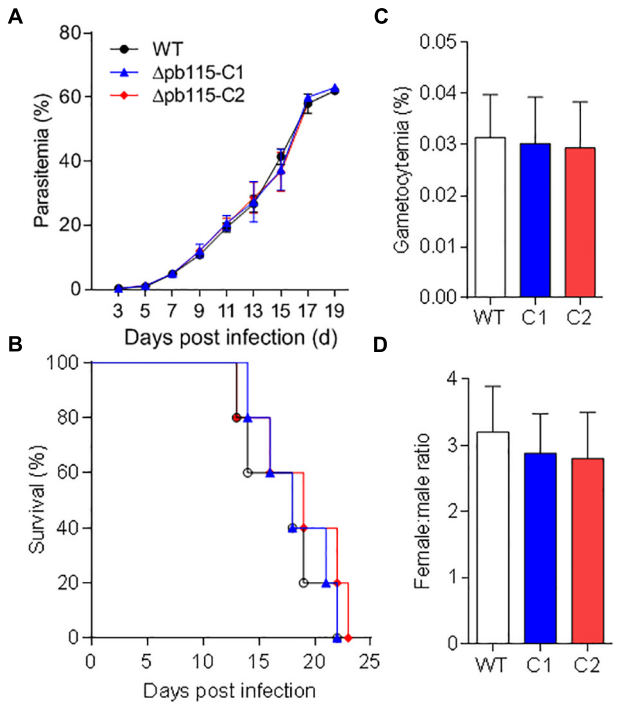

FIGURE 3 | Functional analysis of Pb115 during parasite blood stages. Mice were infected with *P. berghei* or Δ*pb115* parasites Clone 1 (C1) and Clone 2 (C2). **(A)** Growth curve of asexual stages (10 mice per group). **(B)** Survival rates of mice infected with different parasite strains (10 mice per group). **(C)** Gametocytemia on day 3 after infection by different parasite strains (five mice per group). **(D)** Female: male gametocyte ratios on day 3 after infection by WT *P. berghei* and Δ*pb115* clone 1 and 2 (five mice per group). The data are from three biological experiments and are presented as the mean ± SD in each group.

suggesting that Δ*pb115* parasites were defective in fertilization. This finding was further reinforced by results from mosquito feeding experiments, where *A. stephensi* mosquitoes were allowed to feed on WT *P. berghei*- or Δ*pb115*-infected mice and midgut oocysts were quantified. Mosquitoes fed on WT *P. berghei*-infected mice had 88–96% prevalence of infection in three experiments, whereas mosquitoes fed on Δ*pb115*-infected mice had infection prevalence ranging from 12 to 16%, a reduction by 74% ($P < 0.001$; **Table 1**). Similarly, a drastic reduction in oocyst density was observed in mosquitoes fed on Δ*pb115*-infected mice ($P < 0.001$; **Table 1** and **Supplementary Figure S9A**). Specifically, the mean number of oocysts per midgut was 118 in mosquitoes fed on WT-infected mice as compared to <4 on average in those fed on Δ*pb115*-infected mice.

To detect which step of the fertilization process was defective in the Δ*pb115* parasites, we performed detailed observations of the male–female gamete interactions under a phase contrast microscope. Male gametes from both WT and Δ*pb115* parasites exhibited similar motility and interaction with the RBCs, as evidenced by the similar numbers of exflagellation centers formed. In WT parasites, male–female attachments (for >3 s) were readily observed; on average 22 attachments were seen in five experiments (**Figure 4E**). By contrast, the number of gametes forming male–female attachments in the Δ*pb115* parasite lines was drastically reduced (five observed in eight experiments) ($P < 0.01$; **Figure 4E**), indicating that Δ*pb115* gametes were defective in recognition and attachment. To determine whether the resultant defects in gamete attachment in Δ*pb115* were due to either the male or female gamete, we performed *in vitro* cross-fertilization experiments between Δ*pb115* gametocytes and Δ*pbs47* or Δ*pbs48/45* gametocytes. As found in earlier studies (van Dijk et al., 2010), both Δ*pbs47* and Δ*pbs48/45* lines showed a fertilization rate that was decreased by more than 99% compared to WT (**Figure 5**). Since it has been reported that Δ*pbs47* produces normal male but defective female gametes, whereas the Δ*pbs48/45* line produces normal female but defective male gametes, we performed *in vitro* cross-fertilization to confirm that each line only had defects in one sex. As expected, similar numbers of ookinetes were formed in the Δ*pbs47* × Δ*pbs48/45* cross as compared to the WT (**Figure 5**). However, cross-fertilization of Δ*pb115* with either Δ*pbs47* or Δ*pbs48/45* failed to generate an appreciable number of ookinetes as compared with cross-fertilization between Δ*pbs47* and Δ*pbs48/45* ($P < 0.01$; **Figure 5**), suggesting that *pb115* deletion affected both male and female gametes.

Antibodies Against Pb115 Display Apparent TRA

Given that Pb115 was found localized on the PM of gametes and ookinetes, we wanted to test whether Pb115 had TRA. In the *in vitro* ookinete conversion assay, the number of zygotes formed during *in vitro* ookinete culture with the anti-rPb115 mouse sera was 5.3 times lower than those with the control sera ($P < 0.01$; **Figure 6A**). The number of ookinetes formed with the anti-rPb115 mouse sera at 24 h was 5.7 times lower than those with the control sera ($P < 0.01$; **Figure 6B**), suggesting that the immune sera had a major effect on reducing fertilization. In mosquito feeding assays, mice were immunized with rPb115 proteins and then infected with the WT *P. berghei*. Three days post infection, *A. stephensi* mosquitoes were allowed to directly feed on rPb115-immunized and control mice. Mosquitoes fed on control mice had an infection prevalence of 92–96% and oocyst density of 109.9–132.6 oocysts/midgut (**Table 2**). In comparison, mosquitoes fed on rPb115-immunized mice had infection prevalence of 44–52%, a reduction of 44% compared to mosquitoes fed on immunization control mice ($P < 0.001$, Fisher's exact test, **Table 2**). Similarly, moderate levels of reduction (39%) in oocyst density (70–80.1 oocysts/midgut) were also observed in mosquitoes fed on rPb115-immunized mice as compared to those fed on control mice ($P < 0.001$, Mann–Whitney *U* test, **Table 2** and **Supplementary Figure S9B**).

DISCUSSION

Key fertilization factors discovered during functional studies of *Plasmodium* gamete membrane proteins include the male fertility factors Pbs48/45 and Pbs230 and female fertility factor Pbs47, which play critical roles in recognition and attachment to gametes

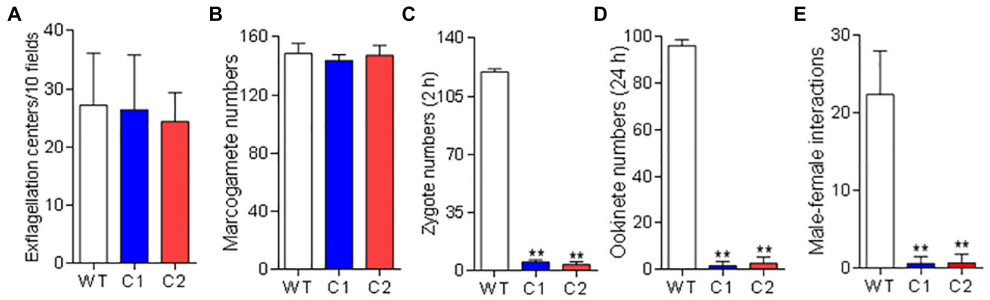

FIGURE 4 | Function analysis of Pb115 in sexual stages. *P. berghei* or Δ*pb115* parasites (Clone 1 and Clone 2)-infected mouse blood on day 3 after infection was incubated in the ookinete culture medium. **(A)** Exflagellation centers of male gametocytes in 10 microscopic fields under a 40× objective. **(B)** Numbers of female gametes in 1 μL of ookinete culture at 15 min post activation **(C)** Numbers of zygotes formed at 2 h during *in vitro* ookinete culture. **(D)** Numbers of ookinetes formed at 24 h during *in vitro* ookinete culture. Data are presented as the mean ± SD for five mice in each group. **(E)** Male–female gamete interactions. Numbers of male gametes attached to females for more than 3 s during 20 min of observation. Data are presented as the mean ± SD from three experiments. ** indicates $P < 0.01$ for comparison with WT parasite (*t* test).

TABLE 1 | Phenotypic comparison between Δ*pb115* and WT *P. berghei* in mosquitoes.

Experiment	Parasites	% infected mosquitoes (infected/dissected)	% reduction in prevalence[a]	Mean% reduction[b]	Oocyst density (mean ± SD)[c]	% reduction in oocyst density[d]	Mean% reduction[e]
I	WT	88.0 (44/50)			131.3 ± 33.2		
	Δ*pb115*	12.0 (6/50)	76.0		2.3 ± 1.0	83.3	
II	WT	92.0 (46/50)			102.9 ± 18.3		
	Δ*pb115*	16.0 (8/50)	76.0		6.3 ± 1.7	93.9	
III	WT	96.0 (48/50)			120.4 ± 22.0		
	Δ*pb115*	16.0 (8/50)	80.0	74***	3.3 ± 1.3	97.5	96.5***

*WT- and Δpb115-infected mice were fed to mosquitoes and prevalence of infection and oocyst density were compared between the two groups. [a]% Reduction of prevalence = % prevalence$_{wt}$ − % prevalence$_{\Delta\ Pb115}$; [b]Fisher's exact test; ***$P < 0.001$; [c]The number of oocysts per midgut (mean ± SD); [d]% Reduction in oocyst density = (mean oocyst density$_{wt}$ − mean oocyst density$_{\Delta\ Pb115}$)/mean oocyst density$_{wt}$ × 100%; [e]Mann–Whitney U test; ***$P < 0.001$.*

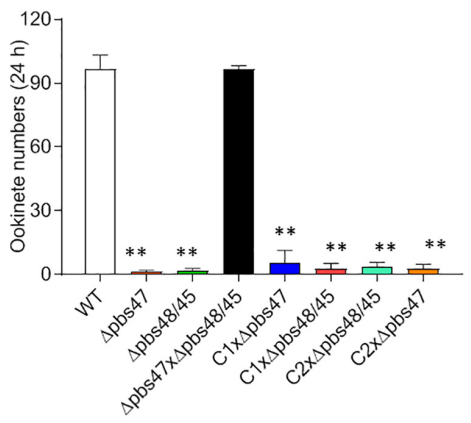

FIGURE 5 | *In vitro* cross-fertilization studies. Δ*pb115* clone C1 and C2 and parasite lines that produce only fertile male (Δ*pbs47*) or only fertile female (Δ*pbs48/45*) gametes were incubated in different combinations during *in vitro* ookinete culture. The numbers of ookinetes formed were counted at 24 h. Data are from three independent experiments. ** indicates $P < 0.01$ for the comparison with WT *P. berghei* (*t* test).

of the opposite sex in the rodent parasite *P. berghei* (van Dijk et al., 2001, 2010). Interestingly, Pfs230 and Pfs47 seem to have divergent functions in *P. falciparum*: Pfs230 mediates erythrocyte binding (Eksi et al., 2006), whereas *Pfs47* is dispensable for female gamete fertility (van Schaijk et al., 2006) but is critical for immune evasion in mosquitoes (Molina-Cruz et al., 2013). Another male fertility factor, HAP2/GCS1, functions after the initial gamete recognition and attachment, since *PbHAP2* deletion lines have normal exflagellation and pairing of the male gametes with female gametes, but lack gamete fusion (Hirai et al., 2008; Liu et al., 2008).

In the current study, we identified a new gamete membrane protein, Pb115, whose deletion affected gamete fertility. The Pb115 protein has a conserved C-terminal MFS domain that is found in the MFS of transporter proteins, the largest superfamily of secondary carriers that are ubiquitously found in all branches of life with nearly 15,000 members. MFS transporters move a myriad of small molecules across biological membranes including sugars, peptides, deleterious substances, organic and inorganic ions (Yan, 2015). Based on the transport mode, MFS transporters are classified into uniporters (transporting a single substrate), symporters (transporting a substrate with a co-transporting ion or solute in the same direction), and antiporters (transporting a substrate with a co-transporting substrate in the opposite direction). They play diverse roles in homeostasis, metabolism and signal transduction (Law et al., 2008). It will be interesting to determine what, if any, compounds are transported by Pb115.

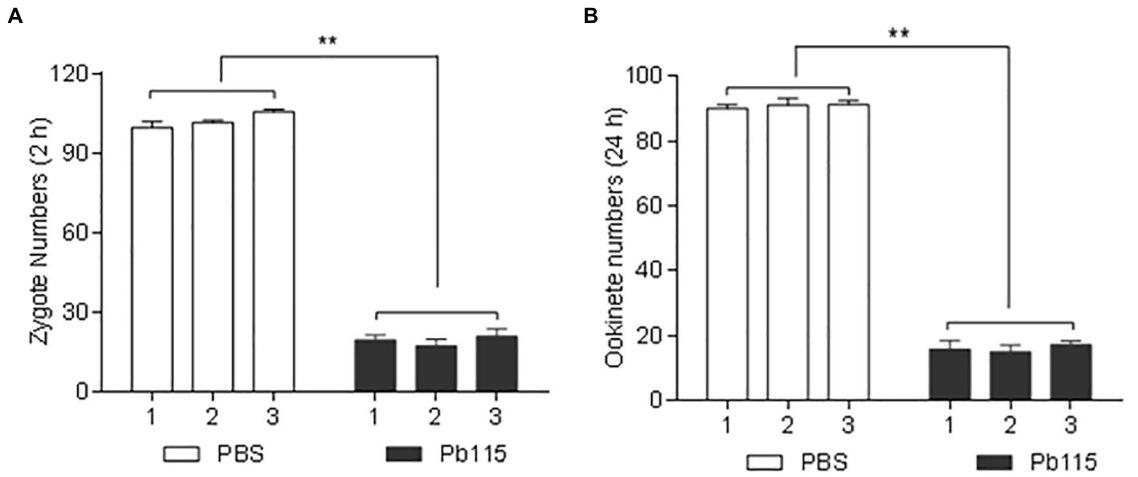

FIGURE 6 | Quantification of TRA of the anti-Pb115 sera *in vitro*. Gametocyte-infected blood on day 3 after infection with *P. berghei* was incubated at 19°C in ookinete culture medium containing 10% anti-Pb115 mouse sera or control sera, and the numbers of zygotes and ookinetes formed at 2 and 24 h were counted. **(A)** Zygote numbers at 2 h. **(B)** Ookinete numbers at 24 h. The data are presented as the mean ± SD. ** indicates $P < 0.01$ for the comparison with the adjuvant control sera (*t* test).

TABLE 2 | *In vivo* evaluation of transmission blocking activity of Pb115.

Experiment	Group	% infected mosquitoes (infected/dissected)	% reduction in prevalence[a]	Mean% reduction[b]	Oocyst density (mean ± SD)[c]	% reduction in oocyst density[d]	Mean% reduction[e]
I	Control	92.0 (46/50)			132.6 ± 21.0		
	rPb115	44.0 (22/50)	48.0		70.0 ± 13.0	47.2	
II	Control	96.0 (48/50)			109.9 ± 16.8		
	rPb115	52.0 (26/50)	44.0		70.8 ± 11.7	35.1	
III	Control	92.0 (46/50)			123.3 ± 21.2		
	rPb115	52.0 (26/50)	40.0	44.0***	80.1 ± 15.8	34.8	39.0***

Mosquitoes were fed on rPb115-immunized and control mice and the prevalence of infection and oocyst density were compared between the two groups. [a] *% Reduction of prevalence = % prevalence$_{Control}$ − % prevalence$_{rPb115}$;* [b] *Fisher's exact test; ***$P < 0.001$;* [c] *The number of oocysts per midgut (mean ± SD);* [d] *% Reduction in oocyst density = mean oocyst density$_{Control}$ − mean oocyst density$_{rPb115}$)/mean oocyst density$_{Control}$ × 100%;* [e] *Mann–Whitney U test; ***$P < 0.001$.*

We learned from the current study that Pb115 is not essential for the intraerythrocytic stages – schizonts and gametocytes – despite its expression in these stages. In addition, gametogenesis in the absence of Pb115 appeared normal. Although the male gametes in the Δ*pb115* parasite showed similar motility to the WT parasites, and made contacts with the female gametes, most of the male–female interactions were transient (lasting less than 3 s) and futile. Furthermore, both male and female gametes were similarly affected by *pb115* deletion, as cross-fertilization with either Δ*pbs48/45* or Δ*pbs47* was not able to restore fertilization in the Δ*pb115* lines. It is noteworthy that despite the very low fertilization rates in the Δ*pb115* parasites, sporozoites dissected from salivary glands of Δ*pb115*-infected mosquitoes were equally infective to mice as the WT sporozoites (data not shown), suggesting the defects observed with Δ*pb115* were probably limited to gamete adhesion. Whether Δ*pb115* affects transport of essential molecules needed for male and/or female gamete functions or whether P115 impacts distribution of key fertility factors described above remains to be determined.

We have demonstrated using IFA that Pb115 was associated with the plasma membrane of gametes and ookinetes. Furthermore, Pb115 appeared to have a membrane localization conformation with its C-terminal domain residing outside the cell, given that the antibodies raised against MFS could detect Pb115 without membrane permeabilization. In addition, anti-HA mAb also detected the Pb115 C-terminal HA tag on gametes and ookinetes in a similar way. Since several gamete membrane proteins such as P48/45 and P230 are primary TBV candidates, the membrane expression of Pb115 during sexual stages prompted us to investigate its transmission-blocking potential. We generated the recombinant MFS domain from yeast and immunized mice to study its TRA using both *in vitro* ookinete conversion and *in vivo* mosquito feeding assays. Antibodies against the synthetic protein could recognize Pb115 in Western blot and IFA, suggesting that the recombinant protein possessed, at least in part, properly folded epitopes. Antisera against rPb115 significantly reduced zygote formation and ookinete conversion. Direct feeding of mosquitoes on rPb115-immunized mice showed 44% reduction in prevalence

and 39% reduction in oocyst intensity as compared to those fed on non-immunized mice. Compared with the TRA of other gamete membrane proteins such as P48/45 (Outchkourov et al., 2008), P230 (Williamson et al., 1995), and HAP2 (Blagborough and Sinden, 2009), the extents of reduction are rather modest and further refinement of the recombinant protein covering important epitopes may help improve the TB activity of Pb115 (Deore et al., 2019). The expression of Pb115 on both gametes and ookinetes suggests that it might be a target for both pre- and post-fertilization immunity. In addition, studies on P115 in human malaria parasites are warranted, given the high degree of conservation of P115 in different *Plasmodium* species.

DATA AVAILABILITY STATEMENT

The raw data supporting the conclusions of this manuscript will be made available by the authors, without undue reservation, to any qualified researcher.

ETHICS STATEMENT

This study was carried out in accordance with the recommendations of the guidelines established by China Medical University, Animal Welfare and Research Ethics Committee. The protocol was approved by the Animal Care and Use Committee of China Medical University.

AUTHOR CONTRIBUTIONS

FL performed the main experiments and wrote the manuscript. QL, CY, YZ, YW, HM, YQ, YJ, and JM provided laboratory assistance. JM took part in most supplemental experiments and revised the manuscript. YC designed the experiments. LC supervised the study and revised the manuscript.

FUNDING

This study was supported by the National Institutes of Health grants (R01AI099611 and U19AI089672) and by the National Natural Science Foundation of China (No. 81429004). The Pbs21 mAb clone 13.1 was a gift from Dr. Hiroyuki Matsuoka.

SUPPLEMENTARY MATERIAL

The Supplementary Material for this article can be found online at: https://www.frontiersin.org/articles/10.3389/fmicb.2019.02193/full#supplementary-material

REFERENCES

Bhatt, S., Weiss, D. J., Cameron, E., Bisanzio, D., Mappin, B., Dalrymple, U., et al. (2015). The effect of malaria control on *Plasmodium falciparum* in Africa between 2000 and 2015. *Nature* 526, 207–211. doi: 10.1038/nature15535

Blagborough, A. M., and Sinden, R. E. (2009). *Plasmodium berghei* HAP2 induces strong malaria transmission-blocking immunity in vivo and in vitro. *Vaccine* 27, 5187–5194. doi: 10.1016/j.vaccine.2009.06.069

Braks, J. A., Franke-Fayard, B., Kroeze, H., Janse, C. J., and Waters, A. P. (2006). Development and application of a positive-negative selectable marker system for use in reverse genetics in *Plasmodium*. *Nucleic Acids Res.* 34:e39. doi: 10.1093/nar/gnj033

Chan, J. A., Fowkes, F. J., and Beeson, J. G. (2014). Surface antigens of *Plasmodium falciparum*-infected erythrocytes as immune targets and malaria vaccine candidates. *Cell. Mol. Life Sci.* 71, 3633–3657. doi: 10.1007/s00018-014-1614-3

Chowdhury, D. R., Angov, E., Kariuki, T., and Kumar, N. (2009). A potent malaria transmission blocking vaccine based on codon harmonized full length Pfs48/45 expressed in *Escherichia coli*. *PLoS One* 4:e6352. doi: 10.1371/journal.pone.0006352

Delves, M. J., Angrisano, F., and Blagborough, A. M. (2018). Antimalarial transmission-blocking interventions: past, present, and future. *Trends Parasitol.* 34, 735–746. doi: 10.1016/j.pt.2018.07.001

Dempsey, E., Prudencio, M., Fennell, B. J., Gomes-Santos, C. S., Barlow, J. W., and Bell, A. (2013). Antimitotic herbicides bind to an unidentified site on malarial parasite tubulin and block development of liver-stage *Plasmodium parasites*. *Mol. Biochem. Parasitol.* 188, 116–127. doi: 10.1016/j.molbiopara.2013.03.001

Deore, S., Kumar, A., Kumar, S., Mittal, E., Lotke, A., and Musti, K. (2019). Erythrocyte binding ligand region VI specific IgA confers tissue protection in malaria infection. *Mol. Biol. Rep.* 46, 3801–3808. doi: 10.1007/s11033-019-04822-7

Ecker, A., Bushell, E. S., Tewari, R., and Sinden, R. E. (2008). Reverse genetics screen identifies six proteins important for malaria development in the mosquito. *Mol. Microbiol.* 70, 209–220. doi: 10.1111/j.1365-2958.2008.06407.x

Eksi, S., Czesny, B., van Gemert, G. J., Sauerwein, R. W., Eling, W., and Williamson, K. C. (2006). Malaria transmission-blocking antigen, Pfs230, mediates human red blood cell binding to exflagellating male parasites and oocyst production. *Mol. Microbiol.* 61, 991–998. doi: 10.1111/j.1365-2958.2006.05284.x

Gardner, M. J., Hall, N., Fung, E., White, O., Berriman, M., Hyman, R. W., et al. (2002). Genome sequence of the human malaria parasite *Plasmodium falciparum*. *Nature* 419, 498–511.

Guttery, D. S., Poulin, B., Ramaprasad, A., Wall, R. J., Ferguson, D. J., Brady, D., et al. (2014). Genome-wide functional analysis of plasmodium protein phosphatases reveals key regulators of parasite development and differentiation. *Cell Host Microbe.* 16, 128–140. doi: 10.1016/j.chom.2014.05.020

Hall, N., Karras, M., Raine, J. D., Carlton, J. M., Kooij, T. W., Berriman, M., et al. (2005). A comprehensive survey of the *Plasmodium* life cycle by genomic, transcriptomic, and proteomic analyses. *Science* 307, 82–86. doi: 10.1126/science.1103717

Hirai, M., Arai, M., Mori, T., Miyagishima, S. Y., Kawai, S., Kita, K., et al. (2008). Male fertility of malaria parasites is determined by GCS1, a plant-type reproduction factor. *Curr. Biol.* 18, 607–613. doi: 10.1016/j.cub.2008.03.045

Kaslow, D. C., Quakyi, I. A., Syin, C., Raum, M. G., Keister, D. B., Coligan, J. E., et al. (1988). A vaccine candidate from the sexual stage of human malaria that contains EGF-like domains. *Nature* 333, 74–76. doi: 10.1038/333074a0

Kocken, C. H., Jansen, J., Kaan, A. M., Beckers, P. J., Ponnudurai, T., Kaslow, D. C., et al. (1993). Cloning and expression of the gene coding for the transmission blocking target antigen Pfs48/45 of *Plasmodium falciparum*. *Mol. Biochem. Parasitol.* 61, 59–68. doi: 10.1016/0166-6851(93)90158-t

Kou, X., Zheng, W., Du, F., Liu, F., Wang, M., Fan, Q., et al. (2016). Characterization of a *Plasmodium berghei* sexual stage antigen PbPH as a new candidate for malaria transmission-blocking vaccine. *Parasit. Vectors* 9:190. doi: 10.1186/s13071-016-1459-8

Lasonder, E., Rijpma, S. R., van Schaijk, B. C., Hoeijmakers, W. A., Kensche, P. R., Gresnigt, M. S., et al. (2016). Integrated transcriptomic and proteomic analyses of *P. falciparum* gametocytes: molecular insight into sex-specific processes and translational repression. *Nucleic Acids Res.* 44, 6087–6101. doi: 10.1093/nar/gkw536

Law, C. J., Maloney, P. C., and Wang, D. N. (2008). Ins and outs of major facilitator superfamily antiporters. *Annu. Rev. Microbiol.* 62, 289–305. doi: 10.1146/annurev.micro.61.080706.093329

Lee, S. M., Wu, C. K., Plieskatt, J. L., Miura, K., Hickey, J. M., and King, C. R. (2017). An N-terminal Pfs230 domain produced in baculovirus as a biological active transmission-blocking vaccine candidate. *Clin. Vaccine Immunol.* 24:e00140-17. doi: 10.1128/CVI.00140-17

Liu, F., Li, L., Zheng, W., He, Y., Wang, Y., Zhu, X., et al. (2018). Characterization of *Plasmodium berghei* Pbg37 as both a pre- and postfertilization antigen with transmission-blocking potential. *Infect. Immun.* 86:e00785-17. doi: 10.1128/IAI.00785-17

Liu, Y., Tewari, R., Ning, J., Blagborough, A. M., Garbom, S., Pei, J., et al. (2008). The conserved plant sterility gene HAP2 functions after attachment of fusogenic membranes in *Chlamydomonas* and *Plasmodium gametes*. *Genes Dev.* 22, 1051–1068. doi: 10.1101/gad.1656508

Molina-Cruz, A., Garver, L. S., Alabaster, A., Bangiolo, L., Haile, A., Winikor, J., et al. (2013). The human malaria parasite Pfs47 gene mediates evasion of the mosquito immune system. *Science* 340, 984–987. doi: 10.1126/science.1235264

Nikolaeva, D., Draper, S. J., and Biswas, S. (2015). Toward the development of effective transmission-blocking vaccines for malaria. *Expert Rev. Vaccines* 14, 653–680. doi: 10.1586/14760584.2015.993383

Outchkourov, N. S., Roeffen, W., Kaan, A., Jansen, J., Luty, A., Schuiffel, D., et al. (2008). Correctly folded Pfs48/45 protein of *Plasmodium falciparum* elicits malaria transmission-blocking immunity in mice. *Proc. Natl. Acad. Sci. U.S.A.* 105, 4301–4305. doi: 10.1073/pnas.0800459105

Sagara, I., Healy, S. A., Assadou, M. H., Gabriel, E. E., Kone, M., Sissoko, K., et al. (2018). Safety and immunogenicity of Pfs25H-EPA/Alhydrogel, a transmission-blocking vaccine against *Plasmodium falciparum*: a randomised, double-blind, comparator-controlled, dose-escalation study in healthy malian adults. *Lancet Infect. Dis.* 18, 969–982. doi: 10.1016/S1473-3099(18)30344-X

Sauerwein, R. W., and Bousema, T. (2015). Transmission blocking malaria vaccines: assays and candidates in clinical development. *Vaccine* 33, 7476–7482. doi: 10.1016/j.vaccine.2015.08.073

Shimp, R. L. Jr., Rowe, C., Reiter, K., Chen, B., Nguyen, V., Aebig, J., et al. (2013). Development of a Pfs25-EPA malaria transmission blocking vaccine as a chemically conjugated nanoparticle. *Vaccine* 31, 2954–2962. doi: 10.1016/j.vaccine.2013.04.034

Tachibana, M., Miura, K., Takashima, E., Morita, M., Nagaoka, H., Zhou, L., et al. (2019). Identification of domains within Pfs230 that elicit transmission blocking antibody responses. *Vaccine* 37, 1799–1806. doi: 10.1016/j.vaccine.2019.02.021

Talaat, K. R., Ellis, R. D., Hurd, J., Hentrich, A., Gabriel, E., Hynes, N. A., et al. (2016). Safety and immunogenicity of Pfs25-EPA/Alhydrogel(R), a transmission blocking vaccine against *Plasmodium falciparum*: an open label study in malaria naive adults. *PLoS One* 11:e0163144. doi: 10.1371/journal.pone.0163144

Tewari, R., Straschil, U., Bateman, A., Bohme, U., Cherevach, I., Gong, P., et al. (2010). The systematic functional analysis of *Plasmodium protein* kinases identifies essential regulators of mosquito transmission. *Cell Host Microbe.* 8, 377–387. doi: 10.1016/j.chom.2010.09.006

Tonkin, C. J., van Dooren, G. G., Spurck, T. P., Struck, N. S., Good, R. T., Handman, E., et al. (2004). Localization of organellar proteins in *Plasmodium falciparum* using a novel set of transfection vectors and a new immunofluorescence fixation method. *Mol. Biochem. Parasitol.* 137, 13–21. doi: 10.1016/j.molbiopara.2004.05.009

Tsuboi, T., Kaslow, D. C., Gozar, M. M., Tachibana, M., Cao, Y. M., and Torii, M. (1998). Sequence polymorphism in two novel *Plasmodium* vivax ookinete surface proteins, Pvs25 and Pvs28, that are malaria transmission-blocking vaccine candidates. *Mol. Med.* 4, 772–782. doi: 10.1007/bf03401770

van Dijk, M. R., Janse, C. J., Thompson, J., Waters, A. P., Braks, J. A., Dodemont, H. J., et al. (2001). A central role for P48/45 in malaria parasite male gamete fertility. *Cell* 104, 153–164. doi: 10.1016/s0092-8674(01)00199-4

van Dijk, M. R., van Schaijk, B. C., Khan, S. M., van Dooren, M. W., Ramesar, J., Kaczanowski, S., et al. (2010). Three members of the 6-cys protein family of *Plasmodium* play a role in gamete fertility. *PLoS Pathog.* 6:e1000853. doi: 10.1371/journal.ppat.1000853

van Schaijk, B. C., van Dijk, M. R., van de Vegte-Bolmer, M., van Gemert, G. J., van Dooren, M. W., Eksi, S., et al. (2006). Pfs47, paralog of the male fertility factor Pfs48/45, is a female specific surface protein in *Plasmodium falciparum*. *Mol. Biochem. Parasitol.* 149, 216–222. doi: 10.1016/j.molbiopara.2006.05.015

Vaughan, J. A. (2007). Population dynamics of *Plasmodium sporogony*. *Trends Parasitol.* 23, 63–70. doi: 10.1016/j.pt.2006.12.009

World Health Organization [WHO] (2018). *World Malaria Report 2017*. Geneva: World Health Organization.

Williamson, K. C., Criscio, M. D., and Kaslow, D. C. (1993). Cloning and expression of the gene for *Plasmodium falciparum* transmission-blocking target antigen, Pfs230. *Mol. Biochem. Parasitol.* 58, 355–358. doi: 10.1016/0166-6851(93)90058-6

Williamson, K. C., Keister, D. B., Muratova, O., and Kaslow, D. C. (1995). Recombinant Pfs230, a *Plasmodium falciparum* gametocyte protein, induces antisera that reduce the infectivity of *Plasmodium falciparum* to mosquitoes. *Mol. Biochem. Parasitol.* 75, 33–42. doi: 10.1016/0166-6851(95)02507-3

Wu, Y., Sinden, R. E., Churcher, T. S., Tsuboi, T., and Yusibov, V. (2015). Development of malaria transmission-blocking vaccines: from concept to product. *Adv. Parasitol.* 89, 109–152. doi: 10.1016/bs.apar.2015.04.001

Yan, N. (2015). Structural biology of the major facilitator superfamily transporters. *Annu. Rev. Biophys.* 44, 257–283. doi: 10.1146/annurev-biophys-060414-033901

Zheng, W., Kou, X., Du, Y., Liu, F., Yu, C., Tsuboi, T., et al. (2016). Identification of three ookinete-specific genes and evaluation of their transmission-blocking potentials in *Plasmodium berghei*. *Vaccine* 34, 2570–2578. doi: 10.1016/j.vaccine.2016.04.011

Zheng, W., Liu, F., He, Y., Liu, Q., Humphreys, G. B., Tsuboi, T., et al. (2017). Functional characterization of *Plasmodium berghei* PSOP25 during ookinete development and as a malaria transmission-blocking vaccine candidate. *Parasit. Vectors* 10:8. doi: 10.1186/s13071-016-1932-4

Zhu, X., Sun, L., He, Y., Wei, H., Hong, M., Liu, F., et al. (2019). Plasmodium berghei serine/threonine protein phosphatase PP5 plays a critical role in male gamete fertility. *Int. J. Parasitol.* 49, 685–695. doi: 10.1016/j.ijpara.2019.03.007

Conflict of Interest: The authors declare that the research was conducted in the absence of any commercial or financial relationships that could be construed as a potential conflict of interest.

frontiers in Microbiology

MINI REVIEW
published: 08 November 2019
doi: 10.3389/fmicb.2019.02652

Erythrocyte Membrane Makeover by *Plasmodium falciparum* Gametocytes

Gaëlle Neveu[1,2] *and Catherine Lavazec*[1,2]*

[1] Inserm U1016, CNRS UMR 8104, Université de Paris, Institut Cochin, Paris, France, [2] Laboratoire d'Excellence GR-Ex, Paris, France

Plasmodium falciparum sexual parasites, called gametocytes, are the only parasite stages responsible for transmission from humans to *Anopheles* mosquitoes. During their maturation, *P. falciparum* gametocytes remodel the structural and mechanical properties of the membrane of their erythrocyte host. This remodeling is induced by the export of several parasite proteins and a dynamic reorganization of the erythrocyte cytoskeleton. Some of these modifications are specific for sexual stages and play a key role for gametocyte maturation, sequestration in internal organs, subsequent release in the bloodstream and ability to persist in circulation. Here we discuss the mechanisms developed by gametocytes to remodel their host cell and the functional relevance of these modifications.

Keywords: gametocytes, erythrocyte membrane and cytoskeleton, mechanical properties, adhesive properties, protein export

OPEN ACCESS

Edited by:
Rhoel Dinglasan, University of Florida, United States

Reviewed by:
Gabriele Pradel, RWTH Aachen University, Germany
Ashley Vaughan, Seattle Children's Research Institute, United States

***Correspondence:**
Catherine Lavazec
catherine.lavazec@inserm.fr

Specialty section:
This article was submitted to Infectious Diseases, a section of the journal Frontiers in Microbiology

Received: *12 September 2019*
Accepted: *30 October 2019*
Published: *08 November 2019*

Citation:
Neveu G and Lavazec C (2019) Erythrocyte Membrane Makeover by Plasmodium falciparum Gametocytes. Front. Microbiol. 10:2652. doi: 10.3389/fmicb.2019.02652

INTRODUCTION

To interact with the external environment, the parasite *Plasmodium falciparum* drastically remodels its erythrocyte host. Such modifications are mediated by the export of parasite proteins into the erythrocyte that alter the architecture of the host cell membrane. By modifying the cytoadherence, deformability and permeability properties of the host cell membrane, these proteins contribute to parasite survival, virulence, and immune evasion. All these processes are extensively described during *P. falciparum* asexual stages, however, they are less characterized in gametocytes, which are the sexual stages responsible for the transmission from humans to mosquitoes. Unlike asexual stages that replicate in a cycle of 48 h, gametocytes develop over a period of 10 days, progressing through five distinct stages of maturation (Hawking et al., 1971). Immature gametocytes from stage I to IV are absent from peripheral circulation and sequester in bone marrow parenchyma (Aguilar et al., 2014; Joice et al., 2014). The mechanisms underlying their sequestration remain poorly understood but are likely drastically different from that of asexual stages, which sequester by cytoadhesion to endothelial cells (Baruch et al., 1995; Smith et al., 1995). At maturation, erythrocytes infected with stage V gametocytes are released in the bloodstream and freely circulate for several days waiting to be taken up by mosquitoes. During this time, gametocytes should be able to circulate through the spleen and avoid immune recognition. To adapt to these different microenvironments, gametocytes express a range of proteins among which more than 10% are

exported to the erythrocyte (Silvestrini et al., 2010). These proteins specifically remodel the erythrocyte membrane to allow gametocytes to interact with the host, indicating that the parasite evolved efficient strategies to renovate its host cell according to the specific needs of each life cycle phase. This review summarizes our current knowledge of the mechanisms developed by gametocytes to remodel the structural and mechanical properties of their erythrocyte host cell. We discuss the functional relevance of these modifications for gametocytes sequestration and circulation within their host.

PROTEIN EXPORT AT THE ERYTHROCYTE MEMBRANE

Upon infection with *P. falciparum*, the architecture of the erythrocyte membrane is deeply altered by parasite proteins (**Figure 1B** and **Table 1**). These proteins are either secreted on the erythrocyte surface by parasite apical organelles during invasion, or are exported by the developing parasite into the erythrocyte cytosol. Secreted proteins include the Ring-infected Erythrocyte Surface Antigen (RESA) contributing to the stabilization of the erythrocyte membrane skeleton (Pei et al., 2007), and the members of the RhopH protein family involved in the new permeability pathway (Counihan et al., 2017; Ito et al., 2017; Sherling et al., 2017). Many of the parasite-exported proteins possess a canonical export motif termed the *Plasmodium* export element (PEXEL) or host-targeting (HT) motif (Hiller et al., 2004; Marti et al., 2004). In addition, the *P. falciparum* exportome also includes a large number of PEXEL-negative exported proteins (PNEPs) (Heiber et al., 2013). To reach the erythrocyte cytosol, all parasite-exported proteins should pass through the parasitophorous vacuole membrane that envelops the parasite and its surrounding vacuole. Both PEXEL proteins and PNEPs cross this membrane through a protein translocon called *Plasmodium* Translocon of EXported proteins (PTEX) (de Koning-Ward et al., 2009), then transit by an exo−membranous trafficking system established by the parasite in the erythrocyte cytosol, and eventually some of them traffic further to the erythrocyte cytoskeleton and plasma membrane. Parasite proteins involved in the export machinery are expressed in both asexual and sexual stages, and proteins containing a PEXEL motif or identified as PNEPs are found at the gametocyte-infected erythrocyte membrane (**Figure 1**; Ingmundson et al., 2014). For instance, early studies showed that the gametocyte-specific giant protein Pf11-1 is exported to the cytoplasm of infected erythrocytes where it interacts with the erythrocyte membrane (Scherf et al., 1992). Later, comparative analysis of the proteome of asexual stages and gametocytes revealed that sexual differentiation is accompanied by an intense export of gametocyte proteins putatively involved in erythrocyte remodeling (Silvestrini et al., 2010). Some of these proteins, over-represented in early gametocytes, were called *P. falciparum* Gametocyte EXported Proteins (PfGEXP) (Silvestrini et al., 2010). The export of several PfGEXPs to the infected erythrocyte has been experimentally validated, including Pfg14.744 (Eksi et al., 2005), PfGECO (Morahan et al., 2011), PfGEXP5 (Tiburcio et al., 2015), and PfGEXP10 (Silvestrini et al., 2010). A recent report confirmed these findings and identified novel exported proteins by proteomics and immune profiling (Dantzler et al., 2019). Trypsin treatment, immunofluorescence and flow cytometry studies demonstrated erythrocyte surface exposure for six antigens, including PfGEXP7 and PfGEXP10. These proteins probably impact the properties of the gametocyte-infected erythrocyte (GIE) membrane, however, it is difficult to predict their function and their role in membrane remodeling due to the lack of any obvious functional annotation for most of the GEXPs. Several GEXPs, as PfGEXP5, belong to the PHIST (*Plasmodium* Helical Interspersed SubTelomeric) protein family (Silvestrini et al., 2010). This family of 89 exported proteins is implicated in various molecular and cellular processes (Warncke et al., 2016), and several PHIST proteins localize to the erythrocyte cytoskeleton during asexual stages where they contribute to erythrocyte remodeling (Parish et al., 2013; Oberli et al., 2016). However, since most of GEPXPs are conserved in asexual and sexual stages, they are unlikely to contribute to the specific needs of gametocytes.

Major specificities of protein export in gametocytes are the absence of the Knob-Associated Histidine Protein (KAHRP) at the erythrocyte skeleton and the reduced levels of the *P. falciparum* erythrocyte membrane protein 1 (PfEMP1) exposed on the erythrocyte surface (Tiburcio et al., 2013) (**Figure 1B**). In contrast, the other multigenic families STEVOR and RIFIN are highly expressed during sexual differentiation (McRobert et al., 2004; Petter et al., 2008; Wang et al., 2010). Immunofluorescence studies with antibodies distinguishing A and B RIFINs revealed that only A-type RIFINs are detectable in the cytoplasm of erythrocytes infected by immature gametocytes and are localized at the erythrocyte membrane (Petter et al., 2008). STEVOR proteins have also been shown to be associated with the erythrocyte membrane in immature gametocytes stages (McRobert et al., 2004; Tiburcio et al., 2012). Although the adhesive domain of STEVOR was detected at the erythrocyte surface in asexual stages where it plays a role in rosetting (Niang et al., 2009; Niang et al., 2014; Singh et al., 2017; Wichers et al., 2019), recent immunofluorescence studies convincingly showed that this domain is not exposed at the surface of erythrocytes infected with immature gametocytes (Neveu et al., 2018). At the mature gametocyte stage, STEVOR proteins are no longer detectable at the erythrocyte membrane, probably as a result of conformational changes upon dephosphorylation (Tiburcio et al., 2012; Naissant et al., 2016; **Figure 1B**). Other parasite proteins also probably disappear from the membrane after stage III since a recent report highlighted that antigens exposed at the surface of stage I/II GIE, but not of mature GIE, are recognized by plasma from naturally exposed individuals (Dantzler et al., 2019). This reduced antigen expression may be due to a decreased in protein export in mature stages. Indeed, PTEX components are expressed in stage I/II gametocytes but undergo degradation during further progression of gametocyte maturation, suggesting that protein export mostly occurs in the first stages of gametocytogenesis (Matthews et al., 2013). This hypothesis would be consistent with the development of the Inner Membrane Complex from stage III onward (Dearnley et al., 2012). Indeed, this system of

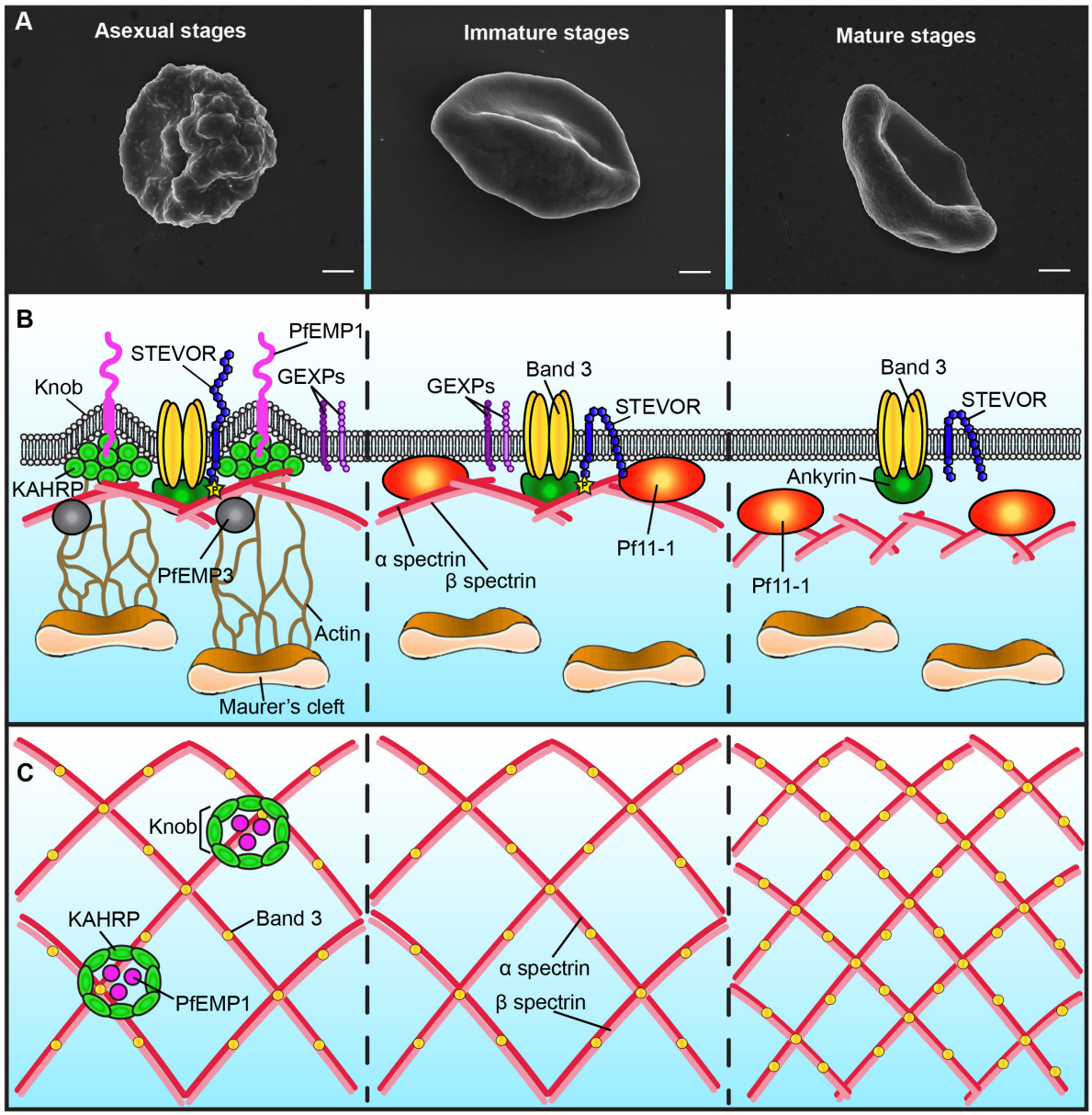

FIGURE 1 | Schematic representation of the plasma membrane and cytoskeleton of *P. falciparum*-infected erythrocytes. Only major differences between different parasite stages are shown. **(A)** Scanning electron microscopy images showing the presence of knobs at the membrane of erythrocytes infected with asexual stages (left panel), but not with gametocytes (middle and right panels). Bars represent 1 μm. **(B)** Schematic representation of the infected-erythrocyte membrane. Left panel: During asexual stages the membrane of infected erythrocytes presents knobs formed by the parasite protein KAHRP. Knobs act as a scaffold for the presentation of PfEMP1 and are connected by actin filaments to the Maurer's clefts. PfEMP3 and STEVOR interact with the spectrin network. The N-terminal domain of STEVOR is exposed at the host cell surface and the C-terminal domain is phosphorylated and linked to the ankyrin complex. GEXPs are exposed at the infected erythrocyte surface of both asexual and gametocyte stages. Middle panel: During immature gametocyte stages, knobs, PfEMP1 and KAHRP are absent from the membrane. The gametocyte-specific protein Pf11-1 is associated to the membrane. Maurer's clefts are not tethered to the membrane by actin. The N-terminal domain of STEVOR is localized at the cytoplasmic face of the infected cell. Right panel: During the mature gametocyte stage, STEVOR is dephosphorylated and its association with the ankyrin complex is abolished. GEXPs are absent from the infected erythrocyte surface. The level of coupling between the membrane skeleton and the plasma membrane decreases. **(C)** Schematic representation of the spectrin meshwork in different parasite stages. During asexual and immature gametocyte stages the length of the spectrin cross-members and the size of the skeletal meshwork are expanded (left and middle panels). Deformable mature GIE exhibit a reduced spectrin meshwork size comparable to that in uninfected erythrocytes (right panel).

flattened membrane compartments underneath the gametocyte plasma membrane could represent a major obstacle for proteins to be trafficked to the erythrocyte cytosol. In addition, the reduction of protein exposure may also result from protease activity or release via extracellular vesicles. Since proteins exposed at the surface of immature GIE may be involved

TABLE 1 | Parasite proteins involved in erythrocyte membrane makeover.

Protein	Localization	Stage	Role in erythrocyte remodeling	References
RESA	Erythrocyte skeleton	Asexual and sexual	Stabilization of the erythrocyte skeleton	Pei et al., 2007
RhopH	Erythrocyte membrane	Asexual	New Permeability Pathway	Counihan et al., 2017; Ito et al., 2017; Sherling et al., 2017
Pf11-1	Erythrocyte cytosol and skeleton	Sexual	Unknown	Scherf et al., 1992
Pfg14.744	Erythrocyte cytosol	Sexual	Unknown	Eksi et al., 2005
PfGECO (PfGEXP1)	Erythrocyte cytosol	Sexual	Unknown	Morahan et al., 2011
PfGEXP5	Erythrocyte cytosol	Sexual	Unknown	Tiburcio et al., 2015
PfGEXP10	Erythrocyte surface	Asexual and sexual	Antigenic exposure, adhesion	Silvestrini et al., 2010; Hermand et al., 2016; Dantzler et al., 2019
PfGEXP7	Erythrocyte surface	Asexual and sexual	Antigenic exposure, adhesion	Silvestrini et al., 2010; Hermand et al., 2016; Dantzler et al., 2019
KAHRP	Erythrocyte skeleton	Asexual	Deformability, knobs formation	Crabb et al., 1997; Glenister et al., 2002; Looker et al., 2019
PfEMP1	MC, erythrocyte surface	asexual	Adhesion, antigenic variation	Baruch et al., 1995; Chen et al., 1998
STEVOR	MC, erythrocyte membrane and surface	Asexual and sexual	Adhesion, deformability, antigenic variation	Niang et al., 2009; Sanyal et al., 2012; Tiburcio et al., 2012; Niang et al., 2014; Naissant et al., 2016; Neveu et al., 2018; Wichers et al., 2019
RIFIN	MC, erythrocyte membrane and surface	Asexual and sexual	Adhesion, immune evasion, antigenic variation	Fernandez et al., 1999; Kyes et al., 1999; Goel et al., 2015
PfEMP3	MC, erythrocyte skeleton	Asexual	Deformability	Glenister et al., 2002

Localization, expression at asexual or sexual stages and involvement in erythrocyte remodeling are indicated with corresponding references. MC: Maurer's Clefts.

in the interactions with the bone marrow parenchyma, their disappearance may contribute to the release of mature GIE in the blood circulation.

REORGANIZATION OF THE ERYTHROCYTE PLASMA MEMBRANE AND CYTOSKELETON

The export of hundreds of parasite proteins to the host cell and the synthesis of novel cellular structures induce a dynamic reorganization of the erythrocyte plasma membrane and of the underlying cytoskeleton. One of the major changes in the plasma membrane of erythrocytes infected with asexual stages is the appearance of thousands of small protrusions at the cell surface termed knobs that act as a scaffold for the presentation of the virulence protein PfEMP1 (**Figure 1A**; Luse and Miller, 1971; Langreth et al., 1978; Crabb et al., 1997). Knobs, whose formation depends on the parasite-derived protein KAHRP, consist of an electron-dense ring-shaped structure underpinned by a spiral structure and connected by multiple links to the actin-spectrin meshwork of the erythrocyte membrane skeleton (**Figure 1C**; Crabb et al., 1997; Looker et al., 2019). Scanning and transmission electron microscopy analyses revealed that the surface of erythrocytes infected by developing gametocytes from stage II to V are devoid of knobs (**Figure 1A**; Sinden, 1982; Tiburcio et al., 2012). In contrast, an early study reported that knobs are present at the surface of stage I GIE (Day et al., 1998). Of note, this study did not benefit from state-of-the-art tools to distinguish asexual from early sexual stages and rather used standard light microscopy for parasite stages differentiation. More recently, transgenic parasites expressing a fluorescent reporter under a gametocyte-specific promoter allowed separation of stage I gametocytes from asexual trophozoites (Silvestrini et al., 2010). Electron microscopy analysis of purified early gametocytes from this transgenic line established that stage I gametocytes do not modify their surface with knob structures (Tiburcio et al., 2013). The erythrocyte membrane modifications induced by gametocyte development rather occur in the cytoskeleton, with remodeling of both lateral and vertical interactions within the skeleton (Dearnley et al., 2016). As observed in asexual stages (Shi et al., 2013), atomic force microscopy of the cytoplasmic surface of the membrane of mechanically sheared infected erythrocytes revealed that the length of the spectrin cross-members and the size of the skeletal meshwork increase in developing immature GIE (**Figure 1C**; Dearnley et al., 2016). This expansion is accompanied by enhanced coupling of the membrane skeleton to the membrane bilayer in immature stages, as evidenced by an altered lateral mobility of Band 3 monitored by microscope-based photobleaching (Parker et al., 2004; Dearnley et al., 2016). In parallel, erythrocytic actin is relocated from the skeleton to the parasite-derived organelles known as Maurer's Clefts (Dearnley et al., 2016). However, in the absence of knobs, which act as anchoring points for these organelles in asexual stages, actin relocation does not tether Maurer's Clefts onto the erythrocyte membrane in gametocytes, thereby increasing their mobility (Cyrklaff et al., 2011; Dearnley et al., 2016). All these modifications are then reversed in stage V GIE, which exhibit a spectrin length and a Band 3 mobile fraction similar to uninfected erythrocytes (**Figure 1C**). A composite model predicting the physical consequences of restructuring the skeletal meshwork revealed that these reversible changes are likely linked to the switch in GIE deformability occurring at the transition from

immature to mature gametocyte stages (Tiburcio et al., 2012; Dearnley et al., 2016).

CHANGES IN ERYTHROCYTE DEFORMABILITY

The profound reorganization of the membrane nanostructure deeply affects the mechanical properties of the infected erythrocyte membrane. During *P. falciparum* asexual development, the infected erythrocyte becomes progressively rigid and the erythrocyte membrane loses its elasticity (Cranston et al., 1984; Nash et al., 1989), in part due to the export of parasite proteins that interact with the erythrocyte skeleton, including KAHRP, PfEMP3, RESA and STEVOR (**Figure 1B** and **Table 1**; Glenister et al., 2002; Mills et al., 2007; Sanyal et al., 2012). Similar biophysical changes occur during gametocytogenesis: an increase in rigidity is observed upon infection with immature gametocytes from stage I to IV, followed by a switch in deformability at the transition between stage IV and stage V (Aingaran et al., 2012; Dearnley et al., 2012; Tiburcio et al., 2012). Increased stiffness of immature GIE may contribute to their sequestration in the bone marrow parenchyma by mechanical retention, whereas the newly acquired deformability of mature GIE leads to a restored ability to cross narrow apertures and may help them survive in the circulation, where they can be picked up by mosquitoes. The regulation of GIE deformability results from a combination of several factors that are beginning to be elucidated. While it has long been thought that immature GIE stiffness was fully dependent on the gametocyte microtubule skeleton, a study reported that disruption of the microtubule network did not influence immature GIE rigidity (Dearnley et al., 2016). These observations suggest that regulation of GIE deformability mainly results from the parasite-induced modifications of its host erythrocyte rather than from the parasite cytoskeleton. In contrast, treatment of immature GIE with cytochalasin D increased GIE deformability, suggesting an important role of the actin cytoskeleton in the GIE membrane stiffness (Dearnley et al., 2016).

As shown in asexual stages, GIE membrane viscoelasticity is affected by the export of parasite proteins to the erythrocyte membrane skeleton. For instance, modulation of GIE deformability is dependent on presence of the parasite proteins STEVOR at the erythrocyte membrane (Tiburcio et al., 2012) and on the interaction of the cytoplasmic domain of STEVOR with erythrocyte proteins composing the ankyrin complex (spectrin α, spectrin β, ankyrin and Band 3) (**Figure 1B**; Naissant et al., 2016). This interaction is dependent on PKA-mediated phosphorylation of the STEVOR cytoplasmic tail and is tightly regulated by the parasite. STEVOR phosphorylation only occurs in immature stages and is due to increased cAMP levels resulting from a low expression of the plasmodial phosphodiesterase δ (PfPDEδ) at this stage. Rising expression of PfPDEδ in mature stages leads to a drop of cAMP levels that reduce the phosphorylation of both STEVORs and their cytoskeletal partner(s) and consequently weaken or abolish their interactions, eventually resulting in an increase of infected erythrocyte deformability (Ramdani et al., 2015; Naissant et al., 2016). In accordance with the key role of PfPDEδ in this mechanism, the marketed PDE inhibitor sildenafil (Viagra®) increases cAMP concentration in mature GIE and impairs their circulation in an *in vitro* model for splenic retention (Ramdani et al., 2015). In line with these observations, treatment of *P. berghei*-infected mice with sildenafil increases gametocytes homing to sequestration sites, suggesting that PDE inhibitors may cause gametocytes to become mechanically trapped in the bone marrow and splenic cords (De Niz et al., 2018).

REMODELING OF ADHESIVES PROPERTIES

To sequester away from the peripheral circulation, asexual parasites deeply modify the adhesive properties of their host erythrocyte membrane and adhere to the host microvasculature via specific ligand-receptor interactions, primarily mediated by the parasite antigen PfEMP1 (Baruch et al., 1995). This adhesin is anchored on knobs at the surface of infected erythrocytes and binds to host endothelial receptors such as ICAM-1 and CD36 (**Figures 1B,C**; Miller et al., 2002). Erythrocytes infected with asexual parasites could also adhere to surrounding non-infected erythrocytes through binding of different antigenic variants of the parasite (PfEMP1, STEVOR and RIFIN) to different receptors on the surface of the erythrocyte, leading to rosette formation (Chen et al., 1998; Niang et al., 2014; Goel et al., 2015). Unlike asexual stages, the adhesive properties of the GIE membrane have long been debated and are still elusive. Early studies produced conflicting data on GIE adhesion efficiency and reported low binding of immature GIE, but not of mature stages, to C32 melanoma or bone marrow stromal cell lines (Rogers et al., 1996; Rogers et al., 2000). This conclusion was, however, not confirmed by another report showing that stage I GIE adhere to CD36-expressing C32 melanoma cells while stage II to V GIE lose their adhesive properties (Day et al., 1998). More recent studies have convincingly shown that immature stage I-IV GIE do not adhere to a panel of endothelial cell lines from various human organs (Silvestrini et al., 2012; Tiburcio et al., 2013). These results are in accordance with the detection of immature gametocytes in extravascular spaces of bone marrow in *ex vivo* and autopsy specimens from malaria-infected patients (Farfour et al., 2012; Joice et al., 2014). The unveiling of the hidden sites for gametocytes maturation led to the hypothesis that they could adhere to non-endothelial bone marrow cells. Recent work using an *in vitro* tridimensional co-culture system revealed that immature GIE adhere to human bone marrow mesenchymal stem cells via trypsin-sensitive parasite ligands exposed on the erythrocyte surface (Messina et al., 2018). This adhesion induces stimulation of mesenchymal cells to secrete a panel of cytokines and growth factors involved in angiogenesis, thus suggesting a mechanism used by the parasite to remodel the bone marrow endothelium. It has been proposed that the GIE surface proteins GEXP7 and GEXP10, which are able to bind CX3CL1, a chemokine expressed on bone marrow stromal cells, may be involved in this

adhesion (Hermand et al., 2016; Messina et al., 2018). However, their insensitivity to trypsin treatment does not support this hypothesis (Dantzler et al., 2019). Although the ligand(s) and receptor(s) promoting such interactions are not identified yet, this mechanism may contribute to immature GIE sequestration in the parenchyma. In contrast, cell-cell adhesion assays with human primary erythroblasts revealed that immature GIE do not specifically adhere to erythroid precursors, despite the fact that some parasite antigens involved in rosetting of asexual stages are expressed by gametocytes and may bind to their receptors present at the surface of erythroblasts (Neveu et al., 2018). The absence of a rosetting-like phenotype in sexual stages is likely due to the reduced levels of PfEMP1 (Tiburcio et al., 2013) and to the failure to detect STEVOR at the surface of immature GIE (Neveu et al., 2018). These observations highlighted that some parasite adhesins may have different role and topology in asexual and sexual stages, which may reflect a strategy that the parasite has evolved to differently modify its host cell to adapt to different microenvironments (Neveu et al., 2018).

CONCLUDING REMARKS

Recent studies have greatly improved our understanding of how *P. falciparum* gametocytes redecorate the surface of their erythrocyte host with parasite antigens and how they remodel the erythrocyte deformability and adhesive properties. Many questions remain outstanding regarding the sequestration mechanisms of immature gametocytes in the bone marrow parenchyma and how erythrocyte remodeling contributes to these processes. The increase in erythrocyte membrane stiffness and the export of adhesive molecules at the erythrocyte surface may contribute to immature GIE sequestration by mechanical retention and by adhesion to bone marrow cells, respectively. Besides these mechanisms, the maintenance of immature gametocytes in the bone marrow parenchyma may also be mediated by the infection of erythroblasts constituting the erythroblastic islands. In support of this hypothesis, the development of asexual parasites can take place in a culture of human erythroblasts and immature gametocytes of stages I and II have been observed in these cells (Tamez et al., 2009; Joice et al., 2014). Whether gametocytes can complete their development in erythroblasts and how the parasite remodels these nucleated cells remains to be investigated.

Our current understanding of the host cell remodeling induced by *P. falciparum* gametocytes opens avenues toward the design of novel interventions to interrupt parasite transmission and the spread of malaria, including transmission-blocking drugs targeting GIE mechanical properties and transmission-blocking vaccines targeting GIE surface antigens.

AUTHOR CONTRIBUTIONS

GN drafted the manuscript. CL edited the manuscript.

FUNDING

GN was supported by a labex GR-Ex fellowship. The labex GR-Ex, reference ANR-11-LABX-0051 is funded by the program "Investissements d'Avenir" of the French National Research Agency, reference ANR-11-IDEX-0005-02. CL and GN acknowledge the financial support from the CNRS, Inserm and the Fondation pour la Recherche Médicale ("Equipe FRM" grant DEQ20170336722).

REFERENCES

Aguilar, R., Magallon-Tejada, A., Achtman, A. H., Moraleda, C., Joice, R., Cistero, P., et al. (2014). Molecular evidence for the localization of *Plasmodium falciparum* immature gametocytes in bone marrow. *Blood* 123, 959–966. doi: 10.1182/blood-2013-08-520767

Aingaran, M., Zhang, R., Law, S. K., Peng, Z., Undisz, A., Meyer, E., et al. (2012). Host cell deformability is linked to transmission in the human malaria parasite *Plasmodium falciparum*. *Cell Microbiol.* 14, 983–993. doi: 10.1111/j.1462-5822.2012.01786.x

Baruch, D. I., Pasloske, B. L., Singh, H. B., Bi, X., Ma, X. C., Feldman, M., et al. (1995). Cloning the P. *falciparum* gene encoding PfEMP1, a malarial variant antigen and adherence receptor on the surface of parasitized human erythrocytes. *Cell* 82, 77–87. doi: 10.1016/0092-8674(95)90054-3

Chen, Q., Barragan, A., Fernandez, V., Sundstrom, A., Schlichtherle, M., Sahlen, A., et al. (1998). Identification of *Plasmodium falciparum* erythrocyte membrane protein 1 (PfEMP1) as the rosetting ligand of the malaria parasite P. *falciparum*. *J. Exp. Med.* 187, 15–23. doi: 10.1084/jem.187.1.15

Counihan, N. A., Chisholm, S. A., Bullen, H. E., Srivastava, A., Sanders, P. R., Jonsdottir, T. K., et al. (2017). *Plasmodium falciparum* parasites deploy RhopH2 into the host erythrocyte to obtain nutrients, grow and replicate. *eLife* 6:e23217. doi: 10.7554/eLife.23217

Crabb, B. S., Cooke, B. M., Reeder, J. C., Waller, R. F., Caruana, S. R., Davern, K. M., et al. (1997). Targeted gene disruption shows that knobs enable malaria-infected red cells to cytoadhere under physiological shear stress. *Cell* 89, 287–296. doi: 10.1016/s0092-8674(00)80207-x

Cranston, H. A., Boylan, C. W., Carroll, G. L., Sutera, S. P., Williamson, J. R., Gluzman, I. Y., et al. (1984). *Plasmodium falciparum* maturation abolishes physiologic red cell deformability. *Science* 223, 400–403. doi: 10.1126/science.6362007

Cyrklaff, M., Sanchez, C. P., Kilian, N., Bisseye, C., Simpore, J., Frischknecht, F., et al. (2011). Hemoglobins S and C interfere with actin remodeling in *Plasmodium falciparum*-infected erythrocytes. *Science* 334, 1283–1286. doi: 10.1126/science.1213775

Dantzler, K. W., Ma, S., Ngotho, P., Stone, W. J. R., Tao, D., Rijpma, S., et al. (2019). Naturally acquired immunity against immature *Plasmodium falciparum* gametocytes. *Sci. Transl. Med.* 11:eaav3963. doi: 10.1126/scitranslmed.aav3963

Day, K. P., Hayward, R. E., Smith, D., and Culvenor, J. G. (1998). CD36-dependent adhesion and knob expression of the transmission stages of *Plasmodium falciparum* is stage specific. *Mol. Biochem. Parasitol.* 93, 167–177. doi: 10.1016/s0166-6851(98)00040-1

de Koning-Ward, T. F., Gilson, P. R., Boddey, J. A., Rug, M., Smith, B. J., Papenfuss, A. T., et al. (2009). A newly discovered protein export machine in malaria parasites. *Nature* 459, 945–949. doi: 10.1038/nature08104

De Niz, M., Meibalan, E., Mejia, P., Ma, S., Brancucci, N. M. B., Agop-Nersesian, C., et al. (2018). *Plasmodium* gametocytes display homing and vascular transmigration in the host bone marrow. *Sci. Adv.* 4:eaat3775. doi: 10.1126/sciadv.aat3775

Dearnley, M., Chu, T., Zhang, Y., Looker, O., Huang, C., Klonis, N., et al. (2016). Reversible host cell remodeling underpins deformability changes in malaria parasite sexual blood stages. *Proc. Natl. Acad. Sci. U.S.A* 113, 4800–4805. doi: 10.1073/pnas.1520194113

Dearnley, M. K., Yeoman, J. A., Hanssen, E., Kenny, S., Turnbull, L., Whitchurch, C. B., et al. (2012). Origin, composition, organization and function of the inner membrane complex of *Plasmodium falciparum* gametocytes. *J. Cell Sci.* 125, 2053–2063. doi: 10.1242/jcs.099002

Eksi, S., Haile, Y., Furuya, T., Ma, L., Su, X., and Williamson, K. C. (2005). Identification of a subtelomeric gene family expressed during the asexual-sexual stage transition in *Plasmodium falciparum*. *Mol. Biochem. Parasitol.* 143, 90–99. doi: 10.1016/j.molbiopara.2005.05.010

Farfour, E., Charlotte, F., Settegrana, C., Miyara, M., and Buffet, P. (2012). The extravascular compartment of the bone marrow: a niche for *Plasmodium falciparum* gametocyte maturation? *Malar J.* 11:285. doi: 10.1186/1475-2875-11-285

Fernandez, V., Hommel, M., Chen, Q., Hagblom, P., and Wahlgren, M. (1999). Small, clonally variant antigens expressed on the surface of the *Plasmodium falciparum*-infected erythrocyte are encoded by the rif gene family and are the target of human immune responses. *J. Exp. Med.* 190, 1393–1404. doi: 10.1084/jem.190.10.1393

Glenister, F. K., Coppel, R. L., Cowman, A. F., Mohandas, N., and Cooke, B. M. (2002). Contribution of parasite proteins to altered mechanical properties of malaria-infected red blood cells. *Blood* 99, 1060–1063. doi: 10.1182/blood.v99.3.1060

Goel, S., Palmkvist, M., Moll, K., Joannin, N., Lara, P., Akhouri, R. R., et al. (2015). RIFINs are adhesins implicated in severe *Plasmodium falciparum* malaria. *Nat. Med.* 21, 314–317. doi: 10.1038/nm.3812

Hawking, F., Wilson, M. E., and Gammage, K. (1971). Evidence for cyclic development and short-lived maturity in the gametocytes of *Plasmodium falciparum*. *Trans. R. Soc. Trop. Med. Hyg.* 65, 549–559. doi: 10.1016/0035-9203(71)90036-8

Heiber, A., Kruse, F., Pick, C., Gruring, C., Flemming, S., Oberli, A., et al. (2013). Identification of new PNEPs indicates a substantial non-PEXEL exportome and underpins common features in *Plasmodium falciparum* protein export. *PLoS Pathog.* 9:e1003546. doi: 10.1371/journal.ppat.1003546

Hermand, P., Ciceron, L., Pionneau, C., Vaquero, C., Combadiere, C., and Deterre, P. (2016). *Plasmodium falciparum* proteins involved in cytoadherence of infected erythrocytes to chemokine CX3CL1. *Sci. Rep.* 6:33786. doi: 10.1038/srep33786

Hiller, N. L., Bhattacharjee, S., van Ooij, C., Liolios, K., Harrison, T., Lopez-Estrano, C., et al. (2004). A host-targeting signal in virulence proteins reveals a secretome in malarial infection. *Science* 306, 1934–1937. doi: 10.1126/science.1102737

Ingmundson, A., Alano, P., Matuschewski, K., and Silvestrini, F. (2014). Feeling at home from arrival to departure: protein export and host cell remodelling during *Plasmodium* liver stage and gametocyte maturation. *Cell Microbiol.* 16, 324–333. doi: 10.1111/cmi.12251

Ito, D., Schureck, M. A., and Desai, S. A. (2017). An essential dual-function complex mediates erythrocyte invasion and channel-mediated nutrient uptake in malaria parasites. *eLife* 6:e23485. doi: 10.7554/eLife.23485

Joice, R., Nilsson, S. K., Montgomery, J., Dankwa, S., Egan, E., Morahan, B., et al. (2014). *Plasmodium falciparum* transmission stages accumulate in the human bone marrow. *Sci. Transl. Med.* 6, 244–245.

Kyes, S. A., Rowe, J. A., Kriek, N., and Newbold, C. I. (1999). Rifins: a second family of clonally variant proteins expressed on the surface of red cells infected with *Plasmodium falciparum*. *Proc. Natl. Acad. Sci. U.S.A.* 96, 9333–9338. doi: 10.1073/pnas.96.16.9333

Langreth, S. G., Jensen, J. B., Reese, R. T., and Trager, W. (1978). Fine structure of human malaria *in vitro*. *J. Protozool.* 25, 443–452.

Looker, O., Blanch, A. J., Liu, B., Nunez-Iglesias, J., McMillan, P. J., Tilley, L., et al. (2019). The knob protein KAHRP assembles into a ring-shaped structure that underpins virulence complex assembly. *PLoS Pathog.* 15:e1007761. doi: 10.1371/journal.ppat.1007761

Luse, S. A., and Miller, L. H. (1971). *Plasmodium falciparum* malaria. Ultrastructure of parasitized erythrocytes in cardiac vessels. *Am. J. Trop. Med. Hyg.* 20, 655–660. doi: 10.4269/ajtmh.1971.20.655

Marti, M., Good, R. T., Rug, M., Knuepfer, E., and Cowman, A. F. (2004). Targeting malaria virulence and remodeling proteins to the host erythrocyte. *Science* 306, 1930–1933. doi: 10.1126/science.1102452

Matthews, K., Kalanon, M., Chisholm, S. A., Sturm, A., Goodman, C. D., Dixon, M. W., et al. (2013). The *Plasmodium* translocon of exported proteins (PTEX) component thioredoxin-2 is important for maintaining normal blood-stage growth. *Mol. Microbiol.* 89, 1167–1186. doi: 10.1111/mmi.12334

McRobert, L., Preiser, P., Sharp, S., Jarra, W., Kaviratne, M., Taylor, M. C., et al. (2004). Distinct trafficking and localization of STEVOR proteins in three stages of the *Plasmodium falciparum* life cycle. *Infect. Immun.* 72, 6597–6602. doi: 10.1128/iai.72.11.6597-6602.2004

Messina, V., Valtieri, M., Rubio, M., Falchi, M., Mancini, F., Mayor, A., et al. (2018). Gametocytes of the malaria parasite *Plasmodium falciparum* interact with and stimulate bone marrow mesenchymal cells to secrete angiogenetic factors. *Front. Cell Infect. Microbiol.* 8:50. doi: 10.3389/fcimb.2018.00050

Miller, L. H., Baruch, D. I., Marsh, K., and Doumbo, O. K. (2002). The pathogenic basis of malaria. *Nature* 415, 673–679. doi: 10.1038/415673a

Mills, J. P., Diez-Silva, M., Quinn, D. J., Dao, M., Lang, M. J., Tan, K. S., et al. (2007). Effect of plasmodial RESA protein on deformability of human red blood cells harboring *Plasmodium falciparum*. *Proc. Natl. Acad. Sci. U.S.A.* 104, 9213–9217. doi: 10.1073/pnas.0703433104

Morahan, B. J., Strobel, C., Hasan, U., Czesny, B., Mantel, P. Y., Marti, M., et al. (2011). Functional analysis of the exported type IV HSP40 protein PfGECO in *Plasmodium falciparum* gametocytes. *Eukaryot Cell* 10, 1492–1503. doi: 10.1128/EC.05155-11

Naissant, B., Dupuy, F., Duffier, Y., Lorthiois, A., Duez, J., Scholz, J., et al. (2016). *Plasmodium falciparum* STEVOR phosphorylation regulates host erythrocyte deformability enabling malaria parasite transmission. *Blood* 127, e42–e53. doi: 10.1182/blood-2016-01-690776

Nash, G. B., O'Brien, E., Gordon-Smith, E. C., and Dormandy, J. A. (1989). Abnormalities in the mechanical properties of red blood cells caused by *Plasmodium falciparum*. *Blood* 74, 855–861. doi: 10.1182/blood.v74.2.855.bloodjournal742855

Neveu, G., Dupuy, F., Ladli, M., Barbieri, D., Naissant, B., Richard, C., et al. (2018). *Plasmodium falciparum* gametocyte-infected erythrocytes do not adhere to human primary erythroblasts. *Sci. Rep.* 8:17886.

Niang, M., Bei, A. K., Madnani, K. G., Pelly, S., Dankwa, S., Kanjee, U., et al. (2014). STEVOR is a *Plasmodium falciparum* erythrocyte binding protein that mediates merozoite invasion and rosetting. *Cell Host Microbe* 16, 81–93. doi: 10.1016/j.chom.2014.06.004

Niang, M., Yan Yam, X., and Preiser, P. R. (2009). The *Plasmodium falciparum* STEVOR multigene family mediates antigenic variation of the infected erythrocyte. *PLoS Pathog.* 5:e1000307. doi: 10.1371/journal.ppat.1000307

Oberli, A., Zurbrugg, L., Rusch, S., Brand, F., Butler, M. E., Day, J. L., et al. (2016). *Plasmodium falciparum Plasmodium* helical interspersed subtelomeric proteins contribute to cytoadherence and anchor P. *falciparum* erythrocyte membrane protein 1 to the host cell cytoskeleton. *Cell Microbiol.* 18, 1415–1428. doi: 10.1111/cmi.12583

Parish, L. A., Mai, D. W., Jones, M. L., Kitson, E. L., and Rayner, J. C. (2013). A member of the *Plasmodium falciparum* PHIST family binds to the erythrocyte cytoskeleton component band 4.1. *Malar J.* 12:160. doi: 10.1186/1475-2875-12-160

Parker, P. D., Tilley, L., and Klonis, N. (2004). *Plasmodium falciparum* induces reorganization of host membrane proteins during intraerythrocytic growth. *Blood* 103, 2404–2406. doi: 10.1182/blood-2003-08-2692

Pei, X., Guo, X., Coppel, R., Bhattacharjee, S., Haldar, K., Gratzer, W., et al. (2007). The ring-infected erythrocyte surface antigen (RESA) of *Plasmodium falciparum* stabilizes spectrin tetramers and suppresses further invasion. *Blood* 110, 1036–1042. doi: 10.1182/blood-2007-02-076919

Petter, M., Bonow, I., and Klinkert, M. Q. (2008). Diverse expression patterns of subgroups of the rif multigene family during *Plasmodium falciparum* gametocytogenesis. *PLoS One* 3:e3779. doi: 10.1371/journal.pone.0003779

Ramdani, G., Naissant, B., Thompson, E., Breil, F., Lorthiois, A., Dupuy, F., et al. (2015). cAMP-signalling regulates gametocyte-infected erythrocyte deformability required for malaria parasite transmission. *PLoS Pathog.* 11:e1004815. doi: 10.1371/journal.ppat.1004815

Rogers, N. J., Daramola, O., Targett, G. A., and Hall, B. S. (1996). CD36 and intercellular adhesion molecule 1 mediate adhesion of developing *Plasmodium falciparum* gametocytes. *Infect. Immun.* 64, 1480–1483.

Rogers, N. J., Hall, B. S., Obiero, J., Targett, G. A., and Sutherland, C. J. (2000). A model for sequestration of the transmission stages of *Plasmodium falciparum*: adhesion of gametocyte-infected erythrocytes to human bone marrow cells. *Infect. Immun.* 68, 3455–3462. doi: 10.1128/iai.68.6.3455-3462.2000

Sanyal, S., Egee, S., Bouyer, G., Perrot, S., Safeukui, I., Bischoff, E., et al. (2012). *Plasmodium falciparum* STEVOR proteins impact erythrocyte mechanical properties. *Blood* 119, e1–e8. doi: 10.1182/blood-2011-08-370734

Scherf, A., Carter, R., Petersen, C., Alano, P., Nelson, R., Aikawa, M., et al. (1992). Gene inactivation of Pf11-1 of *Plasmodium falciparum* by chromosome breakage and healing: identification of a gametocyte-specific protein with a potential role in gametogenesis. *EMBO J.* 11, 2293–2301. doi: 10.1002/j.1460-2075.1992.tb05288.x

Sherling, E. S., Knuepfer, E., Brzostowski, J. A., Miller, L. H., Blackman, M. J., and van Ooij, C. (2017). The *Plasmodium falciparum* rhoptry protein RhopH3 plays essential roles in host cell invasion and nutrient uptake. *eLife* 6:e23239. doi: 10.7554/eLife.23239

Shi, H., Liu, Z., Li, A., Yin, J., Chong, A. G., Tan, K. S., et al. (2013). Life cycle-dependent cytoskeletal modifications in *Plasmodium falciparum* infected erythrocytes. *PLoS One* 8:e61170. doi: 10.1371/journal.pone.0061170

Silvestrini, F., Lasonder, E., Olivieri, A., Camarda, G., van Schaijk, B., Sanchez, M., et al. (2010). Protein export marks the early phase of gametocytogenesis of the human malaria parasite *Plasmodium falciparum*. *Mol. Cell Proteomics* 9, 1437–1448. doi: 10.1074/mcp.M900479-MCP200

Silvestrini, F., Tiburcio, M., Bertuccini, L., and Alano, P. (2012). Differential adhesive properties of sequestered asexual and sexual stages of *Plasmodium falciparum* on human endothelial cells are tissue independent. *PLoS One* 7:e31567. doi: 10.1371/journal.pone.0031567

Sinden, R. E. (1982). Gametocytogenesis of *Plasmodium falciparum in vitro*: an electron microscopic study. *Parasitology* 84, 1–11. doi: 10.1017/s003118200005160x

Singh, H., Madnani, K., Lim, Y. B., Cao, J., Preiser, P. R., and Lim, C. T. (2017). Expression dynamics and physiologically relevant functional study of STEVOR in asexual stages of *Plasmodium falciparum* infection. *Cell Microbiol.* 19:e12715. doi: 10.1111/cmi.12715

Smith, J. D., Chitnis, C. E., Craig, A. G., Roberts, D. J., Hudson-Taylor, D. E., Peterson, D. S., et al. (1995). Switches in expression of *Plasmodium falciparum* var genes correlate with changes in antigenic and cytoadherent phenotypes of infected erythrocytes. *Cell* 82, 101–110. doi: 10.1016/0092-8674(95)90056-x

Tamez, P. A., Liu, H., Fernandez-Pol, S., Haldar, K., and Wickrema, A. (2009). Stage-specific susceptibility of human erythroblasts to *Plasmodium falciparum* malaria infection. *Blood* 114, 3652–3655. doi: 10.1182/blood-2009-07-231894

Tiburcio, M., Dixon, M. W., Looker, O., Younis, S. Y., Tilley, L., and Alano, P. (2015). Specific expression and export of the *Plasmodium falciparum* Gametocyte EXported Protein-5 marks the gametocyte ring stage. *Malar J.* 14:334. doi: 10.1186/s12936-015-0853-6

Tiburcio, M., Niang, M., Deplaine, G., Perrot, S., Bischoff, E., Ndour, P. A., et al. (2012). A switch in infected erythrocyte deformability at the maturation and blood circulation of *Plasmodium falciparum* transmission stages. *Blood* 119, e172–e180. doi: 10.1182/blood-2012-03-414557

Tiburcio, M., Silvestrini, F., Bertuccini, L., Sander, A., Turner, L., Lavstsen, T., et al. (2013). Early gametocytes of the malaria parasite *Plasmodium falciparum* specifically remodel the adhesive properties of infected erythrocyte surface. *Cell Microbiol.* 15, 647–659. doi: 10.1111/cmi.12062

Wang, C. W., Mwakalinga, S. B., Sutherland, C. J., Schwank, S., Sharp, S., Hermsen, C. C., et al. (2010). Identification of a major rif transcript common to gametocytes and sporozoites of *Plasmodium falciparum*. *Malar J.* 9:147. doi: 10.1186/1475-2875-9-147

Warncke, J. D., Vakonakis, I., and Beck, H. P. (2016). *Plasmodium* helical interspersed subtelomeric (PHIST) proteins, at the center of host cell remodeling. *Microbiol. Mol. Biol. Rev.* 80, 905–927. doi: 10.1128/MMBR.00014-16

Wichers, J. S., Scholz, J. A. M., Strauss, J., Witt, S., Lill, A., Ehnold, L. I., et al. (2019). Dissecting the gene expression, localization, membrane topology, and function of the *Plasmodium falciparum* STEVOR protein family. *mBio* 10:e1500-19. doi: 10.1128/mBio.01500-19

Conflict of Interest: The authors declare that the research was conducted in the absence of any commercial or financial relationships that could be construed as a potential conflict of interest.

frontiers in Microbiology

ORIGINAL RESEARCH
published: 15 November 2019
doi: 10.3389/fmicb.2019.02651

Field Relevant Variation in Ambient Temperature Modifies Density-Dependent Establishment of *Plasmodium falciparum* Gametocytes in Mosquitoes

Ashutosh K. Pathak[1,2,3]*, *Justine C. Shiau*[1], *Matthew B. Thomas*[4] and *Courtney C. Murdock*[1,2,3,5,6,7]

[1] Department of Infectious Diseases, College of Veterinary Medicine, University of Georgia, Athens, GA, United States, [2] Center for Ecology of Infectious Diseases, University of Georgia, Athens, GA, United States, [3] Center for Tropical Emerging Global Diseases, University of Georgia, Athens, GA, United States, [4] The Department of Entomology, Center for Infectious Disease Dynamics, The Pennsylvania State University, University Park, PA, United States, [5] Odum School of Ecology, University of Georgia, Athens, GA, United States, [6] Center for Vaccines and Immunology, University of Georgia, Athens, GA, United States, [7] Riverbasin Center, University of Georgia, Athens, GA, United States

OPEN ACCESS

Edited by:
Rhoel Dinglasan,
University of Florida, United States

Reviewed by:
William Stone,
University of London, United Kingdom
Herman Parfait Awono Ambene,
Organisation de Coordination pour la lutte contre les Endémies en Afrique Centrale, Cameroon

***Correspondence:**
Ashutosh K. Pathak
ash1@uga.edu

Specialty section:
This article was submitted to Infectious Diseases, a section of the journal Frontiers in Microbiology

Received: 09 July 2019
Accepted: 30 October 2019
Published: 15 November 2019

Citation:
Pathak AK, Shiau JC, Thomas MB and Murdock CC (2019) Field Relevant Variation in Ambient Temperature Modifies Density-Dependent Establishment of Plasmodium falciparum Gametocytes in Mosquitoes. Front. Microbiol. 10:2651. doi: 10.3389/fmicb.2019.02651

The relationship between *Plasmodium falciparum* gametocyte density and infections in mosquitoes is central to understanding the rates of transmission with important implications for control. Here, we determined whether field relevant variation in environmental temperature could also modulate this relationship. *Anopheles stephensi* were challenged with three densities of *P. falciparum* gametocytes spanning a ∼10-fold gradient, and housed under diurnal/daily temperature range ("DTR") of 9°C (+5°C and −4°C) around means of 20, 24, and 28°C. Vector competence was quantified as the proportion of mosquitoes infected with oocysts in the midguts (oocyst rates) or infectious with sporozoites in the salivary glands (sporozoite rates) at peak periods of infection for each temperature to account for the differences in development rates. In addition, oocyst intensities were also recorded from infected midguts and the overall study replicated across three separate parasite cultures and mosquito cohorts. While vector competence was similar at 20 DTR 9°C and 24 DTR 9°C, oocyst and sporozoite rates were also comparable, with evidence, surprisingly, for higher vector competence in mosquitoes challenged with intermediate gametocyte densities. For the same gametocyte densities however, severe reductions in the sporozoite rates was accompanied by a significant decline in overall vector competence at 28 DTR 9°C, with gametocyte density *per se* showing a positive and linear effect at this temperature. Unlike vector competence, oocyst intensities decreased with increasing temperatures with a predominantly positive and linear association with gametocyte density, especially at 28 DTR 9°C. Oocyst intensities across individual infected midguts suggested temperature-specific differences in mosquito susceptibility/resistance: at 20 DTR 9°C and 24 DTR 9°C, dispersion

(aggregation) increased in a density-dependent manner but not at 28 DTR 9°C where the distributions were consistently random. Limitations notwithstanding, our results suggest that variation in temperature could modify seasonal dynamics of infectious reservoirs with implications for the design and deployment of transmission-blocking vaccines/drugs.

Keywords: malaria transmission, diurnal temperature range, gametocytemia, vector competence, oocysts, sporozoites, parasite aggregation, human infectious reservoir

INTRODUCTION

Targeting transmission of *Plasmodium falciparum* gametocytes to their mosquito vectors is now more pertinent than ever in light of the recent resurgence in disease incidence in sub-Saharan Africa but also for future efforts toward eliminating malaria (World Health Organization., 2018). An improved understanding of the relationship between gametocyte density in the human host and rates of transmission to vectors will benefit efforts to target individuals/sub-groups with dis-proportionately higher contribution to transmission (the "infectious reservoir") (Stone et al., 2015). It will also assist in the development and efficacy assessment of transmission-reducing interventions (Rabinovich et al., 2017).

Assays of the relationship between gametocyte density and infectivity to the vector generally comprise one or more laboratory-reared vector species fed directly on an infected host or via artificial membrane, with/without serum replacement, prior knowledge of gametocyte density, or genotype (Churcher et al., 2013; Stone et al., 2015; Bousema and Drakeley, 2017; Goncalves et al., 2017; Bradley et al., 2018; Grignard et al., 2018; Slater et al., 2019). Taken together, these studies suggest a saturating positive relationship between the density of gametocytes in a human host and the proportion of mosquitoes that become successfully infected. Thus, it is generally assumed that hosts with higher gametocyte density will infect more mosquitoes on average, which in turn shapes recommendations for interventions.

However, significant variability exists around this relationship. For instance, despite the positive relationship between gametocyte density and mosquito infections, there is substantial uncertainty around this relationship. For example, some low density (also referred to as asymptomatic/sub-patent/sub-microscopic) carriers can contribute similar mosquito infection rates in mosquitoes as some high-density (symptomatic/patent/microscopic) carriers (Slater et al., 2019). Further, the saturating nature of the relationship suggests that high-density carriers offer no additional benefits to transmission (Stone et al., 2015; Bradley et al., 2018), which is difficult to reconcile with, for example, the evidence that rates of gametocytogenesis are under such strong selection pressure in sub-Saharan Africa (Duffy et al., 2018; Rono et al., 2018; Usui et al., 2019).

The variation around this relationship is often attributed to variation in host immuno-physiology, different mosquito species/populations, and differences across parasite genotypes in gametocyte investment. Most of the studies investigating the relationship between gametocytemia and infectivity to mosquitoes have been performed in mosquitoes housed at a single, constant temperature (e.g., 26°C) (Bousema et al., 2012; Churcher et al., 2013; Stone et al., 2015, 2018; Bradley et al., 2018; Tadesse et al., 2018; Slater et al., 2019). However, within minutes of ingestion by a mosquito, the malaria parasite is subject to an environment marked by substantial variation in temperature throughout the day, across seasons, and geographic region (Paaijmans et al., 2010; Lahondere and Lazzari, 2012; Murdock et al., 2012, 2014, 2016; Mordecai et al., 2013; Johnson et al., 2015; Ryan et al., 2015; Sinden, 2015; Beck-Johnson et al., 2017). Temperature has strong non-linear effects on mosquito infection rates and overall vector competence (with permissive temperatures for transmission ranging from 20 to 30°C and a predicted thermal optimum of 25°C), and is one of the most reliable environmental predictors of both geographical distribution and seasonal transmission dynamics (Mordecai et al., 2013; Johnson et al., 2015; Reiner et al., 2015; Ryan et al., 2015; Murdock et al., 2016; Shah et al., 2019).

The current study provides proof-of-concept evidence showing how field relevant variation in daily temperatures modulate the interaction between gametocyte density and infectivity to the mosquito vector. Female *Anopheles stephensi* were challenged with three densities of *P. falciparum* NF54 spanning an order of magnitude and housed at thermal regimes pertinent to malaria transmission: daily temperature fluctuations of a total of 9°C (+5°C/−4°C) around mean temperatures of 20, 24, and 28°C, respectively (Paaijmans et al., 2010; Blanford et al., 2013; Murdock et al., 2016). Metrics of parasite infection were assessed as the proportion of mosquitoes with oocysts in the midguts and their corresponding burdens, in addition to the proportions of mosquitoes carrying sporozoites in the salivary glands.

MATERIALS AND METHODS

Study Design

The overall study design is depicted in **Figure 1** with the indicated temperature regimes adapted from a previous study (Murdock et al., 2016). Female *An. stephensi* from the same cohort were sorted into nine groups/cups with each temperature regime receiving three cups each, 24 h prior to the day of infection. On the day of infection, mature gametocytes of *P. falciparum* NF54 generated *in vitro* (Pathak et al., 2018) were serially diluted 3-fold with naïve RBCs to obtain blood-meals representing three final parasite densities with a 9-fold difference between the highest and lowest densities (∼an order

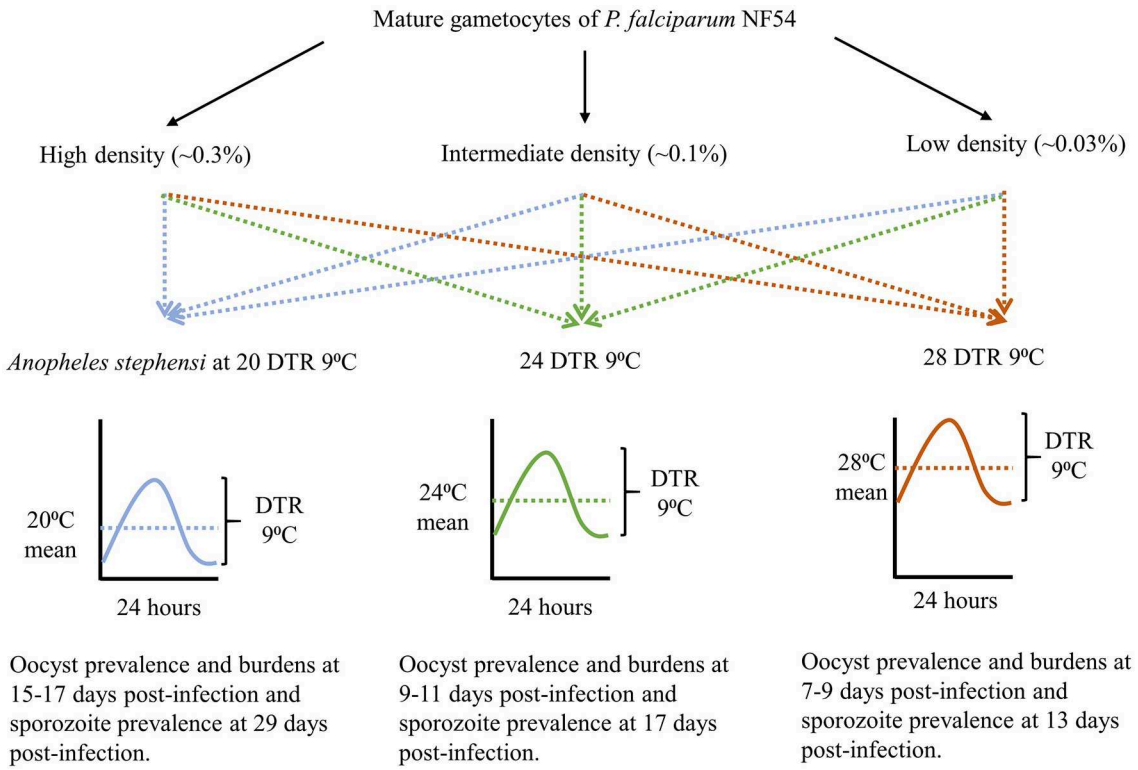

FIGURE 1 | The study design showing gametocyte densities, temperature regimes, and time of sampling for each temperature, to account for the differences in development rates.

of magnitude). Aliquots of the three blood-meals with the varying gametocyte density were offered to the three cups, respectively, at each temperature regime. The experiments were replicated three times with independent mosquito cohorts and parasite cultures. Since the primary objective was to determine the effect of temperature on gametocyte density and vector competence, this experimental design ensured that within each replicate, all three temperature regimes would be assessed simultaneously with the same starting parasite and vector populations in order to reduce any unexpected variations over and above those attributable to temperature. Lastly, all mosquito infections were performed between 1800 and 1900 h which represents "dusk" on a circadian scale when Anopheline mosquitoes are most active (Rund et al., 2016).

All chemicals and consumables were purchased from Fisher Scientific Inc. unless stated otherwise.

In vitro Parasite Cultures

Routine asexual cultures of *P. falciparum* NF54 and induction of gametocytogenesis *in vitro* were performed with cryo-preserved red blood cells (RBCs) as described in detail previously (Pathak et al., 2018). Gametocytogenesis of *P. falciparum* NF54 *in vitro* was monitored with Giemsa staining until 12 days post-culture, after which we assessed cultures for infectiousness through daily assays of male gametogenesis (Pathak et al., 2018). Giemsa stained slides were visualized at a 1000x magnification with an oil immersion lens while gametogenesis was assessed *in vitro* at 400x magnification under differential interference contrast setting on a Leica DM2500 upright microscope. Assays were performed on a 100 μl aliquot of culture re-suspended in fresh media. Infectiousness was determined in duplicate by quantifying male gametogenesis *in vitro* (ex-flagellation) with 10 μl culture volumes on a hemocytometer following incubation in a humidified chamber set to 24°C for 20 min. The remaining culture (~80 μl) was concentrated by centrifugation at 1,800 g for two min at room temperature and Giemsa stained smears prepared as described above.

Mosquito Husbandry and Experimental Infections

An. stephensi colonies (Walter Reed Army Institute of Research, wild-type Indian strain) were housed in a walk-in environmental chamber (Percival Scientific, Perry, IA) at 27°C ± 0.5°C, 80% ± 5% relative humidity, and under a 12 h light: 12 h dark photo-period schedule. Adult mosquitoes were maintained on 5% dextrose (w/v) and 0.05% para-aminobenzoic acid (w/v) and provided whole human blood in glass-jacketed feeders (Chemglass Life Sciences, Vineland, NJ) through parafilm membrane maintained at 37°C to support egg production. Husbandry procedures followed methods outlined previously (Pathak et al., 2018). Briefly, eggs were rinsed twice with 1% house-hold bleach (v/v, final concentration of 0.06% sodium

hypochlorite) before surface-sterilization for 1 min in the same solution at room temperature. Bleached eggs were washed with 4–5 changes of deionized water and transferred to clear plastic trays (34.6 cm L × 21.0 cm W × 12.4 cm H) containing 500 ml of deionized water and 2 medium pellets of Hikari Cichlid Gold fish food (Hikari USA, Hayward, CA) and allowed to hatch for 48 h. Hatched L1 larvae were dispensed into clear plastic trays (34.6 cm L × 21.0 cm W × 12.4 cm H) at a density of 300 larvae/1,000 ml water and provided the same diet until pupation. The feeding regime consisted of 2 medium pellets provided on the day of dispensing (day 0) followed by the provision of a further 2, 4, 4, and 4 medium pellets on days 4, 7, 8, and 9, respectively. This regime allows >85% larval survival and >90% pupation within 11 days with a sex ratio of 1:1 adult males and females (unpublished observations).

Mosquito infections were performed with ∼100, 3, to 7 day old female, host-seeking *An. stephensi* sorted into nine 16/32 oz. soup cups. Three cups each were transferred to the respective temperature regimes and acclimated for ∼24 h. On the day of infection, ex-flagellation was quantified from the cultures, in addition to gametocyte density from 3,000 to 5,000 RBCs stained with Giemsa, as described above. Parasite infected RBCs were collected into a pre-weighed 15 ml conical centrifuge tube and concentrated by centrifugation at 1800 × g for 2 min at low brake setting. The media supernatant was aspirated, and weight of packed, infected RBCs estimated after subtracting the weight of the empty tube. The infected RBC pellet was then resuspended in 3 volumes of a 33% hematocrit suspension of naïve, freshly washed RBCs in human serum to achieve a hematocrit of ∼45–50%. This suspension was then serially diluted 3-fold a further two times by adding 2 volumes of naïve RBCs resuspended in human serum at 45–50% hematocrit to 1 volume of the preceding dilution resulting in three final concentrations of stage V gametocytemia (∼0.3, 0.1, and 0.03%) used throughout this study. This dilution scheme was developed with the objective of achieving a mature gametocytemia of ∼0.2–0.3% at the first dilution based on the gametocytemia recorded in the flasks on the day of infection and was representative of densities collated from independent studies (Adjalley et al., 2011; Miura et al., 2013, 2016; Stone et al., 2013; Eldering et al., 2017).

We then added an equal volume of each concentration of gametocytes to water-jacketed glass feeders maintained at ∼37°C. All nine cups of mosquitoes were placed under the respective feeders and allowed to feed for 20 min. For estimating gametocyte density, smears were prepared from the blood-meal corresponding to the 1:2 dilution for Giemsa staining. Mosquitoes were returned to the respective temperature regimes and starved for a further 48 h to eliminate any partial or non-blood fed individuals after which they were provided cotton pads soaked in 5% dextrose (w/v) and 0.05% para-aminobenzoic acid (w/v) for the remainder of the study, as described previously (Pathak et al., 2018).

Parasite Infection Measurements

Different metrics of parasite infection were estimated at time points corresponding to peak infection intensities specific to each temperature regime. Oocyst and sporozoite rates were measured as the proportion of mosquitoes with oocysts on their midguts or sporozoites in their salivary glands, respectively. Oocyst intensity, or the mean number oocysts per midgut, was used as a metric for overall parasite burden. Specifically, midguts and salivary glands were dissected to assess infection at the following times post-infection: 20 DTR 9°C, 15–17 days post-infection for oocysts and 29 days post-infection for sporozoites; 24 DTR 9°C, 9–11 days post-infection for oocysts and 17 days post-infection for sporozoites; and 28 DTR 9°C, 7–9 days post-infection for oocysts and 13 days post-infection for sporozoites. At each time point, ∼25–30 mosquitoes were vacuum aspirated directly into 70% ethanol and vector competence measured as described previously (Pathak et al., 2018). Briefly, midguts were dissected, and oocysts enumerated at 400× magnification with a Leica DM2500 under DIC optics. For sporozoite rates, salivary glands were dissected into 5 μl of PBS, ruptured by overlaying a 22 mm^2 coverslip and checking for presence/absence of sporozoites at either 100× or 400× magnification with the same microscope.

Data Analyses

All data analyses were performed in RStudio (Version 1.1.463), an integrated development environment for the open-source R package (Version 3.5.2) (RSTUDIO Team, 2016; R Core Team, 2018). Graphical analyses were performed with the "ggplot2" package (Wickham, 2016). Vector competence was statistically modeled using Generalized linear mixed-effects models (GLMMs) with the choice of family/distribution based on the dependent variable—(1) Oocyst and sporozoite rates were modeled as the probability of being infected and infectious, respectively, using a beta-binomial distribution (family = beta-binomial, link = "logit"), and (2) oocyst intensity with a negative binomial distribution (family = nbinom2, link = "log") with the "glmmTMB" package (Brooks et al., 2017). Predictors/fixed effects comprised temperature, gametocyte density and in the case of rates, site of infection, i.e., midguts or salivary glands, with the relationships modeled up to three-way interactions. Temperature and site of infection were classified as categorical fixed effects while density was specified as a continuous variable exerting a linear (x) and quadratic (x^2) effect on the dependent variables (Crawley, 2013). Since technical constraints meant reliable parasite counts were only available for the highest parasite concentrations (1:2 dilution), dilution was used as a proxy for gametocyte density based on the fact that all three biological replicates were performed with the same series of dilutions of the original parasite culture (1:2, 1:6, and 1:18). For all models, the random effect structure allowed for variation in the intercepts between biological replicates and/or between temperatures nested within each replicate.

The choice of family for modeling oocyst intensity was based on likelihood-based information criteria as recommended in the "bbmle" package (Bolker and R Development Core Team, 2017), dispersion characteristics of residuals using the "DHARMa" package (Hartig, 2019), and where possible, the co-efficient of determination ("Pseudo-R-squared") using the "sjstats" package (Lüdecke, 2018). Tests for overdispersion were performed using a predetermined threshold ratio of squared Pearson residuals

over the residual degrees of freedom (overdispersion ratio = <1.5) and a Chi-squared distribution of the squared Pearson residuals with $p > 0.05$, as described previously (Pathak et al., 2018). Once overdispersion was accounted for, the marginal means estimated by each model were then used to perform pairwise comparisons between parasite densities nested within each temperature regime, using Tukey's contrast methods in the "emmeans" package and adjusting for multiple comparisons (Lenth, 2019).

RESULTS

The Effect of Temperature and Gametocyte Density on Oocyst and Sporozoite Rates

Overall, we observed a main effect of temperature on both oocyst and sporozoite rates. Oocyst and sporozoite rates decreased with increasing temperature, with the most notable decline at 28 DTR 9°C (Log-Odds = −1.505, standard error (se) = 0.328, z-value = −4.59, $p < 0.001$) (**Figure 2**, **Table 1**). Sporozoite rates largely

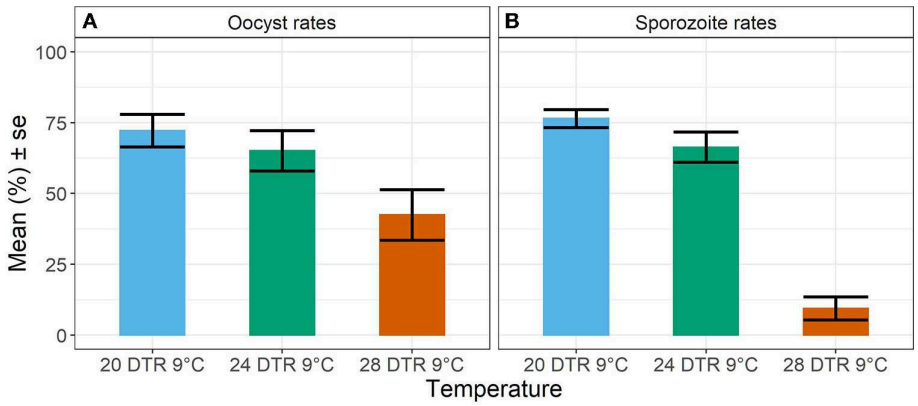

FIGURE 2 | Oocyst rates in midguts **(A)** and sporozoite rates in salivary glands **(B)** at the three temperature regimes. Values represents mean ± standard error (se) of prevalence in percent units from three biological replicates.

TABLE 1 | Statistical models for prevalence of oocysts and sporozoites in midguts and salivary glands respectively.

Predictors (reference group = 20 DTR 9°C)	Log-odds	std. error	Z-value	*p*
(Intercept)	1.065	0.281	3.785	**<0.001**
24 DTR 9°C	−0.359	0.309	−1.162	0.245
28 DTR 9°C	−1.505	0.328	−4.590	**<0.001**
Sporozoite prevalence (vs. oocyst prevalence)	0.148	0.332	0.447	0.655
Gametocyte density (linear trend)	2.116	1.383	1.530	0.126
Gametocyte density (quadratic/"hump-shaped" trend)	−3.720	1.450	−2.566	**0.010**
24 DTR 9°C * sporozoite prevalence (vs. oocyst prevalence)	−0.160	0.430	−0.372	0.710
28 DTR 9°C * sporozoite prevalence (vs. oocyst prevalence)	−2.446	0.561	−4.362	**<0.001**
24 DTR 9°C * Gametocyte density (linear trend)	−1.022	1.854	−0.551	0.582
28 DTR 9°C * Gametocyte density (linear trend)	4.099	2.056	1.993	**0.046**
24 DTR 9°C * Gametocyte density (quadratic/"hump-shaped" trend)	0.256	1.963	0.130	0.896
28 DTR 9°C * Gametocyte density (quadratic/"hump-shaped" trend)	−0.047	2.114	−0.022	0.982
Sporozoite prevalence * Gametocyte density (linear trend)	0.654	2.270	0.288	0.773
Sporozoite prevalence * Gametocyte density (quadratic/"hump-shaped" trend)	3.396	2.173	1.563	0.118
24 DTR 9°C * sporozoite prevalence * Gametocyte density (linear trend)	0.054	2.983	0.018	0.986
28 DTR 9°C * sporozoite prevalence * Gametocyte density (linear trend)	−0.723	3.878	−0.186	0.852
24 DTR 9°C * sporozoite prevalence * Gametocyte density (quadratic/"hump-shaped" trend)	0.451	2.921	0.154	0.877
28 DTR 9°C * sporozoite prevalence * Gametocyte density (quadratic/"hump-shaped" trend)	−3.374	3.954	−0.853	0.394
Random effects				
Random variation in intercepts between temperatures nested within each biological replicate	0.03			
Random variation in intercepts between the three biological replicates	0.08			
Number of observations (i.e., mosquitoes sampled)	1469[#]			
Marginal R^2/Conditional R^2	0.427/0.446			

[#]*For one biological replicate, sporozoite prevalence data for all three densities at 20 DTR 9°C and lowest density at 24 DTR 9°C was not available. Bolded values indicate statistically clear effects based on $p < 0.05$.*

mirrored the oocyst rates at the two cooler temperatures but not at 28 DTR 9°C where sporozoite establishment declined significantly (Log-Odds = −2.446, se = 0.561, z-value = −4.362, $p < 0.001$) (**Figure 2**, **Table 1**). A non-linear quadratic ("hump-shaped") relationship was noted between gametocyte density and overall vector competence (Log-Odds = −3.72, se = 1.45, z-value = −2.566, $p = 0.01$), likely driven by the two cooler temperatures where oocyst rates were highest at intermediate gametocyte densities (**Figure 3**, **Table 1,** and **Supplementary Table 1**). At the warmest temperature of 28 DTR 9°C, gametocyte density showed positive, linear effects on both oocyst and sporozoite rates (Log-Odds = 4.099, se = 2.056, z-value = 1.993, $p = 0.046$) (**Figure 3**, **Table 1,** and **Supplementary Table 1**). Overall, the model was able to explain 44.6% of the variation in the data with the predictors accounting for 42.7% of this fit. Pairwise comparisons of marginal means estimated by the models suggested clear differences between gametocyte density and oocyst rates at 28 DTR 9°C, but not at the two cooler temperatures where the proportion of mosquitoes infected with oocysts was marginally higher at the intermediate relative to the lowest gametocyte densities (**Supplementary Table 2**).

The Effects of Temperature and Gametocyte Density on Oocyst Intensity

In general, the mean number of oocysts per infected mosquito midgut showed significant declines as temperatures warmed, with intensities declining significantly at 24 DTR 9°C (Log-Mean = −0.58, se = 0.168, z-value = −3.449, $p < 0.001$) and especially at 28 DTR 9°C (Log-Mean = −1.386, se = 0.185, z-value = −7.481, $p = 0.001$) (**Figure 4A**). Further, increases in gametocytemia resulted in positive and linear increases in the mean number of oocysts per midgut (Log-Mean = −12.513, se = 1.078, z-value = 11.612, $p < 0.001$) (**Figure 4B**, **Table 2,** and **Supplementary Figure 1**), with weak evidence for a quadratic relationship with highest oocyst intensities at intermediate gametocyte densities (Log-Mean = −3.234, se = 1.072, z-value = −3.016, $p = 0.003$) (**Figure 4B**, **Table 2,** and **Supplementary Table 3**). Of the three temperatures, only the warmest temperature (28 DTR 9°C) showed a positive, linear relationship between gametocyte density and oocyst intensity (Log-Mean = −6.434, se = 2. 432, z-value = −2.747, $p = 0.006$) (**Figure 4B**, **Table 2**). Overall, the model was able to predict a total of 57.9% of the variation, with the predictors

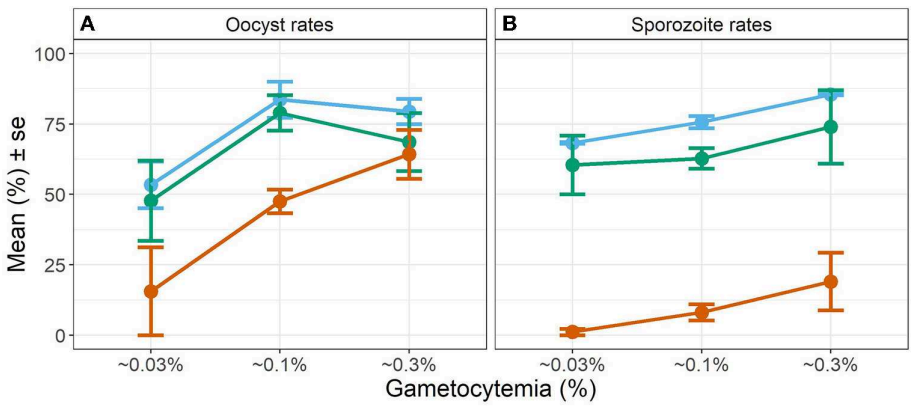

FIGURE 3 | Effect of gametocyte density and temperature on oocyst rates in midguts **(A)** and sporozoite rates in the salivary glands **(B)**. Values represents means ± standard error (se) from three biological replicates. The color scheme is continued from **Figure 2** with blue representing 20 DTR 9°C, green representing 24 DTR 9°C and red/vermillion indicating 28 DTR 9°C.

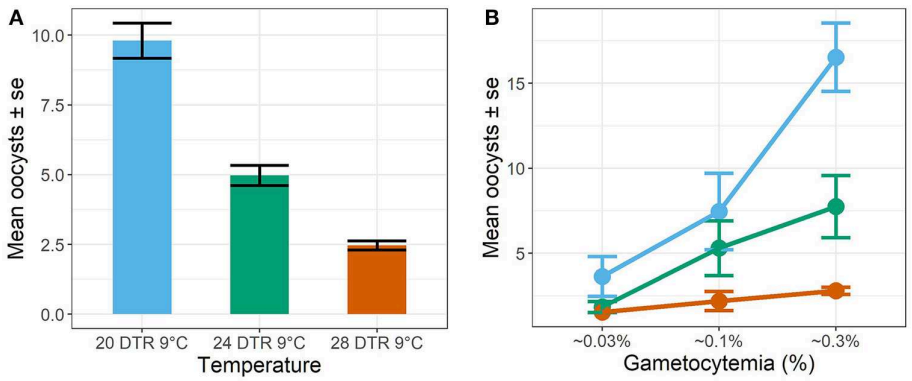

FIGURE 4 | Oocyst intensities (midguts with oocysts ≥1, i.e., infected midguts) across temperatures **(A)** and gametocyte density **(B)**. Values represents means ± standard error (se) from three biological replicates.

contributing 52.2% (**Table 2**). Pairwise comparisons of oocyst intensity suggest clear differences in the mean number of oocysts per midgut across all three gametocyte densities at the two cooler temperatures of 20 and 24 DTR 9°C (**Supplementary Table 4**). At 28 DTR 9°C, only the highest and lowest densities differed significantly in their contribution to burdens, however, this interpretation should be taken with caution since mosquitoes in two of the three experimental replicates at this temperature showed no evidence of infection at the lowest density, which may in turn have affected the pairwise comparisons.

The Effects of Temperature and Gametocytemia on the Distribution of Parasites Across Mosquitoes

Simple phenomenological analyses of the oocyst distribution across individual mosquito midguts suggests strong gametocyte density- and temperature-dependent patterns (**Figure 5** and **Supplementary Figures 1**, **2**). To describe how parasite burdens are distributed across individual mosquito midguts, we quantified the variance to mean ratios (VMR). A VMR of ∼1 indicates a random distribution of oocysts across dissected mosquito midguts while ratios > 1 indicate an uneven or aggregated oocyst distribution, with most midguts exhibiting few to no oocysts and a few midguts displaying high oocyst burdens (Wilson et al., 2002). In general, aggregation decreased with increases in temperature, with oocysts almost randomly distributed at the warmest temperature of 28 DTR 9°C regardless of initial gametocyte density. At the two cooler temperatures, aggregation increased with increasing gametocyte density, with this pattern most pronounced at the coldest temperature of 20 DTR 9°C.

DISCUSSION

Increasing temperatures were detrimental to *P. falciparum* fitness with declines in the mean proportion of mosquitoes infected with oocysts (oocyst rates) and infectious with sporozoites (sporozoite rates), as well as mean oocyst intensities. The main effects of temperature observed in this study fall in line with predicted temperature-vector competence relationships for malaria outlined in previous studies (Mordecai et al., 2013; Johnson et al., 2015; Shapiro et al., 2017). Oocyst and sporozoite rates were similar at the cooler temperatures of 20 and 24 DTR9°C but not at the warmest temperature of 28 DTR 9°C where sporozoite rates declined significantly. We also found oocyst intensity to decrease with increasing temperature. Taken together, our results suggest that the overall efficiency of malaria infection declines at the warmest temperature either due to a direct effect of temperature on parasite sporogony and/or an indirect effect mediated by mosquito immunological or physiological changes.

Interestingly, oocyst rates were comparable across temperatures at the highest gametocyte densities, despite the qualitative differences in the shape of the relationship at each temperature. For example, while the highest oocyst rates were achieved with intermediate gametocyte densities at the two cooler temperatures of 20 and 24 DTR 9°C, high gametocyte densities were required to achieve similar oocyst rates at 28 DTR 9°C and to ensure progression to the salivary glands. At the highest temperature, it is likely that the thermal stress was simply not conducive to sporozoite survival, sporozoite migration, and/or residence in the salivary glands (Mordecai et al., 2013; Johnson et al., 2015; Shapiro et al., 2017). Indeed, while parasite

TABLE 2 | Statistical models for oocyst intensity (infected midguts).

	Oocyst intensity			
Predictors (reference group = 20 DTR 9°C)	**Log-mean**	**std. error**	**Z-value**	***p***
(Intercept)	2.112	0.143	14.772	**<0.001**
24 DTR 9°C	−0.580	0.168	−3.449	**0.001**
28 DTR 9°C	−1.386	0.185	−7.481	**<0.001**
Gametocyte density (linear trend)	12.513	1.078	11.612	**<0.001**
Gametocyte density (quadratic/"hump-shaped" trend)	−3.234	1.072	−3.016	**0.003**
24 DTR 9°C/Gametocyte density (linear trend)	−2.271	1.634	−1.390	0.165
28 DTR 9°C/Gametocyte density (linear trend)	−6.434	2.342	−2.747	**0.006**
24 DTR 9°C/Gametocyte density (quadratic/"hump-shaped" trend)	−2.749	1.624	−1.692	0.091
28 DTR 9°C/Gametocyte density (quadratic/"hump-shaped" trend)	−0.565	2.558	−0.221	0.825
Random effects				
Random variation in intercepts between temperatures within each replicate	0.03			
Random variation in intercepts between replicates	0.1			
Observations	504			
Marginal R^2/Conditional R^2	0.522/0.579			
GLMM family ("link")	Negative binomial with variance increasing quadratically with the mean [glmmTMB family = nbinom2 (link = "log")]			

Bolded values indicate statistically clear effects based on $p < 0.05$.

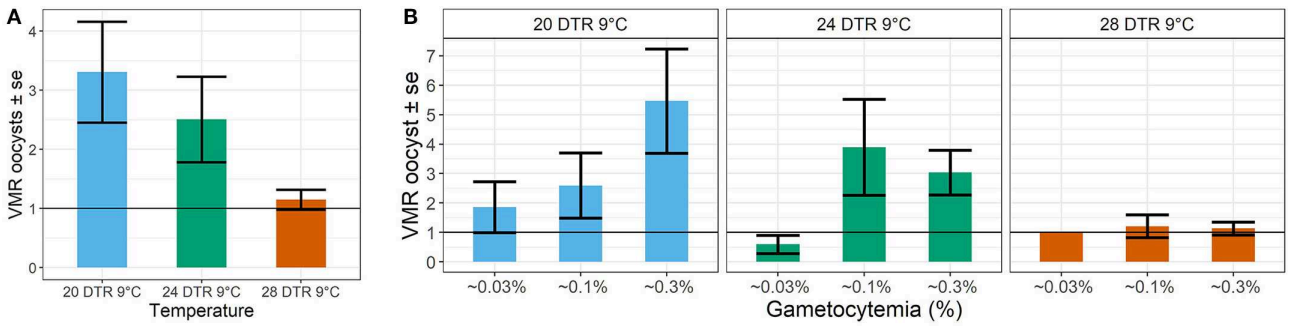

FIGURE 5 | Effect of temperature **(A)** and gametocyte density **(B)** on the distribution of oocyst burdens across individual (infected) midguts at the three temperatures using the Variance to Mean Ratios (VMR) as the measure of dispersion (s^2: m). Values represents means ± standard error (se) of the VMR from three biological replicates.

genotypes are likely to vary in their susceptiblity to high temperatures (Noden et al., 1995), our results appear to contrast with a previous study (Murdock et al., 2016), where vector competence was observed with the same parasite-mosquito combination at temperatures as high as 33°C. However, the gametocyte density offered to the mosquitoes was considerably higher (∼0.8% and unpublished observations) than the highest density from the current study (0.3%) and suggests that this parasite genotype can infect successfully at high temperatures, provided gametocyte densities are high. Additionally, the same study showed similar oocyst and sporozoite rates (∼55%) at 27 DTR 9°C, which corroborates our findings at 28 DTR9°C where high densities promoted parasite progression to the salivary glands. Taken together, the former study complements our current findings and reinforces the notion that variation in environmental temperature alters the relationship between gametocyte density and infection rates in mosquitoes.

In contrast to the effect of gametocyte density on oocyst rates, oocyst intensity in infected midguts showed a generally linear, positive relationship across all temperatures. These distinct midgut responses are in line with other work showing how oocyst burdens rarely saturate with increasing gametocyte density (Eldering et al., 2017; Bradley et al., 2018). However, our results also suggest that temperature can dramatically alter the effects of gametocyte density on the distribution of oocyst burdens across infected midguts. At the gametocyte densities tested here, oocyst distributions showed increased aggregation as gametocyte density increased at the two cooler temperatures, but not at the highest temperature where oocysts were randomly distributed regardless of gametocyte density. These results suggest increased gametocytemia at temperatures permissive for mosquito lifespan and parasite infection rates (Mordecai et al., 2013; Johnson et al., 2015; Shapiro et al., 2017) may increase competition among parasites. Competition can either manifest directly in response to limited host resources or indirectly due to increased host immune responses (Lefevre et al., 2017) resulting in high oocyst burdens in a few, highly nourished or susceptible hosts. In contrast, temperatures above the predicted thermal optimum for vector competence (Mordecai et al., 2013; Johnson et al., 2015; Shapiro et al., 2017) may have direct negative effects on parasite survival resulting in lower infection rates overall, less parasite competition within host, and more random distributions of parasites across hosts.

Our results have several implications for understanding malaria transmission. Identifying human infectious reservoirs and evaluating their contribution to overall transmission for targeted intervention will likely need to consider environmental context. For instance, low-density individuals might contribute as much as high-density carriers in regions of the world or times of season when temperatures are cooler and any intervention may therefore need to cover a relatively larger proportion of the host population. Likewise, the infectious reservoir may shift to high-density carriers in warmer regions of the world or times of season where, in principle, targeting high-density carriers may bring significant returns. Further, if ambient temperature modifies the outcomes of the relationship between gametocyte density and mosquito infection rates as shown here, it could provide an additional rationale for the seasonal and geographical distributions of allelic variants (*gdv1* and/or *AP2-g*), both of which are distinguished primarily by their differential investment in gametocytogenesis (Gadalla et al., 2016; Duffy et al., 2018; Rono et al., 2018; Usui et al., 2019). Finally, while higher temperatures could select for transmission of genotypes capable of higher gametocytogenesis, at lower temperatures the same genotype could be outcompeted due to density-dependent effects (Pollitt et al., 2013).

The interactions between temperature and gametocyte density described here also have several implications for current transmission reducing/blocking interventions. Transmission reducing interventions, such as the anti-gametocidal drug primaquine, could be much more effective in reducing transmission of artemisinin resistant parasites in warmer environments or times of season than in cooler seasons or geographic regions. Further, thermal variation in the field could have implications for current vaccine design and testing pipelines where the rate of reduction in oocyst intensity is the primary method of evaluation (Bompard et al., 2017). For instance, more effective antibody responses may be required at lower temperatures where oocyst intensity and sporozoite

rates are highest. Finally, if transmission blocking vaccines are imperfect as early evidence suggests (Sagara et al., 2018), intermediate gametocytemia in some environmental contexts might actually boost oocyst rates: whether this enhancement will be reflected in subsequent transmission rates will ultimately depend on sporozoite rates, which appear to be less influenced by gametocyte density.

While our proof of concept study has several implications for understanding malaria transmission and control, there are several study limitations that may warrant consideration. *First*, it is likely that the gametocyte densities tested here are more in line with laboratory rather than field-based studies (Koepfli and Yan, 2018). Further, standard membrane feeding assays (SMFAs) are less efficient than direct membrane feeding assays (DMFAs) or direct skin-feeding assays (DFAs) (Bousema et al., 2012). We do not anticipate these effects will change the main result that temperature alters the gametocytemia-infection rate relationship. *Second*, this study was conducted using a "non-native" vector species-parasite genotype combination (Molina-Cruz et al., 2015). However, the effects of temperature on vector competence in *An. gambiae* is correlated with *An. stephensi* (Murdock et al., 2016; Eldering et al., 2017), and the study could prove to be timely considering the recent infestation of *An. stephensi* in cities of Eastern Africa (Faulde et al., 2014; Carter et al., 2018) and contribution to *P. falciparum* transmission (Seyfarth et al., 2019). *Third*, we did not measure sporozoite burdens in the salivary glands, and it is likely that higher temperatures and/or low oocyst intensities may result in reduced sporozoite numbers in the salivary glands (Stone et al., 2013; Miura et al., 2019) with potential implications for transmission to the human host (Churcher et al., 2017). Further, previous work in rodent malaria systems have demonstrated negative relationships between oocyst burdens and the number of sporozoites produced per oocyst (Pollitt et al., 2013; Moller-Jacobs et al., 2014) suggesting density-dependent effects might also influence sporozoite intensity. *Finally*, it is possible that mosquitoes seek particular microclimates, which could mitigate the effects of temperature on this relationship. However, there is limited evidence suggesting this is the case currently (Blanford et al., 2009), and much more work is needed to address this potential limitation.

In this study, we demonstrate that field relevant variation in ambient temperature alters the relationship between density of transmission stages and infection outcomes in the *An. stephensi*—*P. falciparum* system. We emphasize that the role of variation in field relevant factors in shaping this relationship is currently under appreciated, with potentially important implications for understanding malaria transmission and control. Of note, while only one regime was tested here (DTR 9°C), it is possible that the magnitude of fluctuations may result in different parasite fitness phenotypes and collectively argues for further investigating the relationship between gametocytemia and mosquito infection rates under field relevant conditions (Paaijmans et al., 2010; Blanford et al., 2013; Murdock et al., 2016). Further, due to the well-established effects of environmental variation like temperature on other aspects of vectorial capacity (e.g., mosquito mortality, biting rate, and the parasite extrinsic incubation periods), our studies highlight the need to look beyond the human infectious reservoir and mosquito midgut infection rates for characterizing local transmission.

DATA AVAILABILITY STATEMENT

The datasets generated for this study are available on request to the corresponding author.

AUTHOR CONTRIBUTIONS

AP designed the study, collected and analyzed the data, and wrote the manuscript. CM provided critical input on the study design, methods, data analysis, and manuscript preparation, as well as provided infrastructure and resources for the execution of the presented research. JS contributed to the mosquito husbandry and helped AP to collect data. MT provided comments and suggestions during the project and on the manuscript. All authors read and approved the final version of the manuscript.

FUNDING

Funding for this work was provided by the University of Georgia and the NIH (5R01AI110793-04).

ACKNOWLEDGMENTS

The authors would also like to thank members of the Murdock lab for their patience and support.

SUPPLEMENTARY MATERIAL

The Supplementary Material for this article can be found online at: https://www.frontiersin.org/articles/10.3389/fmicb.2019.02651/full#supplementary-material

Supplementary Figure 1 | Effect of gametocytemia on the distribution of oocyst burdens in infected midguts at the three temperature regimes depicted in the respective panes. Each box represents the interquartile range, with the line within each box indicating median oocyst intensities, bounded by the 25th and 75th percentile values. Error bars represent maximum and minimum values from the interquartile range, with the dots representing outliers. Data were aggregated from the three biological replicates.

Supplementary Figure 2 | Effect of gametocytemia on the distribution of oocyst burdens (≥0) across all midguts (infected and un-infected) at 20 DTR 9°C (blue, **top** panes), 24 DTR 9°C (green, **middle** panes) and 28 DTR 9°C (red, **bottom** panes). Gametocyte densities are indicated in the strips above each plot. Values represent data from all 839 mosquito midguts from three biological replicates.

Supplementary Table 1 | Statistical models for prevalence of oocysts and sporozoites in midguts and salivary glands for each temperature and DTR. # Sporozoite prevalence data from one biological replicate was not available. + Sporozoite prevalence data from the lowest density for one biological replicate was not available.

Supplementary Table 2 | Pairwise comparisons of means predicted by the model in **Table 1** in the main text for oocyst and sporozoite prevalence.

Supplementary Table 3 | Statistical models for oocyst intensity (infected midguts) for each temperature.

Supplementary Table 4 | Pairwise comparisons of means predicted by the model in **Table 2** in the main text for oocyst abundance and intensity.

REFERENCES

Adjalley, S. H., Johnston, G. L., Li, T., Eastman, R. T., Ekland, E. H., Eappen, A. G., et al. (2011). Quantitative assessment of *Plasmodium falciparum* sexual development reveals potent transmission-blocking activity by methylene blue. *Proc. Natl. Acad. Sci. U.S.A.* 108, E1214–E1223. doi: 10.1073/pnas.1112037108

Beck-Johnson, L. M., Nelson, W. A., Paaijmans, K. P., Read, A. F., Thomas, M. B., and Bjornstad, O. N. (2017). The importance of temperature fluctuations in understanding mosquito population dynamics and malaria risk. *R. Soc. Open Sci.* 4:160969. doi: 10.1098/rsos.160969

Blanford, J. I., Blanford, S., Crane, R. G., Mann, M. E., Paaijmans, K. P., Schreiber, K. V., et al. (2013). Implications of temperature variation for malaria parasite development across Africa. *Sci. Rep.* 3:1300. doi: 10.1038/srep01300

Blanford, S., Read, A. F., and Thomas, M. B. (2009). Thermal behaviour of *Anopheles stephensi* in response to infection with malaria and fungal entomopathogens. *Malar. J.* 8:72. doi: 10.1186/1475-2875-8-72

Bolker, B., and R Development Core Team (2017). *bbmle: Tools for General Maximum Likelihood Estimation*. R package version 1.0.20. (Vienna). Available online at: https://CRAN.R-project.org/package=bbmle

Bompard, A., Da, D. F., Yerbanga, R. S., Biswas, S., Kapulu, M., Bousema, T., et al. (2017). Evaluation of two lead malaria transmission blocking vaccine candidate antibodies in natural parasite-vector combinations. *Sci. Rep.* 7:6766. doi: 10.1038/s41598-017-06130-1

Bousema, T., Dinglasan, R. R., Morlais, I., Gouagna, L. C., Van Warmerdam, T., Awono-Ambene, P. H., et al. (2012). Mosquito feeding assays to determine the infectiousness of naturally infected *Plasmodium falciparum* gametocyte carriers. *PLoS ONE* 7:e42821. doi: 10.1371/journal.pone.0042821

Bousema, T., and Drakeley, C. (2017). Determinants of malaria transmission at the population level. *Cold Spring Harb. Perspect. Med.* 7:a025510. doi: 10.1101/cshperspect.a025510

Bradley, J., Stone, W., Da, D. F., Morlais, I., Dicko, A., Cohuet, A., et al. (2018). Predicting the likelihood and intensity of mosquito infection from sex specific *Plasmodium falciparum* gametocyte density. *Elife* 7:e34463. doi: 10.7554/eLife.34463

Brooks, M. E., Kristensen, K., Van Benthem, K. J., Magnusson, A., Berg, C. W., Nielsen, A., et al. (2017). glmmTMB balances speed and flexibility among packages for zero-inflated generalized linear mixed modeling. *R J.* 9, 378–400. doi: 10.32614/RJ-2017-066

Carter, T. E., Yared, S., Gebresilassie, A., Bonnell, V., Damodaran, L., Lopez, K., et al. (2018). First detection of *Anopheles stephensi* Liston, 1901 (*Diptera: culicidae*) in Ethiopia using molecular and morphological approaches. *Acta Trop.* 188, 180–186. doi: 10.1016/j.actatropica.2018.09.001

Churcher, T. S., Bousema, T., Walker, M., Drakeley, C., Schneider, P., Ouedraogo, A. L., et al. (2013). Predicting mosquito infection from *Plasmodium falciparum* gametocyte density and estimating the reservoir of infection. *Elife* 2:e00626. doi: 10.7554/eLife.00626

Churcher, T. S., Sinden, R. E., Edwards, N. J., Poulton, I. D., Rampling, T. W., Brock, P. M., et al. (2017). Probability of Transmission of Malaria from Mosquito to Human Is regulated by mosquito parasite density in naive and vaccinated hosts. *PLoS Pathog.* 13:e1006108. doi: 10.1371/journal.ppat.1006108

Crawley, M. J. (2013). *The R Book*. West Sussex: John Wiley and Sons Ltd.

Duffy, C. W., Amambua-Ngwa, A., Ahouidi, A. D., Diakite, M., Awandare, G. A., Ba, H., et al. (2018). Multi-population genomic analysis of malaria parasites indicates local selection and differentiation at the *gdv1* locus regulating sexual development. *Sci. Rep.* 8:15763. doi: 10.1038/s41598-018-34078-3

Eldering, M., Bompard, A., Miura, K., Stone, W., Morlais, I., Cohuet, A., et al. (2017). Comparative assessment of *An. gambiae* and *An. stephensi* mosquitoes to determine transmission-reducing activity of antibodies against *P. falciparum* sexual stage antigens. *Parasit Vectors* 10:489. doi: 10.1186/s13071-017-2414-z

Faulde, M. K., Rueda, L. M., and Khaireh, B. A. (2014). First record of the Asian malaria vector *Anopheles stephensi* and its possible role in the resurgence of malaria in Djibouti, Horn of Africa. *Acta Trop.* 139, 39–43. doi: 10.1016/j.actatropica.2014.06.016

Gadalla, A. A., Schneider, P., Churcher, T. S., Nassir, E., Abdel-Muhsin, A. A., Ranford-Cartwright, L. C., et al. (2016). Associations between season and gametocyte dynamics in chronic *Plasmodium falciparum* infections. *PLoS ONE* 11:e0166699. doi: 10.1371/journal.pone.0166699

Goncalves, B. P., Kapulu, M. C., Sawa, P., Guelbeogo, W. M., Tiono, A. B., Grignard, L., et al. (2017). Examining the human infectious reservoir for *Plasmodium falciparum* malaria in areas of differing transmission intensity. *Nat. Commun.* 8:1133. doi: 10.1038/s41467-017-01270-4

Grignard, L., Goncalves, B. P., Early, A. M., Daniels, R. F., Tiono, A. B., Guelbeogo, W. M., et al. (2018). Transmission of molecularly undetectable circulating parasite clones leads to high infection complexity in mosquitoes post feeding. *Int. J. Parasitol.* 48, 671–677. doi: 10.1016/j.ijpara.2018.02.005

Hartig, F. (2019). *DHARMa: Residual Diagnostics for Hierarchical (Multi-Level/Mixed) Regression Models*. R package version 0.2.4 ed. Available online at: https://CRAN.R-project.org/package=DHARMa

Johnson, L. R., Ben-Horin, T., Lafferty, K. D., Mcnally, A., Mordecai, E., Paaijmans, K. P., et al. (2015). Understanding uncertainty in temperature effects on vector-borne disease: a Bayesian approach. *Ecology* 96, 203–213. doi: 10.1890/13-1964.1

Koepfli, C., and Yan, G. (2018). *Plasmodium* gametocytes in field studies: do we measure commitment to transmission or detectability? *Trends Parasitol.* 34, 378–387. doi: 10.1016/j.pt.2018.02.009

Lahondere, C., and Lazzari, C. R. (2012). Mosquitoes cool down during blood feeding to avoid overheating. *Curr. Biol.* 22, 40–45. doi: 10.1016/j.cub.2011.11.029

Lefevre, T., Ohm, J., Dabiré, K. R., Cohuet, A., Choisy, M., Thomas, M. B., et al. (2017). Transmission traits of malaria parasites within the mosquito: genetic variation, phenotypic plasticity, and consequences for control. *Evol. Appl.* 11, 456–469. doi: 10.1111/eva.12571

Lenth, R. (2019). *emmeans: Estimated Marginal Means, aka Least-Squares Means*. R package version 1.3.3. Available online at: https://CRAN.R-project.org/package=emmeans

Lüdecke, D. (2018). *strengejacke: Load Packages Associated With Strenge Jacke!*. R package version 0.3.0. Available online at: https://github.com/strengejacke/strengejacke

Miura, K., Deng, B., Tullo, G., Diouf, A., Moretz, S. E., Locke, E., et al. (2013). Qualification of standard membrane-feeding assay with *Plasmodium falciparum* malaria and potential improvements for future assays. *PLoS ONE* 8:e57909. doi: 10.1371/journal.pone.0057909

Miura, K., Stone, W. J., Koolen, K. M., Deng, B., Zhou, L., Van Gemert, G. J., et al. (2016). An inter-laboratory comparison of standard membrane-feeding assays for evaluation of malaria transmission-blocking vaccines. *Malar. J.* 15:463. doi: 10.1186/s12936-016-1515-z

Miura, K., Swihart, B. J., Deng, B., Zhou, L., Pham, T. P., Diouf, A., et al. (2019). Strong concordance between percent inhibition in oocyst and sporozoite intensities in a *Plasmodium falciparum* standard membrane-feeding assay. *Parasit. Vectors* 12:206. doi: 10.1186/s13071-019-3470-3

Molina-Cruz, A., Canepa, G. E., Kamath, N., Pavlovic, N. V., Mu, J., Ramphul, U. N., et al. (2015). *Plasmodium* evasion of mosquito immunity and global malaria transmission: the lock-and-key theory. *Proc. Natl. Acad. Sci. U.S.A.* 112, 15178–15183. doi: 10.1073/pnas.1520426112

Moller-Jacobs, L. L., Murdock, C. C., and Thomas, M. B. (2014). Capacity of mosquitoes to transmit malaria depends on larval environment. *Parasit. Vectors* 7:593. doi: 10.1186/s13071-014-0593-4

Mordecai, E. A., Paaijmans, K. P., Johnson, L. R., Balzer, C., Ben-Horin, T., De Moor, E., et al. (2013). Optimal temperature for malaria transmission is dramatically lower than previously predicted. *Ecol. Lett.* 16, 22–30. doi: 10.1111/ele.12015

Murdock, C. C., Blanford, S., Luckhart, S., and Thomas, M. B. (2014). Ambient temperature and dietary supplementation interact to shape mosquito vector competence for malaria. *J. Insect Physiol.* 67, 37–44. doi: 10.1016/j.jinsphys.2014.05.020

Murdock, C. C., Paaijmans, K. P., Cox-Foster, D., Read, A. F., and Thomas, M. B. (2012). Rethinking vector immunology: the role of environmental temperature in shaping resistance. *Nat. Rev. Microbiol.* 10, 869–876. doi: 10.1038/nrmicro2900

Murdock, C. C., Sternberg, E. D., and Thomas, M. B. (2016). Malaria transmission potential could be reduced with current and future climate change. *Sci. Rep.* 6:27771. doi: 10.1038/srep27771

Noden, B. H., Kent, M. D., and Beier, J. C. (1995). The impact of variations in temperature on early *Plasmodium falciparum* development in *Anopheles stephensi*. *Parasitology* 111(Pt 5), 539–545. doi: 10.1017/S0031182000077003

Paaijmans, K. P., Blanford, S., Bell, A. S., Blanford, J. I., Read, A. F., and Thomas, M. B. (2010). Influence of climate on malaria transmission depends on daily temperature variation. *Proc. Natl. Acad. Sci. U.S.A.* 107, 15135–15139. doi: 10.1073/pnas.1006422107

Pathak, A. K., Shiau, J. C., Thomas, M. B., and Murdock, C. C. (2018). Cryogenically preserved RBCs support gametocytogenesis of *Plasmodium falciparum in vitro* and gametogenesis in mosquitoes. *Malar. J.* 17:457. doi: 10.1186/s12936-018-2612-y

Pollitt, L. C., Churcher, T. S., Dawes, E. J., Khan, S. M., Sajid, M., Basanez, M. G., et al. (2013). Costs of crowding for the transmission of malaria parasites. *Evol. Appl.* 6, 617–629. doi: 10.1111/eva,.12048

R Core Team (2018). *R: A Language and Environment for Statistical Computing*. Vienna: R Foundation for Statistical Computing.

Rabinovich, R. N., Drakeley, C., Djimde, A. A., Hall, B. F., Hay, S. I., Hemingway, J., et al. (2017). malERA: an updated research agenda for malaria elimination and eradication. *PLoS Med.* 14:e1002456. doi: 10.1371/journal.pmed.1002456

Reiner, R. C. Jr., Geary, M., Atkinson, P. M., Smith, D. L., and Gething, P. W. (2015). Seasonality of *Plasmodium falciparum* transmission: a systematic review. *Malar. J.* 14:343. doi: 10.1186/s12936-015-0849-2

Rono, M. K., Nyonda, M. A., Simam, J. J., Ngoi, J. M., Mok, S., Kortok, M. M., et al. (2018). Adaptation of *Plasmodium falciparum* to its transmission environment. *Nat. Ecol. Evol.* 2, 377–387. doi: 10.1038/s41559-017-0419-9

RSTUDIO Team (2016). *RStudio: Integrated Development Environment for R*. Boston, MA: RStudio, Inc.

Rund, S. S., O'donnell, A. J., Gentile, J. E., and Reece, S. E. (2016). Daily rhythms in mosquitoes and their consequences for malaria transmission. *Insects* 7:E14. doi: 10.3390/insects7020014

Ryan, S. J., Mcnally, A., Johnson, L. R., Mordecai, E. A., Ben-Horin, T., Paaijmans, K., et al. (2015). Mapping physiological suitability limits for malaria in Africa under climate change. *Vector Borne Zoonot. Dis.* 15, 718–725. doi: 10.1089/vbz.2015.1822

Sagara, I., Healy, S. A., Assadou, M. H., Gabriel, E. E., Kone, M., Sissoko, K., et al. (2018). Safety and immunogenicity of Pfs25H-EPA/Alhydrogel, a transmission-blocking vaccine against *Plasmodium falciparum*: a randomised, double-blind, comparator-controlled, dose-escalation study in healthy Malian adults. *Lancet Infect. Dis.* 18, 969–982. doi: 10.1016/S1473-3099(18)30344-X

Seyfarth, M., Khaireh, B. A., Abdi, A. A., Bouh, S. M., and Faulde, M. K. (2019). Five years following first detection of *Anopheles stephensi* (*Diptera: Culicidae*) in Djibouti, Horn of Africa: populations established-malaria emerging. *Parasitol. Res.* 118, 725–732. doi: 10.1007/s00436-019-06213-0

Shah, M. M., Krystosik, A. R., Ndenga, B. A., Mutuku, F. M., Caldwell, J. M., Otuka, V., et al. (2019). Malaria smear positivity among Kenyan children peaks at intermediate temperatures as predicted by ecological models. *Parasit. Vectors* 12:288. doi: 10.1186/s13071-019-3547-z

Shapiro, L. L. M., Whitehead, S. A., and Thomas, M. B. (2017). Quantifying the effects of temperature on mosquito and parasite traits that determine the transmission potential of human malaria. *PLoS Biol.* 15:e2003489. doi: 10.1371/journal.pbio.2003489

Sinden, R. E. (2015). The cell biology of malaria infection of mosquito: advances and opportunities. *Cell. Microbiol.* 17, 451–466. doi: 10.1111/cmi.12413

Slater, H. C., Ross, A., Felger, I., Hofmann, N. E., Robinson, L., Cook, J., et al. (2019). The temporal dynamics and infectiousness of subpatent *Plasmodium falciparum* infections in relation to parasite density. *Nat. Commun.* 10:1433. doi: 10.1038/s41467-019-09441-1

Stone, W., Bousema, T., Sauerwein, R., and Drakeley, C. (2018). Two-faced immunity? The evidence for antibody enhancement of malaria transmission. *Trends Parasitol.* 35, 140–153. doi: 10.1016/j.pt.2018.11.003

Stone, W., Goncalves, B. P., Bousema, T., and Drakeley, C. (2015). Assessing the infectious reservoir of falciparum malaria: past and future. *Trends Parasitol.* 31, 287–296. doi: 10.1016/j.pt.2015.04.004

Stone, W. J., Eldering, M., Van Gemert, G. J., Lanke, K. H., Grignard, L., Van De Vegte-Bolmer, M. G., et al. (2013). The relevance and applicability of oocyst rates as a read-out for mosquito feeding assays. *Sci. Rep.* 3:3418. doi: 10.1038/srep03418

Tadesse, F. G., Slater, H. C., Chali, W., Teelen, K., Lanke, K., Belachew, M., et al. (2018). The relative contribution of symptomatic and asymptomatic *Plasmodium vivax* and *Plasmodium falciparum* infections to the infectious reservoir in a low-endemic setting in Ethiopia. *Clin. Infect. Dis.* 66, 1883–1891. doi: 10.1093/cid/cix1123

Usui, M., Prajapati, S. K., Ayanful-Torgby, R., Acquah, F. K., Cudjoe, E., Kakaney, C., et al. (2019). *Plasmodium falciparum* sexual differentiation in malaria patients is associated with host factors and GDV1-dependent genes. *Nat. Commun.* 10:2140. doi: 10.1038/s41467-019-10805-w

Wickham, H. (2016). *ggplot2: Elegant Graphics for Data Analysis*. New York, NY: Springer-Verlag.

Wilson, K., Bjørnstad, O. N., Dobson, A. P., Merler, S., Poglayen, G., Randolph, S. E., et al. (2002). "Heterogeneities in macroparasite infections: patterns and processes," in *The Ecology of Wildlife Diseases,* eds P. J. Hudson, A. Rizzoli, B. T. Grenfell, H. Heesterbeek, and Dobson P (Oxford: Oxford University Press), 1–48.

World Health Organization. (2018). *World Malaria Report 2018*. World Health Organization.

Conflict of Interest: The authors declare that the research was conducted in the absence of any commercial or financial relationships that could be construed as a potential conflict of interest.

frontiers in Microbiology

REVIEW
published: 06 December 2019
doi: 10.3389/fmicb.2019.02823

Adaptation of Translational Machinery in Malaria Parasites to Accommodate Translation of Poly-Adenosine Stretches Throughout Its Life Cycle

Jessey Erath, Sergej Djuranovic and Slavica Pavlovic Djuranovic**

Department of Cell Biology and Physiology, Washington University School of Medicine, St. Louis, MO, United States

OPEN ACCESS

Edited by:
Rhoel Dinglasan, University of Florida, United States

Reviewed by:
Scott E. Lindner, Pennsylvania State University (PSU), United States
Vasant Muralidharan, University of Georgia, United States

***Correspondence:**
Sergej Djuranovic
sergej.djuranovic@wustl.edu
Slavica Pavlovic Djuranovic
spavlov@wustl.edu

Specialty section:
This article was submitted to Infectious Diseases, a section of the journal Frontiers in Microbiology

Received: *26 September 2019*
Accepted: *21 November 2019*
Published: *06 December 2019*

Citation:
Erath J, Djuranovic S and Djuranovic SP (2019) Adaptation of Translational Machinery in Malaria Parasites to Accommodate Translation of Poly-Adenosine Stretches Throughout Its Life Cycle. Front. Microbiol. 10:2823. doi: 10.3389/fmicb.2019.02823

Malaria is caused by unicellular apicomplexan parasites of the genus *Plasmodium*, which includes the major human parasite *Plasmodium falciparum*. The complex cycle of the malaria parasite in both mosquito and human hosts has been studied extensively. There is tight control of gene expression in each developmental stage, and at every level of gene synthesis: from RNA transcription, to its subsequent translation, and finally post-translational modifications of the resulting protein. Whole-genome sequencing of *P. falciparum* has laid the foundation for significant biological advances by revealing surprising genomic information. The *P. falciparum* genome is extremely AT-rich (∼80%), with a substantial portion of genes encoding intragenic polyadenosine (polyA) tracks being expressed throughout the entire parasite life cycle. In most eukaryotes, intragenic polyA runs act as negative regulators of gene expression. Recent studies have shown that translation of mRNAs containing 12 or more consecutive adenosines results in ribosomal stalling and frameshifting; activating mRNA surveillance mechanisms. In contrast, *P. falciparum* translational machinery can efficiently and accurately translate polyA tracks without activating mRNA surveillance pathways. This unique feature of *P. falciparum* raises interesting questions: (1) How is *P. falciparum* able to efficiently and correctly translate polyA track transcripts, and (2) What are the specifics of the translational machinery and mRNA surveillance mechanisms that separate *P. falciparum* from other organisms? In this review, we analyze possible evolutionary shifts in *P. falciparum* protein synthesis machinery that allow efficient translation of an AU rich-transcriptome. We focus on physiological and structural differences of *P. falciparum* stage specific ribosomes, ribosome-associated proteins, and changes in mRNA surveillance mechanisms throughout the complete parasite life cycle, with an emphasis on the mosquito and liver stages.

Keywords: plasmodium, ribosomes, mRNA surveillance, AT rich genome, mRNA translation

INTRODUCTION

Plasmodium spp. has been in existence long before humans were on Earth, with an estimated origin of malaria-causing parasites appearing around 165 million years ago. Consequently, mosquitos and malaria had millions of years to co-evolve before either ever interacted with humans (Winegard, 2019). The infection of humans occurred evolutionarily recently, and probably with multiple *Plasmodium* parasite species. *P. falciparum* and *P. vivax* established themselves as a major malaria causing species. *P. falciparum* a most virulent agent in human malaria began speciation around 50,000 years ago followed by the population bottleneck around 5000 years ago but higher level of genetic diversity suggests that *P. vivax* is older (Loy et al., 2018; Otto et al., 2018). *P. malariae*, *P. ovale*, and rare cases of *P. knowlesi* were also reported in human hosts. From the mid-19th century onward, malaria reached its global limits and exacted immensely high numbers in sickness and death. While increased malaria prevention and control treatments have reduced the health burden of malaria, there are still 219 million cases of infection per year resulting in a 435,000 deaths (World Health Organization [WHO], 2018). The complex cycle of the malaria parasite in both mosquito and human hosts has been studied extensively (**Figure 1**). In each of these life cycle stages, gene expression is tightly controlled (Le Roch et al., 2004; Shock et al., 2007; Hughes et al., 2010; Sorber et al., 2011; Bunnik and Le Roch, 2013; Caro et al., 2014; Vembar et al., 2016a; Lu et al., 2017).

It took years of laborious efforts to sequence *P. falciparum* genome (Kooij et al., 2006). Sequences of single or multiple chromosomes as well as complete genome were reported over the course of 4 years (Gardner et al., 1998, 2002a,b; Bowman et al., 1999; Hall et al., 2002; Hyman et al., 2002). The high AT-content of the genome made gap closure in sequences extremely difficult. However, long-read, single molecule, real-time sequencing allowed for complete telomere-to-telomere *de novo* assembly of the *P. falciparum* genome thereby overcoming the problems associated with next generation sequencing of AT-rich genomes (Vembar et al., 2016b). The consequence of AT-richness is the presence of extended tracts of As, Ts, and TAs in introns and intergenic regions (Glöckner, 2000; Szafranski et al., 2005) as well as unusually high number of genes containing coding polyadenosine (polyA) repeats compared to the other species (Habich, 2016; Djuranovic et al., 2018). Repetitions of 12 or more adenosine nucleotides in gene coding sequences, so-called polyA tracks, were recently found to act as negative gene regulation motifs at the level of mRNA translation in all tested organisms (Arthur et al., 2015; Koutmou et al., 2015). Consequently, polyA tracks have been evolutionarily preserved in a select set of genes, but are generally selected against in overall gene coding sequences (Arthur et al., 2015).

Recent analysis of 250 eukaryotic genomes found a median of 2% of transcripts with polyA tracks (Habich, 2016). However, *Plasmodium* species represent an exception to this rule. The percentage of polyA carrying transcripts in the genome exceeds 60% for most *Plasmodium* spp., including *P. falciparum* (64%) (Djuranovic et al., 2018). The pervasive ribosomal stalling and frameshifting found on polyA tracks in other eukaryotes (Arthur et al., 2015; Koutmou et al., 2015; Tournu et al., 2019) would make it almost impossible for the majority of *Plasmodium* proteins to be efficiently and correctly synthesized. However, global studies of *Plasmodium* protein composition (Florens et al., 2002; Silvestrini et al., 2010) and protein synthesis (Le Roch et al., 2004; Bunnik et al., 2013; Caro et al., 2014) do not show any reduction in either the protein or mRNA abundances of polyA track genes. This suggests that both ribosomal stalling and frameshifting in *Plasmodium* are resolved by adaptations in protein synthesis and mRNA quality control systems. In this review, we will discuss how the extreme AT-rich genome of malaria-causing parasite promoted special features in *P. falciparum* ribosomes to enable translation of polyA tracks throughout the complete life cycle. Additionally, genomic changes and parasitic environment have also influenced variation in mRNA surveillance mechanism within the organism resulting in divergence from other Eukaryotes.

EVOLUTION OF AT-RICHNESS IN *P. falciparum*

Extremes in genomic base composition toward GC- or AT-richness exist in all domains of life (Sueoka, 1962; Wernegreen and Funk, 2004; Zilversmit et al., 2010; Wu et al., 2012). The extent of these extremes in nucleotide composition is limited by the necessity of all 20 amino acids and the subsequent requirement of all four nucleotides to encode them. As such, long homopolymeric amino acid repeats appear to be a characteristic of genomes with either bias (Glöckner, 2000; Albà et al., 2007; Muralidharan et al., 2011). Harboring either extreme AT- or GC-richness affects genomic structure, stability, transcriptome, and codon bias of organisms (Wu et al., 2012). As seen in **Table 1**, the *P. falciparum* mean AT-richness of around 80% appears to be one of the highest in all Eukaryotes (Pollack et al., 1982; Musto et al., 1999; Gardner et al., 2002a; Videvall, 2018). Surprisingly, the higher AT-content of the *P. falciparum* genome cannot be fully explained by increased AT-richness in intergenic regions, but rather by contributions of AT-richness in both coding 76.22% (**Table 1**) and non-coding genome 90% (Gardner et al., 2002a). Overall, gene organization patterns in *P. falciparum* are not influenced by the AT-bias (Glöckner, 2000; Szafranski et al., 2005; Djuranovic et al., 2018). However, what distinguishes *Plasmodium* species from other AT-rich organisms is distribution of consecutive adenosine nucleotides resulting in unusually high percentage of polyA track genes (**Table 2**). The genomes of *P. falciparum* and related *Plasmodium* species have apparently evolved independently to reach extreme AT-bias (**Table 2**). Interestingly, while the two groups of *Plasmodium* species can be separated based on their AT-genomic content (median of 75% versus a median of 55% AT-richness), both groups accommodate a considerable amount of polyA tracks within the coding regions (Djuranovic et al., 2018).

Perhaps just as interesting as the consequences of genomic base composition biases are the factors driving it. Previous studies in *P. falciparum* were unable to conclude the primary role of

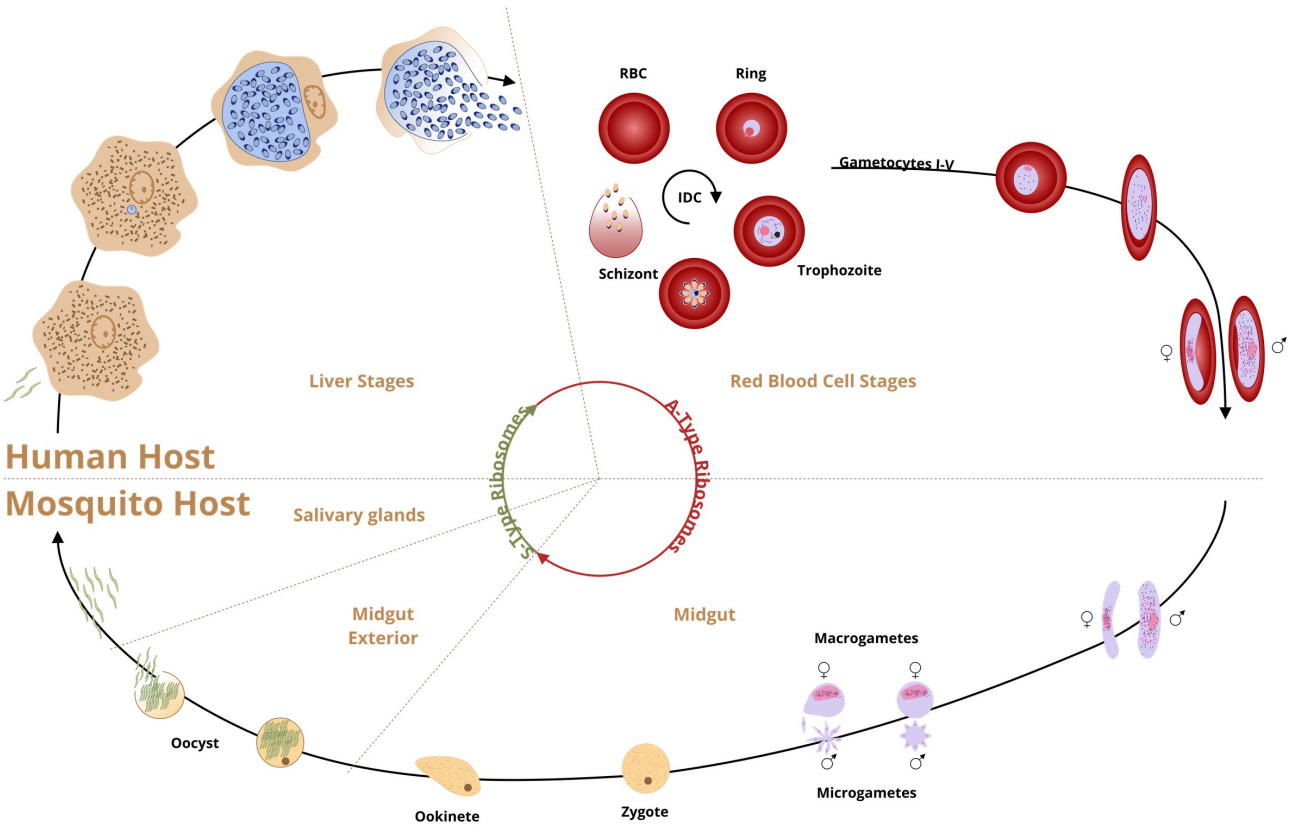

FIGURE 1 | Schematic presentation of *P. falciparum* life cycle and stage-specific ribosomal RNAs (A and S type). Human infection by *P. falciparum* begins when an infected female anopheline mosquito inoculates sporozoites into the bloodstream during feeding. The sporozoites invade liver cells and transform into trophozoites. In 6–8 days one mature schizont will release thousands of liver-stage merozoites into the bloodstream (exoerythrocytic schizogony, the first proliferative stage). The second asexual proliferative stage blood stage (erythrocytic schizogony) starts when the liver-stage merozoites invade the erythrocytes About 14–16 erythrocytic merozoites are generated in a 48-h cycle for re-infection and it is the point when the symptoms start. The merozoites may differentiate into single gametocytes, the initial stage of the sexual reproduction (gametogenesis) or continue the asexual cycle. Mosquito infection begins when the gametocytes are taken by mosquito with the blood meal. The male microgametocyte exflagellates into individual microgametes and fertilizes the female macrogamete. The zygote transforms into a motile ookinete, penetrates the mosquito midgut and develops into an oocyst. After 9–14 days, thousands of sporozoites are differentiated in the mature oocyst (sporogony), the only multiplicative stage in the mosquito. Mature sporozoites invade salivary glands and with the next blood meal the cycle continues.

homopolymeric amino acid repeats in the parasite proteome (Muralidharan et al., 2011; Muralidharan and Goldberg, 2013). Nutrient availability to intracellular parasites – as well as endosymbionts – appears to be a major factor in driving AT-richness, particularly nitrogen availability (Seward and Kelly, 2016; Dietel et al., 2019). *De novo* synthesis of nucleotides comes at great metabolic expense, especially regarding G+C nucleotides (Dietel et al., 2019). A+T nucleotides are less metabolically costly to create and tend to be more abundant. Consequently, A+T nucleotides are easier to scavenge, even in intracellular environments where nutrients may not be readily available. In the case of *P. falciparum*, where *de novo* synthesis of purines does not occur, the parasites must rely upon purine scavenging and salvage pathways (Ting et al., 2005; El Bissati et al., 2006; Quashie et al., 2008). Conversely, pyrimidine *de novo* synthesis occurs using glutamine and aspartic acid precursors. This appears to be the main source for these nucleotides, with the folate pathway being required for thymidine production (Sherman, 1979; Cassera et al., 2011; Hamilton et al., 2017). However, unlike other intracellular organisms referenced above, the intracellular environment for *P. falciparum* is not necessarily nutrient poor, but perhaps nutrient selective; particularly prior to parasite augmentation of the host cell. While *P. falciparum* has multiple means by which amino acids are obtained, much of its initial amino acid supply is from proteolysis of human host red blood cell hemoglobin (Leiriao et al., 2004; Liu et al., 2006; Babbitt et al., 2012).

This brings us to a second major contributor of AT-richness in intracellular organisms: oxidative stress. Reactive nitrogen (RNS) and reactive oxygen species (ROS) generate oxidative stress resulting in 8-oxoguanine production via guanine oxidation. If left unrepaired in DNA, 8-oxoG is able to pair with adenosine; ultimately causing a G:C to T:A conversion. Compounding the process, hemoglobin degradation produces free heme and H_2O_2, which generates further oxidative stress for the parasite (Becker et al., 2004). Additionally, NO and other RNS species may be important factors in the soluble heme-hemozoin equilibration (Ostera et al., 2011). Interestingly, another erythrocytic parasite from *Apicomplexa* phylum, *Babesia microti*, does not degrade

hemoglobin and has a considerably less AT-rich genome (61.02%) and polyA tracks (2.17% of genes with polyA tracks) compared to *P. falciparum* (Cornillot et al., 2012; Djuranovic et al., 2018). Although *Plasmodium* spp. does supply some of its own antioxidants to cope with oxidative assault, the higher than expected G:C to T:A conversion in the organism suggests a lack of full compensation by the biochemical and/or DNA repair safeguards (Hamilton et al., 2017). While 8-oxoG could potentially result in AT-richness imprinted in the DNA sequence, it causes more problems when found in RNA (Simms and Zaher, 2016). The oxidative lesion and incorporation of 8-oxoG in mRNAs reduces the rate of peptide-bond formation by more than three orders of magnitude (Simms et al., 2014). The effect of 8-oxoG nucleotides in mRNAs is independent of its position within the codon, results in stalling of the translational machinery, and finally activation of No-Go decay mRNA surveillance mechanisms (Simms et al., 2014). As such, the presence of oxidative stress may have driven both an increase in genomic AT-richness and changes in mRNA surveillance mechanisms of *P. falciparum*; which are discussed further below.

AT-richness itself appears to provide a feedback loop in the parasite with its increased indel rates, which are thought to be due to DNA replication slippage on AT repeats. These AT tracks provide amplicon breakpoints for copy number variant (CNV) alteration via non-allelic homologous repair-like mechanism that can be advantageous in altering resistance gene CNV numbers (Guler et al., 2013; Hamilton et al., 2017; Huckaby et al., 2019). Altogether, metabolic and biochemical factors continuously drive the parasite genome toward AT richness, which, in turn, drives indels that potentiate genomic plasticity providing an overall platform for relatively rapid adaptive evolution in the parasite. Unarguably, these factors necessitate increased fidelity in DNA replication and RNA transcription. While the exact details specific to *Plasmodium* spp. evolutionary adaptation toward an AT-rich genome, unique codon biases, and polyA encoded lysine stretches remains to be explored, the role ribosomes play as influential factors in this process is certain.

TABLE 1 | Comparison of AT-richness and polyA track gene ratios over selected *Eukaryotic* species.

Organism	CDS % AT richness	PolyA track genes
Plasmodium falciparum	76.22%	63.54%
Plasmodium reichenowi	75.93%	62.93%
Dictyostelium discoideum	72.57%	20.96%
Tetrahymena thermophila	72.50%	28.19%
Saccharomyces cerevisiae	60.39%	5.51%
Plasmodium knowlesi	59.77%	41.42%
Caenorhabditis elegans	57.94%	1.93%
Plasmodium vivax	53.51%	38.85%
Drosophila melanogaster	50.66%	1.10%
Pan troglodytes	50.60%	2.17%
Homo sapiens	49.98%	1.40%
Trypanosoma brucei	49.19%	2.89%
Trypanosoma cruzi	46.83%	2.74%
Toxoplasma gondii	42.88%	1.01%
Leishmania donovani	37.63%	0.19%
Leishmania major	37.52%	0.05%
Leishmania infantum jpcm5	37.50%	0.12%
Acanthamoeba castellanii str neff	37.06%	0.11%
Emiliania huxleyi	31.38%	0.10%
Aureococcus anophagefferens	29.37%	0.33%

The coding region AT-richness from a relevant selection of organisms with high, moderate, and low AT-content was compiled from Habich (2016) and Videvall (2018) and sorted in descending order.

THE rRNA AND SPECIALIZED RIBOSOMES OF *Plasmodium*

The most abundant genes in cells and genomes from bacteria to eukaryotes are those encoding ribosomal RNA. Ribosomal RNA genes in eukaryotic cells form clusters with a highly repetitive structure. *S. cerevisiae*, a single cell organism, has 150 rDNA repeats in one cluster on chromosome XII, while human cells contain five clusters of approximately 70 rDNA

TABLE 2 | Comparison of AT-Richness and polyA track gene ratios over selected *Plasmodium* species.

Organism	CDS % AT richness	PolyA track genes
Plasmodium gallinaceum	78.81%	71.77%
Plasmodium relictum	78.43%	79.18%
Plasmodium berghei	76.26%	68.26%
Plasmodium yoelii 17x	77.03%	64.96%
Plasmodium falciparum	76.22%	63.54%
Plasmodium chabaudi	74.46%	63.37%
Plasmodium reichenowi	75.93%	62.93%
Plasmodium vinckei petteri	74.91%	62.58%
Plasmodium gaboni	77.56%	61.76%
Plasmodium falciparum camp malaysia	76.71%	61.02%
Plasmodium falciparum nf54	76.55%	60.60%
Plasmodium falciparum fch 4	76.67%	60.57%
Plasmodium falciparum ugt5 1	76.49%	60.45%
Plasmodium falciparum santa lucia	76.75%	60.42%
Plasmodium falciparum palo alto uganda	76.56%	60.33%
Plasmodium falciparum nf135 5 c10	76.56%	59.98%
Plasmodium falciparum malips096 e11	76.50%	59.81%
Plasmodium falciparum 7g8	76.65%	59.72%
Plasmodium yoelii yoelii	75.20%	51.06%
Plasmodium knowlesi	59.77%	41.42%
Plasmodium knowlesi strain h	59.76%	41.42%
Plasmodium vivax	53.51%	38.85%
Plasmodium cynomolgi strain b	57.91%	33.83%
Plasmodium inui san antonio 1	56.37%	31.12%

Plasmodium spp. coding region AT-content and the ratio of polyA affected transcripts was collected (Habich, 2016; Videvall, 2018). The data are organized in the table to demonstrate a separation of two groups with high and low coding region AT-content and subsequently the number of polyA track containing transcripts. The separation notably occurs along the line of geographic region with the high AT-content organisms being predominantly found in Africa and the low AT-content group in Asia, Southeast Asia, and Latin America. However, the low AT-content group still exceeds that of most organisms.

repeats on five different chromosomes (Sakai et al., 1995). The organization of rDNA genes in clusters is conserved among most of the eukaryotic organisms (Kobayashi, 2014). Transcription of these clusters is highly coordinated to meet the huge demand for ribosomes, which occupy ∼50% of the total protein mass in a cell (Warner, 1999). *Plasmodium* genomes, however, have only 4–8 single copy rDNA units that are encoded on different chromosomes (Gunderson et al., 1987; Waters et al., 1989; Li et al., 1997). Such a small number of rDNA copies throughout the genome is seen elsewhere only in bacteria. *E. coli* has seven ribosomal RNA genes spread over its circular genome and well positioned in the regions near an origin of replication. This arrangement in *E. coli* enables maximum ribosomal RNA transcription while preventing possible collisions between replication forks and transcription machinery (Ellwood and Nomura, 1982). Thus, while most of the other organisms have optimized ribosome production, how the malaria-causing parasite produces its significant ribosome numbers is still unknown. It might be possible that massive DNA replication that occurs throughout its lifecycle (during shizogeny) in both hosts may accommodate the rRNA production requirements.

Besides this unusual rDNA arrangement, malaria parasites are pioneers in the new era of specialized ribosomes (Walliker et al., 1987; McCutchan et al., 1988; Waters et al., 1989; Velichutina et al., 1998; Xue and Barna, 2012). *Plasmodium* spp. has structurally distinct, stage-specific ribosomes and are the most well-known case of rRNA heterogeneity (McCutchan et al., 1988). The difference in sequence and expression profile during the life cycle classified them into A-type (asexual stage specific) and S-type (sporozoite specific) in the majority of *Plasmodium* species, including *P. falciparum*; with *P. vivax* having a third O-type rRNA (Li et al., 1997). The A-type is present in the liver and blood stage and S-type is sporozoite specific rRNA type that emerges during the mosquito stage and ends during the parasite development in hepatocytes (Zhu et al., 1990). Here, we will focus on the process by which the ribosome types switch and whether ribosomes with distinct rRNA play a selective role in the mRNAs they translate.

Plasmodium spp. have adapted to translation in two different hosts. This requires translation optimization at two distinct temperatures, one of which can be highly variable depending on the mosquito environment. Even though one would think that changes in temperature and hosts would be the reason for development of different rRNAs, the presence of A-type during the early mosquito stage and S-type during early liver stage does not support that idea (Fang and McCutchan, 2002). The rRNA sets are not expressed in an exclusive and binary (on/off) fashion, but more as a dynamic, heterogeneous population whereby one subtype, A or S, is the more dominant rRNA type in a particular lifecycle stage. While the idea of a thermoregulatory nature of the rRNA units has been explored earlier in *P. berghei*, rodent malaria, it has not been followed since (Fang and McCutchan, 2002). *P. berghei*, contains four distinct copies off the rRNA (A, B, C, D) and they are divided into A-type (A and B) and S-type (C and D). A single copy of the S-type gene, C or D was sufficient for life cycle completion, which only affected the parasite fitness. The group was unable to disrupt both S-type genes simultaneously; nor could they disrupt either of A-type genes (van Spaendonk et al., 2001). Interestingly, authors noticed growth retardation in oocyst development, which was more pronounced in D-unit disruption rather than in C-unit (van Spaendonk et al., 2001). Such difference could be explained by difference in ribosomal levels stemming from different transcriptional levels of C- and D-units or functional diversity of C- and D-unit containing ribosomes (Xue and Barna, 2012; Mills and Green, 2017). The disruption of specific S-type rRNA is also associated with oocyst development defects in the second rodent parasite *P. yoelii* (Qi et al., 2015). Finally, van Spaendonk et al. (2001) note a lack in differences between core catalytic components (e.g., GTPase center) of the ribosome large subunit in *P. berghei* that were previously described in *P. falciparum* (Velichutina et al., 1998). These results among species of *Plasmodium* potentiate the question of some aspect of ribosomal specialization (Vembar et al., 2016a).

Previous bacterial work has shown changes in rRNA operon expression in response to stress, resulting in phenotypic changes (Kurylo et al., 2018). The change in *Plasmodium* spp. rRNA population dynamics in response to environmental stress from host transfer is reminiscent of the bacterial changes in rRNA operon expression. However, whether changes in ratios of *Plasmodium* spp. rRNA types drive phenotypic changes is still unknown. Ostensibly, the ribosomes share the same repertoire of ribosomal proteins. RNAseq data shows that while ribosomal protein gene transcription as a whole is fairly persistent throughout the complete life cycle of *P. falciparum*, oscillations in their overall expression pattern match that of stages with increased protein synthesis (**Figure 2**). This does not exclude the highly sought-after notion that a specific set of ribosomes may be optimized for specific mRNA substrates or cell populations that may also exist in *Plasmodium* spp. A recent study in zebrafish showed that embryos have different subtypes of 5.8S, 18S, and 28S rRNAs, creating similar ribosome diversity seen in *Plasmodium* cells (Locati et al., 2017). *In silico* data have shown that the expanded regions of 18S subunit expressed in zebrafish embryos may preferentially bind maternal transcripts when compared to somatic subtypes (Locati et al., 2017). Similarly, a shift in the expression of 16S rRNA ribosome variants created populations of *E. coli* cells that accommodated functional differences in tetracycline binding (Kurylo et al., 2018). As was mentioned before, the rRNA heterogeneity that was mostly known in *Plasmodium* parasites (Gunderson et al., 1987; Waters et al., 1989; Zhu et al., 1990; Rogers et al., 1996; Xue and Barna, 2012) is now recognized in other organisms (Locati et al., 2017; Kurylo et al., 2018). However, the role of different *Plasmodium* rRNAs as a response to different environmental conditions is still not defined.

Plasmodium RIBOSOMES, POLYA AND POLY-LYSINE SEQUENCES

Regardless of the host, all *Plasmodium* spp. rRNA types must contend with the translation of unusually high AU-content and long-coding polyA stretches in mRNAs. RNA-seq data

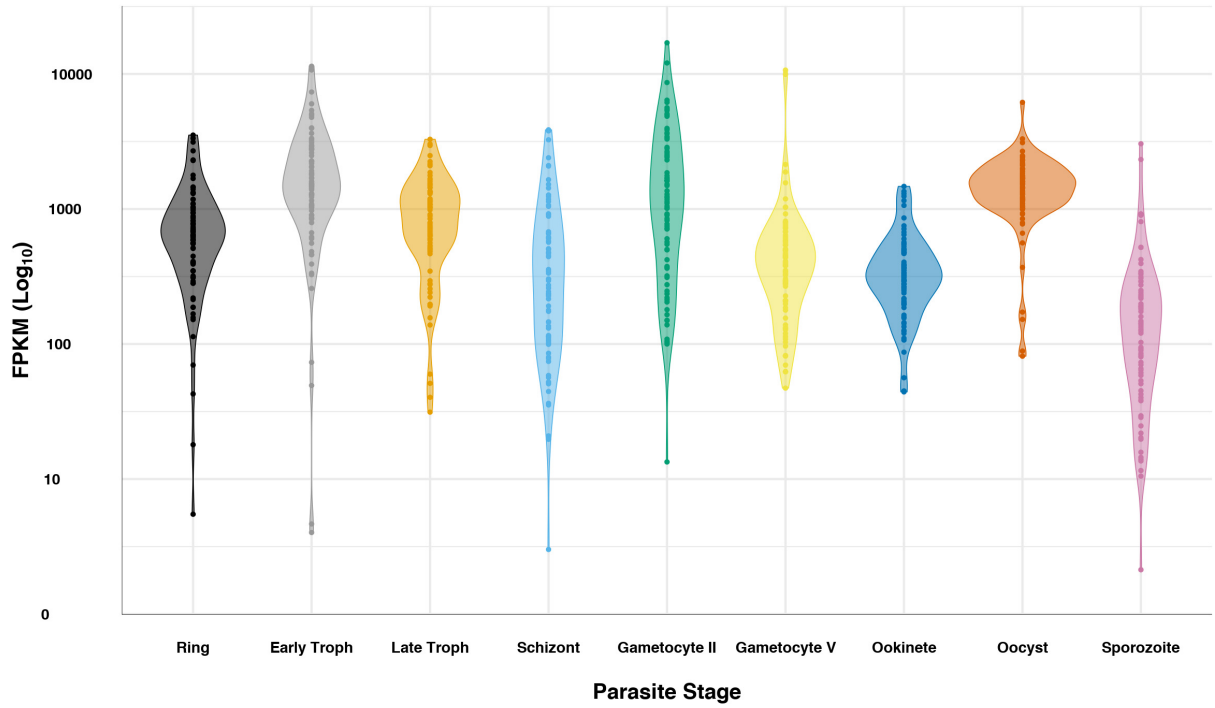

FIGURE 2 | *Plasmodium falciparum* ribosomal protein expression over life cycle. RNAseq data (López-Barragán et al., 2011; Zanghì et al., 2018) for the 82 cytosolic ribosomal proteins was queried from PlasmoDB (Aurrecoechea et al., 2009) for ring, early trophozoite, late trophozoite, schizont, gametocyte II, gametocyte V, ookinete, oocyst, and sporozoite stages. Data is displayed in log scale as a violin plot, showing the general trend of ribosomal protein transcripts. Data for each ribosomal protein is represented as a dot in the plot.

(Le Roch et al., 2004; Shock et al., 2007; Bunnik et al., 2013; Guler et al., 2013; Caro et al., 2014) indicates that the mRNA levels of genes containing polyA stretches follows the same trend as the general gene expression for all stages in both hosts (**Figures 3A–D**). We can conclude that both types of ribosomes expressed in both hosts have features allowing efficient translation of transcripts containing long, coding polyA tracks. This indicates that *P. falciparum* ribosomes have higher fidelity during translation of polyA sequences and are able to accommodate long polybasic peptides coming through their protein-exit channel. Previous ribosome mutagenesis studies in *S. cerevisiae* suggested functional differences in the GTPase centers of *P. falciparum* A- and S-type ribosomes (Velichutina et al., 1998). Despite the differences in yeast viability and growth rates, chimeric yeast ribosomes with either *Plasmodium's* A- or S-type GTPase centers exhibited increased translational accuracy (Velichutina et al., 1998). Even though there are stage-specific ribosomes, there is a group of genes that is present in human and mosquito that contain polyA tracks (**Figure 4**). More recently it was also shown that the *P. falciparum* ribosomes have been altered to accommodate the poly-lysine patches that are prolific throughout the proteome (Djuranovic et al., 2018). To allow these low-complexity, homopolymeric and polybasic amino acid repeats, the parasite ribosome exit channel has been altered by increasing the channel size at key bottle necks, as well as a reduction in the hydrophobicity patches typically seen in bacterial, yeast, or human ribosomes (Djuranovic et al., 2018).

Ribosome profiling and biochemical assays suggest an increased or modified fidelity such that parasite ribosomes do not stall or frameshift on polyA tracks (Djuranovic et al., 2018). The mechanism of this altered fidelity may result from not only modification of the ribosomal RNA sequence, but also via changes to key protein components of ribosomes. Two *P. falciparum* ribosome cryoEM structures suggest a reduced or lost interaction of the receptor for activated C kinase 1 (RACK1) to *Plasmodium* ribosomes (Wong et al., 2014; Sun et al., 2015). RACK1 has been established as an integral ribosomal scaffold protein (Sengupta et al., 2004). Beside other non-ribosome associated functions, RACK1 was found to be important for cap-dependent translation initiation, IRES-mediated translation, and site-specific translation (Majzoub et al., 2014). RACK1 also contributes to the translation arrest that is induced by translation of polyA sequences (Dimitrova et al., 2009; Kuroha et al., 2010), CGA-CGA codons in yeast (Wolf and Grayhack, 2015), or runs of consecutive basic amino-acid (Kuroha et al., 2010). Stalls on polyA tracks can be resolved in mammalian cells by deletion of RACK1 and ZNF598, thus enabling read-through of stall-inducing sequences (Garzia et al., 2017; Juszkiewicz and Hegde, 2017; Sundaramoorthy et al., 2017). *S. cerevisiae* ribosomes lacking the RACK1 homolog Asc1 are able to translate through the CGA-CGA stalling sequences and increase normally attenuated protein output (Wolf and Grayhack, 2015). The increase in amount of synthesized protein from CGA-CGA sequences is a consequence of overall reduced elongation

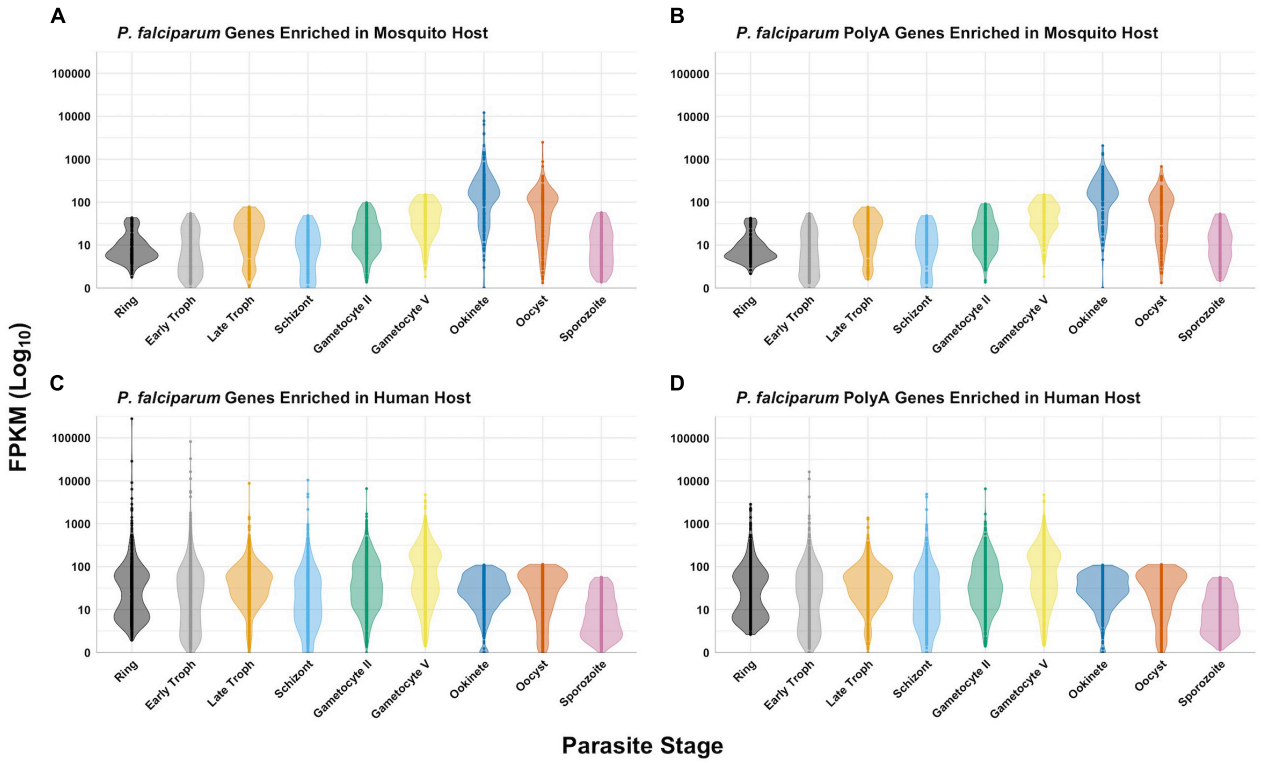

FIGURE 3 | Expression of *P. falciparum* genes in different hosts. The data was queried from PlasmoDB (Aurrecoechea et al., 2009; López-Barragán et al., 2011; Zanghì et al., 2018) for protein-coding genes with expression data greater than or equal to the 80th percentile for ring, early trophozoite, late trophozoite, schizont, gametocyte II, gametocyte V, ookinete, oocyst, and sporozoite stages. *P. falciparum* genes enriched in the mosquito host **(A)**, human host **(C)**, and polyA genes for each (**B** and **D**, respectively) are as previously defined. RNAseq data for all stages in both hosts for these gene sets are displayed in log scale as a violin plot with all data points for comparison.

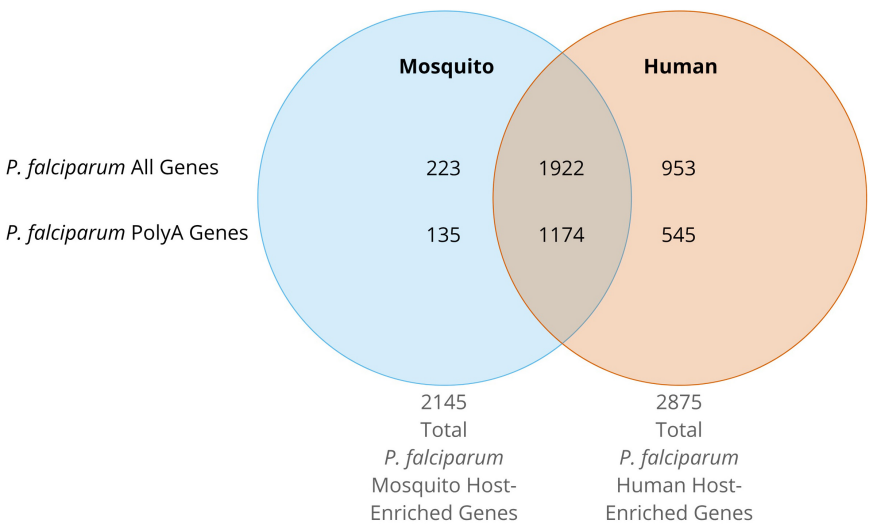

FIGURE 4 | Venn Diagram of *P. falciparum* gene expression from RNAseq data. The expression data greater than or equal to the 80th percentile for ring, early trophozoite, late trophozoite, schizont, gametocyte II, gametocyte V, ookinete, oocyst, and sporozoite stages was queried (López-Barragán et al., 2011; Zanghì et al., 2018). Mosquito stage total genes were defined as those with expression data greater than or equal to the 80th percentile during gametocyte V, ookinete, oocyst, or sporozoite stages. Mosquito host-specific genes are defined as above, but solely in mosquito host stages. Total parasite genes expressed in the human host were defined as those with expression data greater than or equal to the 80th percentile during sporozoite, ring, early trophozoite, late trophozoite, schizont, gametocyte II, or gametocyte V stages. Enriched parasite genes expressed in the human host are defined as above, but solely in human host stages. PolyA genes are those defined as having one or more runs of twelve or more consecutive adenosines in the coding region of the gene.

rates of yeast ribosomes that lack Asc1 (Tesina et al., 2019). Slower elongation rates may also influence cellular responses to ribosome pausing. The position of RACK1/Asc1 near the mRNA exit channel on the ribosome could be important in sensing ribosome collisions that lead to activation of ribosome rescue and mRNA surveillance pathways (Kim et al., 2014; Simms and Zaher, 2016; Tesina et al., 2019). The fact that *Plasmodium* ribosomes lack interaction with PfRACK1 could be beneficial for translation of polyA tracks into poly-lysine runs. However, based on previous conclusions concerning the role of RACK1/Asc1 in correct reading frame maintenance during translation of stalling sequences, the majority of polyA coding sequences in malaria parasites would be predicted to have multiple frameshifted protein products.

Previous studies (Lu and Deutsch, 2008; Kuroha et al., 2010; Brandman et al., 2012) proposed that stalling during the translation of polyA tracks is due to synthesis of the poly-lysine rich nascent peptide. Electrostatic interactions of the polybasic peptide and the peptide exit tunnel in the ribosome would elicit ribosomal stalling (Lu and Deutsch, 2008). Recent studies revealed that an mRNA-mediated mechanism is directly contributing to stalling (Arthur et al., 2015; Koutmou et al., 2015; Tesina et al., 2019). Consecutive adenosines are engaged by the ribosome decoding center nucleotides, are stabilized on both sides by rRNA base stacking interactions (Tesina et al., 2019), and adopt a helical conformation typical for single stranded polyA stretches (Tang et al., 2019). PolyA tracks are highly efficient at causing ribosome stalling, and the inhibitory conformation of polyA mRNA bases can further contribute to a polyA-mediated stalling mechanism. This conclusion is in line with the previous observations that consecutive AAG codons are less efficient at causing stalling than AAA codons (Arthur et al., 2015; Koutmou et al., 2015), despite coding for the same amino acid. Altogether, the charge and conformation of the poly-lysine nascent chain in conjunction with the stacked polyA mRNA nucleotides in the decoding center of the ribosome contribute to the overall stalling mechanism (Tesina et al., 2019). *P. falciparum* ribosomes are again the exception to this rule. The nucleotides that make stacking interactions with polyA repeats are conserved in *P. falciparum* ribosomes. However, both endogenous transcripts and reporter sequences with long runs of polyA tracks are efficiently translated by *Plasmodium* (Lacsina et al., 2011; Bunnik et al., 2013; Djuranovic et al., 2018). Thus, in order to adapt to polyA track translation for production of the polybasic and homopolymeric lysine repeats, the malaria-causing parasite has altered the sequence of its rRNA, its ribosome structure, its ribosomal proteins, and its mRNA translation quality control pathways.

mRNA SURVEILLANCE PATHWAYS IN AU-RICH TRANSCRIPTOME OF *P. falciparum*

The core elements for mRNA translation are highly conserved in *Plasmodium* spp. (Vembar et al., 2016a). The unique features involving protein synthesis in *Plasmodium*, such as different types of ribosomes in different life cycle stages, were noticed even before genome sequencing of the malaria parasite (Gunderson et al., 1987; Zhu et al., 1990; Rogers et al., 1996; van Spaendonk et al., 2001). However, the presence of an unusual number of mRNA binding proteins and the absence of some elements of mRNA surveillance mechanism were noticed upon completion of the *P. falciparum* genome sequence (Gunderson et al., 1987; Waters et al., 1989; Rogers et al., 1996; van Spaendonk et al., 2001; Le Roch et al., 2004; Bunnik and Le Roch, 2013; Cui et al., 2015; Reddy et al., 2015; Lu et al., 2017). A recent review elaborated on the translational regulation in blood-stages of malaria parasites (Vembar et al., 2016a). They focused on cytoplasmic mRNA translation and the fate of mRNAs: decoding of the mRNA messages by the 80S ribosomes, degradation of mRNAs by exo- or endo-nucleases (mRNA decay), and sequestration of mRNAs by protection from mRNA decay or by inhibition of translation. We focus here on the mechanism of activation of mRNA surveillance pathways by aberrant mRNAs in the context of unusual AU-richness and abundance of polyA tracks in *Plasmodium* transcriptome.

Eukaryotic cells have developed mechanisms to protect themselves from the production of the possible toxic proteins due to aberrant mRNA translation events. There are three mRNA quality control systems for translational errors in eukaryotes: Non-sense mediated decay (NMD), No-Go decay (NGD), and Non-Stop decay (NSD). NMD targets transcripts harboring "premature" termination codons (PTC) and nascent polypeptide chains synthesized from such transcripts for efficient degradation (Shoemaker and Green, 2012). Components of NMD pathway distinguishes PTCs from authentic stop codons in the coding sequence. PTCs are usually the product of point-non-sense mutations, ribosomal frameshifting on slippery sequences, aberrant splicing events, or in some cases, the consequence of targeted gene regulation through alternative splicing (Sorber et al., 2011; Yeoh et al., 2019). In higher eukaryotes, PTCs are generally recognized by their proximity to so-called exon-junction complexes (EJCs), which are deposited near exon junctions during pre-mRNA splicing in the nucleus (Shoemaker and Green, 2012).

No-Go decay is an "umbrella term" for the mRNA surveillance pathway that deals with either damaged or difficult to translate mRNA sequences that cause the ribosome to stall during the elongation cycle of translation. Besides the previously mentioned mRNA base damages (8-oxoG) (Simms et al., 2014; Simms and Zaher, 2016), mRNA translation can be stalled by lack of aminoacylated-tRNAs, strong mRNA secondary structure (i.e., stem-loops or long GC-rich regions), or stable interaction of the nascent polypeptide chain with the translating ribosome. Even though Non-Stop Decay (NSD) was discovered earlier than NGD (Doma and Parker, 2006; Izawa et al., 2012; Tsuboi et al., 2012; Saito et al., 2013; Martin et al., 2014; Guydosh and Green, 2017), it became apparent that in mammals and higher eukaryotes, the NSD and NGD pathways share the same effector protein complexes (Saito et al., 2013). The NSD targeted mRNAs that originate from premature 3′ adenylation or cryptic polyadenylation signals found in coding sequences indeed represent a similar group of transcripts that would be

targeted by NGD pathway (Saito et al., 2013; Kashima et al., 2014; Martin et al., 2014). Ribosomes that translate mRNAs without stop codons would eventually stall while translating long polyA tails into poly-lysine repeats, or because they would simply run out of message. Recognition of these types of transcripts, as well as the aforementioned NGD targets, trigger components of NGD/NSD pathways resulting in targeted mRNA cleavage and degradation.

The majority of mRNA surveillance pathway genes have been annotated in the *P. falciparum* genome (**Table 3**; Hughes et al., 2010). However, there are no mechanistic studies to confirm the activity of these pathways. Most of our knowledge on *Plasmodium*'s mRNA surveillance pathways comes from bioinformatic searches using homologous sequences from other eukaryotes. An indirect proof of the existence of NMD in *Plasmodium* is through the studies of alternative splicing of pre-mRNA (Sorber et al., 2011; Yeoh et al., 2019). Regulated alternative splicing events generating transcripts that do not lead to apparent protein synthesis usually carry PTCs, and thus are committed to NMD. Alternative splicing in *P. falciparum* has been reported for several genes like delta-aminolevulinic acid dehydratase (ALAD), stromal processing peptidase (SPP), and chloroquine resistance transporter (*Pf*CRT); among the others. Additionally, studies on the essentiality of *Plasmodium* genes that use the CRISPR/Cas9 technique (Ghorbal et al., 2014) or transposon techniques (Zhang et al., 2018) rely partially on silencing targeted genes through the activation of NMD. In this case, activation of NMD is the consequence of either mutations that are generated during CRISPR/Cas9 DNA cleavage, transposon insertion in the coding sequence, or due to aberrant splicing events caused by transposons landing in introns of targeted genes. As noted above, more than 60% of the *P. falciparum* transcripts harbor polyA track motifs that are seen as mRNA "slippery" sequences during translation (Habich, 2016; Djuranovic et al., 2018). Translation of runs of poly-adenosine nucleotides results in ribosomal frameshifting in most tested organisms causing activation of NMD pathways (Arthur et al., 2015; Koutmou et al., 2015). However, ribosome profiling (Lacsina et al., 2011; Bunnik et al., 2013) and reporter assays (Djuranovic et al., 2018) indicate that *P. falciparum* ribosomes maintain fidelity during translation of rather long polyA stretches (more than 36As in a row). Therefore, while there is indirect evidence that the NMD pathway exists in *Plasmodium*, it seems that this pathway is not upregulated during *Plasmodium* ribosomes' interactions with its polyA runs and AU-rich coding sequences. The most probable reason for this is the above mentioned changes in ribosome structure and fidelity.

Genomic sequencing has also revealed several critical components of surveillance pathways that are missing. According to NCBI, KEGG, and plasmoDB databases, *P. falciparum* and the majority of other *Plasmodium* spp. lack the NGD and NSD decay pathways components Hbs1 (Doma and Parker, 2006) and Cue2-RNA endonuclease (D'Orazio et al., 2019). With the exception of *S. cerevisiae*, the Hbs1/Pelo protein complex rescues stalled ribosomes on mRNAs. It was postulated that stalling events cause ribosome collisions (Simms et al., 2017), generating unique disome units consisting of the stalled ribosome and the following colliding ribosome (Beckman and Inada). The disome, as a minimal ribosome collision unit, is recognized by Ribosome-associated Quality Control (RQC) and NGD pathways (Ito-Harashima et al., 2007; Izawa et al., 2012; Tsuboi et al., 2012; Guydosh and Green, 2017; Juszkiewicz and Hegde, 2017). Activation of RQC and NGD leads to cleavage of stalled mRNA by Cue2, and possibly other unknown endonucleases, which ultimately leads to ribosome rescue by the activity of the Pelo/Hbs1 complex (Ito-Harashima et al., 2007; Tsuboi et al., 2012; Kashima et al., 2014; Matsuda et al., 2014; Sugiyama et al., 2019). In most of the above mentioned RQC and NGD studies,

TABLE 3 | Comparison of translation quality control factors in *P. falciparum* and its mosquito and human hosts.

Pathway	*H. sapiens*	*A. gambiae*	*P. falciparum*
NMD	eRF1, eRF3, UPF1, UPF2, UPF3A/UPF3B, eIF4AIII, MLN51, Y14/MAGOH, BTZ, SMG1, SMG5, SMG6, SMG7, PP2, Musashi, PABP1	eRF1 (AGAP010310), eRF3 (AGAP009310), UPF1 (AGAP001133), UPF2 (AGAP000337), UPF3 (AGAP006649), eIF4AIII (AGAP003089), Y14 (AGAP006365)/MAGOH (AGAP010755), SMG1(AGAP000368), SMG5 (AGAP008181), SMG6 (AGAP000894), PP2A (AGAP004096), Musashi (AGAP001930)	UPF1 (PF3D7_1005500), UPF2 (PF3D7_0925800), UPF3B (PF3D7_1327700), eIF4AIII (PF3D7_0422700) PF3D7_1327700), PP2A(PF3D7_0925400 – KEGG, PF3D7_1319700 – Hs homology, or PF3D7_0927700 – name), Musashi (PF3D7_0916700), PABP1 (PF3D7_1224300), eRF1 (PF3D7_0212300), eRF3 (PF3D7_1123400)
NGD/NSD	Pelota/HBS1L, RACK1, ZNF598, N4BP2 (Cue2)	Pelota (AGAP008269), HBS1L (AGAP002603), RACK1 (AGAP010173), ZNF598 homolog (AGAP007725), N4BP2 homolog (AGAP002516)	Pelota (PF3D7_0722100), RACK1 (PF3D7_0826700), ZNF598 (PF3D7_1450400)
RQC	CNOT4, ABCE1, TRIP4, ASCC2, ASCC3, NEMF, Listerin, UBE2D1, XRN1	CNOT4, ABCE1 (AGAP002182), ASCC2 homolog (AGAP000428), ASCC3 (AGAP001234), NEMF homolog (AGAP002680), Ltn1 (AGAP007143), UBE2D1 homolog (AGAP000145), XRN1	ABCE1 (PF3D7_1368200), NEMF homolog (PF3D7_1202600), Listerin homolog (PF3D7_0615600), CNOT4 (PF3D7_1235300), ASCC3 homolog (PF3D7_1439100), UBE2D1 homolog (PF3D7_1203900) XRN1 (PF3D7_0909400)

Factors associated with NMD, NGD/NSD, and RQC pathways from the literature and KEGG pathway database in human cells were collected (Kanehisa et al., 2019). Homologs in A. gambiae, one of the most common and effected vectors of P. falciparum (Cohuet et al., 2006; Annan et al., 2007; Giraldo-Calderon et al., 2015), were collected using KEGG pathways and performing protein-BLAST searching using VectorBase. Confirmation to FlyBase was also used to confirm vague annotations. P. falciparum factors were similarly documented again using KEGG pathways and PlasmoDB protein-BLAST analysis (Aurrecoechea et al., 2009; Kanehisa et al., 2019; Thurmond et al., 2019). Homologous gene database IDs are listed for reference. Notably, NGD/NSD factors Hbs1L and Cue2 endonuclease are missing in P. falciparum genome.

a typical substrate for ribosomal stalling is a long polyA run, ranging from 36 to 60 adenosines, coding for a peptide with 12–20 consecutive lysine residues. However, long polyA stretches in *P. falciparum* cells are efficiently translated into poly-lysine repeats (Lacsina et al., 2011; Bunnik et al., 2013). Of note, the longest endogenous polyA runs in different *P. falciparum* species range from 88 to 111 nucleotides and code for *Plasmodium* specific and hypothetical proteins (Habich, 2016), which is longer than the length of the normal 3′ polyA tail in either *S. cerevisiae* or human cells (Brown and Sachs, 1998; Chang et al., 2014; Subtelny et al., 2014). As such, many endogenous *Plasmodium* transcripts would be NSD targets in other eukaryotic organisms. It is also a question as to what the signal for NSD pathway is in *Plasmodium* as recent study on 3′ mRNA polyadenylation in apicomplexans did not find any differences in *P. falciparum* polyadenylation complex, polyA binding proteins, or polyA tails when compared to other species (Stevens et al., 2018; Kanehisa et al., 2019). Because *Plasmodium* lacks the components to rescue stalled ribosomes, and because *Plasmodium* ribosomes efficiently translate long polyA runs, the function and mechanism of the NGD/NSD pathway in *P. falciparum* remains a mystery.

CONCLUSION

While it may seem reasonable that *P. falciparum* adapted its ribosomes for higher fidelity on polyA runs and in parallel lost the ability to activate the RQC/NGD/NSD pathways, such a scenario is far from obvious. The absence of mRNA surveillance pathway components or deletion of RQC factors leads to both protein aggregation and proteotoxic stress in yeast cells (Choe et al., 2016; Yonashiro et al., 2016; Jamar et al., 2018). Protein aggregation is observed in *P. falciparum* in the absence of heat shock protein 110 (Muralidharan et al., 2012) but not due to the absence of mRNA surveillance or RQC pathways or as a consequence of increase in both number or length of polyA tracks (Djuranovic et al., 2018). This conflicting result, along with the surprising lack of interaction between the ribosomal scaffold protein RACK1/Asc1 and *Plasmodium* ribosomes (Wong et al., 2014; Sun et al., 2015), argue that the mRNA surveillance pathways in *P. falciparum* are inherently different from those in other eukaryotes. The diversity of rRNAs, *Plasmodium*'s ribosome structure, and the activity of yet unknown ribosome associated factors promote the possibility of "specialized ribosomes" in *Plasmodium* that allow for polyA tracks translation into functional proteins. Each of the aforementioned changes in parasites translational machinery and mRNA quality control pathways come at the cost of self-fitness that would normally be detrimental for survival of *Plasmodium* parasites in both humans and mosquitos. And yet the parasite has persisted in both of these hosts for hundreds of millions of years. Parasitologists and epidemiologists have wondered "How?" for decades; now as translational biologists, we add our voices to the same question.

AUTHOR CONTRIBUTIONS

All authors contributed equally to writing of this review.

FUNDING

This work in Djuranovic's lab was supported by NIH R01 GM112824 to SD and LEAP Awards to SD and SPD. JE was supported by NIH T32 GM007067 and NIMH R01 MH116999.

ACKNOWLEDGMENTS

We are thankful to Caitlin D. Hanlon for critical reading and suggestions on review topic.

REFERENCES

Albà, M. M., Tompa, P., and Veitia, R. A. (2007). Amino acid repeats and the structure and evolution of proteins. *Genome Dyn.* 3, 119–130. doi: 10.1159/000107607

Annan, Z., Durand, P., Ayala, F. J., Arnathau, C., Awono-Ambene, P., Simard, F., et al. (2007). Population genetic structure of *Plasmodium falciparum* in the two main African vectors, *Anopheles gambiae* and *Anopheles funestus*. *Proc. Natl. Acad. Sci. U.S.A.* 104, 7987–7992. doi: 10.1073/pnas.0702715104

Arthur, L., Pavlovic-Djuranovic, S., Smith-Koutmou, K., Green, R., Szczesny, P., and Djuranovic, S. (2015). Translational control by lysine-encoding A-rich sequences. *Sci. Adv.* 1:e1500154. doi: 10.1126/sciadv.1500154

Aurrecoechea, C., Brestelli, J., Brunk, B. P., Dommer, J., Fischer, S., Gajria, B., et al. (2009). PlasmoDB: a functional genomic database for malaria parasites. *Nucleic Acids Res.* 37, D539–D543. doi: 10.1093/nar/gkn814

Babbitt, S. E., Altenhofen, L., Cobbold, S. A., Istvan, E. S., Fennell, C., Doerig, C., et al. (2012). *Plasmodium falciparum* responds to amino acid starvation by entering into a hibernatory state. *Proc. Natl. Acad. Sci. U.S.A.* 109, E3278–E3287. doi: 10.1073/pnas.1209823109

Becker, K., Tilley, L., Vennerstrom, J. L., Roberts, D., Rogerson, S., and Ginsburg, H. (2004). Oxidative stress in malaria parasite-infected erythrocytes: host-parasite interactions. *Int. J. Parasitol.* 34, 163–189. doi: 10.1016/j.ijpara.2003.09.011

Bowman, S., Lawson, D., Basham, D., Brown, D., Chillingworth, T., Churcher, C. M., et al. (1999). The complete nucleotide sequence of chromosome 3 of *Plasmodium falciparum*. *Nature* 400, 532–538.

Brandman, O., Stewart-Ornstein, J., Wong, D., Larson, A., Williams, C. C., Li, G. W., et al. (2012). A ribosome-bound quality control complex triggers degradation of nascent peptides and signals translation stress. *Cell* 151, 1042–1054. doi: 10.1016/j.cell.2012.10.044

Brown, C. E., and Sachs, A. B. (1998). Poly(A) tail length control in Saccharomyces cerevisiae occurs by message-specific deadenylation. *Mol. Cell. Biol.* 18, 6548–6559. doi: 10.1128/mcb.18.11.6548

Bunnik, E. M., and Le Roch, K. G. (2013). An introduction to functional genomics and systems biology. *Adv. Wound Care* 2, 490–498.

Bunnik, E. M., Chung, D. W., Hamilton, M., Ponts, N., Saraf, A., Prudhomme, J., et al. (2013). Polysome profiling reveals translational control of gene expression in the human malaria parasite *Plasmodium falciparum*. *Genome Biol.* 14:R128. doi: 10.1186/gb-2013-14-11-r128

Caro, F., Ahyong, V., Betegon, M., and DeRisi, J. L. (2014). Genome-wide regulatory dynamics of translation in the *Plasmodium falciparum* asexual blood stages. *eLife* 3:e04106. doi: 10.7554/eLife.04106

Cassera, M. B., Zhang, Y., Hazleton, K. Z., and Schramm, V. L. (2011). Purine and pyrimidine pathways as targets in *Plasmodium falciparum*. *Curr. Top. Med. Chem.* 11, 2103–2115. doi: 10.2174/156802611796575948

Chang, H., Lim, J., Ha, M., and Kim, V. N. (2014). TAIL-seq: genome-wide determination of poly(A) tail length and 3′ end modifications. *Mol. Cell.* 53, 1044–1052. doi: 10.1016/j.molcel.2014.02.007

Choe, Y. J., Park, S. H., Hassemer, T., Korner, R., Vincenz-Donnelly, L., Hayer-Hartl, M., et al. (2016). Failure of RQC machinery causes protein aggregation and proteotoxic stress. *Nature* 531, 191–195. doi: 10.1038/nature16973

Cohuet, A., Osta, M. A., Morlais, I., Awono-Ambene, P. H., Michel, K., Simard, F., et al. (2006). *Anopheles* and *Plasmodium*: from laboratory models to natural systems in the field. *EMBO Rep.* 7, 1285–1289.

Cornillot, E., Hadj-Kaddour, K., Dassouli, A., Noel, B., Ranwez, V., Vacherie, B., et al. (2012). Sequencing of the smallest Apicomplexan genome from the human pathogen *Babesia microti*. *Nucleic Acids Res.* 40, 9102–9114. doi: 10.1093/nar/gks700

Cui, L., Lindner, S., and Miao, J. (2015). Translational regulation during stage transitions in malaria parasites. *Ann. N. Y. Acad. Sci.* 1342, 1–9. doi: 10.1111/nyas.12573

Dietel, A. K., Merker, H., Kaltenpoth, M., and Kost, C. (2019). Selective advantages favour high genomic AT-contents in intracellular elements. *PLoS Genet.* 15:e1007778. doi: 10.1371/journal.pgen.1007778

Dimitrova, L. N., Kuroha, K., Tatematsu, T., and Inada, T. (2009). Nascent peptide-dependent translation arrest leads to Not4p-mediated protein degradation by the proteasome. *J. Biol. Chem.* 284, 10343–10352. doi: 10.1074/jbc.M808840200

Djuranovic, S. P., Erath, J., Andrews, R. J., Bayguinov, P. O., Chung, J. J., Chalker, D. L., et al. (2018). PolyA tracks and poly-lysine repeats are the achilles heel of *Plasmodium falciparum*. *bioRxiv* [Preprint]. doi: 10.1101/420109

Doma, M. K., and Parker, R. (2006). Endonucleolytic cleavage of eukaryotic mRNAs with stalls in translation elongation. *Nature* 440, 561–564. doi: 10.1038/nature04530

D'Orazio, K. N., Wu, C. C., Sinha, N., Loll-Krippleber, R., Brown, G. W., and Green, R. (2019). The endonuclease Cue2 cleaves mRNAs at stalled ribosomes during No Go Decay. *eLife* 8:e49117. doi: 10.7554/eLife.49117

El Bissati, K., Zufferey, R., Witola, W. H., Carter, N. S., Ullman, B., and Ben Mamoun, C. (2006). The plasma membrane permease PfNT1 is essential for purine salvage in the human malaria parasite *Plasmodium falciparum*. *Proc. Natl. Acad. Sci. U.S.A.* 103, 9286–9291. doi: 10.1073/pnas.0602590103

Ellwood, M., and Nomura, M. (1982). Chromosomal locations of the genes for rRNA in *Escherichia coli* K-12. *J. Bacteriol.* 149, 458–468.

Fang, J., and McCutchan, T. F. (2002). Thermoregulation in a parasite's life cycle. *Nature* 418:742. doi: 10.1038/418742a

Florens, L., Washburn, M. P., Raine, J. D., Anthony, R. M., Grainger, M., Haynes, J. D., et al. (2002). A proteomic view of the *Plasmodium falciparum* life cycle. *Nature* 419, 520–526. doi: 10.1038/nature01107

Gardner, M. J., Hall, N., Fung, E., White, O., Berriman, M., Hyman, R. W., et al. (2002a). Genome sequence of the human malaria parasite *Plasmodium falciparum*. *Nature* 419, 498–511.

Gardner, M. J., Shallom, S. J., Carlton, J. M., Salzberg, S. L., Nene, V., Shoaibi, A., et al. (2002b). Sequence of *Plasmodium falciparum* chromosomes 2, 10, 11 and 14. *Nature* 419, 531–534.

Gardner, M. J., Tettelin, H., Carucci, D. J., Cummings, L. M., Aravind, L., Koonin, E. V., et al. (1998). Chromosome 2 sequence of the human malaria parasite *Plasmodium falciparum*. *Science* 282, 1126–1132. doi: 10.1126/science.282.5391.1126

Garzia, A., Jafarnejad, S. M., Meyer, C., Chapat, C., Gogakos, T., Morozov, P., et al. (2017). The E3 ubiquitin ligase and RNA-binding protein ZNF598 orchestrates ribosome quality control of premature polyadenylated mRNAs. *Nat. Commun.* 8:16056. doi: 10.1038/ncomms16056

Ghorbal, M., Gorman, M., Macpherson, C. R., Martins, R. M., Scherf, A., and Lopez-Rubio, J. J. (2014). Genome editing in the human malaria parasite *Plasmodium falciparum* using the CRISPR-Cas9 system. *Nat. Biotechnol.* 32, 819–821. doi: 10.1038/nbt.2925

Giraldo-Calderon, G. I, Emrich, S. J., MacCallum, R. M., Maslen, G., Dialynas, E., Topalis, P., et al. (2015). VectorBase: an updated bioinformatics resource for invertebrate vectors and other organisms related with human diseases. *Nucleic Acids Res.* 43, D707–D713. doi: 10.1093/nar/gku1117

Glöckner, G. (2000). Large scale sequencing and analysis of AT rich eukaryote genomes. *Curr. Genom.* 1, 289–299. doi: 10.2174/1389202003351472

Guler, J. L., Freeman, D. L., Ahyong, V., Patrapuvich, R., White, J., Gujjar, R., et al. (2013). Asexual populations of the human malaria parasite, *Plasmodium falciparum*, use a two-step genomic strategy to acquire accurate, beneficial DNA amplifications. *PLoS Pathog.* 9:e1003375. doi: 10.1371/journal.ppat.1003375

Gunderson, J. H., Sogin, M. L., Wollett, G., Hollingdale, M., de la Cruz, V. F., Waters, A. P., et al. (1987). Structurally distinct, stage-specific ribosomes occur in *Plasmodium*. *Science* 238, 933–937. doi: 10.1126/science.3672135

Guydosh, N. R., and Green, R. (2017). Translation of poly(A) tails leads to precise mRNA cleavage. *RNA* 23, 749–761. doi: 10.1261/rna.060418.116

Habich, M. (2016). PATACSDB - The database of polyA translational attenuators in coding sequences. *PeerJ Comput. Sci.* 2:e45. doi: 10.7717/peerj-cs.45

Hall, N., Pain, A., Berriman, M., Churcher, C., Harris, B., Harris, D., et al. (2002). Sequence of *Plasmodium falciparum* chromosomes 1, 3-9 and 13. *Nature* 419, 527–531.

Hamilton, W. L., Claessens, A., Otto, T. D., Kekre, M., Fairhurst, R. M., Rayner, J. C., et al. (2017). Extreme mutation bias and high AT content in *Plasmodium falciparum*. *Nucleic Acids Res.* 45, 1889–1901. doi: 10.1093/nar/gkw1259

Huckaby, A. C., Granum, C. S., Carey, M. A., Szlachta, K., Al-Barghouthi, B., Wang, Y. H., et al. (2019). Complex DNA structures trigger copy number variation across the *Plasmodium falciparum* genome. *Nucleic Acids Res.* 47, 1615–1627. doi: 10.1093/nar/gky1268

Hughes, K. R., Philip, N., Starnes, G. L., Taylor, S., and Waters, A. P. (2010). From cradle to grave: RNA biology in malaria parasites. *Wiley Interdiscip. Rev. RNA* 1, 287–303. doi: 10.1002/wrna.30

Hyman, R. W., Fung, E., Conway, A., Kurdi, O., Mao, J., Miranda, M., et al. (2002). Sequence of *Plasmodium falciparum* chromosome 12. *Nature* 419, 534–537.

Ito-Harashima, S., Kuroha, K., Tatematsu, T., and Inada, T. (2007). Translation of the poly(A) tail plays crucial roles in nonstop mRNA surveillance via translation repression and protein destabilization by proteasome in yeast. *Genes Dev.* 21, 519–524. doi: 10.1101/gad.1490207

Izawa, T., Tsuboi, T., Kuroha, K., Inada, T., Nishikawa, S., and Endo, T. (2012). Roles of dom34:hbs1 in nonstop protein clearance from translocators for normal organelle protein influx. *Cell Rep.* 2, 447–453. doi: 10.1016/j.celrep.2012.08.010

Jamar, N. H., Kritsiligkou, P., and Grant, C. M. (2018). Loss of mRNA surveillance pathways results in widespread protein aggregation. *Sci. Rep.* 8:3894. doi: 10.1038/s41598-018-22183-2

Juszkiewicz, S., and Hegde, R. S. (2017). Initiation of quality control during poly(A) translation requires site-specific ribosome Ubiquitination. *Mol. Cell* 65, 743–750.e4. doi: 10.1016/j.molcel.2016.11.039

Kanehisa, M., Sato, Y., Furumichi, M., Morishima, K., and Tanabe, M. (2019). New approach for understanding genome variations in KEGG. *Nucleic Acids Res.* 47, D590–D595. doi: 10.1093/nar/gky962

Kashima, I., Takahashi, M., Hashimoto, Y., Sakota, E., Nakamura, Y., and Inada, T. (2014). A functional involvement of ABCE1, eukaryotic ribosome recycling factor, in nonstop mRNA decay in drosophila Melanogaster cells. *Biochimie* 106, 10–16. doi: 10.1016/j.biochi.2014.08.001

Kim, H. K., Liu, F., Fei, J., Bustamante, C., Gonzalez, R. L., and Tinoco, I. (2014). A frameshifting stimulatory stem loop destabilizes the hybrid state and impedes ribosomal translocation. *Proc. Natl. Acad. Sci. U.S.A.* 111, 5538–5543. doi: 10.1073/pnas.1403457111

Kobayashi, T. (2014). Ribosomal RNA gene repeats, their stability and cellular senescence. *Proc. JPN Acad. Ser. B Phys. Biol. Sci.* 90, 119–129. doi: 10.2183/pjab.90.119

Kooij, T. W., Janse, C. J., and Waters, A. P. (2006). Plasmodium post-genomics: better the bug you know? *Nat. Rev. Microbiol.* 4, 344–357. doi: 10.1038/nrmicro1392

Koutmou, K. S., Schuller, A. P., Brunelle, J. L., Radhakrishnan, A., Djuranovic, S., and Green, R. (2015). Ribosomes slide on lysine-encoding homopolymeric a stretches. *eLife* 4:e05534. doi: 10.7554/eLife.05534

Kuroha, K., Akamatsu, M., Dimitrova, L., Ito, T., Kato, Y., Shirahige, K., et al. (2010). Receptor for activated C kinase 1 stimulates nascent polypeptide-dependent translation arrest. *EMBO Rep.* 11, 956–961. doi: 10.1038/embor.2010.169

Kurylo, C. M., Parks, M. M., Juette, M. F., Zinshteyn, B., Altman, R. B., Thibado, J. K., et al. (2018). Endogenous rRNA sequence variation can regulate stress response gene expression and phenotype. *Cell Rep.* 25, 236–248.e6. doi: 10.1016/j.celrep.2018.08.093

Lacsina, J. R., LaMonte, G., Nicchitta, C. V., and Chi, J. T. (2011). Polysome profiling of the malaria parasite *Plasmodium falciparum*. *Mol. Biochem. Parasitol.* 179, 42–46. doi: 10.1016/j.molbiopara.2011.05.003

Le Roch, K. G., Johnson, J. R., Florens, L., Zhou, Y., Santrosyan, A., Grainger, M., et al. (2004). Global analysis of transcript and protein levels across the *Plasmodium falciparum* life cycle. *Genom. Res.* 14, 2308–2318. doi: 10.1101/gr.2523904

Leiriao, P., Rodrigues, C. D., Albuquerque, S. S., and Mota, M. M. (2004). Survival of protozoan intracellular parasites in host cells. *EMBO Rep.* 5, 1142–1147. doi: 10.1038/sj.embor.7400299

Li, J., Gutell, R. R., Damberger, S. H., Wirtz, R. A., Kissinger, J. C., Rogers, M. J., et al. (1997). Regulation and trafficking of three distinct 18 S ribosomal RNAs during development of the malaria parasite. *J. Mol. Biol.* 269, 203–213. doi: 10.1006/jmbi.1997.1038

Liu, J., Istvan, E. S., Gluzman, I. Y., Gross, J., and Goldberg, D. E. (2006). *Plasmodium falciparum* ensures its amino acid supply with multiple acquisition pathways and redundant proteolytic enzyme systems. *Proc. Natl. Acad. Sci. U.S.A.* 103, 8840–8845. doi: 10.1073/pnas.0601876103

Locati, M. D., Pagano, J. F. B., Girard, G., Ensink, W. A., van Olst, M., van Leeuwen, S., et al. (2017). Expression of distinct maternal and somatic 5.8S, 18S, and 28S rRNA types during zebrafish development. *RNA* 23, 1188–1199. doi: 10.1261/rna.061515.117

López-Barragán, M. J., Lemieux, J., Quiñones, M., Williamson, K. C., Molina-Cruz, A., Cui, K., et al. (2011). Directional gene expression and antisense transcripts in sexual and asexual stages of *Plasmodium falciparum*. *BMC Genom.* 12:587. doi: 10.1186/1471-2164-12-587

Loy, D. E., Plenderleith, L. J., Sundararaman, S. A., Liu, W., Gruszczyk, J., Chen, Y. J., et al. (2018). Evolutionary history of human. *Proc. Natl. Acad. Sci. U.S.A.* 115, E8450–E8459. doi: 10.1073/pnas.1810053115

Lu, J., and Deutsch, C. (2008). Electrostatics in the ribosomal tunnel modulate chain elongation rates. *J. Mol. Biol.* 384, 73–86. doi: 10.1016/j.jmb.2008.08.089

Lu, X. M., Batugedara, G., Lee, M., Prudhomme, J., Bunnik, E. M., and Le Roch, K. G. (2017). Nascent RNA sequencing reveals mechanisms of gene regulation in the human malaria parasite *Plasmodium falciparum*. *Nucleic Acids Res.* 45, 7825–7840. doi: 10.1093/nar/gkx464

Majzoub, K., Hafirassou, M. L., Meignin, C., Goto, A., Marzi, S., Fedorova, A., et al. (2014). RACK1 controls IRES-mediated translation of viruses. *Cell* 159, 1086–1095. doi: 10.1016/j.cell.2014.10.041

Martin, L., Grigoryan, A., Wang, D., Wang, J., Breda, L., Rivella, S., et al. (2014). Identification and characterization of small molecules that inhibit nonsense-mediated RNA decay and suppress nonsense p53 mutations. *Cancer Res.* 74, 3104–3113. doi: 10.1158/0008-5472.CAN-13-2235

Matsuda, R., Ikeuchi, K., Nomura, S., and Inada, T. (2014). Protein quality control systems associated with no-go and nonstop mRNA surveillance in yeast. *Genes Cells* 19, 1–12. doi: 10.1111/gtc.12106

McCutchan, T. F., de la Cruz, V. F., Lal, A. A., Gunderson, J. H., Elwood, H. J., and Sogin, M. L. (1988). Primary sequences of two small subunit ribosomal RNA genes from *Plasmodium falciparum*. *Mol. Biochem. Parasitol.* 28, 63–68. doi: 10.1016/0166-6851(88)90181-8

Mills, E. W., and Green, R. (2017). Ribosomopathies: there's strength in numbers. *Science* 358:eaan2755. doi: 10.1126/science.aan2755

Muralidharan, V., and Goldberg, D. E. (2013). Asparagine repeats in *Plasmodium falciparum* proteins: good for nothing? *PLoS Pathog.* 9:e1003488. doi: 10.1371/journal.ppat.1003488

Muralidharan, V., Oksman, A., Iwamoto, M., Wandless, T. J., and Goldberg, D. E. (2011). Asparagine repeat function in a *Plasmodium falciparum* protein assessed via a regulatable fluorescent affinity tag. *Proc. Natl. Acad. Sci. U.S.A.* 108, 4411–4416. doi: 10.1073/pnas.1018449108

Muralidharan, V., Oksman, A., Pal, P., Lindquist, S., and Goldberg, D. E. (2012). *Plasmodium falciparum* heat shock protein 110 stabilizes the asparagine repeat-rich parasite proteome during malarial fevers. *Nat. Commun.* 3:1310. doi: 10.1038/ncomms2306

Musto, H., Romero, H., Zavala, A., Jabbari, K., and Bernardi, G. (1999). Synonymous codon choices in the extremely GC-poor genome of *Plasmodium falciparum*: compositional constraints and translational selection. *J. Mol. Evol.* 49, 27–35. doi: 10.1007/pl00006531

Ostera, G., Tokumasu, F., Teixeira, C., Collin, N., Sa, J., Hume, J., et al. (2011). *Plasmodium falciparum*: nitric oxide modulates heme speciation in isolated food vacuoles. *Exp. Parasitol.* 127, 1–8. doi: 10.1016/j.exppara.2010.05.006

Otto, T. D., Gilabert, A., Crellen, T., Böhme, U., Arnathau, C., Sanders, M., et al. (2018). Genomes of all known members of a Plasmodium subgenus reveal paths to virulent human malaria. *Nat. Microbiol.* 3, 687–697. doi: 10.1038/s41564-018-0162-2

Pollack, Y., Katzen, A. L., Spira, D. T., and Golenser, J. (1982). The genome of *Plasmodium falciparum*. I: DNA base composition. *Nucleic Acids Res.* 10, 539–546. doi: 10.1093/nar/10.2.539

Qi, Y., Zhu, F., Eastman, R. T., Fu, Y., Zilversmit, M., Pattaradilokrat, S., et al. (2015). Regulation of *Plasmodium yoelii* oocyst development by strain- and stage-specific small-subunit rRNA. *mBio* 6:e00117. doi: 10.1128/mBio.00117-15

Quashie, N. B., Dorin-Semblat, D., Bray, P. G., Biagini, G. A., Doerig, C., Ranford-Cartwright, L. C., et al. (2008). A comprehensive model of purine uptake by the malaria parasite *Plasmodium falciparum*: identification of four purine transport activities in intraerythrocytic parasites. *Biochem. J.* 411, 287–295. doi: 10.1042/BJ20071460

Reddy, B. P., Shrestha, S., Hart, K. J., Liang, X., Kemirembe, K., Cui, L., et al. (2015). A bioinformatic survey of RNA-binding proteins in *Plasmodium*. *BMC Genom.* 16:890. doi: 10.1186/s12864-015-2092-1

Rogers, M. J., Gutell, R. R., Damberger, S. H., Li, J., McConkey, G. A., Waters, A. P., et al. (1996). Structural features of the large subunit rRNA expressed in *Plasmodium falciparum* sporozoites that distinguish it from the asexually expressed subunit rRNA. *RNA* 2, 134–145.

Saito, S., Hosoda, N., and Hoshino, S. (2013). The Hbs1-Dom34 protein complex functions in non-stop mRNA decay in mammalian cells. *J. Biol. Chem.* 288, 17832–17843. doi: 10.1074/jbc.M112.448977

Sakai, K., Ohta, T., Minoshima, S., Kudoh, J., Wang, Y., de Jong, P. J., et al. (1995). Human ribosomal RNA gene cluster: identification of the proximal end containing a novel tandem repeat sequence. *Genomics* 26, 521–526. doi: 10.1016/0888-7543(95)80170-q

Sengupta, J., Nilsson, J., Gursky, R., Spahn, C. M., Nissen, P., and Frank, J. (2004). Identification of the versatile scaffold protein RACK1 on the eukaryotic ribosome by cryo-EM. *Nat. Struct. Mol. Biol.* 11, 957–962. doi: 10.1038/nsmb822

Seward, E. A., and Kelly, S. (2016). Dietary nitrogen alters codon bias and genome composition in parasitic microorganisms. *Genom. Biol.* 17:226.

Sherman, I. W. (1979). Biochemistry of *Plasmodium* (malarial parasites). *Microbiol. Rev.* 43, 453–495.

Shock, J. L., Fischer, K. F., and DeRisi, J. L. (2007). Whole-genome analysis of mRNA decay in *Plasmodium falciparum* reveals a global lengthening of mRNA half-life during the intra-erythrocytic development cycle. *Genom. Biol.* 8:R134.

Shoemaker, C. J., and Green, R. (2012). Translation drives mRNA quality control. *Nat. Struct. Mol. Biol.* 19, 594–601. doi: 10.1038/nsmb.2301

Silvestrini, F., Lasonder, E., Olivieri, A., Camarda, G., van Schaijk, B., Sanchez, M., et al. (2010). Protein export marks the early phase of gametocytogenesis of the human malaria parasite *Plasmodium falciparum*. *Mol. Cell. Proteomics* 9, 1437–1448. doi: 10.1074/mcp.M900479-MCP200

Simms, C. L., and Zaher, H. S. (2016). Quality control of chemically damaged RNA. *Cell Mol. Life Sci.* 73, 3639–3653. doi: 10.1007/s00018-016-2261-7

Simms, C. L., Hudson, B. H., Mosior, J. W., Rangwala, A. S., and Zaher, H. S. (2014). An active role for the ribosome in determining the fate of oxidized mRNA. *Cell Rep.* 9, 1256–1264. doi: 10.1016/j.celrep.2014.10.042

Simms, C. L., Yan, L. L., and Zaher, H. S. (2017). Ribosome collision is critical for quality control during No-Go Decay. *Mol. Cell* 68, 361–373.e5. doi: 10.1016/j.molcel.2017.08.019

Sorber, K., Dimon, M. T., and DeRisi, J. L. (2011). RNA-Seq analysis of splicing in *Plasmodium falciparum* uncovers new splice junctions, alternative splicing and splicing of antisense transcripts. *Nucleic Acids Res.* 39, 3820–3835. doi: 10.1093/nar/gkq1223

Stevens, A. T., Howe, D. K., and Hunt, A. G. (2018). Characterization of mRNA polyadenylation in the apicomplexa. *PLoS One* 13:e0203317. doi: 10.1371/journal.pone.0203317

Subtelny, A. O., Eichhorn, S. W., Chen, G. R., Sive, H., and Bartel, D. P. (2014). Poly(A)-tail profiling reveals an embryonic switch in translational control. *Nature* 508, 66–71. doi: 10.1038/nature13007

Sueoka, N. (1962). On the genetic basis of variation and heterogeneity of DNA base composition. *Proc. Natl. Acad. Sci. U.S.A.* 48, 582–592. doi: 10.1073/pnas.48.4.582

Sugiyama, T., Li, S., Kato, M., Ikeuchi, K., Ichimura, A., Matsuo, Y., et al. (2019). Sequential Ubiquitination of ribosomal protein uS3 triggers the degradation of non-functional 18S rRNA. *Cell Rep.* 26, 3400–3415.e7. doi: 10.1016/j.celrep.2019.02.067

Sun, M., Li, W., Blomqvist, K., Das, S., Hashem, Y., Dvorin, J. D., et al. (2015). Dynamical features of the *Plasmodium falciparum* ribosome during translation. *Nucleic Acids Res.* 43, 10515–10524. doi: 10.1093/nar/gkv991

Sundaramoorthy, E., Leonard, M., Mak, R., Liao, J., Fulzele, A., and Bennett, E. J. (2017). ZNF598 and RACK1 regulate mammalian ribosome-associated quality control function by mediating regulatory 40S ribosomal Ubiquitylation. *Mol. Cell.* 65, 751–760.e4. doi: 10.1016/j.molcel.2016.12.026

Szafranski, K., Lehmann, R., Parra, G., Guigo, R., and Glöckner, G. (2005). Gene organization features in A/T-rich organisms. *J. Mol. Evol.* 60, 90–98. doi: 10.1007/s00239-004-0201-2

Tang, T. T. L., Stowell, J. A. W., Hill, C. H., and Passmore, L. A. (2019). The intrinsic structure of poly(A) RNA determines the specificity of Pan2 and Caf1 deadenylases. *Nat. Struct. Mol. Biol.* 26, 433–442. doi: 10.1038/s41594-019-0227-9

Tesina, P., Lessen, L. N., Buschauer, R., Cheng, J., Wu, C., Berninghausen, O., et al. (2019). Molecular mechanism of translational stalling by inhibitory codon combinations and poly(A) tracts. *bioRxiv* [Preprint]. doi: 10.1101/755652

Thurmond, J., Goodman, J. L., Strelets, V. B., Attrill, H., Gramates, L. S., Marygold, S. J., et al. (2019). FlyBase 2.0: the next generation. *Nucleic Acids Res.* 47, D759–D765. doi: 10.1093/nar/gky1003

Ting, L. M., Shi, W., Lewandowicz, A., Singh, V., Mwakingwe, A., Birck, M. R., et al. (2005). Targeting a novel *Plasmodium falciparum* purine recycling pathway with specific immucillins. *J. Biol. Chem.* 280, 9547–9554. doi: 10.1074/jbc.m412693200

Tournu, H., Butts, A., and Palmer, G. E. (2019). Titrating gene function in the human fungal pathogen *Candida albicans* through Poly-adenosine tract insertion. *mSphere* 4, e192–e119. doi: 10.1128/mSphere.00192-19

Tsuboi, T., Kuroha, K., Kudo, K., Makino, S., Inoue, E., Kashima, I., et al. (2012). Dom34:hbs1 plays a general role in quality-control systems by dissociation of a stalled ribosome at the 3′ end of aberrant mRNA. *Mol. Cell.* 46, 518–529. doi: 10.1016/j.molcel.2012.03.013

van Spaendonk, R. M., Ramesar, J., van Wigcheren, A., Eling, W., Beetsma, A. L., van Gemert, J., et al. (2001). Functional equivalence of structurally distinct ribosomes in the malaria parasite, *Plasmodium berghei*. *J. Biol. Chem.* 276, 22638–22647. doi: 10.1074/jbc.m101234200

Velichutina, I. V., Rogers, M. J., McCutchan, T. F., and Liebman, S. W. (1998). Chimeric rRNAs containing the GTPase centers of the developmentally regulated ribosomal rRNAs of *Plasmodium falciparum* are functionally distinct. *RNA* 4, 594–602. doi: 10.1017/s1355838298980049

Vembar, S. S., Droll, D., and Scherf, A. (2016a). Translational regulation in blood stages of the malaria parasite *Plasmodium* spp.: systems-wide studies pave the way. *Wiley Interdiscip. Rev. RNA* 7, 772–792. doi: 10.1002/wrna.1365

Vembar, S. S., Seetin, M., Lambert, C., Nattestad, M., Schatz, M. C., Baybayan, P., et al. (2016b). Complete telomere-to-telomere de novo assembly of the *Plasmodium falciparum* genome through long-read (>11 kb), single molecule, real-time sequencing. *DNA Res.* 23, 339–351. doi: 10.1093/dnares/dsw022

Videvall, E. (2018). Plasmodium parasites of birds have the most AT-rich genes of eukaryotes. *Microb. Genom.* 4:e000150. doi: 10.1099/mgen.0.000150

Walliker, D., Quakyi, I. A., Wellems, T. E., McCutchan, T. F., Szarfman, A., London, W. T., et al. (1987). Genetic analysis of the human malaria parasite *Plasmodium falciparum*. *Science* 236, 1661–1666. doi: 10.1126/science.3299700

Warner, J. R. (1999). The economics of ribosome biosynthesis in yeast. *Trends Biochem. Sci.* 24, 437–440. doi: 10.1016/s0968-0004(99)01460-7

Waters, A. P., Syin, C., and McCutchan, T. F. (1989). Developmental regulation of stage-specific ribosome populations in *Plasmodium*. *Nature* 342, 438–440. doi: 10.1038/342438a0

Wernegreen, J. J., and Funk, D. J. (2004). Mutation exposed: a neutral explanation for extreme base composition of an endosymbiont genome. *J. Mol. Evol.* 59, 849–858. doi: 10.1007/s00239-003-0192-z

Winegard, T. C. (2019). *The Mosquito: A Human History of Our Deadliest Predator*. Melbourne: Text Publishing Company.

Wolf, A. S., and Grayhack, E. J. (2015). Asc1, homolog of human RACK1, prevents frameshifting in yeast by ribosomes stalled at CGA codon repeats. *RNA* 21, 935–945. doi: 10.1261/rna.049080.114

Wong, W., Bai, X. C., Brown, A., Fernandez, I. S., Hanssen, E., Condron, M., et al. (2014). Cryo-EM structure of the *Plasmodium falciparum* 80S ribosome bound to the anti-protozoan drug emetine. *eLife* 3:e03080. doi: 10.7554/eLife.03080

World Health Organization [WHO], (2018). *World Malaria Report 2018*. Geneva: World Health Organization.

Wu, H., Zhang, Z., Hu, S., and Yu, J. (2012). On the molecular mechanism of GC content variation among eubacterial genomes. *Biol. Direct* 7:2. doi: 10.1186/1745-6150-7-2

Xue, S., and Barna, M. (2012). Specialized ribosomes: a new frontier in gene regulation and organismal biology. *Nat. Rev. Mol. Cell Biol.* 13, 355–369. doi: 10.1038/nrm3359

Yeoh, L. M., Goodman, C. D., Mollard, V., McHugh, E., Lee, V. V., Sturm, A., et al. (2019). Alternative splicing is required for stage differentiation in malaria parasites. *Genom. Biol.* 20:151. doi: 10.1186/s13059-019-1756-6

Yonashiro, R., Tahara, E. B., Bengtson, M. H., Khokhrina, M., Lorenz, H., Chen, K. C., et al. (2016). The Rqc2/Tae2 subunit of the ribosome-associated quality control (RQC) complex marks ribosome-stalled nascent polypeptide chains for aggregation. *eLife* 5:e11794. doi: 10.7554/eLife.11794

Zanghì, G., Vembar, S. S., Baumgarten, S., Ding, S., Guizetti, J., Bryant, J. M., et al. (2018). A specific PfEMP1 is expressed in *falciparum, P.*, sporozoites and plays a role in hepatocyte infection. *Cell Rep.* 22, 2951–2963. doi: 10.1016/j.celrep.2018.02.075

Zhang, M., Wang, C., Otto, T. D., Oberstaller, J., Liao, X., Adapa, S. R., et al. (2018). Uncovering the essential genes of the human malaria parasite. *Science* 360:eaa7847. doi: 10.1126/science.aap7847

Zhu, J. D., Waters, A. P., Appiah, A., McCutchan, T. F., Lal, A. A., and Hollingdale, M. R. (1990). Stage-specific ribosomal RNA expression switches during sporozoite invasion of hepatocytes. *J. Biol. Chem.* 265, 12740–12744.

Zilversmit, M. M., Volkman, S. K., DePristo, M. A., Wirth, D. F., Awadalla, P., and Hartl, D. L. (2010). Low-complexity regions in *Plasmodium falciparum*: missing links in the evolution of an extreme genome. *Mol. Biol. Evol.* 27, 2198–2209. doi: 10.1093/molbev/msq108

Conflict of Interest: The authors declare that the research was conducted in the absence of any commercial or financial relationships that could be construed as a potential conflict of interest.

frontiers in Microbiology

ORIGINAL RESEARCH
published: 17 January 2020
doi: 10.3389/fmicb.2019.03024

Comprehensive and Durable Modulation of Growth, Development, Lifespan and Fecundity in *Anopheles stephensi* Following Larval Treatment With the Stress Signaling Molecule and Novel Antimalarial Abscisic Acid

*Dean M. Taylor[1], Cassandra L. Olds[1], Reagan S. Haney[1], Brandi K. Torrevillas[1] and Shirley Luckhart[1,2]**

[1] Department of Entomology, Plant Pathology and Nematology, University of Idaho, Moscow, ID, United States, [2] Department of Biological Sciences, University of Idaho, Moscow, ID, United States

OPEN ACCESS

Edited by:
Rhoel Dinglasan, University of Florida, United States

Reviewed by:
Guido Favia, University of Camerino, Italy
Mark R. Brown, University of Georgia, United States

***Correspondence:**
Shirley Luckhart
sluckhart@uidaho.edu

Specialty section:
This article was submitted to Infectious Diseases, a section of the journal Frontiers in Microbiology

Received: *03 October 2019*
Accepted: *17 December 2019*
Published: *17 January 2020*

Citation:
Taylor DM, Olds CL, Haney RS, Torrevillas BK and Luckhart S (2020) Comprehensive and Durable Modulation of Growth, Development, Lifespan and Fecundity in Anopheles stephensi Following Larval Treatment With the Stress Signaling Molecule and Novel Antimalarial Abscisic Acid. Front. Microbiol. 10:3024. doi: 10.3389/fmicb.2019.03024

The larval environment of holometabolous insects determines many adult life history traits including, but not limited to, rate and success of development and adult lifespan and fecundity. The ancient stress signaling hormone abscisic acid (ABA), released by plants inundated with water and by leaf and root fragments in water, is likely ubiquitous in the mosquito larval environment and is well known for its wide ranging effects on invertebrate biology. Accordingly, ABA is a relevant stimulus and signal for mosquito development. In our studies, the addition of ABA at biologically relevant levels to larval rearing containers accelerated the time to pupation and increased death of *A. stephensi* pupae. We could not attribute these effects, however, to ABA-dependent changes in JH biosynthesis-associated gene expression, 20E titers or transcript patterns of *insulin-like peptide* genes. Adult females derived from ABA-treated larvae had reduced total protein content and significantly reduced post blood meal transcript expression of *vitellogenin*, effects that were consistent with variably reduced egg clutch sizes and oviposition success from the first through the third gonotrophic cycles. Adult female *A. stephensi* derived from ABA-treated larvae also exhibited reduced lifespans relative to controls. Collectively, these effects of ABA on *A. stephensi* life history traits are robust, durable and predictive of multiple impacts of an important malaria vector spreading to new malaria endemic regions.

Keywords: *Anopheles*, malaria, abscisic acid, ABA, lifespan, fecundity, development

INTRODUCTION

In 2017, mosquito transmission resulted in 219 million new cases of malaria, 435,000 of which were fatal (World Health Organization [WHO], 2019). A large effort has been made to estimate the burden of malaria in endemic areas using defined parameters including abiotic factors, human clearance of malaria parasites, and mosquito life history traits, such as survival, population density, reproductive output, biting rate, and parasite development (Smith et al., 2018). Many important

mosquito species contribute to parasite transmission, increasing the complexity of both surveillance and control efforts. Our focus is *Anopheles stephensi*, the Indian malaria mosquito, an aggressive malaria vector mosquito that has invaded and become established in Sri Lanka, Djibouti, and Ethiopia, with significant risk for range expansion into Somalia, Eritrea and Sudan (Faulde et al., 2014; Surendran et al., 2018; Seyfarth et al., 2019; Takken and Lindsay, 2019). In Djibouti, *A. stephensi* has been linked to a resurgence of severe infection with the human malaria parasite *Plasmodium falciparum* (Seyfarth et al., 2019), so increased focus on this species is relevant and timely for control.

Larval development in *A. stephensi* is rapid and, under favorable conditions, may be completed within a week from egg hatching. On the other hand, less than ideal larval environments, including for example over-crowding, have been shown to alter life history traits, significantly reducing parasite transmission (Moller-Jacobs et al., 2014; Murdock et al., 2017). Insect development is largely controlled by the regulatory effects of juvenile hormone (JH) and 20-hydroxyecdysone (20E) and our understanding of these details is derived primarily from studies in *Manduca sexta*, *Drosophila melanogaster* and *Aedes aegypti* (Jindra et al., 2013). In particular, JH acts to suppress differentiation of imaginal disk into adult structures when levels of 20E rise, instead maintaining larval structures and inducing larval-larval molts (Riddiford, 2012). In *M. sexta* and *D. melanogaster*, titers of JH decline to undetectable levels in the final larval instar due to reduced JH biosynthesis, elevated JH esterase activity and 20E-dependent transcription that induces metamorphosis (Vince and Gilbert, 1977; Brutis et al., 1990; Riddiford et al., 2000, 2010; Yin and Thummel, 2005; Liu et al., 2009). To date there has been no comprehensive analysis of JH titers over the course mosquito larval development. However, a significant body of work has been published on JH biosynthesis rates and transcriptional regulation of enzymes in adult *A. aegypti* (Noriega, 2014; Van Ekert et al., 2014). In this species, JH acid methyl transferase (JHAMT) is the ultimate enzyme in the principal JH biosynthesis pathway, converting inactive JH acid to active JH (Van Ekert et al., 2014).

Proteins and lipids stored from the larval diet contribute to proper ovarian development in female *A. aegypti*, with approximately half of the lipid stores carried forward to the adult stage (Zhou et al., 2004), such that females with lower larval protein reserves develop smaller follicles (Caroci et al., 2004). In addition to the direct effects of diet, nutrient status of newly emerged adults modulates the effects of insulin/insulin-like growth factor signaling (IIS) on JH synthesis, which remodels the fat body in preparation for a bloodmeal (Raikhel and Lea, 1983; Perez-Hedo et al., 2014). During the first gonotrophic cycle in *A. aegypti*, 80% of the lipids within the ovaries are derived solely from sugar meals acquired as adults (Ziegler and Ibrahim, 2001). Following the blood meal, amino acids derived from blood proteins activate the target of rapamycin (TOR) signaling pathway and ovary ecdysteroidogenic hormone is released from the brain, triggering 20E synthesis and release in the ovaries (Dhara et al., 2013). Following release from the ovaries, 20E signaling is initiated by 20E binding to the heterodimeric receptor comprised of the ecdysone receptor (EcR) and ultraspiracle (USP) to upregulate fat body synthesis of vitellogenin (Vg) that is transported to the developing eggs (Martìn et al., 2001). In the context of these changes, 20E delivered from the male during mating in *Anopheles gambiae* can also interact with the EcR, together with a novel protein Mating-Dependent Regulator of Oogenesis or MISO, to regulate oogenesis and the post-mating switch to monandry and oviposition (Baldini et al., 2013; Gabrieli et al., 2014). While this physiology is presumably conserved in *A. stephensi* based on the presence of an orthologous *miso* gene, both post-feeding and post-mating physiology likely also modulate the switch to physiological sensitivity to oviposition site attractants (Davis and Takahashi, 1980).

Anopheles stephensi females show a breeding habitat preference for natural bodies of water, ranging in size from small puddles to larger calm riverbeds (Manouchehri et al., 1976). Flood and ditch irrigation can impact the ecology of mosquitoes by creating new breeding sites and larval habitats, which are more attractive to gravid female mosquitoes than natural habitats (Mwangangi et al., 2010; Wondwosen et al., 2016). Initial flooding and fast water currents are destructive to larval survival, causing physical harm and reducing critical oxygen tension (Soleimani-Ahmadi et al., 2014). However, following flooding there is an increase in mosquito density and diversity, due to increased temporary breeding habitats (Rodrigures et al., 2017). During flooding, inundated plants can experience high levels of stress, which can result in the release of plant stress hormones into aquatic environments. For example, research has shown flooding of tomato plants increases the concentration of the stress hormone abscisic acid (ABA) in soil water by approximately 2.5-fold over control levels to ∼1.7 μM (Else et al., 1995).

Abscisic acid was first identified in plants, however, it is now recognized as a universal signaling molecule which acts as an effective regulator of stress responses and pathogen biology in plants, parasitic protozoa, sponges, hydroids, insects, and mammals (reviewed in Olds et al., 2018). The interaction of ABA and insects has been studied in several contexts. In the big-headed grasshopper, *Aulocara elliotti,* ingested ABA increased the number of eggs per female, however, eggs derived from ABA-treated females exhibited decreased viability (Visscher, 1980). Injection of ABA reduced protein uptake and Vg concentrations following consumption of a liver meal in the flesh fly *Sarcophaga bullata* (De Man et al., 1981). In addition, ABA injection appeared to act negatively on 20E signaling by delaying the peak of 20E by 16 h (De Man et al., 1981). ABA from nectar and pollen ingested by honeybees (*Apis mellifera*) can be detected in honey (Lipp, 1990) and ingestion of ABA by honeybee larvae can increase cold tolerance and cellular immunity (Negri et al., 2017; Ramirez et al., 2017).

In our previous studies, we observed that ingestion of an ABA-supplemented blood meal by female *A. stephensi* induced signaling kinases associated with a transient metabolic shift in the midgut, fueling immune-mediated killing of *P. falciparum* prior to completion of oocyst development (Glennon et al., 2016, 2017). Interestingly, ingested ABA did not decrease *A. stephensi*

fecundity in the first gonotrophic cycle in contrast to our predictions based on the effects of ABA in *A. elliotti* and in *S. bullata* (Glennon et al., 2017). However, given the effects of ABA on metabolism and homeostasis of the *A. stephensi* midgut, on nutrient stores and 20E levels in other insects, and the potential that ABA in water used for oviposition could impact larval growth, we sought to understand whether ABA, at levels consistent with those released by inundated plants, could affect *A. stephensi* larval development, pupation and fitness of adult females emerging from treated larvae.

Our data show that, at concentrations in water as low as 1 μM, ABA accelerated *A. stephensi* larval development with varying effects on larval 20E levels and increased mosquito death at the time of pupation. Adult females derived from ABA-treated larvae exhibited significantly reduced fecundity over multiple gonotrophic cycles and significantly reduced lifespan, which was not altered by additional treatment of adult females with ABA. Accordingly, the effects of exposure of larval *A. stephensi* to ABA were both striking and durable, suggesting that manipulation of ABA levels in breeding sites, perhaps through nanoparticle release of this natural compound, could be used to reduce mosquito development and reproduction as well as adult survival that is required for completion of the extrinsic incubation period of malaria parasite development.

MATERIALS AND METHODS

Mosquito Rearing

Anopheles stephensi Liston (Indian wild-type strain) were reared and maintained 27°C and 80% humidity with a 16/8-hour light/dark cycle. Adult mosquitoes were housed in 1 ft^3 wire mesh cages and provided continuous access to 10% sucrose-soaked cotton pads. Three days after eclosion, adult female mosquitoes were allowed to feed on live mice sedated with ketamine (50 mg/kg) and xylazine (5 mg/kg) in sterile saline. All animal procedures were approved by the University of Idaho Animal Care and Use Committee. Mosquitoes were provided shallow cups of water to oviposit at 48 h after blood feeding. Eggs were gently washed into 5 L Nalgene pans with shallow water. Larvae were maintained in 5 L Nalgene pans on a solution of 2% powdered fish food (Sera Micron) and baker's yeast in a 2:1 ratio for the first 3 days followed by Game Fish Chow pellet food (Purina) until pupation. Adult mosquitoes were collected for experiments within 12 h post-eclosion and housed in screened, 500 mL polypropylene Nalgene containers.

Effects of ABA on *A. stephensi* Larval Development and Pupation

Larvae were collected at 36 h following transfer of eggs into Nalgene pans to reduce variability in the starting age among larvae used for these studies. For each treatment group, 100 larvae were placed in 500 mL polypropylene Nalgene containers with 200 mL water with or without 1, 10 or 100 μM ABA (Caisson Labs). Due to the light sensitivity of ABA, 50 mL of water from each container was removed daily and replaced with freshly made ABA-supplemented water to yield a final concentration of 1, 10 or 100 μM ABA. Low concentrations of ABA (1 and 10 μM) were based on published soil water concentrations of flooded tomatoes (Else et al., 1995) and on our data from submerged tomato leaves and roots in water (**Supplementary Table S1**); the highest concentration (100 μM) was based on ABA treatment of *A. elliotti* from previous studies (Visscher, 1980). Larvae were fed as above and maintained through pupation and eclosion to adults. After the first pupae were observed, pupae were collected every 12 h until no larvae remained. The numbers of pupae collected each day were recorded as "time to pupation" in days. Collected pupae were placed into cups with untreated water within cartons for adult eclosion; pupal survival was monitored until all adults had emerged and these data were recorded as the proportion of total pupae surviving through to adult eclosion. Based on this design, *A. stephensi* were exposed to ABA during the larval stage only. Five separate cohorts were used to complete biological replicates of this study.

Effects of ABA on Adult *A. stephensi* Lifespan

Female mosquitoes derived from untreated, control larvae or from larvae treated with 1, 10 or 100 μM ABA were maintained in separate cartons with 10% sucrose-soaked cotton pads. At 3–5 days following eclosion, each group of mosquitoes was offered a "human blood meal" of washed human type O + erythrocytes (Interstate Blood Bank) suspended 1:1 (vol:vol) in heat-inactivated human type A + serum (Interstate Blood Bank). A similarly prepared blood meal was offered once weekly via a Hemotek feeder (Hemotek Ltd) until no mosquitoes remained alive. For one lifespan study, emerged adult female *A. stephensi* from each larval control and treatment group were split into two groups and treated as follows. One group of adults received an unsupplemented human blood meal each week whereas the other group was provided a weekly human blood meal supplemented with 100 nM ABA, which approximates the concentration of ABA present in blood in mice and humans with malaria (Glennon et al., 2016, 2018). Two days following blood feeding, females were given the opportunity to oviposit in a shallow water dish. Dead females were counted and removed from each group every 48 h. Two separate cohorts were used to complete biological replicates of the lifespan studies.

Effects of ABA on *A. stephensi* Fecundity

At 3–5 days after adult eclosion from groups prepared as in section "Effects of ABA on Adult *A. stephensi* Lifespan," female *A. stephensi* were allowed to feed on a human blood meal. Following feeding, engorged females were carefully removed and placed into individual 50 mL conical tubes with moist filter paper and allowed to oviposit. Following oviposition, the number of eggs were counted and the females were returned to their respective control or treatment cartons. All females were held until they were fed again the following week. This process of feeding followed by separation and oviposition was repeated until females were no longer receptive to blood feeding. Four separate

cohorts of mosquitoes were used to complete biological replicates of these studies.

qRT-PCR Assays for Relative Gene Expression

Relative transcript levels of *A. stephensi 3-hydroxy-3-methylglutaryl-coa reductase* (*hmg-r*), *juvenile hormone acid methyltransferase* (*jhamt*), *insulin-like peptides 1-5* (*ilp1-5*; Marquez et al., 2011), and *Vg* were determined by qRT-PCR (**Supplementary Table S2**). All data were normalized to transcript levels of *A. stephensi* housekeeping genes *ribosomal protein s7* (*rps7*) and *rps17*. For larval gene expression analyses, five larvae from control and ABA-treated water were collected and pooled for RNA isolation at 1, 2, 4 and 6 h following daily replacement of rearing water as described in section "Effects of ABA on *A. stephensi* Larval Development and Pupation." For *Vg* expression analyses, five adult female *A. stephensi* were collected from control and ABA-treated larvae and pooled at 6, 12, 24, and 48 h post-blood feeding for RNA isolation. Adults were killed by briefly freezing at −20°C and pools of larvae or adults were placed in 500 μL Trizol (Invitrogen). RNA was extracted using the phenol-chloroform method according to manufacturer's instructions. cDNA was synthesized using the QuantiTect reverse transcriptase kit (Qiagen) according to manufacturer's instructions. cDNA concentrations were adjusted to 500 ng/μL with molecular grade water. Data were normalized to housekeeping genes and reported as $\mathrm{Log}_2(2^{-\Delta\ \Delta\ Ct})$. For each treatment group 4-5 replicates were completed, each with three technical replicates.

Effects of ABA on 20-Hydroxyecdysone (20E) Titer

20E titers were measured during larval and pupal development and in adult female *A. stephensi* derived from control and ABA-treated larvae. For these analyses, 40 larvae, 20 pupae or 20 adult female mosquitoes were collected and pooled for each time point from each group. Larval collections started at 3 days post-hatching and continued until pupae were detected at ∼7 days post-hatching. Larvae were collected once a day at 8 h following daily replacement of rearing water as described in section "Effects of ABA on *A. stephensi* Larval Development and Pupation." The pupal stage of *A. stephensi* lasts ∼36 h; pupae were collected every 8 h for the duration of this stage. Adult female mosquitoes were collected within the first 8 h following eclosion. Samples were prepared for analysis by adding 500 μL of 100% chilled methanol to pooled insects, then sonicating on ice (Fisher Scientific Model 100) at level 4 for 5 s intervals. Samples were centrifuged at 5000 × *g* for 5 min and the resulting supernatant transferred to a new tube. Methanol extraction was performed a second time and supernatants were pooled. Pooled supernatants were dried under N_2 stream and stored at −30°C until the 20E titers were measured using 20-hydroxyecdysone EIA kit (Arbor Assays), following manufacturer's instructions. Three separate cohorts of mosquitoes were used to complete biological replicates of these studies.

Effects of ABA on Adult Female *A. stephensi* Protein Content

To measure total protein content of adult female *A. stephensi* derived from control or ABA-treated larvae, 2 mosquitoes within 8 h of eclosion were homogenized in 10 mM dithiothreitol with 1 mM protease inhibitor cocktail (Sigma) in 100 μL loading buffer (Bio-Rad). Samples were boiled for 5 min and then centrifuged at 10,000 × *g* for 10 min at 4°C. Supernatants were transferred to new tubes and stored at −80°C. Total protein content was determined using Bradford reagent (Alfa Aesar) using bovine albumin serum (BSA) as a standard. Three separate cohorts of mosquitoes were used to complete biological replicates of these studies, each with three technical replicates.

Statistical Analyses

All statistical analyses were performed using R statistical software version 3.5.3. Time to pupation and clutch sizes were analyzed by ANOVA and *post hoc* Tukey's test. Proportions of *A. stephensi* laying eggs and dying as pupae were analyzed using likelihood ratio test of independence (GTest). 20E titers by day were analyzed by Student's *t*-test. Data from qRT-PCR assays were normalized by $2^{-\Delta\Delta CT}$, $\log_2$ transformed and analyzed by ANOVA. Lifespan data were analyzed by two stage hazard rate analysis, in which the first stage is a log-rank test, and the second stage is used in cases where the hazard rates are not proportional and cross each other (Qiu and Sheng, 2008). Data across biological replicates within treatments were analyzed by ANOVA; if differences across replicates were not significant, replicate data were combined for analysis. Differences were considered significant at $\alpha \leq 0.05$. All figures were created using the ggplot2 package within R.

RESULTS

ABA Treatment of *A. stephensi* Larvae Reduced Time to Pupation, but Not in Association With Rising 20E Titers

Abscisic acid treatment of larval *A. stephensi* reduced mean time to pupation from 7.22 ± 0.77 days in untreated controls to 7.03 ± 0.67 days (1 μM ABA), 7.01 ± 0.76 days (10 μM ABA) and 7.11 ± 0.68 days (100 μM ABA) in treated larvae (**Figure 1**; ANOVA $p < 0.001$). Times to pupation in larvae treated with 1 and 10 μM ABA were not different (Tukey $p = 0.877$), but exhibited the shortest mean time to pupation relative to control. Larvae treated with 100 μM ABA had higher mean time to pupation relative to larvae treated with 1 μM ABA (Tukey $p < 0.001$) and 10 μM ABA (Tukey $p < 0.001$), but still pupated faster than untreated control larvae (Tukey $p < 0.001$). Although accelerated larval development would be expected to produce smaller adults (Lyimo et al., 1992), larval treatment with 1, 10, and 100 μM ABA was associated with increased size of emerged adult female *A. stephensi* relative to females derived from control untreated larvae (**Supplementary Table S3**).

In *D. melanogaster*, 20E regulates the timing of larval molts and, during the fourth and final instar, 20E titers rise to induce a

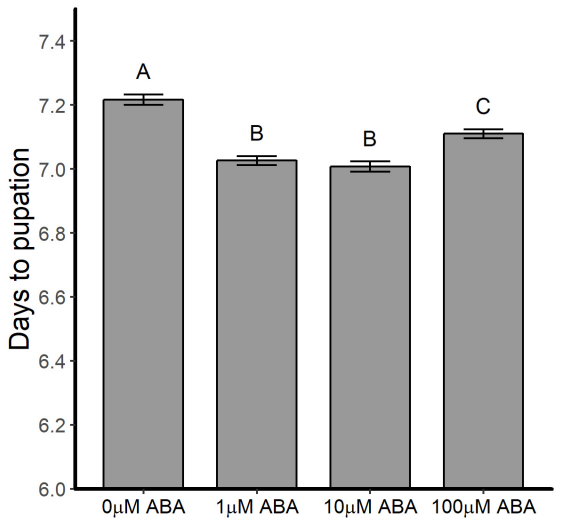

FIGURE 1 | ABA treatment of larval *A. stephensi* reduced time to pupation. Larvae were exposed to 1, 10 or 100 μM ABA in rearing water as described in section "Effects of ABA on *A. stephensi* Larval Development and Pupation." Time to pupation was reduced at all concentrations of ABA compared to control larvae (ANOVA $p < 0.001$). Data from five biological replicates were combined for analysis and are shown as mean ± SEM. Different capitalized letters indicate significant differences among controls and treatments. Control = 1456 larvae, 1 μM ABA = 1403 larvae, 10 μM ABA = 1382 larvae and 100 μM ABA = 1287 larvae.

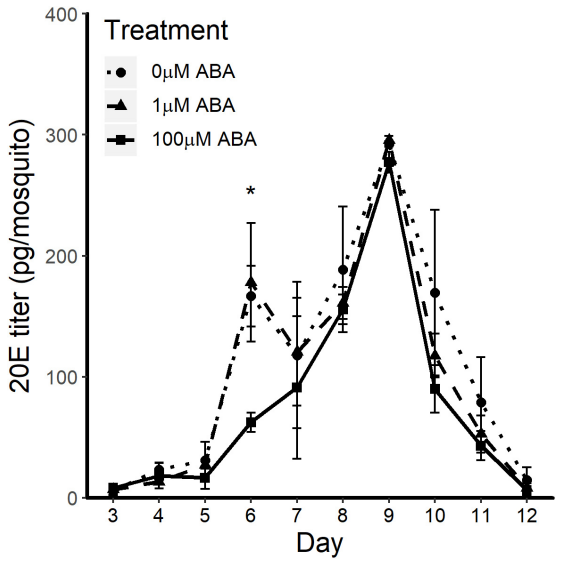

FIGURE 2 | ABA treatment effects on 20E titers through larval development (days 1–7), during the pupal stage (days 8–9) and in newly emerged adult female *A. stephensi* (day 10) were minimal to undetectable. 20-hydroxyecdysone (20E) titers were measured from 20 to 40 individuals each day starting with second instar larvae from 3 days post-egg hatch through to 8 h post-eclosion of adult female mosquitoes. Larval exposure to 100 μM ABA reduced 20E titers on day 6 of larval development relative to controls (*t*-test $p = 0.017$), but no other differences were observed. Each biological sample was analyzed in triplicate to confirm assay reproducibility. Data from three biological replicates were combined for analysis and are shown as mean ± SEM.

cascade of transcriptional responses resulting in the physiological changes during the larval-pupal molt; studies in *A. aegypti* have shown similar 20E titers and expression of 20E-regulated genes (Margam et al., 2006; White and Ewer, 2014). Accordingly, we hypothesized that treatment of larvae with ABA might increase 20E titers earlier than in control larvae, resulting in reduced time to pupation in ABA-treated larvae. Based on the patterns observed in **Figure 1**, we analyzed 20E titers in larvae treated with the lowest (1 μM) and highest concentrations of ABA (100 μM) with untreated controls (**Figure 2**). Larvae exposed to 1 μM ABA showed no differences relative to controls in 20E titers over the course of larval development (days 1–7), during the pupal stage (days 8–9) or in newly emerged adult females (day 10). Larvae exposed to 100 μM ABA, however, had significantly reduced 20E titers on day 6 of larval development relative to controls (*t*-test $p = 0.017$), but no differences at any other timepoints. While there are no reports of 20E titers in *A. stephensi* larvae, our results are within the reported ranges for *A. aegypti* (Margam et al., 2006). These results suggested that the observed reduction in time to pupation in larvae exposed to ABA did not result from significantly elevated 20E titers in the final days of larval development.

ABA Did Not Alter Transcript Expression of JH-Associated Genes in Larval *A. stephensi*

Since ABA treatment was not associated with increased 20E titers, we examined the expression of key genes in the mevalonate pathway and the branch pathway that synthesizes juvenile hormone (JH). Studies in *M. sexta* during larval-larval molts have demonstrated that JH titers remain elevated to suppress expression of 20E target genes and, in the final instar, JH titers decrease to undetectable levels, at which point 20E gene targets are upregulated and the pupal molt is initiated (Boulan et al., 2015). In the insect mevalonate pathway, 3-Hydroxy-3-Methylglutaryl-CoA Reductase (HMGCR) converts HMG-CoA to mevalonate, the precursor of farnesyl-pyrophosphate of the JH pathway. In the latter pathway, JH acid methyl transferase (JHAMT) methylates farnesoic acid to methylfarnesoate and is the terminal enzyme in JH biosynthesis in *A. aegypti* (Shinoda and Itoyama, 2003; Van Ekert et al., 2014). The gene expression profiles of *hmgcr* and *jhamt* were measured hourly for 6 h after daily replacement of rearing water as described in section "Effects of ABA on *A. stephensi* Larval Development and Pupation." If expression levels of *hmgcr* and *jhamt* were down regulated in fourth instar larvae following exposure to ABA this could translate to reduced JH titers and earlier expression of 20E gene targets. However, we did not observe any significant changes in *hmgcr* expression relative to control in fourth instar larvae exposed to 1, 10 or with 100 μM ABA at 1 h (ANOVA $p = 0.070$), 2 h (ANOVA $p = 0.275$), 4 h (ANOVA $p = 0.683$) or 6 h post ABA treatment (ANOVA $p = 0.239$) relative to control (**Supplementary Figure S1**). There were also no significant changes in expression of *jhamt* in fourth instar larvae through

the same 6 h period (ANOVA $p = 0.144$ for 1 h, $p = 0.462$ for 2 h, $p = 0.054$ for 4 h, $p = 0.690$ for 6 h post ABA treatment relative to control) (**Supplementary Figure S1**). Based on these data, it is unlikely that ABA treatment of *A. stephensi* fourth instar larvae alters JH titers in a pattern consistent with the effects of ABA on larval development.

ABA Did Not Alter Expression of *ilp* Genes in *A. stephensi* Larvae

We previously demonstrated that ABA supplementation in a blood meal reduced the expression of *ilp3* and *ilp4* in adult female *A. stephensi* (Glennon et al., 2017), suggesting that ABA might also alter *ilp* expression in the larval stage. In *D. melanogaster* larvae, decreased drosulfakinin (DSK) has been associated with increased feeding and reduced food selectivity, with decreased *dsk* mRNA levels detected in *Dilp2,3,5* triple mutants but not *Dilp5* mutants (Söderberg et al., 2012). Based on these observations and because we saw no increase in 20E titers or changes in transcript expression of *hmgcr* or *jhamt*, we reasoned that ABA might decrease *ilp* expression in *A. stephensi* larvae in the fourth instar, which could increase food intake and trigger earlier pupation. Exposure of *A. stephensi* fourth instar larvae to ABA, however, through 6 h after daily replacement of rearing water as described in section "Effects of ABA on *A. stephensi* Larval Development and Pupation" had no effect on transcript expression of *ilp4* (ANOVA $p = 0.362$ for 1 h, $p = 0.088$ for 2 h, $p = 0.276$ for 4 h, $p = 0.199$ for 6 h post ABA treatment relative to control) or *ilp5* (ANOVA $p = 0.733$ for 1 h, $p = 0.876$ for 2 h, $p = 0.692$ for 4 h, $p = 0.397$ for 6 h post ABA treatment relative to control) (**Supplementary Figure S2**). We also examined expression of *ilp1-3* through the same 6 h period, but no significant differences relative to control were observed (not shown).

ABA Increased the Percentage of *A. stephensi* Pupae Dying Prior to Adult Eclosion

In addition to reducing the time to pupation, treatment of *A. stephensi* larvae with ABA resulted in a higher percentage of dead pupae (out of the total for each treatment group) relative to control. In the absence of ABA treatment, 3.4% of pupae died prior to adult eclosion (**Figure 3**). However, treatment with 10 and 100 μM ABA increased the percentage of dead pupae out of the total for each treatment group to 8.2 and 10.6% relative to control (**Figure 3**) (GTest $p < 0.001$ and $p < 0.001$, respectively). Accordingly, decreased time to pupation in ABA-treated larvae (**Figure 1**) was associated with increased pupal death prior to adult *A. stephensi* eclosion.

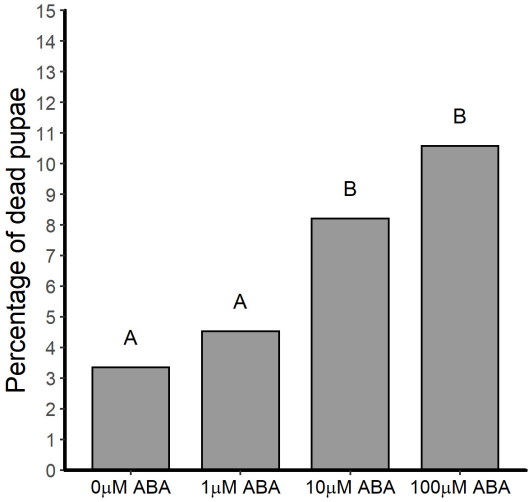

FIGURE 3 | ABA treatment of larval *A. stephensi* increased the percentage of pupae dying prior to adult eclosion. While treatment of *A. stephensi* larvae with 1 μM ABA had no effect on pupae death relative to control (Gtest $p = 0.249$), larvae that were exposed to 10 and 100 μM ABA exhibited increased percentages of pupae death compared to control larvae (Gtest $p < 0.001$ and $p < 0.001$, respectively). Data are represented as percentages of pupae out of the total collected that died prior to adult eclosion. Data from three biological replicates were combined for analysis. Different capitalized letters indicate significant differences among controls and treatments. Control = 776 larvae, 1 μM ABA = 772 larvae, 10 μM ABA = 767 larvae and 100 μM = 700 larvae.

ABA Reduced the Protein Content in Newly Eclosed Female *A. stephensi*

Female mosquitoes break down proteins derived from blood meals to amino acids, activating the TOR pathway, which signals fat body 20E synthesis and the upregulation of yolk protein precursor (YPP) genes in this tissue (Hansen et al., 2005). The nutrients stored during the larval stage are essential for JH-regulated fat body competency to respond to TOR activation such that malnourished mosquitoes exhibit reduced and delayed *Vg* transcript expression (Shiao et al., 2008). Based on these observations, we sought to examine the protein content of newly eclosed female *A. stephensi* to better understand the potential effects of ABA larval treatment on adult life history traits. Protein content of adult female *A. stephensi* derived from untreated control larvae was 9.5 ± 0.92 μg/mosquito (**Figure 4**). In comparison, protein content of adult females derived from larvae treated with 1 μM ABA was 7.7 ± 0.54 μg/mosquito trended downward relative to control but was not significantly different (**Figure 4**). However, protein content of females derived from larvae treated with 100 μM ABA, 6.6 ± 0.38 μg/mosquito, was significantly lower than that in controls, but not significantly different from that of females derived from larvae treated with 1 μM ABA (**Figure 4**). Accordingly, increased body size in adult females derived from larvae treated with 10 and 100 μM ABA (**Supplementary Table S3**) was associated with a trend toward decreased protein content (10 μM ABA) and significantly reduced protein content (100 μM ABA) relative to controls.

Adult Female *A. stephensi* Derived From ABA-Treated Larvae Exhibited Reduced Fecundity

Given the reduction in protein content of newly eclosed female *A. stephensi* derived from ABA-treated larvae and the impact of nutritional status on JH-regulated fat body competency, we

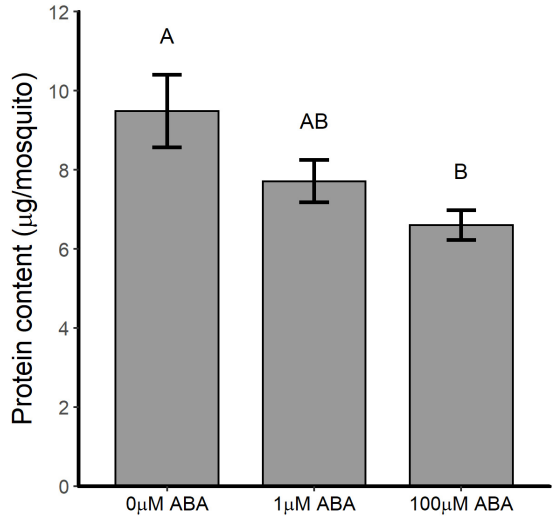

FIGURE 4 | ABA treatment of larval *A. stephensi* reduced the protein content of newly eclosed adult females. Females emerged from larvae treated with 1 μM ABA exhibited a trend toward reduced protein content relative to controls (Tukey $p = 0.214$). Females emerged from larvae treated with 100 μM ABA exhibited reduced protein content relative to controls (Tukey $p = 0.047$), but were not significantly different from females emerged from larvae treated with 1 μM ABA (Tukey $p = 0.493$). Each biological sample was analyzed in triplicate to confirm assay reproducibility. Data from three biological replicates were combined for analysis and are shown as mean ± SEM. Different capitalized letters indicate significant differences among controls and treatments.

examined the fecundity of female *A. stephensi* derived from ABA-treated control larvae. In replicated assays, the percentages of females ovipositing and clutch sizes of female *A. stephensi* derived from ABA-treated larvae compared to females derived from untreated control larvae were variably reduced across three gonotrophic cycles.

For the first gonotrophic cycle adult females derived from larvae treated with 1 and 100 μM ABA had reduced clutch sizes (ANOVA $F = 15.195$, $p < 0.001$; Tukey $p < 0.001$) relative to controls (**Figure 5A**). In addition to smaller clutch sizes in the first gonotrophic cycle, females derived from larvae treated with 100 μM ABA treatment were less likely to oviposit compared to controls (GTest $p = 0.013$) (**Figure 5B**). There was no effect of larval ABA treatment on clutch sizes in the second gonotrophic cycle (ANOVA $F = 0.009$, $p = 0.99$; **Figure 5C**) and an increase in the percentage of ovipositing females derived from larvae treated with 1 μM ABA mosquitoes compared to controls (GTest $p = 0.038$). As in the first gonotrophic cycle, however, there was a decrease in the percentage of ovipositing females derived from larvae treated with 100 μM ABA compared to controls (GTest $p < 0.001$; **Figure 5D**). By the third gonotrophic cycle, clutch sizes from females derived from larvae treated with ABA were again reduced relative to controls (ANOVA $F = 4.49$, $p = 0.012$; Tukey $p = 0.017$ for 1 μM ABA, Tukey $p = 0.034$ for 100 μM ABA; **Figure 5E**). However, in contrast to both prior gonotrophic cycles, there were no differences in the percentages of ovipositing females among the groups (GTest $p = 0.62$; **Figure 5F**).

Post-blood Meal *Vg* Transcript Expression in Adult Female *A. stephensi* Derived From ABA-Treated Larvae Was Delayed Relative to Controls

Based on the effects of ABA larval treatment on adult fecundity, we sought to quantify the expression of *Vg*, the major YPP gene, in adult female *A. stephensi* within the first 48 h following a bloodmeal. The pattern of *Vg* expression in control females derived from untreated larvae followed the expected pattern of expression rising to a peak at 24 h, then declining (**Figure 6**). Adult females derived from larvae treated with 1 and 100 μM ABA showed significantly reduced *Vg* expression at 24 h post-blood meal (ANOVA $p < 0.001$, Tukey $p < 0.001$ for 1 μM ABA; Tukey $p < 0.001$ for 100 μM ABA) (**Figure 6**), suggesting that the effects of ABA larval treatment on adult female fecundity are at least partially explained by a significant reduction in *Vg* expression post-blood meal.

Adult Female *A. stephensi* Derived From ABA-Treated Larvae Exhibited Reduced Lifespan

Based on our observations of reduced protein content (**Figure 4**) and reduced fecundity (**Figure 5**) in adult female *A. stephensi* derived from ABA-treated larvae and evidence for tradeoffs between mosquito lifespan and reproduction (Harshman and Zera, 2007; Faiman et al., 2017), we predicted that ABA treatment of larvae might extend the lifespan of adult female *A. stephensi*. For this study, females derived from untreated control larvae and from larvae treated with 1 and 100 μM ABA received a blood meal once a week with maintenance on 10% sucrose between blood meals. For an additional study, adult females derived from control and treated larvae were each split into two groups, with one group receiving no ABA in the weekly blood meals and the other group receiving 100 nM ABA in the weekly blood meals. In contrast to our prediction, median survival in adult females derived from larvae treated with ABA was reduced to 28 ± 10.78 days (1 μM ABA; log rank $p = 0.028$) and to 30 ± 14.22 days (100 μM ABA; two-stage $p = 0.025$) relative to the untreated control median lifespan of 34 ± 14.2 days (**Figure 7**). Consistent with previous observations of no effect of ABA in blood on adult female lifespan (Glennon et al., 2017), the addition of 100 nM ABA in the blood meal had no effect on adult lifespan nor did it alter the effects of larval treatment with ABA on adult lifespan (**Supplementary Table S4**).

DISCUSSION

Taken together, our data demonstrate that the effects of treating *A. stephensi* larvae with ABA are durable, starting with accelerated pupation and increased pupal death and lasting through multiple gonotrophic cycles to reduce fecundity and adult female survivorship. These effects indicate the potential for multiple population level impacts on mosquito density, biting and pathogen transmission through combined reductions in immature stages, fecundity and lifespan at ABA concentrations

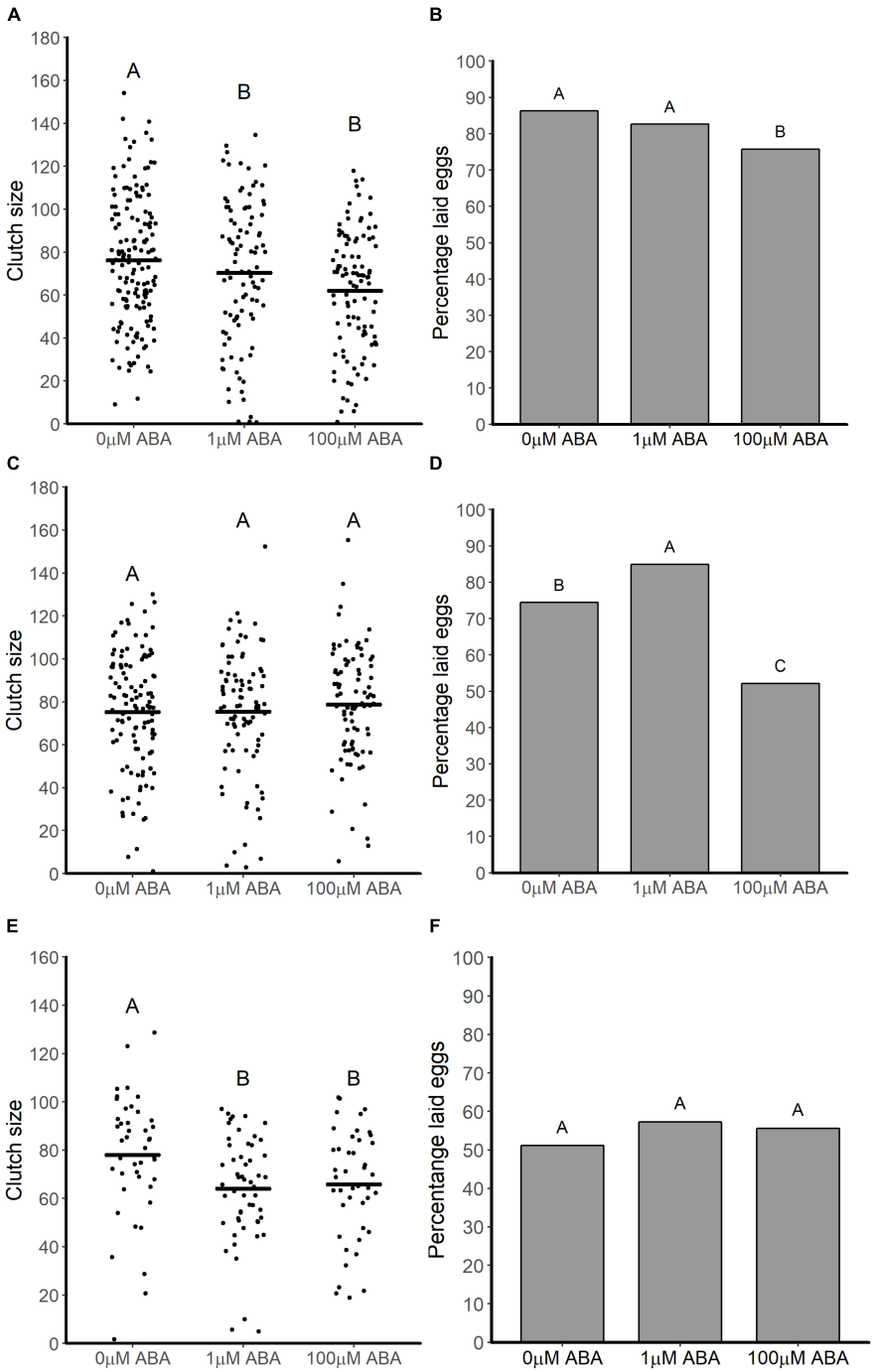

FIGURE 5 | ABA treatment of larval *A. stephensi* variably reduced clutch sizes and percentages of ovipositing adult females across the first **(A,B)**, second **(C,D)** and third **(E,F)** gonotrophic cycles. **(A)** Female mosquitoes derived from larvae treated with 1 and 100 μM ABA had reduced clutch sizes in the first gonotrophic cycle compared to controls (Tukey $p < 0.001$ and $p < 0.001$, respectively). Each dot represents the clutch size of a single female mosquito from four biological replicates; black bars represent means. **(B)** Treatment of larvae with 100 μM ABA reduced the percentage of ovipositing females relative to controls in the first gonotrophic cycle (Gtest $p = 0.013$). Data are shown as the means from three biological replicates, $n = 389$. **(C)** Larval treatment with ABA had no effect on clutch sizes of adult female *A. stephensi* (ANOVA $F = 0.009$, $p = 0.99$) in the second gonotrophic cycle. Each data point represents the clutch size of a single female mosquito from four biological replicates; black bars represents means. **(D)** Treatment of larvae with 1 μM ABA increased the percentage of ovipositing females mosquitoes compared to controls in the (GTest $p = 0.038$), while treatment of larvae with 100 μM ABA reduced the percentage of ovipositing females compared to controls (GTest $p < 0.001$). Data are shown as the means of three biological replicates, $n = 298$. **(E)** Larval treatment with ABA reduced clutch size in the third gonotrophic cycle (ANOVA $p = 0.012$; Tukey $p = 0.017$ for 1 μM ABA, Tukey $p = 0.034$ for 100 μM ABA). Each dot represents the clutch size of a single female mosquito from four biological replicates, black bars represent the mean of each treatment. **(F)** Percentage of fully engorged *A. stephensi* that laid eggs was not affected by larval treatment with ABA (GTest $p = 0.62$). Data are shown as the means of three biological replicates, $n = 141$.

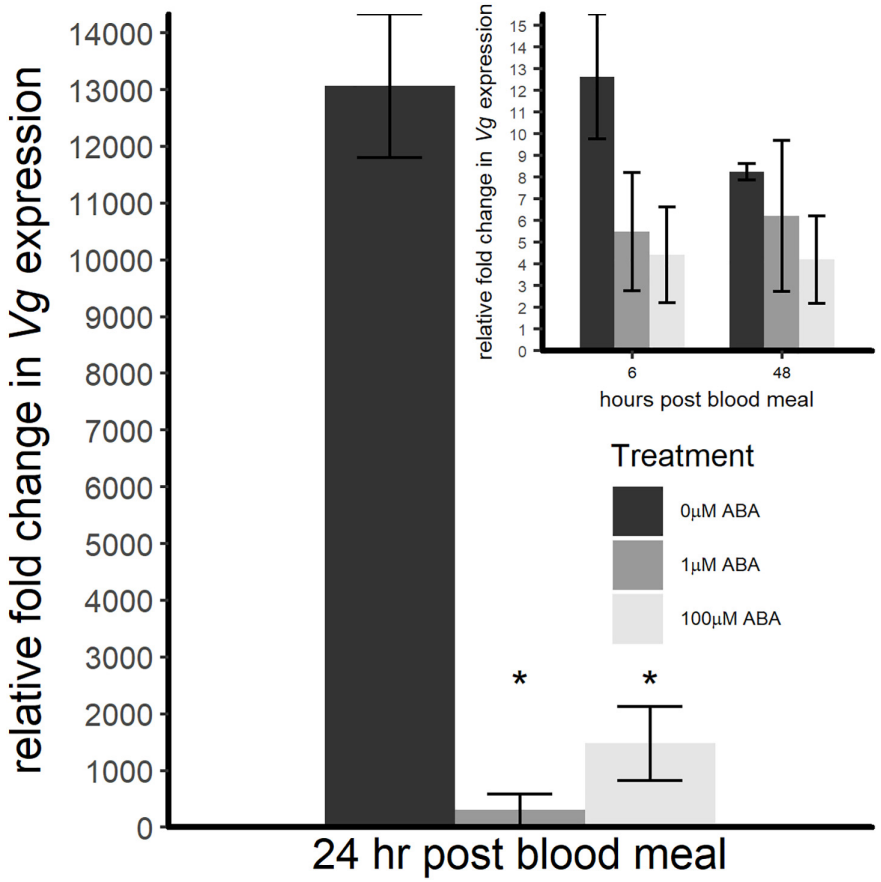

FIGURE 6 | ABA treatment of larval *A. stephensi* reduced *Vg* transcript expression in adult female mosquitoes during the first 24 h following a blood meal. At 6 h post-blood meal (inset), there was no difference in *Vg* expression in females derived from larvae treated with 1 or 100 μM ABA compared to control (ANOVA $F = 0.722$, $p = 0.519$). At 24 h post-blood meal, however, *Vg* expression levels of females derived from larvae treated with 1 μM and 100 μM ABA were significantly reduced relative to controls (ANOVA $F = 56.374$, $p < 0.001$; Tukey $^*p < 0.001$ for 1 μM ABA, Tukey $^*p < 0.001$ for 100 μM ABA). At 48 h post-blood meal (inset), there was no difference in *Vg* expression in either ABA group compared to control (ANOVA $F = 0.518$, $p = 0.616$). Data are shown for three biological replicates as fold change normalized within treatment group to *Vg* expression before the blood meal.

that could occur under natural conditions (Else et al., 1995). In trying to understand these effects of ABA, we examined some obvious developmental cues in our studies. Accelerated pupation in holometabolous insects can result from blocking JH synthesis or activity. For example, removal of the corpora allata, which generates JH, results in precocious pupation in *Manduca sexta* due to a reduction in the critical weight threshold (Nijhout and Williams, 1974). Despite the obvious similarities in accelerated pupation, ABA had no effect on the expression of the JH synthesis-associated genes *hmgcr* and *jhamt*. Further, ABA affected 20E titers on only a single day of larval development (day 6) at the highest concentration of ABA (100 μM), affirming minimal to no effect of ABA on the interacting effects of JH and 20E. Our data contrast with the reported effects of ABA on 20E in adult *S. bullata* (De Man et al., 1981), suggesting the likely possibility that the effects of ABA vary to some degree across insect species. In *D. melanogaster,* reduced food seeking behavior is mediated by the overexpression and release of ILP2 and ILP4 (Wu et al., 2005), suggesting that reduced expression of *ilp*s in our ABA treated larvae might be associated with increased food seeking behavior. However, expression of *ilp* genes in fourth instar *A. stephensi* larvae was not altered by ABA treatment. While the current state of technology is not sufficient to quantify ILPs in *A. stephensi*, we can reasonably conclude that JH, 20E and changes in ILP levels are not mediating the acceleration of development by ABA. Future work regarding potential effects of ABA on *A. stephensi* larval feeding behavior could focus on sulfakinin and neuropeptide F, both of which modulate feeding behavior in *D. melanogaster* larvae (Söderberg et al., 2012; Fadda et al., 2019). Both neuropeptides are also known to be conserved in *A. gambiae* (Strand et al., 2016) and are represented as orthologs in *A. stephensi*[1].

The protein content of newly eclosed adult females derived from larvae treated with ABA was reduced, perhaps as a consequence of accelerated development and increased adult size. Following a blood meal, malnourished mosquitoes have both delayed and reduced *Vg* transcript abundance and may require a second blood meal for proper egg development (Shiao

[1]www.vectorbase.org

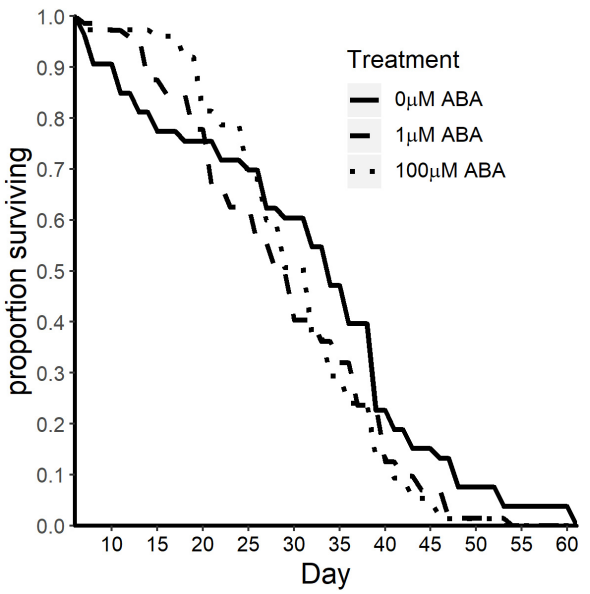

FIGURE 7 | ABA treatment of larval *A. stephensi* reduced adult female survival. Survival curves of adult female mosquitoes derived from control untreated larvae and larvae treated with 1 μM ABA (log-rank $p = 0.028$) and 100 μM ABA (two-stage $p = 0.025$). Median survival was reduced from 34 ± 14.2 days in controls to 28 ± 10.78 days (1 μM ABA) and to 30 ± 14.22 days (100 μM ABA). Data are representative of two biological replicates.

et al., 2008). The reduction in *Vg* expression that we observed is consistent with reduced Vg levels in *S. bullata* injected with ABA (De Man et al., 1981) and reduced Vg levels reported for malnourished *A. aegypti* (Shiao et al., 2008). Reduced protein content has been shown to result in smaller follicle size and increased resorption of oocytes (Caroci et al., 2004; Clifton and Noriega, 2011). Our observed association between reduced *Vg* mRNA expression and decreased fecundity is consistent with other studies showing 50% of Vg depleted mosquitoes still produced mature eggs (Rono et al., 2010). In our studies, reduced protein content of newly eclosed adult females likely contributed to lower clutch sizes and reduced oviposition in the first gonotrophic cycle (following a blood meal at 4 days in week 1). Patterns of oviposition and fecundity in the second and third gonotrophic cycles (weeks 2–3) could reflect the fact that nutrients for optimizing reproduction and preserving the soma are limited. In fact, the inflection points in our lifespan data – which occur at 21 days (**Figure 7**) for 1 μM ABA and 26 days for 100 μM ABA – are consistent with the possibility that the cost of reproduction, even at reduced levels, outweighs any further investment in the soma of females derived from treated larvae relative to controls, which have consistently higher survivorship after these timepoints.

While dietary restriction and the resulting impacts on nutrient stores have been associated with lifespan extension in *Anopheles* mosquitoes (Faiman et al., 2017), we observed reduced survivorship with reduced body protein levels in *A. stephensi* derived from larvae treated with ABA. Reduced survival of ABA-treated mosquitoes was unexpected as weekly supplementation of adults with ABA in blood meals did not change adult female survival (Glennon et al., 2017). Our data indicate that the substantial effect of ABA on adult lifespan carries over from the larval stage and across not one, but two developmental transitions.

Study of the role of plants and plant biology in regulating mosquito life history has focused on the characteristics of oviposition sites that are shaped by both wild and cultivated plant species (Omlin et al., 2007; Overgaard, 2007; Eneh et al., 2016; Wondwosen et al., 2016; Asmare et al., 2017; Wondwosen et al., 2017; Wondwosen et al., 2018), on nectar feeding and its effects on mosquito physiology (Nikbakhtzadeh et al., 2014; Nyasembe et al., 2014; Jacob et al., 2018), the potential role of invasive plants in promoting malaria parasite transmission (Stone et al., 2018), and the utility of plant-derived compounds as novel insecticides (Govindarajan et al., 2008; Nathan et al., 2008; Elango et al., 2009; Elimam et al., 2009). Here, we have taken the relationship between plant biology and mosquito biology a step further, connecting the effects of ABA, a universal signaling molecule first described in and well known from plants (Olds et al., 2018), at concentrations detected in water with submerged plant tissue that can alter substantial features of mosquito growth, development and survivorship across immature and adult stages. Together with our previous studies on the effects of ABA on *P. falciparum* development in *A. stephensi* (Glennon et al., 2017), the association of elevated blood levels of ABA with asymptomatic malaria in humans and reduced infection and disease pathology in our animal model of malaria (Glennon et al., 2018), the effects of ABA on the life cycle of malaria are both comprehensive and complex and will become undoubtedly more so with continued studies of mechanisms underlying this biology.

DATA AVAILABILITY STATEMENT

The datasets generated for this study are available on request to the corresponding author.

ETHICS STATEMENT

All animal procedures were approved by the University of Idaho Animal Care and Use Committee.

AUTHOR CONTRIBUTIONS

DT and SL designed the experiments and wrote the manuscript. RH designed and conducted the fecundity studies. BT assisted in completing various studies and provided input for experimental design. CO contributed to writing and editing the manuscript.

FUNDING

Funding for these studies was provided by the University of Idaho and the UI College of Agricultural and Life Sciences, Moscow, ID, United States.

ACKNOWLEDGMENTS

We would like to thank Sarah M. Garrison and Jason Jackson for their assistance with mosquito rearing and colony maintenance.

SUPPLEMENTARY MATERIAL

The Supplementary Material for this article can be found online at: https://www.frontiersin.org/articles/10.3389/fmicb.2019.03024/full#supplementary-material

REFERENCES

Asmare, Y., Hill, S. R., Hopkins, R. J., Tekie, H., and Ignell, R. (2017). The role of grass volatiles on oviposition site selection by *Anopheles arabiensis* and *Anopheles coluzzii*. *Malar. J.* 16:65. doi: 10.1186/s12936-017-1717-z

Baldini, F., Gabrieli, P., South, A., Valim, C., Mancini, F., and Catteruccia, F. (2013). The interaction between a sexually transferred steroid hormone and a female protein regulates oogenesis in the malaria mosquito *Anopheles gambiae*. *PLoS Biol.* 11:e1001695. doi: 10.1371/journal.pbio.1001695

Boulan, L., Milán, M., and Léopold, P. (2015). The systemic control of growth. *Cold Spring Harb. Perspect. Biol.* 7, 1–29. doi: 10.1101/cshperspect.a019117

Brutis, K. C., Thummel, C. S., James, C. W., Karim, F. D., and Hogness, D. S. (1990). The *Drosophila* 74EF early puff contains *E74*, a complex ecdysone-inducible gene that encodes two *ets*-related proteins. *Cell* 61, 85–91. doi: 10.1016/0092-8674(90)90217-3

Caroci, A. S., Li, Y., and Noriega, F. (2004). Reduced juvenile hormone synthesis in mosquitoes with low teneral reserves reduces ovarian previtellogenic development in *Aedes aegypti*. *J. Exp. Biol.* 207, 2685–2690. doi: 10.1242/jeb.01093

Clifton, M. E., and Noriega, F. G. (2011). Nutrient limitation results in juvenile hormone-mediated resorption of previtellogenic ovarian follicles in mosquitoes. *J. Insect Physiol.* 57, 1274–1281. doi: 10.1016/j.jinsphys.2011.06.002

Davis, E. E., and Takahashi, F. T. (1980). Humoral alteration of chemoreceptor sensitivity in the mosquito. *Olfaction Taste* 7, 139–142.

De Man, W., De Loof, A., Briers, T., and Huybrechts, R. (1981). Effect of abscisic acid on vitellogenesis in *Sarcophaga bullata*. *Entomol. Exp. Appl.* 29, 259–267. doi: 10.1111/j.1570-7458.1981.tb03068.x

Dhara, A., Eum, J., Robertson, A., Gulia-nuss, M., Vogel, K. J., Clark, K. D., et al. (2013). Ovary ecdysteroidogenic hormone functions independently of the insulin receptor in the yellow fever mosquito, *Aedes aegypti*. *Insect Biochem. Mol. Biol.* 43, 1100–1108. doi: 10.1016/j.ibmb.2013.09.004

Elango, G., Bagavan, A., Kamaraj, C., Zahir, A. A., and Rahuman, A. A. (2009). Oviposition-deterrent, ovicidal, and repellent activities of indigenous plant extracts against *Anopheles subpictus* Grassi (Diptera: Culicidae). *Parasitol. Res.* 103, 691–695. doi: 10.1007/s00436-009-1593-8

Elimam, A. M., Elmalik, K. H., and Ali, F. S. (2009). Larvicidal, adult emergence inhibition and oviposition deterrent effects of foliage extract from *Ricinus communis* L. against *Anopheles arabiensis* and *Culex quinquefasciatus* in Sudan. *Trop. Biomed.* 26, 130–139.

Else, M. A., Hall, K. C., Arnold, G. M., Davies, W. J., and Jackson, M. B. (1995). Export of abscisic acid, 1-aminocyclopropane-1-carboxylic acid, phosphate, and nitrate from roots to shoots of flooded tomato plants (accounting for effects of xylem sap flow rate on concentration and delivery). *Plant Physiol.* 107, 377–384. doi: 10.1104/pp.107.2.377

Eneh, L. K., Saijo, H., Karin, A., Karlson, B., Lindh, J. M., and Rajarao, G. K. (2016). Cedrol, a malaria mosquito oviposition attractant is produced by fungi isolated from rhizomes of the grass *Cyperus rotundus*. *Malar. J.* 15:478. doi: 10.1186/s12936-016-1536-7

Fadda, M., Hasakiogullari, I., Temmerman, L., Beets, I., Zels, S., and Schoofs, L. (2019). Regulation of feeding and metabolism by neuropeptide F and short neuropeptide F in invertebrates. *Front. Endocrinol.* 10:64. doi: 10.3389/fendo.2019.00064

Faiman, R., Solon-biet, S., Sullivan, M., Huestis, D. L., and Lehmann, T. (2017). The contribution of dietary restriction to extended longevity in the malaria vector *Anopheles coluzzii*. *Parasit. Vectors* 10:156. doi: 10.1186/s13071-017-2088-6

Faulde, M. K., Rueda, L. M., and Khaireh, B. A. (2014). First record of the Asian malaria vector *Anopheles stephensi* and its possible role in the resurgence of malaria in Djibouti, Horn of Africa. *Acta Trop.* 139, 39–43. doi: 10.1016/j.actatropica.2014.06.016

Gabrieli, P., Kakani, E. G., Mitchell, S. N., Mameli, E., Want, E. J., Anton, A. M., et al. (2014). Sexual transfer of the steroid hormone 20E induces the postmating switch in *Anopheles gambiae*. *Proc. Natl. Acad. Sci. U.S.A.* 111, 16353–16358. doi: 10.1073/pnas.1410488111

Glennon, E. K. K., Adams, L. G., Hicks, D. R., Dehesh, K., and Luckhart, S. (2016). Supplementation with abscisic acid reduces malaria disease severity and parasite transmission. *Am. J. Trop. Med. Hyg.* 94, 1266–1275. doi: 10.4269/ajtmh.15-0904

Glennon, E. K. K., Megawati, D., Torrevillas, B. K., Ssewanyana, I., Huang, L., Aweeka, F., et al. (2018). Elevated plasma abscisic acid is associated with asymptomatic falciparum malaria and with IgG-/caspase-1-dependent immunity in *Plasmodium yoelii*-infected mice. *Sci. Rep.* 8:8896. doi: 10.1038/s41598-018-27073-1

Glennon, E. K. K., Torrevillas, B. K., Morrissey, S. F., Ejercito, J. M., and Luckhart, S. (2017). Abscisic acid induces a transient shift in signaling that enhances NF-κB-mediated parasite killing in the midgut of *Anopheles stephensi* without reducing lifespan or fecundity. *Parasit. Vectors* 10:333. doi: 10.1186/s13071-017-2276-4

Govindarajan, M., Jebanesan, A., Pushpanathan, T., and Samidurai, K. (2008). Studies on effect of *Acalypha indica* L. (Euphorbiaceae) leaf extracts on the malarial vector, *Anopheles stephensi* Liston (Diptera: Culicidae). *Parasitol. Res.* 103, 691–695. doi: 10.1007/s00436-008-1032-2

Hansen, I. A., Attardo, G. M., Roy, S. G., and Raikhel, A. S. (2005). Target of rapamycin-dependent activation of S6 kinase is a central step in the transduction of nutritional signals during egg development in a mosquito. *J. Biol. Chem.* 280, 20565–20572. doi: 10.1074/jbc.M500712200

Harshman, L. G., and Zera, A. J. (2007). The cost of reproduction: the devil in the details. *Trends Ecol. Evol.* 22, 80–86. doi: 10.1016/j.tree.2006.10.008

Jacob, J. W., Tchouassi, D. P., Lagat, Z. O., Mathenge, E. M., Mweresa, C. K., and Torto, B. (2018). Independent and interactive effect of plant- and mammalian- based odors on the response of the malaria vector, *Anopheles gambiae*. *Acta Trop.* 185, 98–106. doi: 10.1016/j.actatropica.2018.04.027

Jindra, M., Palli, S. R., and Riddiford, L. M. (2013). The juvenile hormone signaling pathway in insect development. *Annu. Rev. Entomol.* 58, 181–204. doi: 10.1146/annurev-ento-120811-153700

Lipp, J. (1990). Nachweis und herkunft von abscisinsäure und prolin in honig. *Apidiologie* 21, 249–259. doi: 10.1051/apido:19900310

Liu, Y., Sheng, Z., Liu, H., Wen, D., He, Q., Wang, S., et al. (2009). Juvenile hormone counteracts the bHLH-PAS transcription factors MET and GCE to prevent caspase-dependent programmed cell death in *Drosophila*. *Development* 136, 2015–2025. doi: 10.1242/dev.033712

Lyimo, E. O., Takken, W., and Koella, J. C. (1992). Effect of rearing temperature and larval density on larval survival, age at pupation and adult size of *Anopheles gambiae*. *Entomol. Exp. Appl.* 63, 265–271. doi: 10.1111/j.1570-7458.1992.tb01583.x

Manouchehri, A. V., Javadian, E., Eshghy, N., and Motabar, M. (1976). Ecology of *Anopheles stephensi* Liston in southern Iran. *Trop. Geogr. Med.* 28, 228–232.

Margam, V. M., Gelman, D. B., and Palli, S. R. (2006). Ecdysteroid titers and developmental expression of ecdysteroid-regulated genes during metamorphosis of the yellow fever mosquito, *Aedes aegypti* (Diptera: Culicidae). *J. Exp. Biol.* 52, 558–568. doi: 10.1016/j.jinsphys.2006.02.003

Marquez, A. G., Pietri, J. E., Smithers, H. M., Nuss, A., Antonova, Y., Drexler, A. L., et al. (2011). Insulin-like peptides in the mosquito *Anopheles stephensi*: identification and expression in response to diet and infection with *Plasmodium falciparum*. *Gen. Comp. Endocrinol.* 173, 303–312. doi: 10.1016/j.ygcen.2011.06.005

Martìn, D., Wang, S., and Raikhel, A. S. (2001). The vitellogenin gene of the mosquito *Aedes aegypti* is a direct target of ecdysteroid receptor. *Mol. Cell. Endocrinol.* 173, 75–86. doi: 10.1016/s0303-7207(00)00413-5

Moller-Jacobs, L. L., Murdock, C. C., and Thomas, M. B. (2014). Capacity of mosquitoes to transmit malaria depends on larval environment. *Parasit. Vectors* 7:593. doi: 10.1186/s13071-014-0593-4

Murdock, C. C., Evans, M. V., McClanahan, T. D., Miazgowicz, K. L., and Tesla, B. (2017). Fine-scale variation in microclimate across an urban landscape shapes variation in mosquito population dynamics and the potential of *Aedes albopictus* to transmit arboviral disease. *PLoS Negl. Trop. Dis.* 11:e0005640. doi: 10.1371/journal.pntd.0005640

Mwangangi, J. M., Muriu, S., Mbogo, C. M., Githure, J., Shililu, J., Muturi, E. J., et al. (2010). Anopheles larval abundance and diversity in three rice agro-village complexes Mwea irrigation scheme, central Kenya. *Malar. J.* 9:228. doi: 10.1186/1475-2875-9-228

Nathan, S. S., Hisham, A., and Jayakumar, G. (2008). Larvicidal and growth inhibition of the malaria vector *Anopheles stephensi* by triterpenes from *Dysoxylum malabaricum* and *Dysoxylum beddomei*. *Fitoterapia* 79, 106–111. doi: 10.1016/j.fitote.2007.07.013

Negri, P., Ramirez, L., Quintana, S., Szawarski, N., Maggi, M., Le Conte, Y., et al. (2017). Dietary supplementation of honey bee larvae with arginine and abscisic acid enhances nitric oxide and granulocyte immune responses after trauma. *Insects* 8:E85. doi: 10.3390/insects8030085

Nijhout, H. F., and Williams, C. M. (1974). Control of moulting and metamorphosis in the tobacco hornworm, *Manduca sexta*. *J. Exp. Biol.* 61, 493–501.

Nikbakhtzadeh, M. R., Terbot, J. W. II., Otienoburu, P. E., and Foster, W. A. (2014). Olfactory basis of floral preference of the malaria vector *Anopheles gambiae* (Diptera: Culicidae) among common African plants. *J. Vector Ecol.* 39, 372–383. doi: 10.1111/jvec.12113

Noriega, F. G. (2014). Juvenile hormone biosynthesis in insects: what is new, what do we know, and what questions remain? *Int. Sch. Res. Notices* 2014:967361. doi: 10.1155/2014/967361

Nyasembe, V. O., Teal, P. E. A., Sawa, P., Tumlinson, J. H., Borgemeister, C., and Baldwyn, T. (2014). *Plasmodium falciparum*-infection increases *Anopheles gambiae* attraction to nectar sources and sugar uptake. *Curr. Biol.* 24, 217–221. doi: 10.1016/j.cub.2013.12.022

Olds, C. L., Glennon, E. K. K., and Luckhart, S. (2018). Abscisic acid: new perspectives on an ancient universal stress signaling molecule. *Microbes Infect.* 20, 484–492. doi: 10.1016/j.micinf.2018.01.009

Omlin, F. X., Carlson, J. C., Ogbunugafor, C. B., and Hassanali, A. (2007). *Anopheles gambiae* exploits the treehole ecosystem in western Kenya: a new urban malaria risk? *Am. J. Trop. Med. Hyg.* 77, 264–269. doi: 10.4269/ajtmh.2007.77.264

Overgaard, H. J. (2007). Effect of plant structure on oviposition behavior of *Anopheles minimus* s.l. *J. Vector Ecol.* 32, 193–197.

Perez-Hedo, M., Rivera-Perez, C., and Noriega, F. G. (2014). Starvation increases insulin sensitivity and reduces juvenile hormone synthesis in mosquitoes. *PLoS One* 9:e86183. doi: 10.1371/journal.pone.0086183

Qiu, P., and Sheng, J. (2008). A two-stage procedure for comparing hazard rate. *J. R. Stat. Soc. B* 70, 191–208. doi: 10.1111/j.1467-9868.2007.00622.x

Raikhel, A. S., and Lea, A. O. (1983). Previtellogenic development and vitellogenin synthesis in the fat body of a mosquito: an ultrastructural and immunocytochemical study. *Tissue Cell* 15, 281–299. doi: 10.1016/0040-8166(83)90023-x

Ramirez, L., Negri, P., Sturla, L., Guida, L., Zocchi, E., Vigliarolo, T., et al. (2017). Abscisic acid enhances cold tolerance in honeybee larvae. *Proc. Biol. Sci.* 284:20162140. doi: 10.1098/rspb.2016.2140

Riddiford, L. M. (2012). How does juvenile hormone control insect metamorphosis and reproduction? *Gen. Comp. Endocrinol.* 179, 477–484. doi: 10.1016/j.ygcen.2012.06.001

Riddiford, L. M., Cherbas, P., and Truman, J. W. (2000). Ecdysone receptors and their biological actions. *Vitam. Horm.* 60, 1–73. doi: 10.1016/s0083-6729(00)60016-x

Riddiford, L. M., Truman, J. W., Mirth, C. K., and Shen, Y. (2010). A role for juvenile hormone in the prepupal development of *Drosophila melanogaster*. *Development* 137, 1117–1126. doi: 10.1242/dev.037218

Rodrigues, M. S., Batista, E. P., Silva, A. A., Costa, F. M., Neto, V. A. S., and Gil, L. H. S. (2017). Change in *Anopheles* richness and composition in response to artificial flooding during the creation of the Jirau hydroelectric dam in Porto Velho, Brazil. *Malar. J.* 16, 87. doi: 10.1186/s12936-017-1738-7

Rono, M. K., Whitten, M. M. A., Oulad-abdelghani, M., and Elena, A. (2010). The major yolk protein Vitellogenin interferes with the anti-plasmodium response in the malaria mosquito *Anopheles gambiae*. *PLoS Biol.* 8:e1000434. doi: 10.1371/journal.pbio.1000434

Seyfarth, M., Khaireh, B. A., Abdi, A. A., Bouh, S. M., and Faulde, M. K. (2019). Five years following first detection of *Anopheles stephensi* (Diptera: Culicidae) in Djibouti, Horn of Africa: populations established-malaria emerging. *Parasitol. Res.* 118, 725–732. doi: 10.1007/s00436-019-06213-0

Shiao, S.-H., Hansen, I. A., Zhu, J., Siegleff, D. H., and Raikhel, A. S. (2008). Juvenile hormone connects larval nutrition with target of rapamycin signaling in the mosquito *Aedes aegypti*. *J. Insect Physiol.* 54, 231–239. doi: 10.3390/insects9020060

Shinoda, T., and Itoyama, K. (2003). Juvenile hormone acid methyltransferase: a key regulatory enzyme for insect metamorphosis. *Proc. Natl. Acad. Sci. U.S.A.* 100, 11986–11991. doi: 10.1073/pnas.2134232100

Smith, N. R., Trauer, J. M., Gambhir, M., Richards, J. S., Maude, R. J., Keith, J. M., et al. (2018). Agent-based models of malaria transmission? a systematic review. *Malar. J.* 17:299. doi: 10.1186/s12936-018-2442-y

Söderberg, J. A. E., Carlsson, M. A., and Nässel, D. R. (2012). Insulin-producing cells in the *Drosophila* brain also express satiety-inducing cholecystokinin-like peptide, drosulfakinin. *Front. Endocrinol.* 3:109. doi: 10.3389/fendo.2012.00109

Soleimani-Ahmadi, M., Vatandoost, H., and Zare, M. (2014). Characterization of larval habitats for anopheline mosquitoes in a malarious area under elimination program in the southeast of Iran. *Asian Pac. J. Trop. Biomed.* 4, S73–S80. doi: 10.12980/apjtb.4.2014c899

Stone, C. M., Witt, A. B. R., Walsh, G. C., Foster, W. A., and Murphy, S. T. (2018). Would the control of invasive alien plants reduce malaria transmission? A review. *Parasit. Vectors* 11:76. doi: 10.1186/s13071-018-2644-8

Strand, M. R., Brown, M. R., and Vogel, K. J. (2016). Mosquito peptide hormones: diversity, production, and function. *Adv. Insect Physiol.* 51, 145–188. doi: 10.1016/bs.aiip.2016.05.003

Surendran, S. N., Sivabalakrishnan, K., Gajapathy, K., Arthiyan, S., Jayadas, T., Karvannan, K., et al. (2018). Genotype and biotype of invasive *Anopheles stephensi* in Mannar Island of Sri Lanka. *Parasit. Vectors* 11:3. doi: 10.1186/s13071-017-2601-y

Takken, W., and Lindsay, S. (2019). Increased threat of urban malaria from *Anopheles stephensi* mosquitoes, Africa. *Emerg. Infect. Dis.* 25, 1431–1433. doi: 10.3201/eid2507.190301

Van Ekert, E., Powell, C. A., Shatters, R. G., and Borovsky, D. (2014). Control of larval and egg development in *Aedes aegypti* with RNA interference against juvenile hormone acid methyl transferase. *J. Insect Physiol.* 70, 143–150. doi: 10.1016/j.jinsphys.2014.08.001

Vince, R. K., and Gilbert, L. I. (1977). Juvenile hormone esterase activity in precisely timed last instar larvae and pharate pupae of *Manduca sexta*. *Insect Biochem.* 7, 115–120. doi: 10.1016/0020-1790(77)90003-8

Visscher, S. N. (1980). Regulation of grasshopper fecundity, longevity and egg viability by plant growth hormones. *Experientia* 36, 130–131. doi: 10.1007/bf02004017

White, B. H., and Ewer, J. (2014). Neural and hormonal control of postecdysial behaviors in insects. *Annu. Rev. Entomol.* 59, 363–381. doi: 10.1146/annurev-ento-011613-162028

Wondwosen, B., Birgersson, G., Seyoum, E., Tekie, H., Torto, B., Fillinger, U., et al. (2016). Rice volatiles lure gravid malaria mosquitoes, *Anopheles arabiensis*. *Sci. Rep.* 6:37930. doi: 10.1038/srep37930

Wondwosen, B., Birgersson, G., Tekie, H., Torto, B., Ignell, R., and Hill, S. R. (2018). Sweet attraction: sugarcane pollen-associated volatiles attract gravid *Anopheles arabiensis*. *Malar. J.* 17:90. doi: 10.1186/s12936-018-2245-1

Wondwosen, B., Hill, S. R., Birgersson, G., Seyoum, E., Tekie, H., and Ignell, R. (2017). A(maize)ing attraction: gravid *Anopheles arabiensis* are attracted and oviposit in response to maize pollen odours. *Malar. J.* 16:39. doi: 10.1186/s12936-016-1656-0

World Health Organization [WHO] (2019). *World Malaria Report, ISBN: 978-92-4-156572-1*. Geneva: World Health Organization.

Wu, Q., Zhang, Y., Xu, J., and Shen, P. (2005). Regulation of hunger-driven behaviors by neural ribosomal S6 kinase in *Drosophila*. *Proc. Natl. Acad. Sci. U.S.A.* 102, 13289–13294. doi: 10.1073/pnas.0501914102

Yin, V. P., and Thummel, C. S. (2005). Mechanisms of steroid-triggered programmed cell death in *Drosophila*. *Semin. Cell Dev. Biol.* 16, 237–243. doi: 10.1016/j.semcdb.2004.12.007

Zhou, G., Pennington, J. E., and Wells, M. A. (2004). Utilization of pre-existing energy stores of female *Aedes aegypti* mosquitoes during the first gonotrophic cycle. *Insect Biochem. Mol. Biol.* 34, 919–925. doi: 10.1016/j.ibmb.2004.05.009

Ziegler, R., and Ibrahim, M. M. (2001). Formation of lipid reserves in fat body and eggs of the yellow fever mosquito, *Aedes aegypti*. *J. Insect Physiol.* 47, 623–627. doi: 10.1016/s0022-1910(00)00158-x

Conflict of Interest: The authors declare that the research was conducted in the absence of any commercial or financial relationships that could be construed as a potential conflict of interest.

frontiers in Microbiology

ORIGINAL RESEARCH
published: 24 January 2020
doi: 10.3389/fmicb.2019.03048

The Impact of Antiretroviral Therapy on Malaria Parasite Transmission

*Raquel Azevedo, António M. Mendes and Miguel Prudêncio**

Faculdade de Medicina, Instituto de Medicina Molecular, Universidade de Lisboa, Lisbon, Portugal

Coendemicity between the human immunodeficiency virus (HIV) and *Plasmodium* parasites, the causative agents of acquired immunodeficiency syndrome (AIDS) and malaria, respectively, occurs in several regions around the world. Although the impact of the interaction between these two organisms is not well understood, it is thought that the outcome of either disease may be negatively influenced by coinfection. Therefore, it is important to understand how current first-line antiretroviral therapies (ART) might impact *Plasmodium* infection in these regions. Here, we describe the effect of 18 antiretroviral compounds and of first-line ART on the blood and sporogonic stages of *Plasmodium berghei in vitro* and *in vivo*. We show that the combination zidovudine + lamivudine + lopinavir/ritonavir (LPV/r), employed as first-line HIV treatment in the field, has a strong inhibitory activity on the sporogonic stages of *P. berghei* and that several non-nucleoside reverse transcriptase inhibitors (NNRTI) have a moderate effect on this stage of the parasite's life cycle. Our results expose the effect of current first-line ART on *Plasmodium* infection and identify potential alternative therapies for HIV/AIDS that might impact malaria transmission.

Keywords: *Plasmodium*, HIV, antiretroviral, coinfection, malaria

OPEN ACCESS

Edited by:
Isabelle Morlais, Institut de Recherche pour le Développement (IRD), France

Reviewed by:
Mathilde Gendrin, Institut Pasteur de la Guyane, French Guiana
Ahidjo Ayouba, Institute for Research and Development, Sri Lanka
Arthur Talman, Institut de Recherche pour le Développement (IRD), France

****Correspondence:***
Miguel Prudêncio
mprudencio@medicina.ulisboa.pt

Specialty section:
This article was submitted to Infectious Diseases, a section of the journal Frontiers in Microbiology

Received: *31 October 2019*
Accepted: *18 December 2019*
Published: *24 January 2020*

Citation:
Azevedo R, Mendes AM and Prudêncio M (2020) The Impact of Antiretroviral Therapy on Malaria Parasite Transmission. Front. Microbiol. 10:3048. doi: 10.3389/fmicb.2019.03048

INTRODUCTION

In 2018, an estimated 228 million people suffered from malaria, killing 405,000 (World Health Organization [WHO], 2019a). Malaria is caused by *Plasmodium* parasites that are transmitted to their mammalian host by the bite of female-infected *Anopheles* mosquitoes (Prudêncio et al., 2011). Sporozoites injected into the skin during a blood meal eventually reach the bloodstream and migrate to the liver, initiating the hepatic stage of the infection (Mota et al., 2001). Merozoites formed during parasite replication inside hepatocytes are released into the bloodstream, giving rise to the clinical symptoms of the disease (Prudêncio et al., 2011). When a mosquito takes a blood meal from an infected mammalian host, it ingests *Plasmodium* gametocytes that will subsequently differentiate into female and male gametes and fuse to form a zygote (Sinden et al., 2010). After 18–24 h, the zygote transforms into an ookinete, traverses the midgut epithelium, and settles in the basal lamina of the midgut wall, rounding up into an oocyst (Vinetz, 2005). During the ensuing 10–13 days, oocysts increase in size, producing thousands of sporozoites that will be released in the hemolymph and travel to the mosquito salivary glands, completing the cycle (Baton and Ranford-Cartwright, 2005; Staines and Sanjeev, 2012).

Human immunodeficiency virus (HIV) infects the immune system's $CD4^+$ T cells, inducing chronic inflammation that drives the progression into acquired immune deficiency syndrome (AIDS) (HIV/AIDS, 2019: The Basics Understanding HIV/AIDS). In 2018, 37.9 million people were reported to live with HIV, leading to an estimated 770,000 deaths in that year alone

(World Health Organization [WHO], 2019b). In 2002, the World Health Organization (WHO) issued a set of guidelines to help determine the best usage of antiretroviral (ARV) compounds for the treatment of HIV-positive young adults and adolescents (World Health Organization [WHO], 2016). Since then, these guidelines have been regularly updated, and, since 2016, the recommended first-line antiretroviral therapies (ART) in adults, including pregnant women and adolescents, consist of two nucleoside reverse-transcriptase inhibitors (NRTIs) plus a non-nucleoside reverse transcriptase inhibitors (NNRTI) or an integrase strand transfer inhibitor (INSTI) (World Health Organization [WHO], 2016). The recommendation for children between 3 and 10 years old is the combination of two NRTIs with the NNRTI efavirenz (EFV), while for children under 3 years of age, a combination of the NRTI backbone with the protease inhibitors (PIs) lopinavir/ritonavir (LPV/r) is recommended (World Health Organization [WHO], 2016).

Plasmodium and HIV infections overlap geographically in tropical and subtropical regions, particularly in Sub-Saharan Africa, where 70% of the world's HIV cases and 93% of the malaria cases are concentrated (Kwenti, 2018; World Health Organization [WHO], 2019a). Pregnant women, in whom *Plasmodium* infections are more severe, are at particular risk of coinfection (Kharsany and Karim, 2016; Kwenti, 2018). The outlook of either disease seems to be influenced by coinfection. On the one hand, the low $CD4^+$ cell count of HIV carriers limits their immune system's ability to mount a response against a parasite infection (Skinner-Adams et al., 2008), while on the other hand, *Plasmodium* infection can cause T-cell activation and cytokine release, which can stimulate HIV replication (Xiao et al., 1998; Skinner-Adams et al., 2008). Therefore, it is important to further understand the spectrum of activity of drugs used for treatment of either disease and their possible impact on each other.

Numerous reports describe the effect of ART on the blood and liver stages of *Plasmodium* parasites (Butcher, 1997; Skinner-Adams et al., 2004; Parikh et al., 2005; Hobbs et al., 2009, 2012; Peatey et al., 2010, 2012; Nsanzabana and Rosenthal, 2011; Machado et al., 2017). PIs have been systematically described as the most effective ARVs in inhibiting *Plasmodium* erythrocytic stages (Skinner-Adams et al., 2004; Parikh et al., 2005; Andrews et al., 2006; Lek-Uthai et al., 2008; Peatey et al., 2010; Nsanzabana and Rosenthal, 2011; Hobbs et al., 2013). Their ability to inhibit the growth of drug-susceptible and drug-resistant *Plasmodium falciparum* parasite strains has also been documented (Skinner-Adams et al., 2004; Nsanzabana and Rosenthal, 2011). The PI lopinavir (LPV) has been identified by several studies as the most potent ARV inhibiting *P. falciparum* asexual stages *in vitro* (Parikh et al., 2005; Nsanzabana and Rosenthal, 2011; Hobbs et al., 2013). The PI indinavir (IDV) has also been reported to suppress *Plasmodium cynomolgi* growth and to delay prepatency in monkeys infected with *Plasmodium knowlesi* (Li et al., 2011). *Plasmodium vivax* was found to be more sensitive to the PIs ritonavir (RTV) and saquinavir (SQV) than *P. falciparum* (Lek-Uthai et al., 2008), whereas Peatey et al. (2010) showed that ARV PIs are more active against the trophozoite and schizont stages than against the ring stages of *P. falciparum* asexual parasites in the blood. These authors also showed that the exposure of *P. falciparum* gametocyte cultures to SQV, LPV, RTV, tipranavir, and darunavir (DRV) (PIs) inhibited the formation of gametocytes–gametocytogenesis, but only tipranavir had the ability to kill gametocytes (Peatey et al., 2010). Consistent with these results, Hobbs et al. (2013) showed that prolonged drug exposure to LPV/r, LPV, and SQV reduces early- and late-stage gametocyte viability, with the latter two drugs impacting parasite exflagellation. This impairment in parasite development was also reflected on oocyst infection in the mosquito, when mosquitoes were allowed to feed on blood cultures previously treated with LPV and SQV (Hobbs et al., 2013).

The mechanism of action of PIs on *Plasmodium* is still unknown, but it has been theorized that PIs inhibit the development of malaria parasites by targeting plasmepsins (PMs) in their food vacuole (Savarino et al., 2005; Andrews et al., 2006), where they play an important role in hemoglobin degradation by *P. falciparum* (Liu et al., 2005). More recently, it has been suggested that the these drugs might also target other non-vacuolar PMs (Skinner-Adams et al., 2007; Peatey et al., 2010; Li et al., 2011; Onchieku et al., 2018). Another study suggested that treatment with PIs might affect positively the outcome of malaria infection due to an impairment of parasite sequestration by these drugs. This impairment could be explained by the deficiency in the CD36 receptor observed in some patients treated with ARVs (Nathoo et al., 2003). A recent investigation of the impact of ARVs on the liver stage of *Plasmodium* infection has shown that, consistent with what is observed for erythrocytic stages, the PIs LPV and RTV are potent inhibitors of the parasite's development in hepatic cells (Hobbs et al., 2009). A reduction in the *in vivo Plasmodium yoelii* liver burden by NNRTIs (Hobbs et al., 2012) and of the *in vivo Plasmodium berghei* liver burden by etravirine (ETV) (Machado et al., 2017) have also been reported.

In this study, we employed a recently developed luminescence-based *in vitro* assay (Azevedo et al., 2017) to determine the ability of ARVs and current first-line ARTs to inhibit the development of *Plasmodium* mosquito stages *in vitro*. We further validated those results by assessing the *in vivo* inhibitory activity of the first-line ARTs and selected alternative drug combinations against the sexual stages of the parasite's life cycle, as well as their impact on oocyst infection. This study demonstrates that the current field treatments against HIV have an impact on the mosquito stages of *Plasmodium* and suggest the evaluation of the possible inclusion of both rilpivirine (RPV) and ETV in alternative ARTs.

MATERIALS AND METHODS

Animals and Parasite Lines

Six- to eight-week-old male BALB/cByJ mice were purchased from Charles River Laboratories Inc. (France). The *Pb*CSGFP-Luc (Azevedo et al., 2017) and *Pb*Fluo-frmg (Ponzi et al., 2009) *P. berghei* parasite lines were employed in the experimental work, all of which was carried out under BSL1 or ABSL2 conditions. The former parasite line expresses the fusion gene *gfp-luc* under the control of the *csp* gene promotor (RMgm-152), and the latter

expresses red fluorescent protein and green fluorescent protein (GFP) under the control of stage-specific promotors for female and male gametocytes, respectively (RMgm-164). The genes were integrated by double recombination into the silent *230p* gene locus of the *P. berghei* genome.

Ookinete Production and Culturing

Ookinetes were generated as previously described (Azevedo et al., 2017). Briefly, two male BALB/cBbyJ mice were infected with 10^7 *Pb*CSGFP-Luc-infected red blood cells (RBCs) 3 days posttreatment with 0.1 ml phenylhydrazine (25 mg/ml). On the third day of infection, when three to six exflagellation events/field (1:4 dilution) were observed by light microscopy field (40 × magnification), mice were killed, and ∼2 ml of infected blood was collected by cardiac puncture and added to Roswell Park Memorial Institute (RPMI) 1640 Medium (Sigma) 37°C. After washing with RPMI, 5 μl of blood and 195 μl of ookinete culturing medium [RPMI-1640, 25 mM HEPES, 0.4 mM hypoxanthine, 100 mM xanthurenic acid (Fluka, 85570), 10% fetal bovine serum, pH 7.6] were added per well of a 96-well plate and incubated for 24 h at 19°C for ookinete formation. In parallel, a 1:20 dilution of blood in ookinete medium was cultured in T75 flasks for 22–24 h at 19°C for the production of ookinetes. Ookinetes were purified employing a Nycodenz (Axis-Shield) gradient. The contents of the T75 flask were collected, and the RBCs were lysed for 15 min on ice with 30 volumes of ice-cold 0.17 M ammonium chloride. After removal of the lysed RBCs by washing with RPMI-1640, ookinetes were purified on a 69% Nycodenz gradient by centrifugation at 650 × *g* and 4°C for 30 min. Following centrifugation, ookinetes were collected by aspiration of the dark brown ring formed, washed in RPMI-1640, and resuspended in 1 ml of oocyst medium [Schneider's medium (Sigma S0146), 15% fetal bovine serum, penicillin/streptomycin (50 U/ml, 50 μg/ml), and gentamicin (50 μg/ml)].

Oocyst Cultures

Following purification, ookinetes were cocultured with *Drosophila melanogaster* S2 cells (*Drosophila* Genomics Resource Center, Bloomington, IN, United States) in a 1:10 ratio (10^4 ookinetes and 10^5 S2 cells) in oocyst medium, as previously described (Azevedo et al., 2017). The cultures were maintained in 96-well plates for up to 15 days at 19°C. One quarter of the medium volume was replaced by fresh medium three times a week, and 10^5 S2 cells were added to the medium once per week.

Evaluation of the Activity of ARV Compounds Against *Plasmodium* Mosquito Stages *in vitro*

The activity of 10 μM of each ARV compound was independently assessed against ookinetes and oocysts. This concentration was selected based on the standards established by previous experimental work by Delves et al. (2012) and Azevedo et al. (2017) on the *Plasmodium* transmission blocking effect of various compounds and after a preliminary screen of all the compounds under evaluation at 50, 10, and 1 μM. Eighteen compounds belonging to four different classes of ARVs were evaluated: (1) PI – amprenavir (APV), atazanavir (ATV), DRV, IDV, LPV, nelfinavir (NFV), RTV, and SQV; (2) INSTIs – raltegravir (RAL); (3) NRTIs – abacavir (ABC), tenofovir (TDF), emtricitabine (FTC), zidovudine (AZT), and lamivudine (3TC); and (4) NNRTIs – ETV, nevirapine (NVP), EFV, and RPV. Drug combinations *in vitro* assays contained 10 μM of each compound. ARV compounds were obtained from the NIH AIDS and Reference Reagent Program. Ten millimolars stock solutions of the compounds was prepared in dimethyl sulfoxide (DMSO), and serially diluted compounds were employed for activity assessments. A concentration of DMSO equivalent to that present in the highest compound concentration was also used as a control in all activity assays. The compounds' effect on gametocyte to ookinete transition was determined by adding them to 1-h-old gametocyte cultures. After 24 h, the parasite load was assessed by bioluminescence employing the Firefly Luciferase Assay Kit (Biotium) according to the manufacturer's instructions, with some modifications. Briefly, the well contents were collected, washed with PBS, spun down, and frozen in 50 μl of 1:5 lysis buffer. Thirty microliters of the lysed supernatant was transferred into each well of a white 96-well plate. Fifty microliters of luciferin Firefly Luciferase Assay buffer (1:50 ratio) was added to the samples, and the parasite load was determined by measuring luminescence intensity using a microplate reader (Tecan Infinite M200). To assess their effect on oocyst formation, compounds were mixed with ookinetes and cultured with *D. melanogaster* S2 cells for 3 days, following which the cultures were collected and lysed, and parasite load was determined by luminescence measurement, as described above. The effect of the compounds on oocyst development was assessed by adding them to 3-day-old oocyst cultures, lysing the cultures 12 days later, and determining the parasite load by bioluminescence, as described above.

Evaluation of the Activity of ARV Compounds Against *Plasmodium* Blood and Mosquito Stages *in vivo*

To evaluate the *in vivo* antiplasmodial activity of first-line ARV regimens and proposed modifications, three male BALB/cByJ mice per experimental group were infected with 10^7 infected RBCs of the parasite line *Pb*Fluo-frmg from a donor previously infected from a parasite stock vial. After 24 h, and during the following 4 days, parasitemia and gametocytemia were assessed by the collection of 4 μl of tail blood in 200 μl of PBS. One hundred microliters of the solution was further diluted in PBS at a 1:1 ratio and stored at 4°C, while the remainder was diluted in a 1:1 ratio of PBS containing 1.25 mM of red fluorescent nucleic acid stain Syto® 61 (ThermoFisher Scientific) and incubated for 20 min at room temperature in the dark. The samples were analyzed on an LSR Fortessa X-20 flow cytometer (Becton, Dickinson and Company). Forty-eight hours postinfection, a suspension of the compounds in sunflower oil was administered by oral gavage. Compounds were administered at an allometry-scaled dose, and in accordance with the administration regimen recommended for humans, all the compounds were administered on a 24-h schedule except for ETV, which was administered every 12 h (**Supplementary Table S1**). DMSO in a dosage equivalent to

that present in the highest compound combination was used as a control. On the fifth day of infection, ∼50 previously starved *Anopheles stephensi* mosquitoes per experimental condition were allowed to feed for ∼30 min on anesthetized, infected, drug-treated mice. Mosquitoes were kept in standard dietary conditions, at 20°C with 80% humidity under a 12-h light/dark cycle. Ten days after infection, mosquito midguts were dissected and stained with a solution of 0.025% mercurochrome to quantify oocyst infection by microscopy analysis. Images were acquired on a Leica DM2500 and analyzed with the FIJI software (Schindelin et al., 2012).

Statistical Analysis

Data regarding the compounds' *in vitro* effect and mosquito infection were analyzed using the Kruskal–Wallis test. A chi-squared test was used to compare mosquito infection prevalence. Data on the compounds' effect on parasitemia and gametocytemia *in vivo* were analyzed by non-linear regression analysis. Results were considered significant for $P < 0.05$. All statistical tests were performed using the GraphPad Prism software (version 6.00, GraphPad Software, La Jolla, CA, United States).

Ethics Statement

All work with laboratory animals was performed according to National and European regulations (Directive 2010/63/EU). All protocols were approved by the Animal Experimentation Ethics Committee (AWB_2015_09_MP_Malaria) of the Instituto de Medicina Molecular João Lobo Antunes and are in accordance with the Federation of European Laboratory Animal Science Associations (FELASA) guidelines.

RESULTS

In vitro Activity of ARV Compounds Against Ookinete Formation

The activity of a 10-μM concentration of each of 18 ARV compounds from 4 different drug classes – PI: APV, ATV, DRV, IDV, LPV, NFV, RTV, and SQV; INSTIs: RAL; NRTIs: ABC, FTC, 3TC, TDF, and AZT; and NNRTIs: EFV, ETV, NVP, and RPV – against *P. berghei* sporogonic stages *in vitro* was evaluated (**Figure 1A**). Our results showed that the PIs LPV and RTV led to at least 60% reduction in ookinete formation relative to the controls, whereas the NNRTI ETV inhibited parasite development by ∼40% (**Figure 1B** and **Supplementary Table S2**). Conversely, neither of the NRTI and INSTI compounds under evaluation displayed an inhibitory activity against this stage of the parasite's sporogonic development at the concentration used in this assay (**Figure 1B**).

In vitro Effect of ARVs on Oocyst Formation and Development

We subsequently assessed the activity of the 18 compounds listed above on oocyst formation and development. Our results showed that 10 μM concentrations of the NNRTIs

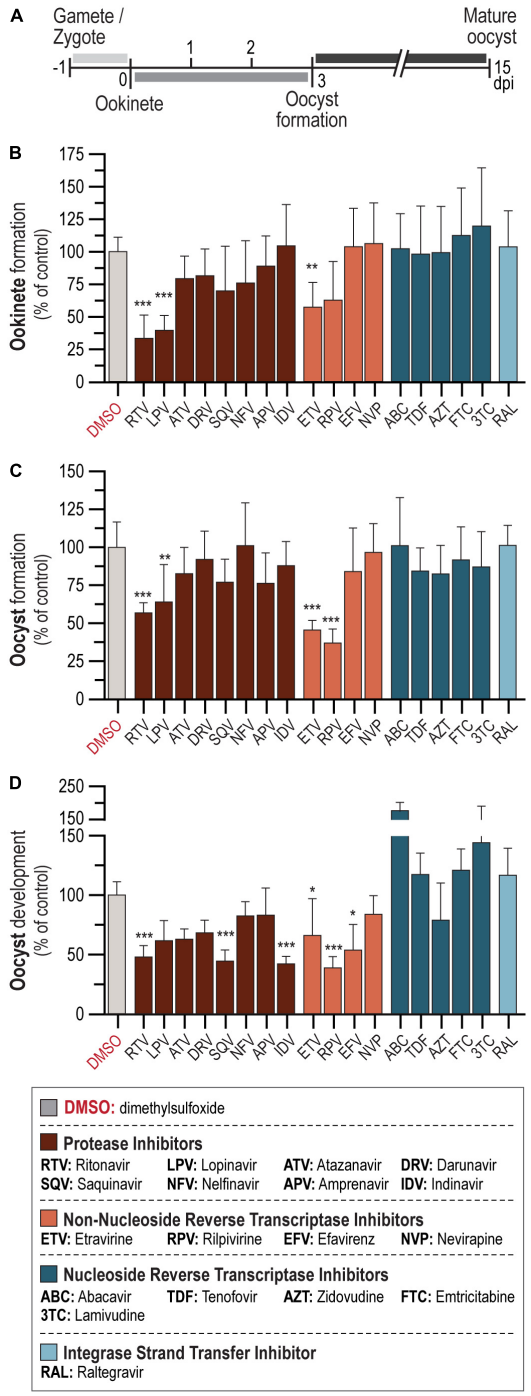

FIGURE 1 | *In vitro* activity of ARV compounds on *P. berghei* sporogonic stages. **(A)** Timeline of *P. berghei* sporogonic development and drug incubation periods. **(B)** Activity of ARV compounds on the conversion of zygotes/gametes into ookinetes. **(C)** Activity of ARV compounds on oocyst formation. **(D)** Activity of ARV compounds on oocyst development. All compounds were employed at 10 μM. Bars correspond to RLU measurements represented as the percentage of RLU of the DMSO control. Results are expressed as the mean ± SD. Statistically significant differences between control and treated conditions were analyzed using the Kruskal–Wallis test. $N = 3$–6. ***$P < 0.001$; **$P < 0.01$; *$P < 0.05$. Detailed statistical analysis is presented in **Supplementary Table S2**.

RPV and ETV inhibited oocyst formation by ∼60 and 50%, respectively. A milder effect has observed for two PIs, with RTV inhibiting oocyst formation by ∼40% and LPV by ∼35% (**Figure 1C** and **Supplementary Table S2**). The PIs IDV, SQV, and RTV, as well as the NNRTI RPV, led to more than 50% inhibition of oocyst development (**Figure 1D** and **Supplementary Table S2**). Smaller effects were observed for the NNRTIs EFV and ETV, which impaired oocyst development by ∼45 and ∼30%, respectively (**Figure 1D** and **Supplementary Table S2**). Interestingly, treatment with the NRTIs ABC and 3TC consistently led to increased parasite loads relative to vehicle-treated controls (**Figure 1D**). None of the remaining compounds under evaluation displayed activity against either oocyst formation or development.

In vitro Activity of First-Line Regimen ART Against *P. berghei* Sporogonic Stages

According to WHO recommendations, ARV should be administered as an integral part of well-established ART regimens. The preferred backbone for first-line treatment against HIV in adults and adolescents is composed of two NRTIs and an NNRTI or INSTI, while for treatment of children <3 years old, WHO's suggested drug combination is AZT + 3TC + LPV/r (World Health Organization [WHO], 2016). We assessed the activity of the first-line ARV regimen for adults and adolescents, TDF (NRTI) + 3TC (NRTI) + EFV (NNRTI), and children, AZT (NNRTI) + 3TC (NNRTI) + LPV/r (PIs), against the parasite's sporogonic development (**Figures 2A–C**). In parallel, informed by our results regarding the activity of individual ARV compounds, we evaluated alternative drug combinations for adults and adolescents where EFV was replaced by either of the NNRTIs ETV or RPV, and alternative drug combinations for children where LPV/r was replaced by either of the best performing PIs in the individual screen, SQV or IDV (**Figures 2A–C**). Our results showed that a combination of 10 μM of the drugs AZT + 3TC + LPV/r displayed a ∼50% inhibitory activity against gametocyte to ookinete transition, whereas the drug combinations TDF + 3TC + ETV and RPV inhibited this process by ∼30% (**Figure 2A**). The combinations AZT + 3TC + LPV/r and TDF + 3TC + RPV markedly inhibited oocyst formation (∼90 and 80% inhibition, respectively), and development (∼50 and ∼40% inhibition, respectively), whereas TDF + 3TC + ETV inhibited oocyst formation by 70% but had no effect on oocyst development. Finally, the combination of TDF + 3TC + EFV also resulted in a ∼50% reduction of oocyst development but showed no effect on oocyst formation (**Figures 2B,C**).

Evaluation of ART Effect on *P. berghei* Sporogonic Stages *in vivo*

To validate our *in vitro* results, the antiplasmodial effect of the first-line drug combinations TDF + 3TC + EFV and AZT + 3TC + LPV/r, were evaluated in an *in vivo* setting (**Figure 3A**). Informed by our *in vitro* data, ETV and RPV were also screened in combination with TDF + 3TC. Our results showed that neither of the drug treatments employed had an impact on *P. berghei* parasitemia and gametocytemia, when compared with vehicle-treated mice (**Figures 3B–D**). Our data further showed that the drug combination AZT + 3TC + LPV/r displayed a strong ∼90% impact on median oocyst infection in the mosquitoes, whereas the remaining drug combinations with EFV, ETV, and RPV led to smaller reductions in the intensity of infection (**Figure 3E** and **Supplementary Table S2**). This reduction does not result from an increase in the number of non-infected mosquitoes, but rather from a reduction in the oocyst load on infected mosquitoes, which is also significant upon treatment with the TDF + 3TC + EFV combination (**Figures 3F,G** and **Supplementary Table S3**).

DISCUSSION

Human immunodeficiency virus and *Plasmodium* coinfections raise serious concerns in the regions where both organisms overlap geographically (Kharsany and Karim, 2016; Kwenti, 2018). It has been hypothesized that the interaction between HIV and *Plasmodium* is both synergistic and bidirectional. Thus, infection with HIV might increase the severity of *Plasmodium* infection, while the HIV viral load has been shown to increase during a *Plasmodium* infection (Nyabadza et al., 2015; Kwenti, 2018). Numerous studies report the effect of HIV ARVs on the different stages of the *Plasmodium* life cycle (Parikh et al., 2005; Andrews et al., 2006; Lek-Uthai et al., 2008; Hobbs et al., 2009, 2012, 2013; Peatey et al., 2010; Li et al., 2011; Nsanzabana and Rosenthal, 2011; Machado et al., 2017). However, little is known about how ARTs may impair the transmission and mosquito stages of *Plasmodium* parasites.

The results presented here show that the several ARV compounds impair various stages of *Plasmodium* sporogonic development *in vitro* and that the WHO-recommended first-line ARTs employed against HIV have a significant impact on *Plasmodium* infection in the mosquito vector (**Figures 3E,G**). However, neither of the current first-line ART nor the alternative combinations evaluated in this work inhibited *P. berghei* asexual and gametocyte stages at clinically relevant concentrations *in vivo* (**Figures 3B–D**). It has been shown that HIV infection leads to an increase in the production of proinflammatory cytokines tumor necrosis factor, interleuking (IL)-1β, and IL-6, which can be partially reversed by ART (Amirayan-Chevillard et al., 2000; Kedzierska and Crowe, 2001), suggesting a possible indirect effect of ART on *Plasmodium* infection. However, the lack of impact of ARVs on the blood stages of *Plasmodium in vivo* suggests that a different mechanism may be responsible for the effects observed on the parasite's sporogony. Our results suggest that PIs might either affect the parasite's fusing process by impairing exflagellation *in vitro*, as previously suggested for *P. falciparum* (Hobbs et al., 2013), or act further downstream of the fertilization process.

Similarly to what has previously been shown for the blood stages of *P. falciparum* (Parikh et al., 2005; Andrews et al., 2006; Peatey et al., 2010; Nsanzabana and Rosenthal, 2011;

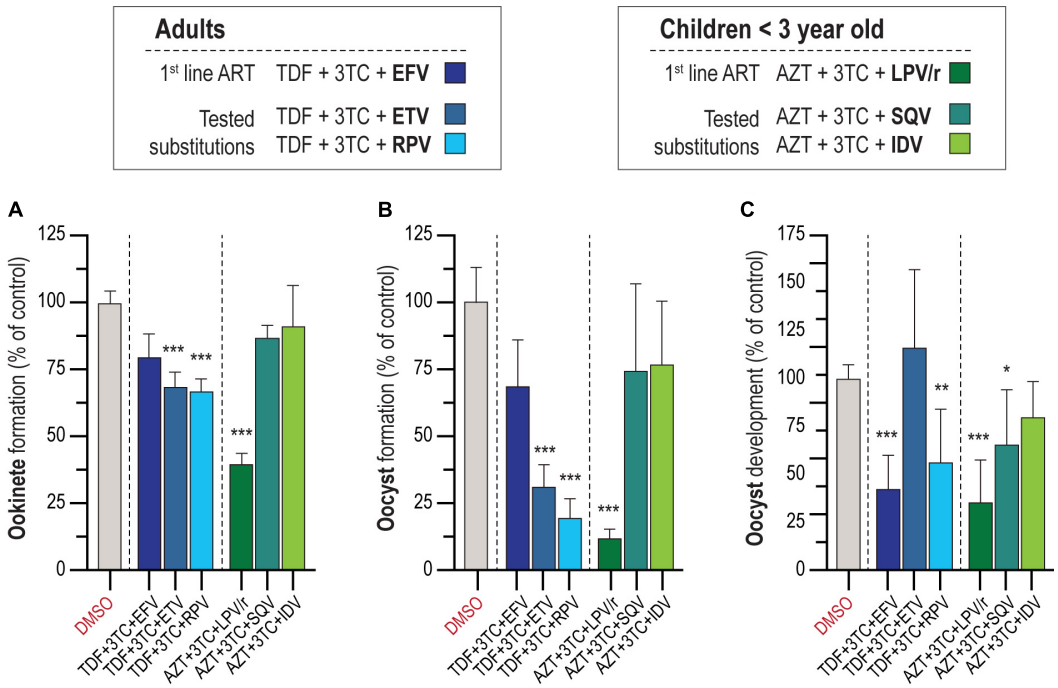

FIGURE 2 | *In vitro* activity of ART on the *P. berghei* sporogonic stages. **(A)** Effect of first-line ART employed for adults and adolescents and for children under 3 years old and suggested substitutions on the conversion of zygotes/gametes into ookinetes. **(B)** Activity of first-line ART and suggested substitutions on oocyst formation. **(C)** Activity of first-line ART and suggested substitutions on oocyst development. All compounds were screened at 10 μM; TDF, tenofovir; 3TC, lamivudine; EFV, efavirenz; ETV, etravirine; RPV, rilpivirine; AZT, zidovudine; LPV/r, lopinavir/ritonavir; SQV, saquinavir; IDV, indinavir. RLU measurements represented as the percentage of RLU of the DMSO control. Statistically significant differences between control and treated conditions were analyzed using the Kruskal–Wallis test. Results are expressed as the mean ± SD. $N = 3–4$. ***$P < 0.001$; **$P < 0.01$; *$P < 0.05$.

Hobbs et al., 2013), our results indicate that PIs display the strongest *in vitro* inhibitory activity against *P. berghei* transition from gametocytes to ookinetes (**Figure 1B**). It has been suggested that PIs act on PMs, a class of *Plasmodium*' aspartic proteases (Parikh et al., 2005; Bonilla et al., 2007; Skinner-Adams et al., 2007; Peatey et al., 2010). Although HIV aspartic proteases are structurally different from *Plasmodium* PMs, several of the latter have been described in the sexual stages of *P. falciparum*, *P. berghei*, and *P. yoelii* (Hall et al., 2005; Young et al., 2005). Our results show that PIs strongly inhibit the formation and development of oocysts *in vitro* (**Figures 1C,D**). Accordingly, the first-line ART containing the PIs LPV/r had the strongest impact on oocyst intensity *in vivo* (**Figures 3E,G**). Although, to the best of our knowledge, the effect of ARVs on ookinetes has not been previously reported, it is known that PMs IV, VII, and X (Li et al., 2010, 2016) are expressed by this parasite stage, thus providing a possible explanation for the effect of PIs on the transformation of ookinetes into oocysts. Moreover, PM VI, whose role is yet undefined, seems crucial for the early oocyst stages of sporogonic development (Li et al., 2016). Thus, the observed inhibition of oocyst formation and development *in vitro* by PIs (**Figures 1C,D**) may suggest that PM VI could be the target of drugs belonging to this class.

We further observed that LPV and RTV had a stronger inhibitory activity on sporogony when tested in combination than individually (**Figures 1B–D** and **2A–C**). RTV is currently administered exclusively as a pharmacokinetic enhancer of other PIs due to its effect on cytochrome P450 3A4 isoenzyme (Hull and Montaner, 2011). However, since this enzyme is absent from the *in vitro* system employed here, the results obtained may be explained by an additive effect of LPV and RTV. We also observed a moderate inhibition of the sporogonic stages of *P. berghei in vitro* by several NNRTIs (**Figures 1A–C**). A reverse transcriptase telomerase has been previously identified and characterized in *P. falciparum* (Figueiredo et al., 2005), and although it differs from HIV's reverse transcriptase, it might contribute to explaining the observed effect of these drugs on the early and late oocyst stage of the parasite's life cycle (**Figures 1C,D**).

Both the first-line ART and the alternative ARV combinations tested here had similar impacts on oocyst infection in the mosquito (**Figures 3E,G**). Our results show that the current first-line ART for children under 3 years old AZT + 3TC + LPV/r is the drug combination that most effectively inhibits the sporogonic stages of *P. berghei in vivo*. Interestingly, previous studies showed that LPV/r inhibits oocyst infection in *P. falciparum* (Hobbs et al., 2013) and reduces parasite *P. yoelii* liver burden (Hobbs et al., 2009). The impact of current first-line ART for adults and adolescents on mosquito infection, which includes EFV, was similar to that of the suggested alternatives employing ETV and RPV. A previous study by Machado et al. (2017)

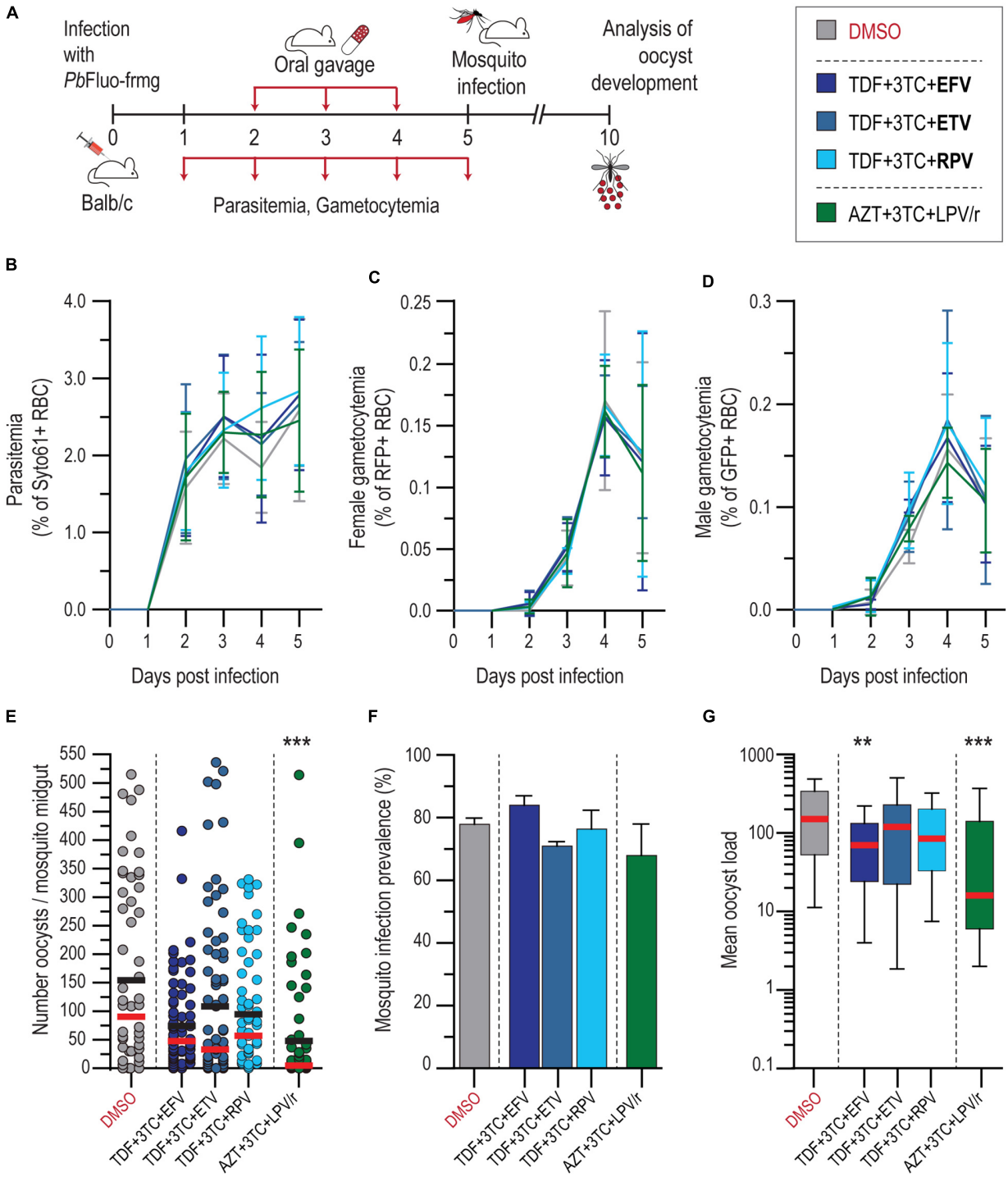

FIGURE 3 | *In vivo* activity of ART on blood and transmission stages of *P. berghei*. **(A)** Schematics of drug administration and sample collection schedules. **(B–D)** Activity of ART and suggested alternative drug combinations on *P. berghei* parasitemia **(B)**, female **(C)**, and male **(D)** gametocytemia in mice. Results are expressed as the mean percentage of syto 61-positive events ± SD for parasitemia, percentage of RFP^+ events for female gametocytemia and percentage of GFP^+ for male gametocytemia. **(E)** Impact of ART and suggested alternatives on *P. berghei* mosquito infection measured as oocyst intensity per mosquito. Results are represented individually by number of parasites per mosquito midgut. Horizontal red and black lines represent median and mean, respectively. **(F)** Prevalence of oocyst infection in mosquitoes infected with *P. berghei* expressed as the mean ± SD. **(G)** Average *P. berghei* oocyst infection intensity upon ART and suggested alternatives in infected mosquitoes. Box plot represent the median and 25th and 75th percentile. $N = 2$. $^{***}P < 0.001$; $^{**}P < 0.01$. In **(B–D)**, statistically significant differences between control and treated conditions for blood stage *P. berghei* development were analyzed using a non-linear regression analysis. In **(E)**, Kruskal–Wallis test was used to calculate *P* values and determine the significance of parasite numbers. A chi-squared test was used to compare infection prevalence values in **(F)**. Detailed statistical analysis is presented in **Supplementary Table S3**.

identified ETV as a stronger inhibitor of the hepatic stages of *P. berghei* than the current recommended ART with EFV.

Overall, our results suggest that both ETV and RPV, as well as other ARVs that may have an impact on *Plasmodium* transmission, should be contemplated when considering alternative ARTs in malaria-endemic regions. However, to fully ascertain the possible impact of these findings in such settings, additional work is required to assess the impact of these compounds on transmission of *P. falciparum* sporozoites. Furthermore, given the importance of the mosquito microbiota on infection by *Plasmodium*, it would be interesting to replicate our results obtained *in vivo* in mosquitoes depleted of microbiota (Dong et al., 2009; Kalappa et al., 2018). Finally, a further understanding of the mechanism of action of ARVs against *Plasmodium* parasites is essential for developing new drugs that might have both ARV and antiplasmodial activity. By identifying the target of HIV PIs on *Plasmodium* parasites, new drugs could be developed that have a stronger impact on *Plasmodium* infection.

DATA AVAILABILITY STATEMENT

The raw data supporting the conclusion of this article will be made available by the authors, without undue reservation, to any qualified researcher.

ETHICS STATEMENT

The animal study was reviewed and approved by the Animal Experimentation Ethics Committee (AWB_2015_09_MP_Malaria) of the Instituto de Medicina Molecular João Lobo Antunes.

AUTHOR CONTRIBUTIONS

RA performed the experimental work. AM and MP designed and supervised the study. RA and MP wrote the manuscript. RA and AM designed the figures.

FUNDING

This work was carried out with the support of grants PTDC-BBB-BMD-2695-2014 and 02/SAICT/2017/29550 from Fundação para a Ciência e Tecnologia, Portugal (FCT) to AM and MP, respectively, and by FCT grant UID/BIM/50005/2019 [Ministério da Ciência, Tecnologia e Ensino Superior (MCTES) through Fundos do Orçamento de Estado]. RA was supported by FCT's fellowship BD/131334/2017. AM was supported by FCT's fellowship SFRH/BPD/80693/2011. MP was supported by FCT's Investigador FCT 2013 and CEEC 2018 fellowships.

ACKNOWLEDGMENTS

We are grateful to Filipa Teixeira for mosquito production, Andreia Santos and Bárbara Oliveira for technical assistance, and Gunnar Mair for sharing the *Pb*Fluo-frmg parasite line. All antiretroviral compounds were obtained through the NIH AIDS Reagent Program, Division of AIDS, NIAID, NIH.

SUPPLEMENTARY MATERIAL

The Supplementary Material for this article can be found online at: https://www.frontiersin.org/articles/10.3389/fmicb.2019.03048/full#supplementary-material

REFERENCES

Amirayan-Chevillard, N., Tissot-Dupont, H., Capo, C., Brunet, C., Dignat-George, F., Obadia, Y., et al. (2000). Impact of highly active anti-retroviral therapy (HAART) on cytokine production and monocyte subsets in HIV-infected patients. *Clin. Exp. Immunol.* 120, 107–112. doi: 10.1046/j.1365-2249.2000.01201.x

Andrews, K. T., Fairlie, D. P., Madala, P. K., Ray, J., Wyatt, D. M., Hilton, P. M., et al. (2006). Potencies of human immunodeficiency virus protease inhibitors in vitro against *Plasmodium falciparum* and in vivo against murine malaria. *Antimicrob. Agents Chemother.* 50, 639–648. doi: 10.1128/AAC.50.2.639-648.2006

Azevedo, R., Markovic, M., Machado, M., Franke-Fayard, B., Mendes, A. M., and Prudêncio, M. (2017). A bioluminescence method for in vitro screening of *Plasmodium* transmission-blocking compounds. *Antimicrob. Agents Chemother.* 61:AAC.2699-2616. doi: 10.1128/AAC.02699-2616

Baton, L. A., and Ranford-Cartwright, L. C. (2005). Spreading the seeds of million-murdering death: metamorphoses of malaria in the mosquito. *Trends Parasitol.* 21, 573–580. doi: 10.1016/j.pt.2005.09.012

Bonilla, J. A., Bonilla, T. D., Yowell, C. A., Fujioka, H., and Dame, J. B. (2007). Critical roles for the digestive vacuole plasmepsins of *Plasmodium falciparum* in vacuolar function. *Mol. Microbiol.* 65, 64–75. doi: 10.1111/j.1365-2958.2007.05768.x

Butcher, G. A. (1997). Antimalarial drugs and the mosquito transmission of *Plasmodium*. *Int. J. Parasitol.* 27, 975–987. doi: 10.1016/S0020-7519(97)00079-79

Delves, M., Plouffe, D., Scheurer, C., Meister, S., Wittlin, S., Winzeler, E. A., et al. (2012). The activities of current antimalarial drugs on the life cycle stages of *Plasmodium*: a comparative study with human and rodent parasites. *PLoS Med.* 9:e1001169. doi: 10.1371/journal.pmed.1001169

Dong, Y., Manfredini, F., and Dimopoulos, G. (2009). Implication of the mosquito midgut microbiota in the defense against malaria parasites. *PLoS Pathog.* 5:e1000423. doi: 10.1371/journal.ppat.1000423

Figueiredo, L., Rocha, E., Mancio-Silva, L., Prevost, C., Hernandez-Verdun, D., and Scherf, A. (2005). The unusually large *Plasmodium* telomerase reverse-transcriptase localizes in a discrete compartment associated with the nucleolus. *Nucleic Acids Res.* 33, 1111–1122. doi: 10.1093/nar/gki260

Hall, N., Karras, M., Raine, J. D., Carlton, J. M., Kooij, T. W. A., Berriman, M., et al. (2005). A comprehensive survey of the *Plasmodium* life cycle by genomic, transcriptomic, and proteomic analyses. *Science* 307, 82–86. doi: 10.1126/science.1103717

HIV/AIDS (2019). *HIV/AIDS: The Basics Understanding HIV/AIDS. AIDSinfo*. Available at: https://aidsinfo.nih.gov/understanding-hiv-aids/fact-sheets/19/45/hiv-aids--the-basics (Accessed August 7, 2019).

Hobbs, C. V., Tanaka, T. Q., Muratova, O., Van Vliet, J., Borkowsky, W., Williamson, K. C., et al. (2013). HIV treatments have malaria gametocyte killing and transmission blocking activity. *J. Infect. Dis.* 208, 139–148. doi: 10.1093/infdis/jit132

Hobbs, C. V., Voza, T., Coppi, A., Kirmse, B., Marsh, K., Borkowsky, W., et al. (2009). HIV protease inhibitors inhibit the development of preerythrocytic-stage *Plasmodium* parasites. *J. Infect. Dis.* 199, 134–141. doi: 10.1086/594369

Hobbs, C. V., Voza, T., De La Vega, P., Vanvliet, J., Conteh, S., Penzak, S. R., et al. (2012). HIV nonnucleoside reverse transcriptase inhibitors and trimethoprim-sulfamethoxazole inhibit *Plasmodium* liver stages. *J. Infect. Dis.* 206, 1706–1714. doi: 10.1093/infdis/jis602

Hull, M. W., and Montaner, J. S. G. (2011). Ritonavir-boosted protease inhibitors in HIV therapy. *Ann. Med.* 43, 375–388. doi: 10.3109/07853890.2011.572905

Kalappa, D. M., Subramani, P. A., Basavanna, S. K., Ghosh, S. K., Sundaramurthy, V., Uragayala, S., et al. (2018). Influence of midgut microbiota in *Anopheles stephensi* on *Plasmodium berghei* infections. *Malar J* 17:385. doi: 10.1186/s12936-018-2535-2537

Kedzierska, K., and Crowe, S. M. (2001). Cytokines and HIV-1: interactions and clinical implications. *Antivir. Chem. Chemother.* 12, 133–150. doi: 10.1177/095632020101200301

Kharsany, A. B. M., and Karim, Q. A. (2016). HIV Infection and AIDS in sub-Saharan Africa: current status, challenges and opportunities. *Open AIDS J.* 10, 34–48. doi: 10.2174/1874613601610010034

Kwenti, T. E. (2018). Malaria and HIV coinfection in sub-Saharan Africa: prevalence, impact, and treatment strategies. *Res. Rep. Trop. Med.* 9, 123–136. doi: 10.2147/RRTM.S154501

Lek-Uthai, U., Suwanarusk, R., Ruengweerayut, R., Skinner-Adams, T. S., Nosten, F., Gardiner, D. L., et al. (2008). Stronger activity of human immunodeficiency virus type 1 protease inhibitors against clinical isolates of *Plasmodium vivax* than against those of *P. falciparum*. *Antimicrob. Agents Chemother.* 52, 2435–2441. doi: 10.1128/AAC.00169-168

Li, F., Bounkeua, V., Pettersen, K., and Vinetz, J. M. (2016). *Plasmodium falciparum* ookinete expression of plasmepsin VII and plasmepsin X. *Malaria J.* 15:111. doi: 10.1186/s12936-016-1161-1165

Li, F., Patra, K. P., Yowell, C. A., Dame, J. B., Chin, K., and Vinetz, J. M. (2010). Apical surface expression of aspartic protease plasmepsin 4, a potential transmission-blocking target of the *Plasmodium* ookinete. *J. Biol. Chem.* 285, 8076–8083. doi: 10.1074/jbc.M109.063388

Li, Y., Qin, L., Peng, N., Liu, G., Zhao, S., He, Z., et al. (2011). Antimalarial effects of human immunodeficiency virus protease inhibitors in rhesus macaques? *Antimicrob. Agents Chemother.* 55, 3039–3042. doi: 10.1128/AAC.00085-11

Liu, J., Gluzman, I. Y., Drew, M. E., and Goldberg, D. E. (2005). The role of *Plasmodium falciparum* food vacuole plasmepsins. *J. Biol. Chem.* 280, 1432–1437. doi: 10.1074/jbc.M409740200

Machado, M., Sanches-Vaz, M., Cruz, J. P., Mendes, A. M., and Prudêncio, M. (2017). Inhibition of plasmodium hepatic infection by antiretroviral compounds. *Front. Cell. Infect. Microbiol.* 7:329. doi: 10.3389/fcimb.2017.00329

Mota, M. M., Pradel, G., Vanderberg, J. P., Hafalla, J. C., Frevert, U., Nussenzweig, R. S., et al. (2001). Migration of *Plasmodium* sporozoites through cells before infection. *Science* 291, 141–144. doi: 10.1126/science.291.5501.141

Nathoo, S., Serghides, L., and Kain, K. C. (2003). Effect of HIV-1 antiretroviral drugs on cytoadherence and phagocytic clearance of *Plasmodium falciparum*-parasitised erythrocytes. *Lancet* 362, 1039–1041. doi: 10.1016/S0140-6736(03)14414-14415

Nsanzabana, C., and Rosenthal, P. J. (2011). in vitro activity of antiretroviral drugs against *Plasmodium falciparum*. *Antimicrob. Agents Chemother.* 55, 5073–5077. doi: 10.1128/AAC.05130-5111

Nyabadza, F., Bekele, B. T., Rúa, M. A., Malonza, D. M., Chiduku, N., and Kgosimore, M. (2015). The implications of HIV treatment on the HIV-Malaria coinfection dynamics: a modeling perspective. *Biomed. Res. Int.* 2015:659651. doi: 10.1155/2015/659651

Onchieku, N. M., Mogire, R., Ndung'u, L., Mwitari, P., Kimani, F., Matoke-Muhia, D., et al. (2018). Deciphering the targets of retroviral protease inhibitors in *Plasmodium berghei*. *PLoS One* 13:e0201556. doi: 10.1371/journal.pone.0201556

Parikh, S., Gut, J., Istvan, E., Goldberg, D. E., Havlir, D. V., and Rosenthal, P. J. (2005). Antimalarial activity of human immunodeficiency virus type 1 protease inhibitors. *Antimicrob. Agents Chemother.* 49, 2983–2985. doi: 10.1128/AAC.49.7.2983-2985.2005

Peatey, C. L., Andrews, K. T., Eickel, N., MacDonald, T., Butterworth, A. S., Trenholme, K. R., et al. (2010). Antimalarial asexual stage-specific and gametocytocidal activities of HIV protease inhibitors. *Antimicrob. Agents Chemother.* 54, 1334–1337. doi: 10.1128/AAC.01512-1519

Peatey, C. L., Leroy, D., Gardiner, D. L., and Trenholme, K. R. (2012). Anti-malarial drugs: how effective are they against *Plasmodium falciparum* gametocytes? *Malaria J.* 11:34. doi: 10.1186/1475-2875-11-34

Ponzi, M., Sidén-Kiamos, I., Bertuccini, L., Currà, C., Kroeze, H., Camarda, G., et al. (2009). Egress of *Plasmodium berghei* gametes from their host erythrocyte is mediated by the MDV-1/PEG3 protein. *Cell. Microbiol.* 11, 1272–1288. doi: 10.1111/j.1462-5822.2009.01331.x

Prudêncio, M., Mota, M. M., and Mendes, A. M. (2011). A toolbox to study liver stage malaria. *Trends Parasitol.* 27, 565–574. doi: 10.1016/j.pt.2011.09.004

Savarino, A., Cauda, R., and Cassone, A. (2005). aspartic proteases of *Plasmodium falciparum* as the target of hiv-1 protease inhibitors. *J. Infect. Dis.* 191, 1381–1382. doi: 10.1086/428781

Schindelin, J., Arganda-Carreras, I., Frise, E., Kaynig, V., Longair, M., Pietzsch, T., et al. (2012). Fiji: an open-source platform for biological-image analysis. *Nat. Meth.* 9, 676–682. doi: 10.1038/nmeth.2019

Sinden, R. E., Talman, A., Marques, S. R., Wass, M. N., and Sternberg, M. J. E. (2010). The flagellum in malarial parasites. *Curr. Opin. Microbiol.* 13, 491–500. doi: 10.1016/j.mib.2010.05.016

Skinner-Adams, T. S., Andrews, K. T., Melville, L., McCarthy, J., and Gardiner, D. L. (2007). Synergistic interactions of the antiretroviral protease inhibitors saquinavir and ritonavir with chloroquine and mefloquine against *Plasmodium falciparum* in vitro. *Antimicrob. Agents Chemother.* 51, 759–762. doi: 10.1128/AAC.00840-846

Skinner-Adams, T. S., McCarthy, J. S., Gardiner, D. L., and Andrews, K. T. (2008). HIV and malaria co-infection: interactions and consequences of chemotherapy. *Trends Parasitol.* 24, 264–271. doi: 10.1016/j.pt.2008.03.008

Skinner-Adams, T. S., McCarthy, J. S., Gardiner, D. L., Hilton, P. M., and Andrews, K. T. (2004). Antiretrovirals as antimalarial agents. *J. Infect. Dis.* 190, 1998–2000. doi: 10.1086/425584

Staines, H. M., and Sanjeev, K. (2012). *Treatment and Prevention of Malaria*, 1st Edn. Basel: Springer.

Vinetz, J. M. (2005). Plasmodium ookinete invasion of the mosquito midgut. *Curr. Top. Microbiol. Immunol.* 295, 357–382. doi: 10.1007/3-540-29088-5_14

World Health Organization [WHO] (2016). *Consolidated Guidelines on the Use of Antiretroviral Drugs for Treating and Preventing HIV Infection: Recommendations for a Public Health Approach*, 2nd Edn. Geneva: World Health Organization.

World Health Organization [WHO] (2019a). *World Malaria Report 2019*. Geneva: World Health Organization.

World Health Organization [WHO] (2019b). *Progress Report on HIV, Viral Hepatitis and Sexually Transmitted Infections*. Geneva: World Health Organization.

Xiao, L., Owen, S. M., Rudolph, D. L., Lal, R. B., and Lal, A. A. (1998). P*lasmodium falciparum* antigen-induced human immunodeficiency virus type 1 replication is mediated through induction of tumor necrosis factor-α. *J. Infect. Dis.* 177, 437–445. doi: 10.1086/514212

Young, J. A., Fivelman, Q. L., Blair, P. L., de la Vega, P., Le Roch, K. G., Zhou, Y., et al. (2005). The *Plasmodium falciparum* sexual development transcriptome: a microarray analysis using ontology-based pattern identification. *Mol. Biochem. Parasitol.* 143, 67–79. doi: 10.1016/j.molbiopara.2005.05.007

Conflict of Interest: The authors declare that the research was conducted in the absence of any commercial or financial relationships that could be construed as a potential conflict of interest.

frontiers in Microbiology

MINI REVIEW
published: 14 February 2020
doi: 10.3389/fmicb.2020.00164

Mining the Human Host Metabolome Toward an Improved Understanding of Malaria Transmission

Regina Joice Cordy[1,2]*

[1] Department of Biology, Wake Forest University, Winston-Salem, NC, United States, [2] Department of Microbiology and Immunology, Wake Forest School of Medicine, Winston-Salem, NC, United States

The big data movement has led to major advances in our ability to assess vast and complex datasets related to the host and parasite during malaria infection. While host and parasite genomics and transcriptomics are often the focus of many computational efforts in malaria research, metabolomics represents another big data type that has great promise for aiding our understanding of complex host-parasite interactions that lead to the transmission of malaria. Recent analyses of the complement of metabolites present in human blood, skin and breath suggest that host metabolites play a critical role in the transmission cycle of malaria. Volatile compounds released through breath and skin serve as attractants to mosquitoes, with malaria-infected hosts appearing to have unique profiles that further increase host attractiveness. Inside the host, fluctuations in the levels of certain metabolites in blood may trigger increased production of transmission-competent sexual stages (gametocytes), setting the stage for enhanced transmission of malaria from human to mosquito. Together, these recent discoveries suggest that metabolites of human blood, skin and breath play critical roles in malaria transmission. This review discusses recent advances in this area, with a focus on metabolites that have been identified to play a role in malaria transmission and methods that may lead to an improved understanding of malaria transmission.

Keywords: plasmodium, malaria, gametocyte, metabolomics, mass spectrometry, transmission, mosquito

OPEN ACCESS

Edited by:
Brandon Keith Wilder, Oregon Health & Science University, United States

Reviewed by:
Jeremy Keith Herren, International Centre of Insect Physiology and Ecology, Kenya
Gabriella Fiorentino, University of Naples Federico II, Italy

***Correspondence:**
Regina Joice Cordy
cordyrj@wfu.edu

Specialty section:
This article was submitted to Infectious Diseases, a section of the journal Frontiers in Microbiology

Received: *30 October 2019*
Accepted: *23 January 2020*
Published: *14 February 2020*

Citation:
Joice Cordy R (2020) Mining the Human Host Metabolome Toward an Improved Understanding of Malaria Transmission. Front. Microbiol. 11:164. doi: 10.3389/fmicb.2020.00164

INTRODUCTION

Technological advancements have been made in recent years in sequencing-based (genomics, transcriptomics, epigenomics) and mass spectrometry-based approaches (proteomics, lipidomics, and metabolomics). These so called 'omics technologies have enabled researchers to explore various biological contexts at multiple levels, and the integration of these technologies is being used to improve our understanding of a range of human diseases (Hasin et al., 2017). An exciting area in which 'omics technology has been applied is in the realm of host-microbe interactions, including the complex interplay between microbes and their hosts in both pathogenic (e.g., viral, bacterial, and parasitic) and commensal (e.g., microbiome) relationships. These such interactions between microbes and their human hosts are often quite complex, resulting from co-evolution over massive time scales.

A highly complex interaction exists between *Plasmodium* (the etiological agent of malaria) and its invertebrate and vertebrate hosts, resulting from tens of thousands of years of co-evolution (Loy et al., 2017). In addition to *Plasmodium's* ability to replicate asexually within the blood cells of vertebrate hosts, *Plasmodium* also undergoes complex stage conversions to successfully transmit itself to the invertebrate host (*Anopheles* mosquito), where it must again undergo a series of stage conversions to be successfully delivered to the next vertebrate host. The propagation of malaria, which is attributed to over 400,000 deaths annually (World Health Organization [WHO], 2018), is therefore highly dependent on the ability of *Plasmodium* to successfully undergo multiple complex stage conversions, and move efficiently between the invertebrate and vertebrates hosts. *Plasmodium* has evolved multiple mechanisms for manipulating its hosts in order to enhance the chances of its successful transmission (Koella, 2005; Cator et al., 2012), and the manipulation of the metabolites present in human blood, skin and breath appears to be one of these such mechanisms.

Metabolomics, the high-throughput profiling of small molecules, has been employed to investigate the role of small molecules (metabolites) in the stage conversions and host exchanges that lead to the successful transmission of malaria. Methods that have been employed to investigate such metabolites run the gamut from functional approaches (e.g., sensory attraction tests), classic metabolic approaches (e.g., fractionation and metabolic labeling), and mass spectrometry-based methods (e.g., gas and liquid chromatography). Within mass-spectrometry-based methods, untargeted big data metabolomics approaches and reference compound-based targeted approaches are both utilized.

In this review, the roles of host metabolites are discussed in the context of malaria transmission, with an emphasis on findings resulting from metabolomics-based investigations. Also discussed are the various ways in which different mass spectrometry-based techniques, computational analyses, and multi-omic modeling approaches can further our knowledge about the impact of host metabolites on malaria transmission.

METABOLIC WINDOWS INTO MALARIA TRANSMISSION

In step with ongoing efforts worldwide to eradicate malaria, there has been an increased focus in recent years on gaining an improved understanding of malaria transmission and in developing novel ways to block and interrupt the cycle. The process of malaria transmission involves complex transitions between mosquito vector and vertebrate host, involving multiple parasite stage transitions.

Initiating a malaria infection in a human begins with the bite of a female *Anopheline* mosquito, which must locate and bite a human host in order to take a bloodmeal (**Figure 1A**). In doing so, the mosquito injects sporozoite stage parasites into the blood of the human host. Once inside the host, and following a period of development within the liver, the parasites begin to replicate asexually within red blood cells. At some point during the infection, a subset of parasites diverge down a path of sexual development, resulting in the formation of mature male and female gametocytes (**Figure 1B**). Importantly, mature gametocytes are the only stages that can be picked up by a mosquito and go on to successfully undergo fertilization and further development within the mosquito. Inside the mosquito, oocysts develop, and eventually burst, and sporozoites are released, migrating to the salivary gland, where they are now ready to be transmitted to the next human host during a subsequent bloodmeal. Adding to the complexity, recent studies suggest that metabolites present in the human host's blood, skin, and breath affect the efficacy of each of the key transition points in the parasite's life cycle, enhancing transmission. Specifically, volatile metabolites in the skin and breath of malaria-infected hosts have been shown to increase attractiveness to the mosquito vector (**Figure 1A**). And upstream of that biting event, metabolites in the host's bloodstream appear to act as signals for parasites to increase their rate of developing transmissible gametocyte stages (**Figure 1B**). The following sections focus on how metabolites in the blood, skin and breath of malaria-infected hosts play key roles in malaria transmission through modulating (a) the attractiveness of hosts to mosquitoes and (b) the rate of gametocyte development within host blood.

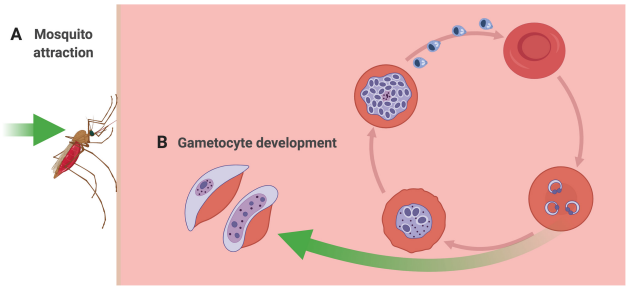

FIGURE 1 | Metabolic windows into malaria transmission. **(A)** Mosquito attraction and feeding. Malaria-infected human hosts produce volatile metabolites (e.g., terpenes and aldehydes) through their skin and/or breath that may serve as attractants for the female *Anopheles* mosquito when she takes her blood meal. **(B)** Gametocyte development. Certain metabolites undergo dynamic fluctuations in the blood plasma during the course of a malaria infection. Some specific metabolite changes have been hypothesized to be detected by parasites *in vivo* and trigger increased conversion to gametocytes (e.g., amino acids and phospholipids).

Metabolites Involved in Mosquito Attraction

It has been known for some time that carbon dioxide (CO_2) and other volatile chemicals help mosquitoes locate their vertebrate hosts and that certain molecules released through the skin, sweat and/or breath of vertebrates are attractive to mosquitoes (Brouwer, 1960; Takken and Kline, 1989). Some of these compounds, such as 1-Octen-3-ol, are routinely manufactured into baited mosquito traps, for example. However, a key question still remaining regarding the transmission of malaria is – *do individuals with malaria have increased attractiveness to mosquitoes, as compared to uninfected people?* (**Figure 1A**).

Gas chromatography mass spectrometry (GCMS) has been employed in efforts to answer this question. A specific type of GCMS called head space gas chromatography mass spectrometry (HS-GCMS) is used to analyze volatile organic compounds (VOCs) in the air space coming off of the subject or sample in question. Human cross-sectional studies using this method in the context of malaria have focused on analyzing VOCs from the breath of malaria-infected individuals. This work, termed "breathprinting," has demonstrated increased levels of multiple terpenes (α-pinene, limonene, and 3-carene), which are known mosquito-attractants (Nyasembe et al., 2012), in the breath of malaria-infected hosts (Kelly et al., 2015; Schaber et al., 2018) (**Table 1**). Additionally, controlled human malaria infection (CHMI) studies have also employed HS-GCMS to study the breath and skin odor composition in malaria-infected subjects (Berna et al., 2015; de Boer et al., 2017). In breath, four thioethers were found to increase in breath alongside increases in malaria parasitemia in blood: allyl methyl sulfide, 1-methylthio-propane, (*Z*)-1-methylthio-1-propene, and (*E*)-1-methylthio-1-propene (Berna et al., 2015). In skin, volatile compounds 2- and 3-methylbutanal, 3-hydroxy-2-butanone, and 6-methyl-5-hepten-2-one were all found to be present at higher levels in human skin odor during malaria infection, and also thought to attract mosquitoes (de Boer et al., 2017). In a further effort to identify VOCs derived from malaria parasites, an analysis of headspace from *in vitro Plasmodium* cultures was performed, and the headspace of the extracellular vesicles (EV) fraction also revealed an enrichment of a previously reported mosquito attractant aldehyde, hexanal (Correa et al., 2017) (**Table 1**).

Taking this concept a step further, a subset of studies have combined HS-GCMS with functional sensory tests in order to identify specific components of the metabolome that are detected by a mosquito's antenna. This approach, termed gas chromatography electroantennography (GC-EAG) involves the coupling of two approaches – chromatography-based compound analysis and an invertebrate sensory functional assessment. In short, as a compound comes off the column, it goes past a mosquito antenna. An olfactory nerve response occurs in the antenna, allowing for the determination of EAG-active metabolites. Example studies using GC-EAG include the analysis of foot odor of malaria-infected individuals, which revealed a set of aldehydes including heptanal, octanal, and nonanal produced at higher levels in malaria-infected individuals and shown to be sensed by mosquitoes (Robinson et al., 2018). Studies involving mammalian hosts including rodents have also used a combination of HS-GCMS and functional sensory tests and have demonstrated that 3-methyl butanoic acid, 2-methyl butanoic acid, hexanoic acid, and tridecane were all elevated at phases of mosquito attraction (De Moraes et al., 2014) (**Table 1**).

Olfactometers, devices used to test for host attractiveness to mosquitoes, have also been used to demonstrate that malaria-infected individuals are more attractive to mosquitoes. Of particular interest, this method has been used to demonstrate that humans carrying *Plasmodium* gametocytes have higher mosquito attractiveness than humans carrying asexual stages alone (Lacroix et al., 2005; Batista et al., 2014; Busula et al., 2017). Importantly this was seen in both *Plasmodium falciparum* and *P. vivax*. In addition, a similar approach was applied in a study of birds, which revealed that birds with chronic malaria are more attractive to mosquito vectors than those with acute malaria (Cornet et al., 2013).

While the production of specific VOCs seems to be linked to the presence of malaria parasites and particularly gametocytes

TABLE 1 | Metabolites associated with enhanced transmission of malaria.

Role	Context	Method	Metabolite	Citation
Increased mosquito attraction/feeding	mouse whole body headspace	GC	*Alkane*: tridecane *Fatty acids*: 3-methyl butanoic acid, 2-methyl butanoic acid, hexanoic acid	De Moraes et al., 2014
	In vitro Plasmodium headspace	GC	*Terpenes*: pinene, limonene	Kelly et al., 2015
	In vitro HMBPP-stimulated RBC headspace	GC	*Aldehydes*: octanal, nonanal, decanal *Terpenes*: α- and β-pinene, limonene *Oxide:* CO_2	Emami et al., 2017
	human skin (foot) headspace	GC	*Aldehyde*: 3-methylbutanal *Ketones*: 6-methyl-5-hepten-2-one, 2- and 3-hydroxy-2-butanone	de Boer et al., 2017
	In vitro Plasmodium headspace	GC	*Aldehyde*: hexanal	Correa et al., 2017
	human skin (foot) headspace	GC-EAG	*Aldehydes:* heptanal, octanal, nonanal	Robinson et al., 2018
	human breath	GC	*Terpenes:* α-pinene and 3-carene	Schaber et al., 2018
	human skin (foot) headspace	GC-EAG	*Aldehydes:* hexanal, nonanal *Aromatic hydrocarbon*: toluene	Stanczyk et al., 2019
Increased gametocyte development	*In vitro Plasmodium*	LC	*α-amino acid:* homocysteine	Beri et al., 2017
	in vitro Plasmodium, human blood	LC	*Phospholipid:* lysophosphotidylcholine	Brancucci et al., 2017; Usui et al., 2019
	In vitro Plasmodium	LC	*Phospholipids:* polyunsaturated fatty acid-containing phospholipids	Tanaka et al., 2019

within the mammalian hosts, the attraction by mosquitoes toward those hosts similarly appears to be affected by the infection status of the *mosquito*. Using olfactometers and neurophysiological assays, mosquitoes of the genus *Anopheles* were found to have a higher attractiveness toward human odors when they were infected with and carrying *Plasmodium* sporozoites than mosquitoes that were uninfected or were infected with those stages of the parasite that were not infectious yet (e.g., oocysts) (Cator et al., 2013; Smallegange et al., 2013). A recent study using GC-EAG to assess this question identified multiple compounds that infected mosquitoes responded to at a higher rate than uninfected mosquitoes, including some of the aldehydes identified in previous studies: hexanal and nonanal (Stanczyk et al., 2019) (**Table 1**). Further work combining olfactory tests with metabolomics approaches are likely to shed light on the full set of volatile chemicals that emanate from malaria-infected individuals, and can lead to broader characterization of compounds that increase host attractiveness to the mosquito vector.

Metabolites Involved in Gametocyte Development

While the attraction of mosquitoes to human hosts is a major part of malaria transmission, another key aspect is the production of gametocytes, which need to be present in the bloodstream of the human host in order to successfully transmit the parasite to the mosquito vector. The process by which asexually reproducing malaria parasites switch to sexual development is called gametocytogenesis and appears to involve both genetic and environmental cues. Specific transcriptional cascades are turned on during the transition from asexual to sexual replication, and environmental changes in host physiology have been long thought to contribute to this process (Josling and Llinás, 2015). A combination of mass spectrometry-based metabolomics, metabolic labeling approaches, and functional assays have implicated a role for exogenous metabolites in triggering sexual development. The primary question here being – *what are the signals in host blood that trigger Plasmodium to undergo gametocytogenesis?* (**Figure 1B**).

Liquid chromatography mass spectrometry (LC-MS) has been utilized in a number of studies to identify metabolites within *in vitro* culture media that are taken up or produced by *Plasmodium* parasites. Studies have been done to investigate the metabolic needs of asexually replicating *Plasmodium* parasites *in vitro* (Olszewski et al., 2009). Additional studies have focused on metabolites in human blood that are altered during malaria infections (Basant et al., 2010; Pappa et al., 2015; Surowiec et al., 2015; Decuypere et al., 2016; Gardinassi et al., 2017; Uppal et al., 2017; Ghosh et al., 2018; Cordy et al., 2019). This body of work has demonstrated the utility of this tool for identifying a wide range of physiological changes that occur in vertebrate hosts during malaria infection.

In addition to these aforementioned studies which focus on asexual replication, a subset of investigations focus on how host metabolites affect disease transmission. For example, a combination of *in vitro* and *in vivo* studies has identified a role for homocysteine in sexual development. This α-amino acid has been shown to accumulate within *Plasmodium*-infected red blood cells *in vitro*, causing redox stress and triggering gametocytogenesis (Chaubey et al., 2014; Beri et al., 2017). Validating the role of this metabolite, homocysteine was also administered to mice with *P. berghei* and an increase in gametocytes was subsequently observed *in vivo* (Beri et al., 2017) (**Table 1**).

Another finding identified through *in vitro* studies paired with LCMS was the discovery that a decline in lysophosphotidylcholine species (lysoPC) in the media was associated with an increased rate of gametocytogenesis (Brancucci et al., 2017). This finding was also supported by LCMS and Flow Injection Analysis (FIA) data from human subjects, demonstrating that *Plasmodium* grown in serum from subjects with lower lysoPC resulted in higher rates of gametocyte development *in vitro* (Usui et al., 2019). Finally, another LCMS-based *in vitro* study examined the difference between human serum and AlbuMAX supplementation in media and found that higher levels of polyunsaturated fatty acid (PUFA)-containing phospholipids in the media were associated with higher rates of gametocyte development *in vitro* (Tanaka et al., 2019) (**Table 1**). Altogether, through the use of LCMS alongside *in vitro* and/or *in vivo* methodologies, multiple host metabolic signals (including α-amino acids and phospholipids) have been identified that appear to trigger gametocyte development, and thus could contribute to malaria transmission.

WHO MAKES WHAT? COMPLEX ORIGINS OF HOST METABOLITES DURING MALARIA INFECTION

Metabolites found in the blood, skin and breath of malaria-infected hosts do not all come from the host. The host, its infecting parasite and even its commensal microbes can all contribute to the metabolome during infection. A key question, therefore, about the metabolites identified in the aforementioned approaches is – *are these metabolites coming from the parasite or the host (or the host's microbiome)?*

Plasmodium exhibits certain metabolic pathways that are not present in the vertebrate host, and chemicals of such pathways are thus known to be produced by the parasite. One such pathway is the 2-*C*-methyl-d-erythritol 4-phosphate (MEP) pathway, and one such chemical is (*E*)-4-hydroxy-3-methyl-but-2-enyl pyrophosphate (HMBPP), a precursor of the parasite's MEP pathway. While HMBPP itself is not a mosquito attractant molecule, HMBPP plays a role in malaria transmission through a complex interaction between the parasite and the host's red blood cells. HMBPP, which is produced by the parasite, has been shown to stimulate host red blood cells to increase their production of CO_2, aldehydes and monoterpenes, thereby indirectly affecting mosquito attractiveness (Emami et al., 2017) (**Table 1**). The volatile metabolites that attract the mosquito are thus host-derived, but the signal that stimulated the metabolite production is of parasite origin.

Commensal microbes of vertebrate hosts also demonstrate complex interplays leading to the production of mosquito

attractant molecules, as has been reviewed previously (Braks et al., 1999). For example, 2- and 3-methylbutanal and 3-hydroxy-2-butanone, mosquito attractants found in the skin odor of malaria-infected individuals (de Boer et al., 2017) (**Table 1**), had been shown previously to be produced by skin microbes (Verhulst et al., 2009). In this study, GCMS identified these metabolites in the headspace of skin-associated microbes which were grown *in vitro* (Verhulst et al., 2009). This work suggests that the host's commensal skin microbes may be the source of several important mosquito-attractant compounds. Future work involving parallel investigations of skin microbiota and skin headspace VOCs during malaria infection may shed light on the significance of skin commensal microbes in the context of malaria transmission.

DATA WRANGLING: BIOINFORMATICS APPROACHES FOR TACKLING THE MALARIA INFECTION METABOLOME

Bioinformatics tools are critically important in the analysis of big data that arises from 'omic technologies. Metabolomics, particularly untargeted metabolomics, can yield a large amount of data on many unique metabolic features which must be sifted out and sorted through in order to determine meaning. A key question here is – *how to find signal within the noise in a metabolomics data set?*

A combination of targeted and untargeted approaches has been used to explore the question of host metabolites in the context of malaria. The strength of untargeted analyses is that these approaches enable the analysis of an extremely large set of metabolic features, allowing for unbiased assessments without setting an *a priori* hypotheses about what may be found. Unsupervised statistical analyses can be applied to these big datasets, such as principal components analysis (PCA) and hierarchical clustering analysis (HCA), and metabolic features that are highly associated with the phenomenon of interest can be identified based on their chemical features (e.g., mass:charge ratio). From that point, computational annotation approaches can be applied to give putative identities, and pathway analysis can be performed to test for significantly perturbed metabolic pathways (Uppal et al., 2016). These approaches can be helpful in the context of exploring new and under-researched questions in the field. Ultimately, however, these approaches should be combined with targeted methods and reference compounds to confirm identities of any putative metabolites (Uppal et al., 2017; Cordy et al., 2019).

Biomarker discovery is another key area in which bioinformatic approaches are applied to metabolomics data. While often used in the context of disease pathogenesis, metabolites could also potentially be identified as biomarkers to indicate malaria transmissibility. To identify metabolite biomarkers of malaria transmission, approaches such as receiver operating curve (ROC) analysis, can be used. More advanced approaches that incorporate multivariate statistics may also be used to help identify robust biomarkers. Importantly these studies require validation in multiple cohorts, and the use of independent datasets on which to build and subsequently apply any given model. Such bioinformatics approaches are likely to lead to the discovery of new biomarkers of transmissibility, that could be highly relevant during the era of malaria eradication.

Potential biomarkers could include those metabolites which have already been found in multiple studies to be associated with enhanced transmissibility. Biomarkers for increased mosquito attraction may include elevated levels of certain terpenes (e.g., pinene) (Kelly et al., 2015; Emami et al., 2017; Schaber et al., 2018) and/or aldehydes (e.g., hexanal, octanal, nonanal) (Correa et al., 2017; Emami et al., 2017; Robinson et al., 2018; Stanczyk et al., 2019) in the headspace of malaria-infected individuals. Biomarkers for increased gametocytogenesis may include altered levels of certain phospholipids (e.g., lysoPC, PUFA-containing phospholipids) (Brancucci et al., 2017; Tanaka et al., 2019; Usui et al., 2019) in the blood of malaria-infected hosts. The utility of such biomarkers is that there may be potential to generate diagnostic tests, particularly non-invasive ones, that detect relevant biomarkers for malaria infection and/or transmissibility. Further, as demonstrated by a recent study of canines identifying malaria-infected individuals through the smell of their socks alone (Guest et al., 2019), it is apparent that volatile chemicals can be detected in a wide variety of ways, and the successful detection of these types of biomarkers may not require expensive equipment.

Finally, in trying to understand the source of these metabolites, data integration across multiple 'omic analyses derived from the same experiment can be helpful toward determining possible sources of metabolites within the complex milieu of the host-parasite-microbial system (Salinas et al., 2014). Data integration techniques can aid in sifting through big datasets to gauge which metabolites are coming from the parasite and which are coming from host (and possibly which from its commensal microbiota). Combining transcriptional data from host, parasite, and microbiota with metabolomics data from the complex host-parasite-microbe system may help to elucidate the ways in which these different components may contribute to the resulting metabolites. Metabolic flux models are particularly helpful for these such joint analyses, as they can combine transcriptional data (which is annotated and thus of known origin) with metabolomics data (from unknown origin). Putting these data together can help to illustrate the predicted activity of various metabolic pathways of either the host or parasite (Chiappino-Pepe et al., 2017; Tang et al., 2018).

CONCLUSION

Plasmodium is a highly complex pathogen which undergoes multiple stage transitions during its passage between its invertebrate and vertebrate hosts. And despite (or more likely, due to) this complexity, transmission of the pathogen results in over 200 million cases of malaria per year (World Health Organization [WHO], 2018). Host, parasite and microbial-derived metabolites, through their impacts on mosquito attractiveness and gametocytogenesis, appear to play a critical

role in ensuring the successful transmission of this devastating parasitic disease. While several recent studies have greatly added to our knowledge in this area, there are still many aspects of malaria transmission biology that are not well understood. Further mining of the host metabolome may help to improve our understanding of the complexities that exist in the malaria host-pathogen system that enhance or hinder transmission.

AUTHOR CONTRIBUTIONS

RJ conceived and wrote the manuscript.

FUNDING

RJ was supported in part by a grant from the U.S. National Institutes of Health (1K01HL143112).

ACKNOWLEDGMENTS

Members of the Malaria Host-Pathogen Interaction Center (MaHPIC) and of the Emory University Clinical Biomarkers Lab are acknowledged for helpful discussions. Figure was created with BioRender.com.

REFERENCES

Basant, A., Rege, M., Sharma, S., and Sonawat, H. M. (2010). Alterations in urine, serum and brain metabolomic profiles exhibit sexual dimorphism during malaria disease progression. *Malar. J.* 9:110. doi: 10.1186/1475-2875-9-110

Batista, E. P., Costa, E. F., and Silva, A. A. (2014). Anopheles darlingi (Diptera: Culicidae) displays increased attractiveness to infected individuals with *Plasmodium vivax* gametocytes. *Parasit. Vectors* 7:251. doi: 10.1186/1756-3305-7-251

Beri, D., Balan, B., Chaubey, S., Subramaniam, S., Surendra, B., and Tatu, U. (2017). A disrupted transsulphuration pathway results in accumulation of redox metabolites and induction of gametocytogenesis in malaria. *Sci. Rep.* 7:40213. doi: 10.1038/srep40213

Berna, A. Z., McCarthy, J. S., Wang, R. X., Saliba, K. J., Bravo, F. G., Cassells, J., et al. (2015). Analysis of breath specimens for biomarkers of *Plasmodium falciparum* infection. *J. Infect. Dis.* 212, 1120–1128. doi: 10.1093/infdis/jiv176

Braks, M. A., Anderson, R. A., and Knols, B. G. (1999). Infochemicals in mosquito host selection: human skin microflora and *Plasmodium parasites*. *Parasitol. Today* 15, 409–413. doi: 10.1016/s0169-4758(99)01514-8

Brancucci, N. M. B., Gerdt, J. P., Wang, C., De Niz, M., Philip, N., Adapa, S. R., et al. (2017). Lysophosphatidylcholine regulates sexual stage differentiation in the human malaria parasite *Plasmodium falciparum*. *Cell* 171:1532-1544.e15. doi: 10.1016/j.cell.2017.10.020

Brouwer, R. (1960). The attraction of carbon dioxide excreted by the skin of the arm for malaria mosquitoes. *Trop. Geogr. Med.* 12, 62–66.

Busula, A. O., Bousema, T., Mweresa, C. K., Masiga, D., Logan, J. G., Sauerwein, R. W., et al. (2017). Gametocytemia and attractiveness of *Plasmodium falciparum*-infected kenyan children to anopheles gambiae mosquitoes. *J. Infect. Dis.* 216, 291–295. doi: 10.1093/infdis/jix214

Cator, L. J., George, J., Blanford, S., Murdock, C. C., Baker, T. C., Read, A. F., et al. (2013). 'Manipulation' without the parasite: altered feeding behaviour of mosquitoes is not dependent on infection with malaria parasites. *Proc. R. Soc. B* 280:20130711. doi: 10.1098/rspb.2013.0711

Cator, L. J., Lynch, P. A., Read, A. F., and Thomas, M. B. (2012). Do malaria parasites manipulate mosquitoes? *Trends Parasitol.* 28, 466–470. doi: 10.1016/j.pt.2012.08.004

Chaubey, S., Grover, M., and Tatu, U. (2014). Endoplasmic reticulum stress triggers gametocytogenesis in the malaria parasite. *J. Biol. Chem.* 289, 16662–16674. doi: 10.1074/jbc.M114.551549

Chiappino-Pepe, A., Tymoshenko, S., Ataman, M., Soldati-Favre, D., and Hatzimanikatis, V. (2017). Bioenergetics-based modeling of *Plasmodium falciparum* metabolism reveals its essential genes, nutritional requirements, and thermodynamic bottlenecks. *PLoS Comput. Biol.* 13:e1005397. doi: 10.1371/journal.pcbi.1005397

Cordy, R. J., Patrapuvich, R., Lili, L. N., Cabrera-Mora, M., Chien, J.-T., Tharp, G. K., et al. (2019). Distinct amino acid and lipid perturbations characterize acute versus chronic malaria. *JCI Insight* 4:125156. doi: 10.1172/jci.insight.125156

Cornet, S., Nicot, A., Rivero, A., and Gandon, S. (2013). Malaria infection increases bird attractiveness to uninfected mosquitoes. *Ecol. Lett.* 16, 323–329. doi: 10.1111/ele.12041

Correa, R., Coronado, L. M., Garrido, A. C., Durant-Archibold, A. A., and Spadafora, C. (2017). Volatile organic compounds associated with *Plasmodium falciparum* infection in vitro. *Parasit. Vectors* 10:215. doi: 10.1186/s13071-017-2157-x

de Boer, J. G., Robinson, A., Powers, S. J., Burgers, S. L., Caulfield, J. C., Birkett, M. A., et al. (2017). Odours of *Plasmodium falciparum*-infected participants influence mosquito-host interactions. *Sci. Rep.* 7:9283. doi: 10.1038/s41598-017-08978-9

De Moraes, C. M., Stanczyk, N. M., Betz, H. S., Pulido, H., Sim, D. G., Read, A. F., et al. (2014). Malaria-induced changes in host odors enhance mosquito attraction. *Proc. Natl. Acad. Sci. U.S.A.* 111, 11079–11084. doi: 10.1073/pnas.1405617111

Decuypere, S., Maltha, J., Deborggraeve, S., Rattray, N. J. W., Issa, G., Bérenger, K., et al. (2016). Towards improving point-of-care diagnosis of non-malaria febrile illness: a metabolomics approach. *PLoS Negl. Trop. Dis.* 10:e0004480. doi: 10.1371/journal.pntd.0004480

Emami, S. N., Lindberg, B. G., Hua, S., Hill, S. R., Mozuraitis, R., Lehmann, P., et al. (2017). A key malaria metabolite modulates vector blood seeking, feeding, and susceptibility to infection. *Science* 355, 1076–1080. doi: 10.1126/science.aah4563

Gardinassi, L. G., Cordy, R. J., Lacerda, M. V. G., Salinas, J. L., Monteiro, W. M., Melo, G. C., et al. (2017). Metabolome-wide association study of peripheral parasitemia in *Plasmodium vivax* malaria. *Int. J. Med. Microbiol.* 307, 533–541. doi: 10.1016/j.ijmm.2017.09.002

Ghosh, S., Pathak, S., Sonawat, H. M., Sharma, S., and Sengupta, A. (2018). Metabolomic changes in vertebrate host during malaria disease progression. *Cytokine* 112, 32–43. doi: 10.1016/j.cyto.2018.07.022

Guest, C., Pinder, M., Doggett, M., Squires, C., Affara, M., Kandeh, B., et al. (2019). Trained dogs identify people with malaria parasites by their odour. *Lancet Infect. Dis.* 19, 578–580. doi: 10.1016/S1473-3099(19)30220-8

Hasin, Y., Seldin, M., and Lusis, A. (2017). Multi-omics approaches to disease. *Genome Biol.* 18:83. doi: 10.1186/s13059-017-1215-1

Josling, G. A., and Llinás, M. (2015). Sexual development in *Plasmodium parasites*: knowing when it's time to commit. *Nat. Rev. Microbiol.* 13:573. doi: 10.1038/nrmicro3519

Kelly, M., Su, C.-Y., Schaber, C., Crowley, J. R., Hsu, F.-F., Carlson, J. R., et al. (2015). Malaria parasites produce volatile mosquito attractants. *mBio* 6:e00235-15. doi: 10.1128/mBio.00235-15

Koella, J. C. (2005). Malaria as a manipulator. *Behav. Process.* 68, 271–273. doi: 10.1016/j.beproc.2004.10.004

Lacroix, R., Mukabana, W. R., Gouagna, L. C., and Koella, J. C. (2005). Malaria infection increases attractiveness of humans to mosquitoes. *PLoS Biol.* 3:e298. doi: 10.1371/journal.pbio.0030298

Loy, D. E., Liu, W., Li, Y., Learn, G. H., Plenderleith, L. J., Sundararaman, S. A., et al. (2017). Out of Africa: origins and evolution of the human malaria parasites *Plasmodium falciparum* and *Plasmodium vivax*. *Int. J. Parasitol.* 47, 87–97. doi: 10.1016/j.ijpara.2016.05.008

Nyasembe, V. O., Teal, P. E. A., Mukabana, W. R., Tumlinson, J. H., and Torto, B. (2012). Behavioural response of the malaria vector *Anopheles gambiae* to host plant volatiles and synthetic blends. *Parasit. Vectors* 5:234. doi: 10.1186/1756-3305-5-234

Olszewski, K. L., Morrisey, J. M., Wilinski, D., Burns, J. M., Vaidya, A. B., Rabinowitz, J. D., et al. (2009). Host-parasite interactions revealed by *Plasmodium falciparum* metabolomics. *Cell Host Microbe* 5, 191–199. doi: 10.1016/j.chom.2009.01.004

Pappa, V., Seydel, K., Gupta, S., Feintuch, C. M., Potchen, M. J., Kampondeni, S., et al. (2015). Lipid metabolites of the phospholipase A2 pathway and inflammatory cytokines are associated with brain volume in paediatric cerebral malaria. *Malar. J.* 14, 513. doi: 10.1186/s12936-015-1036-1

Robinson, A., Busula, A. O., Voets, M. A., Beshir, K. B., Caulfield, J. C., Powers, S. J., et al. (2018). *Plasmodium*-associated changes in human odor attract mosquitoes. *Proc. Natl. Acad. Sci. U.S.A.* 115, E4209–E4218. doi: 10.1073/pnas.1721610115

Salinas, J. L., Kissinger, J. C., Jones, D. P., and Galinski, M. R. (2014). Metabolomics in the fight against malaria. *Mem. Inst. Oswaldo Cruz* 109, 589–597. doi: 10.1590/0074-0276140043

Schaber, C. L., Katta, N., Bollinger, L. B., Mwale, M., Mlotha-Mitole, R., Trehan, I., et al. (2018). Breathprinting reveals malaria-associated biomarkers and mosquito attractants. *J. Infect. Dis.* 217, 1553–1560. doi: 10.1093/infdis/jiy072

Smallegange, R. C., van Gemert, G.-J., van de Vegte-Bolmer, M., Gezan, S., Takken, W., Sauerwein, R. W., et al. (2013). Malaria infected mosquitoes express enhanced attraction to human odor. *PLoS One* 8:e63602. doi: 10.1371/journal.pone.0063602

Stanczyk, N. M., Brugman, V. A., Austin, V., Sanchez-Roman Teran, F., Gezan, S. A., Emery, M., et al. (2019). Species-specific alterations in Anopheles mosquito olfactory responses caused by *Plasmodium* infection. *Sci. Rep.* 9:3396. doi: 10.1038/s41598-019-40074-y

Surowiec, I., Orikiiriza, J., Karlsson, E., Nelson, M., Bonde, M., Kyamanwa, P., et al. (2015). Metabolic signature profiling as a diagnostic and prognostic tool in pediatric *Plasmodium falciparum* malaria. *Open Forum Infect. Dis.* 2:ofv062. doi: 10.1093/ofid/ofv062

Takken, W., and Kline, D. L. (1989). Carbon dioxide and 1-octen-3-ol as mosquito attractants. *J. Am. Mosq. Control Assoc.* 5, 311–316.

Tanaka, T. Q., Tokuoka, S. M., Nakatani, D., Hamano, F., Kawazu, S.-I., Wellems, T. E., et al. (2019). Polyunsaturated fatty acids promote *Plasmodium falciparum* gametocytogenesis. *Biol. Open* 8:bio042259. doi: 10.1242/bio.042259

Tang, Y., Gupta, A., Garimalla, S., MaHPIC Consortium, Galinski, M. R., Styczynski, M. P., et al. (2018). Metabolic modeling helps interpret transcriptomic changes during malaria. *Biochim. Biophys. Acta Mol. Basis Dis.* 1864, 2329–2340. doi: 10.1016/j.bbadis.2017.10.023

Uppal, K., Salinas, J. L., Monteiro, W. M., Val, F., Cordy, R. J., Liu, K., et al. (2017). Plasma metabolomics reveals membrane lipids, aspartate/asparagine and nucleotide metabolism pathway differences associated with chloroquine resistance in *Plasmodium vivax* malaria. *PLoS One* 12:e0182819. doi: 10.1371/journal.pone.0182819

Uppal, K., Walker, D. I., Liu, K., Li, S., Go, Y.-M., and Jones, D. P. (2016). Computational metabolomics: a framework for the million metabolome. *Chem. Res. Toxicol.* 29, 1956–1975. doi: 10.1021/acs.chemrestox.6b00179

Usui, M., Prajapati, S. K., Ayanful-Torgby, R., Acquah, F. K., Cudjoe, E., Kakaney, C., et al. (2019). *Plasmodium falciparum* sexual differentiation in malaria patients is associated with host factors and GDV1-dependent genes. *Nat. Commun.* 10:2140. doi: 10.1038/s41467-019-10172-6

Verhulst, N. O., Beijleveld, H., Knols, B. G., Takken, W., Schraa, G., Bouwmeester, H. J., et al. (2009). Cultured skin microbiota attracts malaria mosquitoes. *Malaria J.* 8:302. doi: 10.1186/1475-2875-8-302

World Health Organization [WHO], (2018). *World Malaria Report 2018*. Geneva: WHO.

Conflict of Interest: The author declares that the research was conducted in the absence of any commercial or financial relationships that could be construed as a potential conflict of interest.

frontiers in Cellular and Infection Microbiology

HYPOTHESIS AND THEORY
published: 03 March 2020
doi: 10.3389/fcimb.2020.00076

Extracellular Vesicles Could Carry an Evolutionary Footprint in Interkingdom Communication

Ricardo Correa[1,2], *Zuleima Caballero*[1], *Luis F. De León*[3] *and Carmenza Spadafora*[1]*

[1] Center of Cellular and Molecular Biology of Diseases, Instituto de Investigaciones Cientificas y Servicios de Alta Tecnologia (INDICASAT AIP), Panama, Panama, [2] Department of Biotechnology, Acharya Nagarjuna University, Guntur, India, [3] Department of Biology, University of Massachusetts, Boston, MA, United States

Extracellular vesicles (EVs) are minute particles secreted by the cells of living organisms. Although the functional role of EVs is not yet clear, recent work has highlighted their role in intercellular communication. Here, we expand on this view by suggesting that EVs can also mediate communication among interacting organisms such as hosts, pathogens and vectors. This inter-kingdom communication via EVs is likely to have important evolutionary consequences ranging from adaptation of parasites to specialized niches in the host, to host resistance and evolution and maintenance of parasite virulence and transmissibility. A potential system to explore these consequences is the interaction among the human host, the mosquito vector and *Plasmodium* parasite involved in the malaria disease. Indeed, recent studies have found that EVs derived from *Plasmodium* infected red blood cells in humans are likely mediating the parasite's transition from the asexual to sexual stage, which might facilitate transmission to the mosquito vector. However, more work is needed to establish the adaptive consequences of this EV signaling among different taxa. We suggest that an integrative molecular approach, including a comparative phylogenetic analysis of the molecules (e.g., proteins and nucleic acids) derived from the EVs of interacting organisms (and their closely-related species) in the malaria system will prove useful for understanding interkingdom communication. Such analyses will also shed light on the evolution and persistence of host, parasite and vector interactions, with implications for the control of vector borne infectious diseases.

Keywords: extracellular vesicles, *Plasmodium falciparum*, interkingdom, communication, evolution, parasites, host, vector

OPEN ACCESS

Edited by:
Matthias Marti,
University of Glasgow,
United Kingdom

Reviewed by:
Ana Maria Jansen,
Oswaldo Cruz Foundation
(Fiocruz), Brazil
Robert P. Hirt,
Newcastle University, United Kingdom

***Correspondence:**
Carmenza Spadafora
cspadafora@indicasat.org.pa

Specialty section:
This article was submitted to Parasite and Host, a section of the journal Frontiers in Cellular and Infection Microbiology

Received: *14 October 2019*
Accepted: *14 February 2020*
Published: *03 March 2020*

Citation:
Correa R, Caballero Z, De León LF and Spadafora C (2020) Extracellular Vesicles Could Carry an Evolutionary Footprint in Interkingdom Communication. Front. Cell. Infect. Microbiol. 10:76. doi: 10.3389/fcimb.2020.00076

INTRODUCTION

The evolution of cell communication is crucial in determining how organisms respond to and interact with each other and their environment. Protozoan parasites also have the ability of releasing membrane–enclosed vesicles toward their extracellular space. These small bodies are collectively known as "extracellular vesicles" (EVs) and can vary in size, composition and origin (Lener et al., 2015). EVs can function as signal carriers for single cell-cell communication or even more complex interactions at the level of tissues and organs (Kim et al., 2015). In this review, we present an overview of what is currently known about these extracellular bodies, the findings reported on protozoarian communication through EVs, their role in pathogenesis, program cell death, communication, and interkingdom coevolution.

HISTORICAL PERSPECTIVE

Despite the use of EV terminology for more than 30 years, starting with the description of exosomes from reticulocytes (Harding et al., 1984), one of the first reports of what would be later referred to as EVs came from the activity of "thromboplastic proteins of the blood" (1946) (Chargaff and West, 1946). These proteins were composed of nanometric vesicles, and were later denominated "platelet dust" (1967) (Wolf, 1967). Other studies were also performed to investigate the activity of cartilage matrix vesicles in bone mineralization in 1969 (Anderson, 1969). Not long after, in 1971, small vesicles originating from RBCs infected with *P. falciparum* were observed using electron microscopy (Luse and Miller, 1971). Later on, studies on the regulatory capacity of EVs from T cells on the immune response triggered a renewed interest due to the potential therapeutic uses of EVs (Raposo et al., 1996). Important advances in the understanding of the role of EVs began to emerge with the identification of key functions such as their role in horizontal genetic transfer, modulation of the immune response, and cell differentiation. This multifunctional activity of EVs stems from their capacity to transport a wide range of distinct biomolecules that can alter the biological functions of target cells (Kalra et al., 2016). Currently, the application of high throughput sequencing tools enables the acquisition of massive data on EV populations from a diverse source of cellular and tissue models, offering new opportunities for the development of novel applications.

EVs have been grouped in a variety of ways (van der Pol et al., 2012; Akers et al., 2013; Raposo and Stoorvogel, 2013; Yanez-Mo et al., 2015; Szatanek et al., 2017). Briefly, EVs originate from cell sacs that are essentially comprised of thousands of different proteins and unique lipids, and which contain not only DNA and mRNA but also small nucleolar RNA (snRNA), Y RNA, mitochondrial RNA, vault RNA and long ncRNA (non-coding RNA) (Lazaro-Ibanez et al., 2014; Kreimer et al., 2015; van Balkom et al., 2015). Thus, EVs have been classified into exosomes, microvesicles and apoptotic bodies, depending on their origin, size and molecular composition. For instance, exosomes range in size from 50 to 150 nm. They are produced by invagination of the endosomal membrane during maturation of multivesicular bodies, and are released outside the cell after fusion with the plasma membrane (Keller et al., 2006; van Niel et al., 2018). Exosome formation is associated with specific proteins located in the endosome, such as tetraspanins, chaperones, and the Rab GTPase family (Ostrowski et al., 2010). A primary component of exosomes is the endosomal sorting complex required for transport (ESCRT), which is involved in the formation of exosomes in the late endosome and in the transportation of cargo (Raposo and Stoorvogel, 2013).

On the other hand, micro vesicles (MVs) are produced after budding directly from the plasma membrane. They have often been referred to in the literature with different names, such as ectosomes, microparticles, or shedding vesicles (Meldolesi, 2018). MVs are formed in cytosolic microdomains produced by the redistribution of phospholipids of the interior side of the plasma membrane, and then released to the extracellular space after vesicle fission (Cocucci and Meldolesi, 2015). MVs have sizes that range from 0.1 to 1 μm, which overlaps with the reported size of exosomes. This indicates that size is not a reliable criterion to differentiate between EVs. In living cells, the redistribution of lipids is facilitated by translocases that allow the movement of phospholipids in both directions across the plasma membrane, such as phophatidyl serine, which induces membrane budding and generation of MVs (Leventis and Grinstein, 2010; van der Heyde et al., 2011; Mantel and Marti, 2014). Additionally, other changes in the endosome and the plasma membrane are involved in the production of MVs, such as overexpression of GTP-binding ARF factor 6 (ADP-ribosylation factor 6), the formation of the complex VPS ATPse E3 ligase, and the interaction of the tumor susceptibility gene 101 (TSG101) with arrestin domain-containing protein 1 (ARRDC1). These modifications produce contractions in the cytoskeletal arrangement and the interaction with phospholipases result in the release of MVs (Muralidharan-Chari et al., 2009; Nabhan et al., 2012).

Finally, apoptotic bodies are released only when apoptosis is triggered in a healthy cell, beginning with chromatin condensation and blebbing of the membrane, followed by proteomic degradation and releasing of apoptotic bodies to the extracellular space (Elmore, 2007). Apoptotic bodies have a larger size in comparison with other types of EVs, ranging from 50 to 5000 μm (Nawaz et al., 2014). Smaller vesicles can be embedded within apoptotic bodies, and may enclose organelles as well as fragmented nuclei, a feature that uniquely separates these particles from other types of EVs. It is still unknown how these smaller vesicles are formed (Bergsmedh et al., 2001; Akers et al., 2013), but the blebbing mechanism of apoptotic bodies has been associated with actin-myosin interaction (Coleman et al., 2001).

EV CHARACTERISTICS DURING PATHOGEN INFECTION

Intracellular and free-living pathogen-derived EVs carry signals that may mediate pathogen-pathogen communication. These signals modulate host biological functions, and induce the production of EVs by host effector cells that have been stimulated by direct contact with the pathogens or by contact with their EVs (Mantel and Marti, 2014). Special attention has been paid to the EVs of intracellular pathogens because this type of pathogen can modify the molecular composition of EVs, changing their function upon release from an infected host cell. For example, macrophages are induced to release inflammatory cytokines after taking up exosomes that were released from other macrophages infected with *Mycobacterium avium* (Bhatnagar and Schorey, 2007). EVs from a wide variety of other pathogens have important activity during infections, such as those produced by *Giardia*, *Chlamydia*, *Trichomonas*, and *Cryptococcus* (Benchimol, 2004; Rodrigues et al., 2008; Frohlich et al., 2012; Twu et al., 2013). Similarly, intracellular protozoan parasites also have an impact on the host, by altering its immune response. For instance, EVs derived from *Toxoplasma gondii* are known to induce

murine macrophages to release inflammatory proteins such as TNF-α, iNOS, and IL-10 (Silva et al., 2018).

EVs IN TRYPANOSOMATIDS

In infections caused by protozoan parasites, the release of EVs can be observed throughout most of the parasite's life cycle, suggesting that EVs are a fundamental component of parasitic infection. As previously reported, EVs are involved in the host–parasite interaction and in communication between parasites, inducing dysfunction in the immune responses or manipulating the physiology and metabolism of the host (Silvester et al., 2017). EVs have been identified in some of the most pathogenic protozoans, those responsible for some of the most widespread, lethal and disabling vector–borne diseases, such as Chagas disease, African trypanosomiasis, and leishmaniasis. Their causative parasites have a complex life cycle, undergoing several transformations during their asexual and sexual stages. As explained below, new findings have determined that EVs play a role in a variety of infective processes, including the immune response of the hosts. The principal findings on the parasite-derived EVs from these major vector–borne diseases are summarized below.

Trypanosoma cruzi, the etiological agent of Chagas disease, infects macrophages during its trypomastigote stage and can generate both exosomes and ectosomes during infection (de Pablos Torro et al., 2018). The parasite then invades new cells and tissues after cellular differentiation and replication. It has been shown that EVs are present in almost all stages of infection (Bayer-Santos et al., 2013). In addition, the modulating activity of EVs is determined by the phase of the disease (acute or chronic), the immune status of patients and the parasite load during infection. During *T. cruzi* infection, EVs can be released from parasites or host cells and can be taken up by both parasites and host cells. For instance, Ramirez et al. (2017) showed that the integration rate of EVs with THP1 monocyte cells is significantly higher upon release from human tissue–cultured trypomastigotes than from insect stage epimastigotes or metacyclic trypomastigotes. If these infected monocyte-derived EVs fuse with other trypomastigotes, they can offer them protection against lysis from the complement system action (Cestari et al., 2012; Ramirez et al., 2017). Likely, this protection originates after trypomastigotes and immune complexes interact with each other through their EVs (Diaz Lozano et al., 2017). The increased incorporation of EVs through a Ca^{2+}-dependent mechanism, in comparison with other stages, is caused by a higher rate of redistribution of phosphatidylserine (PS) in THP-1 monocytes upon interaction with tissue-culture trypomastigotes (Ramirez et al., 2017). Therefore, similar to other cell models, the modulation of the immune response using EV-cargo signals relies on the key role played by PS in facilitating the uptake of EVs from infected host cells. Nevertheless, more studies are required to describe the precise signal cascades involved in the Ca^{2+} efflux and the release of EVs during *T. cruzi* infection. Interestingly, *T. cruzi* proteins are found inside host cells after their incorporation of *T. cruzi* EVs, and this insertion appears to be targeted at specific cells types such as fibroblasts, muscle and neuronal cells. In fact, parasite proteins have not been detected in other types of cells such as lymphocytes or erythrocytes (de Pablos Torro et al., 2018). EVs fusion with THP1 cells produce a higher expression of the genes IKBKB, NR3C1, and TIRAP, which have been associated with an increased generation of reactive oxygen species (ROS) and nitric oxide (NO) (Chowdhury et al., 2017). Additional evidence of the role of EVs in the pathogenicity of trypanosomatids was offered by Trocoli Torrecilhas et al. (2009) who demonstrated that the parasitaemia in BALB/C mice increased following the inoculation of *T. cruzi* EVs prior to infection. Notably, proteomic analysis of EVs from trypomastigotes (host stage) and epimastigotes (vector stage) of *T. cruzi* revealed that most (70%) of the identified EV proteins are present in both stages.

In a similar scenario, EVs play an important role during infection by *Leishmania* parasites, which are transmitted to humans by sandfly bites. Most of the research on EVs from *Leishmania* species has been performed using *L. major* and *L. donovani,* which have different clinical manifestations, with the former developing in the skin and the latter, viscerally. Following the transformation of promastigotes to amastigotes inside macrophages in *in vitro* studies, it has been shown that EVs may be released to the supernatant and present virulence factors such as zinc-metalloproteinase gp63 (Silverman et al., 2008). This protein activates the tyrosine phosphatase SHP-1, which has an inhibitory effect on the pro-inflammatory cytokine response activity of macrophages after inhibiting the host IFN-γ/Jak-STAT1 cascade and the p38-MAPK signaling pathway (Gomez et al., 2009; Mantel and Marti, 2014).

In hepatic cells, protein gp63 also inhibits the enzyme Dicer1, causing the downregulation of the miRNA miR-122, which provokes a change in the lipid metabolism of the host, contributing to the survival of the parasite (Descoteaux et al., 2013). In addition, gp63 participates in the activation of signaling proteins and transcription factors that might be involved in the up/down regulation of several genes in the target macrophage (Hassani and Olivier, 2013). It is not clear yet, however, whether this gp63 action is mediated by EV integration into hepatic cells (Ghosh et al., 2011). On the other hand, EVs from promastigotes have been shown to modify the immune response by decreasing the production of IL-8 and TNF-α, increasing IL-10 and eliminating the dendritic cell capacity to activate Th1 cells (Silverman et al., 2010). In a recent report, EVs were associated with the increased production of cytokines in macrophages and B1 cells as well as with several virulence factors in *L. amazonensis* (Barbosa et al., 2018). What is clear in infections by *Leishmania* parasites is that the EVs from both intracellular and free-living parasites are modulating the immune response of the human host.

EVs IN MALARIA PATHOGENESIS

An early report on malaria EVs focused on their capacity to induce thrombocytopenia, which is associated with cerebral malaria (CM) (Piguet et al., 2002). Later, it was shown

that *P. falciparum* EVs were also present in the sera of infected patients, establishing the occurrence of increased level of EVs in patients ridden with this species of *Plasmodium* (especially associated with coma cases in CM) in comparison with *P. malariae* and *P. ovale* infections (Combes et al., 2004; Pankoui Mfonkeu et al., 2010). In the case of *P. vivax* infections, patients also show elevated levels of EVs derived from erythrocytes, platelets, leucocytes and monocytes, relative to healthy individuals (Campos et al., 2010). Proteomic analyses of circulating EVs in infected patients have identified proteins related to parasite metabolism, invasion and pathogenesis, such as enolase, Hsp 90, lactate dehydrogenase, ADP-ribosylation factor 1, phosphoglycerate kinase and merozoite surface protein 1 (Antwi-Baffour et al., 2016).

Animal models have also served to study the relationship between EVs and malaria pathogenesis and to gain insights into the corresponding host immune response. For example, the high levels of iRBC (infected red blood cell)-derived EVs during CM were reduced after inhibition of the ATP-binding cassette transporter ABCA1 gene, which is a known mediator of MV formation. Specifically, this ABCA1 inhibition reduced TNF-αlevels in sera and cell sequestration of leukocytes into the brain, both features of complicated malaria (Combes et al., 2005). Remarkably, it has been shown that the particular haplotypes of the ABCA1 promoter determine the levels of EV secretion during infections, thus increasing or decreasing the virulence of the parasite (Sahu et al., 2013). Mice models have been used to study the immune response, particularly the inflammatory processes related to macrophage activation in a TLR–dependent manner after *P. berghei*-derived EVs were inoculated into the animals (Couper et al., 2010). Recently, Shrivastava et al. (2017) reported that RBC-derived EVs could be internalized massively by astrocytes along with high levels of CXCL10, a known marker of CM, in *P. berghei*–infected mice (Shrivastava et al., 2017).

On the other hand, after hand *in vitro* studies of *P. falciparum* have also informed the biological function of EVs. For instance, in a model of CM, platelet–derived EVs were associated with the transference of platelet antigens into iRBCs using a PfEMP1-dependent pathway, which resulted in an increase in the binding of infected cells with the endothelium (Faille et al., 2009). In 2013, two independent studies found that *P. falciparum* uses EVs for parasite-parasite and host-parasite communication (Mantel et al., 2013; Regev-Rudzki et al., 2013). These studies elegantly demonstrated several PfEV activities, such as activation of neutrophils, secretion of both pro- and anti-inflammatory cytokines following EV uptake by macrophages, induction of gametocytogenesis, and incorporation of DNA plasmids, which can spread drug resistance among naïve parasites. In addition, MV markers stomatin, GTP-binding protein ARF6 and the disassembly factor VPS4 were identified as cargo of the EVs using proteomic analysis (Mantel et al., 2013). In the context of these findings, the evidence suggested that EVs could be used as indicators during *P. falciparum* infections to estimate parasite density, serve as signals in parasite–parasite communication, and regulate the period of transmissibility to vectors (Mantel and Marti, 2014). Interestingly, recent proteomic analysis identified several proteins that may participate in the invasion of RBCs using molecular mimicry of the host molecules. Particularly, the ring–exported protein 2 (Rex2) and the *Plasmodium*-exported element (PEXEL) present a high molecular similarity to the human RAC2 protein family (Barteneva et al., 2013). Recently, it was also shown that human NK cells activated by iRBC–derived EVs respond by exposing exposed MDA5, a pathogen recognition receptor (Ye et al., 2018).

The origin of *P. falciparum* EVs has been described in asexual stages. Maurer's clefts are important erythrocytic structures formed after invasion by the parasite, participating in protein trafficking and vesicle formation directed at the erythrocyte plasma membrane (Spycher et al., 2006). This was demonstrated when Maurer's cleft proteins were reported as components of released EVs during *P. falciparum in vitro* culture (Mantel et al., 2013). The molecular deletion of Maurer's cleft proteins inhibited the production of EVs, confirming the role of this host-parasite structure in vesicle biogenesis (Regev-Rudzki et al., 2013). Further findings confirmed the participation of the EV cargo in host immune modulation, host vascular function manipulation, gametocytogenesis and gene regulatory functions through small RNAs, DNA, and specific interacting components associated with severe malaria (Mantel et al., 2016; Sisquella et al., 2017; Babatunde et al., 2018). Altogether, these findings revealed that malaria parasites use EVs as an effective communication system that act like cellular "carrier pigeons" to regulate multiple functions of both the parasite population and host homeostasis.

INDIVIDUAL SUICIDE OR COLLECTIVE HOMEOSTASIS? THE ROLE OF EVs

Traditionally, programed cell death (PCD) is defined as a genetically regulated mechanism that is used by multicellular organisms for homeostasis and development (Gunjan et al., 2016). However, in recent years, there has been increasing interest in death regulation in protozoan parasites, generating debate around the traditional classification of programed cell death (PCD) pathways (Proto et al., 2013). In fact, new evidence shows that intracellular parasites can suffer apoptosis (Li et al., 2015; Mandal et al., 2016; de Castro et al., 2017; Gunjan et al., 2018), indicating that PCD is not unique to multicellular organisms. Thus, understanding of the PCD mechanisms that take place during microbial infections is an exciting field of study, given that death signals might be used in therapeutic treatments. For example, *Plasmodium*, *Trypanosoma,* and *Leishmania* parasites present PCD features under distinct experimental conditions (Duszenko et al., 2006; Gunjan et al., 2016; Mandal et al., 2016; Basmaciyan et al., 2017; de Castro et al., 2017; Wei et al., 2018).

Similar to multicellular organisms, these parasites present classic PCD markers, such as DNA fragmentation, cell shrinkage, chromatin condensation, PS translocation and loss of the mitochondrial membrane potential (Reece et al., 2011). Furthermore, several effectors have been suggested

to induce apoptosis in protozoan parasites. For example, prostaglandin D_2 is involved in PCD in *Trypanosoma brucei* procyclic forms, by generating ROS (Duszenko et al., 2006). The description of the gene metacaspases 1 (PfMCA1) and the use of pan caspase inhibitor z-VAD-fmk confirmed the presence of PCD in *P. falciparum* and in *P. vivax* (Meslin et al., 2007; Rezanezhad et al., 2011). In addition, it has been shown that PfMCA1 is regulated by the C2 domain of the calcium-dependent membrane targeting domain and a CARD domain (Caspase Recruitment Domain) (Sow et al., 2015). In *Leishmania* the role of MCA has been identified as being a precursor of PCD, acting on the autophagic protein ATG8 (Casanova et al., 2015). The above evidence makes it clear that protozoan parasites do indeed have PCD mechanisms, albeit distinct from those of multicellular organisms.

Remarkably, EVs can also induce apoptosis during stress and normal development conditions by carrying Fas and TRAIL to different target cells (Janiszewski et al., 2004; Stenqvist et al., 2013). Recently, our group reported that parasite-derived EVs carrying lactate dehydrogenase can induce PCD in *in vitro* cultures of *P. falciparum* during high parasitaemia levels, showing that parasites can likely sense each other and release EVs to regulate the parasite population (Correa et al., 2019). If apoptosis induction involves the pathogen communicating with its kind through EVs, as the evidence suggests, this would represent an important evolutionary force in the adaptation of parasitism to specialized niches in the host. EVs could be involved in the communication strategies used by the parasite to manipulate its hosts and vector in order to maintain its virulence, survival and transmissibility. There is increasing evidence from various fields and approaches suggesting that the study of EVs might help understand the complexity of mammalian host-parasite-vector interactions in protozoan pathogens. We suggest that an integral molecular analysis of EVs could provide a genetic marker(s) that would help answer certain mysteries present in the study of the evolution of interkingdom communication and its role in the adaptation of parasite species and that *P. falciparum* could be a good model to test this hypothesis.

In the case of the malaria parasite, it has been suggested that a mechanism of self-regulation may exist to limit the intensity of the parasitaemia in *in vitro* cultures. Interestingly, in those conditions, the parasitaemia growth of *P. falciparum* can reach a maximum multiplying factor of 8, which is far below a potential factor of 16 (Deponte and Becker, 2004) under ideal conditions. Based on this behavior, it had been suggested that *P. falciparum* uses mechanisms of self-regulation in response to density stress (Mutai and Waitumbi, 2010), and these mechanisms might depend on EVs mediated apoptosis. For instance, recent studies have observed programmed cell death in highly parasitized *in vitro* cultures of *Plasmodium*, and another study that has identified molecules involved in the signaling of death (Totino et al., 2014; Engelbrecht and Coetzer, 2016; Chou et al., 2017; Correa et al., 2019).

THE POSSIBLE ROLE OF EVs IN EVOLUTION BY HORIZONTAL GENE TRANSFER

The basic biochemical composition of EVs includes a phospholipid membrane that forms a sac and can contain conserved proteins, such as enzymes, growth factors, different types of receptors and cytokines, as well as DNA, coding and non-coding RNA and several metabolites (Raposo and Stoorvogel, 2013). Since their discovery, EVs derived from red blood cells infected with *P. falciparum* generated interest regarding their potential role in cell signaling, intra-regulation and communication between host and pathogens (Mutai and Waitumbi, 2010; Proto et al., 2013). Recently, Sundararaman et al. (2016) suggested that EVs could play a role in DNA recombination in the asexual stage of the infection inside the erythrocytes. This indicates that the study of EVs in *P. falciparum* could provide an opportunity to understand host-parasite and parasite-parasite interactions. In particular, its ability to grow in laboratory cultures and its specialized life cycle confined to mosquitoes and humans, makes *P. falciparum* an optimal model system for the study of the evolution of inter-kingdom communication (**Figure 1**).

A series of molecules derived from EVs have been involved in cell signaling and intra-regulation (Mutai and Waitumbi, 2010; Proto et al., 2013), including a variety of proteins and genetic material, and, potentially, transposons (Lefebvre et al., 2016; Preusser et al., 2018), all of which are known to mediate communication between host and pathogens (Schorey et al., 2015). For instance, recent studies on *P. falciparum* show that EVs carry proteins and nucleic acids potentially involved in the horizontal transfer of information parasite$\longleftrightarrow$parasite and/or parasite$\longrightarrow$host (Mantel et al., 2013, 2016; Regev-Rudzki et al., 2013). In addition, the release of EVs from iRBCs has been involved in signaling the transition of the parasite from the asexual to sexual stage as well as its sequestration in micro-capillaries, both of which are transitions that would favor vector transmission (Aingaran et al., 2012; Cornet et al., 2014).

Interkingdom communication via EVs could also play a role in coevolution of interacting organisms. However, the coevolution of cell signaling between different species, such as host-pathogen interactions or mixed infection by related pathogens has not been considered so far. Mixed infections of multiple parasites within a host are common in nature (Krishna et al., 2015; Bernotiene et al., 2016; Graystock et al., 2016). For instance, great apes, and even humans, can host several species of *Plasmodia* parasites (Prugnolle et al., 2010). EVs could mediate communication by facilitating horizontal transfer of genetic information between different *Plasmodia* species (Regev-Rudzki et al., 2013; Kawamura et al., 2017; Otto et al., 2018; Ben-Hur et al., 2019; Plenderleith et al., 2019). Several lines of evidence support this possibility. Indeed, the frequency of EVs found in pathogens suggests that EVs are common in interactions between host and parasites, and are likely to modify the biological functions of the host (Mantel et al., 2016; Zhu et al., 2016). In addition, molecules derived from EVs associated

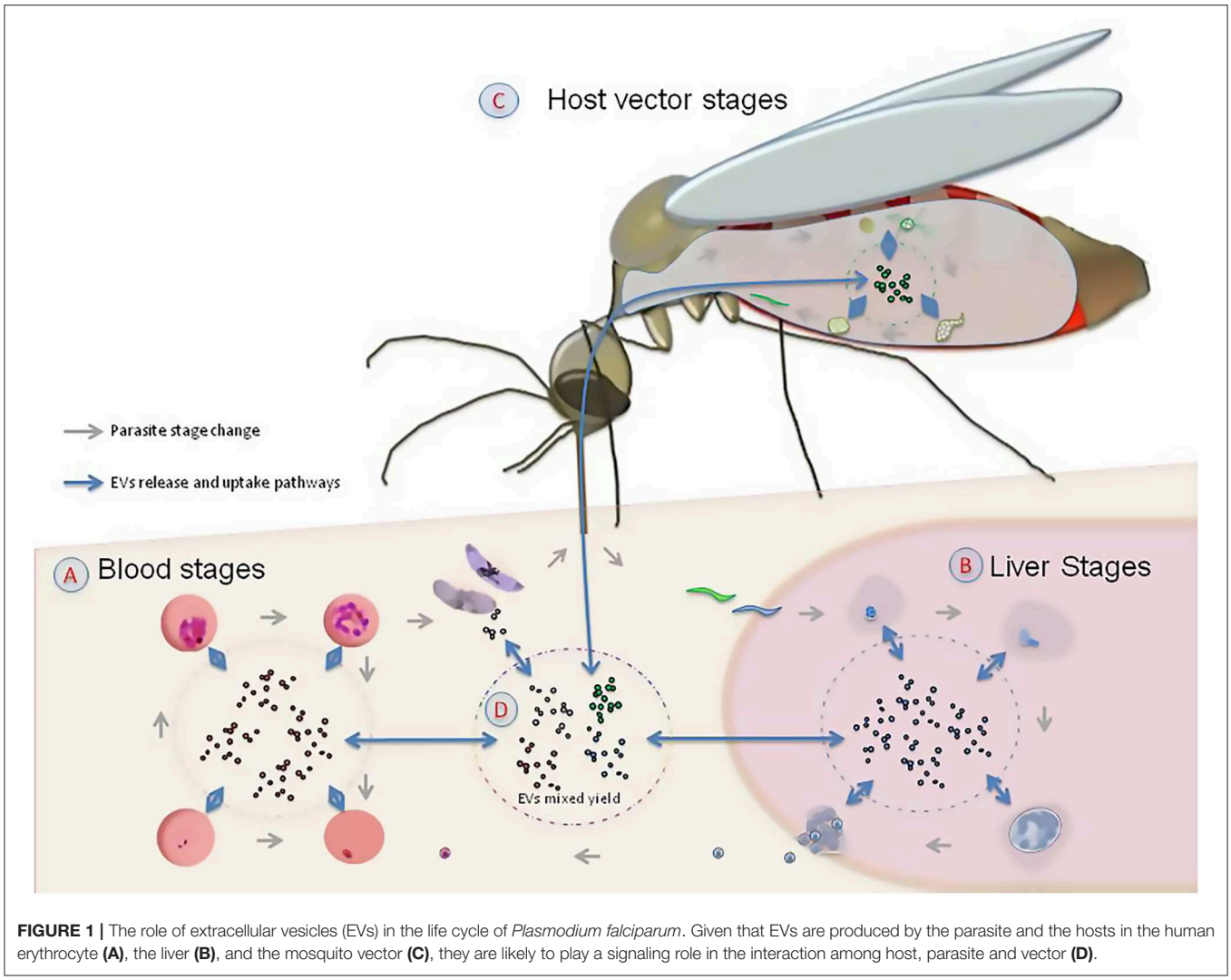

FIGURE 1 | The role of extracellular vesicles (EVs) in the life cycle of *Plasmodium falciparum*. Given that EVs are produced by the parasite and the hosts in the human erythrocyte **(A)**, the liver **(B)**, and the mosquito vector **(C)**, they are likely to play a signaling role in the interaction among host, parasite and vector **(D)**.

with host-pathogen interactions are likely to show a footprint of the reciprocal selection between host and pathogens (Kawamura et al., 2017).

EVOLUTIONARY CONSEQUENCES OF INTERKINGDOM COMMUNICATION

The evolution of interkingdom communication could have several consequences. For example, information transfer in a host with mixed infections (Mantel and Marti, 2014) could facilitate the stable co-existence of multiple pathogen species. This is likely the case in mixed infections of *Plasmodia* spp. in apes, which could be less virulent than a solo *P. falciparum* infection in modern humans, as reported in van Niel et al. (2018). However, it is not yet clear how universal mild infection in apes hosting mixed infections of *Plasmodia* spp. is. Similar to host and parasites, EVs could also facilitate signaling between the *Plasmodium* parasite and the mosquito vector (Deolindo et al., 2013; Twu et al., 2013; Bayer-Santos et al., 2014; Montaner et al., 2014). This information exchange is likely to have played a key role in the initial approach between host and parasite that ended up in the establishment of the infection (**Figure 1D**). However, an integrative examination of EVs derived from infected host, parasite and vector is necessary to shed light on the origins of *P. falciparum* and the development of malaria pathogenesis.

TESTING FOR THE ROLE OF EVs

To test for the role of EVs in the evolution of host-parasite interaction, a deeper analysis of the properties and molecular composition of EVs is necessary. Proteins derived from EVs have already been suggested to mediate communication between host and pathogens, especially in intracellular microorganisms such as *Trypanosoma* spp. (Matthews, 2005; Garcia-Silva et al., 2014), *Leishmania* spp. (Silverman and Reiner, 2011) and *Plasmodium* spp. (Martin-Jaular et al., 2011; Regev-Rudzki et al., 2013). In *Plasmodium* spp., an important number of the molecules have recently been identified (Batista et al., 2011; Correa et al.,

2017). These molecules include a wide range of proteins that are involved in metabolism and immune processes. Sequence variation in these EV proteins and their interacting counterpart in hosts could be examined across tissues infected by the parasite, such as host erythrocytes and mosquito gut lining and salivary glands. Sequence data from these proteins, as well as nucleic acids (e.g., DNA, RNAs) derived from EVs, can be used to infer parallel changes associated with coevolution between parasites and hosts. Some ideas are given in **Table 1**. Additional analyses of these EV molecules could explore patterns of selection acting on aminoacid (or nucleotide) sequence in hosts and parasite. These analyses could be performed using cutting-edge sequencing tools in combination with readily available comparative phylogenetic methods such as parsimony, maximum likelihood, and Bayesian inference (Yang and Bielawski, 2000). From a phylogenetic perspective, comparative analyses could include EV molecules derived from host, parasite and vectors, as well as their closely-related species. These analyses could also reveal whether the communication mechanism via EVs represents a conserved strategy across plasmodia-insect-mammalian species. Finding a conserved communication strategy via EVs could explain the unusual ability of New World mosquitoes to transmit the *Plasmodium* parasite, even though American mosquitoes diverged from their African counterparts 95 million years ago (Molina-Cruz and Barillas-Mury, 2014).

The analyses suggested in **Table 1** might exploit whole-genome sequence tools that have been used recently to study the coevolution of host-parasite interactions. In the absence of known rare genomic changes or other idiosyncratic markers, whole-genome analyses provide a useful tool to circumvent studies with single or low number of markers (Froeschke and von der Heyden, 2014). One example is the use of linkage mapping to perform genetic crosses, useful for localizing phenotypic traits in a range of organisms. Linkage mapping has been applied to *P. falciparum* to identify key genes related to drug resistance and cell development (Ranford-Cartwright and Mwangi, 2012). This method has made it possible to map genes, causing a given phenotype, to genome regions and to find the responsible genes and/or mutations by performing functional genomics experiments (Anderson et al., 2018). Additionally, there are a number of next-generation sequencing tools that can be used to explore the components of the EV cargo as well as the evolutionary history of host-parasite interaction mediated by EVs. This includes parallel sequencing of known (and novel) peptides and nucleic acids derived from the EVs host and parasite. These analyses can also be targeted to specific cell types (e.g., via single cell parallel sequencing), which could facilitate the functional characterization of host and parasite EVs *in vitro* (Turchinovich et al., 2019).

To date, most studies have focused on the interaction between mammalian host and parasites. Nevertheless, the role of parasite EVs in vector attraction to infected cells has received less attention (**Figure 1**). The study of these interactions could help explain the observation that infected mosquitoes can be manipulated by *Plasmodium* in a way that enhances vector attraction to human odor (Lacroix et al., 2005; Smallegange et al., 2013; Batista et al., 2014). In this interaction, a parasite-driven regulation of vector genes (Lu et al., 2007) might activate the receptors used by mosquitoes to detect hosts (Takken and Knols, 1999). EVs could mediate the attraction to the infected

TABLE 1 | Could EVs mediate key aspects of coevolution between parasite and hosts?

Potential role of EV_S in host-parasite interaction	Experimental approach	Prediction
Information (i.e., molecules) delivered by parasites via EVs plays a role in communication that is specific to its host, parasite and vector system.	Characterization of "EVsome" by differential proteomic analysis (e.g., nano LC Mass Spectrometry) and molecular analysis (e.g., DNA, RNA) to identify key signaling molecules from distinct parasite stages of its life cycle.	The composition of EVs has been previously described as "hybrid" (Mantel et al., 2013; Correa et al., 2019) due to the presence of host and parasite proteins. We expect that the composition of EVs can be distinctively associated with its source system (e.g., host, parasite, or vector), suggesting a potential role in information transfer.
EV cargo has functional consequences for the interaction between hosts and parasites.	Experimental assays such as coprecipitation can be used for screening and identification of interacting EV proteins between host and parasite. This will help explore the functional role of interacting EVs components in host and parasite. *In vitro* analyses of gene expression could help identify mRNA molecules in parasite EVs with a role in specific signaling pathways.	Parasite proteins secreted by EVs interact with receptors of the host cell. This interaction leads to detectable changes in enzyme activity, metabolite production, phenotypic change, gene expression, or signaling pathways. Genetic material in the cargo of EVs influence the function of host cells.
The signaling role of EVs could affect coevolution between hosts and parasites.	(i) A comparative analysis of macromolecules in the cargo of EVs of different *Plasmodium* spp. could highlight specific variations as a consequence of an adaptation to the infection of different mammalian hosts. (ii) Homologous sequences of the EVs molecules (e.g., protein, DNA, RNA) across species of the parasite (*Plasmodium* genus) as well as EVs receptors of the host species can be studied using phylogenetic comparative analysis.	Phylogenetic analyses may show coupling of the evolutionary history between parasite proteins secreted by EVs and the receptors of the host cell.

hosts by influencing both gene regulation and activation of other signals during infection (reviewed in Barteneva et al., 2013, Mantel and Marti, 2014). While understanding these signaling pathways is challenging because of the inherent difficulties of studying intracellular pathogens, the specialized nature of the *P. falciparum* life cycle presents a unique opportunity to explore this issue.

A number of reports that suggest coevolution between microbes and hosts can be found in literature (Chapman and Hill, 2012; Mozzi et al., 2018; Quintana-Murci, 2019). The importance of polymicrobial interactions in this occurrence has also been presented (Rioux et al., 2007). Thus, the possible role of EVs on these events would only add another piece to explain coevolution.

CONCLUSIONS

The functional role of EVs has been associated with intercellular communication. However, recent evidence indicates that EVs are also ubiquitous in the interaction among mammalian hosts, parasites and vectors. This suggests that EVs play an important role in interkingdom communication. Thus, communication through EVs is likely to have important evolutionary consequences such as the adaptation of parasitism to specialized niches in the host. EVs could also be involved in the communication strategies used by the parasite to take advantage of its mammalian host and its vector to maintain its virulence, survival and transmissibility. We suggest that the *Plasmodium* parasite involved in the malaria disease represents a potential model system to explore the role of EVs in the evolution of host-parasite interaction and interkingdom communication. Deciphering the cargo composition of EVs derived from parasites, hosts, and vectors will also inform the evolution of the pathogenicity of malaria and other protozoan parasites.

AUTHOR CONTRIBUTIONS

RC conceived the idea and drafted the initial manuscript. ZC and LD wrote sections of the manuscript. RC, ZC, and CS reviewed and worked to produce the final concepts. CS put together the final draft. All authors read, revised, and approved the final manuscript before submission.

FUNDING

CS, ZC, and RC were partially funded by the National System of Research (SNI Panama).

ACKNOWLEDGMENTS

The authors would like to thank Ernst Hempelmann for critically reviewing the manuscript.

REFERENCES

Aingaran, M., Zhang, R., Law, S. K., Peng, Z., Undisz, A., Meyer, E., et al. (2012). Host cell deformability is linked to transmission in the human malaria parasite *Plasmodium falciparum*. *Cell Microbiol.* 14, 983–993. doi: 10.1111/j.1462-5822.2012.01786.x

Akers, J. C., Gonda, D., Kim, R., Carter, B. S., and Chen, C. C. (2013). Biogenesis of extracellular vesicles (EV): exosomes, microvesicles, retrovirus-like vesicles, and apoptotic bodies. *J. Neurooncol.* 113, 1–11. doi: 10.1007/s11060-013-1084-8

Anderson, H. C. (1969). Vesicles associated with calcification in the matrix of epiphyseal cartilage. *J. Cell Biol.* 41, 59–72. doi: 10.1083/jcb.41.1.59

Anderson, T. J. C., LoVerde, P. T., Le Clec'h, W., and Chevalier, F. D. (2018). Genetic crosses and linkage mapping in schistosome parasites. *Trends Parasitol.* 34, 982–996. doi: 10.1016/j.pt.2018.08.001

Antwi-Baffour, S., Adjei, J. K., Agyemang-Yeboah, F., Annani-Akollor, M., Kyeremeh, R., Asare, G. A., et al. (2016). Proteomic analysis of microparticles isolated from malaria positive blood samples. *Proteome Sci.* 15:5. doi: 10.1186/s12953-017-0113-5

Babatunde, K. A., Mbagwu, S., Hernandez-Castaneda, M. A., Adapa, S. R., Walch, M., Filgueira, L., et al. (2018). Malaria infected red blood cells release small regulatory RNAs through extracellular vesicles. *Sci. Rep.* 8:884. doi: 10.1038/s41598-018-19149-9

Barbosa, F. M. C., Dupin, T. V., Toledo, M. D. S., Reis, N., Ribeiro, K., Cronemberger-Andrade, A., et al. (2018). Extracellular vesicles released by leishmania (Leishmania) amazonensis promote disease progression and induce the production of different cytokines in macrophages and B-1 cells. *Front. Microbiol.* 9:3056. doi: 10.3389/fmicb.2018.03056

Barteneva, N. S., Maltsev, N., and Vorobjev, I. A. (2013). Microvesicles and intercellular communication in the context of parasitism. *Front. Cell Infect. Microbiol.* 3:49. doi: 10.3389/fcimb.2013.00049

Basmaciyan, L., Azas, N., and Casanova, M. (2017). Calcein+/PI- as an early apoptotic feature in Leishmania. *PLoS ONE* 12:e0187756. doi: 10.1371/journal.pone.0187756

Batista, B. S., Eng, W. S., Pilobello, K. T., Hendricks-Munoz, K. D., and Mahal, L. K. (2011). Identification of a conserved glycan signature for microvesicles. *J. Proteome Res.* 10, 4624–4633. doi: 10.1021/pr200434y

Batista, E. P., Costa, E. F., and Silva, A. A. (2014). Anopheles darlingi (Diptera: Culicidae) displays increased attractiveness to infected individuals with *Plasmodium vivax* gametocytes. *Parasit. Vectors* 7:251. doi: 10.1186/1756-3305-7-251

Bayer-Santos, E., Aguilar-Bonavides, C., Rodrigues, S. P., Cordero, E. M., Marques, A. F., Varela-Ramirez, A., et al. (2013). Proteomic analysis of *Trypanosoma cruzi* secretome: characterization of two populations of extracellular vesicles and soluble proteins. *J. Proteome. Res.* 12, 883–897. doi: 10.1021/pr300947g

Bayer-Santos, E., Lima, F. M., Ruiz, J. C., Almeida, I. C., and da Silveira, J. F. (2014). Characterization of the small RNA content of *Trypanosoma cruzi* extracellular vesicles. *Mol. Biochem. Parasitol.* 193, 71–74. doi: 10.1016/j.molbiopara.2014.02.004

Benchimol, M. (2004). The release of secretory vesicle in encysting Giardia lamblia. *FEMS Microbiol. Lett.* 235, 81–87. doi: 10.1111/j.1574-6968.2004.tb09570.x

Ben-Hur, S., Biton, M., and Regev-Rudzki, N. (2019). Extracellular vesicles: a prevalent tool for microbial gene delivery? *Proteomics* 19:e1800170. doi: 10.1002/pmic.201800170

Bergsmedh, A., Szeles, A., Henriksson, M., Bratt, A., Folkman, M. J., Spetz, A. L., et al. (2001). Horizontal transfer of oncogenes by uptake of apoptotic bodies. *Proc. Natl. Acad. Sci. U.S.A.* 98, 6407–6411. doi: 10.1073/pnas.101129998

Bernotiene, R., Palinauskas, V., Iezhova, T., Murauskaite, D., and Valkiunas, G. (2016). Avian haemosporidian parasites (Haemosporida): a comparative analysis of different polymerase chain reaction assays in detection of mixed infections. *Exp. Parasitol.* 163, 31–37. doi: 10.1016/j.exppara.2016.01.009

Bhatnagar, S., and Schorey, J. S. (2007). Exosomes released from infected macrophages contain Mycobacterium avium glycopeptidolipids and are proinflammatory. *J. Biol. Chem.* 282, 25779—25789. doi: 10.1074/jbc.M702277200

Campos, F. M., Franklin, B. S., Teixeira-Carvalho, A., Filho, A. L., de Paula, S. C., Fontes, C. J., et al. (2010). Augmented plasma microparticles during acute *Plasmodium vivax* infection. *Malar. J.* 9:327. doi: 10.1186/1475-2875-9-327

Casanova, M., Gonzalez, I. J., Sprissler, C., Zalila, H., Dacher, M., Basmaciyan, L., et al. (2015). Implication of different domains of the Leishmania major metacaspase in cell death and autophagy. *Cell Death Dis.* 6:e1933. doi: 10.1038/cddis.2015.288

Cestari, I., Ansa-Addo, E., Deolindo, P., Inal, J. M., and Ramirez, M. I. (2012). *Trypanosoma cruzi* immune evasion mediated by host cell-derived microvesicles. *J. Immunol.* 188, 1942–1952. doi: 10.4049/jimmunol.1102053

Chapman, S. J., and Hill, A. V. (2012). Human genetic susceptibility to infectious disease. *Nat. Rev. Genet.* 13,175–188. doi: 10.1038/nrg3114

Chargaff, E., and West, R. (1946). The biological significance of the thromboplastic protein of blood. *J. Biol. Chem.* 166, 189–197.

Chou, E. S., Abidi, S. Z., Teye, M., Leliwa-Sytek, A., Rask, T. S., Cobbold, S. A., et al. (2017). A high parasite density environment induces transcriptional changes and cell death in *Plasmodium falciparum* blood stages. *FEBS J.* 285, 848–870. doi: 10.1111/febs.14370

Chowdhury, I. H., Koo, S. J., Gupta, S., Liang, L. Y., Bahar, B., Silla, L., et al. (2017). Gene expression profiling and functional characterization of macrophages in response to circulatory microparticles produced during *Trypanosoma cruzi* infection and chagas disease. *J. Innate. Immun.* 9, 203–216. doi: 10.1159/000451055

Cocucci, E., and Meldolesi, J. (2015). Ectosomes and exosomes: shedding the confusion between extracellular vesicles. *Trends Cell Biol.* 25, 364–372. doi: 10.1016/j.tcb.2015.01.004

Coleman, M. L., Sahai, E. A., Yeo, M., Bosch, M., Dewar, A., and Olson, M. F. (2001). Membrane blebbing during apoptosis results from caspase-mediated activation of ROCK I. *Nat. Cell. Biol.* 3, 339–345. doi: 10.1038/35070009

Combes, V., Coltel, N., Alibert, M., van Eck, M., Raymond, C., Juhan-Vague, I., et al. (2005). ABCA1 gene deletion protects against cerebral malaria: potential pathogenic role of microparticles in neuropathology. *Am. J. Pathol.* 166, 295–302. doi: 10.1016/S0002-9440(10)62253-5

Combes, V., Taylor, T. E., Juhan-Vague, I., Mege, J. L., Mwenechanya, J., Tembo, M., et al. (2004). Circulating endothelial microparticles in malawian children with severe falciparum malaria complicated with coma. *JAMA* 291, 2542–2544. doi: 10.1001/jama.291.21.2542-b

Cornet, S., Nicot, A., Rivero, A., and Gandon, S. (2014). Evolution of plastic transmission strategies in avian malaria. *PLoS Pathog.* 10:e1004308. doi: 10.1371/journal.ppat.1004308

Correa, R., Coronado, L., Caballero, Z., Faral, P., Robello, C., and Spadafora, C. (2019). Extracellular vesicles carrying lactate dehydrogenase induce suicide in increased population density of *Plasmodium falciparum in vitro*. *Sci. Rep.* 9:5042. doi: 10.1038/s41598-019-41697-x

Correa, R., Coronado, L. M., Garrido, A. C., Durant-Archibold, A. A., and Spadafora, C. (2017). Volatile organic compounds associated with *Plasmodium falciparum* infection *in vitro*. *Parasit. Vectors.* 10:215. doi: 10.1186/s13071-017-2157-x

Couper, K. N., Barnes, T., Hafalla, J. C., Combes, V., Ryffel, B., Secher, T., et al. (2010). Parasite-derived plasma microparticles contribute significantly to malaria infection-induced inflammation through potent macrophage stimulation. *PLoS Pathog.* 6:e1000744. doi: 10.1371/journal.ppat.1000744

de Castro, E., Reus, T. L., de Aguiar, A. M., Avila, A. R., and de Arruda Campos Brasil de Souza, T. (2017). Procaspase-activating compound-1 induces apoptosis in *Trypanosoma cruzi*. *Apoptosis* 22, 1564–1577. doi: 10.1007/s10495-017-1428-5

de Pablos Torro, L. M., Retana Moreira, L., and Osuna, A. (2018). Extracellular vesicles in chagas disease: a new passenger for an old disease. *Front. Microbiol.* 9:1190. doi: 10.3389/fmicb.2018.01190

Deolindo, P., Evans-Osses, I., and Ramirez, M. I. (2013). Microvesicles and exosomes as vehicles between protozoan and host cell communication. *Biochem. Soc. Trans.* 41, 252–257. doi: 10.1042/BST20120217

Deponte, M., and Becker, K. (2004). *Plasmodium falciparum*—do killers commit suicide? *Trends Parasitol.* 20, 165–169. doi: 10.1016/j.pt.2004.01.012

Descoteaux, A., Moradin, N., and Arango Duque, G. (2013). Leishmania dices away cholesterol for survival. *Cell Host Microbe.* 13, 245–247. doi: 10.1016/j.chom.2013.02.018

Diaz Lozano, I. M., De Pablos, L. M., Longhi, S. A., Zago, M. P., Schijman, A. G., and Osuna, A. (2017). Immune complexes in chronic Chagas disease patients are formed by exovesicles from *Trypanosoma cruzi* carrying the conserved MASP N-terminal region. *Sci. Rep.* 7:44451. doi: 10.1038/srep44451

Duszenko, M., Figarella, K., Macleod, E. T., and Welburn, S. C. (2006). Death of a trypanosome: a selfish altruism. *Trends Parasitol.* 22, 536–542. doi: 10.1016/j.pt.2006.08.010

Elmore, S. (2007). Apoptosis: a review of programmed cell death. *Toxicol. Pathol.* 35, 495–516. doi: 10.1080/01926230701320337

Engelbrecht, D., and Coetzer, T. L. (2016). *Plasmodium falciparum* exhibits markers of regulated cell death at high population density *in vitro*. *Parasitol. Int.* 65(6 Pt A), 715–727. doi: 10.1016/j.parint.2016.07.007

Faille, D., Combes, V., Mitchell, A. J., Fontaine, A., Juhan-Vague, I., Alessi, M. C., et al. (2009). Platelet microparticles: a new player in malaria parasite cytoadherence to human brain endothelium. *FASEB J.* 23, 3449–3458. doi: 10.1096/fj.09-135822

Froeschke, G., and von der Heyden, S. (2014). A review of molecular approaches for investigating patterns of coevolution in marine host-parasite relationships. *Adv. Parasitol.* 84, 209–252. doi: 10.1016/B978-0-12-800099-1.00004-1

Frohlich, K., Hua, Z., Wang, J., and Shen, L. (2012). Isolation of Chlamydia trachomatis and membrane vesicles derived from host and bacteria. *J. Microbiol. Methods* 91, 222–230. doi: 10.1016/j.mimet.2012.08.012

Garcia-Silva, M. R., das Neves, R. F., Cabrera-Cabrera, F., Sanguinetti, J., Medeiros, L. C., Robello, C., et al. (2014). Extracellular vesicles shed by *Trypanosoma cruzi* are linked to small RNA pathways, life cycle regulation, and susceptibility to infection of mammalian cells. *Parasitol. Res.* 113, 285–304. doi: 10.1007/s00436-013-3655-1

Ghosh, J., Lal, C. S., Pandey, K., Das, V. N., Das, P., Roychoudhury, K., et al. (2011). Human visceral leishmaniasis: decrease in serum cholesterol as a function of splenic parasite load. *Ann. Trop. Med. Parasitol.* 105, 267–271. doi: 10.1179/136485911X12899838683566

Gomez, M. A., Contreras, I., Halle, M., Tremblay, M. L., McMaster, R. W., and Olivier, M. (2009). Leishmania GP63 alters host signaling through cleavage-activated protein tyrosine phosphatases. *Sci. Signal.* 2:ra58. doi: 10.1126/scisignal.2000213

Graystock, P., Meeus, I., Smagghe, G., Goulson, D., and Hughes, W. O. (2016). The effects of single and mixed infections of *Apicystis bombi* and deformed wing virus in *Bombus terrestris*. *Parasitology* 143, 358–365. doi: 10.1017/S0031182015001614

Gunjan, S., Sharma, T., Yadav, K., Chauhan, B. S., Singh, S. K., Siddiqi, M. I., et al. (2018). Artemisinin derivatives and synthetic trioxane trigger apoptotic cell death in asexual stages of plasmodium. *Front. Cell Infect. Microbiol.* 8:256. doi: 10.3389/fcimb.2018.00256

Gunjan, S., Singh, S. K., Sharma, T., Dwivedi, H., Chauhan, B. S., Imran Siddiqi, M., et al. (2016). Mefloquine induces ROS mediated programmed cell death in malaria parasite: Plasmodium. *Apoptosis* 21, 955–964. doi: 10.1007/s10495-016-1265-y

Harding, C., Heuser, J., and Stahl, P. (1984). Endocytosis and intracellular processing of transferrin and colloidal gold-transferrin in rat reticulocytes: demonstration of a pathway for receptor shedding. *Eur. J. Cell Biol.* 35, 256–263.

Hassani, K., and Olivier, M. (2013). Immunomodulatory impact of leishmania-induced macrophage exosomes: a comparative proteomic and functional analysis. *PLoS Negl. Trop. Dis.* 7:e2185. doi: 10.1371/journal.pntd.0002185

Janiszewski, M., Do Carmo, A. O., Pedro, M. A., Silva, E., Knobel, E., and Laurindo, F. R. (2004). Platelet-derived exosomes of septic individuals possess proapoptotic NAD(P)H oxidase activity: a novel vascular redox pathway. *Crit. Care Med.* 32, 818–825. doi: 10.1097/01.CCM.0000114829.17746.19

Kalra, H., Drummen, G. P., and Mathivanan, S. (2016). Focus on extracellular vesicles: introducing the next small big thing. *Int. J. Mol. Sci.* 17:170. doi: 10.3390/ijms17020170

Kawamura, Y., Yamamoto, Y., Sato, T. A., and Ochiya, T. (2017). Extracellular vesicles as trans-genomic agents: emerging roles in disease and evolution. *Cancer Sci.* 108, 824–830. doi: 10.1111/cas.13222

Keller, S., Sanderson, M. P., Stoeck, A., and Altevogt, P. (2006). Exosomes: from biogenesis and secretion to biological function. *Immunol. Lett.* 107, 102–108. doi: 10.1016/j.imlet.2006.09.005

Kim, D. K., Lee, J., Kim, S. R., Choi, D. S., Yoon, Y. J., Kim, J. H., et al. (2015). EVpedia: a community web portal for extracellular vesicles research. *Bioinformatics* 31, 933–939. doi: 10.1093/bioinformatics/btu741

Kreimer, S., Belov, A. M., Ghiran, I., Murthy, S. K., Frank, D. A., and Ivanov, A. R. (2015). Mass-spectrometry-based molecular characterization of extracellular vesicles: lipidomics and proteomics. *J. Proteome Res.* 14, 2367–2384. doi: 10.1021/pr501279t

Krishna, S., Bharti, P. K., Chandel, H. S., Ahmad, A., Kumar, R., Singh, P. P., et al. (2015). Detection of mixed infections with *Plasmodium* spp. by PCR, India, 2014. *Emerg. Infect. Dis.* 21, 1853–1857. doi: 10.3201/eid2110.150678

Lacroix, R., Mukabana, W. R., Gouagna, L. C., and Koella, J. C. (2005). Malaria infection increases attractiveness of humans to mosquitoes. *PLoS Biol.* 3:e298. doi: 10.1371/journal.pbio.0030298

Lazaro-Ibanez, E., Sanz-Garcia, A., Visakorpi, T., Escobedo-Lucea, C., Siljander, P., Ayuso-Sacido, A., et al. (2014). Different gDNA content in the subpopulations of prostate cancer extracellular vesicles: apoptotic bodies, microvesicles, and exosomes. *Prostate* 74, 1379–1390. doi: 10.1002/pros.22853

Lefebvre, F. A., Benoit Bouvrette, L. P., Perras, L., Blanchet-Cohen, A., Garnier, D., Rak, J., et al. (2016). Comparative transcriptomic analysis of human and Drosophila extracellular vesicles. *Sci. Rep.* 6:27680. doi: 10.1038/srep27680

Lener, T., Gimona, M., Aigner, L., Borger, V., Buzas, E., Camussi, G., et al. (2015). Applying extracellular vesicles based therapeutics in clinical trials - an ISEV position paper. *J. Extracell Vesicles* 4:30087. doi: 10.3402/jev.v4.30087

Leventis, P. A., and Grinstein, S. (2010). The distribution and function of phosphatidylserine in cellular membranes. *Annu. Rev. Biophys.* 39, 407–427. doi: 10.1146/annurev.biophys.093008.131234

Li, M., Wang, H., Liu, J., Hao, P., Ma, L., and Liu, Q. (2015). The Apoptotic role of metacaspase in *Toxoplasma gondii*. *Front. Microbiol.* 6:1560. doi: 10.3389/fmicb.2015.01560

Lu, T., Qiu, Y. T., Wang, G., Kwon, J. Y., Rutzler, M., Kwon, H. W., et al. (2007). Odor coding in the maxillary palp of the malaria vector mosquito Anopheles gambiae. *Curr. Biol.* 17, 1533–1544. doi: 10.1016/j.cub.2007.07.062

Luse, S. A., and Miller, L. H. (1971). *Plasmodium falciparum* malaria. Ultrastructure of parasitized erythrocytes in cardiac vessels. *Am. J. Trop. Med. Hyg.* 20, 655–660. doi: 10.4269/ajtmh.1971.20.655

Mandal, A., Das, S., Roy, S., Ghosh, A. K., Sardar, A. H., Verma, S., et al. (2016). Deprivation of L-Arginine induces oxidative stress mediated apoptosis in leishmania donovani promastigotes: contribution of the polyamine pathway. *PLoS. Negl. Trop. Dis.* 10:e0004373. doi: 10.1371/journal.pntd.0004373

Mantel, P. Y., Hjelmqvist, D., Walch, M., Kharoubi-Hess, S., Nilsson, S., Ravel, D., et al. (2016). Infected erythrocyte-derived extracellular vesicles alter vascular function via regulatory Ago2-miRNA complexes in malaria. *Nat. Commun.* 7:12727. doi: 10.1038/ncomms12727

Mantel, P. Y., Hoang, A. N., Goldowitz, I., Potashnikova, D., Hamza, B., Vorobjev, I., et al. (2013). Malaria-infected erythrocyte-derived microvesicles mediate cellular communication within the parasite population and with the host immune system. *Cell Host Microbe.* 13, 521–534. doi: 10.1016/j.chom.2013.04.009

Mantel, P. Y., and Marti, M. (2014). The role of extracellular vesicles in Plasmodium and other protozoan parasites. *Cell. Microbiol.* 16, 344–354. doi: 10.1111/cmi.12259

Martin-Jaular, L., Nakayasu, E. S., Ferrer, M., Almeida, I. C., and Del Portillo, H. A. (2011). Exosomes from *Plasmodium yoelii*-infected reticulocytes protect mice from lethal infections. *PLoS ONE* 6:e26588. doi: 10.1371/journal.pone.0026588

Matthews, K. R. (2005). The developmental cell biology of Trypanosoma brucei. *J. Cell Sci.* 118(Pt 2), 283–290. doi: 10.1242/jcs.01649

Meldolesi, J. (2018). Exosomes and ectosomes in intercellular communication. *Curr. Biol.* 28, R435–R444. doi: 10.1016/j.cub.2018.01.059

Meslin, B., Barnadas, C., Boni, V., Latour, C., De Monbrison, F., Kaiser, K., et al. (2007). Features of apoptosis in *Plasmodium falciparum* erythrocytic stage through a putative role of PfMCA1 metacaspase-like protein. *J. Infect Dis.* 195, 1852–1859. doi: 10.1086/518253

Molina-Cruz, A., and Barillas-Mury, C. (2014). The remarkable journey of adaptation of the *Plasmodium falciparum* malaria parasite to New World anopheline mosquitoes. *Mem. Inst. Oswaldo Cruz.* 109, 662–667. doi: 10.1590/0074-0276130553

Montaner, S., Galiano, A., Trelis, M., Martin-Jaular, L., Del Portillo, H. A., Bernal, D., et al. (2014). The role of extracellular vesicles in modulating the host immune response during parasitic infections. *Front. Immunol.* 5:433. doi: 10.3389/fimmu.2014.00433

Mozzi, A., Pontremoli, C., and Sironi, M. (2018). Genetic susceptibility to infectious diseases: current status and future perspectives from genome-wide approaches. *Infect. Genet. Evol.* 66, 286–307. doi: 10.1016/j.meegid.2017.09.028

Muralidharan-Chari, V., Clancy, J., Plou, C., Romao, M., Chavrier, P., Raposo, G., et al. (2009). ARF6-regulated shedding of tumor cell-derived plasma membrane microvesicles. *Curr. Biol.* 19, 1875–1885. doi: 10.1016/j.cub.2009.09.059

Mutai, B. K., and Waitumbi, J. N. (2010). Apoptosis stalks *Plasmodium falciparum* maintained in continuous culture condition. *Malar. J.* 9(Suppl. 3):S6. doi: 10.1186/1475-2875-9-S3-S6

Nabhan, J. F., Hu, R., Oh, R. S., Cohen, S. N., and Lu, Q. (2012). Formation and release of arrestin domain-containing protein 1-mediated microvesicles (ARMMs) at plasma membrane by recruitment of TSG101 protein. *Proc. Natl. Acad. Sci. U.S.A.* 109, 4146–4151. doi: 10.1073/pnas.1200448109

Nawaz, M., Camussi, G., Valadi, H., Nazarenko, I., Ekstrom, K., Wang, X., et al. (2014). The emerging role of extracellular vesicles as biomarkers for urogenital cancers. *Nat. Rev. Urol.* 11, 688–701. doi: 10.1038/nrurol.2014.301

Ostrowski, M., Carmo, N. B., Krumeich, S., Fanget, I., Raposo, G., Savina, A., et al. (2010). Rab27a and Rab27b control different steps of the exosome secretion pathway. *Nat. Cell Biol.* 12, 19–30. doi: 10.1038/ncb2000

Otto, T. D., Gilabert, A., Crellen, T., Bohme, U., Arnathau, C., Sanders, M., et al. (2018). Genomes of all known members of a Plasmodium subgenus reveal paths to virulent human malaria. *Nat. Microbiol.* 3, 687–697. doi: 10.1038/s41564-018-0162-2

Pankoui Mfonkeu, J. B., Gouado, I., Fotso Kuate, H., Zambou, O., Amvam Zollo, P. H., Grau, G. E., et al. (2010). Elevated cell-specific microparticles are a biological marker for cerebral dysfunctions in human severe malaria. *PLoS ONE* 5:e13415. doi: 10.1371/journal.pone.0013415

Piguet, P. F., Kan, C. D., and Vesin, C. (2002). Thrombocytopenia in an animal model of malaria is associated with an increased caspase-mediated death of thrombocytes. *Apoptosis* 7, 91–98. doi: 10.1023/A:1014341611412

Plenderleith, L. J., Liu, W., Learn, G. H., Loy, D. E., Speede, S., Sanz, C. M., et al. (2019). Ancient introgression between two ape malaria parasite species. *Genome. Biol. Evol.* 11, 3269–3274. doi: 10.1093/gbe/evz244

Preusser, C., Hung, L. H., Schneider, T., Schreiner, S., Hardt, M., Moebus, A., et al. (2018). Selective release of circRNAs in platelet-derived extracellular vesicles. *J. Extracell. Vesicles* 7:1424473. doi: 10.1080/20013078.2018.1424473

Proto, W. R., Coombs, G. H., and Mottram, J. C. (2013). Cell death in parasitic protozoa: regulated or incidental? *Nat. Rev. Microbiol.* 11, 58–66. doi: 10.1038/nrmicro2929

Prugnolle, F., Durand, P., Neel, C., Ollomo, B., Ayala, F. J., Arnathau, C., et al. (2010). African great apes are natural hosts of multiple related malaria species, including *Plasmodium falciparum*. *Proc. Natl. Acad. Sci. U.S.A.* 107, 1458–1463. doi: 10.1073/pnas.0914440107

Quintana-Murci, L. (2019). Human immunology through the lens of evolutionary genetics. *Cell* 177,184–199. doi: 10.1016/j.cell.2019.02.033

Ramirez, M. I., Deolindo, P., de Messias-Reason, I. J., Arigi, E. A., Choi, H., Almeida, I. C., et al. (2017). Dynamic flux of microvesicles modulate parasite-host cell interaction of *Trypanosoma cruzi* in eukaryotic cells. *Cell. Microbiol.* (2017) 19:e12672. doi: 10.1111/cmi.12672

Ranford-Cartwright, L. C., and Mwangi, J. M. (2012). Analysis of malaria parasite phenotypes using experimental genetic crosses of *Plasmodium falciparum*. *Int. J. Parasitol.* 42, 529–534. doi: 10.1016/j.ijpara.2012.03.004

Raposo, G., Nijman, H. W., Stoorvogel, W., Liejendekker, R., Harding, C. V., Melief, C. J., et al. (1996). B lymphocytes secrete antigen-presenting vesicles. *J. Exp. Med.* 183, 1161–1172. doi: 10.1084/jem.183.3.1161

Raposo, G., and Stoorvogel, W. (2013). Extracellular vesicles: exosomes, microvesicles, and friends. *J. Cell. Biol.* 200, 373–383. doi: 10.1083/jcb.201211138

Reece, S. E., Pollitt, L. C., Colegrave, N., and Gardner, A. (2011). The meaning of death: evolution and ecology of apoptosis in protozoan parasites. *PLoS Pathog.* 7:e1002320. doi: 10.1371/journal.ppat.1002320

Regev-Rudzki, N., Wilson, D. W., Carvalho, T. G., Sisquella, X., Coleman, B. M., Rug, M., et al. (2013). Cell-cell communication between malaria-infected red blood cells via exosome-like vesicles. *Cell* 153, 1120–1133. doi: 10.1016/j.cell.2013.04.029

Rezanezhad, H., Menegon, M., Sarkari, B., Hatam, G. R., and Severini, C. (2011). Characterization of the metacaspase 1 gene in *Plasmodium vivax* field isolates from southern Iran and Italian imported cases. *Acta Trop*. 119, 57–60. doi: 10.1016/j.actatropica.2011.03.010

Rioux, J. D., Xavier, R. J., Taylor, K. D., Silverberg, M. S., Goyette, P., Huett, A., et al. (2007). Genome-wide association study identifies new susceptibility loci for Crohn disease and implicates autophagy in disease pathogenesis: *Nat. Genet*. 39, 596–604. doi: 10.1038/ng2032

Rodrigues, M. L., Nakayasu, E. S., Oliveira, D. L., Nimrichter, L., Nosanchuk, J. D., Almeida, I. C., et al. (2008). Extracellular vesicles produced by Cryptococcus neoformans contain protein components associated with virulence. *Eukaryot. Cell* 7, 58–67. doi: 10.1128/EC.00370-07

Sahu, U., Mohapatra, B. N., Kar, S. K., and Ranjit, M. (2013). Promoter polymorphisms in the ATP binding cassette transporter gene influence production of cell-derived microparticles and are highly associated with susceptibility to severe malaria in humans. *Infect. Immun*. 81, 1287–1294. doi: 10.1128/IAI.01175-12

Schorey, J. S., Cheng, Y., Singh, P. P., and Smith, V. L. (2015). Exosomes and other extracellular vesicles in host-pathogen interactions. *EMBO Rep*. 16, 24–43. doi: 10.15252/embr.201439363

Shrivastava, S. K., Dalko, E., Delcroix-Genete, D., Herbert, F., Cazenave, P. A., and Pied, S. (2017). Uptake of parasite-derived vesicles by astrocytes and microglial phagocytosis of infected erythrocytes may drive neuroinflammation in cerebral malaria. *Glia* 65, 75–92. doi: 10.1002/glia.23075

Silva, V. O., Maia, M. M., Torrecilhas, A. C., Taniwaki, N. N., Namiyama, G. M., Oliveira, K. C., et al. (2018). Extracellular vesicles isolated from *Toxoplasma gondii* induce host immune response. *Parasite Immunol.* 40:e12571. doi: 10.1111/pim.12571

Silverman, J. M., Chan, S. K., Robinson, D. P., Dwyer, D. M., Nandan, D., Foster, L. J., et al. (2008). Proteomic analysis of the secretome of Leishmania donovani. *Genome. Biol*. 9:R35. doi: 10.1186/gb-2008-9-2-r35

Silverman, J. M., Clos, J., Horakova, E., Wang, A. Y., Wiesgigl, M., Kelly, I., et al. (2010). Leishmania exosomes modulate innate and adaptive immune responses through effects on monocytes and dendritic cells. *J. Immunol*. 185, 5011–5022. doi: 10.4049/jimmunol.1000541

Silverman, J. M., and Reiner, N. E. (2011). Leishmania exosomes deliver preemptive strikes to create an environment permissive for early infection. *Front. Cell Infect. Microbiol*. 1:26. doi: 10.3389/fcimb.2011.00026

Silvester, E., Young, J., Ivens, A., and Matthews, K. R. (2017). Interspecies quorum sensing in co-infections can manipulate trypanosome transmission potential. *Nat. Microbiol.* 2, 1471–1479. doi: 10.1038/s41564-017-0014-5

Sisquella, X., Ofir-Birin, Y., Pimentel, M. A., Cheng, L., Abou Karam, P., Sampaio, N. G., et al. (2017). Malaria parasite DNA-harbouring vesicles activate cytosolic immune sensors. *Nat. Commun*. 8:1985. doi: 10.1038/s41467-017-02083-1

Smallegange, R. C., van Gemert, G. J., van de Vegte-Bolmer, M., Gezan, S., Takken, W., Sauerwein, R. W., et al. (2013). Malaria infected mosquitoes express enhanced attraction to human odor. *PLoS ONE* 8:e63602. doi: 10.1371/journal.pone.0063602

Sow, F., Nyonda, M., Bienvenu, A. L., and Picot, S. (2015). Wanted *Plasmodium falciparum*, dead or alive. *Microb. Cell* 2, 219–224. doi: 10.15698/mic2015.07.211

Spycher, C., Rug, M., Klonis, N., Ferguson, D. J., Cowman, A. F., Beck, H. P., et al. (2006). Genesis of and trafficking to the Maurer's clefts of *Plasmodium falciparum*-infected erythrocytes. *Mol. Cell Biol*. 26, 4074–4085. doi: 10.1128/MCB.00095-06

Stenqvist, A. C., Nagaeva, O., Baranov, V., and Mincheva-Nilsson, L. (2013). Exosomes secreted by human placenta carry functional Fas ligand and TRAIL molecules and convey apoptosis in activated immune cells, suggesting exosome-mediated immune privilege of the fetus. *J. Immunol*. 191, 5515–5523. doi: 10.4049/jimmunol.1301885

Sundararaman, S. A., Plenderleith, L. J., Liu, W., Loy, D. E., Learn, G. H., Li, Y., et al. (2016). Genomes of cryptic chimpanzee Plasmodium species reveal key evolutionary events leading to human malaria. *Nat. Commun*. 7:11078. doi: 10.1038/ncomms11078

Szatanek, R., Baj-Krzyworzeka, M., Zimoch, J., Lekka, M., Siedlar, M., and Baran, J. (2017). The methods of choice for extracellular vesicles (EVs) characterization. *Int. J. Mol. Sci*. 18:E1153. doi: 10.3390/ijms18061153

Takken, W., and Knols, B. G. (1999). Odor-mediated behavior of Afrotropical malaria mosquitoes. *Annu. Rev. Entomol*. 44, 131–157. doi: 10.1146/annurev.ento.44.1.131

Totino, P. R., Magalhaes, A., Alves, E. B., Costa, M. R., de Lacerda, M. V., Daniel-Ribeiro, C. T., et al. (2014). *Plasmodium falciparum*, but not *P. vivax*, can induce erythrocytic apoptosis. *Parasit. Vectors* 7:484. doi: 10.1186/PREACCEPT-1516774475118464

Trocoli Torrecilhas, A. C., Tonelli, R. R., Pavanelli, W. R., da Silva, J. S., Schumacher, R. I., de Souza, W., et al. (2009). *Trypanosoma cruzi*: parasite shed vesicles increase heart parasitism and generate an intense inflammatory response. *Microbes. Infect*. 11, 29–39. doi: 10.1016/j.micinf.2008.10.003

Turchinovich, A., Drapkina, O., and Tonevitsky, A. (2019). Transcriptome of extracellular vesicles: state-of-the-art. *Front. Immunol*. 10:202. doi: 10.3389/fimmu.2019.00202

Twu, O., de Miguel, N., Lustig, G., Stevens, G. C., Vashisht, A. A., Wohlschlegel, J. A., et al. (2013). Trichomonas vaginalis exosomes deliver cargo to host cells and mediate hostratioparasite interactions. *PLoS Pathog*. 9:e1003482. doi: 10.1371/journal.ppat.1003482

van Balkom, B. W., Eisele, A. S., Pegtel, D. M., Bervoets, S., and Verhaar, M. C. (2015). Quantitative and qualitative analysis of small RNAs in human endothelial cells and exosomes provides insights into localized RNA processing, degradation and sorting. *J. Extracell. Vesicles* 4:26760. doi: 10.3402/jev.v4.26760

van der Heyde, H. C., Gramaglia, I., Combes, V., George, T. C., and Grau, G., E. (2011). Flow cytometric analysis of microparticles. *Methods Mol. Biol.* 699, 337–354. doi: 10.1007/978-1-61737-950-5_16

van der Pol, E., Boing, A. N., Harrison, P., Sturk, A., and Nieuwland, R. (2012). Classification, functions, and clinical relevance of extracellular vesicles. *Pharmacol. Rev*. 64, 676–705. doi: 10.1124/pr.112.005983

van Niel, G., D'Angelo, G., and Raposo, G. (2018). Shedding light on the cell biology of extracellular vesicles. *Nat. Rev. Mol. Cell. Biol.* 19, 213–228. doi: 10.1038/nrm.2017.125

Wei, M., Lu, L., Sui, W., Liu, Y., Shi, X., and Lv, L. (2018). Inhibition of GLUTs by WZB117 mediates apoptosis in blood-stage Plasmodium parasites by breaking redox balance. *Biochem. Biophys. Res. Commun*. 503, 1154–1159. doi: 10.1016/j.bbrc.2018.06.134

Wolf, P. (1967). The nature and significance of platelet products in human plasma. *Br. J. Haematol.* 13, 269–288. doi: 10.1111/j.1365-2141.1967.tb08741.x

Yanez-Mo, M., Siljander, P. R., Andreu, Z., Zavec, A. B., Borras, F. E., Buzas, E. I., et al. (2015). Biological properties of extracellular vesicles and their physiological functions. *J. Extracell. Vesicles* 4:27066. doi: 10.3402/jev.v4.27066

Yang, Z., and Bielawski, J. P. (2000). Statistical methods for detecting molecular adaptation. *Trends Ecol. Evol*. 15, 496–503. doi: 10.1016/S0169-5347(00)01994-7

Ye, W., Chew, M., Hou, J., Lai, F., Leopold, S. J., Loo, H. L., et al. (2018). Microvesicles from malaria-infected red blood cells activate natural killer cells via MDA5 pathway. *PLoS Pathog*. 14:e1007298. doi: 10.1371/journal.ppat.1007298

Zhu, L., Liu, J., Dao, J., Lu, K., Li, H., Gu, H., et al. (2016). Molecular characterization of S. japonicum exosome-like vesicles reveals their regulatory roles in parasite-host interactions. *Sci. Rep*. 6:25885. doi: 10.1038/srep25885

Conflict of Interest: The authors declare that the research was conducted in the absence of any commercial or financial relationships that could be construed as a potential conflict of interest.

frontiers in Microbiology

ORIGINAL RESEARCH
published: 03 March 2020
doi: 10.3389/fmicb.2020.00246

Uptake of *Plasmodium falciparum* Gametocytes During Mosquito Bloodmeal by Direct and Membrane Feeding

*Arthur M. Talman[1,2], Dinkorma T. D. Ouologuem[3], Katie Love[1], Virginia M. Howick[1], Charles Mulamba[1], Aboubecrin Haidara[3], Niawanlou Dara[3], Daman Sylla[3], Adama Sacko[3], Mamadou M. Coulibaly[3], Francois Dao[3], Cheick P. O. Sangare[3], Abdoulaye Djimde[3] and Mara K. N. Lawniczak[1]**

[1] Wellcome Sanger Institute, Hinxton, United Kingdom, [2] MIVEGEC, IRD, CNRS, University of Montpellier, Montpellier, France, [3] Malaria Research and Training Centre, University of Science, Techniques and Technologies of Bamako, Bamako, Mali

OPEN ACCESS

Edited by:
Brandon Keith Wilder, Oregon Health & Science University, United States

Reviewed by:
Robert Sinden, Imperial College London, United Kingdom
Chris Drakeley, University of London, United Kingdom

***Correspondence:**
Mara K. N. Lawniczak
mara@sanger.ac.uk

Specialty section:
This article was submitted to Infectious Diseases, a section of the journal Frontiers in Microbiology

Received: *03 September 2019*
Accepted: *03 February 2020*
Published: *03 March 2020*

Citation:
Talman AM, Ouologuem DTD, Love K, Howick VM, Mulamba C, Haidara A, Dara N, Sylla D, Sacko A, Coulibaly MM, Dao F, Sangare CPO, Djimde A and Lawniczak MKN (2020) Uptake of Plasmodium falciparum Gametocytes During Mosquito Bloodmeal by Direct and Membrane Feeding. Front. Microbiol. 11:246. doi: 10.3389/fmicb.2020.00246

Plasmodium falciparum remains one of the leading causes of child mortality, and nearly half of the world's population is at risk of contracting malaria. While pathogenesis results from replication of asexual forms in human red blood cells, it is the sexually differentiated forms, gametocytes, which are responsible for the spread of the disease. For transmission to succeed, both mature male and female gametocytes must be taken up by a female *Anopheles* mosquito during its blood meal for subsequent differentiation into gametes and mating inside the mosquito gut. Observed circulating numbers of gametocytes in the human host are often surprisingly low. A pre-fertilization behavior, such as skin sequestration, has been hypothesized to explain the efficiency of human-to-mosquito transmission but has not been sufficiently tested due to a lack of appropriate tools. In this study, we describe the optimization of a qPCR tool that enables the relative quantification of gametocytes within very small input samples. Such a tool allows for the quantification of gametocytes in different compartments of the host and the vector that could potentially unravel mechanisms that enable highly efficient malaria transmission. We demonstrate the use of our gametocyte quantification method in mosquito blood meals from both direct skin feeding on *Plasmodium* gametocyte carriers and standard membrane feeding assay. Relative gametocyte abundance was not different between mosquitoes fed through a membrane or directly on the skin suggesting that there is no systematic enrichment of gametocytes picked up in the skin.

Keywords: malaria, transmission, gametocyte, mosquito feeding, *Plasmodium falciparum*

INTRODUCTION

Transmission of *Plasmodium falciparum* from humans to mosquitoes depends on the sexual phase of the parasite's life cycle. Both male and female gametocytes have to be picked up in the mosquito blood meal in order to mate and colonize the mosquito. Relatively low circulating gametocyte densities are typically observed (Bousema and Drakeley, 2011), and yet transmission remains efficient even at gametocyte densities for which random

sampling of the host cannot explain successful infection of the mosquito (Lawniczak and Eckhoff, 2016). Sub-patently infected carriers that harbor parasites below the limit of detection by microscopy can readily infect mosquitoes (Schneider et al., 2007; Ouédraogo et al., 2009). Mosquitoes fed directly on the skin have also been found to be infected more readily than by a direct membrane feeding assay (Bonnet et al., 2000; Diallo et al., 2008). These findings have led to the hypothesis of gametocyte biology and behavior that enhance their transmission but have yet to be described (Pichon et al., 2000; Bousema and Drakeley, 2011). A pre-fertilization behavior, whereby malaria gametocytes associate in the circulating blood and/or adhere to sub-dermal capillaries could enhance their probability of being ingested in sufficient quantities. Intriguingly, two early studies revealed that gametocytes were on average three times more concentrated in skin biopsies than in the venous circulation (Chardome and Janssen, 1952; Van Den Berghe et al., 1954), although these experiments lacked appropriate controls. Whilst associative behaviors have been hypothesized, they have never been explicitly tested. Comparing gametocyte uptake in skin-fed and membrane-fed mosquitoes could determine if the patterns differ between these blood sources. Such an undertaking, however, requires a sensitive detection tool able to accurately measure gametocyte densities in individual mosquito blood meals. The most commonly used gametocyte molecular detection tools, albeit of good sensitivity, only detect female gametocytes in human blood sample (Schneider et al., 2015). In this study, we describe a molecular assay capable of measuring relative gametocyte densities directly in mosquito bloodmeals and investigate the uptake of gametocytes during natural and artificial blood feeding of symptomatic malaria patients.

MATERIALS AND METHODS

Gametocyte Specific Transcript Selection for Ultrasensitive Detection and Multiplex Rt qPcr

In order to find a suitable gametocyte biomarker, 107 transcripts displaying a 25-fold enrichment in gametocytes compared to rings in a published stage-specific RNAseq study were selected (López-Barragán et al., 2011; **Supplementary Table S1**). qPCR primers to each of these transcripts were designed using the IDT PrimerQuest® Tool. *P. falciparum* isolate NF54 was maintained in O+ blood in RPMI 1640 culture medium (GIBCO) supplemented with 25 mM HEPES (SIGMA), 10 mM D-Glucose (SIGMA), 50 mg/L hypoxanthine (SIGMA), and 10% human serum in a gas mix containing 5% O_2, 5% CO_2, and 90% N_2. Human O+ erythrocytes were obtained from NHS Blood and Transplant, Cambridge, United Kingdom. None of the blood products used contained identifying information from donors. *Plasmodium* culture using human serum and erythrocytes from donors has been approved by the NHS Cambridgeshire 4 Research Ethics Committee (REC reference 15/EE/0253) and the Wellcome Sanger Institute Human Materials and Data Management Committee. Pure ring stage parasites (10^9) were produced by double Percoll-sorbitol synchronization (Moll et al., 2008), followed by negative selection on a MACs LS column (Miltenyi Biotec). Pure stage V gametocyte samples (10^8) were produced and purified on a MACs LS column (Ribaut et al., 2008). Parasite counts were established by Giemsa staining and hematocrit was measured with a hemocytometer. RNA was extracted with TRIzol according to the manufacturer's recommendations. RNAs were treated with DNA-free DNAse Turbo kit (Ambion) and reverse transcribed with the high capacity reverse transcriptase kit (Thermo Fisher), supplemented with oligo-dts (Thermo Fisher) at a final concentration of 2.5 μM. SYBR-green qPCR (Roche) was conducted on a Lightcycler 480 (Roche) for each of these transcripts on pure gametocyte and ring duplicate cDNAs. The DNA-free DNAse Turbo kit removes gDNA, a reverse transcriptase-less control was run with each extraction batch and was verified to be negative before inclusion of samples in the dataset. Enrichment of transcripts in gametocytes was estimated using the delta-delta *Ct* method for each 107 transcript and the housekeeping gene glucose-6-phosphate dehydrogenase-6-phosphogluconolactonase (PF3D7_1453800) as a control. A probe-based multiplex assay was designed to allow relative quantification and comparison of gametocytes within mosquito bloodmeals. A triplex qPCR assay was devised: it detected the gametocyte biomarker (*MDV-1*, PF3D7_1216500, cy5), an asexual transcript (*Mahrp2*, PF3D7_1353200, HEX) and a human transcript (*hsGAPDH*, FAM) (**Supplementary Table S2**). The *Mahrp2* transcript was selected because it was the most enriched transcript in rings compared to gametocytes by RNAseq; if one excludes *Hrp2* or *Hrp3,* two gene*s* that have been shown to be deleted in some populations of parasites and are therefore not suitable (Watson et al., 2017). An alternative assay using the human transcript *UBA-1* was included to validate *hsGAPDH* as a suitable loading control for leukocytes. Multiplex primer efficiencies were calculated on qPCRs of gDNA serial dilutions for all primer/probe combinations (**Supplementary Table S3**). The qPCR conditions were as follows, the samples were first incubated for 10 min at 95°C, then 45 cycles were performed (95°C for 10 s, 60°C for 10 s, and 68°C for 20 s), followed by a melting curve step to ensure single product amplification. Single amplification was observed for all samples. The melting temperature were chosen as that recommended by the assay manufacturer without alteration. The *Ct* calculated by the relative quantification protocol of the Light cycle 480 software were used. Fold changes were calculated by the delta-delta *Ct* method corrected for primer efficiency (Pfaffl, 2004; p. 96 equation 3.5).

Mock Blood Meals With a Gametocyte Serial Dilution

To test the triplex qPCR assay with differing concentrations of gametocytes, *in vitro* cultured asexual and sexual parasites were artificially fed to mosquitoes. A serial dilution of gametocytes (10–100,000 per blood meal) was spiked with 10,000 rings per μl, placed in whole blood and spun at 800 *g* for 5 min, heat-inactivated serum was used to resuspend the pellet to 50% hematocrit and aliquoted into a heated plastic membrane

feeder covered with stretched parafilm (Bemis NA). Eight female *Anopheles coluzzii* (N'Gousso strain) were allowed to feed on each dilution for 12 min and were immediately sacrificed in 70% ethanol. Fed mosquitoes were tapped briefly on absorbent paper to remove excess ethanol and immediately immersed in 50 µl of TriZol in RNAse-free 1.5 ml tubes and stored at −80°C. Upon thawing, 450 µl of fresh TriZol was added to each 50 µl sample, and mosquitoes were homogenized with a clean pestle and RNA extraction and cDNA generation were conducted as described above.

Study Site and Ethical Approval

To test the assay in natural conditions, we recruited *P. falciparum* positive patients in Faladie, Mali. Faladie is situated in the Koulikoro region of Mali and is characterized by a seasonal hyperendemic transmission of mostly *P. falciparum* malaria. Patients, aged 6–14 years, with symptomatic non-severe malaria were recruited from November to December 2016 (**Table 1**). Patients were screened by thick smear microscopy during which the asexual parasite (rings) and gametocyte counts (stage V) were recorded for 1000 leukocytes. A standard concentration of 8000 leukocytes per µl was used to calculate parasitemia and gametocytaemias. The protocol was approved by an IRB from the Faculty Of Medicine, Pharmacy and Odontostomatology de Pharmacy; Université des Sciences, Techniques et Technologies of Bamako (IRB approval letter No. 2016/133/CE/FMPOS).

Mosquito Feeding Assay

To compare the number of gametocytes acquired in the mosquito bloodmeal from feeding on the skin or peripheral bloodstream, a peripheral blood sample was first obtained from *P. falciparum* gametocyte carriers in a vacutainer with EDTA and immediately placed into two plastic membrane feeders covered with parafilm (600 µl each). 50 starved *A. coluzzii* females were allowed to feed on each feeder (n = 100 total). Membrane feedings were allowed to proceed for 12 min. Concomitantly 2 pots of 25 mosquitoes were allowed to direct skin-feed on each volunteer (back of left calf, right calf) until repletion (8 min approximatively). Following the feeds, all mosquitoes were immediately sacrificed with 70% ethanol. Mosquitoes were each transferred to 50 µl of TriZOl and kept in liquid nitrogen or at −80°C until extraction.

Mosquito Sample Processing for Parasite Quantification

For RNA extraction, upon thawing, 450 µl of fresh TriZol was added to each 50 µl sample, and mosquitoes were homogenized with a clean pestle. RNA extraction and cDNA generation were conducted as above. Two assays per sample were run: the triplex mentioned above (*MDV-1*, *hsGAPDH*, and *Mahrp2)* and a duplex with the alternative human transcript *hsUBA-1* (FAM) and a control mosquito transcript (ribosomal protein S7, HEX). Samples that yielded $Ct > 38$ for *MDV-1* or *hsGAPDH* were discarded. Fold changes were calculated using the delta-delta *Ct* method corrected for primer efficiency (Pfaffl, 2004; **Supplementary Table S4**); the test gene was always *MDV-1*

TABLE 1 | Feed data for six patients. Parasitemia and gametocytemia were established by microscopy.

Patient number	Parasitemia-day 0 (Microscopy) (/µl)	Gametocytemia day 0 (Microscopy) (/µl)	Membrane feeder 1 (positive blood meals/total)	Membrane feeder 2 (positive blood meals/total)	Skin feed left (positive blood meals/total)	Skin feed right (positive blood meals/total)	Variance (*F*-test)		*t*-test	
							Variance in skinfed than membrane fed	*p*-value	Mean fold change in skinfed vs membrane fed	*p*-value
EGF006	14,680	520	16/17	15/17	16/17	12/13	Greater	0.03091	NS	0.1986
EGF007	37,640	48	17/18	6/8	19/20	14/15	Greater	0.006914	NS	0.05617
EGF009	4800	144	15/15	11/12	17/19	10/10	NS	0.1377	NS	0.617
EGF014	1440	360	16/17	9/9	15/15	19/20	Greater	0.01363	NS	0.2308
EFG017	512	296	21/21	20/21	23/23	23/23	Less	0.01764	NS	0.3374
EFG020	17,520	96	14/21	12/17	9/21	11/24	Less	2.545E-06	less	3.06E-05
Overall	NA	NA	NA	NA	NA	NA	Less	8.138e-06	NS	0.05251

Number of fed mosquitoes with a positive MDV-1 Ct (<38) is given together with the total number of mosquitoes for each feed.

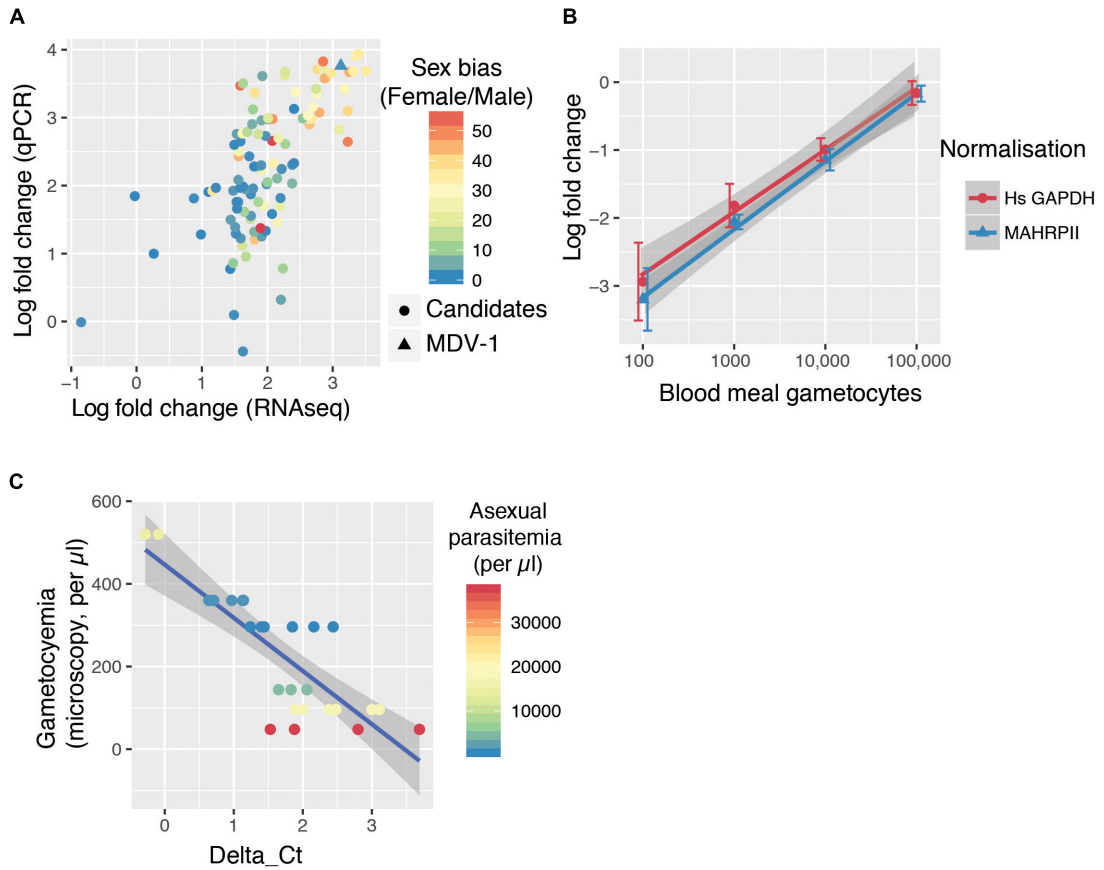

FIGURE 1 | The GQA, a multiplex assay capable of sensitively detecting gametocyte uptake by mosquitoes. **(A)** RNAseq (López-Barragán et al., 2011) and qPCR fold change of 107 transcripts in gametocytes compared to ring stage parasites. The color scale indicates sex-bias in expression based on (Lasonder et al., 2016) with high female:male ratios in red and balanced ratios in blue. **(B)** Relative abundance of MDV-1 in blood meals of mosquitoes fed on a serial dilution of gametocytes compared to the maximum gametocyte input (100,000/bloodmeal). Error bars represent the standard deviation. **(C)** Relationship between observed gametocyte numbers by microscopy and delta *Ct* of test and control gene in 10 µl blood samples from symptomatic malaria patients colored by asexual parasitemia (26 samples from 6 patients).

whilst the control genes used were either *hsUBA-1*, *Mahrp2* or *hsGAPDH*.

Sampling and Statistical Evaluation

Statistical analyses were conducted in R and using package "car" for the ANOVA (Fox and Weisberg, 2018). *F*-tests were run with the var.test() function.

RESULTS

An Assay to Measure Gametocyte Uptake in the Bloodmeal

Because a mosquito bloodmeal is composed of only a few microliters of blood, we reasoned that maximum sensitivity in detecting bloodmeal gametocyte density will be achieved by detecting the most abundant transcripts found in gametocytes. We selected 107 transcripts that were at least 25-fold enriched in gametocytes over the ring form from a previous bulk RNAseq study (López-Barragán et al., 2011). We designed individual RT-qPCR for the candidate transcripts in order to confirm their relative abundance. Previous bulk RNAseq work and our specific qPCR results on 107 transcripts were in good agreement (**Figure 1A**). We also overlaid a sex-specific transcriptome analysis (Lasonder et al., 2016), which revealed that the most abundant transcripts tend to be contributed by female gametocytes (**Figure 1A**). The most abundant transcript by both qPCR and RNAseq that did not show a sex bias was *MDV-1* (sex-bias = 1.01).

We tested the sensitivity of this potential gametocyte biomarker by qRT-PCR with a serial dilution of *in vitro* cultured gametocytes mixed with purified ring stage parasites in whole blood (spanning the range of 10–100 k per bloodmeal with a blood meal considered to be 2 µl). *A. coluzzii* females were fed on this serial dilution and immediately sacrificed, and whole mosquitoes were used to generate cDNA. *MDV-1* transcript abundance was normalized with either *Mahrp2*, which is a ring stage transcript, or with *hsGAPDH*, which is transcript present in human leukocyte. The gametocyte numbers estimated to be present in each dilution was significantly correlated to the fold

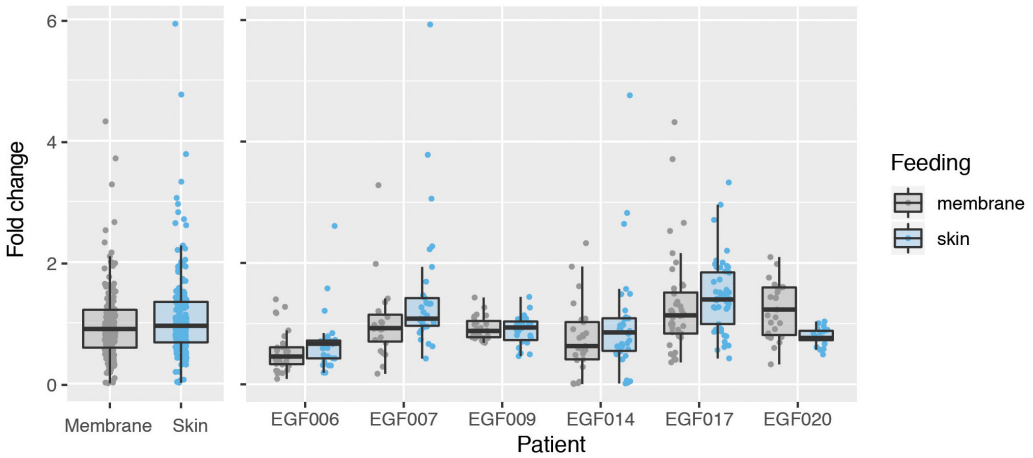

FIGURE 2 | Comparison of gametocyte density in natural and artificial mosquito blood meals. Gametocyte detected in mosquitoes fed on six patients either by direct skin feeding or membrane feeding. The left panel shows the data pooled across patients and the right displays results for each individual. Hinges correspond to the first and third quartiles, whiskers extend 1.5 interquartile range on either side of the hinges. Jitter points are overlaid, those beyond the whiskers are outlying points.

changes normalized with *Mahrp2* ($r = 0.79$, p-values < 0.001 by Pearson's correlation) and *hsGAPDH* ($r = 0.76$, p-values < 0.001 by Pearson's correlation), indicating that the gametocytemia can be relatively quantified by these assays within 8 individual mosquito bloodmeals per condition over a wide dynamic range (10–100,000 gametocytes per blood meal) (**Figure 1B**). We found only 3 of 8 mosquitoes fed on a blood meal with 10 gametocytes had a signal below the limit of detection threshold ($Ct < 38$), suggesting the limit of reliable detection for the assay is between 10 and 100 gametocytes per bloodmeal. We named this assay gametocyte quantification assay (GQA).

We next tested the GQA on mock blood meals composed of 10 μl of venous blood from 6 symptomatic gametocyte carriers recruited in Faladje and one unfed mosquito (**Table 1**). We observed that peripheral gametocytemia as measured by microscopy is highly correlated with the delta Ct from the GQA ($r = -0.82$, $p = 3.567e\text{-}07$ by Pearson's correlation) and was independent of peripheral asexual parasitemia (**Figure 1C**). No single nucleotide polymorphism with a minor allele frequency superior to 0.002 was found in the MDV-1 region targeted by the GQA > 3000 genomes (MalariaGEN Plasmodium falciparum Community Project, 2016), indicating that genetic diversity in natural populations is unlikely to affect the performance of the GQA. Altogether these results indicate that the GQA can be used to measure relative gametocytaemias in minute quantities of blood in both cultured parasites and for wild populations of parasites, it should be noted that the assay will be most useful for densities of gametocytes detectable by microscopy and not sensitive enough for subpatent gametocyte carriage.

TABLE 2 | ANOVA full results.

Reference gene	Model component	*F*-value	Pr(>*F*)
GAPDH	Feed	0.7305	0.39331
GAPDH	Patient	6.6312	6.461e-06
GAPDH	Feed × patient	2.7878	0.01744
UBA-1	Feed	1.7948	0.18121
UBA-1	Patient	5.5182	6.612e-05
UBA-1	Feed × patient	2.6143	0.02445
Mahrp2	Feed	0.1488	0.6999
Mahrp2	Patient	1.7555	0.1214
Mahrp2	Feed × patient	1.4370	0.2102

Uptake of Gametocytes During Natural and Artificial Bloodmeals

We next used the GQA to measure the relative uptake of gametocytes during mosquito blood feeding either directly from the skin or through an artificial membrane to test the potential role of the skin in gametocyte transmission biology. For the aforementioned six patients, we performed the GQA measurement after direct or membrane feeding. Control samples used in the quantification for each volunteer were mock blood meal samples (see above). We used the linear model: *fold change* ~ *feed* + *patient* + *feed* × *patient* (where *feed* is the feeding mode, skin or membrane). Relative gametocyte abundance was not different between mosquitoes fed through a membrane or directly on the skin when normalized to human *GAPDH* (type III ANOVA, $p = 0.39331$) (**Figure 2** and **Supplementary Table S4**), an alternative human transcript *UBA-1* (type III ANOVA, $p = 0.18121$), or the asexual transcript *Mahrp2* (type III ANOVA, $p = 0.6999$) (**Table 2**). This is indicative that there was no difference in density of gametocytes during natural or artificial blood meals. We did, however, note a patient-dependent effect on feeding mode but with inconsistent directionality (type III ANOVA, feed × patient: $p = 0.01744$). We, therefore, tested differences in the fold change of the gametocyte marker for each patient and found no difference in skin-fed vs membrane-fed except in the case of one patient (EGF020, **Table 1**). We also note that the variance observed between skin-fed and membrane-fed in each patient

were different in 5 of the 6 patients but again with inconsistent directionality (**Table 1**).

DISCUSSION

Malaria transmission from human to mosquito is a very efficient process that is still not completely understood (Bousema and Drakeley, 2011). In this study, we have established a new tool to study *P. falciparum* transmission in natural infections. The GQA detects a new biomarker of *P. falciparum* gametocytes (*MDV-1*) which is both sensitive and detects both males and female gametocytes. The GQA is particularly apt at comparing blood samples originating from the same individual because gametocyte densities can be normalized to either asexual parasite or leukocyte transcripts, which should be good loading controls within an infection. The GQA will, therefore, be extremely useful to assess the spatial and temporal heterogeneity in gametocyte densities within an infection. Moreover, this assay requires very little initial input, therefore it can be used for finger prick blood samples, skin punctures or mosquito blood meals, as we have shown in this study. It should be noted that the GQA is used at relatively high gametocytaemias (>100 gametocyte/μl) compared to lower gametocytaemias that may still yield successful mosquito infections.

Associative behaviors of gametocyte pre-fertilization have been postulated as a mechanism for enhanced transmission (Pichon et al., 2000; Lawniczak and Eckhoff, 2016; Nixon, 2016). In this study we have not seen a different density of gametocytes in mosquito bloodmeals taken through skin feeding versus membrane feeding on volunteers with patent gametocytemia. Therefore, in our gametocyte concentration window of observation (48–520 gametocytes/μl) there may not be a differential uptake of gametocytes during skin feeding. Another recent study comparing capillary and venous gametocyte densities also found no difference (Sandeu et al., 2017). Gametocyte clustering in the skin has previously been hypothesized to potentially enhance transmission (Pichon et al., 2000; Bousema and Drakeley, 2011; Lawniczak and Eckhoff, 2016). The effect of feeder type on the variance observed between mosquitoes was also patient dependent. Therefore, if clustering mechanisms do occur, they may not be specifically associated with the skin or may be only observed post-fertilization. There does not appear to be an association between higher variance in skin feeding vs membrane feeding and parasitemia or gametocytemia, noting that our study only examined six patients. Our results warrant further examination of these questions over a larger sample size both in terms of patients and fed mosquitoes and also on volunteers with a wider range of gametocytemia, including those without light microscopy detectable gametocytemia. Indeed, pre-fertilization behaviors might only be apparent at lower gametocyte concentration when the likelihood of infection is low. Additionally, associative behaviors between the sexes that ensure the presence of a male and a female in a blood meal but don't alter local gametocyte densities, for instance syzygy as observed in a species of *Leucocytozoon* might also be occurring (Barraclough et al., 2008).

Overall the skin has been implicated as an organ that can enhance vector-borne pathogens, including malaria transmission to (Chardome and Janssen, 1952; Van Den Berghe et al., 1954) and from the mosquito (Gueirard et al., 2010) as well as in trypanosomes (Capewell et al., 2016). Conducting a full-scale investigation of the role of this organ in pathogen transmission is an important endeavor and will be facilitated by sensitive tools such as the GQA and may allow a deeper understanding of the infectious reservoir of malaria and how to eliminate it.

DATA AVAILABILITY STATEMENT

All datasets generated for this study are included in the article/**Supplementary Material**.

ETHICS STATEMENT

The studies involving human participants were reviewed and approved by the Faculty of Medicine, Pharmacy and Odontostomatology de Pharmacy; Université des Sciences, Techniques et Technologies of Bamako (IRB approval letter no. 2016/133/CE/FMPOS). Written informed consent to participate in this study was provided by the participants' legal guardian/next of kin.

AUTHOR CONTRIBUTIONS

AT, DO, AD, and ML designed the study. AT, DO, CM, AH, ND, DS, AS, MC, FD, and CS conducted the field work. AT and KL performed the molecular biology. VH provided statistical expertise. AT, VH, and ML wrote the manuscript with contributions from other authors. All authors read and approved the manuscript.

FUNDING

The Wellcome Sanger Institute is funded by the Wellcome Trust (grant 206194/Z/17/Z). ML was supported by an MRC Career Development Award (G1100339).

ACKNOWLEDGMENTS

We thank all the participants in the study.

SUPPLEMENTARY MATERIAL

The Supplementary Material for this article can be found online at: https://www.frontiersin.org/articles/10.3389/fmicb.2020.00246/full#supplementary-material

TABLE S1 | List of genes tested as gametocyte biomarkers.

TABLE S2 | Primer sequences in the multiplex assay.

TABLE S3 | Primer efficiencies.

TABLE S4 | Full qPCR data of skin and membrane feeds.

REFERENCES

Barraclough, R. K., Duval, L., Talman, A. M., Ariey, F., and Robert, V. (2008). Attraction between sexes: male-female gametocyte behaviour within a *Leucocytozoon toddi* (Haemosporida). *Parasitol. Res.* 102, 1321–1327. doi: 10.1007/s00436-008-0913-8

Bonnet, S., Gouagna, C., Safeukui, I., Meunier, J.-Y., and Boudin, C. (2000). Comparison of artificial membrane feeding with direct skin feeding to estimate infectiousness of *Plasmodium falciparum* gametocyte carriers to mosquitoes. *Trans. R. Soc. Trop. Med. Hyg.* 94, 103–106. doi: 10.1016/s0035-9203(00)90456-5

Bousema, T., and Drakeley, C. (2011). Epidemiology and infectivity of *Plasmodium falciparum* and *Plasmodium vivax* gametocytes in relation to malaria control and elimination. *Clin. Microbiol. Rev.* 5:17716.

Capewell, P., Cren-Travaillé, C., Marchesi, F., Johnston, P., Clucas, C., Benson, R. A., et al. (2016). The skin is a significant but overlooked anatomical reservoir for vector-borne African trypanosomes. *Elife* 5:e17716. doi: 10.7554/eLife.17716

Chardome, M., and Janssen, P. J. (1952). Enquete sur l'incidence malarienne par la methode dermique dans la region du Lubilash(Congo Belge). *Ann. Soc. Belg. Med. Trop.* 32, 209–211.

Diallo, M., Touré, A. M., Traoré, S. F., Niaré, O., Kassambara, L., Konaré, A., et al. (2008). Evaluation and optimization of membrane feeding compared to direct feeding as an assay for infectivity. *Malar. J.* 7:248.

Fox, J., and Weisberg, S. (2018). *An R Companion to Applied Regression*. Thousand Oaks, CA: SAGE Publications.

Gueirard, P., Tavares, J., Thiberge, S., Bernex, F., Ishino, T., Milon, G., et al. (2010). Development of the malaria parasite in the skin of the mammalian host. *Proc. Natl. Acad. Sci. U.S.A.* 107, 18640–18645. doi: 10.1073/pnas.1009346107

Lasonder, E., Rijpma, S. R., van Schaijk, B. C. L., Hoeijmakers, W. A. M., Kensche, P. R., Gresnigt, M. S., et al. (2016). Integrated transcriptomic and proteomic analyses of *P. falciparum* gametocytes: molecular insight into sex-specific processes and translational repression. *Nucleic Acids Res.* 44, 6087–6101. doi: 10.1093/nar/gkw536

Lawniczak, M. K. N., and Eckhoff, P. A. (2016). A computational lens for sexual-stage transmission, reproduction, fitness and kinetics in *Plasmodium falciparum*. *Malar. J.* 15, 487.

López-Barragán, M. J., Lemieux, J., Quiñones, M., Williamson, K. C., Molina-Cruz, A., Cui, K., et al. (2011). Directional gene expression and antisense transcripts in sexual and asexual stages of *Plasmodium falciparum*. *BMC Genom.* 12:587. doi: 10.1186/1471-2164-12-587

MalariaGEN Plasmodium falciparum Community Project, (2016). Genomic epidemiology of artemisinin resistant malaria. *eLife* 5:8714. doi: 10.7554/eLife.08714

Moll, K., Ljungström, I., Perlmann, H., Scherf, A., Wahlgren, M., and Manassas, V. (2008). *Methods IN Malaria Research*. Available at: https://www.researchgate.net/profile/Abhinav_Sinha/publication/312495167_Tight_synchronisation_protocol_for_in_vitro_cultures_of_Plasmodium_falciparum/links/587f233808ae9275d4ebaab5.pdf (accessed October 01, 2016).

Nixon, C. P. (2016). *Plasmodium falciparum* gametocyte transit through the cutaneous microvasculature: a new target for malaria transmission blocking vaccines? *Hum. Vaccin. Immunother.* 12, 3189–3195. doi: 10.1080/21645515.2016.1183076

Ouédraogo, A. L., Bousema, T., Schneider, P., de Vlas, S. J., Ilboudo-Sanogo, E., Cuzin-Ouattara, N., et al. (2009). Substantial contribution of submicroscopical *Plasmodium falciparum* gametocyte carriage to the infectious reservoir in an area of seasonal transmission. *PLoS One* 4:e8410. doi: 10.1371/journal.pone.0008410

Pfaffl, M. W. (2004). "Quantification strategies in real-time PCR," in *A-Z of Quantitative PCR*, ed. S. A. Bustin, (La Jolla, CA: International University Line), 87–112.

Pichon, G., Awono-Ambene, H. P., and Robert, V. (2000). High heterogeneity in the number of *Plasmodium falciparum* gametocytes in the bloodmeal of mosquitoes fed on the same host. *Parasitology* 121(Pt 2), 115–120. doi: 10.1017/s0031182099006277

Ribaut, C., Berry, A., Chevalley, S., Reybier, K., Morlais, I., Parzy, D., et al. (2008). Concentration and purification by magnetic separation of the erythrocytic stages of all human *Plasmodium* species. *Malar. J.* 7:45. doi: 10.1186/1475-2875-7-45

Sandeu, M. M., Bayibéki, A. N., Tchioffo, M. T., Abate, L., Gimonneau, G., Awono-Ambéné, P. H., et al. (2017). Do the venous blood samples replicate malaria parasite densities found in capillary blood? A field study performed in naturally-infected asymptomatic children in Cameroon. *Malar. J.* 16:345.

Schneider, P., Bousema, J. T., Gouagna, L. C., Otieno, S., van de Vegte-Bolmer, M., Omar, S. A., et al. (2007). Submicroscopic *Plasmodium falciparum* gametocyte densities frequently result in mosquito infection. *Am. J. Trop. Med. Hyg.* 76, 470–474. doi: 10.4269/ajtmh.2007.76.470

Schneider, P., Reece, S. E., van Schaijk, B. C. L., Bousema, T., Lanke, K. H. W., Meaden, C. S. J., et al. (2015). Quantification of female and male *Plasmodium falciparum* gametocytes by reverse transcriptase quantitative PCR. *Mol. Biochem. Parasitol.* 199, 29–33. doi: 10.1016/j.molbiopara.2015.03.006

Van Den Berghe, L., Chardome, M., and Peel, E. (1954). Superiority of preparations from skin scarification over preparations of peripheral blood for the diagnosis of malaria. *An. Inst. Med. Trop.* 9, 553–562.

Watson, O. J., Slater, H. C., Verity, R., Parr, J. B., Mwandagalirwa, M. K., Tshefu, A., et al. (2017). Modelling the drivers of the spread of *Plasmodium falciparum* hrp2 gene deletions in sub-Saharan Africa. *eLife* 6:25008. doi: 10.7554/eLife.25008

Conflict of Interest: The authors declare that the research was conducted in the absence of any commercial or financial relationships that could be construed as a potential conflict of interest.

frontiers in Microbiology

ORIGINAL RESEARCH
published: 17 March 2020
doi: 10.3389/fmicb.2020.00269

Critical Steps of *Plasmodium falciparum* Ookinete Maturation

Giulia Siciliano[1†], Giulia Costa[2†], Pablo Suárez-Cortés[1,2†], Angelo Valleriani[2,3], Pietro Alano[1] and Elena A. Levashina[2*]*

[1] *Dipartimento di Malattie Infettive, Istituto Superiore di Sanità, Rome, Italy,* [2] *Vector Biology, Max Planck Institute for Infection Biology, Berlin, Germany,* [3] *Department of Theory and Bio-Systems, Max Planck Institute of Colloids and Interfaces, Potsdam, Germany*

The egress and fertilization of *Plasmodium* gametes and development of a motile ookinete are the first crucial steps that mediate the successful transmission of the malaria parasites from humans to the *Anopheles* vector. However, limited information exists about the cell biology and regulation of this process. Technical impediments in the establishment of *in vitro* conditions for ookinete maturation in *Plasmodium falciparum* and other human malaria parasites further constrain a detailed characterization of ookinete maturation. Here, using fluorescence microscopy and immunolabeling, we compared *P. falciparum* ookinete maturation in *Anopheles coluzzii* mosquitoes *in vivo* and in cell culture *in vitro*. Our results identified two critical steps in ookinete maturation that are regulated by distinct mosquito factors, thereby highlighting the role of the mosquito environment in the transmission efficiency of malaria parasites.

Keywords: malaria parasite transmission, *Plasmodium falciparum*, *Anopheles coluzzii*, ookinete maturation, time course of zygote development, developmental bottleneck

OPEN ACCESS

Edited by:
Rhoel Dinglasan, University of Florida, United States

Reviewed by:
Michael Delves, University of London, United Kingdom
Ryan Smith, Iowa State University, United States
Henrique Silveira, New University of Lisbon, Portugal

***Correspondence:**
Pietro Alano
pietro.alano@iss.it
Elena A. Levashina
levashina@mpiib-berlin.mpg.de

[†] *These authors have contributed equally to this work*

Specialty section:
This article was submitted to Infectious Diseases, a section of the journal Frontiers in Microbiology

Received: *21 November 2019*
Accepted: *06 February 2020*
Published: *17 March 2020*

Citation:
Siciliano G, Costa G, Suárez-Cortés P, Valleriani A, Alano P and Levashina EA (2020) Critical Steps of Plasmodium falciparum Ookinete Maturation. Front. Microbiol. 11:269. doi: 10.3389/fmicb.2020.00269

INTRODUCTION

Malaria is a mosquito-borne disease, mainly caused by the protozoan parasite *Plasmodium falciparum*, which kills 429,000 people annually (World Health Organization [WHO], 2018). A key component of the global initiative to eliminate malaria is the transmission block of malaria parasites from humans to the mosquito vector. *Plasmodium* transmission is initiated within minutes after blood ingestion by the *Anopheles* mosquito. Within the mosquito midgut, the gametocytes transform into mature extracellular female and male gametes. The product of fertilization, the zygote, takes one day to transform into a motile ookinete, which then traverses the midgut epithelium to establish oocyst infection on the basal side. About 10–12 days later, each oocyst releases thousands of sporozoites that migrate to and invade the salivary glands, ready to be injected into a human at the next mosquito bite. During the first 24 h after blood meal, the parasites undergo a series of radical tightly regulated morphological changes: gamete roundup, egress and exflagellation, formation of a zygote, emergence of an elongated protuberance and transformation of a round zygote into a crescent-shaped motile ookinete. The early stages of gametocyte-to-gamete transformation are triggered by the mosquito-derived metabolite xanthurenic acid, which together with the temperature drop signals for gamete egress and exflagellation (Billker et al., 1998). Although fertilization and post-fertilization steps are critical for *Plasmodium* establishment in the mosquito, very little is known about molecular mechanisms and signals that orchestrate parasite sexual reproduction. Field studies suggested that pre-fertilization events do not reliably predict the outcome of mosquito infection, as the numbers of the blood-circulating gametocytes do not always correlate with the donor infectiousness

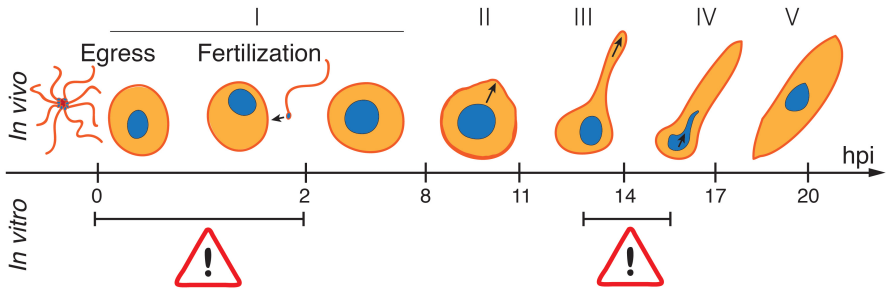

GRAPHICAL ABSTRACT | Ookinete development within the mosquito blood bolus is a critical step in malaria transmission. Using time-series approaches, we identified two limiting steps of *Plasmodium falciparum* ookinete development *in vitro*: (i) inhibition of transition from round forms (stage I) to knobs (stage II), likely caused by an inefficient fertilization, and (ii) arrest of transition between stages III and IV, associated with morphological abnormalities during protuberance elongation and enlargement. The abnormal protuberance at stage IV prevents further nuclear migration from the round body to the appendage.

to the insect vector (Bousema and Drakeley, 2011). Are post-fertilization events (the transition from zygote to ookinete) a more accurate proxy to forecast the efficiency of *Plasmodium* transmission?

To better characterize the post-fertilization events, several studies attempted to establish *P. falciparum* ookinete cultures *in vitro* (Carter et al., 1987; Warburg and Schneider, 1993; Bounkewa et al., 2010; Ghosh et al., 2010; Delves et al., 2017). While such cultures were successful for the rodent malaria parasite *Plasmodium berghei* (Janse et al., 1985; Sinden et al., 1985), the efficiency of *P. falciparum* conversion from round-shaped parasites to mature ookinetes is surprisingly low (0.45 to 16%) as compared to the estimated 50% efficiency *in vivo* (Carter et al., 1987; Bounkewa et al., 2010; Delves et al., 2017). The poor efficiency of *P. falciparum* gamete fertilization was identified as a major obstacle to efficient ookinete production *in vitro* (Ghosh et al., 2010; Delves et al., 2017). As the factors that promote fertilization *in vivo* remained obscure, a series of culture conditions (lipids, glucose, mosquito pupal extract, and red blood cell lysate additives, variations in hematocrit, pH, and gas; etc.) were tested to rescue the block in fertilization, albeit without success (Ghosh et al., 2010; Delves et al., 2017).

In spite of low efficiency, culturing *in vitro* provided a first classification of ookinete development based on morphology of Giemsa-stained cells (Ghosh et al., 2010). Besides the round-shaped zygote, five ookinete stages have been described: (I and II) retorts with a short protuberance attached to the round body; (III) retort with enlarged but not fully elongated protuberance; (IV) retorts with the thin protuberance at maximum elongation; (V) crescent or fluke-shaped mature ookinetes. The drawback of this classification was the unspecific basis of the Giemsa staining, which could not distinguish between residual non-activated gametocytes, developmentally blocked degenerated parasites, and mature ookinetes. Application of monoclonal antibodies that bound the zygote/ookinete surface antigen Pfs25 and/or the ookinete-specific intracellular enzyme chitinase helped the identification of mature ookinetes (Carter et al., 1987; Bounkewa et al., 2010; Ghosh et al., 2010; Delves et al., 2017). However, the antibodies were used only to count the mature ookinetes at a late time point or at the very beginning and very end of the process, thereby preventing a faithful reconstruction of the ookinete maturation stages.

Here, using live immunofluorescence microscopy, we report the temporal characterization of the zygote to ookinete development in the *P. falciparum*-infected *Anopheles coluzzii* mosquitoes and in cell culture *in vitro*. By comparing the time series of the zygote development *in vivo* and *in vitro*, we demonstrate a requirement of mosquito-derived factor(s) for gamete fertilization and identify a new critical stage of ookinete maturation.

MATERIALS AND METHODS

Parasite Cultures

Plasmodium falciparum NF54 parasites were cultured in O^+ human red blood cells (Haema, Berlin), at 37°C, in a 3% O_2, 5% CO_2, and 92% N_2 atmosphere. Asexual cultures (0.5–5% of parasitemia) were maintained at 3–4% hematocrit in the complete medium composed of RPMI 1640 with L-glutamine and 25 mM HEPES, supplemented with 10% human A^+ serum (Haema, Berlin), 10 mM hypoxanthine (c-c-Pro), and 20 μg/ml of gentamicin (Sigma). For gametocyte production, asynchronous asexual parasites were seeded at 1% parasitemia and 5% hematocrit, and complete medium without gentamicin was replaced daily for 15 days until mosquito infections. Stage V gametocytes were enumerated in a counting chamber (Neubauer) 14 days post seeding. On the same day, a sample from the culture was incubated for 15 min at room temperature in the presence of 20 μM of xanthurenic acid (Sigma), and exflagellating clusters were enumerated in a counting chamber (Neubauer). The exflagellation rate was calculated as follows:

$$\frac{\text{No. of exflagellating clusters/m1}}{\text{No. of stage V gametocytes/m1}}$$

P. falciparum NF54 clone originated from Prof. Sauerwein's laboratory, Radboud University Medical Center, Nijmegen, The Netherlands, and was authenticated for *Pfs47* by PCR on genomic DNA. *P. falciparum* asexual cultures were monthly tested for *Mycoplasma* contamination.

Mosquito Rearing and Parasite Infections

Anopheles coluzzii (Ngousso S1 strain) was maintained at 29°C 70–80% humidity 12/12-h day/night cycle. For *P. falciparum* infections, mosquitoes were fed for 15 min on a membrane feeder with stage V gametocytes diluted in fresh red blood cells and human serum to 3.7×10^6 stage V gametocytes/ml and 50% hematocrit. Infected mosquitoes were kept in a secured S3 laboratory at 26°C for up to 11 days according to national regulations (Landesamt für Gesundheit und Soziales, project number 297/13). Unfed mosquitoes were removed shortly after infection.

Mosquito Dissections

For ookinete analyses, midguts of decapitated mosquitoes were dissected in 1 × phosphate-buffered saline (PBS) at the indicated time points (20 midguts per time point for each experimental condition). For oocyst counts, mosquitoes were killed in ethanol 70% at 11 dpi, midguts were dissected and incubated in 1% mercurochrome (Sigma) in water for 5–10 min. The oocyst numbers were enumerated under a light microscope Leica DM2000 LED.

Ookinete Cultures *in vitro* and *ex vivo*

For *in vitro* experiments, ookinete cultures were set up by diluting gametocyte cultures 15 days post seeding in fresh complete medium to 5×10^6 stage V gametocytes/ml, supplemented with 20 μM xanthurenic acid and incubated at 26°C in a siliconized tube until analyses.

For *ex vivo* experiments, midguts of infected mosquitoes were homogenized in complete medium containing 40 μg/ml of gentamicin and 5 μg/ml of Fungizone (Gibco) to decrease the microbial charge, incubated for 2 min at room temperature, washed (300 *g*, 4 min), resuspended in 500 μl of complete medium containing 40 μg/ml of gentamicin (Alpha Laboratories), and incubated at 26°C in a siliconized tube for an additional 21 h. Control *in vivo* samples were collected from mosquito bolus 23 h post infection (hpi), while control *in vitro* ookinete cultures were set up with the same gametocyte suspension prepared for mosquito infections, diluted 1:25 in complete medium without gentamicin and incubated at 26°C for 23 h. As mock control, one aliquot from *in vitro* cultures was subjected 2 h post seeding to the same gentamicin/Fungizone treatment used *ex vivo* and then cultured for an additional 21 h (**Supplementary Figure 4**).

Ookinete Staining and Quantification

Hybridoma cells expressing anti-Pfs25 IgG (clone 4B7) were obtained from BEI Resources. IgG fraction was purified using Protein G Sepharose columns (GE Healthcare) and labeled to Alexa Fluor 568 (Life Technologies) in the Central Laboratory Facility (Deutsches Rheuma-Forschungszentrum, Berlin). Ookinetes were stained with anti-Pfs25-Alexa Fluor 568 antibody (7.5 μg/ml at 2 hpi and 1.5 μg/ml at 23 hpi) and Hoechst 1:500 (Molecular Probes) for 30 min at 4°C in PBS. Samples were washed (300 *g*, 4 min) and resuspended in PBS. The numbers of Pfs25-positive parasites were enumerated in a counting chamber (Neubauer) using a Leica DMRB fluorescence microscope and classified into stages using an Axio Observer Z1 fluorescence microscope equipped with an Apotome module (Zeiss) (**Figure 1**).

Ookinete conversion was defined as follows:

$$\frac{\text{No. of converted ookinetes (Stage II to IV)}}{\text{No. of Pfs25-positive parasites}}$$

The proportion of mature ookinete was defined as follows:

$$\frac{\text{No. of mature ookinetes (Stage V)}}{\text{No. of Pfs25-positive parasites}}$$

Representative pictures were acquired with the Apotome module, and images were deconvoluted and corrected for phase contrast and local bleaching using ZEN 2012 software (Zeiss).

Statistical Analysis

No samples were excluded from the analyses. Mosquitoes from the same batches were randomly allocated to the experimental groups (age range: 1–2 days). The experimenters were not blinded to the group allocation during the experiment and/or when assessing the outcome. Statistical analysis for **Figure 2** was performed with GraphPad Prism 8, and *p*-values below 0.05 were considered significant ($^*p < 0.05$) as indicated in the figures. The specific tests used are indicated in the figure legend.

Statistical analyses for **Figures 3**, **4** were performed by comparing the fraction of each single ookinete stage between two growth conditions at the same time point. The method (see below) takes both the biological variability and the sample sizes into account and allows estimation of the errors associated with the average percentages, which are then compared using a *z*-test. We defined f1, f2, and f3 as the fractions of the morphology for three independent experiments under one growth condition and s1, s2, and s3 as the corresponding sample sizes. For each of the three sample sizes, we take one fraction at random and generate one number of ookinetes from a binomial distribution with probability given by the chosen fraction and population size given by the sample size. As an illustrative example, suppose that we associate f3 to s1, f1 to s2, and f1 to s3 for a certain ookinete stage (e.g., knob) at a certain time (e.g., 17 hpi) and a certain condition (e.g., *in vivo*). We then generate three random numbers from binomial distributions with the parameters given by the

TABLE 1 | *p*-values computed from the *z*-test for the comparison *in vivo* versus *in vitro* as shown in **Figures 3C,D**.

hpi	II	III	IV	V
14	2e−4	2e−4	0.11	–
17	0.03	1e−4	3e−4	0.02
20	2e−3	1e−4	0.32	1e−4
36	0.31	1e−4	0.49	1e−4

Significant p-values (smaller than 0.001, in green) indicate the arrest of development at stage III in vitro compared to in vivo, where instead the ookinetes reach the mature stage at 20 h post infection (hpi). p-values smaller than the inverse of the product of the sample sizes have been replaced with 1e−4.

TABLE 2 | *p*-values computed with a *z*-test for the comparison *in vivo*, *in vitro*, and *ex vivo* at 23 h post infection (hpi) as shown in **Figure 4B**.

	I	II	III	IV	V
in vivo vs. *in vitro*	1e−4	3e−3	1e−4	1e−4	1e−4
in vivo vs. *ex vivo*	0.09	0.22	1e−4	1e−4	1e−4
in vitro vs. *ex vivo*	1e−4	0.06	1e−4	0.50	0.04

Significant p-values (smaller than 0.001, in green) indicate that in vitro ookinetes are arrested at stage I, whereas in vivo and ex vivo cells have a similar stage I and II development. Both in vitro and ex vivo ookinetes have a further blockage point at stage III compared to the in vivo conditions. p-values smaller than 1e−4 have been replaced with 1e−4.

fraction and sample size. These three numbers (n1, n2, and n3) are the number of ookinetes found for the three samples. This corresponds to a simulated replica of the same experiment under the condition that the fractions (f1, f2, and f3) and the sample sizes (s1, s2, and s3) are the same as found in the experiment. The corresponding fraction of ookinete will then be g1 = n1/s1, g2 = n2/s2, and g3 = n3/s3.

We repeat this procedure M times, for M = 3e+6. After this procedure, the data contain M triplets of random numbers g1, g2, and g3 that represent simulated outcomes of the same experiments given the data obtained in the experimental work. The average of each of the triplets produces M average fractions E[g] = (g1 + g2 + g3)/3. The mean E[E(g)] of all these M average fractions and the variance Var[E(g)] of the M average fractions are the mean fraction and its variance associated with the ookinete stage at that given time point and under the given condition. We repeat this procedure for the each ookinete stage, time point, and condition and then compare the means of two conditions in pairs, taking the variances thus computed into account. The z-test applied to the two means and their variances finally delivers the p-value. Based on the above-mentioned procedure, the generated p-values are summarized in the **Table 1** (refer to **Figures 3C,D**) and **Table 2** (refer to **Figure 4**). The raw data used for this analysis are reported in **Supplementary Tables 4–6**.

RESULTS

Stages of *P. falciparum* Ookinete Development in *A. coluzzii*

To characterize the major stages of zygote development, we performed a time course fluorescence live microscopy analysis of the blood bolus content of *A. coluzzii* mosquitoes infected with gametocyte cultures of *P. falciparum*. Live parasites within the mosquito bolus were dissected at 11, 14, 17, 20, 23, and 36 hpi and stained with the Hoechst nuclear dye and anti-Pfs25 antibodies. We identified five parasite developmental stages based on morphology, fluorescence patterns, and nuclear position (**Figure 1A**). Specifically, all immature stages were round shaped and displayed differences in the length of the protuberance that eventually gave the elongated shape to mature ookinetes. Stage I lacked the protuberance and was indistinguishable from egressed female gametes; stage II featured a short protuberance that did not exceed in length the radius of the main spherical body (knob); stage III had an elongated well-developed protuberance of at least the length of the radius of the main spherical body (stem); stage IV had a round nucleated body of reduced size and a wide long protuberance; stage V acquired the characteristic elongated shape with or without attached residual spherical body (**Figure 1A**). Importantly, stages I–IV displayed nuclear staining in the round body. Nuclear translocation from the residual round body to the well-formed elongated protuberance was observed during the transition from stage IV to stage V (**Supplementary Figure 1**). We also detected parasites that were suggestive of a degenerated form of a mature ookinete with disrupted Pfs25 surface signal and named them ghosts (**Figure 1A**). As these forms were only observed after appearance of mature ookinetes at the late time point of ookinete development *in vivo*, we speculate that ghosts represent ookinetes undergoing degradation probably due to the harsh environment of the mosquito midgut. This classification was used to measure the proportion of each stage in the mosquito blood bolus at six time points after infection. We found no obvious morphological changes in the round-shaped parasites until 11 hpi. During the next 3–14 h, the zygotes progressively developed protuberance, translocated the nucleus from the shrinking round body to the protuberance, and converted into mature ookinetes. We established the following kinetics of the ookinete development: stage II dominated at 14 hpi, stage III at 17 hpi, and stage IV between 17 and 23 hpi (**Figures 1B,C** and **Supplementary Table 2**). Mature ookinetes appeared at 17 hpi, peaked at 23 hpi, and persisted in the blood bolus until 36 hpi, whereas the ghost forms accumulated between 23 and 36 hpi (**Figures 1B,C** and **Supplementary Table 2**). The absolute number of Pfs25-positive parasites per mosquito blood bolus remained constant until 23 hpi but decreased at 36 hpi (**Supplementary Figure 2** and **Supplementary Table 2**), likely reflecting the ookinete traversal of the mosquito midgut. Interestingly, only half of bolus-resident parasites developed into ookinetes, suggesting that at some stages, parasite development was restricted by the mosquito environment. We concluded that the observed progressive changes in proportions of developmental stages were not caused by parasite mortality but represented the dynamics of ookinete development in the mosquito.

Development of Mature Ookinetes in the Mosquito Blood Bolus Reliably Predicts Successful Mosquito Infection

As only half of the ingested parasites transformed into mature ookinetes (**Figure 1B**), we next evaluated how well the exflagellation rate of a given gametocyte culture, the conversion rate of egressed gametes into all ookinete stages (stages II to V) or into mature ookinetes only (stage V), predicted the success of oocyst formation. Ookinete development was monitored by anti-Pfs25 staining at 24 hpi as described above, whereas oocysts were labeled by mercurochrome staining for counting at 11 days post infection (dpi). In line with the field studies, gametocyte exflagellation rate (accounting only for male gametocytes) was a poor predictor of oocyst prevalence (**Figure 2A**). We found that

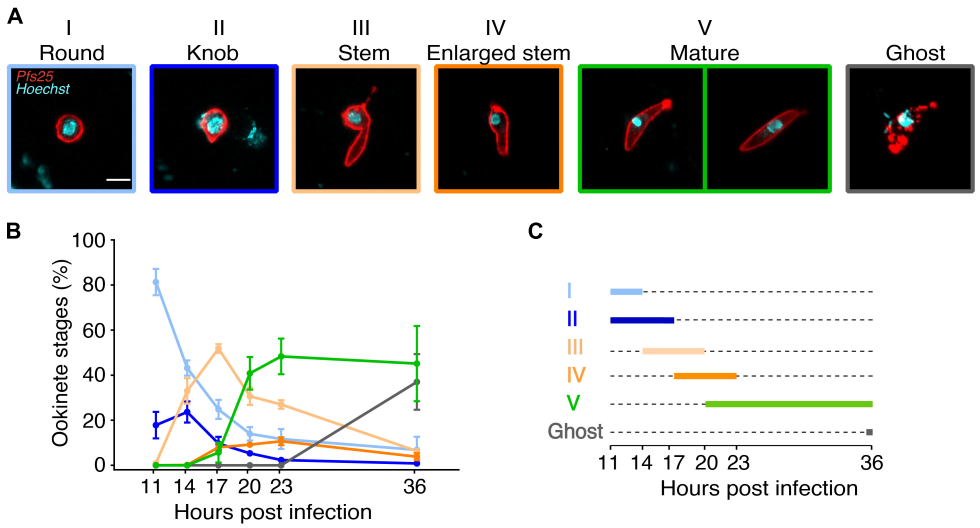

FIGURE 1 | Kinetics of *Plasmodium falciparum* ookinete maturation in the mosquito bolus. *Anopheles coluzzii* mosquitoes were infected with *P. falciparum* gametocytes. Live parasites were isolated from a pool of 20 mosquito boluses and stained with anti-Pfs25 antibody at 11, 14, 17, 20, 23, and 36 h post infection (hpi). **(A)** Representative pictures of Pfs25-positive and Hoechst-stained ookinete stages as referred throughout this study (scale bar: 5 μm). Stage I: Round, indistinguishable from egressed female gamete. Stage II: Knob, small protuberance not exceeding in length the radius of the main spherical body. Stage III: Stem, elongated protuberance longer than the radius of the main spherical body. Stage IV: Enlarged stem, the elongated protuberance–still containing the nucleus–increasing in width. Stage V: Mature, terminally differentiated elongated form with or without residual spherical body; the nucleus has migrated from the residual spherical body to the stem. Ghost: elongated degenerated forms with non-continuous surface Pfs25 signal. **(B)** *In vivo* ookinete forms were classified as in **(A)**. Proportion of ookinete stages out of total Pfs25-positive parasites is indicated for each time point. Every point represents the mean ± SEM of three independent experiments ($N = 3$, $n = 200$ parasites counted per time point). **(C)** Schematic representation of the duration of ookinete stages in the mosquito vector described in **(A)**.

oocyst prevalence (number of oocyst-positive mosquitoes/total number of blood fed mosquitoes) correlated significantly with the ookinete conversion rate [number of converted ookinetes (stages II to V)/total Pfs25-positive parasites] and the proportion of mature ookinetes [number of mature ookinetes (stage V)/total Pfs25-positive parasites] (**Figures 2B,C** and **Supplementary Table 3**). We concluded that similar to natural infections, ookinete conversion is a more reliable predictor of parasite development in the mosquito than exflagellation rate, pointing to some critical steps that regulate gamete fusion and early stages of zygote development.

Critical Stages of Ookinete Development *in vitro*

To identify developmental bottlenecks in ookinete conversion, we compared the dynamics of *in vivo* and *in vitro* ookinete development using the same initial gametocyte culture for mosquito infections and ookinete culture. At selected time points, parasites were isolated from the mosquito bolus or collected from the culture, stained with anti-Pfs25 antibodies and staged as described above. The absolute number of Pfs25-positive parasites stayed overall constant in all conditions until 23 hpi (**Supplementary Figure 3**). As expected, at 23 hpi, the majority of zygotes in the mosquito bolus developed protuberances, and 40% of them converted into mature ookinetes. In contrast, at the same time point *in vitro*, most of the detected Pfs25-positive forms remained at stage I (**Figures 3A,B**). As gametocytes efficiently egressed in both conditions (**Supplementary Table 1**), our findings are consistent with the previous reports that proposed a block in gamete fertilization *in vitro*. Focusing the analysis on the small proportion of ookinetes that developed from stage II onward, we observed an accumulation of stage III parasites. While this stage was dominant at the 14 h post culture setup, the corresponding samples *in vivo* showed a higher proportion of stage II parasites (**Figures 3C,D**, p-values = 0.0002, paired z-test). Interestingly, stage III parasites continued to accumulate in cultures *in vitro* at later time points, and only a small proportion of the parasites developed into mature ookinetes. In contrast, slower development of stage III forms *in vivo* was accompanied by swift progression to stage IV and V ookinetes. Our results identified a specific critical step in ookinete development after fertilization–the rate of stage III to stage IV transition–morphologically corresponding to a proper enlargement of the ookinete protuberance.

We next attempted to rescue *ex vivo* the critical step of ookinete development blocked *in vitro*. In these experiments, mosquitoes were infected with the gametocyte cultures, and 2 h later, the parasites were extracted from the insect gut and put into culture *in vitro* for an additional 21 h. In parallel, we examined the dynamics of ookinete development from the same gametocyte culture *in vivo* and *in vitro* as described above (**Figure 4A**). As the mosquito environment is not sterile, the *ex vivo* isolated parasites were treated with an antibiotic/antimycotic mix to prevent the overgrowth of the microbes inhabiting the mosquito midgut. This antimicrobial treatment had no effect on parasite development (**Supplementary Figure 4**). We found that the proportion of

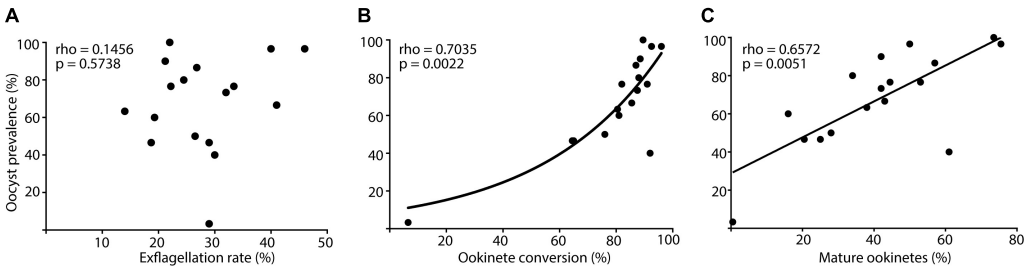

FIGURE 2 | Correlation between male gamete activation and ookinete development rates with oocyst prevalence. *Anopheles coluzzii* mosquitoes were fed with *Plasmodium falciparum* gametocytes. Live parasites were isolated from the mosquito bolus and stained with anti-Pfs25 antibody at 24 h post infection (hpi), while oocysts were stained with mercurochrome and counted at 11 days post infection (dpi). Correlation between oocyst prevalence and **(A)** exflagellation rate (exflagellation clusters ml^{-1}/gametocyte stage V ml^{-1}) of gametocyte cultures 24 h before infection, **(B)** percentage of ookinete conversion (stages II to V ookinetes/total Pfs25-positive parasites), and **(C)** percentage of mature ookinetes (mature stage V ookinetes/total Pfs25-positive parasites). Every dot represents one independent experiment (N = 17), Pfs25-positive parasites (n = 200) were counted in pooled samples of 20 blood boluses, and oocyst prevalence was analyzed in dissected midguts (n = 30) per experiment. Rho- and p-values (Spearman correlation) are indicated on the top left corner of every graph, and lines show data trends for significant correlations **(B)**, exponential growth curve; **(C)**, linear regression.

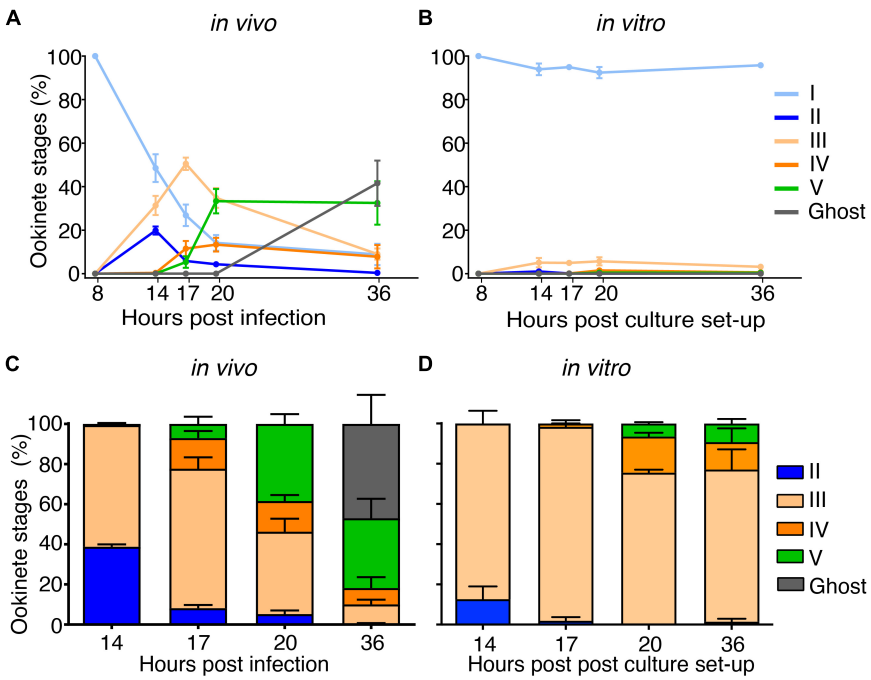

FIGURE 3 | Parallel time course highlights two limiting steps in *in vitro* ookinete development. The same preparation of *Plasmodium falciparum* gametocytes was diluted and fed to mosquitoes or induced to undergo gametogenesis in a parallel time course of *in vivo* versus *in vitro* development. Parasites were isolated from a pool of 20 mosquito boluses or collected from the *in vitro* culture and stained with anti-Pfs25 antibody at 8, 14, 17, 20, and 36 h after feeding or culture setup. Ookinete forms were classified as in **Figure 2A**, and the proportions of ookinete stages on total Pfs25-positive parasites *in vivo* **(A)** or *in vitro* **(B)** are indicated for each time point. Every point represents the mean ± SEM of three independent experiments (**A:** n = 200, **B:** n = 500 parasites counted per time point). Relative proportions of ookinete stages out of total Pfs25-posititve parasites excluding round forms (stages II to V and ghosts) per each time point are shown *in vivo* **(C)** and *in vitro* **(D)**. Bar plots represent the mean proportions ± SEM of three independent experiments **(C)**, n = 309, 439, 515, and 449 and **(D)**, n = 91, 76, 114, and 63 Pfs25-positive parasites were analyzed per time point. The z-test was used to compare the mean proportion of each ookinete stage and its variances *in vivo* versus *in vitro*.

ookinetes that bypassed stage I was not significantly different in *in vivo* versus *ex vivo* conditions, demonstrating that the first 2 h of *in vivo* development rescued the fertilization block *in vitro* to the levels observed *in vivo* (**Figure 4B**, p-value = 0.09, paired z-test). However, the majority of the *ex vivo* parasites remained at stage III at 23 hpi, with only a minor fraction developing into mature ookinetes (p-value = 0.0001, paired z-test). The arrested stage III parasites featured a much thinner protuberance than those obtained *in vivo* (**Figure 4C**). Altogether, our results describe a new critical step in ookinete development. Further

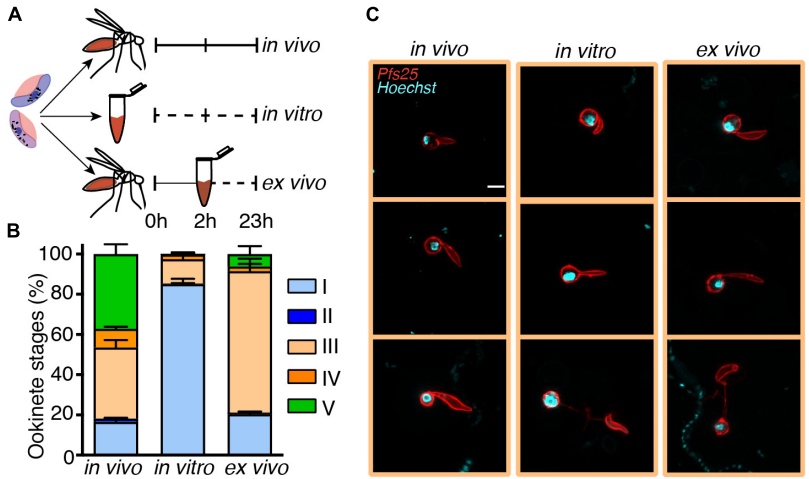

FIGURE 4 | Ookinete development *in vitro* is critically impaired at the stage III-to-IV transition. The same *Plasmodium falciparum* gametocyte culture was used for mosquito infections or for *in vitro* ookinete development. To bypass the fertilization block, 20 mosquito blood boluses per time point were pooled and dissected 2 h post infection (hpi), and the residing parasites were transferred into *in vitro* cultures and incubated for 21 h (*ex vivo* conditions). Parasites developed in the mosquito bolus or in cultures *in vitro* were stained with anti-Pfs25 antibody at 2 and 23 hpi or post culture setup and were classified according to stages. **(A)** Schematic overview of the experiment. **(B)** Proportional composition of Pfs25-positive parasite stages developed *in vivo*, *in vitro*, and *ex vivo* 23 hpi or post culture as depicted in **(A)**. Bar plots represent the mean proportions ± SEM ($N = 3$, $n = 200$ parasites counted per time point). **(C)** Representative images of anti-Pfs25-positive and Hoechst-stained stage III ookinetes 23 hpi or post culture developed in three conditions (scale bar-5 μm). The *z*-test was used to perform pairwise comparison of mean proportions of each ookinete stage and their variances *in vivo*, *in vitro*, and *ex vivo*.

studies should investigate cellular mechanisms that control protuberance emergence and enlargement in *P. falciparum*.

DISCUSSION

The human-to-mosquito *Plasmodium* transition is essential for transmission of malaria parasites and a promising target of drug- or antibody-mediated transmission-blocking interventions. With both pharmacological and immunological interventions receiving increased attention, the absence of robust ookinete *in vitro* culturing methods poses a major roadblock for identification of potent inhibitory targets. Here, by comparing the dynamics of ookinete development *in vivo* and *in vitro*, we characterize mosquito-regulated critical steps in early ookinete maturation. The first mosquito factor shaping host-to-vector transmission was identified almost 40 years ago and was shown to increase exflagellation efficiency of male gametocytes in the avian malaria parasite *Plasmodium gallinaceum* (Nijhout, 1979). Later on, this factor was purified from mosquito extracts and identified as xanthurenic acid (Billker et al., 1998). The results reported here postulate an existence of additional mosquito factors that promote gamete fertilization and zygote morphogenesis.

We found that the rate of gamete conversion to ookinetes was a good predictor of oocyst production in the mosquito, whereas the rate of production of male gametes (exflagellation) was not. These observations indicate that the first 24 h are crucial for *Plasmodium* establishment in its vector. These results are in line with the field studies that showed that numbers of circulating gametocytes do not always predict parasite infectiousness to the insect vector (Bousema and Drakeley, 2011). A meta-analysis of the infectiousness of *P. falciparum*-infected blood samples from children from Burkina Faso and Tanzania to *A. gambiae*, and a similar study with *P. vivax* and *A. dirus*, revealed a non-linear relationship between the gametocyte titers in the donors' blood and infection prevalence in the mosquito (Churcher et al., 2013; Kiattibutr et al., 2017). Furthermore, a recent meta-analysis conducted on *P. falciparum* gametocyte carriers in Mali, Burkina Faso, and Cameroon revealed a broad positive correlation between circulating female gametocytes and infected mosquitoes, while circulating male gametocytes contributed to mosquito infection only at low gametocyte densities (Bradley et al., 2018). These findings provide an additional proof that the *Plasmodium* exflagellation rate, which corresponds to the fraction of mature male gametocytes, is a poor predictor of carrier infectivity to mosquitoes.

We propose that the poor predictive properties of gamete activation are linked to variability in mosquito factors that control fertilization and zygote development. The importance of the mosquito environment is supported by two observations: (i) rescue of gamete fertilization block by within-mosquito development during the first 2 h after infection and (ii) abnormal morphogenesis of stage III parasites *in vitro* that results in narrow protuberance, which may block nuclear migration at stage IV. Interestingly, the defined here ordering of stages III and IV differs from that proposed by Ghosh et al. (2010), where the ookinetes with enlarged stem (stage IV here) were positioned before the forms with the elongated stem (stage III here). Therefore, the systematic time-series approach applied here contributed to a better understanding of the timing and order of the crucial steps in ookinete development.

The synchronous comparison of *in vivo* and *in vitro* ookinete maturation confirmed that *P. falciparum* gamete fertilization is very inefficient *in vitro* (Delves et al., 2017) (**Graphical Abstract**). Here, we demonstrate that this block is completely reverted by allowing *in vivo* parasite within-mosquito development within the first 2 h. Our cultures *in vitro* contained xanthurenic acid, and we detected no differences in gamete egress between *in vivo* and *in vitro* conditions. Therefore, we propose that gamete fusion requires other mosquito factor(s). Currently, the nature of these factors is unknown. Interestingly, our conclusions are in line with an earlier study which used a computational approach to model ookinete development (Lawniczak and Eckhoff, 2016).

In contrast to fertilization, the short pulse of *in vivo* development did not rescue the second block in the ookinete maturation *in vitro*. Instead of delay, we observed faster development of the protuberance and, hence, accumulation of stage III *in vitro*. However, this faster development translated into morphological abnormalities, as stage III developed thinner protuberance *in vitro*. This observation could be explained by higher concentrations of some permissive factor(s) in the culture medium as compared to the natural mosquito environment. Identification of the factor(s) not only will allow optimization of *in vitro* conditions but also will inform how within-mosquito variability in this factor affects ookinete development *in vivo*. In conclusion, the results presented here suggest that successful *P. falciparum* fertilization and ookinete maturation require the continuous presence of multiple as yet unknown mosquito factors. Identification of these factors should benefit the establishment of *P. falciparum* ookinete culture *in vitro* and uncover the mechanisms that regulate early stages of transmission of this deadly parasite.

DATA AVAILABILITY STATEMENT

All datasets generated for this study are included in the article/**Supplementary Material**.

AUTHOR CONTRIBUTIONS

GS, GC, and PS-C conceived and performed the experiments, analyzed the results, and wrote the manuscript. AV performed statistical analyses and wrote the manuscript. PA and EL conceived experiments, analyzed the data, and wrote the manuscript.

FUNDING

GS was supported by the grant ISARP "Farmaci di nuova generazione contro la trasmissione di *Plasmodium falciparum* per la eradicazione della malaria" from the Italian Ministry of Foreign Affairs and International Cooperation and Istituto Superiore di Sanità. This study has received funding from the European Union's Horizon 2020 Research and Innovation Programme under grant agreement no. 731060.

ACKNOWLEDGMENTS

We thank M. Andres, D. Eyermann, H. Ahmed, and L. Spohr (Vector Biology Unit, Max Planck Institute for Infection Biology, Berlin) for mosquito rearing, parasite culturing, and *P. falciparum* infections. The following reagent was obtained through BEI Resources, NIAID, NIH: Hybridoma 4B7 Anti-*Plasmodium falciparum* 25 kDa Gamete Surface Protein (Pfs25), MRA-315, contributed by Louis H. Miller and Allan Saul. We thank Tuula Geske (Central Laboratory Facility, Deutsches Rheuma-Forschungszentrum, Berlin) for anti-Pfs25 IgG production, purification, and labelling.

SUPPLEMENTARY MATERIAL

The Supplementary Material for this article can be found online at: https://www.frontiersin.org/articles/10.3389/fmicb.2020.00269/full#supplementary-material

REFERENCES

Billker, O., Lindo, V., Panico, M., Etienne, A. E., Paxton, T., Dell, A., et al. (1998). Identification of xanthurenic acid as the putative inducer of malaria development in the mosquito. *Nature* 392, 289–292. doi: 10.1038/32667

Bounkewa, V., Li, F., and Vinetz, J. M. (2010). In vitro generation of *Plasmodium falciparum* ookinetes. *Am. J. Trop. Med. Hyg.* 83, 1187–1194. doi: 10.4269/ajtmh.2010.10-0433

Bousema, T., and Drakeley, C. (2011). Epidemiology and infectivity of *Plasmodium falciparum* and *Plasmodium vivax* gametocytes in relation to malaria control and elimination. *Clin. Microbiol. Rev.* 24, 377–410. doi: 10.1128/CMR.00051-10

Bradley, J., Stone, W., Da, D. F., Morlais, I., Dicko, A., Cohuet, A., et al. (2018). Predicting the likelihood and intensity of mosquito infection from sex specific *Plasmodium falciparum* gametocyte density. *eLife* 7:e34463. doi: 10.7554/eLife.34463

Carter, E. H., Suhrbier, A., Beckers, P. J., and Sinden, R. E. (1987). The *in vitro* cultivation of *P. falciparum* ookinetes and their enrichment on Nycodenz density gradients. *Parasitology* 95, 25–30. doi: 10.1017/s0031182000057516

Churcher, T. S., Bousema, T., Walker, M., Drakeley, C., Schneider, P., Ouédraogo, A. L., et al. (2013). Predicting mosquito infection from *Plasmodium falciparum* gametocyte density and estimating the reservoir of infection. *eLife* 2:e00626. doi: 10.7554/eLife.00626

Delves, M. J., Marques, S. R., Ruecker, A., Straschil, U., Miguel-Blanco, C., López-Barragá, M. J., et al. (2017). Failure of in vitro differentiation of *Plasmodium falciparum* gametocytes into ookinetes arises because of poor gamete fertilisation. *bioRxiv[Preprint]*

Ghosh, A. K., Dinglasan, R. R., Ikadai, H., and Jacobs-Lorena, M. (2010). An improved method for the *in vitro* differentiation of *Plasmodium falciparum* gametocytes into ookinetes. *Malar. J.* 9:194. doi: 10.1186/1475-2875-9-194

Janse, C. J., Mons, B., Rouwenhorst, R. J., Van der Klooster, P. F., Overdulve, J. P., and Van der Kaay, H. J. (1985). *In vitro* formation of ookinetes and functional maturity of *Plasmodium berghei* gametocytes. *Parasitology* 91(Pt 1), 19–29. doi: 10.1017/s0031182000056481

Kiattibutr, K., Roobsoong, W., Sriwichai, P., Saeseu, T., Rachaphaew, N., Suansomjit, C., et al. (2017). Int. *J. Parasitol.* 47, 163–170. doi: 10.1016/j.ijpara.2016.10.006

Lawniczak, M. K., and Eckhoff, P. A. (2016). A computational lens for sexual-stage transmission, reproduction, fitness and kinetics in *Plasmodium falciparum*. *Malar J.* 15, 487. doi: 10.1186/s12936-016-1538-5

Nijhout, M. M. (1979). *Plasmodium gallinaceum*: exflagellation stimulated by a mosquito factor. *Exp. Parasitol.* 48, 75–80. doi: 10.1016/0014-4894(79)90056-0

Sinden, R. E., Hartley, R. H., and Winger, L. (1985). The development of *Plasmodium* ookinetes *in vitro*: an ultrastructural study including a description of meiotic division. *Parasitology* 91, 227–244. doi: 10.1017/s0031182000057334

Warburg, A., and Schneider, I. (1993). In vitro culture of the mosquito stages of Plasmodium falciparum. *Exp Parasitol.* 76, 121–126. doi: 10.1006/expr.1993.1014

World Health Organization [WHO] (2018). *World Malaria Report*. Geneva: WHO.

Conflict of Interest: The authors declare that the research was conducted in the absence of any commercial or financial relationships that could be construed as a potential conflict of interest.

Advantages of publishing in Frontiers

OPEN ACCESS
Articles are free to read for greatest visibility and readership

FAST PUBLICATION
Around 90 days from submission to decision

HIGH QUALITY PEER-REVIEW
Rigorous, collaborative, and constructive peer-review

TRANSPARENT PEER-REVIEW
Editors and reviewers acknowledged by name on published articles

Frontiers
Avenue du Tribunal-Fédéral 34
1005 Lausanne | Switzerland

Visit us: www.frontiersin.org
Contact us: info@frontiersin.org | +41 21 510 17 00

REPRODUCIBILITY OF RESEARCH
Support open data and methods to enhance research reproducibility

DIGITAL PUBLISHING
Articles designed for optimal readership across devices

FOLLOW US
@frontiersin

IMPACT METRICS
Advanced article metrics track visibility across digital media

EXTENSIVE PROMOTION
Marketing and promotion of impactful research

LOOP RESEARCH NETWORK
Our network increases your article's readership